Development of new polyesters by organometallic and enzymatic catalysis

Thibaud Debuissy

UNIVERSITÉ DE STRASBOURG

ÉCOLE DOCTORALE Physique – Chimie Physique

ICPEES - UMR 7515

THÈSE présentée par :

Thibaud DEBUISSY

Soutenue le : **10 mai 2017**

pour obtenir le grade de : **Docteur de l'Université de Strasbourg**

Discipline/ Spécialité : Chimie des Polymères

Développement de nouveaux polyesters par catalyse organométallique et enzymatique

THÈSE dirigée par :

M. AVEROUS Luc	Professeur, Université de Strasbourg

RAPPORTEURS :

M. CRAMAIL Henryi	Professeur, Université de Bordeaux
M. FLEURY Etienne	Professeur, INSA Lyon

AUTRES MEMBRES DU JURY :

Mme DELAITE Christelle	Professeur, Université de Haute-Alsace

MEMBRE INVITE :

M. POLLET Eric	Maître de Conférences, Université de Strasbourg

ICPEES, Institut de Chimie et Procédés pour l'Energie, l'Environnement et la Santé – UMR 7515

25 rue Becquerel – 67087 Strasbourg Cedex 2

COMMUNICATIONS LIÉES AUX TRAVAUX DE THÈSE

Publications

Les résultats présentés dans cette thèse font l'objet de 10 articles et d'une revue bibliographique.

Articles publiés :

- Debuissy T., Pollet E., Avérous L. – "Synthesis of potentially biobased copolyesters based on adipic acid and butanediols: kinetic study between 1,4- and 2,3-butanediol and their influence on crystallization and thermal properties", *Polymer, 2016, 99, 204-213.*
- Debuissy T., Pollet E., Avérous L. – "Enzymatic synthesis of a biobased copolyester from poly(butylene succinate) and poly[(*R*)-3-hydroxybutyrate]: Study of reaction parameters on the transesterification rate", *Biomacromolecules, 2016, 17 (12), 4054–4063.*
- Debuissy T., Pollet E., Avérous L. – "Synthesis and characterization of biobased poly(butylene succinate-*ran*-butylene adipate). Analysis of the composition-dependent physicochemical properties", *European Polymer Journal, 2017, 87, 84-98.*
- Perez-Camargo R. A., Fernandez-d'Arlas B., Cavallo D., Debuissy T., Pollet E., Avérous, L., Muller A. J. – "Tailoring the Structure, Morphology, and Crystallization of Isodimorphic Poly(butylene succinate-*ran*-butylene adipate) Random Copolymers by Changing Composition and Thermal History", *Macromolecules, 2017, 50 (2), 597–608.*
- Debuissy T., Pollet E., Avérous L.– "Titanium-catalyzed transesterification as a route to the synthesis of fully biobased poly(3-hydroxybutyurate-*co*-butylene dicarboxylate) copolyesters, from their homopolyesters", *European Polymer Journal, 2017, 90, 92-104.*
- Debuissy T., Pollet E., Avérous L., – "Synthesis and characterization of block poly(ester-ether-urethane)s from bacterial poly(3-hydroxybutyrate) oligomers.", *Journal of Polymer Science Part A: Polymer Chemistry, 2017, 55 (11), 1949-1961.*
- Debuissy T., Pollet E., Avérous L., – "Enzymatic synthesis of biobased poly(1,4-butylene succinate-*ran*-2,3-butylene succinate) copolyesters and characterization. Influence of 1,4- and 2,3-butanediol contents", *European Polymer Journal, 2017, 93, 103-115.*
- Debuissy T., Sangwan P., Pollet E., Avérous L., – "Study on the structure-properties relationship of biodegradable and biobased aliphatic copolyesters based on 1,3-propanediol, 1,4-butanediol, succinic and adipic acids", *Polymer, 2017, 122, 105-116.*
- Debuissy T., Pollet E., Avérous L.– "Synthesis and characterization of fully biobased poly(propylene succinate-*ran*-propylene adipate). Analysis of the architecture-dependent physicochemical behavior", *Journal of Polymer Science Part A: Polymer Chemistry, 2017, DOI:10.1002/pola.28668.*

Articles soumis :

- Debuissy T., Pollet E., Avérous L., – "Enzymatic synthesis of potentially biobased and biodegradable aliphatic copolyesters: effect of the monomer length on the lipase reactivity and copolyester properties." *Soumis dans European Polymer Journal*.

Articles qui seront soumis ultérieurement :

- Debuissy T., Pollet E., Avérous L., – "Abiotic and biotic synthesis of biobased polyesters from short building blocks – A review".

Conférences

Les résultats présentés dans cette thèse ont fait l'objet d'une communication orale dans une conférence internationale :

- Debuissy T., Pollet E., Avérous L. – "New fully biobased macromolecular architectures: analysis of the structure-properties relationship of synthesized terpolyesters from building blocks", *communication orale*, 23rd Bio-Environmental Polymer Society, Karlsruhe (Allemagne, 14 octobre 2015).

LISTE DES ABRÉVIATIONS

[α]	Specific optical rotation
1,10-DCO	1,10-decanediol
1,3-PDO	1,3-propanediol
1,4-BDO	1,4-butanediol
1,6-HDO	1,6-hexanediol
2,3-BDO	2,3-butanediol
4,4'-MDI	4,4'-diphenylmethylene diisocyanate
AA	Adipic acid (ou acide adipique)
As	Aspartate
CALB	*Candida antarctica* lipase B (ou lipase B de *Candida antarctica*)
$CDCl_3$	Deuterated chloroform
CES	Chromatographie d'exclusion stérique
Cl-TMDP	2-chloro-4,4,5,5-tetramethyl-1,3,2-dioxaphospholane
COOH	Carboxylic acid end-group
DBE	Dibenzyl ether
DBTL	Dibutyl tin (II) dilaurate
DEA	Diethyl adipate (ou diéthyle adipate)
DEPT	Distortionless enhancement by polarization transfer
DES	Diethyl succinate (ou diéthyle succinate)
DMA	Dimethyl adipate (ou diméthyle adipate)
DMAP	4-dimethylaminopyridine
DMS	Dimethyl succinate (ou diméthyle succinate)
DMSO-d_6	Deuterated dimethyl sulfoxide
DPE	Diphenyl ether
DP_n	Number-average degree of polymerization
DSC	Differential scanning calorimetry
D_t	Degree of biodegradability
DTG	Derivative thermogravimetric analysis
Đ	Dispersity
E_a	Energy of activation
EDIPA	*N*-ethyl-*N*,*N*-diisopropylamine
EG	Ethylene glycol
eq.	Molar equivalent (ou equivalent molaire)
FTIR	Fourrier transform infra-red
Glu	Glutamate
HCl	Hydrogen chloride
HDI	1,6-hexamethylene diisocyanate
HiC	*Humicola insolens* cutinase
His	Histidine
HSQC-NMR	Heteronuclear single quantum coherence nuclear magnetic resonance
IUPAC	International Union of Pure and Applied Chemistry
log P	Logarithm of the partition coefficient between 1-octanol and water
L_{XX}	Average sequence length of XX units
MALDI-ToF MS	Matrix-assisted laser desorption-ionization – time of flight - mass spectrometry
mcl	Medium-chain-length
MHS	Mark-Houwink-Sakurada
M_n	Number-average molar mass (ou masse molaire moyenne en nombre)
mol.%	Mol percent
M_w	Weight-average molar mass (ou masse molaire moyenne en poids)
N435	Novozym® 435
NMR	Nuclear magnetic resonance
OH	Hydroxyl end-group
p	Extent of reaction
P(3HB-*co*-3HHx)	Poly(3-hydroxybutyrate-*co*-3-hydroxyhexanoate)
P(3HB-*co*-3HV)	Poly(3-hydroxybutyrate-*co*-3-hydroxyvalerate)
P(3HB-*co*-4HB)	Poly(3-hydroxybutyrate-*co*-4-hydroxybutyrate)
PB'A	Poly(2,3-butylene adipate)
PB'S	Poly(2,3-butylene succinate)
PBA	Poly(1,4-butylene adipate)

PBAT	Poly(butylene adipate-co-butylene terephthalate)
PBAT	Poly(butylene adipate-*co*-butylene terephthalate)
PBB'A	Poly(1,4-butylene adipate-*co*-2,3-butylene adipate)
PBB'S	Poly(1,4-butylene succinate-*co*-2,3-butylene succinate)
PBS	Poly(1,4-butyene succinate)
PBSA	Poly(1,4-butylene succinate-*co*-1,4-butylene adipate)
PCL	Poly(ε-caprolactone)
pds.%	Pourcentage en masse
PEEU	Poly(ester-ether-urethane) (ou poly(ester-éther-uréthane))
PEF	Poly(ethylene furanoate)
PEG	Poly(ethylene glycol)
PET	Poly(ethylene terephthalate)
P_{ether}	Polyether-diol
PHA	Poly(hydroxyalkanoate) (ou poly(hydroxyalcanoate))
PHB	Poly[(*R*)-3-hydrobutyrate]
PHB-diol	Telechelic hydroxylated poly(3-hydrobutyrate) oligomers
PLA	Poly(lactic acid)
PLA	Poly(lactic acid)
Poly(HB-*co*-BA)	Poly(3-hydroxybutyrate-co-butylene adipate)
Poly(HB-*co*-BS)	Poly(3-hydroxybutyrate-co-butylene succinate)
PPA	Poly(1,3-propylène adipate)
PPBA	Poly(1,3-propylene adipate-*co*-1,4-butylene adipate)
PPBS	Poly(1,3-propylene succinate-*co*-1,4-butylene succinate)
PPG-PEG-PPG	Poly(propylene glycol)-*block*-poly(ethylene glycol)-*block*-poly(propylene glycol)
PPS	Poly(1,3-propylene succinate)
PPSA	Poly(1,3-propylene succinate-*co*-1,3-propylene adipate)
R	Degree of randomness
RMN	Résonance magnétique nucléaire
ROP	Ring-opening polymerization
rpm	Round per minute
SA	Succinic acid (ou acide succinique)
sc	Supercirtical fluids
scl	Short-chain-length
SEC	Size exclusion chromatography
Ser	Serine
$SnCl_2$	Tin (II) chloride
SSP	Solid-state polymerization
T_b	Boiling temperature
T_c	Crystallization temperature
T_{cc}	Cold-crystallization temperature
$T_{d,2\%}$	2 wt.% degradation temperature
$T_{d,50\%}$	50 wt.% degradation temperature
$T_{deg,max}$	Maximal degradation rate temperature
TEA	Triéthylamine
$T_{ébu}$	Température d'ébulittion
T_f	Température de fusion
T_g	Glass transition temperature
TGA	Thermogravimetric analysis
$THCO_2$	Theoretical amount of carbon dioxide
T_m	Melting temperature
TPU	Thermoplastic polyurethane
US-DoE	United States Department of Energy
WAXS	Wide angle X-ray scattering
wt.%	Weight percent
X_c	Degree of crystallinity
ΔH_c	Crystallization enthalpy
ΔH_{cc}	Cold-crystallization enthalpy
ΔH_m	Melting enthalpy
$\Delta H_m°$	Melting enthalpy of a 100% pure crystalline polymer

SOMMAIRE

LISTE DES ILLUSTRATIONS

Figures

Introduction générale

Chapitre 1

Chapitre 2

Chapitre 3

Chapitre 4

Conclusion

Annexes

Tableaux

Chapitre 1

Chapitre 2

Chapitre 3

Chapitre 4

Annexes

Schémas

Chapitre 1

Chapitre 2

Chapitre 3

Chapitre 4

Annexes

INTRODUCTION GÉNÉRALE

Les matériaux fossiles et notamment les polymères sont aujourd'hui très utilisés dans de nombreuses applications de par leur facilité de mise en œuvre et leurs propriétés. Cependant l'accès de plus en plus limité à certaines fractions de ressources fossiles, l'évolution des normes environnementales ainsi que globalement la prise de conscience écologique des citoyens poussent les industriels à mettre sur le marché des produits plus respectueux de l'environnement, et ceci du « berceau » (ressource) à la « tombe » (fin de vie des matériaux). En effet, une large réflexion sur l'impact environnemental de nos modes de vie actuels s'est engagée au cours des dernières décennies. Afin de limiter l'utilisation de produits toxiques pour notre environnement, les pratiques actuelles dans le secteur des matériaux et de la chimie sont en pleine mutation. Le développement durable devient un axe majeur de notre économie moderne et s'appuie sur une « chimie verte » en plein essor. Ce concept repose sur 12 principes fondateurs introduits en 1998 par les chimistes américains Paul Anastas et John C. Warner (Anastas and Warner, 2000), de l'EPA (United States Environmental Protection Agency), parmi lesquels on trouve notamment l'utilisation de ressources renouvelables (septième principe), la recherche de procédés de synthèse pas ou peu toxiques pour l'homme et son environnement (troisième et quatrième principes), la recherche de procédés en conditions douces (troisième principe) ou encore l'utilisation préférentielle de procédés catalytiques (neuvième principe).

L'application du septième principe de la chimie verte favorise le développement de polymères biosourcés qui connaissent depuis quelques années un développement rapide avec une capacité de production mondiale qui est passée de 180 milliers de tonnes en 2008 à près de 2 millions de tonnes en 2015, avec une croissance à 2 chiffres pour un marché global qui s'exprime en milliards d'euros. Cette croissance a pu être soutenue grâce au développement de bioraffineries qui permettent à partir de diverses biomasses (*i.e.*, matériaux produits par la croissance de microorganismes, plantes ou animaux, selon la définition donnée par IUPAC) l'obtention (i) de molécules plateformes équivalentes à celles obtenues à partir de ressources fossiles, ou (ii) de nouvelles molécules plateformes (par exemple : isosorbide, furanes).

La demande mondiale croissante en bioplastiques (*i.e.*, matières plastiques biosourcées) a permis le développement industriel de nombreux matériaux biosourcés et notamment des polyesters comme l'acide polylactique, le poly(butylène succinate) et plus récemment le poly(éthylène furanoate) (PEF). Cependant, les polymères biosourcés sont aujourd'hui encore loin de pouvoir se substituer largement à leurs équivalents pétrosourcés soit pour des raisons de coût, soit pour des problèmes de disponibilité de la biomasse correspondante, mais souvent et globalement parce qu'ils n'atteignent pas les caractéristiques requises par les cahiers de charges industriels actuels. Malgré cela, pour répondre à l'explosion pressentie de la demande (Figure I.1), qui d'après les données du Nova Institute pourrait être multipliée par deux d'ici 2021 (Aeschelmann and Carus, 2016), la recherche et l'investissement dans ce domaine se développent rapidement et de nouvelles solutions biosourcées émergent à court ou à moyen terme.

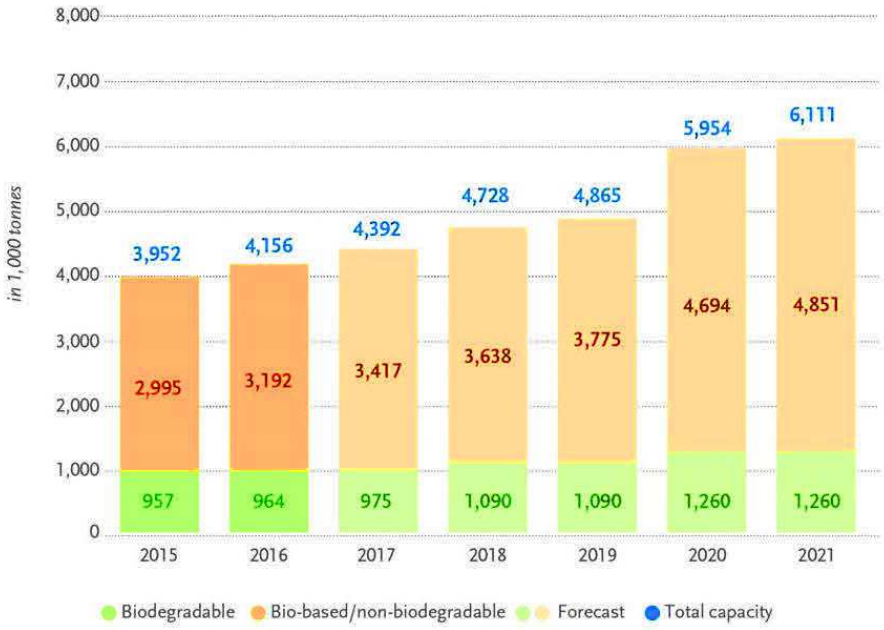

Figure I.1 : Projection de l'évolution de la capacité de production mondiale en bioplastiques (source : Nova-Institute, 2016).

C'est dans ce contexte de développement durable qu'a vu le jour ce projet de thèse mené par l'équipe BioTeam dirigée par le Pr. Luc Avérous au sein de l'Institut de Chimie et Procédés pour l'Energie, l'Environnement et la Santé (ICPEES – UMR 7515 – Université de Strasbourg). Ce projet, intitulé « Synthèse de polyesters par catalyse organométallique et enzymatique », s'inscrit dans le cadre du projet européen SYNPOL (« Biopolymers from Syngas Fermentation ») du 7ème PCRD comprenant une quinzaine de partenaires académiques et industriels en Europe (www.Synpol.org) et qui a démarré fin 2012 pour 4 ans. Ce projet a pour finalité la création d'une plateforme technologique intégrant la pyrolyse de bio-déchets complexes et la synthèse de polymères/matériaux biosourcés par des procédés technologiques avancés, notamment par fermentation biologique de syngas. Le schéma général de ce projet est présenté dans la Figure I.2. Le projet s'articule en plusieurs parties :

1. Synthèse de syngas par pyrolyse contrôlée de bio-déchets complexes (déchets solides municipaux/commerciaux, résidus lignocellulosiques, boues d'épuration).
2. Développement de procédés et des souches pour la synthèse bactérienne et enzymatique de polyhydroxyalcanoates (PHA) et de synthons biosourcés stratégiques (acide succinique, butanediol, acide hydroxybutyrique…).
3. Synthèse de copolyesters biosourcés et de poly(ester-uréthane)s par catalyse chimique, organométallique et enzymatique à partir des synthons et PHAs développés en amont.
4. Développement de matériaux composites à partir de PHAs par renfort de charges et de fibres naturelles.

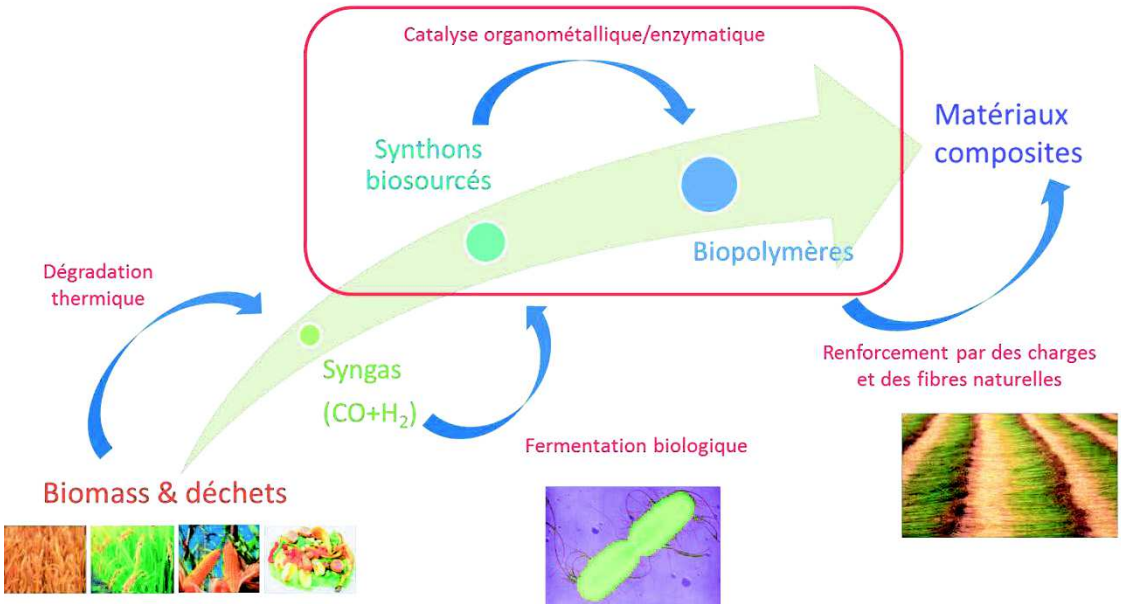

Figure I.2 : Schéma récapitulatif du projet européen SYNPOL.

Cette étude s'inscrit donc dans la troisième partie du projet SYNPOL. Ce travail de doctorat en utilisant une approche d'ingénierie macromoléculaire s'est focalisé dans un premier temps sur la synthèse de copolyesters thermoplastiques aliphatiques à partir de diacides biosourcés (acide succinique et acide adipique), de diols biosourcés à chaînes courtes (1,3-propanediol, 1,4-butanediol et 2,3-butanediol) et de PHAs par catalyse organométallique et enzymatique, et porte dans un second temps sur la caractérisation et l'étude des relations structures-propriétés des copolymères synthétisés. La structure des polymères synthétisés a été déterminée par RMN (^{1}H, ^{13}C, DEPT 135, HSQC-2D et ^{31}P) et FTIR. La stabilité thermique et la dégradation thermique ont quant à elles été évaluées par ATG sous atmosphère inerte (hélium) La structure cristalline et les propriétés thermiques ont été déterminées par DRX et DSC.

De plus, ce travail a fait l'objet de différentes interactions et collaborations avec des laboratoires internationaux. Par exemple, une étude spécifique de biodégradation en compost de certains de ces polyesters a été menée en collaboration avec le Dr. Parween Sangwan (CSIRO, Clayton, Australie). En collaboration avec le Pr. Alejandro J. Müller (UPV, San Sebastian, Espagne) une étude fine a été développée sur l'influence des compositions molaires et de l'histoire thermique des copolyesters synthétisés par catalyse organométallique sur la structure, la morphologie et la cristallisation de ces matériaux.

Ce sujet de thèse transversal associe ainsi la synthèse des polymères (catalyse organométallique et/ou enzymatique) et la caractérisation (structure chimique, structure cristalline, propriétés thermiques, stabilité thermique) des différentes architectures obtenues (copolyesters aliphatiques biosourcés) afin de développer des outils d'ingénierie macromoléculaire permettant notamment d'analyser l'impact des structures chimiques et teneurs des synthons obtenus par bioproduction (biotechnologie blanche) sur les propriétés des matériaux finaux.

Organisation du manuscrit :

Ce manuscrit s'articulera en quatre grands chapitres (Figure I.3) organisés autour de différents articles scientifiques rédigés en anglais qui seront encadrés par des textes d'introduction et des conclusions en français.

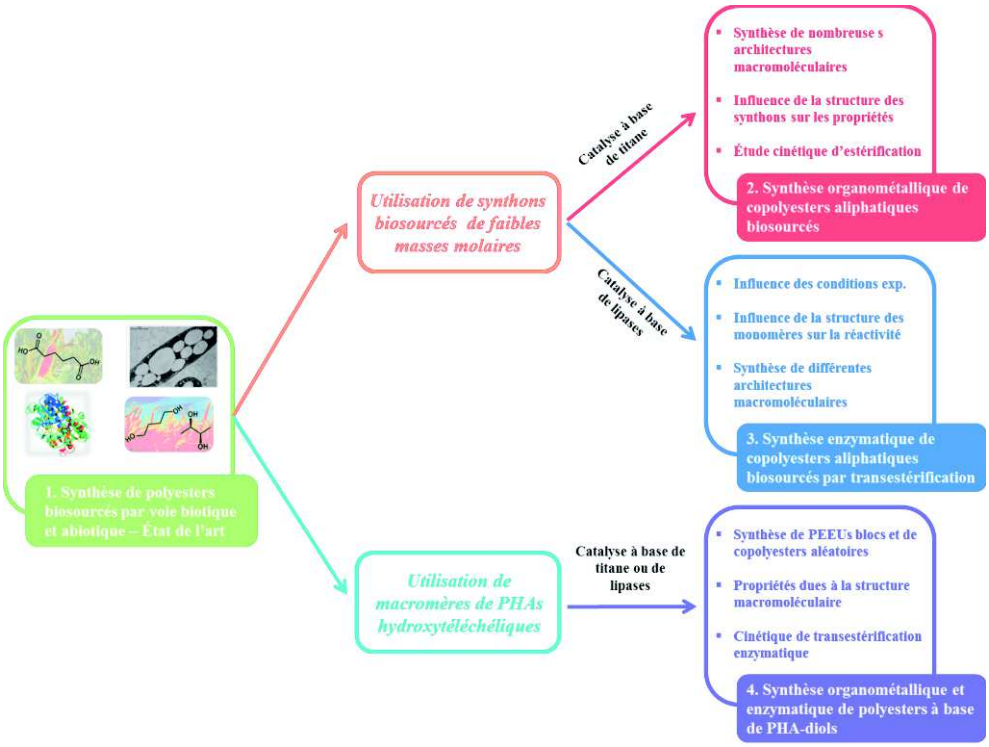

Figure I.3 : Récapitulatif de la stratégie développée au cours de la thèse.

Tout d'abord, un premier chapitre s'attachera à faire un état de l'art de la synthèse de copolyesters aliphatiques biosourcés par les différentes voies catalytiques (principalement organométallique et enzymatique) en se concentrant principalement sur l'estérification et la transestérification de monomères multifonctionnels (diols et diacides ou leurs dérivés). Cet état de l'art permettra de mettre en évidence la richesse des architectures synthétisées ainsi que les paramètres clés de la synthèse organométallique et enzymatique.

Le deuxième chapitre, composé de plusieurs sous-chapitres, présentera les résultats relatifs à la synthèse et à l'étude de la relation « structure-propriété » de différents copolyesters obtenus par **catalyse organométallique** à partir de synthons biosourcés. Ainsi, un premier sous-chapitre (2.1) se focalisera sur le poly(butylène succinate-*co*-butylène adipate) (PBSA) et mettra en évidence le comportement isodimorphique de ce copolyester. Pour sa part, le sous-chapitre 2.2 se concentrera sur la synthèse du poly(propylène succinate-*co*-propylène adipate) (PPSA) et montrera notamment l'influence du 1,3-propanediol sur la cinétique de cristallisation et celui du diacide sur la stabilité thermique du matériau. Par la suite, le sous-chapitre 2.3 étudiera l'influence de la composition sur les propriétés du poly(propylène succinate-*co*-butylène succinate) (PPBS) et du poly(propylène adipate-*co*-butylène adipate) (PPBA). Pour conclure ce deuxième chapitre, le sous-chapitre 2.4 portera exclusivement sur le poly(1,4-butylène adipate-*co*-2,3-

butylène adipate) (PBB'A) issu d'un diol ayant des fonctions hydroxyles secondaires (2,3-butanediol) et mettra en évidence la plus faible réactivité de ce dernier comparé au diol porteur de fonctions hydroxyles primaires, entrainant ainsi des structures de plus faibles masses molaires. L'influence du 2,3-butanediol sur la cristallinité du copolyester sera également étudiée. L'ensemble des copolyesters synthétisés et étudiés lors de ce chapitre est présenté dans la Figure I.4.

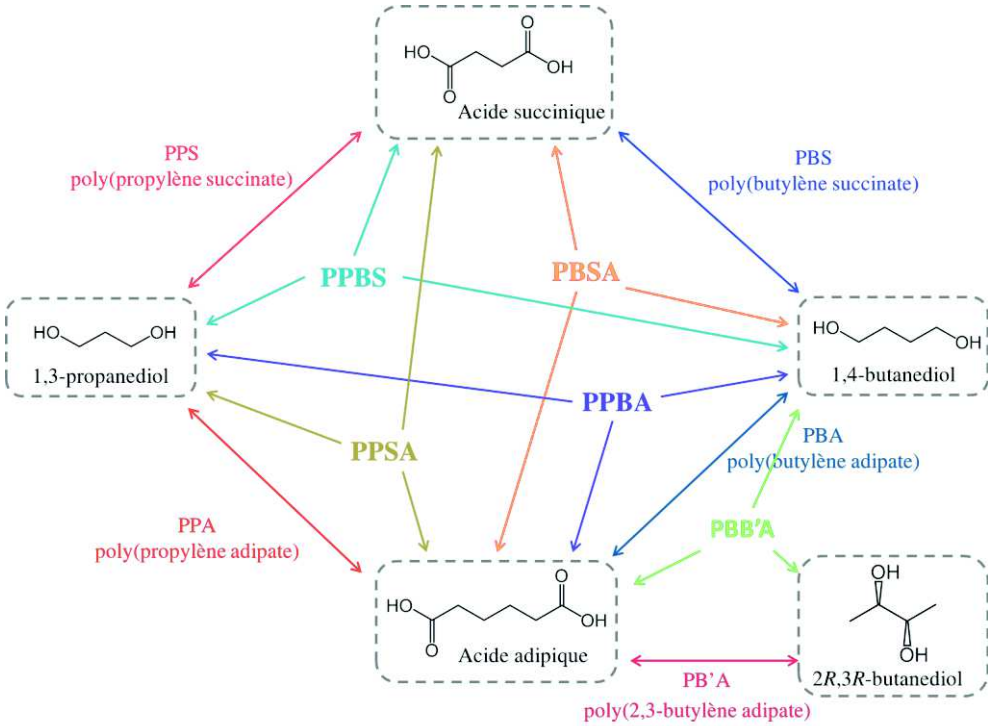

Figure I.4 : Schéma récapitulatif des copolyesters issus des synthons biosourcés.

La troisième partie de ce manuscrit (chapitre 3), composée de trois sous-chapitres, présentera les résultats portant sur la synthèse par **catalyse enzymatique** de copolyesters issus de synthons biosourcés. Tout d'abord, le sous-chapitre 3.1 est axé sur le développement de la méthodologie et des voies de transestérification par catalyse enzymatique en solution ou en masse pour la synthèse de polyesters tels que le poly(butylène succinate) ou le poly(butylène adipate). Ensuite, le sous-chapitre 3.2 discutera de la réactivité du 2,3-butanediol, qui est un synthon asymétrique et court, lors de la synthèse enzymatique du poly(1,4-butylène succinate-*co*-2,3-butylène succinate) (PBB'S) et son impact sur les propriétés de ce dernier. Pour finir, le sous-chapitre 3.3 portera sur la synthèse enzymatique en solution de PBSA et de PPBS, et permettra de comparer les structures obtenues par catalyse organométallique et enzymatique. La cinétique de transestérification et l'influence de la longueur de chaîne des monomères seront particulièrement discutées.

Le quatrième et dernier chapitre sera dédié à la synthèse de copolymères par voie organométallique et enzymatique à partir de PHAs bactériens, plus particulièrement le poly((*R*)-3-hydroxybutyrate) (PHB). Pour commencer, le sous-chapitre 4.1 porte sur la synthèse d'oligomères de PHB téléchéliques à terminaisons hydroxyles (PHA-diol) par alcoolyse organométallique et son utilisation comme « macrodiol » dans la synthèse de poly(ester-éther-uréthane)s. Après l'étude de la cinétique d'alcoolyse, l'influence de la

masse molaire des PHA-diols et celle du ratio « segment dur/segment souple » sur les propriétés des poly(ester-éther-uréthane)s sont tout particulièrement discutées. Ensuite, le sous-chapitre 4.2 étudiera la synthèse enzymatique de poly(3-hydroxybutyrate-*co*-butylène succinate) soit en une seule étape à partir des synthons correspondant, soit par transestérification de PHA-diols avec du poly(butylène succinate) préalablement synthétisé par catalyse enzymatique. L'étude portera tout particulièrement sur l'influence des conditions réactionnelles sur la structure des copolyesters obtenus et les propriétés des matériaux correspondants. Pour finir, le sous-chapitre 4.3 se focalisera sur la synthèse organométallique de copolyesters à partir d'oligomères de PHA et de poly(butylène dicarboxylate)s de masse molaires importantes par transestérification organométallique. Une attention particulière sera portée au procédé de synthèse afin de limiter la dégradation thermique des PHAs durant la synthèse des copolyesters. L'ensemble des réactions réalisées à partir de PHAs lors de ce chapitre est schématisé dans la Figure I.5.

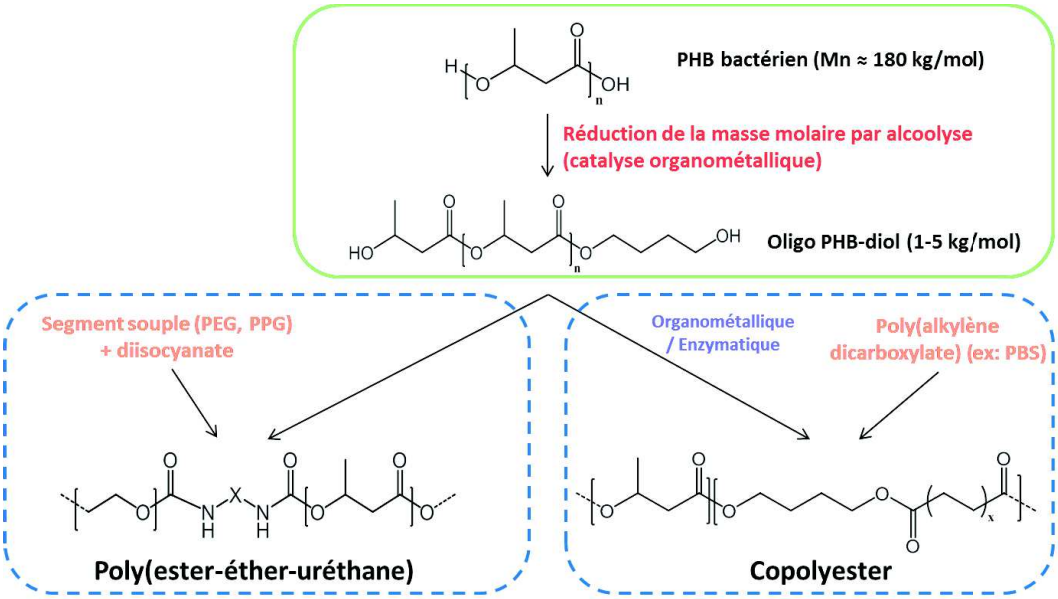

Figure I.5 : Schéma des synthèses de copolyesters et poly(ester-éther-uréthane)s à partir d'oligo PHB-diols.

Références :

Aeschelmann, F., Carus, 2016. Bio-based Building Blocks and Polymers - Global Capacities and Trends 2016 – 2021. Nova-Institute, Germany.

Anastas, P.T., Warner, J.C., 2000. Green chemistry: theory and practice. Oxford Univ. Press, Oxford.

CHAPITRE 1: SYNTHÈSE DE POLYESTERS BIOSOURCÉS PAR VOIE ABIOTIQUE ET BIOTIQUE – ETAT DE L'ART

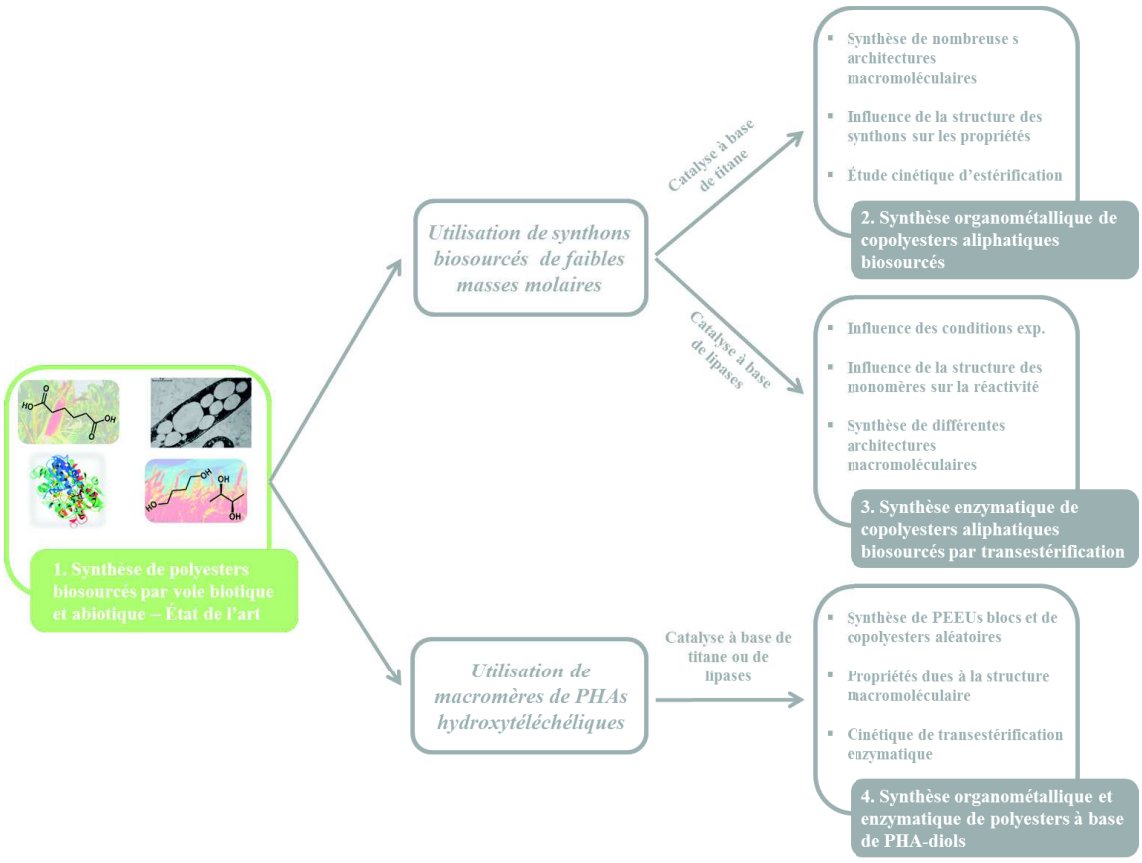

Introduction du chapitre 1

La synthèse bibliographique présentée dans ce chapitre est consacrée à l'étude de la production de polyesters biosourcés par catalyse chimique (abiotique) ou biologique (biotique). Elle se présente sous la forme d'une revue intitulée «Abiotic and biotic synthesis of biobased polyesters from short building blocks – A review » qui sera soumise dans un journal ultérieurement.

Dans un premier temps, un rapide aperçu sur la production industrielle actuelle de polyesters biosourcés ou potentiellement biosourcés est présenté, ainsi que les principaux synthons issus de la biomasse qui sont utilisés pour la synthèse de ces polyesters. Ensuite, un état de l'art sur la synthèse de polyesters par estérification/transestérification à partir de synthons plurifonctionnels par catalyse chimique (ou abiotique), dite « traditionnelle », en utilisant principalement des catalyseurs à base de métaux de transition est exposé. Le procédé en masse à partir de diacide (ou de diesters des diacides correspondants) et de diols est tout particulièrement étudié car c'est celui qui a été utilisé lors notre étude. Toutefois, d'autres types de catalyseur et d'autres procédés de synthèse sont également évoqués. Puis, le procédé de synthèse par catalyse enzymatique est présenté en s'intéressant tout particulièrement à la réaction de transestérification. Après un rapide aperçu des différentes enzymes démontrant une activité catalytique pour ce type de réaction, les différents paramètres impliqués lors la synthèse enzymatique par transestérification sont étudiés. Par la suite, les polyesters bactériens, connus sous le nom de polyhydroxyalcanoates (PHAs), obtenus par fermentation sont présentés. Une attention particulière est prêtée aux architectures complexes (*i.e.*, copolyesters) qui peuvent être obtenues par fermentation d'une part ou par voie de synthèse à partir d'oligomères de PHAs d'autre part. Pour finir, des perspectives sont énoncées, en soulignant d'une part la richesse des architectures macromoléculaires susceptibles d'être synthétisées et le caractère extrêmement prometteur de la synthèse de polyesters par catalyse enzymatique d'autre part, même si cette voie de synthèse nécessite encore de nombreuses améliorations.

Abiotic and biotic synthesis of biobased polyesters from short building blocks – A review

Thibaud Debuissy, Eric Pollet and Luc Avérous*

BioTeam/ICPEES-ECPM, UMR CNRS 7515, Université de Strasbourg, 25 rue Becquerel, 67087 Strasbourg Cedex 2, France

*Corresponding author: luc.averous@unistra.fr

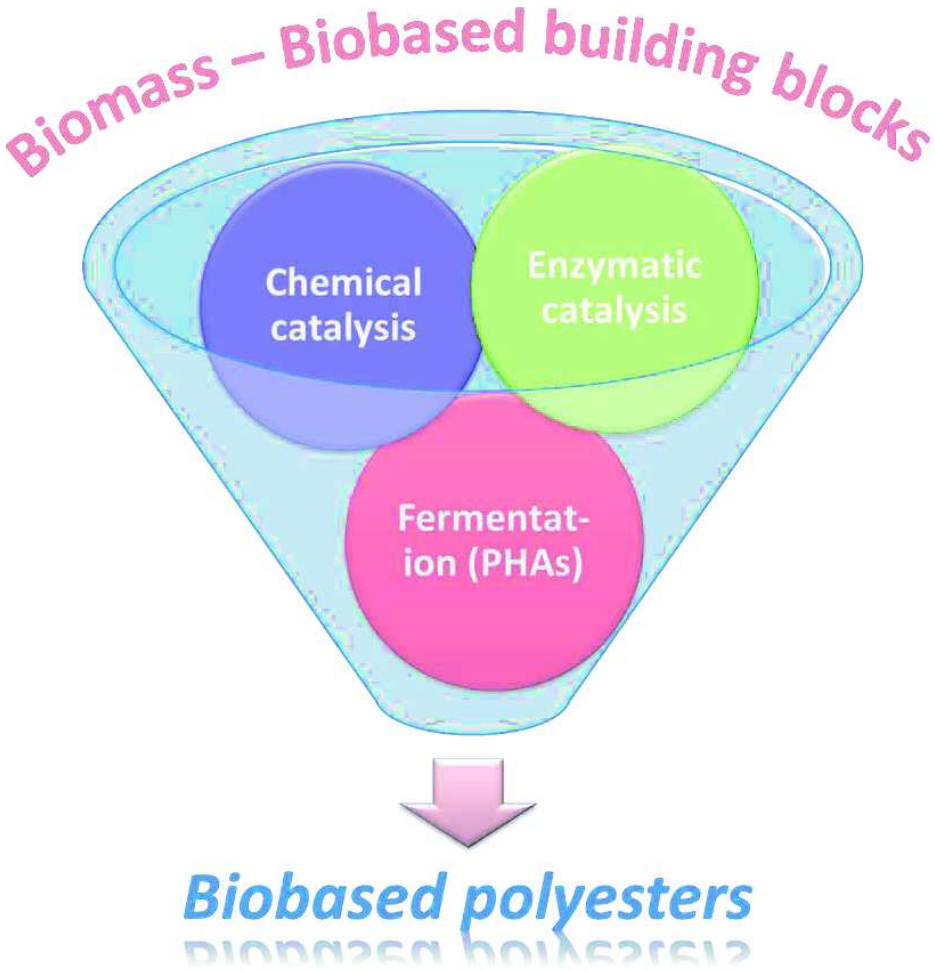

1. Towards the development of biobased polymers

Polymers are one of the most important materials developed by mankind, which play an essential role in our modern life with a multitude of applications. They are large macromolecules that are composed of many small molecular fragments known as repeating units. They are used in a large range of applications such as plastics, rubbers, fibers, coatings, adhesives and foams. According to their synthesis and origin, polymers can be registered as biopolymers or synthetic polymers. Biopolymers (IUPAC's definition: macromolecules formed by living organisms) are biosynthesized in "nature" *via* in vivo reactions, where biocatalysts, mostly enzymes, are inevitably involved in the synthetic process. Biopolymers can be found in all living organisms: plants, animals, and microorganisms such as bacteria or fungi. Examples of biopolymers include cellulose, lignins, chitin, starch, proteins, DNA, natural rubbers and polyhydroxyalkanoates (PHAs).

Synthetic polymers are commonly produced *via* polymerization of fossil-based chemicals having simple structures. Chemical catalysts, especially metal-based catalysts, are normally used in the synthesis of synthetic polymers. Because of (i) the high development of the petrochemical industry, (ii) the availability of cheap fossil resources and (iii) the establishment and development of polymerization techniques, numerous synthetic polymers have been developed, such as, phenol-formaldehyde resins, polyolefins, polyvinyl chloride, silicones, polystyrene, polyesters, polyamides, polyurethanes… Synthetic polymers became important in common usage since the early 20th century and are widely used as bottles, bags, boxes, textile fibers, films, insulation…

Today, there is huge demand for polymers. The global production of plastics increased from 230 million tons in 2004 to 322 million tons in 2015 (Figure 1.1), and the worldwide polymer production is expected to reach about 400 million tons in 2020 (Aeschelmann and Carus, 2016). This huge polymer consumption leads to a high demand for fossil oils for the polymer industry (about 4% of the global oil production), which brings some significant issues. On one side, fossil resources are depleting resources with limited reserve and their generation requires millions of years. There is a great concern that fossil resources will be exhausted in about 100 years. Moreover, the extreme volatility of oil prices, which are related to unstable politics, is another drawback. On the other side, hazardous waste and emissions are generated in high amount with the consumption of fossil resources causing severe environmental issues such as the increase of the greenhouse effect and atmospheric pollution which induces a major health issue. Due to the growing environmental concern, it is necessary to develop more eco-friendly polymers for reducing the current dependence on fossil resources and also decreasing the production of pollutant.

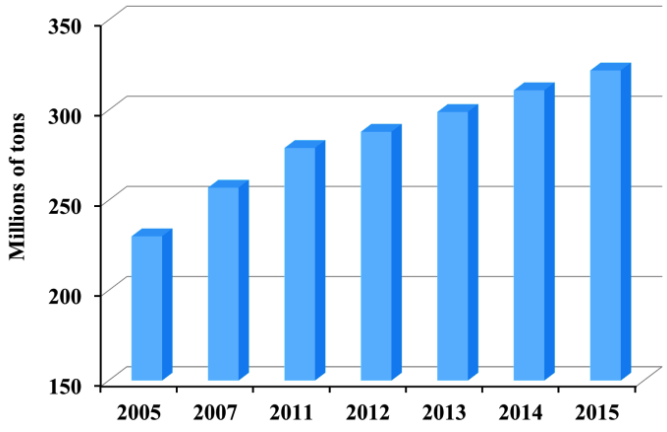

Figure 1.1 : Worldwide production evolution of plastics from 2005 to 2015.

The concept of biorefinery in which renewable resources (biomass) are used to overcome environmental challenges and simultaneously finding an alternative to limited fossil resources have been developed extensively through the world (Corma et al., 2007). Biorefinery is defined as an "sustainable and integral upstream, midstream, and downstream processing of biomass into a range of marketable products (food, feed, materials, chemicals) and energy (fuels, power, heat)" by the International Energy Agency (IEA), whereas sustainability is defined as "the development which meets the needs of the present time without compromising the ability of future generations to meet their own needs". Through a biorefinery scheme, many chemicals can be produced from widely available and renewable resources by chemical or

biotechnological processes as they are traditionally produced in petroleum refinery. Ideally, a biorefinery can use all kinds of biomass from forestry, agriculture, aquaculture, and residues from industry and households. Biomass production by nature is estimated at 170 million tons per year, which only 3.5% are used by humans. Among these 3.5%, most of the production is used for food, 33% for energy, paper, furniture and construction, and only 5% (*i.e.*, 300 ktons) are used for other non-food applications such as chemicals and clothing. Important aspects to take into consideration is the valorization of biomass residues and process by-products avoiding the competition with the food production, such as the adaptation of existing industrial plant technologies to produce new biobased materials to the greatest feasible extent.

Among chemical commodities, polymers, the main component of plastics, are one of the most used fossil-based products in several sectors. Considering the growing demand of polymers, the profitable business around such materials, their relatively low cost and unique properties, it is clear that replacing oil with renewable resources in polymer resources in polymer production within the biorefinery concept is a necessary objective toward a sustainable development.

Polymers from renewable resources, from biomass (IUPAC's definition: material produced by the growth of microorganisms, plants or animals) also named "biobased polymers" are pointed out to be the most interesting alternative to petroleum-based polymers. They can be defined as "a commercial or industrial product (other than food or feed) that is composed, in whole or in significant part, of biological products or renewable domestic agricultural materials (including plant, animal, and marine materials) or forestry materials" (United States Department of Agriculture, 2011). Biobased polymers can be produced by (i) direct extraction from biomass (*e.g.*, starch, cellulose, alginates), (ii) classical chemical synthesis from biobased building blocks produced *via* a biorefinery route (*e.g.*, poly(lactic acid), polyamides, polyesters), or (iii) fermentation processes using microorganisms (*e.g.*, PHAs) (Avérous and Pollet, 2012). On way to determine the biobased content of a polymer is linked to the quantification of C^{14} content (ASTM 6866).

The concept of obtaining polymers from renewable resources is not new since biobased polymers have been used for food, furniture and clothing for hundreds of years. Some biopolymers such as starch, cellulose or natural rubber are useful materials for centuries, but they are limited in variety, and their properties and applications are also limited as they are determined by their chemical structure. Moreover, physical or chemical modifications of these natural polymers still possess some drawbacks such as a rather poor solubility, process difficulties and unwanted impurities which are difficult to remove. In bottom line, these impurities can greatly influence the properties and so their applications. However, the conversion of rich and diverse biomass feedstocks into building blocks is the most promising way for the large production of polymer products. The term "building block" is defined by the US Department of Energy (US-DoE) as "a molecule with multiple functional groups that possess the potential to be transformed into new families of useful molecules" (Werpy et al., 2004).

These building blocks can be then transformed into a wide range of platform molecules *via* chemical processes such as oxidation, reduction, hydrogenolysis, dehydration or direct polymerization (Corma et al., 2007; Sheldon et al., 2008). These platform chemicals can be used as precursors for the production of a large variety of chemicals and materials such as solvents, fibers, antifreeze, and polymers (Bozell, 2008; Yixiang Xu et al., 2008; Yang et al., 2013). Most common building blocks used for the polymer industry are diols (*e.g.*, ethylene glycol, propanediols, butanediols), dicarboxylic acids (*e.g.*, oxalic, malonic, succinic, glutaric, fumaric, itaconic, adipic, 2,5-furanedicarboxylic, sebacic acid), hydroxyacids (*e.g.*, lactic acid, 3-hydroxypropionic acid, malic acid or levulinic acid) and diamines (*e.g.*, ethylenediamine, putrecine or cadaverine) (Becker et al., 2015; Belgacem and Gandini, 2008; Harmsen et al., 2014; Holmberg et al., 2014). Moreover, the huge development of biomass feedstock conversion in recent years, promoted by economic and environmental reasons, has permitted to increase the access of many building blocks with various chemical structures allowing the synthesis of not only sustainable alternative to oil-based polymers with similar structures, but also in novel green polymers with new macromolecular architectures (*e.g.*, furans and sorbitol) that cannot be produced from oil-based building blocks. Some of these biobased building blocks are already or will soon become commercially available due to the fast development of biotechnologies and with the forthcoming scaling-up their prices will be competitive compared to those obtained from fossil resources. Whereas the global production of biobased polymers in 2016 is estimated to reach 6.6 million tons which represent about 2% of the total polymer production capacity, a sustained development of biobased polymers in the near future is expected.

2. Polyesters from renewable resources

2.1. Development of polyesters

Polyesters are polymers in which the backbone is composed of aliphatic or aromatic moieties (R_1 and R_2) linked together by ester groups.

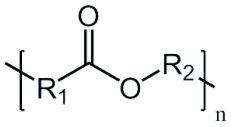

Figure 1.2 : General formula of polyesters.

The polyester family is extremely large and depending on the nature of R_1 and R_2, exhibits a colossal variety of macromolecular structures, properties and thus applications. It has been known since early 19th century that heating carboxylic polyacids with glycerol resulted in aliphatic resinous compounds. After that, it is only in the 1910-1920s, that the General Electric Company led extensive research on alkyd resins. These kinds of resins have still applications in coatings, paints and varnishes. However, the modern history of polyesters began when Carothers studied reactions between aliphatic dicarboxylic acids and diols, and established the worldwide-known step-growth relationships (Carothers, 1929; Carothers and Arvin, 1929; Carothers, 1931, 1936).

In order to increase the polyester melting point and to approach thermomechanical properties of nylons (polyamides), semi-aromatic polyesters using aromatic monomers, such as terephthalic acid, and aliphatic diols were developed in early 1940s. Poly(ethylene terephthalate) (PET) is now one of the most produced polymers for packaging (*e.g.*, bottles) and textile applications, whereas poly(butylene terephthalate) et poly(propylene terephthalate) found applications in solid-state molding resin and the textile industry, respectively.

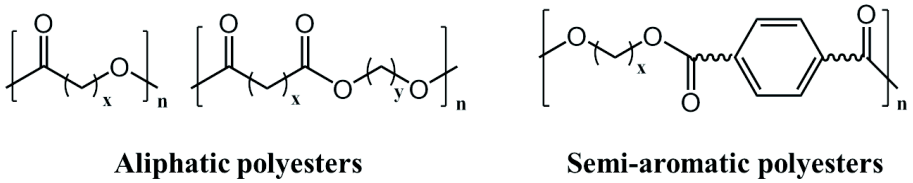

Figure 1.3 : Schematic chemical structure of aliphatic and semi-aromatic polyesters.

A new type of thermoset resins, based on unsaturated polyesters, was developed at the end of the 1930s. These resins were obtained by dissolving these polyesters in unsaturated monomers, such as styrene, capable of undergoing free-radical copolymerization with the unsaturation contained in the polyester chains and leading to insoluble crosslinked network. These resins found an application in combination with glass fibers for protective radar domes during World War II and are now one of the most important matrix resins for glass-fiber-reinforced composite materials (Fradet and Tessier, 2003).

Then, in the 1960s, low molar mass hydroxyl-terminated aliphatic polyesters were used as macromers for the polyurethane industry by reaction with diisocyanate. Despite the fact that aliphatic polyesters were fully characterized, they did not find commercial application until then. In the 1970s, poly(ester-ether) block copolymers having characteristics of thermoplastic elastomers were commercialized by Dupont under the tradename Hytrel (Holden and Adams, 1996).

In the 1990s, environmental concerns began to be gaining ground. The versatility of the ester linkage, able to undergo hydrolysis in some conditions, makes polyesters a perfect choice of polymers for the increasing demand for recyclable and biodegradable polymers (Albertsson and Varma, 2003; Tokiwa et al., 2009). This has resulted in a new interest for aliphatic polyesters such as poly(lactide)s, poly(lactone)s, poly(alkylene dicarboxylate)s, poly(hydroxyalkanoate)s or copolyesters containing aliphatic moieties.

Moreover, the fact that nowadays most of aliphatic polyesters, and even some semi-aromatic polyesters, can be synthesized from biobased monomers increased their attractiveness in the environmental concern discussed previously. Furthermore, aliphatic polyesters are (bio)degradable materials in which ester linkage can be easily cleaved by hydrolysis *via* alkaline, acid or enzymatic catalysis (Rydz et al., 2014). Therefore, aliphatic polyesters can be disposed, recycled, composted or incinerated with a low environmental impact. Furthermore, the fact that aliphatic polyesters are mainly used as thermoplastics or thermoset resins permits now to use these polymers in numerous commodities and specialty applications.

2.2. Biobased polyesters

The most known biobased aliphatic polyester is poly(lactic acid) (PLA), whose monomers are produced by microorganisms from carbohydrates feedstocks (mainly starch), and it is biotically degraded by microorganisms to produce in the end CO_2 and H_2O. This polymer can be therefore considered as one of the best example of fully environmentally-friendly polymer. PLA finds applications mostly as fibers and food packaging materials. The global demand for PLA was around 200,000 tons in 2013 with an average annual growth of 10%. The PLA market is projected to reach a market of 5.2 billion $ by 2020 (Rydz et al., 2014).

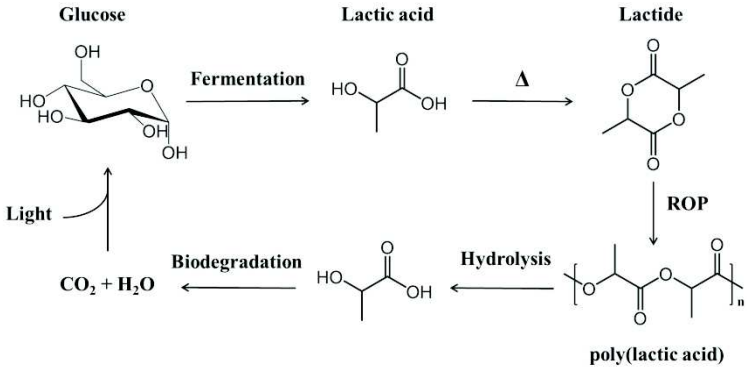

Scheme 1.1 : Schematic view of PLA life cycle.

Poly(butylene succinate) (PBS) is another important commodity polyester which is also biodegradable and potentially 100% biosourced. It has been produced since 1990s, firstly by Showa Denko K.K. (Japan) under the tradename Bionolle™. PBS is synthesized from succinic acid and 1,4-butanediol, which can nowadays be both obtained from natural feedstocks. The global PBS production capacity was about 125,000 tons in 2014 by about 8 different companies including in particular Showa Denko K.K. (Japan), PTT MCC Biochem (Thailand), Mitsubishi Chemical (Japan) and Ire Chemical (South Korean). Until a few years ago, PBS was only produced from petroleum-based monomers. However, since the important development of the bio-succinic acid production by fermentation of carbohydrates feedstocks, some of the PBS producers started producing PBS from biobased monomers. PBS is used mainly as films/sheets for food packaging and agriculture. Moreover, PBS finds new applications in automotive or biodegradable fish nets.

Poly(butylene succinate-*co*-butylene adipate) (PBSA) is a well-known copolyester of PBS which is prepared with adipic acid (AA) to source materials of PBS. Interestingly, PBSA degrades faster than PBS. Compared to PBSA, PBS has a higher crystallinity and is better suited for molding. PBSA with a lower crystallinity is better suited for film applications (Niaounakis, 2014). Even if AA is nowadays petroleum-based and thus PBSA is not 100% biobased, PBSA could be fully biobased in a near future.

Polyhydroxyalkanoates (PHA)s are a large family of thermoplastic biopolyesters synthesized by fermentation using various bacteria from different substrates such as glucose or sucrose. The richness of PHAs monomers allows the development of various macromolecular architectures, even if poly((*R*)-3-hydroxybutyrate) (PHS) is the most known and produced PHA. In addition to the richness of PHA structures, their excellent biodegradability and biocompatibility permit the use of PHA for a large range of applications such in packaging, agriculture and the biomedical area (Doi, 1990; Bordes et al., 2009a; Chen, 2010).

Today, many biobased polyesters are already commercially available such as PLA, PHAs, PBS, PBSA, poly(butylene adipate-*co*-butylene terephthalate) (PBAT), poly(ethylene terephthalate) (PET) and poly(ethylene furanoate) (PEF) (Table 1.1) (Niaounakis, 2014; Rudnik, 2010).

Table 1.1 : Some commercially available biobased polyesters and their manufacturers.

Polyester	Biosourcing (%)	Manufacturer	Trademark
PLA	up to 100	NatureWorks (USA)	Ingeo™, NatureWorks®
		Mitsui Chemicals (Japan)	LACEA®
		Corbion Purac (Netherlands)	Luminy®, Purasorb®
		Futerro (Belgium)	Futerro®
		Shimadzu Corporation (Japan)	Lacty®
		Teijin (Japan)	BioFront™
PHA	100	Metabolix (USA)	Mirel™
		PHB Industrial (Brazil)	Biocyle ®
		Tianjin Green Bioscience (China)	GreenBio
		Tianan Biological (China)	ENMAT ™
		Meredian (USA)	Nodax ™
		Kaneka Co. (Japan)	Kaneka PHBH
		Mitsubishi Chemical (Japan)	BioGreen®
PBS	up to 100	ShowaDenko K.K. (Japan)	Bionolle™
		IRE Chemicals (South Korean)	Enpol®
		SK Chemicals (South Korean)	Skygreen ®
		Mitsubishi Chemical (Japan)	GS PLA®
		PTT MCC Biochem (Thailand)	BioPBS™
PBSA	up to 100	ShowaDenko K.K. (Japan)	Bionolle™
		IRE Chemicals (South Korean)	Enpol®
		SK Chemicals (South Korean)	Skygreen ®
PBAT	30-70	BASF (Germany)	Ecoflex®
		Dupont (USA)	Biomax®
		Novamont (Italy)	Origo-Bi®
		IRE Chemicals (South Korean)	Enpol®
PET	up to 100	Coca Cola (USA)	PlantBottle™
		Toyota Tsusho (Japan)	Globio®
		Toray Industries (Japan)	BioView™
		Teijin Limited (Japan)	ECO CIRCLE™
PEF	up to 100	Avantium (Netherlands)	-

Most of these biobased polyesters, except for PHAs, are produced using short biobased building blocks from dicarboxylic acids and diols.

2.3. Short biobased building blocks for the polyester synthesis

Thanks to the huge development of biorefinery through the world, many biobased building blocks, such as dicarboxylic acids and polyols, can be now produced from various substrates, by biotechnological pathways, to synthesize some of the polyesters cited above. Among the numerous potentially biobased of dicarboxylic acids and polyols, the main developments for the synthesis of biopolyesters concern succinic, fumaric, itaconic and adipic acids on one hand, and ethylene glycol, 1,3-propanediol, 1,4-butanediol, 2,3-butanediol and glycerol on the other hand. The structures of these main biobased building blocks are presented in Figure 1.4.

2.3.1. Main biobased dicarboxylic acids

Succinic acid (SA) is a dicarboxylic acid which has been listed, in 2004, by the US-DoE as one of the "Top Value Added Chemicals from Biomass" (Werpy et al., 2004). This list identifies the potential building blocks that could be produced from biomass *via* biological or chemical conversions, which will have a significant importance in the future. Nowadays, SA is predominantly produced commercially through petrochemical routes by catalytic hydrogenation of maleic acid or anhydride with a global production of 30-50 ktons per year (Jansen and van Gulik, 2014). However, SA can also be produced by fermentation of carbohydrates or glycerol using engineered bacteria or yeast. The current bio-routes for SA are based on *Basfia succiniciproducens*, *E. Coli* and yeasts (*i.e.*, *Saccharomyces cerevisiae* and possibly

Candida krusei) (Bechthold et al., 2008; Becker et al., 2015). Currently, four companies have built up industrial facilities for the production of biobased SA: BioAmber, Succinity, Reverdia and Myriant (Choi et al., 2015). The high interest in SA is based on its wide range of application as building block for the synthesis of polyesters (Debuissy et al., 2017a) or resins, or as a molecule platform (Bozell, 2008).

Fumaric acid is an unsaturated dicarboxylic acid classified in the top building blocks (Werpy et al., 2004). Currently, fumaric acid is mainly produced chemically from fossil resources, but the biotechnological production using *Saccharomyces cerevisiae*, *Rhizopus, Aspergillus* or *Escherichia coli* species is developing rapidly since the last few years (Jiménez-Quero et al., 2016a; Roa Engel et al., 2008; Shah et al., 2016; Song and Lee, 2015). As an example, Myriant is developing a biobased fumaric acid production facility for the production of unsaturated polyester resins (Smitthipong et al., 2014). Moreover, fumaric acid is widely used in food industry as additive for acidity regulation, or as a platform molecule (Bechthold et al., 2008; Wojcieszak et al., 2015).

Itaconic acid is an attractive unsaturated building block that has already been produced industrially by sugar fermentation using *Aspergillus terreus* in the 1960s. Such as SA and fumaric acid, it was listed as one of the top building blocks from renewable resources by the US-DoE (Werpy et al., 2004). The current production of itaconic acid is around 80,000 tons per year (Okabe et al., 2009; Choi et al., 2015), with a potential increase up to 400,000 tons per year in 2020 (Medway and Sperry, 2014). To reduce the cost and increase the sustainability, current studies mainly focus on microorganisms strain improvement , development of more cost-effective processes and the use of cheaper substrate than glucose, such as cellulolytic biomass (El-Imam and Du, 2014; Jiménez-Quero et al., 2016b, 2016a; Okabe et al., 2009). Itaconic acid can be used as a building block for the synthesis of curable polyesters or polyamides resins (Jiang et al., 2015a; Pellis et al., 2015b). Moreover, itaconic acid can be used as a platform molecule to obtain *via* hydrogenation/reduction reactions a large range of chemical derivatives, such as γ-butyrolactone, methacrylic acid and pyrrolidones (Le Nôtre et al., 2014; Qi et al., 2016).

Adipic acid (AA) is one of the most important commodity chemicals with a global market of about 4 million tons per year, which is mainly used for the production of nylon 6,6 or polyesters (Harmsen et al., 2014; Debuissy et al., 2017a, 2016a). At present times, AA is mostly manufactured industrially by oxidation of cyclohexanol or cyclohexanone (Bart and Cavallaro, 2015; Beerthuis et al., 2015; Deng et al., 2016). Nevertheless, different companies (*i.e.*, Verdezyme, Genomatica, Renovia, BioAmber) have already started the production or are currently developing plants for producing biobased AA. In recent years, two biosynthetic pathways to biobased AA have been developed: (i) the chemo-catalytic conversion of biologically derived precursors such as *cis,cis*-muconic acid or glucaric acid by a hydrogenation process (Vardon et al., 2015; Becker et al., 2015), and (ii) the direct biological conversion of vegetal oils and sugars using yeast and bacteria (Picataggio et al., 1992; Polen et al., 2013; Yu et al., 2014).

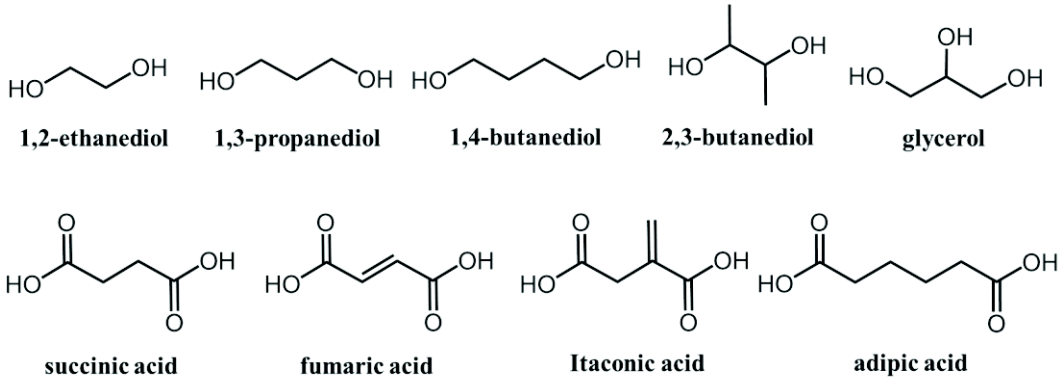

Figure 1.4 : Chemical structures of the main biobased polyols and dicarboxylic acids.

2.3.2. Main biobased aliphatic polyols

1,3-propanediol (1,3-PDO) is a commodity chemical used in a wide range of possible applications, especially as anti-freeze and monomer for polyester synthesis (Biebl et al., 1999). Until a few years ago, there were only chemical processes for the industrial production of 1,3-PDO, starting from oil-based ethylene glycol and acrolein (Kraus, 2008;

Stegmann, 2014). Nowadays biobased 1,3-PDO can be synthesized from glucose using a genetically engineered *E. Coli* with a production up to a concentration of 135 g/L. In addition, biobased 1,3-PDO can be obtained from biomass-derived glycerol using a bacterial fermentation process from various strains (Jiang et al., 2016; Kaur et al., 2012; Przystałowska et al., 2015; Silva et al., 2014; Sun et al., 2015).

1,4-butanediol (1,4-BDO) is a widely used chemicals for the polymer synthesis, especially polyesters, polyamides and polyurethanes, with an annual global market of over 2.5 millions tons (Yim et al., 2011). The industrial production of 1,4-BDO depends mostly on petroleum-based chemicals such as maleic anhydride, acetylene, butane, propylene and butadiene. Nowadays, biobased 1,4-BDO is industrially obtained *via* a chemical process of hydrogenation from biobased SA (Bechthold et al., 2008; Bozell and Petersen, 2010; Choi et al., 2015). In addition, Genomatica (USA) has developed genetically modified *E. Coli* to obtain the straight bioproduction of 1,4-BDO from sugars (Yim et al., 2011; Barton et al., 2014; Sun et al., 2015). Recently, the successful production of bio-based 1,4-BDO on a commercial scale (*i.e.*, 2,000 tons) was achieved from the partnership between Genomatica and DuPont Tate & Lyle.

2,3-butanediol (2,3-BDO), composed of only secondary hydroxyl functions contrary to the previous diols, has been industrially produced by a fermentative process since the 20th century. The strong interest of this bioprocess is driven by the large number of industrial applications of 2,3-BDO and its derivatives (*e.g.*, plasticizers, printing inks, perfumes, fumigants, softening agents and pharmaceutical products) (Celińska and Grajek, 2009; Köpke et al., 2011). Interestingly, 2,3-BDO can be produced from many species of bacteria, like *Klebsiella sp.* and *Paenibacillus polymyxa*, using different bio-resources such as xylose, sugar cane molasses, glucose and corn (Wang et al., 1996; Ji et al., 2011; J.-Y. Dai et al., 2015). Recently, 2,3-BDO has found a real interest for the polyesters synthesis (Noordover et al., 2006; Erik Gubbels et al., 2013; Debuissy et al., 2016a).

Glycerol, which is a triol compared to previous diols, was mainly produced from petroleum-based resources since 1950s, even if its microbial production has been known for more than 100 years. Such as SA, glycerol was listed by the US-DoE as one of "Top Value Added Chemicals from Biomass" (Werpy et al., 2004). Recently, biobased glycerol has found a new attractiveness and is obtained as the main byproduct of biodiesel production from vegetable oils and fats (Hoekman et al., 2012). Moreover, in addition of a very interesting building blocks for hyperbranched polymers (Uyama et al., 2001; Fu et al., 2003; Zhang and Grinstaff, 2014; Loh et al., 2015), glycerol is a molecules platform for the synthesis of a large amount of chemicals such as 1,3-PDO, glycerol carbonate, ethylene glycol, epichlorohydrin…(Bozell and Petersen, 2010; Isikgor and Becer, 2015)

Ethylene glycol (EG) is an important diol for the polymer industry since it is one of the two components of poly(ethylene terephthalate) (PET), which can be obtained from glycerol *via* a catalytic hydrogenolysis. Nowadays, petroleum-based EG is produced at industrial level by the oxidation of ethylene followed by water addition (Isikgor and Becer, 2015). Since it is possible to produce biobased ethylene from ethanol, biobased EG can also be obtained by this pathway. Besides the ethanol route, other possibilities to produce biobased EG have been developed from sugars such as glucose or xylose *via* a catalytic hydrogenolysis (Harmsen et al., 2014), although this pathway still require further development to be competitive. Nowadays, considerable efforts are being developed by the soft drink industry (*e.g.*, Coca Cola, Pepsi) for the so called "bio-PET", bottle that is produced partially (EG) or entirely (EG and terephthalic acid) from renewable resources (Sheldon, 2014).

2.4. Synthetic routes for polyester synthesis

Synthetic polyesters can be obtained according to three main polymerization modes: (i) step-growth polycondensation of dicarboxylic acids with diols or hydroxyacids, (ii) ring-opening polymerization (ROP) of lactones or lactides, and (iii) a combination of ROP and polycondensation (or ring-opening addition-condensation polymerization) of carboxylic anhydride with diols. The three different routes are presented in Scheme 1.2.

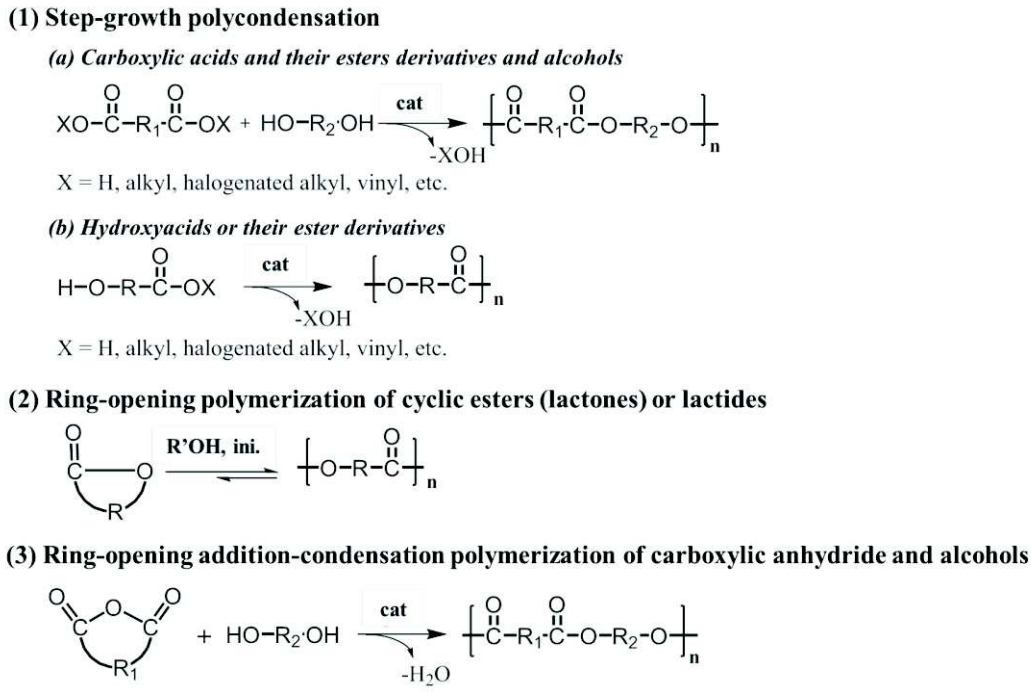

Scheme 1. 2 : Main polymerization modes for the synthesis of polyesters.

All these methods have their own advantages and drawbacks. On one hand, building blocks for the step-growth polymerization are generally easy to obtain at a relatively low price. However, elevated reaction temperatures, long reaction times, high vacuum and heavy metal catalysts are generally required for polycondensation. In addition, side reactions, thermal degradation and monomer volatilization may occur at elevated temperature under vacuum. On the other hand, the removal of bio-products is not required for ROP or ring-opening addition-condensation polymerization reactions allowing the production of high molar mass polyesters under relatively mild conditions in a matter of minutes. Moreover, side reactions can be greatly contained. However, heavy metals catalysts and additional synthetic step are required for the preparation of starting monomers (*i.e.*, lactones or lactides).

Since this work is based mostly on the study of poly(alkylene dicarboxylate)s synthesized from functional building blocks, the ROP polymerization, and the combination of ROP and polycondensation will be not detailed in this chapter. These different reactions can be catalyzed by either traditional chemical (abiotic) or biological (biotic) catalysts. Traditional catalysts include protic species, organometallic compounds, metal oxides and salts, whereas biological catalysts refer to enzymes.

3. Abiotic synthesis of polyesters via a step-growth polymerization process

3.1. Two-step melt polymerization

The synthesis of polyesters from functional monomers according the step-growth polymerization is carried out by a stoichiometric stepwise reaction between bifunctional reactants, which is accompanied by the formation of a low molar condensate.

Polyesters are typically manufactured by two routes in melt: (i) direct esterification of a dicarboxylic acid with a diol (or a hydroxyacid) followed by polycondensation to form the high molar mass polymer, or (ii) transesterification of a diester dicarboxylate with a diol (or a hydroxyester). Direct esterification and transesterification are rather slow at low temperature and must be carried out at high temperature and high end-group (*i.e.*, reactive group) concentration, preferably in bulk. Vacuum is generally applied during the last steps of reaction to distill off reactions condensate (*i.e.*, water in direct polyesterification or a volatile alcohol in transesterification polymerization) and to continuously shift the reaction toward the formation of high molar mass polyesters. That is why, diester dicarboxylate are preferentially

dimethyl dicarboxylates. Monomer excess accidentally or deliberately introduced in the reaction mixture can be eliminated at high temperature and under vacuum during the last steps of the reaction. The presence of a catalyst is usually requested to obtain high molar mass polyesters. Metal salts (*e.g.*, $Zn(OAc)_2$, $SnCl_2$, $HfCl_4$ and $ZrCl_4$) and oxides (*e.g.*, GeO_2, Sb_2O_3), and organometallic compounds, mainly titanium, tin and zirconium alkoxides, are the preferred catalysts for bulk polyesterifications usually carried out in the 160-250 °C temperature range (Fradet and Maréchal, 1982).

The direct esterification is the most straightforward method of polyesters synthesis, which is based on the work of Carothers in the 1930s, and it is still a very widely used method for the synthesis of polyesters from diacids and diols, or from hydroxyacids. As an example, poly(ethylene succinate) synthesis by direct polyesterification in bulk from SA and EG is described in Scheme 1.3. The reaction is performed in two steps. In the first one (esterification), SA is reacted with an excess of 1,4-BDO (typically 1:1.05 - 1:1.5) at 150-210 °C for few hours with elimination of water under a low flow of an inert gas, until having oligomers of sufficient length to avoid any sublimation phenomena during the last steps. The use of an excess of alcohol groups compared to carboxylic one is due to the will to form preferentially hydroxylated-terminated oligomers and to counterbalance the potential loss by cyclization of some diols (*i.e.*, 1,4-BDO). In the second step (polycondensation), the catalyst is added to the reaction mixture and the medium is then heated up to 250 °C under reduced pressure (typically < 10 mbar) until unreacted 1,4-BDO is removed, and high molar mass polyesters are obtained.

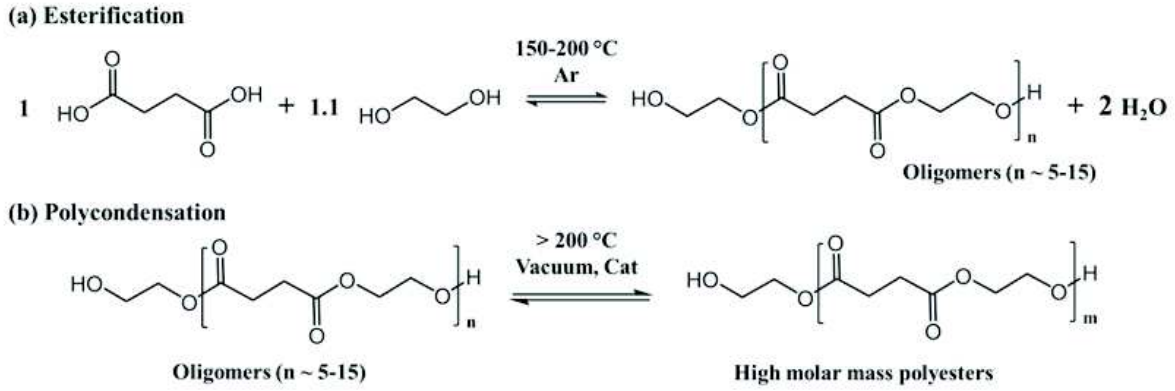

Scheme 1.3 : Reaction scheme of the two-step melt polycondensation synthesis of poly(ethylene succinate).

The transesterification reaction from diester dicarboxylates and diols plays also a predominant role in most industrial process to synthesize aliphatic and semi-aromatic polyesters. Regarding to the synthesis of poly(butylene succinate) (Table 1.1), the monomers for the transesterification reaction are dimethyl succinate and 1,4-BDO. Such as for the direct esterification, the reaction is carried out in two stages with a high vacuum during the second step. For this type of reaction, most of the time, the catalyst is added since the initial step of the reaction.

This two-step melt polycondensation method can be efficiently used for a large number of different biobased monomers with various metal-based catalysts allowing the synthesis of a wide range of biobased polyesters (Table 1.2). As observed in Table 1.2, the alkane chain length of aliphatic saturated building blocks does not have an influence on the reactivity. However, the presence of unsaturation (*e.g.*, itaconic acid), aromatic rings (*i.e.*, 2,5-furandicarboxylic acid), secondary hydroxyl functions (*e.g.*, 2,3-butanediol) have drastic negative influence on the lengthening of the polyester chains leading to mostly polyesters of low molar masses (M_n < 5,000 g/mol).

Table 1.2 : Organometallic-catalyzed synthesis of some biobased aliphatic or semi-aromatic polyesters in melt.

Diol	Diacid	Catalyst	Temperature (°C) 1st/2nd step	Pressure (2nd step)	M_n (kg/mol)	References
1,2-ethanediol	succinic acid	titanium (IV) butoxide	190 / 230	5 Pa	17.1	(Bikiaris and Achilias, 2006)
		titanium (IV) isopropoxide	170 / 220	1 mmHg	105	(Tsai et al., 2008)
			230 / 230	0.5 mmHg	40	(Cao et al., 2002)
		germanium (IV) butoxide	200 / 240	0.5 mmHg	59	(Mochizuki et al., 1997)
	itaconic acid	dibutyl tin (II) dilaurate	160 / 160	> 100 mbar	1	(J. Dai et al., 2015)
	adipic acid	titanium (IV) butoxide	180 / 210	0.02 mmHg	40	(Jin et al., 2000a)
	suberic acid	titanium (IV) isopropoxide	220 / 220	0.5 mmHg	82	(Qiu and Qiu, 2016)
	azelaic acid	titanium (IV) butoxide	190 / 230	5 Pa	21	(Papageorgiou et al., 2011)
	sebacic acid	titanium (IV) isopropoxide	150/180	not spec.	54	(H. Park et al., 2012)
		zinc acetate dihydrate	155/185	5 mmHg	9.2	(Mohsen-Nia and Memarzadeh, 2013)
1,3-propanediol	succinic acid	titanium (IV) butoxide	190 / 230	5 Pa	14.5	(Bikiaris and Achilias, 2006)
			190 / 240	5 Pa	29.5	(Papageorgiou et al., 2008)
			190 / 230	5 Pa	13	(Bikiaris et al., 2008)
			150 / 200	1 mmHg	11.3	(Yongxiang Xu et al., 2008)
		titanium (IV) isopropoxide	190 / 210	1 mmHg	119	(Chen et al., 2010)
	dimethyl succinate	titanium (IV) butoxide	190 / 215	0.5 mmHg	3.9	(Ghassemi and Schiraldi, 2014)
			180 / 210	0.1 mbar	36.4	(Soccio et al., 2007)
	itaconic acid	titanium (IV) butoxide	170 / 170	10 mbar	6.8 (M_w)	(Wibowo et al., 2017)
	glutaric acid	titanium (IV) butoxide	190 / 230	5 Pa	14	(Bikiaris et al., 2008)
	dimethyl glutarate	titanium (IV) butoxide	180 / 210	0.1 mbar	43.5	(Soccio et al., 2007)
	adipic acid	titanium (IV) butoxide	190 / 230	5 Pa	14	(Bikiaris et al., 2008)
	dimethyl adipate	titanium (IV) butoxide	180 / 210	0.1 mbar	31.2	(Soccio et al., 2007)
	pimelic acid	titanium (IV) butoxide	190 / 230	5 Pa	19	(Bikiaris et al., 2008)
	suberic acid	titanium (IV) butoxide	190 / 230	5 Pa	15	(Bikiaris et al., 2008)
	azelaic acid	titanium (IV) butoxide	190 / 230	5 Pa	25	(Bikiaris et al., 2008)
	dimethyl azelate	titanium (IV) butoxide	180 / 210	0.1 mbar	36	(Soccio et al., 2007)
	sebacic acid	titanium (IV) butoxide	190 / 230	5 Pa	26	(Bikiaris et al., 2008)
2,3-butanediol	dimethyl-2,5-furandicarboxylate	titanium (IV) butoxide	180 / 220	not spec.	2 - 3	(E. Gubbels et al., 2013)
		tin (II) ethylhexanoate	180 / 220	not spec.	7 - 13	(E. Gubbels et al., 2013)
		zirconium (IV) butoxide	180 / 220	not spec.	2.4	(E. Gubbels et al., 2013)
	2,5-furandicarboxylic acid	titanium (IV) butoxide	180 / 220	not spec.	2.5	(E. Gubbels et al., 2013)
		tin (II) 2- ethylhexanoate	180 / 220	not spec.	3.7	(E. Gubbels et al., 2013)
		zirconium (IV) butoxide	180 / 220	not spec.	2.0	(E. Gubbels et al., 2013)
	dimethyl-2,5-furandicarboxylate	titanium (IV) butoxide	180 / 220	not spec.	3.1	(Gubbels et al., 2014)
	adipic acid	titanium (IV) isopropoxide	150 / 180	1-3 mbar	3.8	(Debuissy et al., 2016a)
1,4-butanediol	succinic acid	titanium (IV) butoxide	190 / 250	20 mbar	25.3	(Mincheva et al., 2013)
			200 / 240	0.5 mmHg	59	(Mochizuki et al., 1997)
			190 / 230	5 Pa	17.1	(Bikiaris and Achilias, 2006)
			150 / 200	1 mmHg	21.4	(Yongxiang Xu et al., 2008)
			170 / 240	1 mbar	29.1	(Kint et al., 2003)
			180 / 210	0.02 mmHg	38	(Jin et al., 2000a)
		titanium (IV) isopropoxide	240 / 240	< 10 Pa	85	(Tachibana et al., 2010)
			230 / 230	0.5 mmHg	65	(Cao et al., 2002)
			190 / 220	< 67 Pa	77	(Ahn et al., 2001)
			190 / 210	1 mmHg	30	(Chen et al., 2010)
			210 / 230	1-3 mbar	39.2	(Debuissy et al., 2017a)
		scandium triflate	180 / 180	3-30 mbar	30.7	(Takasu et al., 2003)
	dimethyl succinate	titanium (IV) butoxide	180 / 215	0.1 mbar	51.2	(Gigli et al., 2013)
			180 / 240	1 mmHg	28	(Montaudo and Rizzarelli, 2000)
			190 / 215	0.5 mmHg	23.2	(Ghassemi and Schiraldi, 2014)
			180 / 230	0.08 mbar	50.6	(Fortunati et al., 2017)
			150 / 200	< 1.5 mmHg	26	(Nikolic and Djonlagic, 2001)
			180 / 200	0.15 mbar	59.5	(Tserki et al., 2006b)
		titanium (IV) isopropoxide	215 / 215	< 10 Pa	43	(Tachibana et al., 2010)
			120 / 180	0.1 mmHg	61	(Shirahama et al., 2001)
		titanium (IV) ethoxide	120 / 180	0.1 mmHg	16.2	(Shirahama et al., 2001)
		niobium (V) ethoxide	120 / 180	0.1 mmHg	20.3	(Shirahama et al., 2001)
		tantalum (V) ethoxide	120 / 180	0.1 mmHg	11.4	(Shirahama et al., 2001)
		zirconium (IV) n-butoxide	120 / 180	0.1 mmHg	10.5	(Shirahama et al., 2001)
	itaconic acid	dibutyl tin (II) dilaurate	160 / 160	> 100 mbar	0.8	(J. Dai et al., 2015)
	dimethyl glutarate	titanium (IV) isopropoxide	120 / 180	0.1 mmHg	59.1	(Shirahama et al., 2001)

Table 1.2 (continuation): Organometallic-catalyzed synthesis of some biobased aliphatic or semi-aromatic polyesters in melt.

Diol	Diacid	Catalyst	Temperature (°C) 1st/2nd step	Pressure (2nd step)	M_n (kg/mol)	References
1,4-butanediol	adipic acid	titanium (IV) butoxide	200 / 230	200 Pa	45	(Wu et al., 2014)
			190 / 220	< 67 Pa	62	(Ahn et al., 2001)
		titanium (IV) isopropoxide	150 / 180	1-3 mbar	31.2	(Debuissy et al., 2016a)
			210 / 230	1-3 mbar	33.3	(Debuissy et al., 2017a)
	dimethyl adipate	titanium (IV) butoxide	210 / 250	0.15 mbar	36	(Celli et al., 2013)
			180 / 200	0.15 mbar	31.1	(Tserki et al., 2006b)
			150 / 200	< 1.5 mmHg	17	(Nikolic and Djonlagic, 2001)
			180 / 240	1 mmHg	36.2	(Montaudo and Rizzarelli, 2000)
		titanium (IV) isopropoxide	120 / 180	0.1 mmHg	26.9	(Shirahama et al., 2001)
			130 / 180	not spec.	24.2	(Lindström et al., 2004)
	dimethyl pimelate	titanium (IV) isopropoxide	120 / 180	0.1 mmHg	35.6	(Shirahama et al., 2001)
	suberic acid	titanium (IV) butoxide	190 / 230	not spec.	18.6	(Cui and Qiu, 2015)
	dimethyl suberate	titanium (IV) isopropoxide	120 / 180	0.1 mmHg	52.6	(Shirahama et al., 2001)
	azelaic acid	titanium (IV) butoxide	180 / 200	not spec.	37	(Kong et al., 2014)
	dimethyl azelate	titanium (IV) butoxide	190 / 250	20 mbar	42.5	(Mincheva et al., 2013)
		titanium (IV) isopropoxide	120 / 180	0.1 mmHg	45.4	(Shirahama et al., 2001)
	sebacic acid	titanium (IV) butoxide	180 / 200	not spec.	28	(Kong et al., 2014)
	dimethyl sebacate	titanium (IV) butoxide	180 / 240	1 mmHg	33.6	(Montaudo and Rizzarelli, 2000)
		titanium (IV) isopropoxide	120 / 180	0.1 mmHg	37.8	(Shirahama et al., 2001)

3.2. Effective catalysts for the melt polycondensation

3.2.1. Non- and acid-catalyzed direct esterification

First of all, the non-catalyzed esterification of diacids and diols leads to the formation of only oligomers in which the molar mass depends on the [COOH]/[OH] molar ratio according Carothers law. As an example, poly(propylene dicarboxylate)s polyesters of molar mass lower than 2,500 g/mol are synthesized from the non-catalyzed esterification of 1,3-PDO and succinic or adipic acids (Chandure and Umare, 2007). This method is, thus, not adapted to the synthesis of high molar mass polyesters. However, the use of an acid catalyst, such as *p*-toluenesulfonic (Witt et al., 1994) or dodecylbenzenesulfonic (Saam, 1998) acids, and using equimolar proportion of reactive groups permits to increase the M_n up to 10,000 g/mol. Nevertheless, these two kinds of reactions are mainly used as the first step of the reaction scheme previously described.

3.2.2. Transition metal alkoxides

Many transition metal alkoxides compounds show remarkable activity towards esterification and transesterification reactions. Moreover, these catalysts often exhibit an optimal activity under solventless conditions which are favorable and preferred for the industrial production of polyesters. Typical metals for these catalysts are tin (II), antimony (III), bismuth (III), titanium (IV), zirconium (IV) and hafnium (IV).

Industrially, the most common strategy is to use an efficient catalyst, such as titanium, in a relatively high amount (*i.e.*, Ti = 100-360 ppm, Sb = 350-450 ppm, and Sn = 450-1,500 ppm) to limit the exposition of the polymer to high temperatures as much as possible, to prevent its degradation inside the reactor and thus the coloration of the material.

For the synthesis of poly(ethylene terephthalate), the most studied polyester, titanium (IV) compounds display the highest catalytic activity leading to the highest molar mass (Otton et al., 1988). However, due to the higher amount of side reactions and the yellowish generated by titanium compounds, most commercially available semi-aromatic polyesters are produced using antimony, germanium oxides or a mixture of metals (Bersot et al., 2011). Nevertheless, germanium oxides, known for their good catalytic efficiency and thermo-oxidative stability (Mochizuki et al., 1997; Aharoni, 2002), are quite expensive catalysts due to the rather low natural abundance of this element (*i.e.*, 0.0001%).

In the academic studies on the synthesis of aliphatic polyesters according the two-step melt polycondensation or transesterification, titanium (IV) n-butoxide and titanium (IV) isopropoxide are the most used organometallic catalysts, as showed in Table 1.2. Indeed, such as for poly(ethylene terephthalate), Jacquel *et al*. showed that titanium (IV)

compounds display higher activity for the synthesis of poly(butylene succinate) from 1,4-BDO and SA than other catalysts, with the following trend: Ti >> Zr ~ Sn > Hf > Sb > Bi (Jacquel et al., 2011). Moreover, this highly active catalyst is used in much lower amount than other organometallic catalysts which is beneficial from an economic point of view. In addition, Shirahama *et al.* proved that the transesterification of dimethyl succinate with 1,4-BDO was much more efficient with titanium (IV) isopropoxide as catalyst (M_n = 61,000 g/mol) than using other catalysts (*i.e.*, zirconium (IV) n-butoxide, titanium (IV)-, nobium (V)- and tantalum (V) ethoxide) (Shirahama et al., 2001). Some organometallic catalysts are presented in Figure 1.5.

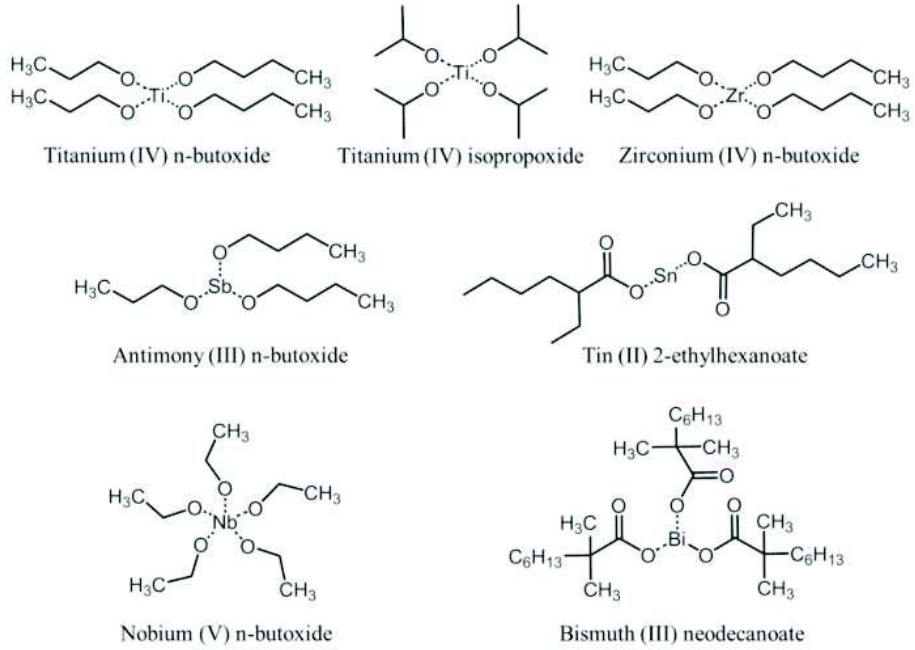

Figure 1.5 : Some organometallic catalysts for the synthesis of polyesters by step-growth polymerization.

In addition, it has been shown that the structure of the catalyst also has a significant influence on its activity. However, some exceptions on the catalyst activity trends are sometimes observed surely due to the chemical structure of monomers and the reaction type (*i.e.*, esterification or transesterification). As an example, a tin catalyst allows to reach higher molar mass for the transesterification of dimethyl succinate with 2,3-butanediol than using titanium or zirconium compounds (E. Gubbels et al., 2013).

Furthermore, the titanium (IV) catalyst should not be added before the polycondensation step (*i.e.*, 2nd step), otherwise its efficiency decreases markedly due to the partial deactivation of the catalyst by water produced during the esterification step (Jacquel et al., 2011). Nevertheless, some studies reported the use of the catalyst since the first step but it is then sometimes necessary to add a second amount of catalyst at the end of the esterification step. This method is not the best synthetic pathway since the very high amount of organometallic catalyst contained in the polymer may favor undesired side reactions. To circumvent this issue, sometimes heat stabilizer additives, such as poly(phosphoric acid), are used (Papageorgiou and Bikiaris, 2005a).

3.2.3. Strong metal-based Lewis acids

In addition to the typical metal alkoxides, new strong Lewis acid catalysts have been recently developed that are based on rare-earth or transition metals, such as scandium (*e.g.*, scandium triflate ($Sc(OTf)_3$), scandium perfluorooctanesulfonate ($Sc(OPf)_3$) or scandium triflyimide ($Sc(NTf_2)_3$)), neodymium (*e.g.*, $Nd(OTf)_3$), thulium (*e.g.*, $Tm(OTf)_3$) or yttrium (*e.g.*, $Y(OTf)_3$). These catalysts have exhibited remarkable activities under mild condition (mostly temperatures < 80 °C) for the synthesis of polyesters by (i) ROP of lactones (*i.e.*, ε-caprolactone, δ-valerolactone, lactide) (Agarwal et al., 2000; Deng et al., 1999; Kunioka et al., 2005; Wang et al., 2003; Wang and Kunioka, 2005), (ii) a combination of ROP and polycondensation (Tang et al., 2013; Yashiro et al., 2009a) and (iii) step-growth polycondensation or transesterification (Takasu et al., 2003, 2005b, 2009; Garaleh et al., 2009; Zhu et al., 2007).

As an example, the reaction between SA and 1,4-BDO catalyzed in bulk by scandium triflate ($Sc(OTf)_3$) under vacuum at 180 °C leads to PBS up to 31,000 g/mol (Table 1.2) (Takasu et al., 2003). Even if this catalyst is highly active at low temperature, an increase of the reaction temperature permits to obtain polyester chains of higher molar mass. Similarly, Kircheldorf *et al*. reported the successful use of bismuth compounds for the synthesis of aliphatic polyesters from dimethyl ester (Kricheldorf et al., 2005), succinic anhydrides (Yashiro et al., 2009a) or from the direct polycondensation of dicarboxylic acid (Kricheldorf et al., 2005; Buzin et al., 2008). M_n values up to 30,000 g/mol were obtained from the bulk polymerization at 80 °C for over 48 h. Bismuth is particularly interesting since it combines two advantages compared to scandium: a lower toxicity and a higher efficiency as esterification catalyst (Buzin et al., 2008).

Moreover, these metal-based Lewis acid catalysts are particularly interesting for monomers containing vinyl functions, such as maleic anhydride (Tang et al., 2013) or citraconic acid (Takasu et al., 2005a), which can undergo cross-linking at high temperature. Rare-earth catalysts, which are highly reactive under mild conditions compared to classical organometallic compounds, are thus adapted catalysts for reactions involving these unsaturated monomers. Nevertheless, the high cost of these catalysts strongly limits their use at the industrial scale.

3.3. Chain-extension

The melt polycondensation suffers from the increase of the reaction mixture viscosity during the process limiting the polymer chains growth. To circumvent this issue and to synthesize high molar mass polyesters, a chain-extension can be performed on the α,ω-dihydroxy-terminated oligomers. The chain-extension procedure can be performed using phosgene (Penco et al., 1998) (Penco et al., 1998; Ranucci et al., 2000), dicarbonate (Kawai et al., 1995; Miura et al., 1998), diisocyanate (Tserki et al., 2006a), *bis*(2-oxazoline) (Huang et al., 2010; Luo et al., 2006; Xu et al., 2011) and *bis*-caprolactamate (Luo et al., 2006).

The chain-extension of α,ω-dihydroxy-terminated polyesters oligomers (M_n ~ 1,000-3,000 g/mol) using phosgene is performed in solution (mostly in chloroform) at low temperature (0-5 °C) using N-ethyl-N,N-diisopropylamine (EDIPA) and 4-dimethylaminopyridine (DMAP) as acid acceptor and acylation catalyst, respectively (Scheme 1.4). For this, EDIPA as acid acceptor is a better choice than the more usual trimethylamine since EDIPA is less prone to undergo side reactions with acylating agents, due to its larger steric hindrance. In the same spirit, the use of DMAP as catalyst was found to give far superior results over pyridine. In fact, polymers produced by the chain-extension with phosgene are, strictly speaking, poly(ester-carbonate)s. As an example, poly(propylene succinate) and poly(lactic-glycolic acid) polyesters up to 30,000 and 90,000 g/mol have been obtained after such chain-extension, respectively (Penco et al., 1998; Ranucci et al., 2000). However, due to the high toxicity of phosgene (and difficulties to handle) this method is rarely used. As an alternative, diphenyl carbonate is sometimes used (Kawai et al., 1995; Miura et al., 1998).

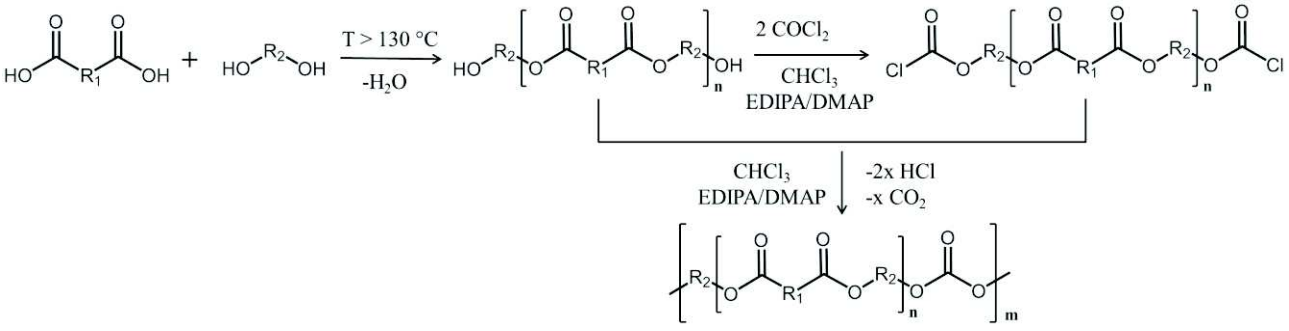

Scheme 1.4 : Synthesis of high molar mass polyesters using chain-extension of phosgene (Penco et al., 1998).

Chain-extension by diisocyanate (*e.g.*, 1,6-hexamethylene diisocyanate) as coupling agent is the most used method. Contrary to the process using phosgene, which is carried out in solution, the chain-extension with diisocyanate is performed under solventless conditions, which is a great advantage. This process is industrially used since twenty years by Showa Denko, for example, for the synthesis of high molar mass chain-extended poly(butylene succinate) by 1,6-hexamethylene diisocyanate. Synthesized polymers produced by the chain-extension with diisocyanate are, strictly speaking, poly(ester-urethane)s with a low amount of urethane linkages. Two strategies were studied. In the first one,

α,ω-dihydroxy-terminated polyester oligomers of M_n ~ 3,000-4,000 g/mol were synthesized by esterification and then submitted to such chain-extension by diisocyanate to reach high molar mass (up to 81,000 g/mol for the synthesis of PBS)) (Zheng et al., 2011). In the second one, the chain-extension is carried out on polyesters of much higher molar mass (> 15,000 g/mol), synthesized *via* the two-step melt polycondensation method, and permits to roughly double the molar mass (Mani et al., 2002; Shirahama et al., 2001; Tserki et al., 2006a). This second strategy is more based on a post-polymerization reaction to increase the molar mass, which can improve mechanical properties of materials (Tserki et al., 2006a).

In addition to these two main techniques, *bis*(2-oxazoline) (Huang et al., 2010; Luo et al., 2006; Xu et al., 2011) or *bis*-caprolactamate molecules (Luo et al., 2006) have been more recently used as coupling agent. These two routes are presented in Scheme 1.5. Such as the previous chain-extension method (*i.e.*, diisocyanate), these two coupling agents are used in solventless conditions. *Bis*(2-oxazoline) and *bis*-caprolactamate are chain extenders for carboxyl- and hydroxyl-terminated oligomers, respectively.

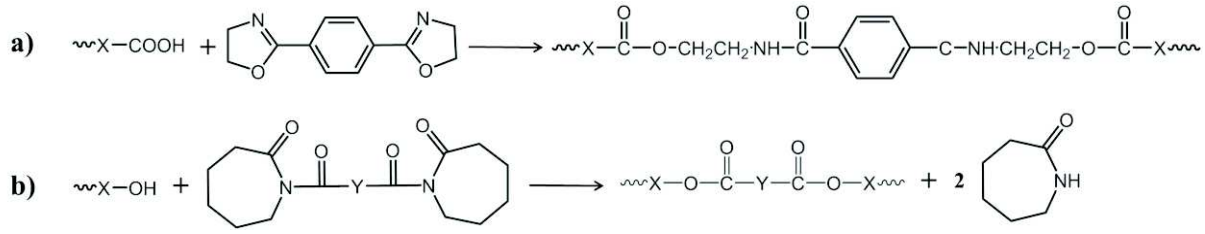

Scheme 1.5 : Reaction schemes of polyesters chain-extension by (a) bis(2-oxazoline) and (b) bis-caprolactamate.

Finally, the chain-coupling has a huge advantage since it permits to easily synthesize block copolyesters macromolecular architectures contrary to the organometallic or rare-earth catalysts which produce random copolyesters structures, even by starting from already synthesized homopolyesters.

3.4. Solid-state polymerization

In solid-state polymerization (SSP), starting materials are heated to a temperature higher than the glass transition temperature (T_g), but lower than the melting temperature (T_m), to avoid particle agglomeration, so that end-groups are mobile enough to react. The polycondensation progresses through chain-ends reactions in the amorphous phase or at the surface of the crystalline phase of the semi-crystalline polymer. (Vouyiouka et al., 2005; Papaspyrides and Vouyiouka, 2009). It is generally accepted that chemical reactions which occur in solid state during the SSP and the melt polycondensation are the same. The advantages of SSP include the use of low reaction temperatures, which decrease highly side reactions such as cyclization and thermal degradation of the product, while requiring inexpensive equipment. SSP is mainly carried out in glass tubes, fixed and fluidized bed reactors, and rotation flasks. This method is, thus, practical for the synthesis of semi-crystalline polymer displaying a low thermal stability or having very high melting temperatures such as semi-aromatic polyesters. Moreover, molar masses of polymers achieved by SSP are much higher than those obtained by melt polycondensation which are limited due to the increase of the viscosity. As an example, the SSP process for poly(ethylene terephthalate) is performed at approximatively 220-230 °C for 10-30 h (Duh, 2001, 2002). The increase of the molar mass during SSP is coupled with the increase of the crystallinity and crystal perfection (Srinivasan et al., 1994), while drying the polymer is very important since the moisture content has a bad influence on the processability. The removal of by-products is favored to drive the reaction to the esterification, thanks to the application of a vacuum or the convection of an inert gas (*e.g.*, N_2, Ar, CO_2 and He) (Mallon et al., 1998; Shi et al., 2001a, 2001b, Gross et al., 1999, 2000). Disadvantages of SSP mainly concern the low reaction rates compared to the melt polycondensation since the chain-end required mobility is significantly restricted, and the possible agglomeration of particles, especially at high temperature (Kampouris and Papaspyrides, 1985).

3.5. Polymerization in solution

Whereas the abiotic synthesis of polyesters is mainly performed in bulk (in the molten state), the use of a solvent can be required in some specific cases.

3.5.1. Acyl chlorides as monomer

Since some diols involved in the synthesis of polyesters are not enough reactive under melt polycondensation conditions, usually they are made to react with a more reactive acid derivative, *i.e.,* a chloride. The reaction between diacyl chlorides and aliphatic diols or diphenolic compounds commonly take place in solution and a low or moderate temperature (mostly until 100 °C) (Kwolek and Morgan, 1964). Nevertheless, some high temperature solution reactions have also been reported for less soluble aromatic polyesters (Liaw et al., 2000). The solution polymerization from diacyl chlorides and diphenols is usually carried out in the presence of tertiary amines such as trimethylamine or pyridine, which play a role of both reaction catalyst and a HCl acceptor (Vasnes et al., 1990). The by-product of the reaction, *i.e.,* HCl, precipitates in the form of its quaternary ammonium salt and cannot participate in the reverse reaction. Without the use of a HCl acceptor, HCl stay under its gaseous form and thus is removed from the reaction mixture. Nevertheless, due to the high corrosiveness of this gas, the process without a HCl acceptor owns some drawbacks and should be performed with care. This also prevents possible proton-catalyzed side reactions during the process. The existence of such side reactions is the reason why high-temperature bulk processes involving diacyl chlorides, although possible, are not commonly applied to the synthesis of polyesters. However, the extensive use of solvents and environmentally unfriendly reagents makes solution polymerization not suitable to be applied at an industrial scale (Fradet and Tessier, 2003). More recently, this method has been used for preparing biscyclocarbonate macromers for the synthesis of non-isocyanate poly(urethane)s (Carré et al., 2014) or carried out for the modification of cellulose (Reulier et al., 2016).

3.5.2. Metal salts catalysts

Direct polycondensation can be catalyzed by metal salts. Even if these catalysts exhibit good efficiency for this kind of reaction, leading to high molar mass polyesters, no recent studies have been reported for the synthesis of polyesters in the last decade. These reactions are performed in solvent (*e.g.*, dimethyl benzene or *o*-xylene) under reflux with a Dean-Stark or a water trap containing molecular sieve apparatus. Using $SnCl_2$ as catalyst in dimethyl benzene, PBS with M_n up to 31,000 g/mol was synthesized from equimolar amount of 1,4-BDO and SA (Zhu et al., 2003), whereas the polycondensation of different hydroxyacids or diacids with diols in o-xylene catalyzed by $Hf(Cl)_4$ leads to M_n up to 17,000 g/mol (Ishihara et al., 2000). However, the use of high volumes of solvents and long reaction times (24-80 h) do not make this method an industrially viable process.

3.5.3. Distannoxanes catalysts

Similarly to the direct polycondensation using metal salts, different distannoxanes catalysts have been used for the synthesis of high molar mass polyesters under azeotropic conditions. Distannoxanes is a class of organotin complexes $[R_3SnOSnR_3]_2$ (Figure 1.6) that are used as catalyst, especially for the synthesis of polyesters *via* ROP (Hori et al., 1993a, 1993b, 1995) and step-growth polycondensation (Takahashi et al., 2000; Ishii et al., 2001) or transesterification (Campistron et al., 1997).

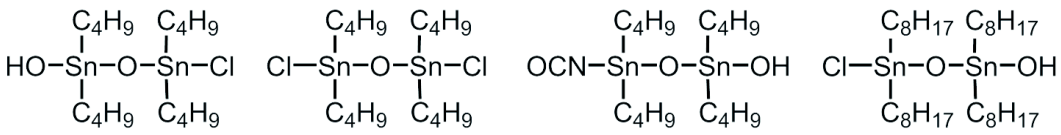

Figure 1.6 : Chemical structure of some distannoxane catalysts.

Different aliphatic polyesters were synthesized from dicarboxylic acids and diols under reflux in nonane, decalin or dodecane using a Dean-Stark apparatus for 24-72 h (Takahashi et al., 2000; Ishii et al., 2001). Under these conditions, distannoxanes showed much higher catalytic activities than metal salts catalysts (*i.e.*, $SnCl_2$) and titanium organo-

compounds. The solvent also had a huge impact of the polycondensation process. As an example, the M_n of PBS increased with the boiling temperature of solvent, until M_n of 150,000 g/mol. Moreover, distannoxanes should be used in small amount (*i.e.*, 0.01 mol.%) for an optimal catalytic activity. The optimal process proceeds in a two-phase system of solvent and molten polymer. This two-phase system is especially effective in keeping the concentration of the reactants in the polymerization system high (Ishii et al., 2001). The main advantage of distannoxane-catalyzed esterification is that the reverse reaction hydrolysis cannot occur probably due to the surface alkyl groups of distannoxanes preventing water molecules from approaching the catalytic core sites (Otera et al., 1991). In addition, , the bulk polycondensation using distannoxanes as catalyst was performed, but led to only low molar mass polyesters (*i.e.*, M_n = 9,000 g/mol) (Takahashi et al., 2000). This is the reason why this process is performed preferentially in solution. As for the metal salts, the use of high volumes of solvents and long reaction times do not make this method a viable process, even if very high molar masses can be obtained.

4. Enzymatic synthesis of polyesters

4.1. Enzymes

Enzymes are indispensable substances in living cells, which catalyze all *in vivo* metabolic reactions to produce essential biomacromolecules to maintain the living systems. Several thousand types of enzymes are known and until now, many investigations have been carried out on enzymatic reactions. The enzymatic catalysis is used not only for the synthesis of macromolecules, but also for their modifications using enzymes-based selective reactions. The enzymatic catalysis can bring, normally, an acceleration of the reaction of about 10^6-10^{12} fold, but can reached 10^{20} fold in some specific cases (Borman, 2004).

Enzymes are proteins, *i.e.,* high molar mass polymers composed of many different amino-acids, which possess a specific 3D structure which gives them their catalytic activities and their specificities. Within each enzyme there is a small region were catalysis takes place, the so-called “active site”. The electrostatic properties and spatial arrangement of amino-acids surrounding the catalytically active residues determine the specificity of the enzyme.

Enzymes are divided into six main classes as shown in Table 1.3. Many of them are actually used for industrial production in the areas of food, pharmacology, medicine, textile industry, etc. Nevertheless, only four enzyme classes (*i.e.*, oxidoreductases, transferases, hydrolases and ligases) are able to catalyze polymerization reactions (Loos, 2010).

Table 1.3 : Enzyme classes and typical examples for their use in polymer synthesis.

Enzyme class	Reaction catalyzed	Typical enzymes	Macromolecules synthesized
Oxidoreductases	Oxidation/Reduction $AH_2 + B \rightarrow A + BH_2$	peroxidase, laccase, glucose oxidase, tyrosinase, oxygenase	polyphenols, polyanilines, polythiophene, vinyl polymers
Transferases	Group transfer $AX + B \rightarrow A + BX$	phosphorylase, acyltransferase, glycoltransferase, transaminase, PHA synthase	polysaccharides, hyaluronan, polyesters, amylose
Hydrolases	Hydrolysis by H_2O $AB + H_2O \rightarrow AH + BOH$	glycosidase (cellulase, amylase, chitinase, xylanase), protease, lipase, peptidase, papain	polysaccharides, polyesters, polyamides, polycarbonates, polythioesters, polyphosphates, poly(amino acids)
Lyases	Bond cleavage $A \rightarrow B + C$	decarboxylase, aldolase, dehydratase	
Isomerases	Isomerization/Racemization $A \rightarrow B$	racemase, epimerase, isomerase, tautomerase	
Ligases	Bond formation $A + B \rightarrow AB$	ligase, synthase, acyl CoA synthase, DNA ligase, cyanophycin synthetase	DNA, cyanophycin

The concept of “green chemistry” became well-known since the book of Anastas and Warner was published (Anastas and Warner, 2000). These authors orientated the future direction of the chemistry research and the chemical industry. The enzymatic synthesis falls directly in this domain. Indeed, enzymes are nontoxic, renewable, natural catalysts, which

are metal-free in most cases (*i.e.*, without the addition of a co-factor), and are used under mild conditions (*i.e.*, low temperature, around neutral pH and mainly under atmospheric pressure). The enzyme-catalyzed reactions are highly selective with many respects on enantio-, chemo-, regio- and choro-selectivities, and hence they give a clean reaction pathway with producing a minimal of by-products. Moreover, in some cases, enzymes are robust enough to be used in combination with other chemical catalysts allowing new chemo-enzymatic processes (Patel, 2008; Pion et al., 2015). Furthermore, one of the limiting factor in the use of enzymes in chemistry, especially for the polymer synthesis; is generally their low stability towards both high temperatures and organic solvents. Because many chemical compounds can only be dissolved in organic solvents, one way to improve the enzyme stability in organic solvents is immobilization. Enzymes can be immobilized wide range of different supports allowing the increase of the enzyme activity (up to a factor of 100) in organic solvents and the enzyme to be recovered and repeatedly used, thus permitting the decrease of the production cost at the industrial scale (Guisan et al., 2009; Jesionowski et al., 2014; Mohamad et al., 2015). Finally, enzymes are able to catalyze very complicated reactions, when the monomer is adequately designed to the specific enzyme.

4.2. Enzymes for the synthesis of polyesters: hydrolases

Hydrolases (EC.3) are naturally occurring macromolecular organic catalysts that cleave bonds of substrate in the presence of water molecules. They are the most commonly used enzymes in organic synthesis due to their acceptance towards a large variety of substrates, considerable stability in organic solvents, direct use without a co-factor, and the fact that many of them are commercially available. The use of hydrolases as catalysts for producing macromolecular organic materials is commonly performed. Until now, four different families (*i.e.*, lipase, cutinase, esterase, PHB depolymerase) of enzymes has shown a specific activity for the synthesis of polyesters.

4.2.1. Lipases

Lipases (E.C. 3.1.1.3.) are the most studied enzymes for the ring-opening polymerization (ROP) or the esterification/transesterification reactions for the synthesis of polyesters. They can be found in most organisms from the microbial, vegetal and animal kingdom (Schmid and Verger, 1998a). They are serine hydrolase that catalyze ester bound cleavage of lipids in aqueous medium (their physiological action is the cleavage of triglyceride as illustrated in Scheme 1.6, but they are also able to catalyze ester bond formation in organic medium (reverse reaction) (Albertsson and Srivastava, 2008). Moreover, in addition to the esterification, lipases can catalyze, in organic solvents, other reactions such as transesterification, interesterification, amidation, transamidation, aminolysis, aldol condensation and Michael addition (Gotor-Fernández and Vicente, 2007). So far, lipases are the most frequently employed enzymes as catalyst for the synthesis of macromolecules.

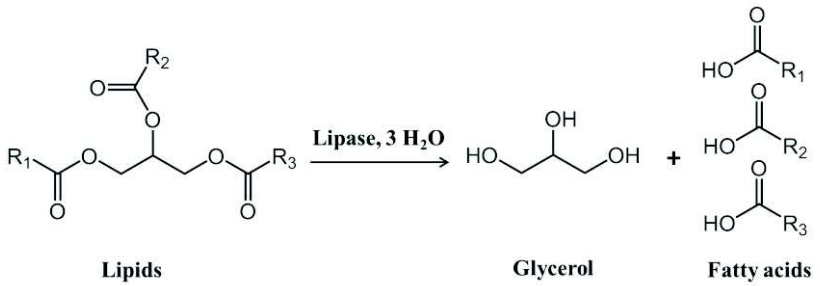

Scheme 1.6 : Hydrolysis of fatty acids catalyzed by lipase.

The enzyme activity is closely related to its tridimensional structure. Despite their different sources, all lipases possess a very similar α/β hydrolase fold. The α/β hydrolase fold consists of a β-sheet core of five to eight parallels stands connected on both sides by α -helices, forming also a α/β/α sandwich-like shape (Ollis et al., 1992; Nardini and Dijkstra, 1999; Hotelier et al., 2004).

Since the structure of enzymes is well adapted to natural substrates, the enzyme surface presents a large apolar area to allow the formation of an acyl-enzyme complex with fatty acids or fatty esters. Lipases can be classified into 3 major groups depending on the form of their binding site (Pleiss et al., 1998), which are presented in Figure 1.7. They can

present either a tunnel shape binding site (*e.g.*, *Candida rugosa*), a crevice-like binding site (*e.g.*, *Rhizomucor miehei*), or a funnel-shaped binding site (*e.g.*, *Candida antarctica* and *Fusarium solani pisi*). Generally, lipases having a funnel-like binding site are those presenting the highest efficiency for the synthesis of polyesters. In addition, some lipases have the capacity to change their structure, *i.e.,* to switch from an open to a closed state of the binding site with the presence of a lid near it (Kapoor and Gupta, 2012; Rehm et al., 2010). The lid controls the access of substrate molecules to the lipase catalytic center. In the presence of a lipid-water interface, the lid opens the active center and thus the active site becomes accessible. However, without the lipid-water interface, the lid is in a closed conformation and, thus, the active center is not accessible making the enzyme inactive.

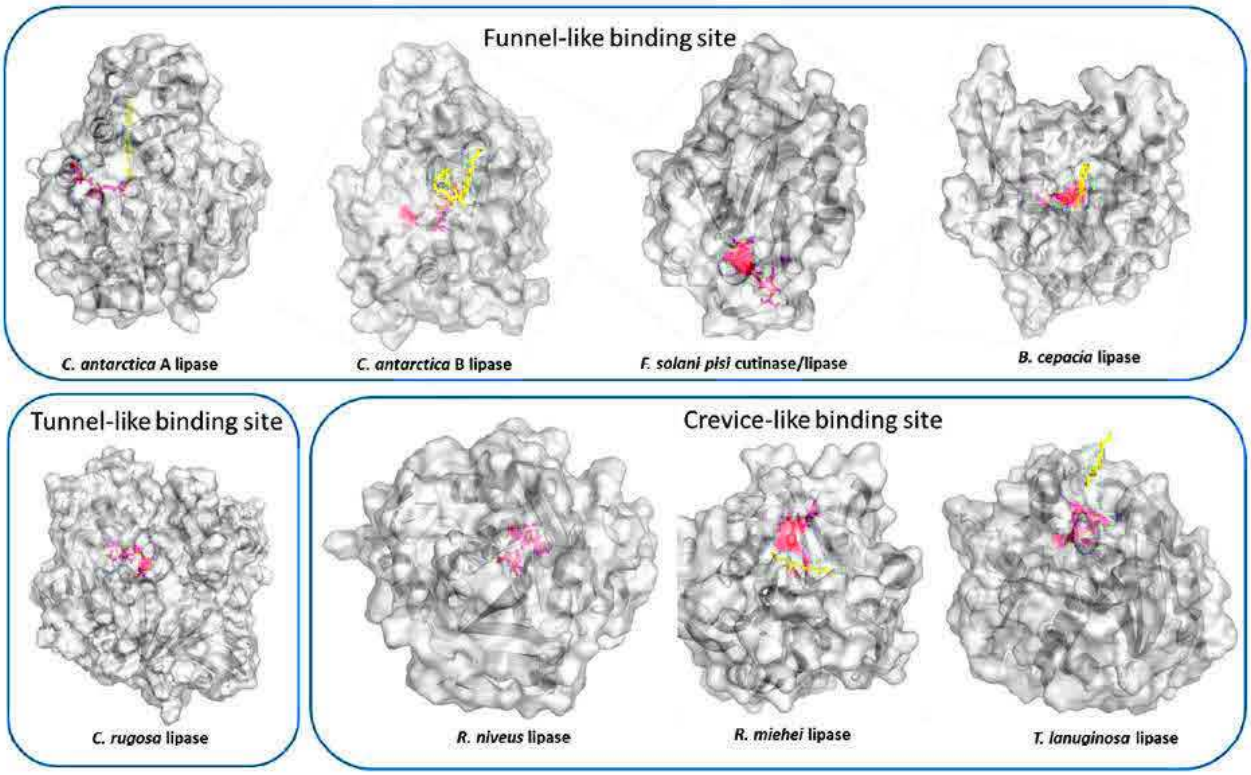

Figure 1.7 : Lipases structures with their different binding sites (Pleiss et al., 1998).

Lipases are serine hydrolases. This means that they all have the same catalytic mechanism, involving a catalytic triad composed of a serine (Ser), a histidine (His) and a glutamate or an aspartate (Glu/Asp). The esterification mechanism catalyzed by serine hydrolase has been well described. Prior to binding, the substrate of the His accepts a proton from the Ser creating a nucleophile at the Ser. Then, His tautomerizes and is stabilized by the Glu/As amino-acid (Hedstrom, 2002), as described in Scheme 1.7. Close to the nucleophilic residue (*i.e.*, serine), a so-called oxyanion hole is formed that can form the tetrahedral intermediates during the hydrolysis or the polyester synthesis.

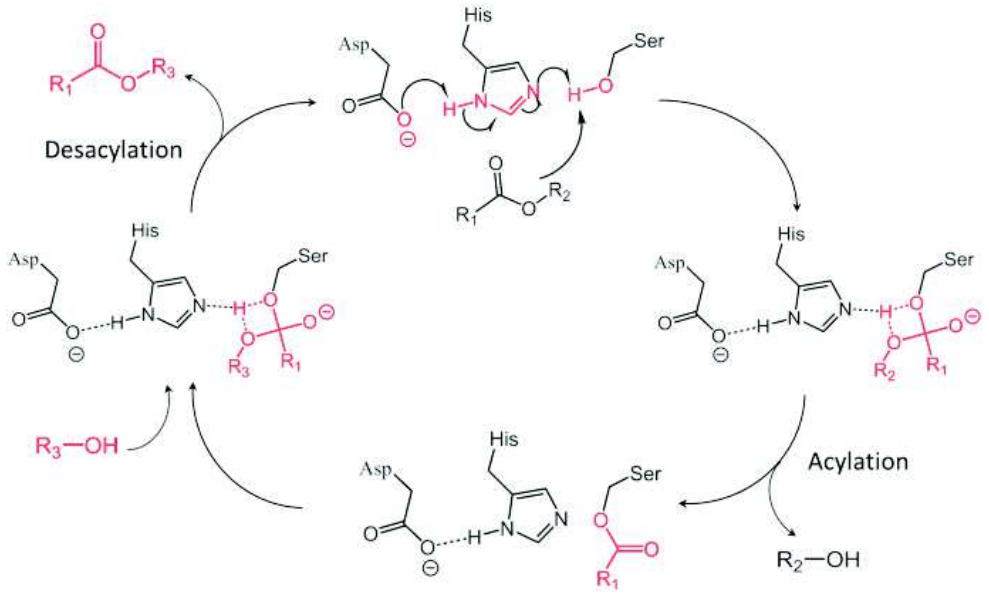

Scheme 1.7 : Proposed mechanism for the lipase-catalyzed transesterification reaction.

Candida antarctica lipase B (CALB), isolated from the yeast of *Candida antarctica*, is the most famous lipase for the synthesis of macromolecules. This yeast also produces another lipase: the lipase A. Moreover, its expression in *Aspergillus oryzae* and *Aspergillus niger* allowed the production of these enzymes in large scale (Høegh et al., 1995).

The crystal structure of the lipase B was elucidated and CALB is composed of 317 amino acids with a molar mass of 33 kDa (Uppenberg et al., 1994). The active site is accessible through a 12Å narrow channel. The CALB active site has two distinct parts: the acyl-binding side and the alcohol binding side. The last one being stereospecific for secondary alcohols due to a stereospecific pocket that can accommodate a methyl side group (Uppenberg et al., 1995).

CALB is commercially available as a free enzyme or in its immobilized form. At present, the most known commercially available immobilized CALB formulation is Novozym® 435 (N435) produced by Novozymes (Denmark) in which CALB are immobilized by adsorption on macroporous acrylic. The CALB immobilization increases the thermostability of the lipase so that it can be used at temperatures up to 100 °C (Kumar and Gross, 2000a; Poojari and Clarson, 2013). Also, the stability towards organic solvents is greatly improved by the immobilization. The heterogeneous catalyst (*i.e.*, N435), containing about 10 wt.% of CALB, consists of physically immobilized CALB on small macroporous acrylic resin (Lewatit VP OC 1600) beads of poly(methyl methacrylate-*co*-divinylbenzene). Lewatit beads have a reported average particle size of 315–1000 μm, a surface area of 130 m^2/g and a pore diameter of approximatively 150Å (Mei et al., 2003). Due to the immobilization method of CALB on the support, lipases are situated near the surface, as showed in Figure 1.8. Moreover, pore size is about 10 times higher than the volume of CALB permitting the increase of the surface area and the substrate diffusion throughout the bead to obtain a maximum catalytic activity. N435 has been already employed in many organic solvents such as toluene, dioxane, hexane, isooctane, cyclooctane, benzene, cyclohexane, diphenyl ether, isopropyl ether, tert-butanol, tetrahydrofuran, ionic liquids and supercritical CO_2 (Uyama and Kobayashi, 2006; Miletić et al., 2010; Kobayashi, 2015).

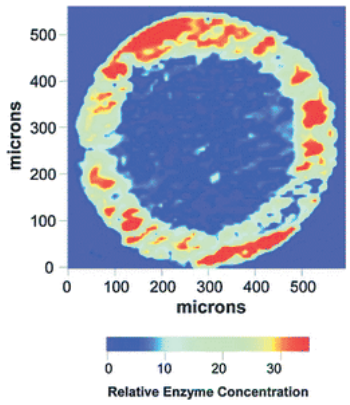

Figure 1.8 : Cross-section of a N435 bead showing the CALB distribution (Mei et al., 2003).

4.2.2. Cutinases

In addition to lipases, cutinases (EC.3.1.1.74) have also been tested for the synthesis of polyesters. Cutinase (*i.e.*, cutin hydrolase) is a serin esterase that catalyzes the hydrolysis of cutin. Cutin is the structural component of plant cuticle and is an insoluble polymer composed of hydroxyl fatty acids and contains up to three hydroxyl groups. Cutinases can be found in pathogenic fungus such as *Fusarium solani pisi* and *Humicola insulens*. Like lipases, they display an α/β hydrolase fold. *Fusarium solani pisi* cutinase is composed of 197 amino acids and has a molar mass of 22-25 kDa (Martinez et al., 1992). It possesses a catalytic triad composed of Ser120, Asp175 and His188. Cutinase, as CALB, does not display an interfacial activation because the active site is not buried under a lip and is therefore accessible to solvents (Martinez et al., 1992; Schrag and Cygler, 1997). Studies on the dynamics of *Fusarium solani pisi* cutinase *via* structural comparison of different crystal forms revealed that the absence of any significant structural rearrangement upon binding highlights the important feature of cutinase (Martinez et al., 1994), which is probably shared only by CALB (Longhi et al., 1996). In addition, kinetic studies of cutinases showed similar kinetic behavior to lipases (Egmond and de Vlieg, 2000).

Studies on the applications of cutinases have been performed for their uses in industry. They have been used in various reactions such as hydrolysis (Murphy et al., 1996; Silva et al., 2005; Gamerith et al., 2017; Alessandro Pellis et al., 2016b), esterification (de Barros et al., 2009a, 2009b, 2010), transesterification (Badenes et al., 2011), and as a lypotic enzyme for a detergent to remove fats (Carvalho et al., 1998, 1999).

Cutinases are not only successfully used for the polymer degradation or the surface modification of polyacrylonitrile, PLA and polyamides fibers (Pio and Macedo, 2009; Pellis et al., 2015a; Ortner et al., 2017), but also as catalyst for the synthesis of polymers, for example in the synthesis of polyesters. Gross and coworkers have used the *Humicola insolens* cutinase (HiC) in its immobilized form for the synthesis of polyesters by ROP (Hunsen et al., 2008) and by polycondensation of aliphatic monomers (Hunsen et al., 2007; Feder and Gross, 2010). Nevertheless, even if HiC exhibited similar reactivity for (i) the ROP of ε-caprolactone and ω-pentadecalactone, and (ii) the esterification of hydroxyl-acids with 12 and 16 carbons chain lengths than CALB, its reactivity became negligible for polycondensation reactions of hydroxy-acids or diol/diacids with aliphatic chain lengths below 10 carbons, contrary to CALB. Recently, Gardossi and coworkers reported the use of cutinase from *Thermobifida cellulosilytica* for transesterification reaction. The synthesis, under thin film conditions, led to only low molar mass oligomers (*i.e.*, < 2,000 g/mol), but higher than with HiC and CALB (A. Pellis et al., 2016).

4.2.3. PHB depolymerases

Other hydrolase enzymes, depolymerases, was found to synthesize polyesters but only *via ROP* reactions *in vitro*. Poly(hydroxybutyrate) (PHB) depolymerases (EC 3.1.1.75) were extracted from *Pseudomonas stutzeri*, *Alcaligenes faecalis* and *Pseudomonas lemoignei,* and show a promising activity for the ROP of lactones, especially on short ring size lactone (4 to 5 ring members) (Suzuki et al., 2001; Santos et al., 2012; Suzuki et al., 2000). As an example, *Alcaligenes faecalis* PHB depolymerase exhibits the highest polymerization activity (93% yield) with β-butyrolactone,

resulting in the formation of polyesters with a M_w = 16,000 g/mol (Suzuki et al., 2003). On the other hand, medium and large lactones (ε-caprolactone, 11-undecanolide, and 12-dodecanolide), which are readily polymerized by lipases, were scarcely polymerized by PHB depolymerases. However, until now, no study on the synthesis of polyesters by polycondensation or transesterification exhibited positive results.

4.2.4. Proteases

Proteases (EC.3.4), present in every living organism, are hydrolysis enzymes catalyzing the hydrolysis of proteins with L-amino acids residues. They catalyze also the peptide bond formation, leading to polymer production (Patil et al., 1991; Hedstrom, 2001, 2002). Enzymes of this class naturally cleave amide bonds, but considering the chemical similarity between ester and amides functions, it is logical that some of these enzymes exhibit esterases activity and are able to produce polyesters even if mixed results were obtained so far.

The alkaline protease of *Bacillus licheniformis* allowed the polycondensation of (i) bis(2,2,2-trifluoroethyl) adipate with sucrose resulting in a linear polyester molar mass up to 13,000 g/mol (M_n = 1,600 g/mol) without showing any cross-linking reactions (Patil et al., 1991), and (ii) a terephthalic acid diester with 1,4-BDO of M_n = 1,000 g/mol (Park et al., 1994). In the same vein, protease catalyzed the oligomerization of alkyl D- and L-lactates leading to oligo(L-lactic acid)s (dimers to pentamers) with moderate yields (Ohara et al., 2011). It is noteworthy that the L-enantioselectivity of the protease is opposite to the one of lipases (Ohara et al., 2010), which is used for the PLA depolymerization hydrolysis (Hedstrom, 2002; Kawai et al., 2011).

Moreover, in addition to the relative activity of protease for polycondensation reactions, the ROP of 1,4-dioxan-2-one by the protease of *Bacillus thermoproteolyticus rokko* led to a poly(1,4-dioxan-2-one) polyester with a M_n of 8,600 g/mol, whereas the ROP of D,L-lactide by proteinase K had a low monomer conversion (40%) and led to a M_n of only 1,900 g/mol.

Finally, even if proteases exhibited a relative activity for the synthesis of polyester by polycondensation and ROP reactions, molar masses of synthesized polyesters are not up to expectations. Nevertheless, proteases such as papain, bromelain, trypsin and α-chymotrypsin showed a much higher reactivity towards the synthesis of polyamides (Shoda et al., 2016).

4.3. Enzymatic step-growth polymerization of polyesters

Such as for the chemical polymerization, three polymerization modes can be envisaged for the lipase-catalyzed polyester synthesis: (i) step-growth polycondensation, (ii) enzymatic ring-opening polymerization (ROP) and (iii) a combination of ROP and polycondensation. Among them, enzyme-catalyzed polycondensation and ROP are the most common methods used for biocatalytic polyester synthesis. However, since ROP reactions have been already largely investigated (Albertsson and Srivastava, 2008; Kobayashi, 2015; Miletić et al., 2010; Y. Yang et al., 2011) and they are not studied in this thesis, they will not be detailed.

Four modes of elemental reactions may occur during the lipase-catalyzed polyester synthesis by the step-growth polycondensation: (i) hydrolysis, (ii) esterification, (iii) transesterification (alcoholysis and acidolysis) and (iv) interesterification (Scheme 1.8). These reactions are all, in principle, reversible. Therefore, to facilitate the ester formation, it is crucial to remove the remaining water and by-products like alcohols from the reaction mixture, for example, by adding absorbing and drying agents such as molecular sieve, by applying reduced pressure, by using azeotropic distillation conditions, and so on.

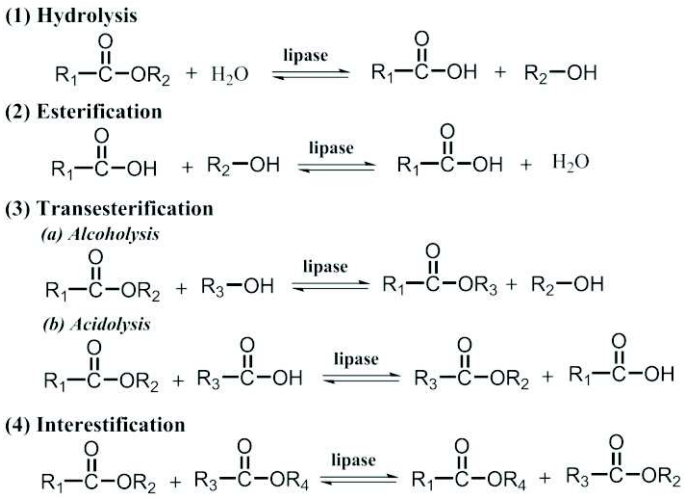

Scheme 1.8 : Basic modes of elemental lipase-catalyzed reactions in biocatalytic polyesters synthesis (Jiang and Loos, 2016).

The enzymatic step-growth polymerization occurred under mild conditions (T < 100 °C) in organic solvent or in bulk from mainly dicarboxylic acid or derivatives (mainly diester dicarboxylate) with diols.

Early results (about 20 years ago) described the synthesis of polyesters using various free lipases such as *CALB*, porcine pancreas lipase and lipases from *Pseudomonas cepacia*, *Pseudomonas fluorescens*, *Rhizomucor miehei*, *Aspergillus niger* and *Candida cylindracea*. The use of free enzymes led to (i) a rapid decrease of the biocatalytic activity leading to long reaction times (Wu et al., 1996), (ii) the use of a very high amount of biocatalyst (up to almost 100 wt.% of the total weight of substrates, (iii) low reactions yields and (iv) mostly low molar mass (Chaudhary et al., 1997b). However, some lipases such as CALB or lipases from *Rhizomucor miehei* and *Pseudomonas cepacia* exhibited interesting results with M_n > 10,000 g/mol for divinyl dicarboxylates substrates (Uyama et al., 1999).

To shift the equilibrium toward the product polymer more effectively, activation of esters was conducted using a halogenated alcohol like 2-chloroethanol, 2,2,2-trifluoroethanol and 2,2,2-trichloroethanol. Compared with water-, methanol- or ethanol- leaving groups, the halogenated moiety increased the electrophilicity of the acyl carbonyl and avoided significant alcoholysis of the products by decreasing the nucleophilicity of the leaving alkoxy groups. As an example, for the polycondensation/transesterification, *Rhizomucor miehei* lipase relative affinity order with bis(2,2,2-triflurorethyl) was the following: sebacate > sebacic acid > diethyl sebacate (Linko et al., 1995a). This halogenation method was widely used in the early studies when processes were not already optimized. However, this method increases highly the price of the substrate.

In the same vein, an irreversible ester-formation process was also developed. For this purpose, vinyl and enol esters of dicarboxylic acids were used as the activated acid form in the enzyme-catalyzed polyester synthesis. The by-products resulting from polymerization of enol or vinyl esters tautomerize to respectively ketones or aldehydes, preventing the back-reaction, thereby shifting the equilibrium towards the synthesis of polyesters.

Thereafter, the major breakthrough on the enzymatic catalysis was the used of high boiling point solvents, such as diphenyl ether or veratrole (1,2-dimethoxybenzene), under vacuum to remove more efficiently the by-product of the reaction and shifting thus the equilibrium towards the synthesis of polyesters. Molar mass could be thus quadrupled by modifying only the pressure in the reaction mixture (Linko et al., 1995a).

The other breakthrough in this method was the use of immobilized enzymes. The immobilization of an enzyme on a support (*e.g.*, porous acrylic beads, porous ceramic or other polymers carriers) permits to highly increase its stability allowing the synthesis of polyesters with much higher molar masses. N435 is the best example of CALB immobilization. For instance, the solvent-free polycondensation of AA and 1,8-octanediol with immobilized CALB led to polyester with at least the double of the molar mass achieved using free CALB (Mahapatro et al., 2004). Moreover, the effect of the catalyst load on the final polymer molar mass was studied and showed that M_n increased with the N435 load from 0.1 to 10 wt.%, even if the increase was not so important between 1 and 10 wt.% (Mahapatro et al., 2004). The higher activity of N435 (CALB) than Lipozyme (immobilized form of lipase from *Rhizomucor miehei*) has been

reported (Mezoul et al., 1995; Linko et al., 1998). Recently, some interesting enzyme immobilizations on nanoclays were reported, providing interesting perspectives for using inorganic supports as reactive fillers (Düşkünkorur et al., 2015; Öztürk Düşkünkorur et al., 2014; Öztürk et al., 2016). Enzymes immobilization is being developed to improve the biocatalytic activity and decrease the production cost of enzymatic catalysts (Jesionowski et al., 2014). Since the late 1990s, N435 became the working horse in biocatalytic polyester synthesis due to it commercially availability and it good catalytic activity.

Nowadays, the synthesis of polyesters by polycondensation/transesterification reactions is carried out either in bulk or in high boiling point solvents with mostly N435 as catalyst under vacuum using various dicarboxylic acids or diester dicarboxylates with diols. Likewise, the synthesis of polyesters in diphenyl ether achieved higher molar masses than in bulk since the major drawback on the bulk polymerization is the significant increase of the viscosity decreasing highly the reaction rate after reaching a certain level (Azim et al., 2006; Mahapatro et al., 2003).

4.4. Effects of some reaction parameters on polyester synthesis

4.4.1. Influence of the solvent

Since the polyester synthesis is driven by the reverse reaction of lipases, the water content in the system is a key factor. Minimal water content should thus be present in the reaction mixture.

Kumar and Gross investigated the influence of the solvent hydrophobicity on the N435 activity on the ROP of ε-caprolactone (Kumar and Gross, 2000a). None of tested solvents having a log P (logarithm of the water/octanol coefficient partition) value below 1.5 were suitable solvents leading to the low conversion of monomers and low polymer molar masses. A partial explanation of this may be the deactivation of the enzyme in polar media due to the conformational change. However, between the different suitable solvents for this reaction (*i.e.,* isopropyl ether, toluene, butyl ether, isooctane), no tendency was observed, which may do think that the observed differences cannot be explained simply by considering log P values. They claimed also that a better understanding of how the solvent geometry, dipole moments, solubilization of substrates, and other factors influence the physicochemical and catalytic properties of enzymes is needed. Yao et al. reported the same tendency for the N435-catalyzed polycondensation of 1,8-octanediol, AA and L-maleic acid, with high molar mass achieved only for solvents having a log P value higher than 2 (Yao et al., 2011).

Among the numerous amount of apolar solvents tested for the enzymatic synthesis of by polycondensation/transesterification such as toluene, dioxane, hexane, isooctane, cyclooctane, benzene, cyclohexane, dodecane, isopropyl ether…, many studies have proved that diphenyl ether under vacuum is the preferred solvent for CALB and *Rhizomucor miehei* (Linko et al., 1995a, 1995b; Wang et al., 1996; Mahapatro et al., 2003; Azim et al., 2006; Jiang et al., 2013).

4.4.2. Influence of the substrate concentration

The substrate concentration in solvent enzymatic process is an important parameter since (i) a low concentration mays lead to the cyclization of oligomers to form macrocycles (Sugihara et al., 2006; Yagihara and Matsumura, 2012; Champagne et al., 2017) and (b) not optimal conditions can decrease significantly the molar mass.

As an example, Linko et al. determined that 350 wt.% of diphenyl ether (vs. total mass of monomers) was optimal for the transesterification of bis(2,2,2-triflurorethyl) sebacate with 1,4-BDO at 37 °C by the crude *Rhizomucor miehei* lipase. On their side, Jiang et al. showed that 150 wt.% of diphenyl ether was the optimal solvent amount for the N435-catalyzed transesterification reaction of diethyl succinate, dimethyl itaconate and 1,4-BDO in diphenyl ether at 80 °C (Jiang et al., 2013).

The determination of the optimal substrate concentration is thus an important parameter to achieve the synthesis of polyesters of high molar mass, but the value depends highly on the other reaction parameters (*e.g.*, substrate, solvent) and so is characteristic of a given system.

4.4.3. Influence of the substrate length

Since the basic biological activity of lipases is to cleave lipids into fatty acids, lipases have naturally a preference for hydrophobic substrate with a long linear alkane chain length. Lipases have shown a preference toward substrates with a pronounced hydrophobic character. For this reason, in polyester synthesis, lipases exhibit globally an increase of the catalytic activity with the diol and dicarboxylic acid chain length. Moreover, an increase of the alkyl chain length gives a higher flexibility to the substrate, which permits an easier access to the active site of enzymes.

As an example, the molar mass of a semi-aromatic polyesters synthesized by N435 in diphenyl ether from the transesterification of dimethyl-2,5-furandicarboxylate with various diols increased with the diol chain length according to C10 > C8 > C6 > C4 > C2 (Jiang et al., 2015b).

Likewise, Mahapatro *et al.* showed that the polyester molar mass from the N435-catalyzed polycondensation of AA increased with the diol chain length from 1,4-BDO to 1,8-octanediol both in bulk and in diphenyl ether (Mahapatro et al., 2003). Moreover, the N435 relative activity for the polycondensation of 1,8-octanediol with different dicarboxylic acid in diphenyl ether and in bulk was sebacic ~ adipic > glutaric ~ succinic acids. Interestingly, the reaction in bulk and in diphenyl ether followed the same trend.

Linko et al. exhibited the increase of crude *Rhizomucor miehei* lipase activity with the diol length from C2 to C5 then a slight decrease for C6 for the transesterification at 37 °C in diphenyl ether with bis(2,2,2-triflurorethyl) sebacate (Linko et al., 1995b).

Similarly the molar mass for the transesterification of divinyl adipate with several diols by *Pseudomonas fluorescens* lipase in isopropyl ether for 48 increased with the diol length from EG to 1,6-hexanediol (Uyama and Kobayashi, 1994). However, M_n values decreased markedly with 1,10-decanediol, which confirms that the increase of the lipase activity with the substrate length is more a general trend than an "universal law".

On their side, Feder and Gross studied the effect of the diol and the dicarboxylic acid chain length with N435 and the immobilized cutinase of *Humicola insolens* (HiC) (Feder and Gross, 2010). The activity order for the polycondensation of sebacic acid (C10-diacid) with different diols with 3-, 4-, 5-, 6,- and 8-carbon chain lengths was C8 > C6 with HiC, whereas smaller diols did not polymerized efficiently (*i.e.*, Mn < 2,000 g/mol). N435 relative activity for diol substrates was C8 = C6 = C5 > C4 > C3 without big differences between all values. HiC activity for the polycondensation of 1,8-octanediol with various dicarboxylic acid with 6,- , 8-, 9-, 10-, and 13-carbon chain lengths was the highest for C13 = C10, but it showed little activity for C6, C8 and C9 diacids. On the contrary, N435 displayed similar activity toward all these diacid chain lengths. Thus, N435 can accommodate a broader substrate range than HiC. Similarly, Hunsen *et al.* presented a similar tendency for the HiC-catalyzed polycondensation in bulk of AA with diols (*i.e.*, C8 > C6 > C4) (Hunsen et al., 2007).

Generally, the lipase activity increases with the substrate alkane chain length up to 8-10 carbons length. However, experimental studies exhibited several exceptions due to the specificity of the biocatalyst, the substrate and the reactional conditions.

4.4.4. Influence of the reaction temperature

Generally, lipase-catalyzed synthesis of polyesters is performed at temperature up to 95 °C to avoid the protein denaturation and the loss of catalytic activity. Crude enzymes, which have been widely used in the early stages, are used mostly at low temperature (*i.e.*, 35-60 °C) according to the species (Kobayashi et al., 1998; Uyama et al., 1999; Uyama and Kobayashi, 1994; Wu et al., 1996). However, the use of immobilized enzyme permits to reach higher reaction temperature, for substantial times.

For the ROP reaction of ε-caprolactone in toluene, N435 exhibited its highest activity at 90 °C, whereas HiC exhibited the highest activity at 70 °C (Hunsen et al., 2007; Kumar and Gross, 2000a). Moreover, a significant decrease of the monomer conversion was observed between 70 and 80 °C for HiC due to the significant denaturation of the enzyme at temperature higher than 70 °C (Hunsen et al., 2008). HiC exhibited thus a much lower thermal stability than N435.

For the step-growth polycondensation, N435 exhibited an optimal activity in bulk or in solvent system at 80-90 °C for various substrates (Li et al., 2008). Similarly, the lipase of *Burkholderia cepacia* immobilized on diatomaceous earth

exhibited an optimal activity at 80 °C for the transesterification of dimethyl itaconate, 12-hydroxystearate and 1,4-BDO in toluene (Yasuda et al., 2010).

Furthermore, the temperature had a significant influence in the regioselectivity of N435. An increase of the temperature decreased highly the preference of the biocatalyst to primary hydroxyl functions of glycerol during its transesterification with divinyl adipate leading to a hyperbranched polymer instead of a linear one at lower temperature (Taresco et al., 2016).

In bottom line, all reactional parameters are inter-dependent which complicates highly the determination of optimal reaction conditions (Figure 1.9). That is why, most of the time, each research group used almost always the same reactional conditions, even for different polyesters structures, after an optimization of a first system.

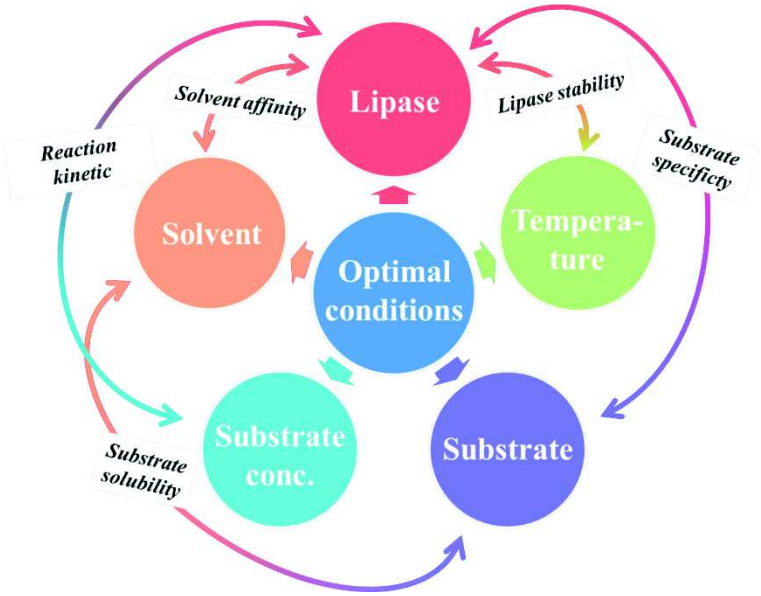

Figure 1.9 : Different key parameters of the lipase-catalyzed synthesis of polyesters.

4.5. New strategies for the improvement of the enzymatic catalysis

In addition to classical methods of enzymatic polymerization, some other less conventional methods, including microwave irradiation, ultrasound activation, reactive extrusion and the use of new solvents (*i.e.*, ionic liquids and supercritical fluids), has been tested to improve the lipase activity and address the above issues.

4.5.1. Microwave-assisted polymerization

Although microwave-assisted reactions are widely applied in various domains of organic chemistry, their use in the area of enzymatic chemistry has been rather limited, due to the high temperatures associated with the microwave heating. Microwave irradiation, allowing an important decrease of the overall reaction time, has been tested for a lot of hydrolysis, esterification and transesterification reactions in organic solvents or bulk conditions with different enzymes (*i.e.*, lipases and cutinases). However, mixed results were obtained (Rejasse et al., 2007). As an example, the esterification of oleic acid by methanol catalyzed by immobilized CALB under microwave irradiation in bulk did not show any improvements (Bukhari et al., 2014). Just the opposite, the transesterification of β-ketoesters by N435 under microwave irradiation worked very well in solvent-free conditions (Risso et al., 2012). Due to mixed results of the enzyme-catalyzed reactions under microwave irradiation, until now only a limited number of studies was performed on the polyester synthesis. The combination of N435 and microwave irradiation for the ROP of ε-caprolactone did not lead to a significant improvement compared to the classical reaction heated with an oil bath (Kerep and Ritter, 2006, 2007). A slight increase of the ROP reaction rate in diethyl ether was observed, whereas a decrease was observed with the considered better solvents, such as toluene and benzene, or in bulk. For their part, Matos *et al.* reported the successful use of the microwave heating for the ROP of ε-caprolactone in solvent-free conditions (90 °C, 240 min, 50 W) and showed a four-fold increase of the M_n when microwave irradiation was used compared to conventional heating *via* an

oil bath (Matos et al., 2011). Recently, the transesterification reaction of dimethyl succinate or dimethyl adipate with 1,4-BDO in bulk or in diethyl ether catalyzed by N435 exhibited similar or lower molar mass than with the conventional heating (Alessandro Pellis et al., 2016a). Finally, up to now, the enzyme-catalyzed synthesis of polyester by microwave irradiation did not show improvements.

4.5.2. Ultrasound-assisted polymerization

Use of ultrasound holds a substantial potential for enhancing the performance of biocatalytic processes with saving time (Chisti, 2003), but sonication has not been widely evaluated for lipase mediated polymerization. On one side, the ultrasonic irradiation leads to the significant improvement of the N435-catalyzed ROP of ε-caprolactone in ionic liquid with final polyester with molar mass and monomer conversion respectively three and seven times greater than in classical conditions (Gumel et al., 2012). Moreover, the sonication permits the reaction to continue longer in a bulk process due to the lower influence of the viscosity as sonication takes place (Gumel et al., 2013). On the other side, the ultrasonic-assisted synthesis of poly(ethylene glutarate) from diethyl glutarate and ethylene glycol diacetate in bulk with N435 as catalyst led to polyesters chains with the same degree of polymerization as the ones polymerized without sonication, but in 7 h instead of 24 h (Zhao et al., 2016).

4.5.3. Reactive extrusion

More recently, the reactive extrusion process has been tested for the hydrolysis of poly(butylene succinate) (Jbilou et al., 2015) and the ROP polymerization reaction of ω-pentadecalactone (Spinella et al., 2015) using N435 as catalyst for both reactions. This process exhibited a remarkable activity of CALB leading to a fast decrease of the PBS molar mass from 82,000 to 4,500 g/mol in only 5 min in the presence of 1 wt.% of lipase. For a reaction time of 30 min and 10 wt.% of lipase, up to 44% free SA has been released. In the opposite direction, the ROP of ω-pentadecalactone showed an almost total conversion of monomers (*i.e.*, > 99%) in only 15 min, resulting in 80,000 g/mol polyesters. To obtain similar results in a classical batch in toluene, the reaction must be 72 hours long, whereas the bulk polymerization led to only 22,000 g/mol polyesters. Nevertheless, to the best of our knowledge, till now, no synthesis of polyesters by polycondensation/transesterification has been reported by this process, even if it would be interesting to try.

4.5.4. New solvents with special properties

In the past few years, ionic liquids have been investigated as an alternative to classical organic solvents. Indeed, many polyesters are poorly soluble in apolar organic solvents that are suitable for the enzymatic synthesis of polyesters, which causes premature precipitation of the formed polymer leading to low molar mass. However, due to the unconventional properties of ionic liquids allowing abtter polymer solubility, they offer the possibility of enzymatic polymerization. Since fifteen years, ionic liquids have been used for enzyme-catalyzed polymerization mostly by ROP with mixed results (Uyama et al., 2002; Chanfreau et al., 2010; Mena et al., 2010, 2013; Piotrowska and Sobczak, 2014). However, transesterification reactions have been much less studied, surely due to the fact that molar mass were much lower (*i.e.*, M_n up to only 5,900 g/mol) than using conventional solvents, that have highly decreased the interest of these solvents (Uyama et al., 2002; Marcilla et al., 2006).

The use of supercritical (sc) fluids, especially $scCO_2$, is another way to substitute organic solvents. It has been widely explored as a promising green method, allowing the reduction of the reaction temperature. Such as for ionic liquids, supercritical fluids have been mostly used for the investigation of ROP reactions of lactones, but results do not show better results than using classical solvents (Loeker et al., 2004; Nakaoki et al., 2005; Guzmán-Lagunes et al., 2012; Thurecht et al., 2006; Takamoto et al., 2013; Comim Rosso et al., 2013). On his side, the step-growth polymerization process in sc-fluids yielded only polymers of low molar masses (*i.e.*, M_n < 4,000 g/mol) (Chaudhary et al., 1995; Takamoto et al., 2013).

5. Bacterial polyesters: the poly(hydroxyalkanoate)s

In addition to the two synthetic pathways described previously for the synthesis of polyesters, bacterial polyesters, known as poly(hydroxyalkanoate)s (PHAs), can be obtained directly by fermentation using bacteria.

5.1. Structure of bacterial PHAs

PHAs are aliphatic polyesters synthesized as intracellular carbon and energy reserve by various microorganisms (or bacteria) (Pollet and Avérous, 2011). Within the cytoplasm of the bacteria cells, PHAs are stored in form of granules, which are insoluble, amorphous and osmotically inert inclusions. Bacteria use carbon sources to produce PHA granules in condition of nutriment limitation (nitrogen, phosphorous or oxygen) to prevent starvation ensuring the bacteria cells growth (Sudesh et al., 2000).

PHAs are natural and fully biobased thermoplastic polyesters that are also biodegradable in almost all environments including soils and sea water (Doi, 1990; Sudesh et al., 2000). Moreover, their biocompatibility is a huge advantage since it permits targeting biomedical applications for these materials (Bordes et al., 2009a). These natural polymers have typically a molar mass that ranges from 200,000 to 3,000,000 g/mol according to the bacteria strain and growth conditions (Zinn et al., 2001).

The working horse of PHAs is the homopolyester poly((*R*)-3-hydroxybutyrate) (PHB), which was described in the mid-twenties by the French microbiologist Maurice Lemoigne who isolated and characterized this polymer from *Bacillus megaterium* bacteria (Lemoigne, 1926).

Since the PHB discovery, a great number of bacteria strains (over 300 species) capable of PHA synthesis and more than 150 types of monomers were discovered thanks to the significant development of biotechnology (Laycock et al., 2013). Nevertheless, the amount of bacterial strains which can be used to synthesize PHAs at an industrially acceptable level of production remains limited. Among the most efficient bacteria that have been tested for an industrial production, one can cite recombinant *Escherichia coli*, *Cupriavidus necator*, *Alcaligenes latus, Aeromonas hydrophila* and *Pseudomonas oleovorans* (Chen, 2010).

PHAs are composed of monomers containing from 3 to 18 carbon atoms with a general structure presented in Figure 1.10 where x is 1 for most PHAs and R can be a hydrogen atom or a hydrocarbon chain of variable length with sometimes some functionalities (unsaturation, carboxylic acid group, hydroxyl group, methyl ester function, epoxy function). Moreover, some PHA monomers contain in the side chain halogen atoms or aromatic cycles (Steinbüchel and Valentin, 1995).

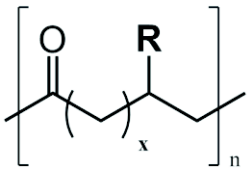

x = 1	**R =**	**hydrogen**	**Poly-3-hydroxypropionate (P3HP)**
		methyl	**Poly-3-hydroxybutyrate (P3HB)**
		ethyl	**Poly-3-hydroxyvalerate (P3HV)**
		propyl	**Poly-3-hydroxyhexanoate (P3HHx)**
		butyl	**Poly-3-hydroxyheptanoate (P3HHp)**
		penthyl	**Poly-3-hydroxyoctanoate (P3HO)**
		heptyl	**Poly-3-hydroxydecanoate (P3HD)**
		nonyl	**Poly-3-hydroxydodecanoate (P3HDD)**
x = 2	**R =**	**hydrogen**	**Poly-4-hydroxybutyrate (P4HB)**
		methyl	**Poly-4-hydroxyvalerate (P4HV)**
x = 3	**R =**	**hydrogen**	**Poly-5-hydroxyvalerate (P3HV)**

Figure 1.10 : Structures of main polyhydroxyalkanoates.

According to the number of carbon atoms in the monomer units, two mains classes of PHAs are usually designed: (i) short-chain-length (scl) PHAs when monomers have 3-5 carbon atoms or (ii) medium-chain-length (mcl) PHAs when monomers have 6 to 18 carbon atoms (Lee, 1996; Laycock et al., 2013). The chemical nature of PHAs produced depends strongly on the carbon substrate and the bacterial strain used (S. J. Park et al., 2012). For example, *Cupriavidus necator* (formerly known as *Ralstonia eutropha)* produces only scl-PHAs, whereas *Pseudomonas putida* synthesizes only mcl-PHAs. The first class (*i.e.*, scl-PHAs) generally displays thermoplastic material properties similar to polypropylene (Holmes, 1985; Tsuge, 2002), whereas mcl-PHAs have elastic material properties similar to rubber and elastomer. Moreover, most of PHA monomers are optically active chemicals due to the presence of a chiral carbon

linked to the side chain of the PHA monomer and they show only a *R*-configuration, even if some linear monomers such as 3-hydroxypropionate, 4-hydroxybutyrate or 5-hydroxyvalerate can be produced.

5.2. PHA fermentation and recovery

In most bacteria, PHB is produced *via* the acetyl-CoA pathway by a sequence of three enzyme-catalyzed reactions; acetyl-CoA C-acetyltransferase catalyzes the condensation of two acetyl-CoA molecules to form acetoacetyl-CoA; then NADPH-dependent acetoacetyl-CoA reductase reduces acetoacetyl-CoA to (*R*)-3-hydroxybutyryl-CoA; finally PHB synthase catalyzes the polymerization of (*R*)-3-hydroxybutyryl-CoA monomers to PHB (Peoples and Sinskey, 1989a, 1989b). When the bacteria are under condition of nutriment limitation, polymer degradation occurs due to the PHB depolymerase and PHB is transformed to acetoacetyl-CoA by enzyme-catalyzed reactions to close the cyclic PHB metabolic process (Doi, 1990). The biological pathway of PHB is summarized in Scheme 1.9.

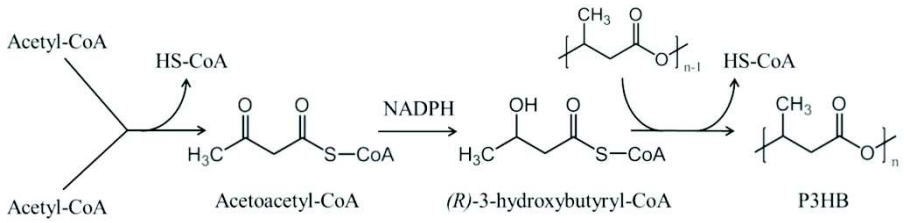

Scheme 1.9 : Simplified mechanism of the bacterial fermentation production of PHB.

Currently, PHAs are produced at an industrial level using feedstocks such as glucose, sucrose and fatty acids fermented by pure cultures of either natural or genetically modified engineered microorganisms such as the recombinant strains of *Escherichia coli* (Fidler and Dennis, 1992; Kahar et al., 2005) or *Cupriavidus necator* (Kahar et al., 2004). The fermentation process are most often operated in two-stage in a batch reactor where the bacteria cells firstly grow in a media enriched in nutrient and carbon source (growth phase) and then a limitation of one of an essential nutrient (phosphorous, oxygen or ammonium) activates the production of PHAs which are accumulated during the second stage (accumulation phase). Bacteria cells can accumulate PHA granules up to 90% of their cell dry weight (Laycock et al., 2013). A great effort has been made to improve the fermentation process efficiency of PHA production and, thus, to lower the production cost essential to broaden their uses by using inexpensive carbon substrate and mixed microbial cultures (*e.g.*, activated sludge). Different renewable vegetal oils and various waste products have been successfully used as carbons sources such as corn oil, palm oil (Fukui and Doi, 1998; Lee et al., 2008), soybean oil (Kahar et al., 2004), waste frying oils (Verlinden et al., 2011) and molasses (Solaiman et al., 2006a, 2006b). Mixed cultures allow important advantages compared to simpler process since no requirement of strict sterilization conditions are needed and offer a better adaptability to complex waste feedstocks. Moreover, some kind of reactor simulating feast and famine sequential conditions for bacteria, called sequential batch reactors, were developed since their represent a very promising solution for the industrial PHA production with higher yields obtained (Beun et al., 2002; Johnson et al., 2009; Villano et al., 2014).

The fermentation process is followed by the PHA recovery by extraction from cells and purification which increases significantly the production cost. The oldest technique to recover PHA is by using an organic solvent such as chloroform in which the polymer is soluble, then precipitate it in a PHA non-solvent and finally recover the polymer by classical techniques such as centrifugation or filtration. Despite the fact that the basic method permits both high yields and high degree of purity, the method is not environmentally friendly and not economically interesting for large-scale productions since this method consumes a large volume of solvent. Many alternatives processes have been developed in which it is the non-PHA cell mass (NPCM) that is solubilized (digestion treatment) (Roy and Visakh, 2014). This method includes the use of surfactants (Kim et al., 2003; Y.-H. Yang et al., 2011), surfactants with alkali (Lo et al., 2011) or chelates (Chen et al., 1999, 2001), alkali alone (Anis et al., 2012; Choi and Lee, 1999a) or in combination with acids (Yu and Chen, 2006), enzymes (Kapritchkoff et al., 2006; Neves and Müller, 2012) and chemicals (Kathiraser et al., 2007; Koning and Witholt, 1997). In addition to chemical disruption, mechanical (high pressure homogenization, beads mill) or physical (*e.g.*, freezing, osmotic shock, ultrasonication) treatments can be employed even if they are

expensive and not easily industrially scalable (Harrison, 1991; Geciova et al., 2002). More recently, supercritical fluids, which have unique physicochemical properties that make them suitable solvents for the PHA extraction, have been used. However, this method is costly compared to other techniques (Hejazi et al., 2003). Moreover, another particularly interesting method is the spontaneous liberation (or autolysis) of PHA from cells that has been developed on some strains such as *E. coli*. This method naturally shows a great interest since no chemicals are used in this process (Jung et al., 2005).

5.3. PHA copolymers

Historically, PHB was the main PHA industrially produced, but it limited properties have driven the development of PHA copolymers which can present interesting properties. Indeed, PHA random copolymers with different monomer structure and composition can be synthesized thanks to the addition of suitable co-substrates to the carbon sources in the medium during the fermentation process. The most known random PHA copolymer is poly(3-hydroxybutyrate-*co*-3-hydroxyvalerate) (P(3HB-*co*-3HV)), composed of monomers with side groups R = methyl and R = ethyl (Figure 1.10), which permits to adjust the properties of PHB (Chen et al., 2014; Du et al., 2001). In the same way, random poly(3-hydroxybutyrate-*co*-4-hydroxybutyrate) (P(3HB-*co*-4HB)) and random poly(3-hydroxybutyrate-*co*-3-hydroxyhexanoate) (P(3HB-*co*-3HHx)) are also produced at large scale (Chen, 2009). However, the high cost of using precursors for the non 3HB monomers in the copolymers increases the price of these copolymers. For example, propionic acid, 1,4-BDO and lauric acid are used for the formation of 3HV, 4HB, and 3HHx in their respective copolymers based on 3HB (Choi and Lee, 1999b; Zhang et al., 2009). Moreover, some of these precursors are difficult to handle during the cell growth period or present some toxicity for the bacteria. Nevertheless, some recent developments involving metabolic engineering of strains and screenings permit to use only glucose, which is a rather low cost substrate, for the synthesis of random PHA copolymers which will increase the competitiveness of these PHAs compared to petroleum-based polymers according to their production cost (Aldor et al., 2002; Li et al., 2010; Valappil et al., 2008).

Furthermore, PHA block copolymers with two or more unique blocks can be produced allowing such block structure copolymer to possess the properties of each block which can generate new properties that cannot be available by polymer blending (Pederson et al., 2006) or in the random copolymer counterparts. They are obtained by using periodic co-substrate addition to the growth medium (Pederson et al., 2006; Tripathi et al., 2013). Block copolymers can display structures such as AB diblock, ABC triblock or $(AB)_n$ repeating multiblocks, among others (Bates, 1991). The bacterial synthesis of PHA block copolymers is less common due to the specificity of PHA synthases which produced mostly random structures. As an example, *Cupriavidus necator* allows the production of P(HB-*b*-HV) block copolymer under certain conditions and this particular structure permits to prevent the polymer aging which is one of the main issue of PHB (McChalicher and Srienc, 2007). Nevertheless, due to the close properties of both parent homopolymers, P(3HB-*b*-3HV), being a scl-block copolymer, still shows brittleness drawbacks. On the contrary, one may expect that scl-mcl block copolymers could display improved properties. Indeed, the P(3HB-*b*-(3HV-*co*-3HHp)) block copolymer containing a first block of PHB and another block made of a random P(3HV-*co*-3HHp) copolymer exhibited improved mechanical properties (Li et al., 2011). Likewise, P(3HB-*b*-4HB), P(3HB-*b*-3HHx), and P(3HHx-*b*-(3HD-*co*-3HDD)) block copolymers have been synthesized (Hu et al., 2011; Tripathi et al., 2012; Gao et al., 2011; Chen et al., 2015). The block copolymerization opens, thus, a new area in the production of new macromolecular structures of PHAs displaying tuned and improved properties.

5.4. Thermal stability of PHAs

The major disadvantage of PHAs, especially for scl-PHAs (*i.e.*, PHB and P(3HB-*co*-3HV)), is their poor thermal stability which makes their processing by conventional techniques quite challenging. The thermal degradation of PHAs occurs mainly by a cis-elimination reaction which leads to the formation of crotonic acid and linear oligomers containing crotonyl chain ends as volatile products (Grassie et al., 1984a, 1984b; Aoyagi et al., 2002). In the case of PHB, due to its high melting temperature, the thermal degradation occurs already at temperature below its minimal

procession temperature (*i.e.*, 190 °C) and, thus, a non-negligible decomposition is impossible to avoid and results in the decrease of molar mass which has a detrimental effect on the material properties (*e.g.*, mechanical properties) (Hoffmann et al., 1994). A common way to reduce the melt temperature of PHB is through the incorporation of a co-monomer such as valerate moieties, in sufficient amount, in PHBV copolymers. Moreover, at processing temperatures, transesterification reactions can occur when PHB is blended with other polymers containing reactive moieties (*e.g.*, ester, carboxyl, hydroxyl…).

5.5. PHA-based copolymers

To overcome the thermal stability drawbacks of PHAs, PHA-based copolymers have been developed *via* bio- or chemosynthesis. In order to obtain these structures, controlled PHA oligomers must be obtained by PHA molar mass reduction with functionalization to obtain telechelic hydroxyl-terminated PHAs (PHA-diol). These oligomers can be synthesized by either organometallic- (Hirt et al., 1996) and acid-catalyzed (Deng and Hao, 2001) alcoholysis or sodium borohydrate reduction (Baran et al., 2002; Bergamaschi et al., 2011).

From PHA oligomers, different tailored materials can be obtained including block poly(ester-urethanes), block poly(ester-ether-urethane)s and block or random copolyesters based on PHA blocks with others blocks (Ke, 2015; Ravenelle and Marchessault, 2002). Block poly(ester-urethane)s and block poly(ester-ether-urethane)s are obtained by the use of diisocyanates (*e.g.*, 1,6-hexamethylene diisocyanate, toluene diisocyanate, methylene diphenyl diisocyanate or L-Lysine methyl ester diisocyanate) as coupling agent of PHA-diols with others blocks, such as poly(ε-caprolactone), poly(ethylene glycol), poly(butylene adipate) or PBS (Ke, 2015).

On his side, block, micro-block and random copolyesters are obtained by different processes. Block copolyesters are synthesized *via* (i) either the chemical (Reeve et al., 1993; Wu et al., 2010) or enzymatic (Dai and Li, 2008) ROP of lactones/lactides from PHA-diol oligomers or (ii) chain coupling using an acyl chloride (e.g., terephthaloyl chloride) or 1,3-*N,N*-dicyclohexylcarbodiimide/4-(dimethylamino) pyridine (Li et al., 2003). Micro-block and random copolyesters with different compositions have also been synthesized by (i) acid-catalyzed transesterification in solution (Impallomeni et al., 2013, 2002), (ii) titanium-catalyzed transesterification in bulk (Debuissy et al., 2017b) and (iii) CALB-catalyzed transesterification in diphenyl ether (Debuissy et al., 2016b).

5.6. Applications

PHAs have seen their range of applications increased significantly since the past twenty years. Whereas, at the beginning, applications of PHAs were limited mainly to the agriculture or packaging area (*e.g.*, shampoo bottles, cosmetics containers, milk cartons and films …) (Griffin, 1994; Smith, 2005) and bulk chemical production from depolymerized PHA (Brandl et al., 1988; Lee et al., 1999; Madison and Huisman, 1999). More recently, the PHA industry has been focused on the medical area due to the biocompatibility of PHAs using PHAs derivatives. This includes their usage as cardiovascular products (repair patches, scaffold for bone generation, vascular graft), dental and maxillofacial treatment (dental floss, bone generation, guiding tissue), drug delivery systems (tablets, implants, micro-carriers), nutrition and sutures (Steinbüchel and Hofrichter, 2001; Valappil et al., 2006; Philip et al., 2007).

6. Conclusions

Biobased polyesters, especially poly(alkylene dicarboxylate)s, have gaining a great interest in the last few years due to the environmental concerns and the possibility to obtain new macromolecular architectures from biomass. The development of biorefineries from different feedstocks and biological processes allows, now, the access to many biobased building blocks, among which some of them are already commercially available because competitive compared to fossil-sourced ones. Moreover, the richness of available macromolecular structures permits to target a wide range of applications, whence the large development observed recently.

Synthetic polyesters are, for the moment, still mainly produced by the chemical route using for the most part metal-based catalysts and a two-step melt polycondensation reaction under harsh conditions which is sometimes used in tandem with chain-extension processes. This allows the fast production of high molar mass polyesters. In the case of

high melting temperature polyesters such as semi-aromatic polyesters, the solid-state polymerization process was used. However, recently a more eco-friendly pathway is developing based on the use of biological catalysts such as the enzymes. Among them, lipases have shown a remarkable activity and the capacity to synthesize polyesters under mild conditions. Compared to the chemical pathway, the enzymatic synthesis of polyesters is still in development and the technology is not already mature. However, the biotic pathway has shown to be a powerful and versatile approach for the synthesis of various macromolecular architectures.

Benefits of using the enzymatic pathway include the use of non-toxic natural catalysts contrary to organometallic ones. This allows thus the use of some of the polyesters produced from these syntheses for applications requiring the absence of toxic moieties, such as in biomedical or cosmetic. Moreover, the use of immobilized enzymes permits to reuse the catalyst several times without a drastic decrease of the enzyme activity, allowing a reduction of the polymer production cost. Then, since enzyme is a biological molecule, it has a low thermal stability and thus polymerization should be performed under mild conditions allowing energy savings. In addition, the reaction at low temperatures permits to almost suppress all thermal degradation occurring during the melt polycondensation reaction. It has a huge interest for the synthesis of unsaturated polyester resins using building blocks, such as itaconic or fumaric acids, since reaction temperature are much lower than ones initiating the cross-linking. Besides, since lipases exhibit high stereo-selectivity, an excellent control can be obtained allowing the synthesis of precise macromolecular architectures, especially by using polyols with primary and secondary hydroxyl functions.

Nevertheless, since this technology is still not fully mature, some drawbacks remain and need to be overcome. Nowadays, best results are obtained using non-ecofriendly solvents such as toluene or diphenyl ether. Likewise, the enzymatic process is very long to obtain high molar mass polymer, especially for step-growth polymerizations which last few days. Moreover, molar masses obtained using the biological process are lower than the ones obtained, in shorter time, from the conventional chemical route. Besides, compared to the two-step melt polycondensation, the atom efficiency is rather low when ester or vinyl derivatives are used as substrates instead of acids since leaving groups of ester or vinyl derivatives (*i.e.*, alcohols or aldehydes) are bigger than the one of acids (*i.e.*, H_2O). Furthermore, nowadays the price of the enzyme catalysts is still high. The purity of substrate in a biological process is also a key parameter in order to avoid the poisoning of the reaction mixture. Finally, the enzymatic polymerization involving monomers with short chain length (*e.g.*, ethylene glycol or 1,3-PDO), secondary hydroxyl functions (*e.g.*, 2,3-BDO or isoborbide) and aromatic rings (*e.g.*, furans) generally results in low molar mass polymers.

In addition to synthetic polyesters which can be obtained *via* an abiotic or a biotic pathway, PHA bacterial polyesters have gained a significant interest since they are high molar mass polyesters produced by bacteria in large fermenter from rather cheap substrates. In addition, a large amount of PHA derivatives can be produced from PHA-diol oligomers allowing the development of new macromolecular architectures. Moreover, the richness of monomer structures (more than 150 different monomers) permits considering a wide range of application for these polyester family, even if the current tendency is to use them for the packaging or agriculture due to is biodegradable ability or in the biomedical field due to it biocompatibility.

In the near future, thanks to the fast development of biorefineries from different biomasses, biobased polyesters from biobased building blocks will take a significant importance by using either biobased monomers instead of their oil-based equivalent (*e.g.*, for the synthesis of PBS, PBSA, PBAT, PET) or using novel green polymers with new macromolecular architectures (*e.g.*, furans and sorbitol) that cannot be produced from oil-based building blocks and which can replace oil-based polyesters from certain applications (*e.g.*, replacement of biobased PEF instead of oil-based PET). In addition, the enzymatic catalysis has still a long way to develop in order to obtain a better understanding of the mechanisms governing this process and the synergy between different reaction parameters. The main research axis will focus on the development of more active and stable catalysts facilitating the synthesis of high molar mass polymers and the recycle of the enzyme. This should decrease the cost of this technology necessary to transferring this pathway from the laboratory to the industrial scale. To increase the enzymatic activity in terms of units of polymer obtained per unit of enzyme used, enzymes should be modified by genetic engineering to improve their kinetic characteristics. On their side, PHA-based materials will have strong development driven by the research of complex architectures using PHA-macromers obtained by the controlled PHA depolymerization from the wide variety of PHAs available. The development of PHA-based materials, permitting tailoring properties, allows thus new interesting and promising valorization routes.

7. References

Aeschelmann, F., Carus, 2016. Bio-based Building Blocks and Polymers - Global Capacities and Trends 2016 – 2021. Nova-Institute, Germany.

Agarwal, S., Mast, C., Dehnicke, K., Greiner, A., 2000. Macromol. Rapid Commun. 21, 195–212.

Aharoni, S.M., 2002. Industrial-Scale Production of Polyesters, Especially Poly(Ethylene Terephthalate), in: DSc, S.F. (Ed.), Handbook of Thermoplastic Polyesters. Wiley-VCH Verlag GmbH & Co. KGaA, pp. 59–103.

Ahn, B.D., Kim, S.H., Kim, Y.H., Yang, J.S., 2001. J. Appl. Polym. Sci. 82, 2808–2826.

Albertsson, A.-C., Srivastava, R.K., 2008. Adv. Drug Deliv. Rev., Design and Development Strategies of Polymer Materials for Drug and Gene Delivery Applications 60, 1077–1093.

Albertsson, A.-C., Varma, I.K., 2003. Biomacromolecules 4, 1466–1486.

Aldor, I.S., Kim, S.-W., Prather, K.L.J., Keasling, J.D., 2002. Appl. Environ. Microbiol. 68, 3848–3854.

Anastas, P.T., Warner, J.C., 2000. Green chemistry: theory and practice. Oxford Univ. Press, Oxford.

Anis, S.N.S., Nurhezreen, M.I., Sudesh, K., Amirul, A.A., 2012. Appl. Biochem. Biotechnol. 167, 524–535.

Aoyagi, Y., Yamashita, K., Doi, Y., 2002. Polym. Degrad. Stab. 76, 53–59.

Avérous, L., Pollet, E., 2012. Biodegradable Polymers, in: Avérous, L., Pollet, E. (Eds.), Environmental Silicate Nano-Biocomposites, Green Energy and Technology. Springer London, pp. 13–39.

Azim, H., Dekhterman, A., Jiang, Z., Gross, R.A., 2006. Biomacromolecules 7, 3093–3097.

Badenes, S.M., Lemos, F., Cabral, J.M.S., 2011. Biotechnol. Bioeng. 108, 1279–1289.

Baran, E.T., Özer, N., Hasirci, V., 2002. J. Microencapsul. 19, 363–376.

de Barros, D.P.C., Fonseca, L.P., Cabral, J.M.S., Weiss, C.K., Landfester, K., 2009a. Biotechnol. J. 4, 674–683.

de Barros, D.P.C., Fonseca, L.P., Fernandes, P., Cabral, J.M.S., Mojovic, L., 2009b. J. Mol. Catal. B Enzym. 60, 178–185.

de Barros, D.P.C., Lemos, F., Fonseca, L.P., Cabral, J.M.S., 2010. J. Mol. Catal. B Enzym. 66, 285–293.

Bart, J.C.J., Cavallaro, S., 2015. Ind. Eng. Chem. Res. 54, 1–46.

Barton, N.R., Burgard, A.P., Burk, M.J., Crater, J.S., Osterhout, R.E., Pharkya, P., Steer, B.A., Sun, J., Trawick, J.D., Dien, S.J.V., Yang, T.H., Yim, H., 2014. J. Ind. Microbiol. Biotechnol. 42, 349–360.

Bates, F.S., 1991. Science 251, 898–905.

Bechthold, I., Bretz, K., Kabasci, S., Kopitzky, R., Springer, A., 2008. Chem. Eng. Technol. 31, 647–654.

Becker, J., Lange, A., Fabarius, J., Wittmann, C., 2015. Curr. Opin. Biotechnol. 36, 168–175.

Beerthuis, R., Rothenberg, G., Shiju, N.R., 2015. Green Chem. 17, 1341–1361.

Belgacem, M.N., Gandini, A. (Eds.), 2008. Monomers, polymers and composites from renewable resources, 1st ed. ed. Elsevier, Amsterdam ; Boston.

Bergamaschi, J.M., Pilau, E.J., Gozzo, F.C., Felisberti, M.I., 2011. Macromol. Symp. 299–300, 10–19.

Bersot, J.C., Jacquel, N., Saint-Loup, R., Fuertes, P., Rousseau, A., Pascault, J.P., Spitz, R., Fenouillot, F., Monteil, V., 2011. Macromol. Chem. Phys. 212, 2114–2120.

Beun, J.J., Dircks, K., Van Loosdrecht, M.C.M., Heijnen, J.J., 2002. Water Res. 36, 1167–1180.

Biebl, H., Menzel, K., Zeng, A.-P., Deckwer, W.-D., 1999. Appl. Microbiol. Biotechnol. 52, 289–297.

Bikiaris, D.N., Achilias, D.S., 2006. Polymer 47, 4851–4860.

Bikiaris, D.N., Papageorgiou, G.Z., Giliopoulos, D.J., Stergiou, C.A., 2008. Macromol. Biosci. 8, 728–740.

Bordes, P., Pollet, E., Avérous, L., 2009. Potential Use of Polyhydroxyalkanoate (PHA) for Biocomposite Development, in: Nano- and Biocomposites. CRC Press, Boca Raton, pp. 193–226.

Borman, S., 2004. Chem. Eng. News 82, 35–39.

Bozell, J.J., 2008. CLEAN – Soil Air Water 36, 641–647.

Bozell, J.J., Petersen, G.R., 2010. Green Chem. 12, 539.

Brandl, H., Gross, R.A., Lenz, R.W., Fuller, R.C., 1988. Appl. Environ. Microbiol. 54, 1977–1982.

Bukhari, A., Idris, A., Atta, M., Loong, T.C., 2014. Chin. J. Catal. 35, 1555–1564.

Buzin, P., Lahcini, M., Schwarz, G., Kricheldorf, H.R., 2008. Macromolecules 41, 8491–8495.

Campistron, I., Reyx, D., Hamza, M., Oulmidi, A., 1997. Macromol. Symp. 122, 329–334.

Cao, A., Okamura, T., Nakayama, K., Inoue, Y., Masuda, T., 2002. Polym. Degrad. Stab. 78, 107–117.

Carothers, W.H., 1929. J. Am. Chem. Soc. 51, 2548–2559.

Carothers, W.H., 1931. Chem. Rev. 8, 353–426.

Carothers, W.H., 1936. Trans Faraday Soc 32, 39–49.

Carothers, W.H., Arvin, J.A., 1929. J. Am. Chem. Soc. 51, 2560–2570.

Carré, C., Bonnet, L., Avérous, L., 2014. RSC Adv 4, 54018–54025.

Carvalho, C.M.L., Aires-Barros, M.R., Cabral, J.M.S., 1998. Electron. J. Biotechnol. 1, 160–173.

Carvalho, C.M.L., Aires-Barros, M.R., Cabral, J.M.S., 1999. Biotechnol. Bioeng. 66, 17–34.

Celińska, E., Grajek, W., 2009. Biotechnol. Adv. 27, 715–725.

Celli, A., Marchese, P., Sisti, L., Dumand, D., Sullalti, S., Totaro, G., 2013. Polym. Int. 62, 1210–1217.

Champagne, É., Lévaray, N., Zhu, X.X., 2017. ACS Sustain. Chem. Eng. 5, 689–695.

Chandure, A.S., Umare, S.S., 2007. Int. J. Polym. Mater. Polym. Biomater. 56, 339–353.

Chanfreau, S., Mena, M., Porras-Domínguez, J.R., Ramírez-Gilly, M., Gimeno, M., Roquero, P., Tecante, A., Bárzana, E., 2010. Bioprocess Biosyst. Eng. 33, 629–638.

Chaudhary, A., Beckman, E.J., Russell, A.J., 1995. J. Am. Chem. Soc. 117, 3728–3733.

Chaudhary, A.K., Lopez, J., Beckman, E.J., Russell, A.J., 1997. Biotechnol. Prog. 13, 318–325.

Chen, C.-H., Peng, J.-S., Chen, M., Lu, H.-Y., Tsai, C.-J., Yang, C.-S., 2010. Colloid Polym. Sci. 288, 731–738.

Chen, G.-Q., 2009. Chem. Soc. Rev. 38, 2434–2446.

Chen, G.-Q. (Ed.), 2010. Plastics from bacteria: natural functions and applications, Microbiology monographs. Springer, Berlin.

Chen, G.-Q., Hajnal, I., Wu, H., Lv, L., Ye, J., 2015. Trends Biotechnol. 33, 565–574.

Chen, Y., Chen, J., Yu, C., Du, G., Lun, S., 1999. Process Biochem. 34, 153–157.

Chen, Y., Li, M., Meng, F., Yang, W., Chen, L., Huo, M., 2014. Environ. Technol. 35, 1791–1801.

Chen, Y., Yang, H., Zhou, Q., Chen, J., Gu, G., 2001. Process Biochem. 36, 501–506.

Chisti, Y., 2003. Trends Biotechnol. 21, 89–93.

Choi, J., Lee, S.Y., 1999a. Biotechnol. Bioeng. 62, 546–553.

Choi, J., Lee, S.Y., 1999b. Appl. Environ. Microbiol. 65, 4363–4368.

Choi, S., Song, C.W., Shin, J.H., Lee, S.Y., 2015. Metab. Eng. 28, 223–239.

Comim Rosso, S.R., Bianchin, E., de Oliveira, D., Oliveira, J.V., Ferreira, S.R.S., 2013. J. Supercrit. Fluids, Special Issue – 10th International Symposium on Supercritical FluidsSpecial Issue – 10th International Symposium on Supercritical Fluids 79, 133–141.

Corma, A., Iborra, S., Velty, A., 2007. Chem. Rev. 107, 2411–2502.

Cui, Z., Qiu, Z., 2015. Polymer 67, 12–19.

Dai, J., Ma, S., Wu, Y., Han, L., Zhang, L., Zhu, J., Liu, X., 2015. Green Chem. 17, 2383–2392.

Dai, J.-Y., Zhao, P., Cheng, X.-L., Xiu, Z.-L., 2015. Appl. Biochem. Biotechnol. 175, 3014–3024.

Dai, S., Li, Z., 2008. Biomacromolecules 9, 1883–1893.

Debuissy, T., Pollet, E., Avérous, L., 2016a. Polymer 99, 204–213.

Debuissy, T., Pollet, E., Avérous, L., 2016b. Biomacromolecules 17, 4054–4063.

Debuissy, T., Pollet, E., Avérous, L., 2017a. Eur. Polym. J. 87, 84–98.

Debuissy, T., Pollet, E., Avérous, L., 2017b. Eur. Polym. J. 90, 92–104.

Deng, X.M., Hao, J.Y., 2001. Eur. Polym. J. 37, 211–214.

Deng, X.M., Yuan, M.L., Xiong, C.D., Li, X.H., 1999. J. Appl. Polym. Sci. 71, 1941–1948.

Deng, Y., Ma, L., Mao, Y., 2016. Biochem. Eng. J. 105, Part A, 16–26.

Doi, Y., 1990. Microbial polyesters, John Wiley & Sons, Inc. ed. VCH, New York.

Du, G.C., Chen, J., Yu, J., Lun, S., 2001. Biochem. Eng. J. 8, 103–110.

Duh, B., 2001. J. Appl. Polym. Sci. 81, 1748–1761.

Duh, B., 2002. Polymer 43, 3147–3154.

Düşkünkorur, H.Ö., Bégué, A., Pollet, E., Phalip, V., Güvenilir, Y., Avérous, L., 2015. J. Mol. Catal. B Enzym. 115, 20–28.

Egmond, M.R., de Vlieg, J., 2000. Biochimie, Lipase 2000 82, 1015–1021.

El-Imam, A.A., Du, C., 2014. J. Biodivers. Bioprospecting Dev.

Feder, D., Gross, R.A., 2010. Biomacromolecules 11, 690–697.

Fidler, S., Dennis, D., 1992. FEMS Microbiol. Rev. 9, 231–235.

Fortunati, E., Gigli, M., Luzi, F., Dominici, F., Lotti, N., Gazzano, M., Cano, A., Chiralt, A., Munari, A., Kenny, J.M., Armentano, I., Torre, L., 2017. Carbohydr. Polym. 165, 51–60.

Fradet, A., Maréchal, E., 1982. Kinetics and mechanisms of polyesterifications, in: Polymerizations and Polymer Properties. Springer, Berlin, Heidelberg, pp. 51–142.

Fradet, A., Tessier, M., 2003. Polyesters, in: Rogers, rtin E., Long, T.E. (Eds.), Synthetic Methods in Step-Growth Polymers. John Wiley & Sons, Inc., pp. 17–134.

Fu, H., Kulshrestha, A.S., Gao, W., Gross, R.A., Baiardo, M., Scandola, M., 2003. Macromolecules 36, 9804–9808.

Fukui, T., Doi, Y., 1998. Appl. Microbiol. Biotechnol. 49, 333–336.

Gamerith, C., Zartl, B., Pellis, A., Guillamot, F., Marty, A., Acero, E.H., Guebitz, G.M., 2017. Process Biochem.

Gao, X., Chen, J.-C., Wu, Q., Chen, G.-Q., 2011. Curr. Opin. Biotechnol., 22/6 Chemical biotechnology and Pharmaceutical biotechnology 22, 768–774.

Garaleh, M., Lahcini, M., Kricheldorf, H.R., Weidner, S.M., 2009. J. Polym. Sci. Part Polym. Chem. 47, 170–177.

Geciova, J., Bury, D., Jelen, P., 2002. Int. Dairy J. 12, 541–553.

Ghassemi, H., Schiraldi, D.A., 2014. J. Appl. Polym. Sci. 131, n/a-n/a.

Gigli, M., Lotti, N., Gazzano, M., Finelli, L., Munari, A., 2013. Polym. Eng. Sci. 53, 491–501.

Gotor-Fernández, V., Vicente, G., 2007. Use of Lipases in Organic Synthesis, in: Polaina, J., MacCabe, A.P. (Eds.), Industrial Enzymes. Springer Netherlands, pp. 301–315.

Grassie, N., Murray, E.J., Holmes, P.A., 1984a. Polym. Degrad. Stab. 6, 47–61.

Grassie, N., Murray, E.J., Holmes, P.A., 1984b. Polym. Degrad. Stab. 6, 127–134.

Griffin, G.J.L. (Ed.), 1994. Chemistry and technology of biodegradable polymers, 1st ed. ed. Blackie Academic & Professional, London ; New York.

Gross, S.M., Flowers, D., Roberts, G., Kiserow, D.J., DeSimone, J.M., 1999. Macromolecules 32, 3167–3169.

Gross, S.M., Roberts, G.W., Kiserow, D.J., DeSimone, J.M., 2000. Macromolecules 33, 40–45.

Gubbels, E., Drijfhout, J.P., Posthuma-van Tent, C., Jasinska-Walc, L., Noordover, B.A.J., Koning, C.E., 2014. Prog. Org. Coat. 77, 277–284.

Gubbels, E., Jasinska-Walc, L., Koning, C.E., 2013. J. Polym. Sci. Part Polym. Chem. 51, 890–898.

Gubbels, Erik, Jasinska-Walc, L., Noordover, B.A.J., Koning, C.E., 2013. Eur. Polym. J. 49, 3188–3198.

Guisan, J.M., Betancor, L., Fernandez-Lorente, G., Flickinger, M.C., 2009. Immobilized Enzymes, in: Encyclopedia of Industrial Biotechnology. John Wiley & Sons, Inc.

Gumel, A.M., Annuar, M.S.M., Chisti, Y., 2013. Ultrason. Sonochem. 20, 937–947.

Gumel, A.M., Annuar, M.S.M., Chisti, Y., Heidelberg, T., 2012. Ultrason. Sonochem. 19, 659–667.

Guzmán-Lagunes, F., López-Luna, A., Gimeno, M., Bárzana, E., 2012. J. Supercrit. Fluids 72, 186–190.

Harmsen, P.F.H., Hackmann, M.M., Bos, H.L., 2014. Biofuels Bioprod. Biorefining 8, 306–324.

Harrison, S.T.L., 1991. Biotechnol. Adv. 9, 217–240.

Hedstrom, L., 2001. An Overview of Serine Proteases, in: Current Protocols in Protein Science. John Wiley & Sons, Inc.

Hedstrom, L., 2002. Chem. Rev. 102, 4501–4524.

Hejazi, P., Vasheghani-Farahani, E., Yamini, Y., 2003. Biotechnol. Prog. 19, 1519–1523.

Hirt, T.D., Neuenschwander, P., Suter, U.W., 1996. Macromol. Chem. Phys. 197, 1609–1614.

Høegh, I., Patkar, S., Halkier, T., Hansen, M.T., 1995. Can. J. Bot. 73, 869–875.

Hoekman, S.K., Broch, A., Robbins, C., Ceniceros, E., Natarajan, M., 2012. Renew. Sustain. Energy Rev. 16, 143–169.

Hoffmann, A., Kreuzberger, S., Hinrichsen, G., 1994. Polym. Bull. 33, 355–359.

Holden, G., Adams, R.K. (Eds.), 1996. Thermoplastic elastomers, 2. ed. ed. Hanser [u.a.], Munich.

Holmberg, A.L., Reno, K.H., Wool, R.P., Thomas H. Epps, I.I.I., 2014. Soft Matter 10, 7405–7424.

Holmes, P.A., 1985. Phys. Technol. 16, 32.

Hori, H., Takahashi, H., Yamaguchi, A., Hagiwara, T., 1995. Can. J. Microbiol. 41, 282–288.

Hori, Y., Suzuki, M., Yamaguchi, A., Nishishita, T., 1993a. Macromolecules 26, 5533–5534.

Hori, Y., Takahashi, Y., Yamaguchi, A., Nishishita, T., 1993b. Macromolecules 26, 4388–4390.

Hotelier, T., Renault, L., Cousin, X., Negre, V., Marchot, P., Chatonnet, A., 2004. Nucleic Acids Res. 32, D145–D147.

Hu, D., Chung, A.-L., Wu, L.-P., Zhang, X., Wu, Q., Chen, J.-C., Chen, G.-Q., 2011. Biomacromolecules 12, 3166–3173.

Huang, C.Q., Luo, S.Y., Xu, S.Y., Zhao, J.B., Jiang, S.L., Yang, W.T., 2010. J. Appl. Polym. Sci. 115, 1555–1565.

Hunsen, M., Abul, A., Xie, W., Gross, R., 2008. Biomacromolecules 9, 518–522.

Hunsen, M., Azim, A., Mang, H., Wallner, S.R., Ronkvist, A., Xie, W., Gross, R.A., 2007. Macromolecules 40, 148–150.

Impallomeni, G., Carnemolla, G.M., Puzzo, G., Ballistreri, A., Martino, L., Scandola, M., 2013. Polymer 54, 65–74.

Impallomeni, G., Giuffrida, M., Barbuzzi, T., Musumarra, G., Ballistreri, A., 2002. Biomacromolecules 3, 835–840.

Ishihara, K., Ohara, S., Yamamoto, H., 2000. Science 290, 1140–1142.

Ishii, M., Okazaki, M., Shibasaki, Y., Ueda, M., Teranishi, T., 2001. Biomacromolecules 2, 1267–1270.

Isikgor, F.H., Becer, C.R., 2015. Polym. Chem., Polymer Chemistry 6, 4497–4559.

Jacquel, N., Freyermouth, F., Fenouillot, F., Rousseau, A., Pascault, J.P., Fuertes, P., Saint-Loup, R., 2011. J. Polym. Sci. Part Polym. Chem. 49, 5301–5312.

Jansen, M.L., van Gulik, W.M., 2014. Curr. Opin. Biotechnol., Chemical biotechnology • Pharmaceutical biotechnology 30, 190–197.

Jbilou, F., Dole, P., Degraeve, P., Ladavière, C., Joly, C., 2015. Eur. Polym. J. 68, 207–215.

Jesionowski, T., Zdarta, J., Krajewska, B., 2014. Adsorption 20, 801–821.

Ji, X.-J., Huang, H., Ouyang, P.-K., 2011. Biotechnol. Adv. 29, 351–364.

Jiang, W., Wang, S., Wang, Y., Fang, B., 2016. Biotechnol. Biofuels 9, 57.

Jiang, Y., Loos, K., 2016. Polymers 8, 243.

Jiang, Y., Woortman, A.J.J., van Ekenstein, G.O.R.A., Loos, K., 2013. Biomolecules 3, 461–480.

Jiang, Y., Woortman, A.J.J., Ekenstein, G.O.R.A. van, Loos, K., 2015a. Polym. Chem. 6, 5451–5463.

Jiang, Y., Woortman, A.J.J., Ekenstein, G.O.R.A. van, Loos, K., 2015b. Polym. Chem. 6, 5198–5211.

Jiménez-Quero, A., Pollet, E., Zhao, M., Marchioni, E., Avérous, L., Phalip, V., 2016a. J. Microbiol. Biotechnol. 26, 1557–1565.

Jiménez-Quero, A., Pollet, E., Zhao, M., Marchioni, E., Averous, L., Phalip, V., 2016b. J. Microbiol. Biotechnol.

Jin, H.-J., Lee, B.-Y., Kim, M.-N., Yoon, J.-S., 2000. Eur. Polym. J. 36, 2693–2698.

Johnson, K., Jiang, Y., Kleerebezem, R., Muyzer, G., van Loosdrecht, M.C.M., 2009. Biomacromolecules 10, 670–676.

Jung, I.L., Phyo, K.H., Kim, K.C., Park, H.K., Kim, I.G., 2005. Res. Microbiol. 156, 865–873.

Kahar, P., Agus, J., Kikkawa, Y., Taguchi, K., Doi, Y., Tsuge, T., 2005. Polym. Degrad. Stab. 87, 161–169.

Kahar, P., Tsuge, T., Taguchi, K., Doi, Y., 2004. Polym. Degrad. Stab. 83, 79–86.

Kampouris, E.M., Papaspyrides, C.D., 1985. Polymer 26, 413–417.

Kapoor, M., Gupta, M.N., 2012. Process Biochem. 47, 555–569.

Kapritchkoff, F.M., Viotti, A.P., Alli, R.C.P., Zuccolo, M., Pradella, J.G.C., Maiorano, A.E., Miranda, E.A., Bonomi, A., 2006. J. Biotechnol. 122, 453–462.

Kathiraser, Y., Aroua, M.K., Ramachandran, K.B., Tan, I.K.P., 2007. J. Chem. Technol. Biotechnol. 82, 847–855.

Kaur, G., Srivastava, A.K., Chand, S., 2012. Biochem. Eng. J. 64, 106–118.

Kawai, F., Nakadai, K., Nishioka, E., Nakajima, H., Ohara, H., Masaki, K., Iefuji, H., 2011. Polym. Degrad. Stab. 96, 1342–1348.

Kawai, R., Miura, M., Takakuwa, K., Isahaya, Y., Fujimori, T., Suito, J., Nakamura, M., Kawai, R., Miura, M., Takakuwa, K., Isahaya, Y., Fujimori, T., Suito, J., Nakamura, M., 1995. Aliphatic polyester carbonate and process for producing the same. EP0684270 (A2).

Ke, Y., 2015. Express Polym. Lett. 10, 36–53.

Kerep, P., Ritter, H., 2006. Macromol. Rapid Commun. 27, 707–710.

Kerep, P., Ritter, H., 2007. Macromol. Rapid Commun. 28, 759–766.

Kim, M., Cho, K.-S., Ryu, H.W., Lee, E.G., Chang, Y.K., 2003. Biotechnol. Lett. 25, 55–59.

Kint, D.P.R., Alla, A., Deloret, E., Campos, J.L., Muñoz-Guerra, S., 2003. Polymer 44, 1321–1330.

Kobayashi, S., 2015. Polym. Adv. Technol. 26, 677–686.

Kobayashi, S., Uyama, H., Namekawa, S., 1998. Polym. Degrad. Stab., Biodegradable Polymers and Macromolecules 59, 195–201.

Kong, X., Qi, H., Curtis, J.M., 2014. J. Appl. Polym. Sci. 131, n/a-n/a.

Koning, G.J.M. de, Witholt, B., 1997. Bioprocess Eng. 17, 7–13.

Köpke, M., Mihalcea, C., Liew, F., Tizard, J.H., Ali, M.S., Conolly, J.J., Al-Sinawi, B., Simpson, S.D., 2011. Appl. Environ. Microbiol. 77, 5467–5475.

Kraus, G.A., 2008. CLEAN – Soil Air Water 36, 648–651.

Kricheldorf, H.R., Behnken, G., Schwarz, G., 2005. Polymer 46, 11219–11224.

Kumar, A., Gross, R.A., 2000. Biomacromolecules 1, 133–138.

Kunioka, M., Wang, Y., Onozawa, S., 2005. Macromol. Symp. 224, 167–180.

Kwolek, S.L., Morgan, P.W., 1964. J. Polym. Sci. A 2, 2693–2703.

Laycock, B., Halley, P., Pratt, S., Werker, A., Lant, P., 2013. Prog. Polym. Sci., Topical Issue on Biorelevant Polymers 38, 536–583.

Le Nôtre, J., Witte-van Dijk, S.C.M., van Haveren, J., Scott, E.L., Sanders, J.P.M., 2014. ChemSusChem 7, 2712–2720.

Lee, S.Y., 1996. Trends Biotechnol. 14, 431–438.

Lee, S.Y., Lee, Y., Wang, F., 1999. Biotechnol. Bioeng. 65, 363–368.

Lee, W.-H., Loo, C.-Y., Nomura, C.T., Sudesh, K., 2008. Bioresour. Technol. 99, 6844–6851.

Lemoigne, M., 1926. Bull Soc Chim Bio 8, 770–782.

Li, G., Yao, D., Zong, M., 2008. Eur. Polym. J. 44, 1123–1129.

Li, J., Li, X., Ni, X., Leong, K.W., 2003. Macromolecules 36, 2661–2667.

Li, S.Y., Dong, C.L., Wang, S.Y., Ye, H.M., Chen, G.-Q., 2011. Appl. Microbiol. Biotechnol. 90, 659–669.

Li, Z.-J., Shi, Z.-Y., Jian, J., Guo, Y.-Y., Wu, Q., Chen, G.-Q., 2010. Metab. Eng. 12, 352–359.

Liaw, D.-J., Liaw, B.-Y., Hsu, J.-J., Cheng, Y.-C., 2000. J. Polym. Sci. Part Polym. Chem. 38, 4451–4456.

Lindström, A., Albertsson, A.-C., Hakkarainen, M., 2004. Polym. Degrad. Stab. 83, 487–493.

Linko, Y.-Y., Lämsä, M., Wu, X., Uosukainen, E., Seppälä, J., Linko, P., 1998. J. Biotechnol., Biocatalysis 66, 41–50.

Linko, Y.-Y., Wang, Z.-L., Seppälä, J., 1995a. J. Biotechnol. 40, 133–138.

Linko, Y.-Y., Wang, Z.-L., Seppälä, J., 1995b. Enzyme Microb. Technol. 17, 506–511.

Lo, C.-W., Wu, H.-S., Wei, Y.-H., 2011. J. Taiwan Inst. Chem. Eng. 42, 240–246.

Loeker, F.C., Duxbury, C.J., Kumar, R., Gao, W., Gross, R.A., Howdle, S.M., 2004. Macromolecules 37, 2450–2453.

Loh, X.J., Karim, A.A., Owh, C., 2015. J. Mater. Chem. B Mater. Biol. Med. 3, 7641–7652.

Longhi, S., Nicolas, A., Creveld, L., Egmond, M., Verrips, C.T., de Vlieg, J., Martinez, C., Cambillau, C., 1996. Proteins Struct. Funct. Bioinforma. 26, 442–458.

Loos, K. (Ed.), 2010. Front Matter, in: Biocatalysis in Polymer Chemistry. Wiley-VCH Verlag GmbH & Co. KGaA.

Luo, S.Y., Zhang, Y., Zhao, J.B., 2006. Adv. Mater. Res. 11–12, 387–390.

Madison, L.L., Huisman, G.W., 1999. Microbiol. Mol. Biol. Rev. MMBR 63, 21–53.

Mahapatro, A., Kalra, B., Kumar, A., Gross, R.A., 2003. Biomacromolecules 4, 544–551.

Mahapatro, A., Kumar, A., Kalra, B., Gross, R.A., 2004. Macromolecules 37, 35–40.

Mallon, F., Beers, K., Ives, A., Ray, W.H., 1998. J. Appl. Polym. Sci. 69, 1789–1791.

Mani, R., Bhattacharya, M., Leriche, C., Nie, L., Bassi, S., 2002. J. Polym. Sci. Part Polym. Chem. 40, 3232–3239.

Marcilla, R., de Geus, M., Mecerreyes, D., Duxbury, C.J., Koning, C.E., Heise, A., 2006. Eur. Polym. J. 42, 1215–1221.

Martinez, C., De Geus, P., Lauwereys, M., Matthyssens, G., Cambillau, C., 1992. Nature 356, 615–618.

Martinez, C., Nicolas, A., van Tilbeurgh, H., Egloff, M.P., Cudrey, C., Verger, R., Cambillau, C., 1994. Biochemistry (Mosc.) 33, 83–89.

Matos, T.D., King, N., Simmons, L., Walker, C., McClain, A.R., Mahapatro, A., Rispoli, F.J., McDonnell, K.T., Shah, V., 2011. Green Chem. Lett. Rev. 4, 73–79.

McChalicher, C.W.J., Srienc, F., 2007. J. Biotechnol. 132, 296–302.

Medway, A.M., Sperry, J., 2014. Green Chem. 16, 2084–2101.

Mei, Y., Miller, L., Gao, W., Gross, R.A., 2003. Biomacromolecules 4, 70–74.

Mena, M., Chanfreau, S., Gimeno, M., Bárzana, E., 2010. Bioprocess Biosyst. Eng. 33, 1095–1101.

Mena, M., López-Luna, A., Shirai, K., Tecante, A., Gimeno, M., Bárzana, E., 2013. Bioprocess Biosyst. Eng. 36, 383–387.

Mezoul, G., Lalot, T., Brigodiot, M., Maréchal, E., 1995. J. Polym. Sci. Part Polym. Chem. 33, 2691–2698.

Miletić, N., Loos, K., Gross, R.A., 2010. Enzymatic Polymerization of Polyester, in: Loos, K. (Ed.), Biocatalysis in Polymer Chemistry. Wiley-VCH Verlag GmbH & Co. KGaA, pp. 83–129.

Mincheva, R., Delangre, A., Raquez, J.-M., Narayan, R., Dubois, P., 2013. Biomacromolecules 14, 890–899.

Miura, M., Takakuwa, K., Fujimori, S., Ito, M., 1998. Aliphatic Polyestercarbonate and Its Production. JPH1045884 (A).

Mochizuki, M., Mukai, K., Yamada, K., Ichise, N., Murase, S., Iwaya, Y., 1997. Macromolecules 30, 7403–7407.

Mohamad, N.R., Marzuki, N.H.C., Buang, N.A., Huyop, F., Wahab, R.A., 2015. Biotechnol. Biotechnol. Equip. 29, 205–220.

Mohsen-Nia, M., Memarzadeh, M.R., 2013. Polym. Bull. 70, 2471–2491.

Montaudo, G., Rizzarelli, P., 2000. Polym. Degrad. Stab. 70, 305–314.

Murphy, C.A., Cameron, J.A., Huang, S.J., Vinopal, R.T., 1996. Appl. Environ. Microbiol. 62, 456–460.

Nakaoki, T., Kitoh, M., Gross, R.A., 2005. Enzymatic Ring Opening Polymerization of ε-Caprolactone in Supercritical CO2, in: Polymer Biocatalysis and Biomaterials, ACS Symposium Series. American Chemical Society, pp. 393–404.

Nardini, M., Dijkstra, B.W., 1999. Curr. Opin. Struct. Biol. 9, 732–737.

Neves, A., Müller, J., 2012. Biotechnol. Prog. 28, 1575–1580.

Niaounakis, M., 2014. Biopolymers: Processing and Products. William Andrew.

Nikolic, M.S., Djonlagic, J., 2001. Polym. Degrad. Stab. 74, 263–270.

Noordover, B.A.J., van Staalduinen, V.G., Duchateau, R., Koning, C.E., van Benthem, Mak, M., Heise, A., Frissen, A.E., van Haveren, J., 2006. Biomacromolecules 7, 3406–3416.

Ohara, H., Nishioka, E., Yamaguchi, S., Kawai, F., Kobayashi, S., 2011. Biomacromolecules 12, 3833–3837.

Ohara, H., Onogi, A., Yamamoto, M., Kobayashi, S., 2010. Biomacromolecules 11, 2008–2015.

Okabe, M., Lies, D., Kanamasa, S., Park, E.Y., 2009. Appl. Microbiol. Biotechnol. 84, 597–606.

Ollis, D.L., Cheah, E., Cygler, M., Dijkstra, B., Frolow, F., Franken, S.M., Harel, M., Remington, S.J., Silman, I., Schrag, J., 1992. Protein Eng. 5, 197–211.

Ortner, A., Pellis, A., Gamerith, C., Yebra, A.O., Scaini, D., Kaluzna, I., Mink, D., Wildeman, S. de, Acero, E.H., Guebitz, G.M., 2017. Green Chem. 19, 816–822.

Otera, J., Danoh, N., Nozaki, H., 1991. J. Org. Chem. 56, 5307–5311.

Otton, J., Ratton, S., Vasnev, V.A., Markova, G.D., Nametov, K.M., Bakhmutov, V.I., Komarova, L.I., Vinogradova, S.V., Korshak, V.V., 1988. J. Polym. Sci. Part Polym. Chem. 26, 2199–2224.

Öztürk Düşkünkorur, H., Pollet, E., Phalip, V., Güvenilir, Y., Avérous, L., 2014. Polymer 55, 1648–1655.

Öztürk, H., Pollet, E., Phalip, V., Güvenilir, Y., Avérous, L., 2016. Polymers 8, 416.

Papageorgiou, G.Z., Bikiaris, D.N., 2005. Polymer 46, 12081–12092.

Papageorgiou, G.Z., Bikiaris, D.N., Achilias, D.S., Papastergiadis, E., Docoslis, A., 2011. Thermochim. Acta 515, 13–23.

Papageorgiou, G.Z., Vassiliou, A.A., Karavelidis, V.D., Koumbis, A., Bikiaris, D.N., 2008. Macromolecules 41, 1675–1684.

Papaspyrides, C.D., Vouyiouka, S.N. (Eds.), 2009. Solid state polymerization. Wiley, Hoboken, N.J.

Park, H., Seo, J., Lee, H.-Y., Kim, H.-W., Wall, I.B., Gong, M.-S., Knowles, J.C., 2012. Acta Biomater. 8, 2911–2918.

Park, H.G., Chang, H.N., Dordick, J.S., 1994. Biocatalysis 11, 263–271.

Park, S.J., Kim, T.W., Kim, M.K., Lee, S.Y., Lim, S.-C., 2012. Biotechnol. Adv., Special issue on ACB 2011 30, 1196–1206.

Patel, R.N., 2008. Expert Opin. Drug Discov. 3, 187–245.

Patil, D.R., Rethwisch, D.G., Dordick, J.S., 1991. Biotechnol. Bioeng. 37, 639–646.

Pederson, E.N., McChalicher, C.W.J., Srienc, F., 2006. Biomacromolecules 7, 1904–1911.

Pellis, A., Acero, E.H., Weber, H., Obersriebnig, M., Breinbauer, R., Srebotnik, E., Guebitz, G.M., 2015a. Biotechnol. J. 10, 1739–1749.

Pellis, A., Corici, L., Sinigoi, L., D'Amelio, N., Fattor, D., Ferrario, V., Ebert, C., Gardossi, L., 2015b. Green Chem. 17, 1756–1766.

Pellis, A., Ferrario, V., Zartl, B., Brandauer, M., Gamerith, C., Acero, E.H., Ebert, C., Gardossi, L., Guebitz, G.M., 2016. Catal. Sci. Technol. 6, 3430–3442.

Pellis, Alessandro, Guebitz, G.M., Farmer, T.J., 2016a. Molecules 21, 1245.

Pellis, Alessandro, Haernvall, K., Pichler, C.M., Ghazaryan, G., Breinbauer, R., Guebitz, G.M., 2016b. J. Biotechnol., Special Issue on ACIB, Dedicated to the Occasion of Prof. Dr. Helmut Schwab's 65th Birthday 235, 47–53.

Penco, M., Ranucci, E., Ferruti, P., 1998. Polym. Int. 46, 203–216.

Peoples, O.P., Sinskey, A.J., 1989a. J. Biol. Chem. 264, 15293–15297.

Peoples, O.P., Sinskey, A.J., 1989b. J. Biol. Chem. 264, 15298–15303.

Philip, S., Keshavarz, T., Roy, I., 2007. J. Chem. Technol. Biotechnol. 82, 233–247.

Picataggio, S., Rohrer, T., Deanda, K., Lanning, D., Reynolds, R., Mielenz, J., Eirich, L.D., 1992. Nat. Biotechnol. 10, 894–898.

Pio, T.F., Macedo, G.A., 2009. Chapter 4 Cutinases:: Properties and Industrial Applications, in: Microbiology, B.-A. in A. (Ed.), . Academic Press, pp. 77–95.

Pion, F., Reano, A.F., Oulame, M.Z., Barbara, I., Flourat, A.L., Ducrot, P.-H., Allais, F., 2015. Chemo-enzymatic Synthesis, Derivatizations, and Polymerizations of Renewable Phenolic Monomers Derived from Ferulic Acid and Biobased Polyols: An Access to Sustainable Copolyesters, Poly(ester-urethane)s, and Poly(ester-alkenamer)s, in: Green Polymer Chemistry: Biobased Materials and Biocatalysis, ACS Symposium Series. American Chemical Society, pp. 41–68.

Piotrowska, U., Sobczak, M., 2014. Molecules 20, 1–23.

Pleiss, J., Fischer, M., Schmid, R.D., 1998. Chem. Phys. Lipids 93, 67–80.

Polen, T., Spelberg, M., Bott, M., 2013. J. Biotechnol., Research on Industrial Biotechnology within the CLIB-Graduate Cluster - Part III 167, 75–84.

Pollet, E., Avérous, L., 2011. Production, Chemistry and Properties of Polyhydroxyalkanoates, in: Plackett, D. (Ed.), Biopolymers – New Materials for Sustainable Films and Coatings. John Wiley & Sons, Ltd, Chichester, pp. 65–86.

Poojari, Y., Clarson, S.J., 2013. Biocatal. Agric. Biotechnol. 2, 7–11.

Przystałowska, H., Lipiński, D., Słomski, R., 2015. Acta Biochim. Pol. 62, 23–34.

Qi, P., Chen, H.-L., Nguyen, H.T.H., Lin, C.-C., Miller, S.A., 2016. Green Chem. 18, 4170–4175.

Qiu, S., Qiu, Z., 2016. J. Appl. Polym. Sci. 133, n/a-n/a.

Ranucci, E., Liu, Y., Söderqvist Lindblad, M., Albertsson, A.-C., 2000. Macromol. Rapid Commun. 21, 680–684.

Ravenelle, F., Marchessault, R.H., 2002. Biomacromolecules 3, 1057–1064.

Reeve, M.S., McCarthy, S.P., Gross, R.A., 1993. Macromolecules 26, 888–894.

Rehm, S., Trodler, P., Pleiss, J., 2010. Protein Sci. 19, 2122–2130.

Rejasse, B., Lamare, S., Legoy, M.-D., Besson, T., 2007. J. Enzyme Inhib. Med. Chem. 22, 519–527.

Reulier, M., Perrin, R., Avérous, L., 2016. J. Appl. Polym. Sci. 133, n/a-n/a.

Risso, M., Mazzini, M., Kröger, S., Saenz-Méndez, P., Seoane, G., Gamenara, D., 2012. Green Chem. Lett. Rev. 5, 539–543.

Roa Engel, C.A., Straathof, A.J.J., Zijlmans, T.W., van Gulik, W.M., van der Wielen, L.A.M., 2008. Appl. Microbiol. Biotechnol. 78, 379–389.

Roy, I., Visakh, P.M. (Eds.), 2014. Polyhydroxyalkanoate (PHA) Based Blends, Composites and Nanocomposites, RSC Green Chemistry. Royal Society of Chemistry, Cambridge.

Rudnik, E., 2010. Compostable Polymer Materials. Elsevier.

Rydz, J., Sikorska, W., Kyulavska, M., Christova, D., 2014. Int. J. Mol. Sci. 16, 564–596.

Saam, J.C., 1998. J. Polym. Sci. Part Polym. Chem. 36, 341–356.

Santos, M., Gangoiti, J., Llama, M.J., Serra, J.L., Keul, H., Möller, M., 2012. J. Mol. Catal. B Enzym. 77, 81–86.

Schmid, R.D., Verger, R., 1998. Angew. Chem. Int. Ed. 37, 1608–1633.

Schrag, J.D., Cygler, M., 1997. [4] Lipases and αβ hydrolase fold, in: Enzymology, B.-M. in (Ed.), Lipases, Part A: Biotechnology. Academic Press, pp. 85–107.

Shah, M.V., van Mastrigt, O., Heijnen, J.J., van Gulik, W.M., 2016. Yeast Chichester Engl. 33, 145–161.

Sheldon, R.A., 2014. Green Chem. 16, 950–963.

Sheldon, R.A., Arends, I., Hanefeld, U., 2008. Green chemistry and catalysis, Repr. ed, Green chemistry. Wiley-VCH, Weinheim.

Shi, C., DeSimone, J.M., Kiserow, D.J., Roberts, G.W., 2001a. Macromolecules 34, 7744–7750.

Shi, C., Gross, S.M., DeSimone, J.M., Kiserow, D.J., Roberts, G.W., 2001b. Macromolecules 34, 2060–2064.

Shirahama, H., Kawaguchi, Y., Aludin, M.S., Yasuda, H., 2001. J. Appl. Polym. Sci. 80, 340–347.

Shoda, S., Uyama, H., Kadokawa, J., Kimura, S., Kobayashi, S., 2016. Chem. Rev. 116, 2307–2413.

Silva, C.M., Carneiro, F., O'Neill, A., Fonseca, L.P., Cabral, J.S.M., Guebitz, G., Cavaco-Paulo, A., 2005. J. Polym. Sci. Part Polym. Chem. 43, 2448–2450.

Silva, G.P. da, Contiero, J., Neto, Á., Marcelo, P., Lima, C.J.B. de, 2014. Quím. Nova 37, 527–534.

Smith, R. (Ed.), 2005. Biodegradable polymers for industrial applications. Woodhead ; CRC Press, Cambridge : Boca Raton.

Smitthipong, W., Chollakup, R., Nardin, M., 2014. Bio-Based Composites for High-Performance Materials: From Strategy to Industrial Application. CRC Press.

Soccio, M., Lotti, N., Finelli, L., Gazzano, M., Munari, A., 2007. Polymer 48, 3125–3136.

Solaiman, D.K.Y., Ashby, R.D., Foglia, T.A., Marmer, W.N., 2006a. Appl. Microbiol. Biotechnol. 71, 783–789.

Solaiman, D.K.Y., Ashby, R.D., Hotchkiss, A.T., Foglia, T.A., 2006b. Biotechnol. Lett. 28, 157–162.

Song, C.W., Lee, S.Y., 2015. Appl. Microbiol. Biotechnol. 99, 8455–8464.

Spinella, S., Ganesh, M., Re, G.L., Zhang, S., Raquez, J.-M., Dubois, P., Gross, R.A., 2015. Green Chem. 17, 4146–4150.

Srinivasan, R., Desai, P., Abhiraman, A.S., Knorr, R.S., 1994. J. Appl. Polym. Sci. 53, 1731–1743.

Stegmann, P., 2014. The environmental performance of biobased 1,3-propanediol production from glycerol compared to conventional production pathways - A Life Cycle Assessment (Master's Thesis). University of Utrecht, Utrecht, Netherlands.

Steinbüchel, A., Hofrichter, M. (Eds.), 2001. Biopolymers, Polyesters III - Applications and Commercial Products. Wiley-VCH, Weinheim ; Chichester.

Steinbüchel, A., Valentin, H.E., 1995. FEMS Microbiol. Lett. 128, 219–228.

Sudesh, K., Abe, H., Doi, Y., 2000. Prog. Polym. Sci. 25, 1503–1555.

Sugihara, S., Toshima, K., Matsumura, S., 2006. Macromol. Rapid Commun. 27, 203–207.

Sun, X., Shen, X., Jain, R., Lin, Y., Wang, Jian, Sun, J., Wang, Jia, Yan, Y., Yuan, Q., 2015. Chem. Soc. Rev. 44, 3760–3785.

Suzuki, Y., Ohura, T., Kasuya, K., Toshima, K., Doi, Y., Matsumura, S., 2000. Chem. Lett. 29, 318–319.

Suzuki, Y., Taguchi, S., Hisano, T., Toshima, K., Matsumura, S., Doi, Y., 2003. Biomacromolecules 4, 537–543.

Suzuki, Y., Taguchi, S., Saito, T., Toshima, K., Matsumura, S., Doi, Y., 2001. Biomacromolecules 2, 541–544.

Tachibana, Y., Masuda, T., Funabashi, M., Kunioka, M., 2010. Biomacromolecules 11, 2760–2765.

Takahashi, H., Hayakawa, T., Ueda, M., 2000. Chem. Lett. 29, 684–685.

Takamoto, T., Uyama, H., Kobayashi, S., 2013. E-Polym. 1, 19–24.

Takasu, A., Iio, Y., Mimura, T., Hirabayashi, T., 2005a. Polym. J. 37, 946–953.

Takasu, A., Iio, Y., Oishi, Y., Narukawa, Y., Hirabayashi, T., 2005b. Macromolecules 38, 1048–1050.

Takasu, A., Makino, T., Yamada, S., 2009. Macromolecules 43, 144–149.

Takasu, A., Oishi, Y., Iio, Y., Inai, Y., Hirabayashi, T., 2003. Macromolecules 36, 1772–1774.

Tang, T., Moyori, T., Takasu, A., 2013. Macromolecules 46, 5464–5472.

Taresco, V., Creasey, R.G., Kennon, J., Mantovani, G., Alexander, C., Burley, J.C., Garnett, M.C., 2016. Polymer 89, 41–49.

Thurecht, K.J., Heise, A., deGeus, M., Villarroya, S., Zhou, J., Wyatt, M.F., Howdle, S.M., 2006. Macromolecules 39, 7967–7972.

Tokiwa, Y., Calabia, B.P., Ugwu, C.U., Aiba, S., 2009. Int. J. Mol. Sci. 10, 3722–3742.

Tripathi, L., Wu, L.-P., Chen, J., Chen, G.-Q., 2012. Microb. Cell Factories 11, 44.

Tripathi, L., Wu, L.-P., Meng, D., Chen, J., Chen, G.-Q., 2013. Biomacromolecules 14, 862–870.

Tsai, C.-J., Chang, W.-C., Chen, C.-H., Lu, H.-Y., Chen, M., 2008. Eur. Polym. J. 44, 2339–2347.

Tserki, V., Matzinos, P., Pavlidou, E., Panayiotou, C., 2006a. Polym. Degrad. Stab. 91, 377–384.

Tserki, V., Matzinos, P., Pavlidou, E., Vachliotis, D., Panayiotou, C., 2006b. Polym. Degrad. Stab. 91, 367–376.

Tsuge, T., 2002. J. Biosci. Bioeng. 94, 579–584.

United States Department of Agriculture, 2011. Biobased Economy Indicators - A report to the U.S. Congress. Washington DC.

Uppenberg, J., Hansen, M.T., Patkar, S., Jones, T.A., 1994. Structure 2, 293–308.

Uppenberg, J., Oehrner, N., Norin, M., Hult, K., Kleywegt, G.J., Patkar, S., Waagen, V., Anthonsen, T., Jones, T.A., 1995. Biochemistry (Mosc.) 34, 16838–16851.

Uyama, H., Inada, K., Kobayashi, S., 2001. Macromol. Biosci. 1, 40–44.

Uyama, H., Kobayashi, S., 1994. Chem. Lett. 23, 1687–1690.

Uyama, H., Kobayashi, S., 2006. Enzymatic Synthesis of Polyesters via Polycondensation, in: Kobayashi, S., Ritter, H., Kaplan, D. (Eds.), Enzyme-Catalyzed Synthesis of Polymers, Advances in Polymer Science. Springer Berlin Heidelberg, pp. 133–158.

Uyama, H., Takamoto, T., Kobayashi, S., 2002. Polym. J. 34, 94–96.

Uyama, H., Yaguchi, S., Kobayashi, S., 1999. J. Polym. Sci. Part Polym. Chem. 37, 2737–2745.

Valappil, S.P., Misra, S.K., Boccaccini, A.R., Roy, I., 2006. Expert Rev. Med. Devices 3, 853–868.

Valappil, S.P., Rai, R., Bucke, C., Roy, I., 2008. J. Appl. Microbiol. 104, 1624–1635.

Vardon, D.R., Franden, M.A., Johnson, C.W., Karp, E.M., Guarnieri, M.T., Linger, J.G., Salm, M.J., Strathmann, T.J., Beckham, G.T., 2015. Energy Env. Sci 8, 617–628.

Vasnes, V.A., Ignatov, V.N., Vinogradova, S.V., Tseitlin, H.M., 1990. Makromol. Chem. 191, 1759–1763.

Verlinden, R.A., Hill, D.J., Kenward, M.A., Williams, C.D., Piotrowska-Seget, Z., Radecka, I.K., 2011. AMB Express 1, 11.

Villano, M., Valentino, F., Barbetta, A., Martino, L., Scandola, M., Majone, M., 2014. New Biotechnol., Polyhydroxyalkanoate (PHA) by Mixed Microbial Cultures: Fermentation, Control and Downstream Processing 31, 289–296.

Vouyiouka, S.N., Karakatsani, E.K., Papaspyrides, C.D., 2005. Prog. Polym. Sci. 30, 10–37.

Wang, Y., Kunioka, M., 2005. Macromol. Symp. 224, 193–206.

Wang, Y., Onozawa, S., Kunioka, M., 2003. Green Chem. 5, 571–574.

Wang, Z.-L., Hiltunen, K., Orava, P., Seppälä, J., Linko, Y.-Y., 1996. J. Macromol. Sci. Part A 33, 599–612.

Werpy, T.A., Holladay, J.E., White, J.F., 2004. Top Value Added Chemicals from Biomass: I. Results of Screening for Potential Candidates from Sugars and Synthesis Gas (No. PNNL-14808). Pacific Northwest National Laboratory (PNNL), Richland, WA (US).

Wibowo, A.H., Crysandi, R., Verdina, A., Makhnunah, N., Wijayanta, A.T., Storz, H., 2017. Mater. Chem. Phys. 186, 552–560.

Witt, U., Müller, R.-J., Augusta, J., Widdecke, H., Deckwer, W.-D., 1994. Macromol. Chem. Phys. 195, 793–802.

Wojcieszak, R., Santarelli, F., Paul, S., Dumeignil, F., Cavani, F., Gonçalves, R.V., 2015. Sustain. Chem. Process. 3, 9.

Wu, B., Xu, Y., Bu, Z., Wu, L., Li, B.-G., Dubois, P., 2014. Polymer 55, 3648–3655.

Wu, L., Wang, L., Wang, X., Xu, K., 2010. Acta Biomater. 6, 1079–1089.

Wu, X.Y., Seppäl↠, J., Linko, Y.-Y., 1996. Biotechnol. Tech. 10, 793–798.

Xu, S.Y., Shi, Y.H., Zhao, J.B., Jiang, S.L., Yang, W.T., 2011. Polym. Adv. Technol. 22, 2360–2367.

Xu, Yixiang, Hanna, M.A., Isom, L., 2008. Open Agric. J. 2, 54–61.

Xu, Yongxiang, Xu, J., Liu, D., Guo, B., Xie, X., 2008. J. Appl. Polym. Sci. 109, 1881–1889.

Yagihara, T., Matsumura, S., 2012. Polymers 4, 1259–1277.

Yang, S.-T., El Enshasy, H., Thongchul, N. (Eds.), 2013. Bioprocessing technologies in biorefinery for sustainable production of fuels, chemicals, and polymers. AIChE : John Wiley & Sons, Inc, Hoboken, New Jersey.

Yang, Y., Yu, Y., Zhang, Y., Liu, C., Shi, W., Li, Q., 2011. Process Biochem. 46, 1900–1908.

Yang, Y.-H., Brigham, C., Willis, L., Rha, C., Sinskey, A., 2011. Biotechnol. Lett. 33, 937–942.

Yao, D., Li, G., Kuila, T., Li, P., Kim, N.H., Kim, S.-I., Lee, J.H., 2011. J. Appl. Polym. Sci. 120, 1114–1120.

Yashiro, T., Kricheldorf, H.R., Huijser, S., 2009. Macromol. Chem. Phys. 210, 1607–1616.

Yasuda, M., Ebata, H., Matsumura, S., 2010. Enzymatic Synthesis and Properties of Novel Biobased Elastomers Consisting of 12-Hydroxystearate, Itaconate and Butane-1,4-diol, in: Green Polymer Chemistry: Biocatalysis and Biomaterials, ACS Symposium Series. American Chemical Society, pp. 237–251.

Yim, H., Haselbeck, R., Niu, W., Pujol-Baxley, C., Burgard, A., Boldt, J., Khandurina, J., Trawick, J.D., Osterhout, R.E., Stephen, R., Estadilla, J., Teisan, S., Schreyer, H.B., Andrae, S., Yang, T.H., Lee, S.Y., Burk, M.J., Van Dien, S., 2011. Nat. Chem. Biol. 7, 445–452.

Yu, J., Chen, L.X.L., 2006. Biotechnol. Prog. 22, 547–553.

Yu, J.-L., Xia, X.-X., Zhong, J.-J., Qian, Z.-G., 2014. Biotechnol. Bioeng. 111, 2580–2586.

Zhang, H., Grinstaff, M.W., 2014. Macromol. Rapid Commun. 35, 1906–1924.

Zhang, L., Shi, Z.-Y., Wu, Q., Chen, G.-Q., 2009. Appl. Microbiol. Biotechnol. 84, 909–916.

Zhao, X., Bansode, S.R., Ribeiro, A., Abreu, A.S., Oliveira, C., Parpot, P., Gogate, P.R., Rathod, V.K., Cavaco-Paulo, A., 2016. Ultrason. Sonochem. 31, 506–511.

Zheng, L., Li, C., Zhang, D., Guan, G., Xiao, Y., Wang, D., 2011. Polym. Int. 60, 666–675.

Zhu, C., Zhang, Z., Liu, Q., Wang, Z., Jin, J., 2003. J. Appl. Polym. Sci. 90, 982–990.

Zhu, K., Zhu, W.-P., Gu, Y.-B., Shen, Z.-Q., Chen, W., Zhu, G.-X., 2007. Chin. J. Chem. 25, 1581–1583.

Zinn, M., Witholt, B., Egli, T., 2001. Adv. Drug Deliv. Rev., Polymeric Materials for Advanced Drug Delivery 53, 5–21.

Conclusion du chapitre 1

La synthèse bibliographique présentée dans ce chapitre a montré, en premier lieu, la richesse des architectures des polyesters aliphatiques partiellement ou totalement biosourcés synthétisés par différentes voies catalytiques (chimique et enzymatique) à partir de synthons plurifonctionnels ou par fermentation bactérienne. Bien que la part des polyesters biosourcés est encore faible à l'heure actuelle, son dévellopement rapide en fait un des matériaux de première importance dans le domaine de la recherche.

Concernant la synthèse de polyesters à partir de synthons plurifonctionnels par catalyse chimique, celle-ci s'effectue majoritairement selon le procédé en masse à l'aide d'un catalyseur à base de métaux de transition, tel que le titane, car cela permet d'obtenir de hautes masses molaires rapidement. Toutefois, l'état de l'art a également montré que d'autres catalyseurs (*e.g.*, acides forts de Lewis) et des procédés en solution à l'aide de chlorures d'acyle, de sels métalliques ou de distannoxanes sont parfois utilisés.

Plus récemment, un procédé plus écologique a été développé en utilisant des catalyseurs biologiques pour la sythèse de polyesters aliphatiques sous conditions douces. Parmi ces catalyseurs biologiques, les lipases et notamment la lipase B de *Candida antarctica* montre une remarquable activité pour les réactions de polycondensation ou de transestérification. Toutefois d'autres enzymes (*e.g.*, cutinases, protéases et PHB dépolymérases) ont démontré une activité pour ces réactions. Les différents paramètres clés (*i.e.*, nature du solvant, concentration des substrats, structure des substrats, nature de l'enzyme et température) régissant la catalyse enzymatique ont été présentés en insitant particulièrment sur leur effet sur la masses molaire des polyesters synthétisés. Il apparait ainsi que l'utilisation de la lipase B de *Candida antarctica* immobilisée dans un solvent apolaire, et notamment le diphényl éther, à une température de 70-90 °C permet la synthèse de polyesters de masses molaires correctes. Cependant, il est à noter que l'activité de l'enzyme diminue fortement avec le raccourcissement de la chaîne alkyle des substrats et donc que la masse molaire des architectures diminue de la même manière.

En plus des deux voies de synthèses présentées auparavant, les polyhydroxyalcaonates (PHA) qui sont des polyesters issus de fermentation bactérienne ont vu leur intérêt grandement augmenter ces dernières années du fait de leur procédé de synthèse à partir de substrats relativement bon marché, leurs grands nombres de structures possibles (plus de 150 monomères différents), leurs grandes variétés d'architectures macromoléculaires (*i.e.*, homopolyesters, copolyesters aléatoires ou copolyesters blocs), leur biodégradabilité et leur biocompatibilité, permettant ainsi l'acces à de nombreux matériaux aux propriétés variées pouvant être utilisés dans de nombreuses applications. De plus, un grande nombres de matériaux dérivés de ces PHAs peuvent être synthétisés permettant le développement d'une nouvelle gamme de matériaux.

La suite de ce travail a donc consisté à synthétiser, en premier lieu, par catalyse organométallique de nombreux (co)polyesters avec différentes architectures afin d'étudier l'influence de la structure des monomères sur leur réactivité durant la synthèse d'une part et sur les propriétés du matériau d'autre part (chapitre 2). Ensuite, l'influence de la structure des monomères sur l'activité enzymatique de la lipase B de *Candida antarctica* a été étudiée afin de synthétiser différentes architectures macromoléculaires. Enfin, de nouvelles architectures macromoléculaires à base d'oligomères de PHAs ont pu être synthétisés et étudiées par couplage de chaîne à l'aide de diisocyanate d'une part et par transestérification organométallique ou enzymatique d'autre part.

CHAPITRE 2: SYNTHÈSE ORGANOMÉTALLIQUE DE COPOLYESTERS ALIPHATIQUES BIOSOURCÉS

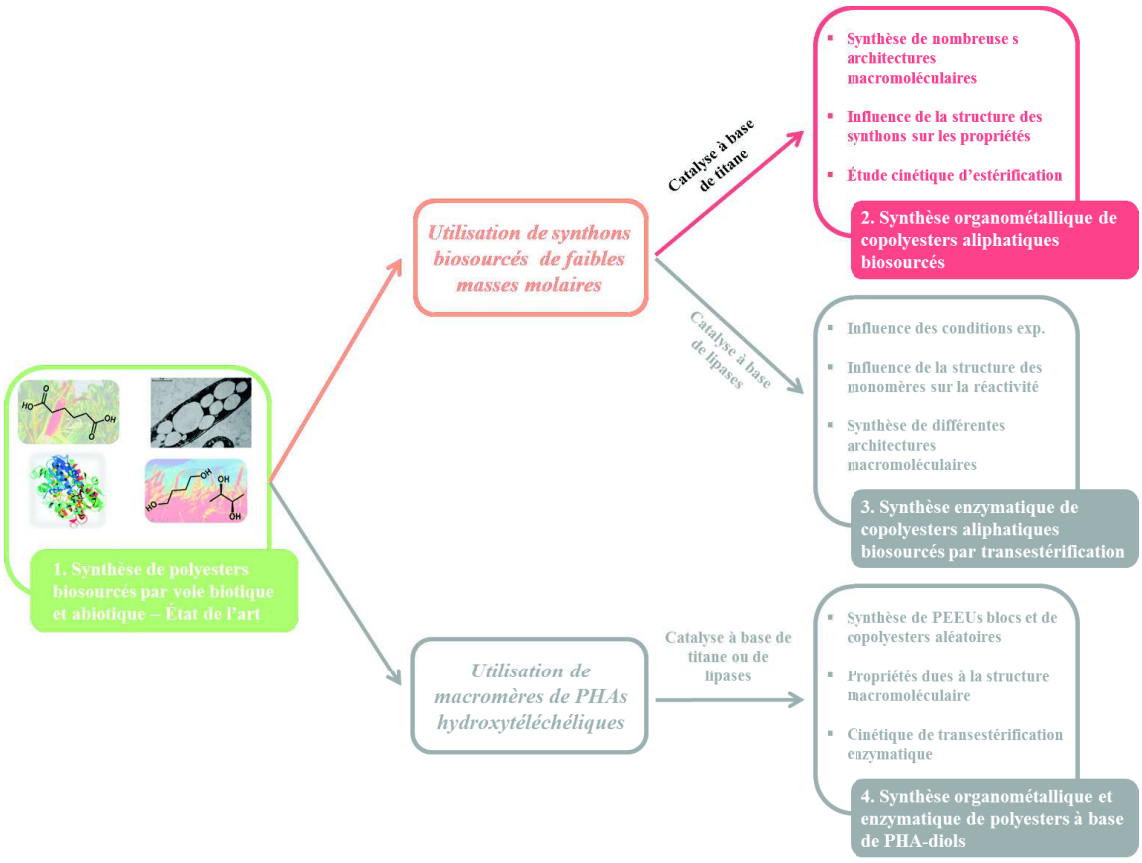

Introduction du chapitre 2

L'étude bibliographique a montré d'une part la richesse des structures macromoléculaires des (co)polyesters biosourcés permettant ainsi d'obtenir des matériaux aux propriétés variées et d'autre part les nombreux progrès réalisés dans les laboratoires académiques et industriels pour la production durable de ces architectures macromoléculaires par voie biotique et abiotique.

Les polyesters de type « poly(alkylene dicarboxylate) » ont vu leur intérêt fortement grandir dans les dernières années à cause notamment du fort développement des nombreux synthons biosourcés permettant ainsi de développer de nombreuses architectures macromoléculaires lesquelles influent directement sur les propriétés (thermique, mécanique, optique…) des matériaux. Les propriétés de ces polyesters peuvent alors être ajustées par copolymérisation selon la nature chimique de ces synthons et leur composition.

Le chapitre 2 décrit l'étude de la synthèse de (co)polyesters de différentes structures macromoléculaires à partir de synthons bifonctionnels (acide succinique, acide adipique, 1,3-propanediol, 1,4-butanediol et 2,3-butanediol) biosourcés par catalyse organométallique à l'aide d'un catalyseur à base de titane. Dans ce cadre, les structures macromoléculaires et les propriétés (stabilité thermique, structure cristalline, propriétés thermiques) du poly(butylène succinate-*co*-butylène adipate) (PBSA), du poly(propylène succinate-*co*-propylène adipate) (PPSA), du poly(propylène succinate-*co*-butylène succinate) (PPBS), du poly(propylène adipate-*co*-butylène adipate) (PPBA) et du poly(1,4-butylène adipate-*co*-2,3-butylène adipate) (PBB'A) ont été étudiées et déterminées. De plus, grâce à deux collaborations internationales, la biodégradabilité dans le sol de certains polyesters et l'isodimorphisme du PBSA ont pu être étudiés plus en détail.

Ce chapitre est découpé en quatre sous-chapitres qui sont chacun présentés sous forme d'une publication :

- Le sous-chapitre 1 présentera une étude sur le PBSA dans laquelle la structure, la stabilité thermique et les propriétés thermiques du copolyester seront déterminées sous la forme d'un article intitulé « Synthesis and characterization of biobased poly(butylene succinate-*ran*-butylene adipate). Analysis of the composition-dependent physicochemical properties » et publié dans *European Polymer Journal.*
- Le sous-chapitre 2 exposera une étude sur la synthèse et la caractérisation de PPSA en mettant notamment en évidence la faible vitesse de cristallisation de ce copolyester sous la forme d'unepublication intitulée « Synthesis and characterization of fully biobased poly(propylene succinate-*ran*-propylene adipate). Analysis of the architecture-dependent physicochemical behavior » et publiée dans *Journal of Polymer Science Part A: Polymer Chemistry.*
- Le sous-chapitre 3 présentera, quant à lui, une étude sur le PPBS et le PPBA en se focalisant particulièrement sur l'influence de la structure des synthons sur les propriétés des copolyesters et se conclura sur une étude de biodégradation de certains (co)polyesters dans un sol. Cette étude se présentera sous la forme d'un article intitulé « Synthesis and characterization of biodegradable and biobased copolyesters. Influence of the building blocks length » qui sera soumis sous peu.
- Le sous-chapitre 4 présentera tout d'abord une étude sur la cinétique d'estérification entre un diacide dicarboxylique avec des diols primaires et secondaires, puis une étude sur la synthèse et la caractérisation thermique et optique de poly(1,4-butylène adipate-*ran*-2,3-butylène adipate) sous la forme d'une publication intitulée «Synthesis of potentially biobased copolyesters based on adipic acid and butanediols: kinetic study between 1,4- and 2,3-butanediol and their influence on crystallization and thermal properties » et publiée dans *Polymer*.

Sub-chapter 2.1. Synthesis and characterization of biobased poly(butylene succinate-ran-butylene adipate). Analysis of the composition-dependent physicochemical properties

Thibaud Debuissy, Eric Pollet and Luc Avérous*

BioTeam/ICPEES-ECPM, UMR CNRS 7515, Université de Strasbourg, 25 rue Becquerel, 67087 Strasbourg Cedex 2, France

*Corresponding author: luc.averous@unistra.fr

Published by European Polymer Journal, 2017, 87, 84-98

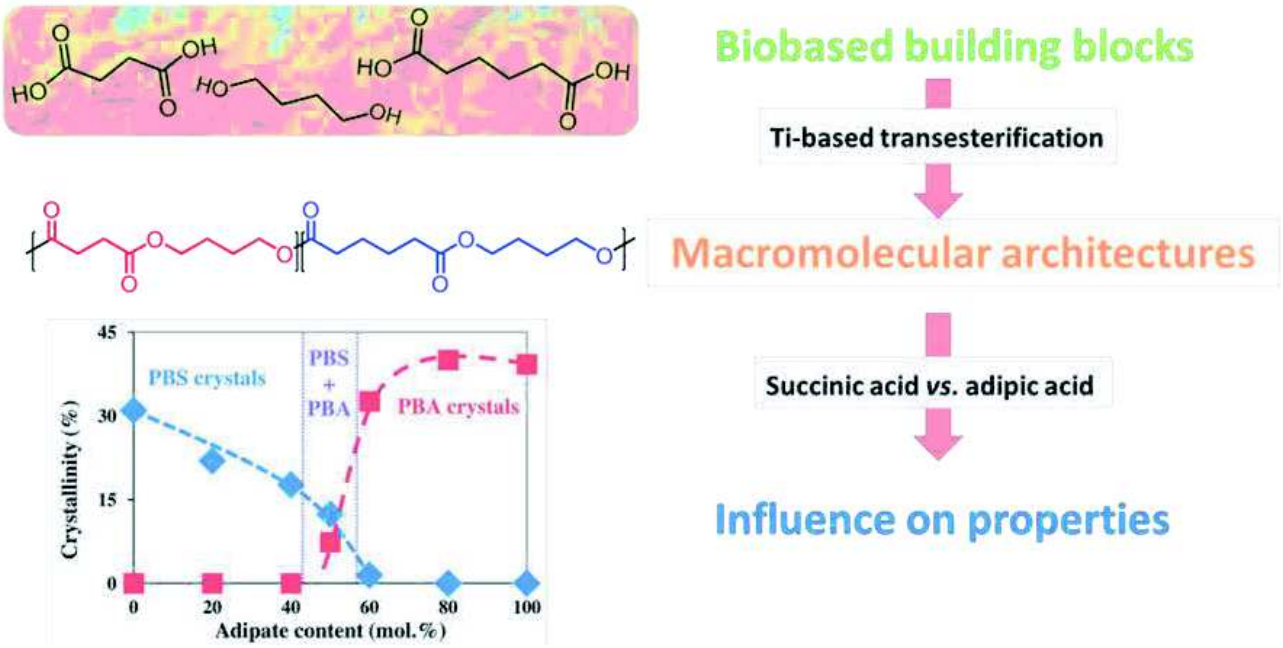

1. Abstract

Fully biobased aliphatic random poly(butylene succinate-ran-butylene adipate) (PBSA) copolyesters and the corresponding homopolyesters (poly(butylene succinate) (PBS) and poly(butylene adipate) (PBA)) with high molar mass, were synthesized with different succinic acid/adipic acid (SA/AA) molar ratio by transesterification in melt, using titanium (IV) isopropoxide as an effective catalyst. All synthesized copolyesters were fully characterized by various chemical and physicochemical techniques including NMR, SEC, FTIR, WAXS, DSC and TGA. The final copolyesters molar compositions were identical to the feed ones. The different sequences based on succinate and adipate were randomly distributed along the chains. All the corresponding copolyesters showed an excellent thermal stability with a degradation onset temperature higher than 290 °C and a thermal degradation profile driven by the major diacid component. Glass transition temperatures of copolyesters decreased with the adipate content due to the decrease of the chain mobility, following the Gordon-Taylor relation. PBSA showed a pseudo-eutectic melting behavior characteristic of an isodimorphic character. Besides, the presence of both crystalline phases was observed for adipate content in the range 50-60 mol.%.

2. Introduction

Over the last decades, renewable polymers from biomass have attracted considerable attention, as a sustainable alternative to fossil-based materials. These biobased polymers can bring new macromolecular architectures with the corresponding advanced properties. Among them, poly(lactic acid) (Avérous, 2004), poly(butylene succinate) (PBS) (Xu and Guo, 2010), poly(hydroxyalkanoates) (Pollet and Avérous, 2011) have seen their interest growing on an industrial point of view with various applications such as packaging, agriculture, sanitary or in biomedical engineering.

The development of biorefinery through the world was a huge step in the production of corresponding biobased monomers or building blocks, such as succinic acid (SA), 1,4-butanediol (1,4-BDO), adipic acid (AA), furans, glycerol and others (Becker et al., 2015; Bozell and Petersen, 2010). SA is a well-known short dicarboxylic acid, listed by the US-DoE as one of the strategic platform chemicals from renewable resources (Becker et al., 2015; Werpy et al., 2004; Bechthold et al., 2008; Choi et al., 2015). Biobased SA is commercialized by different companies (*e.g.*, BioAmber, Myriant, Succinity and Reverdia) and has seen its interest also growing for the production of polyesters (*e.g.*, PBS), polyamides…(Bechthold et al., 2008; Becker et al., 2015) 1,4-BDO is a short diol mainly obtained *via* a chemical process of hydrogenation from SA (Bechthold et al., 2008; Bozell and Petersen, 2010; Choi et al., 2015). However, recently Genomatica has genetically modified *E. Coli* for the direct bioproduction of 1,4-BDO from sugars (Barton et al., 2014). Produced at an industrial level by different companies (Novamont, BioAmber, Genomatica-BASF), biobased 1,4-BDO is largely used, for instance, as chain extender in the polyurethane synthesis (Bueno-Ferrer et al., 2012; Reulier and Avérous, 2015) or as building block for the synthesis of various polyesters and polyamides (Debuissy et al., 2016a). AA is a very interesting aliphatic six-carbon diacid also used as building block in the synthesis of polyamides, polyurethanes and polyesters (Avérous and Fringant, 2001; Debuissy et al., 2016a). Recently, new biological pathways were discovered for the bioproduction of AA from different biomass such as glucose (Polen et al., 2013), lignin (Vardon et al., 2015) and fatty acids (Picataggio et al., 1992).

Biobased aliphatic polyesters have attracted increasing interest mainly since around two decades. They have been studied from both academic and industrial perspectives, due to their excellent properties and also very often, biodegradability. PBS is one of the most interesting aliphatic polyesters due to its very high melting point, excellent mechanical properties close to some polyolefins (Tokiwa et al., 2009), biodegradability and easy processability. From the different chemical structures and the large availability of biobased building blocks, various other polyesters can be obtained such as poly(butylene adipate) (PBA) which has a lower melting point and is more readily biodegraded than PBS (Tokiwa et al., 2009). As a route to develop materials with improved properties, tailor-made aliphatic copolyesters were synthesized combining different biobased building blocks. Biodegradable aliphatic polyesters such as PBS and poly(butylene succinate-co-butylene adipate) (PBSA) copolymer have been developed at an industrial level since 1990 by Showa Denko (Japan) under tradename “Bionolle”. PBSA copolyester has an excellent processability (Takiyama and Fujimaki, 1994) and also present lower melting temperature, lower degree of crystallinity and higher biodegradability than PBS (Ren et al., 2005).

Through the literature, different PBSA copolyesters with various compositions have been synthesized either by polycondensation from 1,4-BDO and diacids (SA and AA) (Ahn et al., 2001) or by transesterification from 1,4-BDO and dimethyl esters of SA and AA (Montaudo and Rizzarelli, 2000; Nikolic and Djonlagic, 2001; Tserki et al., 2006b). The influence of the PBSA composition on its physical, thermal, mechanical and biodegradation properties was investigated (Ahn et al., 2001; Montaudo and Rizzarelli, 2000; Nikolic and Djonlagic, 2001; Tserki et al., 2006b). Nevertheless, different parameters and properties such the sequence distribution, the thermal degradation, the isodimorphism and the co-crystallization of PBSA were not studied in details in these previous works, which were more particularly focused on degradation or biodegradation analysis by hydrolytic (Ahn et al., 2001) or enzymatic ways (Nikolic and Djonlagic, 2001; Tserki et al., 2006b; Montaudo and Rizzarelli, 2000; Tserki et al., 2006a) in different media such as soil (Tserki et al., 2006b), landfill (Ahn et al., 2001)…

To synthesize high molar mass aliphatic polyesters from diacid and diol buildings blocks, the transesterification polycondensation reaction from the melt with an organometallic catalyst is the most used and promising way (Ahn et al., 2001; Debuissy et al., 2016a). Moreover, the literature shows that titanium-based catalysts are the most efficient organometallic catalysts for the transesterification reaction, compared to other zirconium, tin, hafnium or antinomy-based catalysts (Jacquel et al., 2011).

The aim of this study was, thus, to synthesize and characterize high molar mass PBSA copolyesters and the corresponding homopolyesters (PBS and PBA. They were produced by transesterification polycondensation reaction in melt, with a titanium-based organometallic catalyst, and with different SA/AA ratios. Chemical and physicochemical properties of these different macromolecular architectures were fully investigated by ^{1}H-, ^{13}C-, ^{31}P-NMR, SEC and FTIR. The thermal stability, crystalline structure and thermal properties were analyzed by TGA, WAXS and DSC, respectively. The effect of the SA/AA molar composition on the physicochemical properties was particularly discussed.

3. Experimental part

3.1. Materials

Biobased succinic acid (SA) (99.5%) was kindly supplied by BioAmber (France). SA was bioproduced by fermentation of glucose (from wheat or corn) and obtained after a multistep process based on several purifications, evaporation and crystallization stages. 1,4-butanediol (1,4-BDO), methanol (≥99.6%), chloroform (99.0-99.4%), chromium (III) acetyl acetonate (97%), 2-chloro-4,4,5,5-tetramethyl-1,3,2-dioxaphospholane (Cl-TMDP, 95%) and cholesterol (> 99%) were purchased from Sigma-Aldrich. Pyridine HPLC grade (99.5+%) was purchased from Alfa Aesar. Adipic acid (AA) (99%), titanium (IV) isopropoxide (TTIP) (98+%) and extra dry toluene (99.85%) were supplied by Acros. All reactants were used without further purification. All solvents used for the analytical methods were of analytical grade.

3.2. Synthesis of copolyesters

Different aliphatic copolyesters were synthesized by a two-stage melt polycondensation method (esterification and transesterification). Syntheses were performed in a 50 mL round bottom flask with a distillation device in order to remove all the by-products from the reaction (mostly water). All reactions were carried out with a diol (1,4-BDO)/acid (SA and/or AA) molar ratio of 1.1/1.

During the first step (esterification), the reaction mixture was maintained under a constant argon flux and magnetically stirred at 300 rpm. The temperature of the reactor was set to 210 °C for 3 h. After 3 h of oligomerization, the remaining by-product of the reaction was distilled off by reducing the pressure to 200 mbar for 5 min, and then the proper amount (0.1 mol.% *vs*. the respective amount of diacid) of a 5 wt.% solution of TTIP in extra dry toluene was introduced inside the reactor. The reaction mixture was stirred at the same temperature as before under a constant argon flux for 45 min. In a second step (transesterification), the temperature of the reactor was slowly increased to 230 °C and the pressure was decreased stepwise over periods of 5 min at 100, 50 and 25 mbar, respectively, in order to avoid excessive foaming and to minimize oligomer sublimation, which is a potential issue during the melt polycondensation. Finally, the pressure was decreased to 1-3 mbar and the transesterification continued for about 3-4 h. The global reaction scheme and conditions involved are summarized in Scheme 2.1.1. At the end, the synthesized polyester had a slightly yellowish color. The reaction mixture was cooled down, dissolved in chloroform, precipitated into a large volume of vigorously

stirred dry ice-cold methanol. Thereafter, the precipitate was filtered with a fine (0.45 μm) filter, washed with cold methanol and dried under reduced pressure in an oven at 40 °C for 24 h. Ivory white solid polyesters were finally recovered.

Several poly(butylene succinate-*co*-butylene adipate) (PBSA) copolyesters were synthesized with different SA/AA molar ratios (100/0, 80/20, 60/40, 50/50, 40/60, 20/80 and 0/100). Samples are named "PBSxAy" with x and y as the molar proportion of succinate and adipate determined by ^{1}H-NMR, respectively. The two homopolyesters ($PBS_{100}A_0$ and PBS_0A_{100}) are also named as PBS and PBA, respectively.

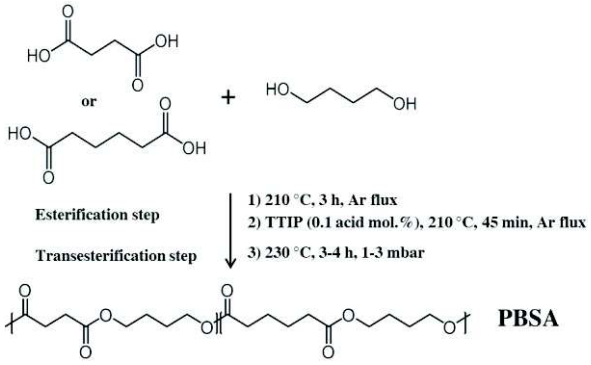

Scheme 2.1.1 : Reaction procedure for PBSA organometallic synthesis.

3.3. General methods and analysis

^{1}H- and ^{13}C-NMR spectra of polyesters were obtained on a Bruker 400 MHz spectrometer. $CDCl_3$ was used as solvent to prepare solutions with concentrations of 8-10 and 30-50 mg/mL for ^{1}H-NMR and ^{13}C-NMR, respectively. The number of scans was set to 128 for ^{1}H-NMR and at least 5,000 for ^{13}C-NMR. Calibration of the spectra was performed using the $CDCl_3$ peak (δ_H = 7.26 ppm, δ_C = 77.16 ppm).

^{31}P-NMR was performed after phosphitylation of the samples, according to standard protocols (Spyros et al., 1997). An accurately weighed amount of sample (approx. 100 mg) was dissolved in 500 μL of anhydrous $CDCl_3$. 100 μL of a standard solution of cholesterol (0.1 M in an anhydrous $CDCl_3$/pyridine (1/1.6) solution) containing Cr(III) acetyl acetonate as relaxation agent was then added. Finally, 50 μL of 2-chloro-4,4,5,5-tetramethyl-1,3,2-dioxaphospholane (Cl-TMDP) were added and the mixture was stirred at room temperature for 2 h. Spectra were recorded on a Bruker 400 MHz spectrometer (256 scans at 20 °C). All chemical shifts reported are relative to the reaction product of water with Cl-TMDP, which gives a sharp signal in pyridine/$CDCl_3$ at 132.2 ppm. The quantitative analysis of end-groups and the calculation of molar masses by ^{31}P-NMR were performed based on previous reports (Siotto et al., 2013; Spyros et al., 1997).

Size exclusion chromatography (SEC) was performed to determine the number-average molar mass (M_n), the mass-average molar mass (M_w) and the dispersity (Đ) of the samples. A Shimadzu liquid chromatograph was equipped with PLGel Mixed-C and PLGeL 100 Å columns and a refractive index detector. Chloroform was used as eluent at a flow rate of 0.8 ml/min. The instrument was calibrated with linear polystyrene standards from 162 to 1,650,000 g/mol.

Infrared spectroscopy (IR) was performed with a Nicolet 380 Fourier transformed infrared spectrometer (Thermo Electron Corporation) used in reflection mode and equipped with an ATR diamond module (FTIR-ATR). The FTIR-ATR spectra were collected at a resolution of 4 cm^{-1} and with 64 scans per run.

Differential scanning calorimetry (DSC) was performed using a TA Instrument Q 200 under nitrogen (flow rate of 50 mL/min), calibrated with high purity standards. Samples of 2-3 mg were sealed in aluminum pans. A three-step procedure with a 10 °C/min ramp was applied that involved: (1) heating up from room temperature to 130 °C and holding for 3 min to erase the thermal history, (2) cooling down to -80 °C and holding for 3 min and (3) heating (second heating) from -80 °C to 130 °C. To determine the glass transition temperature (T_g), (co)polyesters samples in pans were melted at 130 °C, quickly quenched in liquid nitrogen in order to obtain fully amorphous (co)polyesters and then heated from -80 to 0 °C at 10 °C/min. The degree of crystallinity (X_c) of (co)polyesters was calculated according to Equation (2.1.1),

$$X_c(\%) = \frac{\Delta H_m}{\Delta H_m{}^0} \times 100 \qquad (2.1.1)$$

where the melting enthalpy (ΔH_m) is taken from the first heating run and $\Delta H_m{}^0$ is the melting enthalpy of a 100% pure crystalline polyester.

Thermal degradations were studied by thermogravimetric analyses (TGA). Measurements were conducted under helium atmosphere (flow rate of 25 mL/min) using a Hi-Res TGA Q5000 apparatus from TA Instruments. Samples (1-3 mg) were heated from room temperature up to 600 °C at a rate of 20 °C/min.

Wide angle X-ray Scattering (WAXS) data were recorded on a Siemens D5000 diffractometer using Cu K_α radiation (1.5406 Å) at 25-30 °C in the range of 2θ = 14-32° at 0.4°.min^{-1}. Analyses are performed on compression-molded sheets.

3.4. Ester function density

The ester function density of polyesters is defined by the number of ester function by repetitive unit on the number of carbons in the main chain by repetitive unit. The ester function density of PBSA copolyesters ($D_{ester,PBSA}$) is defined by Equation (2.1.2),

$$D_{ester,PBSA} = \chi_{SA} \times D_{ester,PBS} + \chi_{AA} \times D_{ester,PBA} \qquad (2.1.2)$$

where χ_{SA} and χ_{AA} are the succinate and adipate contents in copolyester, respectively; $D_{ester,PBS}$ and $D_{ester,PBA}$ are ester function densities of PBS and PBA, respectively.

4. Results

4.1. Characterization of macromolecular architectures of synthesized copolyesters

Different PBSA copolyesters were produced by a two-step melt polycondensation method (Scheme 2.1.1). In the first step, the non-catalyzed esterification reaction between 1,4-BDO and a mixture of diacid (SA/AA) resulted in formation of oligomers, which reached M_n of about 2,000-3,000 g/mol (determined by SEC) after 3 h of esterification, necessary to avoid any removal phenomenon (*e.g.* monomer sublimation) during the next step. Then, TTIP was added into the reaction mixture and the transesterification, under vacuum, of the previously synthesized oligomers resulted in a significant increase of copolyesters molar masses. The corresponding molar masses are presented in Table 2.1.1. The synthesized copolyesters could be considered as high molar mass polyesters since the samples have M_n higher than 27,000 g/mol, with a dispersity (Đ) of about 1.4-1.9. Đ were slightly lower than the expected value of 2, especially for the 20/80 (SA/AA) composition. One can suppose a small loss of the shortest oligomers during the dissolution/precipitation process even if maximum care (small filter, dry ice cold methanol) was taken to recover the maximum amount of product. Polymerization yields determined after precipitation of samples were rather high and only varied in a narrow range (approx. 85–90%).

The final (co)polyester chemical structures were analyzed by ^{1}H-, ^{13}C-, ^{31}P-NMR and FTIR. ^{1}H-NMR results are presented in Figure 2.1.1-a. In ^{1}H-NMR spectra, the presence of ester functions was verified by the signal at δ = 4.10 ppm assigned to COO-C$\underline{H}_2$-CH$_2$- protons from 1,4-BDO repeating units. This signal is complex due to the influence of neighboring dicarboxylate units (*i.e.,* two triplets at 4.11 and 4.09 ppm were detected for the neighboring succinate (SA) and adipate (AA) units, respectively). ^{1}H chemical shifts at δ = 1.65, 1.70, 2.32 and 2.62 ppm were ascribed to CO-CH$_2$-C$\underline{H}_2$- protons from AA repeating units, to O-CH$_2$-C$\underline{H}_2$- protons from 1,4-BDO repeating units, to CO-C$\underline{H}_2$-CH$_2$- protons from AA repeating units and to CO-C$\underline{H}_2$-protons from SA repeating units, respectively. Interestingly, the hydroxyl terminal group (HO-C$\underline{H}_2$-) signal was detected at δ = 3.67 ppm, with low intensities, in agreement with the relatively high molar mass of the samples. The succinate (χ_{SA}) and adipate (χ_{AA}) contents of synthesized copolyesters was calculated from ^{1}H-NMR spectra using relative intensities of methylene protons in α of ester functions in succinate (δ = 2.62 ppm) and adipate (δ = 2.32 ppm) segments (more details in Annex 1). Determined χ_{SA} and χ_{AA} contents in the chains are given in Table 2.1.1. All synthesized copolyesters presented SA/AA molar ratio equivalent to the initial feed ones. The chosen pathway allows to perform an accurate fabrication of copolyesters with a targeted composition.

Previous studies showed that the non-catalyzed esterification rate with AA were much lower than with SA, for small chain length aliphatic diols (Makay-Bödi, E. and Vancso-Szercsanyi, I., 1969; Vancsó-Szmercsányi et al., 1969). This can be explained by the small pKa difference of both diacids (*i.e.,* $pKa_{,1}/pKa_{,2}$ of 4.16/5.61 and 4.43/5.41 for SA and AA, respectively) which permitted to dissociate an higher proportion of acidic protons inside the reaction mixture, allowing an higher rate of the auto-catalytic reaction. However, the presence of an excess of hydroxyl (OH) functions compared to carboxylic acid (COOH) functions increased the overall esterification rate permitting a higher diacid conversion (Kuo and Chen, 1989; Lin and Hsieh, 1977). Moreover, the esterification time was set to 3 h in order to avoid remaining free diacid residual monomers in the system. Finally, these experimental conditions permitted to override the reactivity difference and convert all feed diacid into oligomers before the second reactive step under high vacuum.

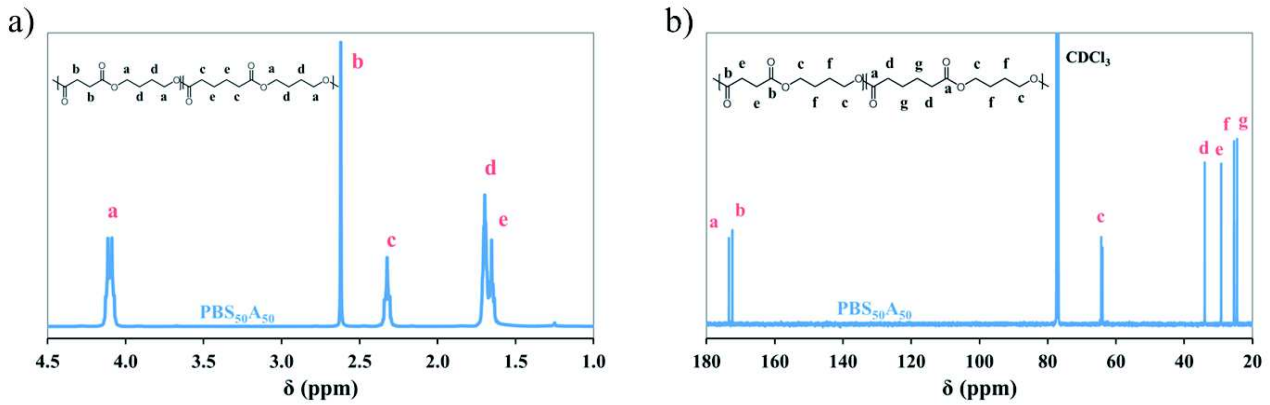

Figure 2.1.1 : (a) ^{1}H- and (b) ^{13}C-NMR of $PBS_{50}A_{50}$ in $CDCl_3$.

To obtain more detailed information about the PBSA architecture, ^{13}C-NMR was performed. ^{13}C-NMR results are presented in Figure 2.1.1-b. ^{13}C chemical shifts at δ = 24.5, 34.0 and 173.4 ppm were ascribed to CO-CH_2-$\underline{C}H_2$-, CO-$\underline{C}H_2$-CH_2- and $\underline{C}$O-CH_2-CH_2- carbons from AA repeating units, whereas ones at δ = 29.1 and 172.4 ppm were ascribed to CO-$\underline{C}H_2$-and $\underline{C}$O-CH_2- carbons from SA repeating units, respectively. Finally, ^{13}C chemical shifts at δ = 25.4 (three peaks), 64.0 (two peaks) and 64.3 (two peaks) ppm were assigned to O-CH_2-$\underline{C}H_2$-, O-$\underline{C}H_2$-CH_2- next to an adipate repetitive units and O-$\underline{C}H_2$-CH_2- next to a succinate repetitive units, respectively. The sensitivity of the ^{13}C-NMR to small differences in the chemical environment enabled us to identify the different triads SBS, SBA, and ABA (with S, B and A standing for SA, 1,4-BDO diol and AA, respectively) presented in Figure 2.1.2-a. 1,4-BDO moieties are present in all three triads at distinctly different resonance absorptions close to chemical shifts of PBS ($PBS_{100}A_0$) or PBA (PBS_0A_{100}). Such results, with the splitting of the two signals (carbon atoms a_1, a_2, a_3 and a_4 in Figure 2.1.2), enable the calculation of the average sequence length of BS and BA units (L_{BS} and L_{BA}, respectively) and the degree of randomness (R) using Equations (2.1.3) to (2.1.5),

$$L_{BS} = 1 + \frac{2 \times I_{SBS}}{I_{SBA-S} + I_{SBA-A}} \qquad (2.1.3)$$

$$L_{BA} = 1 + \frac{2 \times I_{ABA}}{I_{SBA-S} + I_{SBA-A}} \qquad (2.1.4)$$

$$R = \frac{1}{L_{BS}} + \frac{1}{L_{BA}} \qquad (2.1.5)$$

where I_{SBS}, $I_{SBA\text{-}S}$, $I_{SBA\text{-}A}$ and I_{ABA} are intensities of peaks assigned to methylene carbons in α of the ester function in butyl segments (δ ~ 64 ppm) of SBS, SBA-S side, SBA-A side and ABA triads in PBSA copolyesters. The corresponding data are listed in Table 2.1.1.

For fully random copolymers, R is equal to 1, whereas it is equal to 2 for strictly alternating, and close to 0 for block copolymers. According to the SA/AA ratio, L_{BS} and L_{BA} varied between 1.3 and 4.8. PBSA copolyesters, composed of both diacids, all showed a randomness degree of about 1.0 meaning a random distribution between succinate and adipate segments along the polyester chain, as it was expected by using titanium-based organometallic catalyst (Chen et al., 2010; Debuissy et al., 2016a).

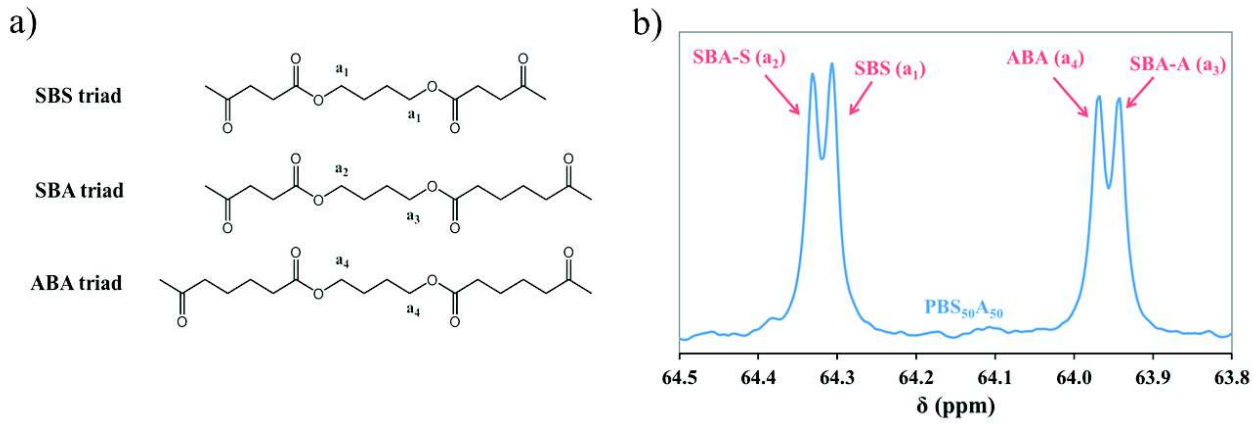

Figure 2.1.2 : (a) Possible triads of PBSA copolyesters, (b) ^{13}C-NMR spectra of $PBS_{50}A_{50}$ with high number of scans centered at δ ~ 64 ppm.

^{31}P-NMR analyses were performed in $CDCl_3$ with cholesterol as standard, and presented in Figure 2.1.3-a. All copolyesters showed COOH (134.9 ppm) and primary OH (147.4 ppm) end-groups. The majority of the end-groups were OH functions (due to the higher amount of OH initially introduced into the reaction mixture, compared to COOH). However, an important disparity of OH end-groups proportion was determined. Since reported values correspond to one sample by composition and not an average value, results should be considered with care. Moreover, it was interesting to note that SA (134.85 ppm) and AA (134.90 ppm) end-groups were separated in ^{31}P-NMR spectra. The proportion of AA end-groups seemed to be slightly superior to the global adipate content into the chain, for almost all copolyesters containing a mixture of diacids (Table SI.1 in Annex 1). This latest result was surprising if we take into account the effect of the transesterification, with the corresponding random structure. One can suppose that the difference could come from measurement uncertainty, the small acid signal overlapping (Figure SI.1 in Annex 1) and the possible difference of stability of both acid end-groups with the phosphorus reactant (Korntner et al., 2015).

The calculated M_n of copolyesters by ^{31}P-NMR ($M_{n,31P\text{-}NMR}$), reported in Table 2.1.1, were approx. 2-3 times smaller compared to the one obtained by SEC, the latter being overestimated partly due to the calibration based on PS standards. M_n determined by ^{31}P-NMR varied between 9,500 and 17,000 g/mol. This technique gave a more accurate estimation of aliphatic copolyesters molar mass. However, this method based on the quantification of end-groups did not take into account the possible macrocycles that could have been produced during the polyester synthesis, but undetectable by ^{31}P-NMR analysis (Charlier, Q. et al., 2015; Yashiro et al., 2009b). Furthermore, a new method to calculate the molar mass was developed using (i) ^{1}H-NMR specific signals of AA, SA, OH end-groups and 1,4-BDO repetitive units at 2.32, 2.62, 3.67 and 4.10 ppm, respectively, and (ii) the OH end-groups proportion determined by ^{31}P-NMR. $M_{n,1H\text{-}NMR}$ was calculated according to Equation (2.1.6),

$$M_{n,1H-NMR} = \frac{\frac{I_{4.12}}{4} \times 88.10 + \chi_{SA} \times \frac{I_{2.62}}{4} \times 84.07 + \chi_{AA} \times \frac{I_{2.32}}{4} \times 112.13 + \frac{I_{3.67}}{2} \times 89.11}{0.5 \times \frac{I_{3.67}}{2}} \times X_{OH} \quad (2.1.6)$$

where $I_{4.12}$, $I_{2.62}$, $I_{2.32}$ and $I_{3.67}$ are intensities of 1,4-BDO, SA, AA and OH end-groups respectively; 88.10, 84.07, 112.13 and 89.11 are molar mass of 1,4-BDO, SA, AA and OH end-groups units respectively; χ_{SA} and χ_{AA} are the succinate and adipate contents in copolyester, respectively; X_{OH} is the OH end-groups proportion determined by ^{31}P-NMR. $M_{n,1H\text{-}NMR}$ results are reported in Table 2.1.1.

Due to the impossibility to quantify COOH end-groups, X_{OH} was used as correcting factor. This method was based on the quantification of OH end-groups and, such as $M_{n,31P\text{-}NMR}$. $M_{n,1H\text{-}NMR}$ of PBSA copolyesters varied between 9,500 and 20,000 g/mol. $M_{n,1H\text{-}NMR}$ values were mostly close to the one calculated according to ^{31}P-NMR with relative M_n difference, lower than 15%, except for $PBS_{79}A_{21}$ (around 30%).

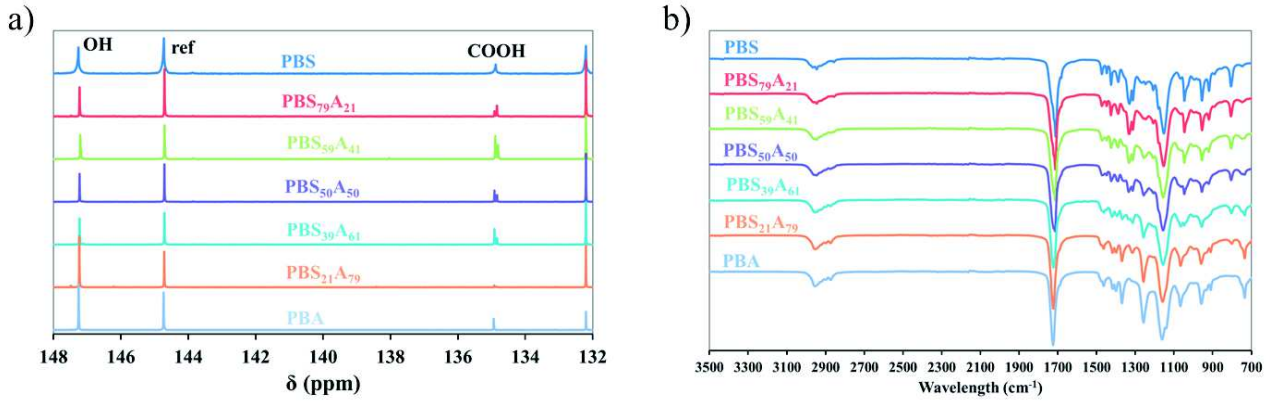

Figure 2.1.3 : (a) ^{31}P-NMR and (b) FTIR spectra of PBSA copolyesters.

The FTIR analysis of copolyesters showed some interesting results. FTIR spectra of all copolyesters are presented in Figure 2.1.3-b. First, in all copolyesters, no broad signals around 3200-3400 cm^{-1} assigned to the O-H vibration of COOH and OH end-groups were observed due to the high molar mass of the synthesized copolyesters. Then, all samples exhibited a sharp signal at approx. 1710-1725 and 1150-1160 cm^{-1} assigned to the C=O and asymmetric –COO- stretching vibration from ester groups confirming the synthesis of esters functions, respectively. One can observe that the C=O stretching ester vibration slightly shifted from 1710 to 1725 for PBS (or $PBS_{100}A_0$) to PBA (or PBS_0A_{100}), respectively. Moreover signals at 2850-3000 cm^{-1} were assigned to C-H stretching vibrations of methylene carbons. Finally, signals at 1330, 1045 and 805 cm^{-1} assigned to the symmetric C-O stretching, O-CH_2- stretching and -CH_2- rocking vibrations shifted to 1255, 1055 and 735 cm^{-1} with the increase of the adipate content in copolyesters, respectively. There was, thus, a modification of the FTIR spectra profile with the SA/AA composition.

Table 2.1.1 : Molar composition and molar masses of synthesized PBSA copolyesters.

Sample	Feed SA/AA composition	^{1}H-NMR		SEC		^{31}P-NMR		^{13}C-NMR		
		Determined SA /AA composition	$M_{n,1H\text{-}NMR}$	$M_{n,SEC}$	Đ	$M_{n,31P\text{-}NMR}$	OH end-groups	L_{PS}	L_{PA}	R
	mol.%	mol.%	kg/mol	kg/mol		kg/mol	%			
PBS ($PBS_{100}A_0$)	100 / 0	100 / 0	19.7	39.2	1.7	17.3	78	-	-	-
$PBS_{79}A_{21}$	80 / 20	79.2 / 20.8	15.5	39.7	1.9	16.4	65	4.8	1.3	1.00
$PBS_{59}A_{41}$	60 / 40	58.6 / 41.4	12.3	26.8	1.8	9.5	41	2.6	1.6	1.01
$PBS_{50}A_{50}$	50 / 50	49.7 / 50.3	11.4	44.5	1.6	13.7	60	2.0	2.0	1.00
$PBS_{39}A_{61}$	40 / 60	39.1 / 60.9	12.2	41.4	1.6	12.0	55	1.8	2.4	0.99
$PBS_{21}A_{79}$	20 / 80	20.9 / 79.1	9.4	27.4	1.4	10.7	94	1.3	4.2	1.04
PBA (PBS_0A_{100})	0 / 100	0 / 100	13.7	33.3	1.8	13.6	79	-	-	-

4.2. Thermal degradation

TGA traces of PBSA samples are shown in Figure 2.1.4 with their corresponding derivatives curves (DTG). Data are summarized in Table 2.1.2. Under helium, all copolyesters degraded into two main steps which involve competitive mechanisms. First, a small mass loss was observed at 260-315 °C due to the degradation of low molar mass chains along with the cyclization at the chain-ends and back-biting reactions that are responsible for CO_2 and H_2O release, which are produced from the decomposition of COOH and OH chain-ends, respectively (Scheme SI.1 in Annex 1) (Chrissafis et al., 2006a; Persenaire et al., 2001). Secondly, a major degradation occurred at 315-425 °C with a substantial mass loss of approx. 90% corresponding to the thermal degradation of polyesters chains, mostly by β- and α-hydrogen bond scissions. These reactions are responsible for the decomposition of polyesters into small compounds such as diacids, vinyl compounds, aldehydes and anhydrides (Bikiaris et al., 2007; Persenaire et al., 2001). After this decomposition step, mass residue of approx. 4% still remained. This multi-steps degradation is in agreement with previous reports (Debuissy et al., 2016a; Zorba et al., 2007).

The 2% mass degradation temperature ($T_{d,2\%}$) of all copolyesters were about 290-315 °C. By taking $T_{d,2\%}$ as criterion for the thermal stability of polyesters, PBS possessed the lowest thermal stability, whereas PBA showed the highest one. The 50 % mass loss degradation temperature ($T_{d,50\%}$) and the maximal degradation temperature ($T_{deg,max}$) were approx. 365-385 and 375-400 °C, respectively, and both decreased with the adipate content.

Results showed that it seemed appropriate to class copolyesters into two groups according to their composition. PBSA with adipate content of 60 mol.% or higher exhibited a $T_{d,50\%}$ and $T_{deg,max}$ of approx. 370 and 375 °C, whereas PBSA with adipate content lower than 60 mol.% exhibited a $T_{d,50\%}$ and $T_{deg,max}$ of approx. 380-385 and 395 °C, respectively. The thermal degradation profile of "adipate rich" copolyesters was, thus, sharper compared to "succinate rich" copolyesters. DTG curves of $PBS_{79}A_{21}$, $PBS_{59}A_{41}$ and $PBS_{50}A_{50}$ exhibited first a shoulder at approx. 350-360 °C assigned to the degradation of adipate units and, then the degradation assigned to succinate units at 380-400 °C. In conclusion, the thermal degradation profile of PBSA depended highly on the SA/AA molar ratio. This result was in contradiction with a previous study which showed that the degradation mechanism depended highly on the type of diol unit, whereas the influence of the carboxylic acid unit was less important (Plage and Schulten, 1990). Therefore, since the same diol was used in this study, its influence on the degradation was not investigated and, thus, the influence on the diol *vs.* the influence of the diacid was not possible. Nevertheless, the present results proved that the influence of the diacid was not negligible.

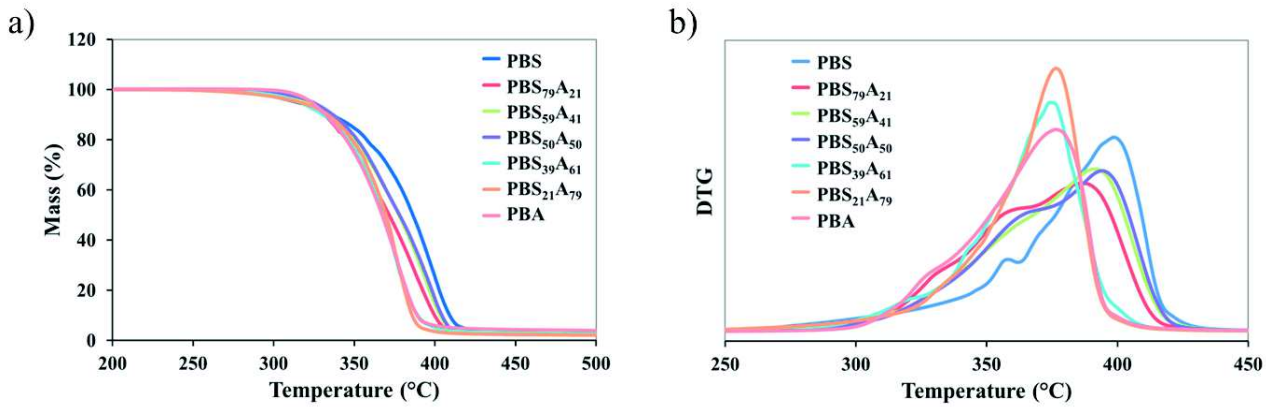

Figure 2.1.4 : (a) Mass loss and (b) DTG curves of PBS, PBSA copolyesters and PBA under helium at 20 °C/min.

Table 2.1.2 : TGA results of PBSA copolyesters in helium with a heating rate of 20 °C/min.

Sample	D_{ester}	$T_{d,2\%}$	$T_{d,50\%}$	$T_{deg,max}$	Residue at 500 °C
	%	°C	°C	°C	wt.%
$PBS_{100}A_0$ (PBS)	25.0	293	386	398	2.7
$PBS_{79}A_{21}$	24.0	302	371	387	2.8
$PBS_{59}A_{41}$	23.0	300	378	394	2.2
$PBS_{50}A_{50}$	22.5	308	378	397	2.2
$PBS_{39}A_{61}$	22.0	297	368	374	3.2
$PBS_{21}A_{79}$	21.0	294	370	376	2.2
PBS_0A_{100} (PBA)	20.0	314	367	377	4.0

4.3. WAXS and DSC results

To investigate the crystalline structure of copolyesters, a WAXS study was first performed. The patterns of PBSA copolyesters are shown in Figure 2.1.5. WAXS patterns of the copolyesters appeared to be characterized by well-defined diffraction peaks over the whole composition range. The patterns of semi-crystalline copolyesters could be divided into three groups according to the adipate content: copolyesters containing 50 mol.% or less of adipate units are characterized by X-ray patterns very similar to PBS, indicating that the crystal structure in these copolyesters has the same characteristics as the PBS lattice. On the contrary, samples containing more than 61 mol.% of adipate units crystallized according to the PBA lattice. Finally, it was interesting to note that $PBS_{39}A_{61}$ seemed to exhibit both crystalline phases.

The crystal structure of PBS was in agreement with previous reports and defined in α-form characterized by monoclinic unit cell (Pan and Inoue, 2009). The reflections for PBS appeared at 2θ = 19.4, 21.7, 22.4 and 28.7°. The crystal structure of PBA has been already studied (Pan and Inoue, 2009). Two crystalline forms were identified such as (i) the α-form which is characterized by a monoclinic unit cell, mainly formed at low cooling rate (thermodynamically favored) and high temperature of crystallization (T_c) (> 32 °C), and (ii) the β-form which is characterized by chains in a planar zigzag conformation packed in a orthorhombic unit cell, formed at high cooling rate (kinetically favored) and low T_c (< 28 °C). Our sample of PBA exhibited reflections at 2θ = 21.3 and 24.4° assigned to β-form crystals, but also reflections at 2θ = 21.6, 22.3 and 24.1° assigned to α-form crystals. PBS exhibited thus α + β mixed crystals (Gan et al., 2002).

$PBS_{79}A_{21}$, $PBS_{59}A_{41}$, $PBS_{50}A_{50}$ and $PBS_{39}A_{61}$ showed diffraction patterns similar to PBS, but with lower intensities. The co-monomeric unit (adipate in this case) incorporated in minor amount was found to be excluded from the PBS crystal lattice or only partially integrated in it. This phenomenon decreased the crystal strength and lamellae sizes due to the presence of "adipate defects" inside the chain and, thus, the degree of crystallinity decreased with the adipate content. The presence of defects in the chain led to a small modification of the crystalline structure proved by the quite larger and slightly shifted copolyesters diffraction peaks compared to those of homopolyesters. Contrary to PBA, $PBS_{21}A_{79}$ and $PBS_{39}A_{61}$ seemed to show only β-form crystals of PBA. One can suppose that this could be due to the inclusion of succinate units inside the PBA crystalline phase which disrupted the homogeneity of the polyester chain, slowed down the crystallization rate and, thus, only kinetically-favored β-form crystals of PBA were formed during the crystallization of $PBS_{21}A_{79}$ and $PBS_{39}A_{61}$. Finally, in $PBS_{39}A_{61}$, the β-form PBA crystalline phase was dominant but a small PBS crystalline phase was also present in the sample. The presence of both crystalline phases could be explained by the close unit cells and structures of PBS and PBA, and by the high amount of both segments at this composition.

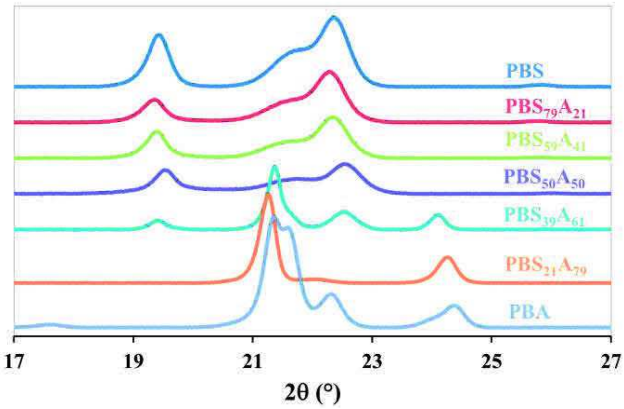

Figure 2.1.5 : WAXS patterns of PBS, PBSA copolyesters and PBA.

In complement to WAXS analysis, the degree of crystallinity and thermal properties of copolyesters were studied by DSC. Prior to this, it has been verified, from TGA results, that no significant degradation occurred on the samples in the DSC analyses temperature range. Cooling and second heating run curves are presented in Figure 2.1.6 and all corresponding data are summarized in Table 2.1.3. Figure 2.1.7-a plotted the crystallization temperatures (T_c) and enthalpies (ΔH_c) of (co)polyesters, measured during the cooling run, as a function of the adipate content, whereas Figure 2.1.7-b plotted T_g of (co)polyesters as a function of the adipate content. The melting temperatures (T_m) and enthalpies (ΔH_m) of (co)polyesters, measured during the second heating run, as a function of the adipate content are plotted in Figure 2.1.8. The variation of thermal properties is also discussed as a function of D_{ester}, calculated according to Equation (2).

At the beginning, all (co)polyesters were melted in order to erase the thermal history. During the cooling run from the melt at controlled speed (10 °C/min), all samples showed an exothermic phenomenon attributed to the crystallization. T_c decreased with the adipate content from 83 °C for PBS until reaching a minimal T_c of -16 °C for $PBS_{50}A_{50}$. Then, T_c increased again to reach 32°C for PBA. Figure 2.1.7-a exhibited, thus, a pseudo-eutectic behavior for T_c, but also another pseudo-eutectic behavior for ΔH_c with a minimal value for the $PBS_{39}A_{61}$ copolyester. The addition of a co-monomeric unit in the homopolyester matrix disrupted the structure and, thus, decreased the lamellae size and crystal

strength. Moreover, crystallization peaks became larger with the increase of the co-monomeric unit content in the homopolyester, which reduced the crystal homogeneity as observed in WAXS.

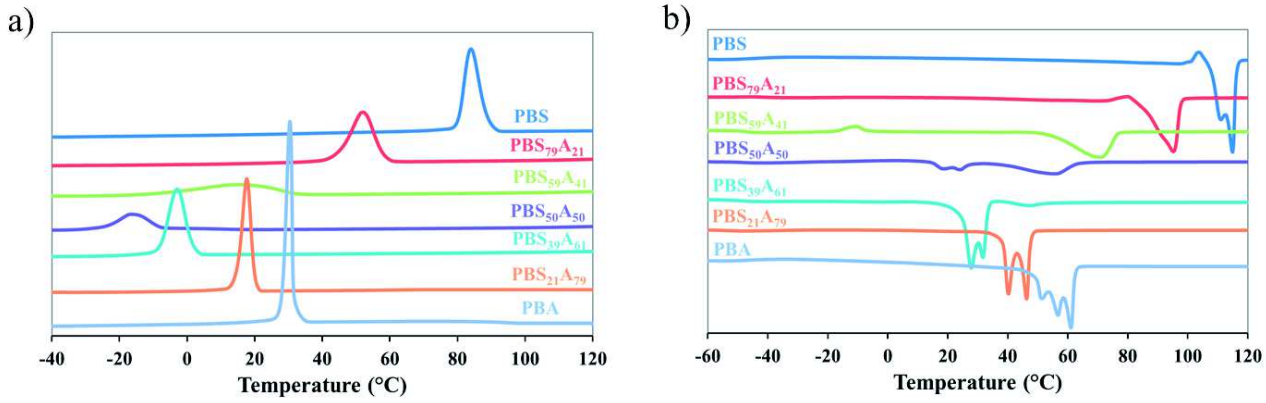

Figure 2.1.6 : (a) Cooling and (b) second heating run curves of PBS, PBSA copolyesters and PBA at 10 °C/min.

The second heating run was characterized by a small endothermal baseline deviation associated to the glass-transition phenomenon and an endothermic peak at higher temperature, associated to a melting phenomenon. Moreover, $PBS_{59}A_{41}$ exhibited, in addition to these two phenomena, an exothermic signal attributed to a cold-crystallization at approx. -11 °C. The presence of the cold-crystallization phenomena was due to an incomplete crystallization during the cooling run. One can conclude that $PBS_{59}A_{41}$ had, thus, the lowest crystallization rate.

T_g values are summarized in Table 2.1.3 and are plotted in Figure 2.1.7-b as a function of the adipate content. As can be seen, T_g was influenced by the amount of adipate unit in the copolyester chain. T_g decreased continuously from -35 to -59 °C for adipate content of 0 and 100%, respectively. Indeed, by increasing the amount of adipate unit in the copolyester, D_{ester} decreased. Moreover, it is well known that the second-order transition temperature is considered as a measure of the chain flexibility of the polymer chain. The more flexible the chains are, the lower the T_g is. By decreasing D_{ester} of the copolyester chain, a lower amount of intra or inter-chain interactions between ester groups were possible, whence the increase of chain mobility leading to the decrease of T_g.

In random copolyesters, T_g is usually a monotonic function of composition. The most common relationship used to predict T_g as a function of a co-monomer content is the Fox equation (Fox, 1956), defined by Equation (2.1.7),

$$\frac{1}{T_{g,copo}} = \frac{w_1}{T_{g,1}} + \frac{w_2}{T_{g,2}} \qquad (2.1.7)$$

where $T_{g,1}$ and $T_{g,2}$ are the glass transition temperature of pure homopolyesters, and w_1 and w_2 respective mass fractions. However, as one can observe in Figure 2.1.7-b, the Fox equation did not fit at all the experimental data. Thus, an alternative relationship has been considered for copolymers by using a mixing law, the Gordon-Taylor equation (Gordon and Taylor, 2007), defined by Equation (2.1.8),

$$T_{g,copo} = \frac{w_1\, T_{g,1} + k(1-w_1)\, T_{g,2}}{w_1 + k(1-w_1)} \qquad (2.1.8)$$

where $T_{g,1}$ and $T_{g,2}$ are the glass transition temperature of pure homopolyesters, w_1 the respective mass fraction of the pure homopolyester 1 and k the Gordon-Taylor parameter.

As shown in Figure 2.1.7-b, the Gordon-Taylor equation fitted well the experimental data with k = 0.83. In the original version of volume additivity, the parameter $k = \rho_1\Delta\alpha_2/\rho_2\Delta\alpha_1$ has a well-defined significance (ρ_i is the density and $\Delta\alpha_i = \alpha_{melt} - \alpha_{glass}$ is the increment at T_g of the expansion coefficient of the respective component i). But generally k is considered a real fitting parameter (Penzel et al., 1997). T_g of the copolyesters could be, thus, predicted for all the composition range using this relation.

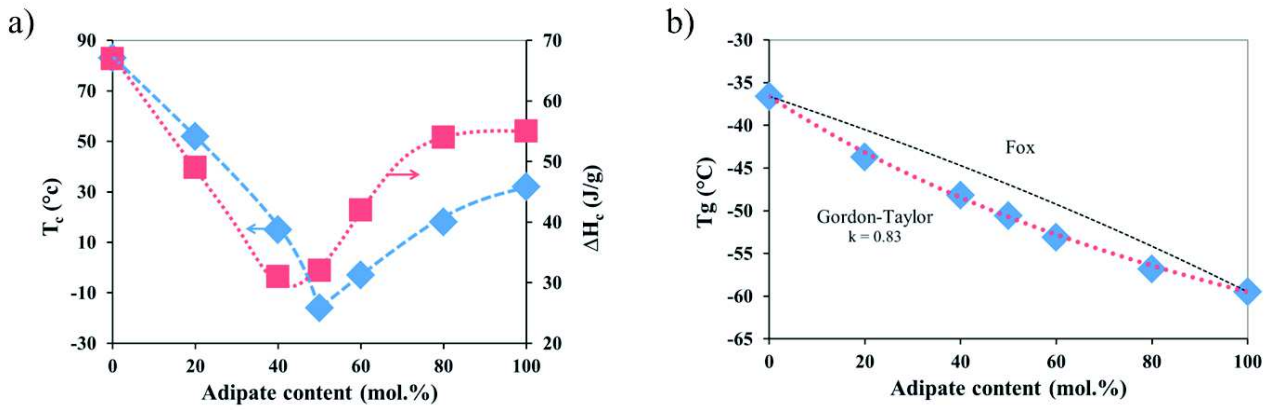

Figure 2.1.7 : (a) Variation of T_c and ΔH_c of copolyesters vs. adipate content and (b) variation of T_g vs. adipate content in PBSA.

Figure 2.1.6-b highlighted that PBS had the highest T_m at approx. 115 °C. In detail, one can observe that the melting phenomena spread on a large temperature range (100-120 °C) and was composed of two peaks. Moreover, a small cold-crystallization signal was observed just before the melting. These multiple peaks were attributed to the crystallite reorganization during the heating by a fusion-recrystallization phenomenon (Chivrac et al., 2007; Debuissy et al., 2016a; Nikolic and Djonlagic, 2001). Such as PBS, PBA melting area spread on a large temperature range (45-65 °C) with three endothermic peaks. They were due, such as PBS, to the fusion-recrystallization phenomenon, but also to the polymorphism of PBA (Pan and Inoue, 2009). The copolyesters showed also fusion-recrystallization phenomena. During the second heating run, $PBS_{50}A_{50}$ exhibited two melting phenomena at approx. 24 and 56 °C even if only one crystallization signal was observed during the cooling run. One can suppose the presence of two crystalline phases (*i.e.,* PBS and PBA), even if the presence of PBA crystals was not highlighted by WAXS. Nevertheless, WAXS analysis was performed on compressed-molded samples which were quenched during the process and not slowly cooled at 10 °C/min. This can explain the difference of the crystalline structure. Likewise, $PBS_{39}A_{61}$ showed first an intense melting phenomenon at 20-35 °C assigned to the fusion of PBA crystals, followed by a small fusion at approx. 45 °C assigned to the fusion of PBS crystals observed in WAXS.

Figure 2.1.8 showed that T_m and ΔH_m of PBS crystals decreased with the adipate content until $PBS_{39}A_{61}$. On the same way, T_m of PBA crystals decreased with the SA content until $PBS_{50}A_{50}$. $PBS_{50}A_{50}$ and $PBS_{39}A_{61}$ showed the presence of both crystalline phases by DSC in our conditions. However, $PBS_{50}A_{50}$ and $PBS_{39}A_{61}$ crystalline phases are mostly based on PBS and PBA crystals, respectively. This result was in agreement with WAXS results. The variations of T_m and ΔH_m with the composition both showed pseudo-eutectic behaviors with minimal values near the 50/50-40/60 (SA/AA) composition. Moreover, the plot of ΔH_m of copolyesters as a function of the adipate content for the sum of both crystalline phases are presented in Figure SI.2 (in Annex 1) and showed such as before a pseudo-eutectic behavior with minimal values for adipate content of approx. 39-50 mol.%. The presence of both melting and melting enthalpy pseudo-eutectic points and the presence of different crystalline phases according to the molar composition highlighted the isodimorphic co-crystallization behavior of PBSA as observed for other aliphatic random copolyesters (Arandia et al., 2015; Díaz et al., 2014).

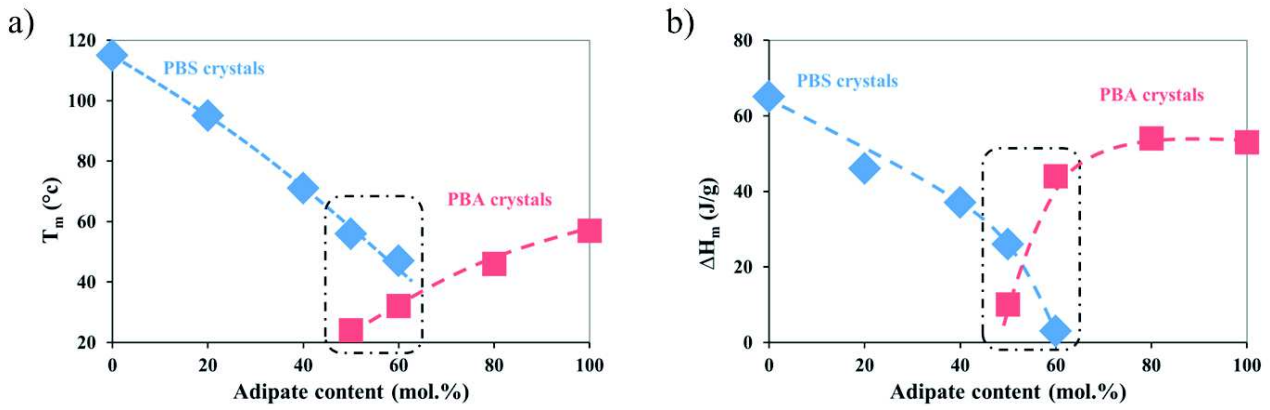

Figure 2.1.8 : Variation of (a) T_m and (a) ΔH_m of copolyesters during the second heating run vs. the adipate content.

The melting enthalpy value of 100% crystalline phase ($\Delta H_m°$) is determined from the groups contribution method as proposed by Van Krevelen (Van Krevelen, 1997) for PBA (135 J/g), and from experimental data (Papageorgiou and Bikiaris, 2005a) for PBS (210 J/g). WAXS results showed that most samples exhibited only one crystal lattice by sample. The degree of crystallinity (X_c) of copolyesters was calculated from the first and second heating scans and values are summarized in Table 2.1.3. X_c was plotted as a function of the adipate content and shown in Figure 2.1.9. X_c of PBA was slightly higher than the one of PBS. One can suppose that the decrease of D_{ester} due to adipate units with more methylene groups bring more flexibility to the chain and thus facility to crystallize contrary to succinate units. However, results should be taken with care since $\Delta H_m°$ values of PBA and PBS were theoretically and experimentally calculated, respectively. X_c followed the same trend as the melting and crystallization enthalpies with a global decrease of the copolyester degree of crystallinity with the addition of a co-monomeric unit (reduction of block length inside the chain). However, one can observe that the X_c of $PBS_{21}A_{79}$ during the second heating run is similar (even slightly higher) than the one of PBA. We can suppose that this was more likely due to the lower M_n of $PBS_{21}A_{79}$ than PBA. Nevertheless, during the first heating scan, X_c of $PBS_{21}A_{79}$ was lower than the one of PBA confirming the decrease of the copolyester degree of crystallinity with the addition of a co-monomeric unit.

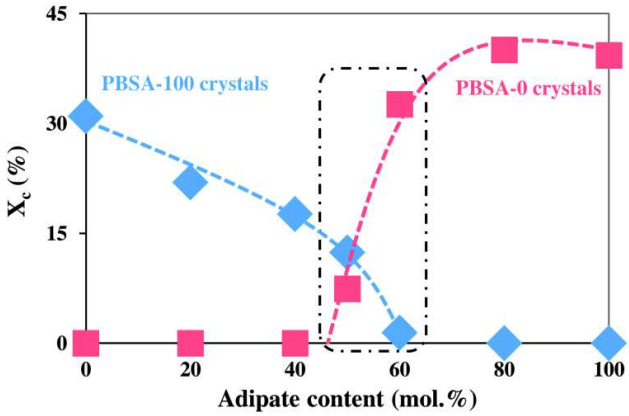

Figure 2.1.9 : Degree of crystallinity during the second heating run of PBSA copolyesters in function of adipate content.

Table 2.1.3 : DSC results of PBSA copolyesters with heating and cooling rate of 10 °C/min.

Sample	D_{ester}	first heating			cooling		T_g [a]	second heating				
		T_m	ΔH_m	X_c	T_c	ΔH_c		T_{cc}	ΔH_{cc}	T_m	ΔH_m	X_c
	%	°C	J/g	%	°C	J/g	°C	°C	J/g	°C	J/g	%
PBS ($PBS_{100}A_0$)	25.0	116	81	39	83	67	-37	-	-	115	65	31
$PBS_{79}A_{21}$	24.0	95	47	22	52	49	-44	-	-	95	46	22
$PBS_{59}A_{41}$	23.0	72	42	20	15	31	-48	-11	4	71	37	18
$PBS_{50}A_{50}$	22.5	51	41	20	-16	32	-51	-	-	24/56*	10/26*	7/12*
$PBS_{39}A_{61}$	22.0	43	26	19	-3	42	-53	-	-	32/47*	44/3*	33/2*
$PBS_{21}A_{79}$	21.0	49	66	49	18	54	-57	-	-	46	54	40
PBA (PBS_0A_{100})	20.0	58	80	59	32	55	-60	-		57	53	39

[a] T_g values were determined after a quenching from the melt. * Presence of two crystalline phases (PBA phase / PBS phase).

5. Conclusion

Different biobased copolyesters (PBSA) and homopolymers (PBS and PBA) based on renewable building blocks were successfully synthesized in melt, using TTIP as an effective catalyst, with different compositions. The optimized synthetic pathway permitted to obtain (i) high molar masses, (ii) final copolyesters with the same molar compositions than the initial feed ratios and (iii) a random distribution between succinate and adipate segments along the polyester chain.

PBSA copolyesters exhibited excellent thermal stability until approx. 300 °C. Moreover, the thermal degradation profile of PBSA copolyesters was driven by the major diacid component, resulting in an acceleration of the degradation rate, after the onset, for “adipate rich” copolyesters.

Furthermore, PBSA copolyesters showed an isodimorphic co-crystallization behavior characterized by the presence of one crystalline phase for each sample according to the composition, except for copolyesters with adipate content of 50-60 mol.% which showed the presence of both crystalline phases, and a pseudo-eutectic melting behavior. T_g of copolyesters decreased with the adipate content according to the Gordon-Taylor relation with a calculated Gordon-Taylor parameter, k, of 0.83. The decrease of T_g was ascribed to the increase in copolyester chain mobility resulting from the decrease of the ester function density.

The PBSA copolyester is, thus, an excellent example to demonstrate the importance of the macromolecular engineering to tailor the right material, to open new areas of applications. The PBSA copolyesters family is a nice and promising sustainable material series for some applications such as agriculture, packaging or for some biomedical devices but also for uses where the biodegradation or biocompatibility is not needed such as in automotive or building applications. However, to fulfill the strict requirements of these different fields, some additional tests must be carried out, such as: the study of the biodegradability, biocompatibility, fire retardancy, and specific mechanical and ageing behaviors.

6. References

Ahn, B.D., Kim, S.H., Kim, Y.H., Yang, J.S., 2001. J. Appl. Polym. Sci. 82, 2808–2826.

Arandia, I., Mugica, A., Zubitur, M., Arbe, A., Liu, G., Wang, D., Mincheva, R., Dubois, P., Müller, A.J., 2015. Macromolecules 48, 43–57.

Avérous, L., 2004. J. Macromol. Sci. Part C 44, 231–274.

Avérous, L., Fringant, C., 2001. Polym. Eng. Sci. 41, 727–734.

Barton, N.R., Burgard, A.P., Burk, M.J., Crater, J.S., Osterhout, R.E., Pharkya, P., Steer, B.A., Sun, J., Trawick, J.D., Dien, S.J.V., Yang, T.H., Yim, H., 2014. J. Ind. Microbiol. Biotechnol. 42, 349–360.

Bechthold, I., Bretz, K., Kabasci, S., Kopitzky, R., Springer, A., 2008. Chem. Eng. Technol. 31, 647–654.

Becker, J., Lange, A., Fabarius, J., Wittmann, C., 2015. Curr. Opin. Biotechnol. 36, 168–175.

Bikiaris, D.N., Chrissafis, K., Paraskevopoulos, K.M., Triantafyllidis, K.S., Antonakou, E.V., 2007. Polym. Degrad. Stab. 92, 525–536.

Bozell, J.J., Petersen, G.R., 2010. Green Chem. 12, 539.

Bueno-Ferrer, C., Hablot, E., Garrigós, M. del C., Bocchini, S., Averous, L., Jiménez, A., 2012. Polym. Degrad. Stab., 3rd International Conference on Biodegradable and Biobased Polymers (BIOPOL-2011) - Strasbourg 2011 97, 1964–1969.

Charlier, Q., Girard, E., Freyermouth, F., Vandesteene, M, Jacquel, N., Ladavière, C., Rousseau, A., Fenouillot, F., 2015. Express Polym. Lett. 9, 424–434.

Chen, C.-H., Peng, J.-S., Chen, M., Lu, H.-Y., Tsai, C.-J., Yang, C.-S., 2010. Colloid Polym. Sci. 288, 731–738.

Chivrac, F., Pollet, E., Avérous, L., 2007. J. Polym. Sci. Part B Polym. Phys. 45, 1503–1510.

Choi, S., Song, C.W., Shin, J.H., Lee, S.Y., 2015. Metab. Eng. 28, 223–239.

Chrissafis, K., Paraskevopoulos, K.M., Bikiaris, D.N., 2006. Thermochim. Acta 440, 166–175.

Debuissy, T., Pollet, E., Avérous, L., 2016. Polymer 99, 204–213.

Díaz, A., Franco, L., Puiggalí, J., 2014. Thermochim. Acta 575, 45–54.

Fox, T., 1956. Bull. Am. Phys. Soc. 1, 123–132.

Gan, Z., Abe, H., Doi, Y., 2002. Macromol. Chem. Phys. 203, 2369–2374.

Gordon, M., Taylor, J.S., 2007. J. Appl. Chem. 2, 493–500.

Jacquel, N., Freyermouth, F., Fenouillot, F., Rousseau, A., Pascault, J.P., Fuertes, P., Saint-Loup, R., 2011. J. Polym. Sci. Part Polym. Chem. 49, 5301–5312.

Korntner, P., Sumerskii, I., Bacher, M., Rosenau, T., Potthast, A., 2015. Holzforschung 69, 807–814.

Kuo, C.-T., Chen, S.-A., 1989. J. Polym. Sci. Part Polym. Chem. 27, 2793–2803.

Lin, C.C., Hsieh, K.H., 1977. J. Appl. Polym. Sci. 21, 2711–2719.

Makay-Bödi, E., Vancso-Szercsanyi, I., 1969. Eur. Polym. J. 5, 145.

Montaudo, G., Rizzarelli, P., 2000. Polym. Degrad. Stab. 70, 305–314.

Nikolic, M.S., Djonlagic, J., 2001. Polym. Degrad. Stab. 74, 263–270.

Pan, P., Inoue, Y., 2009. Prog. Polym. Sci. 34, 605–640.

Papageorgiou, G.Z., Bikiaris, D.N., 2005. Polymer 46, 12081–12092.

Penzel, E., Rieger, J., Schneider, H.A., 1997. Polymer 38, 325–337.

Persenaire, O., Alexandre, M., Degée, P., Dubois, P., 2001. Biomacromolecules 2, 288–294.

Picataggio, S., Rohrer, T., Deanda, K., Lanning, D., Reynolds, R., Mielenz, J., Eirich, L.D., 1992. Nat. Biotechnol. 10, 894–898.

Plage, B., Schulten, H.R., 1990. Macromolecules 23, 2642–2648.

Polen, T., Spelberg, M., Bott, M., 2013. J. Biotechnol., Research on Industrial Biotechnology within the CLIB-Graduate Cluster - Part III 167, 75–84.

Pollet, E., Avérous, L., 2011. Production, Chemistry and Properties of Polyhydroxyalkanoates, in: Plackett, D. (Ed.), Biopolymers – New Materials for Sustainable Films and Coatings. John Wiley & Sons, Ltd, pp. 65–86.

Ren, M., Song, J., Song, C., Zhang, H., Sun, X., Chen, Q., Zhang, H., Mo, Z., 2005. J. Polym. Sci. Part B Polym. Phys. 43, 3231–3241.

Reulier, M., Avérous, L., 2015. Eur. Polym. J. 67, 418–427.

Siotto, M., Zoia, L., Tosin, M., Degli Innocenti, F., Orlandi, M., Mezzanotte, V., 2013. J. Environ. Manage. 116, 27–35.

Spyros, A., Argyropoulos, D.S., Marchessault, R.H., 1997. Macromolecules 30, 327–329.

Takiyama, E., Fujimaki, T., 1994. Biodegradable plastics and polymers, in: Doi, Y., Fukuda, K. (Eds.), Biodegradable Plastics and Polymers. Elsevier Science, Burlington, p. 150.

Tokiwa, Y., Calabia, B.P., Ugwu, C.U., Aiba, S., 2009. Int. J. Mol. Sci. 10, 3722–3742.

Tserki, V., Matzinos, P., Pavlidou, E., Panayiotou, C., 2006a. Polym. Degrad. Stab. 91, 377–384.

Tserki, V., Matzinos, P., Pavlidou, E., Vachliotis, D., Panayiotou, C., 2006b. Polym. Degrad. Stab. 91, 367–376.

Van Krevelen, D.W., 1997. Chapter 5 - Calorimetric properties, in: Properties of Polymers (Third, Completely Revised Edition). Elsevier, Amsterdam, pp. 109–127.

Vancsó-Szmercsányi, I., Maros-Gréger, K., Makay-Bödi, E., 1969. Eur. Polym. J. 5, 155–161.

Vardon, D.R., Franden, M.A., Johnson, C.W., Karp, E.M., Guarnieri, M.T., Linger, J.G., Salm, M.J., Strathmann, T.J., Beckham, G.T., 2015. Energy Env. Sci 8, 617–628.

Werpy, T.A., Holladay, J.E., White, J.F., 2004. Top Value Added Chemicals from Biomass: I. Results of Screening for Potential Candidates from Sugars and Synthesis Gas (No. PNNL-14808). Pacific Northwest National Laboratory (PNNL), Richland, WA (US).

Xu, J., Guo, B.-H., 2010. Biotechnol. J. 5, 1149–1163.

Yashiro, T., Kricheldorf, H.R., Huijser, S., 2009. Macromol. Chem. Phys. 210, 1607–1616.

Zorba, T., Chrissafis, K., Paraskevopoulos, K.M., Bikiaris, D.N., 2007. Polym. Degrad. Stab. 92, 222–230.

7. Collaboration

N.B: In addition to this study, a successful collaboration was performed with the team of Pr. Alejandro Müller (Unisversity of Basque-Country, Spain), who investigated in details the isodimorphic and the co-cristallization behaviors of PBSA. This collaboration led to the publication of an article named "Tailoring the Structure, Morphology, and Crystallization of Isodimorphic Poly(butylene succinate-ran-butylene adipate) Random Copolymers by Changing Composition and Thermal History" in *Macromolecules* (*2017, 50 (2), 597–608*). This article is given in Annex 10.

Sub-chapter 2.2. Synthesis and characterization of fully biobased poly(propylene succinate-*ran*-propylene adipate). Analysis of the architecture-dependent physicochemical behavior

Thibaud Debuissy, Eric Pollet and Luc Avérous*

BioTeam/ICPEES-ECPM, UMR CNRS 7515, Université de Strasbourg, 25 rue Becquerel, 67087 Strasbourg Cedex 2, France

*Corresponding author: luc.averous@unistra.fr

Accepted in Journal of Polymer Science Part A: Polymer Chemistry, 2013, DOI:10.1002/pola.28668

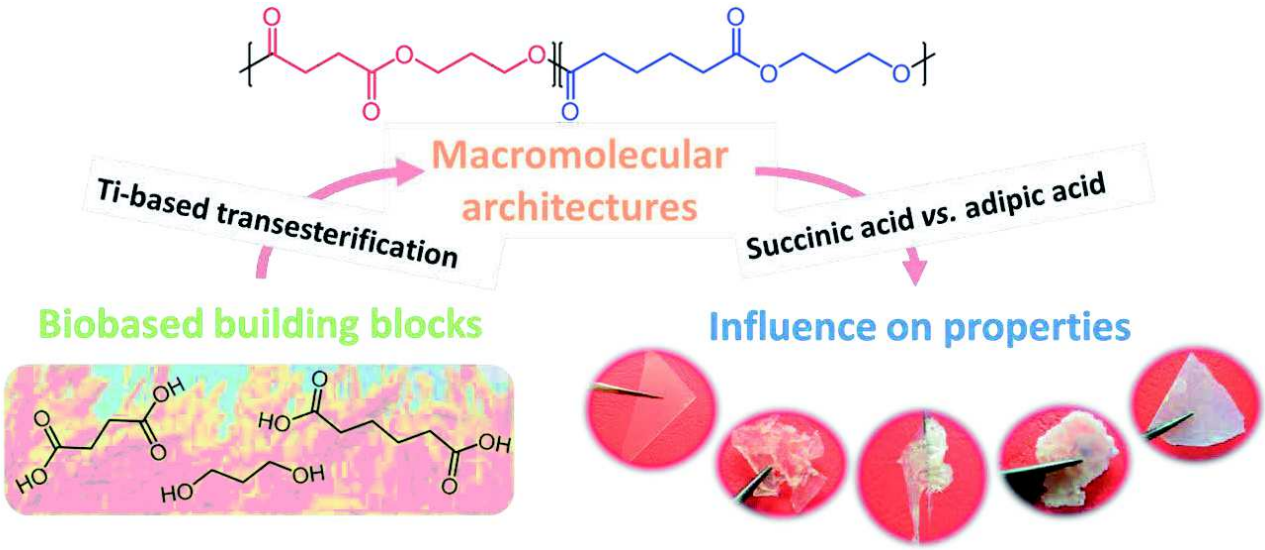

1. Abstract

Fully biobased aliphatic random [poly(1,3-propylene succinate-*ran*-1,3-propylene adipate) (PPSA) copolyesters with high molar mass were synthesized with different macromolecular architectures based on various succinic acid/adipic acid (SA/AA) molar ratio, by transesterification in melt. Titanium (IV) isopropoxide was used as an effective catalyst. All synthesized copolyesters were fully characterized by different chemical and physicochemical techniques including NMR, SEC, FTIR, WAXS, DSC and TGA. The final copolyesters molar compositions were identical to the feed ones. The different sequences based on succinate and adipate segments were randomly distributed along the chains. All the corresponding copolyesters showed an excellent thermal stability with a degradation onset temperature higher than 290 °C, which increased with the adipate content. According to their compositions and architectures, PPSA copolyesters can exhibit or not a crystalline phase, at room temperature. Glass transition temperatures of copolyesters decreased with the adipate content due to the decrease of the chains mobility, following the Gordon-Taylor relation. PPSA showed a pseudo eutectic melting behavior characteristic of an isodimorphic character. Finally, PPSA copolyesters were not able to crystallize during the cooling or the second heating run, due to the 1,3-propanediol chemical structure, which led to amorphous materials with the exception of the polyester based solely on adipic acid.

2. Introduction

Over the last decades, renewable polymers have attracted considerable attention, as an alternative to fossil-based materials. These biobased polymers can bring new macromolecular architectures with the corresponding advanced properties (Vilela et al., 2014a; Alessandro Pellis et al., 2016c; Stempfle et al., 2016). Among them, poly(lactic acid) (PLA) (Avérous, 2004), poly(ε-caprolactone), poly(butylene succinate) (PBS) (Debuissy et al., 2017a; Xu and Guo, 2010), poly(hydroxyalkanoates) (PHA) (Pollet and Avérous, 2011) have seen their interest growing on an industrial point of view with various applications such as packaging, agriculture, sanitary or in biomedical engineering.

Up to now, biobased 1-3 propanediol (1,3-PDO) was not largely available in the market at low cost with sufficient purity for chemical purposes. These limiting factors have been recently overcome by the development of new bioprocesses, using biological pathways mainly from glycerol, which permit an increase of the industrial production (Biebl et al., 1999; Drożdżyńska et al., 2011). The strong development of worldwide biorefineries has been a huge step forward for the bioproduction of 1,3-PDO, and other interesting biobased monomers or building blocks, such as succinic acid (SA), adipic acid (AA), furans, glycerol and others (Becker et al., 2015; Bozell and Petersen, 2010; Werpy et al., 2004). SA is a well-known short dicarboxylic acid, listed by the US-DoE as one of the strategic platform chemicals from renewable resources (Becker et al., 2015; Werpy et al., 2004; Bechthold et al., 2008; Choi et al., 2015). Biobased SA is commercialized by different companies (*e.g.,* BioAmber, Myriant, Succinity-Reverdia) and has seen its interest also growing for the production of polyesters (*e.g.*, PBS), polyamides…(Bechthold et al., 2008; Becker et al., 2015) AA is a very interesting aliphatic six-carbon diacid used as building block in the synthesis of polyamides, polyurethanes and polyesters (Avérous and Fringant, 2001; Debuissy et al., 2016a). Recently, new biological pathways were discovered for the bioproduction of AA from different biomass such as glucose (Polen et al., 2013), lignin (Vardon et al., 2015) and fatty acids (Picataggio et al., 1992).

Aliphatic polyesters based on 1,3-propanediol (1,3-PDO) have attracted increasing interest in the last twenty years. They have been studied from both academic and industrial perspectives, due to the excellent properties of 1,3-PDO-based polyesters. For example, poly(1,3-propylene terephthalate) (PPT), one of the first and most studied 1,3-PDO-based polyesters, is commercially available (Sorona®, Dupont) since a decade (Ho et al., 2000; Wang et al., 2001). Due to the odd number of methylene groups of the diol segment, PPT chains have a more angular structure than the more conventional poly(1,2-ethylene terephthalate) (PET) or poly(1,4-butylene terephthalate) (PBT). However and for instance, PPT fibers present a better resilience and higher stress recovery than PET or PBT (Ward et al., 1976). Unfortunately and as these latter, PPT is not susceptible to biodegrade in natural environment.

More recently, several biodegradable aliphatic polyesters based on 1,3-PDO such as poly(1,3-propylene succinate) (PPS), poly(1,3-propylene adipate) (PPA), poly(1,3-propylene glutarate), poly(1,3-propylene azelate) have been studied (Soccio et al., 2007; Bikiaris et al., 2008; Umare et al., 2007; Papageorgiou and Bikiaris, 2005a). Different copolyesters as a route to prepare tailor-made aliphatic copolyesters with improved properties were investigated. For example,

poly(1,3-propylene succinate-*co*-1,4-butylene succinate) copolyesters has been extensively studied in connection to the excellent properties of both corresponding homopolyesters (*i.e.,* PPS and PBS) (Papageorgiou and Bikiaris, 2007; Xu et al., 2007; Yongxiang Xu et al., 2008; Lu et al., 2010, 2012; Chen et al., 2010). For the same reason, poly(1,2-ethylene succinate-*co*-1,3-propylene succinate) (Papageorgiou and Bikiaris, 2009), poly(caprolactone-*block*-1,3-propylene adipate) (Nanaki et al., 2011) and poly(1,3-propylene succinate-*co*-1,3-propylene adipate) (PPSA) (Soccio et al., 2009; Umare et al., 2007) copolyesters were also recently synthesized and studied. The PPSA copolyesters exhibited some interesting structural properties. Nevertheless, Umare *et al* synthesized and studied only oligomers of PPSA with low molar mass (lower than 4,000 g/mol) (Umare et al., 2007). Soccio *et al* studied both block and random architectures synthesized from PPS and PPA blends, and not from the initial building blocks (Soccio et al., 2009).

To synthesize high molar mass aliphatic polyesters from diacid and diol buildings blocks, the transesterification polycondensation reaction from the melt with an organometallic catalyst is the most used and promising way (Bikiaris et al., 2006; Debuissy et al., 2016a; Papageorgiou and Bikiaris, 2005a; Soccio et al., 2007). Moreover, the literature shows that titanium-based catalysts are the most efficient organometallic catalysts for the transesterification reaction, compared to other zirconium, tin, hafnium or antinomy-based catalysts (Jacquel et al., 2011).

The aim of this study was, thus, to synthesize and characterize high molar mass biobased PPSA copolyesters of various SA/AA compositions, produced by the transesterification polycondensation reaction process in melt, with a titanium-based organometallic catalyst. Chemical and physicochemical properties of the different macromolecular structures were fully investigated. The molar mass of the corresponding copolyesters were determined by ^{1}H-, ^{13}C-, ^{31}P-NMR, SEC and FTIR. The thermal stability, crystalline structure and thermal properties were analyzed by TGA, WAXS and DSC, respectively. The effect of the SA/AA molar composition on copolyesters properties was particularly discussed.

3. Experimental part

3.1. Materials

Biobased succinic acid (SA) (99.5%) was kindly supplied by BioAmber (France). SA was bioproduced by fermentation of glucose (from wheat or corn) and obtained after a multistep process based on several purifications, evaporation and crystallization stages. Methanol (≥99.6%), chloroform (99.0-99.4%), chromium(III) acetyl acetonate (97%), tetramethyl-1,3,2-dioxaphospholane (Cl-TMDP, 95%) and cholesterol (> 99%) were purchased from Sigma-Aldrich. 1,3-propanediol (1,3-PDO) (98%) and pyridine HPLC grade (99.5+%) were purchased from Alfa Aesar. Adipic acid (AA) (99%), titanium (IV) isopropoxide (TTIP) (98+%) and extra dry toluene (99.85%) were supplied by Acros. All reactants were used without further purification. All solvents used for the analytical methods were of analytical grade.

3.2. Synthesis of copolyesters

Aliphatic copolyesters were synthesized by a two-stage melt polycondensation method (esterification and transesterification). Syntheses are performed in a 50 mL round bottom flask with a distillation device in order to remove all the by-products from the reaction (mostly water). All reactions were performed with a diol (1,3-PDO)/acid (SA and/or AA) molar ratio of 1.1/1.

During the first step (esterification), the reaction mixture was maintained under a constant argon flux and stirred at 300 rpm. The temperature of the reactor was set to 190 °C for 3 h. After 3 h of oligomerization, the remaining by-product of the reaction was distilled off by reducing the pressure to 200 mbar for 5 min, and then the proper amount (0.1 mol.% *vs.* the respective amount of diacid) of a 5 wt.% solution of TTIP in extra dry toluene was introduced inside the reactor. The reaction mixture was heated to 210 °C under a constant argon flux for 45 min. In the second step (transesterification), the temperature of the reactor was slowly increased to 230 °C and the pressure was decreased stepwise over periods of 5 min at 100, 50 and 25 mbar, respectively, in order to avoid excessive foaming and to minimize oligomer sublimation, which is a potential issue during the melt polycondensation. Finally, the pressure was decreased to 1-3 mbar and the transesterification continued for about 3-4 h. The global reaction scheme and conditions involved are summarized in Scheme 2.2.1. At the end, the synthesized polyester was cooled down, dissolved in chloroform and precipitated into a large volume of vigorously stirred cold methanol. Thereafter, the precipitate was

filtered, washed with methanol and dried under reduced pressure in an oven at 40 °C for 24h. Ivory white or pale yellow polyesters were finally obtained.

Several poly(propylene succinate-*co*-propylene adipate) (PPSA) were synthesized with different SA/AA molar ratios (100/0, 80/20, 50/50, 20/80 and 0/100). Samples are named "PPSxAy" with x and y as the molar proportion of succinate and adipate, respectively. The two homopolyesters ($PPS_{100}A_0$ and PPS_0A_{100}) are also named as PPS and PPA, respectively.

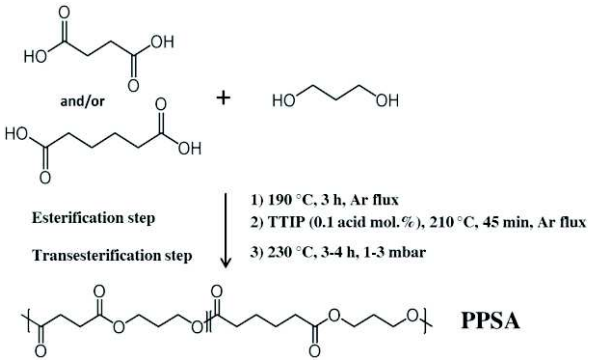

Scheme 2.2.1 : Reaction procedure for PPSA organometallic synthesis.

3.3. General methods and analysis

^{1}H- and ^{13}C-NMR spectra of polyesters were obtained with a Bruker 400 MHz spectrometer. $CDCl_3$ was used as solvent to prepare solutions with concentrations of 8-10 and 30-50 mg/mL for ^{1}H-NMR and ^{13}C-NMR, respectively. The number of scans was set to 128 for ^{1}H-NMR and at least 5,000 for ^{13}C-NMR. Calibration of the spectra was performed using the $CDCl_3$ peak (δ_H = 7.26 ppm, δ_C = 77.16 ppm).

^{31}P-NMR was performed after phosphitylation of the samples, according to standard protocols (Spyros et al., 1997). An accurately weighed amount of sample (approx. 100 mg) was dissolved in 500 µL of anhydrous $CDCl_3$. 100 µL of a standard solution of cholesterol (0.1 M in an anhydrous $CDCl_3$/pyridine (1/1.6) solution) containing Cr(III) acetyl acetonate as relaxation agent was then added. Finally, 50 µL of 2-chloro-4,4,5,5-tetramethyl-1,3,2-dioxaphospholane (Cl-TMDP) were added and the mixture was stirred at room temperature for 2 h. Spectra were recorded on a Bruker 400 MHz spectrometer (256 scans at 20 °C). All chemical shifts reported are relative to the reaction product of water with Cl-TMDP, which gives a sharp signal in pyridine/$CDCl_3$ at 132.2 ppm. The quantitative analysis of end-groups and the calculation of molar masses by ^{31}P-NMR were performed based on previous reports (Siotto et al., 2013; Spyros et al., 1997).

The number-average molar mass (M_n), the mass-average molar mass (M_w) and the dispersity (Đ) of the polyesters samples were determined in chloroform by Size Exclusion Chromatography (SEC), using a Shimadzu liquid chromatograph. The columns used were PLGel Mixed-C and PLGeL 100 Å. A refractive index detector was used. Chloroform was used as eluent at a flow rate of 0.8 ml/min. The apparatus was calibrated with linear polystyrene standards from 162 to 1,650,000 g/mol.

Infrared spectroscopy (IR) was performed with a Fourier transformed infrared spectrometer Nicolet 380 (Thermo Electron Corporation) used in reflection mode and equipped with an ATR diamond module (FTIR-ATR). The FTIR-ATR spectra were collected at a resolution of 4 cm^{-1} and with 64 scans per run.

Differential scanning calorimetry (DSC) was performed using a TA Instrument Q 200 under nitrogen (flow rate of 50 mL/min), calibrated with high purity standards. Samples of 2-3 mg were sealed in aluminum pans. Samples were stored at room temperature for at least two months prior to DSC analysis in order to let the polyester reach the crystallization equilibrium state. A three-step procedure was applied with a 10 °C/min ramp: (1) heating up from room temperature to 90 °C and holding for 3 min to erase the thermal history; (2) cooling down to -80 °C and holding for 3 min; (3) heating (second heating) from -80 °C to 90°C. The degree of crystallinity (X_c) was calculated according to Equation (2.2.1),

$$X_c(\%) = \frac{\Delta H_m}{\Delta H_m{}^0} \times 100 \qquad (2.2.1)$$

where ΔH_m is the melting enthalpy of samples and $\Delta H_m{}^0$ is the melting enthalpy of a 100% crystalline homopolyester.

Thermal degradations were studied by thermogravimetric analyses (TGA). Measurements were conducted under helium atmosphere (flow rate of 25 mL/min) using a Hi-Res TGA Q5000 apparatus from TA Instruments. Samples (1-3 mg) were heated from room temperature up to 600 °C at a rate of 20 °C/min. Isothermal degradation was performed for 2 h at 230 °C under an helium atmosphere.

Wide angle X-ray Scattering (WAXS) data were recorded on a Siemens D5000 diffractometer using Cu K_α radiation (1.5406 Å) at 25-30 °C in the range of 2θ = 14-32° at 0.4 °.min^{-1}. Analyses are performed on compression-molded sheets.

3.4. Ester function density

The ester function density of polyesters is defined by the number of ester function by repetitive unit on the number of carbons in the main chain by repetitive unit. The ester function density of PPSA copolyesters ($D_{ester,copo,PPSA}$) is defined by Equation (2.2.2),

$$D_{ester,copo,PPSA} = \chi_{SA} \times D_{ester,PPS} + \chi_{AA} \times D_{ester,PPA} \qquad (2.2.2)$$

where χ_{SA} and χ_{AA} are the succinate and adipate contents in copolyester, respectively. $D_{ester,PPS}$ and $D_{ester,PPA}$ are ester function densities of PPS and PPA, respectively.

4. Results

4.1. Characterization of macromolecular architectures of synthesized copolyesters

Different PPSA copolyesters were produced following a two-step melt polycondensation method (Scheme 2.2.1). In the first step, the non-catalyzed esterification reaction between 1,3-PDO and a mixture of diacids (SA/AA) resulted in formation of oligomers, which reached M_n of about 2,000-3,000 g/mol (determined by SEC) after 3 h of esterification, necessary to avoid any removal phenomenon during the next step. In the second step, the transesterification of previously synthesized oligomers using TTIP under vacuum resulted in a significant increase of copolyesters molar masses. The molar masses of final synthesized copolyesters determined by SEC are presented in Table 2.2.1. The synthesized copolyesters could be considered as high molar mass polyesters since the samples have M_n higher than 24,000 g/mol, with a dispersity of about 1.6-1.9. Polymerization yields determined after precipitation of samples are rather high and only vary in a narrow range (approx. 80–90%).

The final chemical structure of copolyesters was verified by ^{1}H-, ^{13}C-NMR and FTIR. ^{1}H-NMR of PPSA copolyesters is presented in Figure 2.2.1-a. In ^{1}H-NMR spectra, the presence of ester functions was verified by the signal at δ = 4.20-4.10 ppm assigned to COO-C$\underline{H_2}$-CH$_2$- protons from 1,3-PDO repeating units. This signal is complex due to the influence of neighboring dicarboxylate units (*i.e.*, two triplets at 4.17 and 4.14 ppm were detected for the neighboring succinate and adipate units, respectively). ^{1}H chemical shifts at δ = 1.70, 1.97, 2.32 and 2.61 ppm were ascribed to CO-CH$_2$-C$\underline{H_2}$- protons from adipate repeating units, to COO-CH$_2$-C$\underline{H_2}$- protons from 1,3-PDO repeating units, to CO-C$\underline{H_2}$-CH$_2$- protons from adipate repeating units and to CO-C$\underline{H_2}$-protons from succinate repeating units, respectively. Interestingly, the hydroxyl terminal group (HO-C$\underline{H_2}$-) signal was detected at δ = 3.67 ppm with low intensity, in agreement with the relatively high molar mass of the samples. The molar composition (SA/AA) of synthesized copolyesters was calculated from ^{1}H-NMR spectra using relative intensities of methylene protons in α of ester functions in succinate (δ = 2.62 ppm) and adipate (δ = 2.32 ppm) segments (more details in Annex 2). Determined SA and AA contents in the chains are given in Table 2.2.1. All synthesized copolyesters present SA/AA molar ratio equivalent to the initial feed ones, allowing a simple fabrication of copolyesters with a targeted composition. Previous studies showed that the non-catalyzed esterification rate with AA were much lower than with SA, for short aliphatic diols (Makay-Bödi, E. and Vancso-Szercsanyi, I., 1969; Vancsó-Szmercsányi et al., 1969). This can be explained by the small pKa difference of both diacids (*i.e.*, pKa_1/pKa_2 of 4.16/5.61 and 4.43/5.41 for SA and AA, respectively) which permitted to dissociate an higher proportion of acidic protons inside the reaction mixture, allowing an higher rate of auto-catalytic reaction. However, the presence of an excess of hydroxyl (OH) functions compared to carboxylic acid (COOH)

functions increased the overall esterification rate permitting a higher diacid conversion (Kuo and Chen, 1989; Lin and Hsieh, 1977). Moreover, the esterification time was set to 3 h in order to avoid free diacid residual monomer in the system. Finally, these experimental conditions permitted to override the reactivity difference and convert all feed diacid into oligomers before the second reactive step under high vacuum.

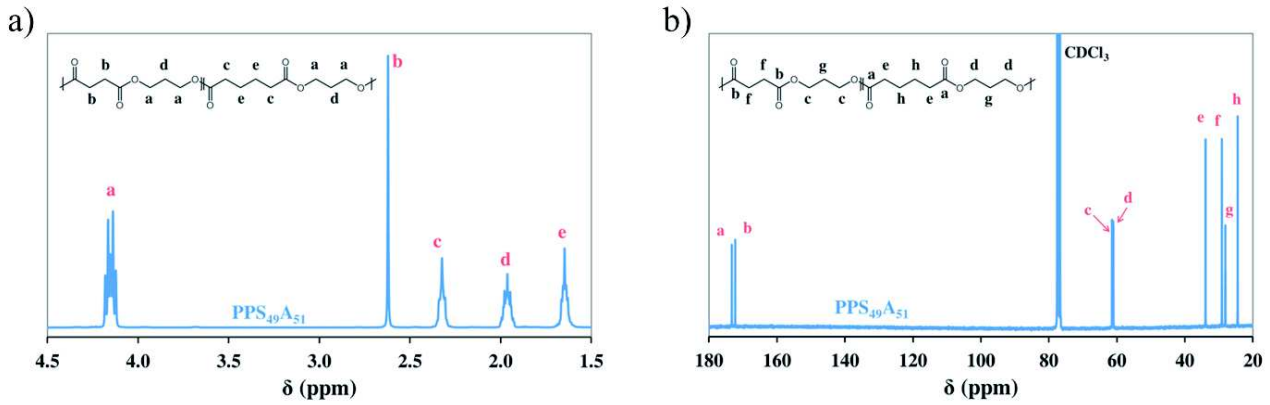

Figure 2.2.1 : (a) ^{1}H- and (b) ^{13}C-NMR of $PPS_{49}A_{51}$.

To obtain more detailed information about the structure of PPSA, ^{13}C-NMR was performed. ^{13}C-NMR of PPSA copolyesters is presented in Figure 2.2.1-b. ^{13}C chemical shifts at δ = 24.5, 33.9 and 173.3 ppm were ascribed to CO-CH_2-$\underline{C}H_2$-, CO-$\underline{C}H_2$-CH_2- and $\underline{C}$O-CH_2-CH_2- carbons from adipate repeating units, whereas ones at δ = 29.1 and 172.3 ppm were ascribed to CO-$\underline{C}H_2$-and $\underline{C}$O-CH_2- carbons from succinate repeating units, respectively. Finally, ^{13}C chemical shifts at δ = 28.1 (three peaks), 61.1 (two peaks) and 61.4 (two peaks) ppm were assigned to COO-CH_2-$\underline{C}H_2$-, COO-$\underline{C}H_2$-CH_2- next to an adipate repetitive unit and COO-$\underline{C}H_2$-CH_2- next to a succinate repetitive unit, respectively. The sensitivity of the ^{13}C-NMR to small differences in the chemical environment enabled us to identify the different triads SPS, SPA, and APA (with S, P and A standing for SA, 1,3-PDO and AA, respectively) presented in Figure 2.2.2-a. 1,3-PDO moieties are present in all three triads at distinctly different resonance absorptions close to chemical shifts of PPS ($PPS_{100}A_0$) or PPA (PPS_0A_{100}). Such results, with the splitting of the two signals (carbon atoms a_1, a_2, a_3 and a_4 in Figure 2.2.2), enable the calculation of the average sequence length of propylene-succinate (PS) and propylene-adipate (PA) units (L_{PS} and L_{PA}, respectively) and the degree of randomness (R) using Equations (2.2.3) to (2.2.5),

$$L_{PS} = 1 + \frac{2 \times I_{SPS}}{I_{SPA-S} + I_{SPA-A}} \qquad (2.2.3)$$

$$L_{PA} = 1 + \frac{2 \times I_{APA}}{I_{SPA-S} + I_{SPA-A}} \qquad (2.2.4)$$

$$R = \frac{1}{L_{PS}} + \frac{1}{L_{PA}} \qquad (2.2.5)$$

where I_{SPS}, $I_{SPA\text{-}S}$, $I_{SPA\text{-}A}$ and I_{APA} are intensities of peaks assigned to methylene carbons in α of the ester function in propyl segments (δ ~ 61.0-61.5 ppm) of SPS, SPA-S side, SPA-A side and APA triads in PPSA copolyesters. The corresponding data are listed in Table 2.2.1.

For fully random copolymers, R is equal to 1, whereas it is equal to 2 for strictly alternating and close to 0 for block copolymers. According to the SA/AA ratio, L_{PS} and L_{PA} varied between 1.4 and 4.6. PPSA copolyesters, composed of both diacids, all showed a randomness degree of about 1.0 meaning a random distribution between succinate and adipate segments along the polyester chain, as it was expected by using titanium-based organometallic catalyst (Chen et al., 2010; Debuissy et al., 2016a).

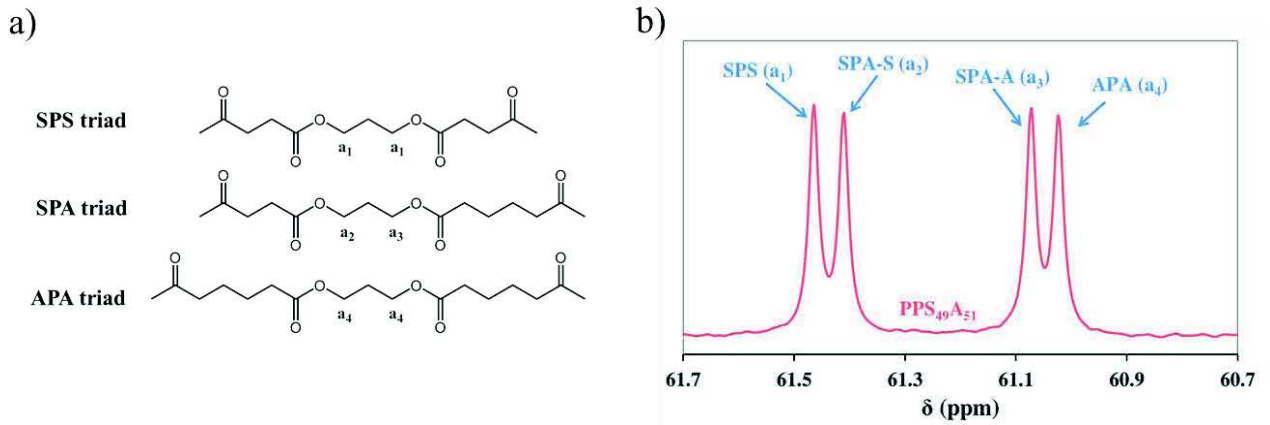

Figure 2.2.2 : (a) Potential triads of PPSA copolyesters, (b) ^{13}C-NMR spectra of $PPS_{49}A_{51}$ with high number of scans centered at δ ~ 61 ppm.

^{31}P-NMR analyses of PPSA copolyesters were performed in $CDCl_3$ with cholesterol as standard and ^{31}P-NMR spectra of copolyesters are presented in Figure 2.2.3-a. The ^{31}P-NMR analysis exhibited that all copolyesters showed COOH (134.9 ppm) and primary OH (147.4 ppm) end-groups. The majority of end-groups were OH functions (due to the higher amount of OH initially introduced in the reaction mixture compared to COOH). It was interesting to note that SA (134.85 ppm) and AA (134.90 ppm) end-groups were separated in ^{31}P-NMR spectra. The proportion of AA end-groups seemed to be slightly superior to the global AA content into the chain, for all copolyesters containing a mixture of diacids (Table SI.2 in Annex 2). From the transesterification and the corresponding random structure obtained, this latest result was surprising and unexpected.

The calculated M_n of copolyesters by ^{31}P-NMR were approx. 2-3 times smaller compared to the one obtained by SEC, the latter being overestimated partly due to the calibration based on PS standards. M_n determined by ^{31}P-NMR varied between 8,500 and 15,000 g/mol and this technique gave a more accurate estimation of the aliphatic copolyesters molar mass. However, this method based on the quantification of end-groups did not take into account the possible macrocycles that could have been produced during the polyester synthesis and were present on the polymer matrix but undetectable by ^{31}P-NMR analysis (Charlier, Q. et al., 2015; Yashiro et al., 2009b).

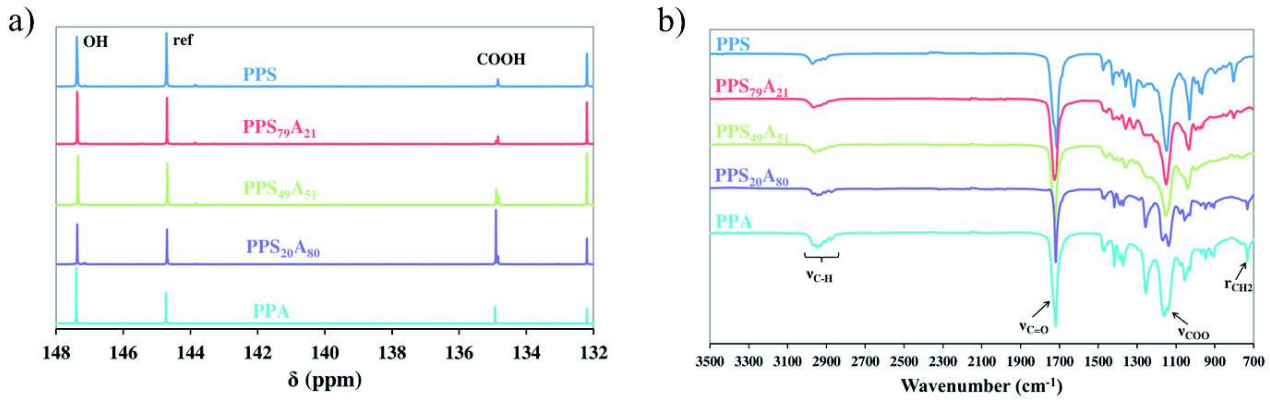

Figure 2.2.3 : (a) ^{31}P-NMR and (b) FTIR spectra of PPSA copolyesters.

The FTIR analysis of PPSA copolyesters showed some interesting results. FTIR spectra of all copolyesters are presented in Figure 2.2.3-b. First, in all copolyesters, no broad signals around 3200-3400 cm^{-1} assigned to the O-H vibration of COOH and OH end-groups were observed confirming the high molar mass of the synthesized copolyesters. Then, all samples exhibited a sharp signal at approx. 1725 cm^{-1} assigned to the C=O stretching vibration from ester groups confirming the synthesis of esters functions, whereas signals at 2850-3000 cm^{-1} were assigned to C-H stretching vibrations of methylene carbons. In PPSA copolyesters, signals at 1315, 1030 and 805 cm^{-1} assigned to the symmetric C-O stretching, O-CH_2- stretching and -CH_2- rocking vibrations shifted to 1255, 1055 and 735 cm^{-1} with the increase of the adipate content in copolyesters, respectively. There was, thus, a modification of the FTIR spectra profile with the

SA/AA composition. Finally, the intensity of the strong asymmetric –COO- stretching vibration of PPS at 1150 cm^{-1} decreased and the signal split into two bands at approx. 1140-1160 cm^{-1} when adipate units became majority.

Table 2.2.1 : Molar composition and molar masses of synthesized PPSA copolyesters.

Sample	Feed SA/AA composition	^{1}H-NMR	SEC			^{31}P-NMR		^{13}C-NMR		
		Det. SA/AA composition	M_n	M_w	Đ	M_n	OH end-groups	L_{PS}	L_{PA}	R
	mol.%	mol.%	kg/mol	kg/mol		kg/mol	%			
$PPS_{100}A_0$	100 / 0	100 / 0	35.2	57.9	1.6	15.5	88	-	-	-
$PPS_{79}A_{21}$	80 / 20	79.4 / 20.6	38.2	64.4	1.7	14.4	82	4.6	1.3	1.00
$PPS_{49}A_{51}$	50 / 50	49.2 / 50.8	36.4	68.1	1.9	11.8	67	2.0	2.0	1.01
$PPS_{20}A_{80}$	20 / 80	20.4 / 79.6	24.0	40.6	1.7	8.5	44	1.3	4.5	1.02
PPS_0A_{100}	0 / 100	0 / 100	28.6	46.5	1.6	10.1	77	-	-	-

4.2. Thermal degradation

TGA traces of PPSA samples are shown in Figure 2.2.4 with their corresponding derivative curves (DTG). Data are summarized in Table 2.2.2. Under helium, all copolyesters degraded in two main steps which involve competitive mechanisms. First, a small mass loss was observed at 260-315 °C due to the degradation of low molar mass chains along with the cyclization at the chain-ends and back-biting reactions that are responsible for CO_2 and H_2O release, which are produced from the decomposition of COOH and OH chain-ends, respectively (Scheme SI.1 in Annex 1) (Chrissafis et al., 2006a; Persenaire et al., 2001). Secondly, a major degradation occurred at 315-425 °C with a substantial mass loss of approx. 90% corresponding to the thermal degradation of polyesters chains, mostly by β- and α-hydrogen bond scissions. These reactions are responsible for the decomposition of polyesters into small compounds such as diacids, vinyl compounds, aldehydes and anhydrides (Bikiaris et al., 2007; Persenaire et al., 2001). After this decomposition step, mass residue of approx. 4% still remains. This multi-step degradation is in agreement with previous reports (Debuissy et al., 2016a; Zorba et al., 2007).

The 2% mass loss degradation temperature ($T_{d,2\%}$) of all copolyesters were about 290-310 °C and seemed to increase with the adipate content. By taking $T_{d,2\%}$ as criterion for the thermal stability of polyesters, PPS ($PPS_{100}A_0$) possessed the lowest thermal stability. The 50 % mass loss degradation temperature ($T_{d,50\%}$) and the maximal degradation temperature ($T_{deg,max}$) were approx. 365-380 and 375-395 °C, respectively. Both degradation temperatures decreased with the adipate content. In conclusion, the thermal degradation profile of PPSA depended highly on the SA/AA molar composition and the degradation profile was sharper with adipate rich copolyesters compared to succinate rich copolyesters. This result was in contradiction to a previous study which showed that the degradation mechanism depended highly on the diol unit, whereas the influence of the carboxylic acid unit was minor (Plage and Schulten, 1990). Since only one diol was used along this study, its influence on the degradation cannot be investigated. Nevertheless, this study had clearly proved that the influence of the diacid was far to be negligible. The simplest way to interpret our results is to consider that aliphatic polyesters can be modeled to polyethylene chains containing esters groups. It is well established that the introduction of esters into a polyethylene chain reduces its thermal stability, the effect being proportional to their concentration (Vinogradova and Korshak, 1965). Therefore, it was not surprising that the thermal stability of copolyesters increased with the adipate content. Indeed, by increasing the amount of adipate unit in the copolyester, the relative ester function density (D_{ester}), determined by Equation (2.2.2), decreased.

The isothermal mass loss curves at 230 °C (*i.e.*, transesterification step reaction temperature) under helium of copolyesters are presented in Figure 2.2.5. The isothermal degradation of PPS, $PPS_{79}A_{21}$ and $PPS_{49}A_{51}$ exhibited a linear decrease of the sample mass for 2 h, whereas the isothermal degradation profile of $PPS_{20}A_{80}$ and PPA were rather composed of two linear segments with an increase of the degradation rate after 1 h. One can suppose the presence of two mechanisms for $PPS_{20}A_{80}$ and PPA, contrary to other copolyesters, the first one at the beginning of the thermal degradation and the second one after the thermal degradation initiation. The presence of two mechanisms for the thermal degradation of PPA was previously stated, even if this result was obtained from a non-isothermal degradation

and not an isothermal degradation (Zorba et al., 2007). This could explain the difference on the appearance of the second mechanism which started after a mass loss of approx. 3-4% whereas in the literature it is reported to start only after a 30% mass loss. In the case of PPS, two degradation mechanisms were reported in the literature with the second one starting after a 10% mass loss (Chrissafis et al., 2006b). However, according to our results no second mechanism was observed. But, as for PPA, the difference of behavior could be due to the difference on the thermal degradation process used and to the fact that the temperature of isothermal degradation was much lower than temperatures reached during the non-isothermal degradation.

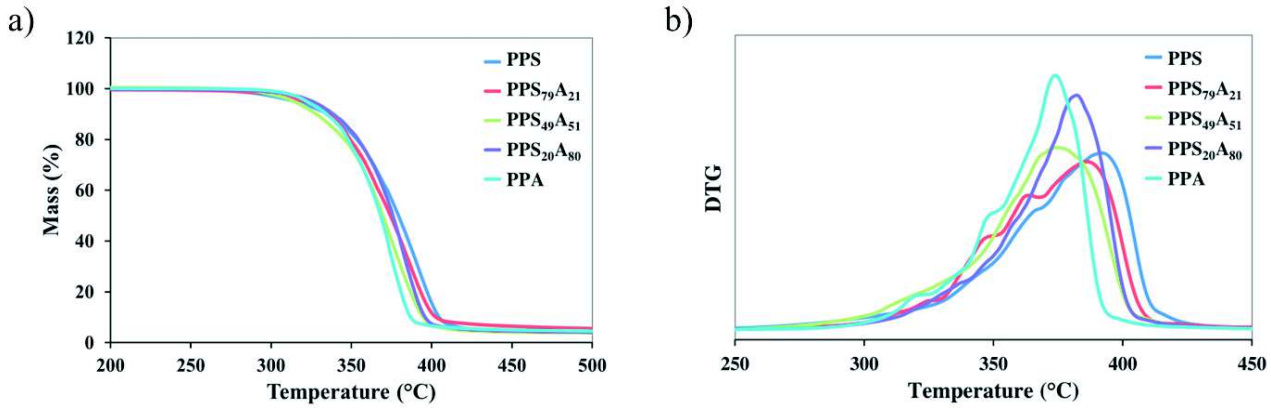

Figure 2.2.4 : (a) Mass loss and (b) DTG curves of PPSA copolyesters under helium at 20 °C/min.

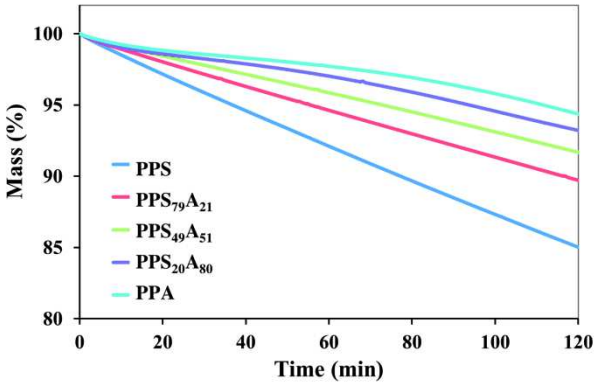

Figure 2.2.5 : Mass loss curves of PPSA copolyesters during the isothermal degradation at 230 °C under helium.

Table 2.2.2 : TGA results of PPSA copolyesters thermal degradation under helium.

		Non-isothermal degradation (20°C/min)				Isothermal degradation	
						1st mechanism	2nd mechanism
Sample	D_{ester}	$T_{d,2\%}$	$T_{d,50\%}$	$T_{deg,max}$	Residue at 500 °C	Mass loss rate (x10^2)	Mass loss rate (x10^2)
	%	°C	°C	°C	wt.%	wt.% / min	wt.% / min
PPS ($PPS_{100}A_0$)	28.6	292	379	392	3.4	11.9	-
$PPS_{79}A_{21}$	27.3	300	374	386	3.9	8.2	-
$PPS_{49}A_{51}$	25.4	299	370	374	3.9	6.9	-
$PPS_{20}A_{80}$	23.5	309	376	382	4.1	3.5	6.7
PPA (PPS_0A_{100})	22.2	311	368	374	4.3	2.7	6.5

4.3. Crystalline structure and thermal properties

To investigate the crystalline structure of copolyesters, a WAXS study was first performed. The patterns of PPSA copolyesters are shown in Figure 2.2.6. WAXS patterns of the copolyesters appeared to be characterized by well-defined diffraction peaks over the whole composition range, excepted for $PPS_{49}A_{51}$ which was amorphous at room

temperature. According to profile shapes, it could be deduced that, in each sample, only one crystalline phase was present. The patterns of semi-crystalline copolyesters could be divided into two groups according to the adipate content. Copolyesters containing 21 mol.% or less of adipate units are characterized by X-ray patterns very similar to PPS, indicating that the crystal structure in these copolyesters has the same characteristics as the PPS lattice. On the contrary, samples containing 80 mol.% or more of adipate units crystallized according to the PPA lattice. The crystal structure of PPS exhibited diffraction peaks at 2θ = 17.9, 19.4, 20.3, 22.3 and 25.9°, whereas PPA showed diffraction peaks at 2θ = 18.9, 20.2, 21.0, 22.1, 24.3 and 26.8°, respectively. The diffraction patterns of these two homopolyesters were similar to previously reported ones (Papageorgiou and Bikiaris, 2007; Soccio et al., 2007). However, until now, no clear crystal lattice parameters of PPS and PPA homopolyesters have been reported. On one hand, Hernandez *et al.* claimed that the PPS and PPA crystallized according to the monoclinic unit cell with different crystal unit cell parameters for PPS (a = 0.4493 nm, b = 0.9254 nm, c = 1.0500 nm and α = 75°) and PPA (a = 0.5067 nm, b = 0.9420 nm, c = 1.2600 nm and α = 57°) (Hernández et al., 2010). However, on the other hand, Jourdan *et al.* claimed that polyesters which have an odd number of methylene groups in the glycol or in the acid segment adopt an orthorhombic unit cell (Jourdan et al., 1995). $PPS_{79}A_{21}$ and $PPS_{20}A_{80}$ showed diffraction patterns similar to PPS and PPA, respectively, but with lower intensities. For $PPS_{79}A_{21}$, the co-monomeric unit (adipate in this case) incorporated in minor amount was found to be excluded from the PPS crystal lattice or only partially integrated. This phenomenon decreased the crystal strength and lamellae sizes due to the presence of "adipate defects" inside the chain and, thus, the $PPS_{79}A_{21}$ degree of crystallinity decreased compared to PPS. Similar phenomenon was observed for $PPS_{20}A_{80}$, with succinate units being excluded or only partially integrated inside the PPA crystal lattice. The presence of defects in the chain led to a small modification of the crystalline structure proved by the quite larger and small shifts of copolyesters diffraction peaks compared to those of homopolyesters.

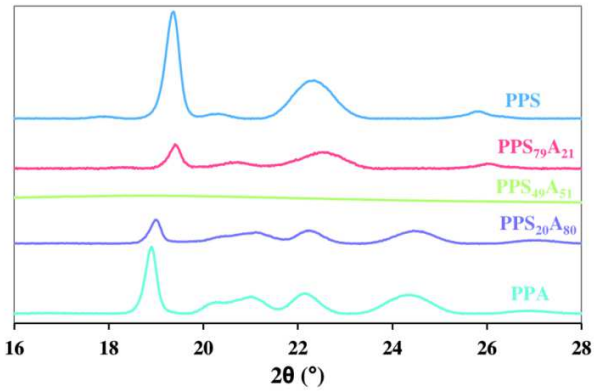

Figure 2.2.6 : WAXS patterns of PPSA copolyesters.

In complement to WAXS analysis, the degree of crystallinity and thermal properties of copolyesters were studied by DSC. Prior to this, it has been verified, from TGA results, that no significant degradation occurred for the copolyesters in the DSC analyses temperature range. The melting temperatures (T_m) and melting enthalpies (ΔH_m) of copolyesters, taken from the first heating scan, were plotted in Figure 2.2.7 in function of the adipate content. The second heating scan curves are presented in Figure 2.2.8-a and all corresponding data are summarized in Table 2.2.3. The variation of thermal properties is also discussed as a function of D_{ester}.

From the first heating scan, one can see that $PPS_{79}A_{21}$ shows lower T_m and ΔH_m values compared to PPS. As observed in WAXS, the crystal strength and lamellae sizes decreased with the incorporation of the adipate co-monomeric unit making crystals easier to melt. The same phenomenon was observed with $PPS_{20}A_{80}$ which showed lower T_m and ΔH_m values than PPA due to the succinate units acting as "defects". One can observe, thus, a classical thermal profile for random copolyesters in which both T_m and ΔH_m seemed to exhibit a pseudo-eutectic point. The presence of both T_m and ΔH_m pseudo-eutectic points as well as the presence of only one crystalline phase for each sample let suppose the presence of an isodimorphic co-crystallization behavior as observed for other aliphatic random copolyesters (Arandia et al., 2015; Díaz et al., 2014; Papageorgiou and Bikiaris, 2007).

The melting enthalpy value of 100% crystalline phase ($\Delta H_m°$) is determined from the groups contribution method as proposed by Van Krevelen (Van Krevelen, 1997) for PPA (124 J/g) and from experimental data (Papageorgiou and

Bikiaris, 2005a) for PPS (140 J/g). WAXS results showed that each copolyester exhibited only one type of crystal lattice. The degree of crystallinity (X_c) of copolyesters was calculated from the first heating scan and values are summarized in Table 2.2.3. X_c of PPA was higher than the one of PPS. One can suppose that, contrary to succinate units, the adipate units bring more flexibility to the chain which facilitates the crystallization

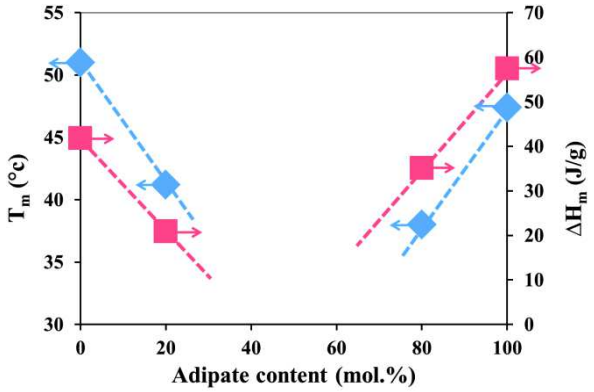

Figure 2.2.7 : Variation of T_m and ΔH_m vs. adipate content during the 1st heating scan at 10 °C/min.

During the cooling run at controlled rate (10 °C/min), none of PPSA samples were able to crystallize and, thus, the second heating run was characterized only by an intense endothermal baseline deviation associated to the glass-transition phenomenon, with the exception of PPA. DSC curves of the latter, beside the T_g, also exhibited a cold-crystallization exotherm at approx. 7 °C and a fusion endotherm at 31 °C. At a lower cooling/heating rate of 5 °C/min (Table SI.3 in Annex 2), only PPA showed a partial crystallization phenomenon during the cooling run, which was completed by a cold-crystallization during the heating run. T_m (42 °C) and ΔH_m (40 J/g) of PPA crystals formed at 5 °C/min were higher than for the cooling/heating runs at 10 °C/min due to the higher degree of crystallinity. Moreover, PPS exhibited tiny cold-crystallization and melting phenomena of 1 J/g. All other compositions were unable to crystallize at cooling/heating rate of 5 °C/min. This result proved the decrease of the crystallization rate with the introduction of a co-monomer acting as "defects" in the chain, even if this co-monomer has a higher ability to crystallize.

T_g values are summarized in Table 2.2.3 and are plotted in Figure 2.2.8-b as a function of the adipate content. As can be seen, T_g was influenced by the amount of adipate unit in the copolyester chain and decreased continuously from -29 to -54 °C for adipate content ranging from 0 to 100%, respectively. Indeed, by increasing the amount of adipate unit in the copolyester, D_{ester} decreased. Moreover, it is well known that the second-order transition temperature is considered as a measure of the chain flexibility of the polymer chain. The more flexible the chains are, the lower the T_g is. By decreasing D_{ester} of the copolyester chain, a lower amount of intra or inter-chain interactions between ester groups were possible, whence the increase of chain mobility leading to the decrease of T_g.

In random copolyesters, T_g is usually a monotonic function of composition and the most common relationship used to predict T_g as a function of a co-monomer content is the Fox equation (Fox, 1956), defined by Equation (2.2.6).

$$\frac{1}{T_{g,copo}} = \frac{w_1}{T_{g,1}} + \frac{w_2}{T_{g,2}} \qquad (2.2.6)$$

where $T_{g,1}$ and $T_{g,2}$ are the glass transition temperatures of homopolyesters, and w_1 and w_2 their respective mass fractions.

However, as one can observe in Figure 2.2.8-b, the Fox equation did not fit with the experimental data when using the T_g experimentally measured on PPS and PPA. Although Soccio *et al.* used this relation to describe the T_g evolution of PPSA in function of adipate content (Soccio et al., 2009). However, a doubt could be permitted on these reported data since their graph scale was large. Another relationship is used for copolymers with a mixing law, the Gordon-Taylor equation (Gordon and Taylor, 2007), defined by Equation (2.2.7),

$$T_{g,copo} = \frac{w_1\, T_{g,1} + k(1-w_1)\, T_{g,2}}{w_1 + k(1-w_1)} \qquad (2.2.7)$$

where $T_{g,1}$ and $T_{g,2}$ are the glass transition temperatures of homopolyesters, w_1 is the respective mass fraction of the homopolyester 1 and k the Gordon-Taylor parameter.

As shown in Figure 2.2.8-b, the Gordon-Taylor equation fitted well the experimental data with k = 0.61. In the original version of volume additivity, the parameter $k = \rho_1\Delta\alpha_2/\rho_2\Delta\alpha_1$ has a well-defined significance (ρ_i is the density and $\Delta\alpha_i = \alpha_{melt} - \alpha_{glass}$ is the increment at T_g of the expansion coefficient of the respective component i). But generally k is considered a real fitting parameter (Penzel et al., 1997). T_g of PPSA could be, thus, predicted for all the composition range using this relation.

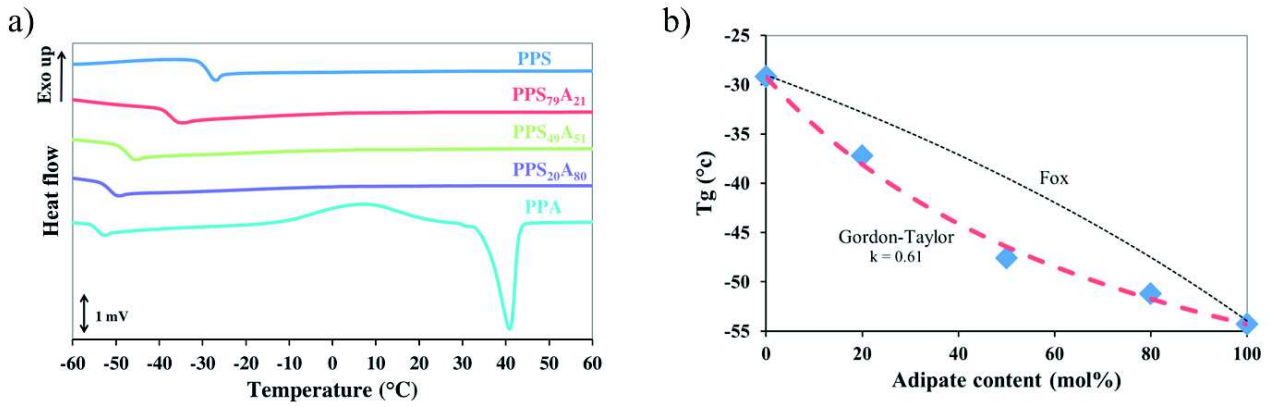

Figure 2.2.8 : (a) 2nd heating DSC curves and (b) variation of the copolyester T_g vs. adipate content in PPSA.

Table 2.2.3 : DSC results of PPSA copolyesters with heating and cooling rate of 10 °C/min.

Sample	D_{ester}	1st heating			cooling		2nd heating					
		T_m	ΔH_m	χ	T_c	ΔH_c	T_g	T_{cc}	ΔH_{cc}	T_m	ΔH_m	χ
	%	°C	J/g	%	°C	J/g	°C	°C	J/g	°C	J/g	%
PPS ($PPS_{100}A_0$)	28.6	51	42	30	-	-	-29	-	-	-	-	-
$PPS_{79}A_{21}$	27.3	41	21	15	-	-	-37	-	-	-	-	-
$PPS_{49}A_{51}$	25.4	-	-	-	-	-	-47	-	-	-	-	-
$PPS_{20}A_{80}$	23.5	38	35	28	-	-	-51	-	-	-	-	-
PPA (PPS_0A_{100})	22.2	47	58	46	-	-	-54	7	17	31	18	15

5. Conclusion

Different biobased copolyesters (PPSA) based on renewable building blocks were successfully synthesized, at different compositions and architectures, in melt using TTIP as an effective catalyst. The selected synthetic pathway permitted to obtain (i) high molar masses polymers, (ii) final copolyesters with the same molar compositions than the initial feed ratios and (iii) a random distribution between succinate and adipate segments along the chains.

PPSA copolyesters exhibited a good thermal stability which slightly increased with the adipate content. Moreover, the thermal degradation profile of PPSA copolyesters was driven by the major diacid component, resulting in an acceleration of the degradation rate after the onset in copolyesters based principally on adipate. Furthermore, the isothermal degradation of copolyesters with 50 mol.% or less of adipate showed a degradation mechanism in one step, whereas copolyesters with 80 mol.% or more of adipate showed a mechanism in two steps with an acceleration of the degradation rate after the thermal degradation initiation.

Furthermore, PPSA copolyesters seemed to show an isodimorphic behavior characterized by the presence of only one crystalline phase for each sample and a pseudo-eutectic melting behavior. Moreover, the very slow crystallization rate

of PS or PA phases due to the presence of 1,3-PDO, induced an absence of crystallization or cold-crystallization phenomena for almost all compositions, except the one fully based on adipate (PPA), leading to mostly amorphous material after the second heating run. T_g of copolyesters decreased with the adipate content according to the Gordon-Taylor relation with a calculated Gordon-Taylor parameter, k, of 0.61. The decrease of T_g was ascribed to the increase in copolyester chain mobility resulting from the decrease of the ester function density.

The synthesis of PPSA copolyesters is, thus, an excellent example to highlight the influence of the macromolecular engineering on material properties. Indeed, the use of 1,3-PDO as a "crystallization retardant" could be very interesting for some applications such as adhesives or for specific biomedical properties, even if the macromolecular engineering must be pursued in order to obtain the adequate tailor-made properties. Additional tests should be carried out to determine biodegradability and biocompatibility of these biobased macromolecular architectures.

6. References

Arandia, I., Mugica, A., Zubitur, M., Arbe, A., Liu, G., Wang, D., Mincheva, R., Dubois, P., Müller, A.J., 2015. Macromolecules 48, 43–57.

Avérous, L., 2004. J. Macromol. Sci. Part C 44, 231–274.

Avérous, L., Fringant, C., 2001. Polym. Eng. Sci. 41, 727–734.

Bechthold, I., Bretz, K., Kabasci, S., Kopitzky, R., Springer, A., 2008. Chem. Eng. Technol. 31, 647–654.

Becker, J., Lange, A., Fabarius, J., Wittmann, C., 2015. Curr. Opin. Biotechnol. 36, 168–175.

Biebl, H., Menzel, K., Zeng, A.-P., Deckwer, W.-D., 1999. Appl. Microbiol. Biotechnol. 52, 289–297.

Bikiaris, D.N., Chrissafis, K., Paraskevopoulos, K.M., Triantafyllidis, K.S., Antonakou, E.V., 2007. Polym. Degrad. Stab. 92, 525–536.

Bikiaris, D.N., Papageorgiou, G.Z., Achilias, D.S., 2006. Polym. Degrad. Stab. 91, 31–43.

Bikiaris, D.N., Papageorgiou, G.Z., Giliopoulos, D.J., Stergiou, C.A., 2008. Macromol. Biosci. 8, 728–740.

Bozell, J.J., Petersen, G.R., 2010. Green Chem. 12, 539.

Charlier, Q., Girard, E., Freyermouth, F., Vandesteene, M, Jacquel, N., Ladavière, C., Rousseau, A., Fenouillot, F., 2015. Express Polym. Lett. 9, 424–434.

Chen, C.-H., Peng, J.-S., Chen, M., Lu, H.-Y., Tsai, C.-J., Yang, C.-S., 2010. Colloid Polym. Sci. 288, 731–738.

Chen, M.S., Chang, S.J., Chang, R.S., Kuo, W.F., Tsai, H.B., 1990. J. Appl. Polym. Sci. 40, 1053–1057.

Choi, S., Song, C.W., Shin, J.H., Lee, S.Y., 2015. Metab. Eng. 28, 223–239.

Chrissafis, K., Paraskevopoulos, K.M., Bikiaris, D.N., 2006a. Thermochim. Acta 440, 166–175.

Chrissafis, K., Paraskevopoulos, K.M., Bikiaris, D.N., 2006b. Polym. Degrad. Stab. 91, 60–68.

Debuissy, T., Pollet, E., Avérous, L., 2016a. Polymer 99, 204–213.

Debuissy, T., Pollet, E., Avérous, L., 2016b. Biomacromolecules 17, 4054–4063.

Debuissy, T., Pollet, E., Avérous, L., 2017. Eur. Polym. J. 87, 84–98.

Díaz, A., Franco, L., Puiggalí, J., 2014. Thermochim. Acta 575, 45–54.

Drożdżyńska, A., Leja, K., Czaczyk, K., 2011. BioTechnologia 1, 92–100.

Fox, T., 1956. Bull. Am. Phys. Soc. 1, 123–132.

Gordon, M., Taylor, J.S., 2007. J. Appl. Chem. 2, 493–500.

Hernández, J.J., Rueda, D.R., García-Gutiérrez, M.C., Nogales, A., Ezquerra, T.A., Soccio, M., Lotti, N., Munari, A., 2010. Langmuir 26, 10731–10737.

Ho, R.-M., Ke, K.-Z., Chen, M., 2000. Macromolecules 33, 7529–7537.

Jacquel, N., Freyermouth, F., Fenouillot, F., Rousseau, A., Pascault, J.P., Fuertes, P., Saint-Loup, R., 2011. J. Polym. Sci. Part Polym. Chem. 49, 5301–5312.

Jourdan, N., Deguire, S., Brisse, F., 1995. Macromolecules 28, 8086–8091.

Kuo, C.-T., Chen, S.-A., 1989. J. Polym. Sci. Part Polym. Chem. 27, 2793–2803.

Lin, C.C., Hsieh, K.H., 1977. J. Appl. Polym. Sci. 21, 2711–2719.

Lu, S.-F., Chen, M., Chen, C.H., 2012. J. Appl. Polym. Sci. 123, 3610–3619.

Lu, S.-F., Chen, M., Shih, Y.-C., Chen, C.H., 2010. J. Polym. Sci. Part B Polym. Phys. 48, 1299–1308.

Makay-Bödi, E., Vancso-Szercsanyi, I., 1969. Eur. Polym. J. 5, 145.

Nanaki, S.G., Pantopoulos, K., Bikiaris, D.N., 2011. Int. J. Nanomedicine 6, 2981–2995.

Papageorgiou, G.Z., Bikiaris, D.N., 2005. Polymer 46, 12081–12092.

Papageorgiou, G.Z., Bikiaris, D.N., 2007. Biomacromolecules 8, 2437–2449.

Papageorgiou, G.Z., Bikiaris, D.N., 2009. Macromol. Chem. Phys. 210, 1408–1421.

Pellis, A., Herrero Acero, E., Gardossi, L., Ferrario, V., Guebitz, G.M., 2016. Polym. Int. 65, 861–871.

Penzel, E., Rieger, J., Schneider, H.A., 1997. Polymer 38, 325–337.

Pérez-Camargo, R.A., Fernández-d'Arlas, B., Cavallo, D., Debuissy, T., Pollet, E., Avérous, L., Müller, A.J., 2017. Macromolecules.

Persenaire, O., Alexandre, M., Degée, P., Dubois, P., 2001. Biomacromolecules 2, 288–294.

Picataggio, S., Rohrer, T., Deanda, K., Lanning, D., Reynolds, R., Mielenz, J., Eirich, L.D., 1992. Nat. Biotechnol. 10, 894–898.

Plage, B., Schulten, H.R., 1990. Macromolecules 23, 2642–2648.

Polen, T., Spelberg, M., Bott, M., 2013. J. Biotechnol., Research on Industrial Biotechnology within the CLIB-Graduate Cluster - Part III 167, 75–84.

Pollet, E., Avérous, L., 2011. Production, Chemistry and Properties of Polyhydroxyalkanoates, in: Plackett, D. (Ed.), Biopolymers – New Materials for Sustainable Films and Coatings. John Wiley & Sons, Ltd, Chichester, pp. 65–86.

Siotto, M., Zoia, L., Tosin, M., Degli Innocenti, F., Orlandi, M., Mezzanotte, V., 2013. J. Environ. Manage. 116, 27–35.

Soccio, M., Lotti, N., Finelli, L., Gazzano, M., Munari, A., 2007. Polymer 48, 3125–3136.

Soccio, M., Lotti, N., Finelli, L., Gazzano, M., Munari, A., 2009. Eur. Polym. J. 45, 3236–3248.

Spyros, A., Argyropoulos, D.S., Marchessault, R.H., 1997. Macromolecules 30, 327–329.

Stempfle, F., Ortmann, P., Mecking, S., 2016. Chem. Rev. 116, 4597–4641.

Umare, S.S., Chandure, A.S., Pandey, R.A., 2007. Polym. Degrad. Stab. 92, 464–479.

Van Krevelen, D.W., 1997. Chapter 5 - Calorimetric properties, in: Properties of Polymers (Third, Completely Revised Edition). Elsevier, Amsterdam, pp. 109–127.

Vancsó-Szmercsányi, I., Maros-Gréger, K., Makay-Bödi, E., 1969. Eur. Polym. J. 5, 155–161.

Vardon, D.R., Franden, M.A., Johnson, C.W., Karp, E.M., Guarnieri, M.T., Linger, J.G., Salm, M.J., Strathmann, T.J., Beckham, G.T., 2015. Energy Env. Sci 8, 617–628.

Vilela, C., Sousa, A.F., Fonseca, A.C., Serra, A.C., Coelho, J.F.J., Freire, C.S.R., Silvestre, A.J.D., 2014. Polym. Chem. 5, 3119–3141.

Vinogradova, S.V., Korshak, V.V., 1965. , in: Polyesters, Chapt. 6. Pergamon Press, Oxford.

Wang, B., Li, C.Y., Hanzlicek, J., Cheng, S.Z.D., Geil, P.H., Grebowicz, J., Ho, R.-M., 2001. Polymer 42, 7171–7180.

Ward, I.M., Wilding, M.A., Brody, H., 1976. J. Polym. Sci. Polym. Phys. Ed. 14, 263–274.

Werpy, T.A., Holladay, J.E., White, J.F., 2004. Top Value Added Chemicals from Biomass: I. Results of Screening for Potential Candidates from Sugars and Synthesis Gas (No. PNNL-14808). Pacific Northwest National Laboratory (PNNL), Richland, WA (US).

Xu, J., Guo, B.-H., 2010. Biotechnol. J. 5, 1149–1163.

Xu, Y., Xu, J., Guo, B., Xie, X., 2007. J. Polym. Sci. Part B Polym. Phys. 45, 420–428.

Xu, Y., Xu, J., Liu, D., Guo, B., Xie, X., 2008. J. Appl. Polym. Sci. 109, 1881–1889.

Yamadera, R., Murano, M., 1967. J. Polym. Sci. [A1] 5, 2259–2268.

Yashiro, T., Kricheldorf, H.R., Huijser, S., 2009. Macromol. Chem. Phys. 210, 1607–1616.

Zorba, T., Chrissafis, K., Paraskevopoulos, K.M., Bikiaris, D.N., 2007. Polym. Degrad. Stab. 92, 222–230.

Sub-chapter 2.3. Study on the structure-properties relationship of biodegradable and biobased aliphatic copolyesters based on 1,3-propanediol, 1,4-butanediol, succinic and adipic acids.

Thibaud Debuissy[1], Parveen Sangwan[2], Eric Pollet[1] and Luc Avérous[1]*

[1] BioTeam/ICPEES-ECPM, UMR CNRS 7515, Université de Strasbourg, 25 rue Becquerel, 67087 Strasbourg Cedex 2, France

[2] CSIRO Manufacturing Flagship, Private Bag 10, Clayton South, Victoria, 3169, Australia

*Corresponding author: luc.averous@unistra.fr

Published by Polymer, 2017, 122, 105-116

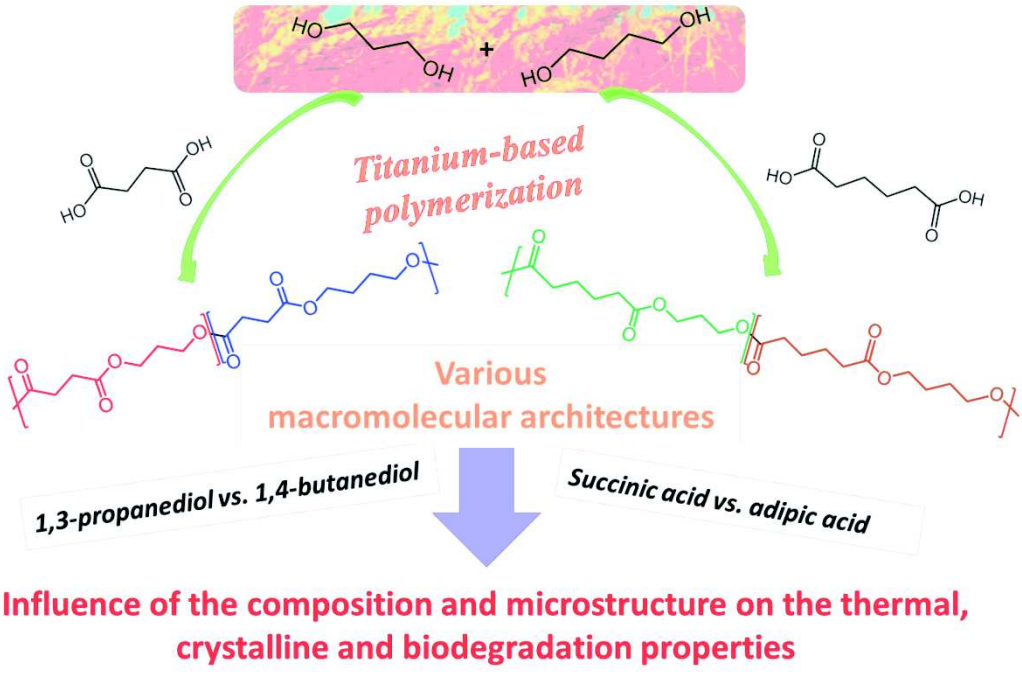

1. Abstract

Two series of high molar mass biobased aliphatic copolyesters [poly(1,3-propylene succinate-ran-1,4-butylene succinate) (PPBS) and poly(1,3-propylene adipate-ran-1,4-butylene adipate) (PPBA) were synthesized with different 1,3-propanediol/1,4-butanediol (1,3-PDO/1,4-BDO) molar ratio by transesterification in melt, using titanium (IV) isopropoxide as catalyst. NMR, SEC, FTIR, WAXS, TGA and DSC analyses and aerobic biodegradation in soil measurements were used to fully characterize copolyesters. Their compositions were similar to the feed ones with random distribution of 1,3-PDO and 1,4-BDO segments along chains. Copolyesters exhibited an excellent stability until at least 275 °C with a degradation profile dependent only of the diacid structure. Moreover, the shortening of the diacid and diol lengths induced an increase of Tg and a decrease of the crystallization rate, especially with 1,3-PDO, until having amorphous copolyesters for 1,3-PDO content of 60-100 and 80 mol.% for PPBS and PPBA, respectively. Furthermore, both copolyesters showed an isodimorphic co-crystallization behavior characterized by a pseudo-eutectic melting behavior and the presence of only one crystalline phase, except for PPBA with 1,3-PDO content of 50-59 mol.% which were in molten state. Lastly, the aerobic biodegradation rate in soil increased with the increase of the diacid length from succinic to adipic acids and the diol length from 1,3-propanediol to 1,4-butanediol monomers without showing any residual ecotoxicity.

2. Introduction

Over the last decades, renewable polymers as an alternative to petroleum-based materials have attracted considerable attention from both academic and industrial groups. These biobased polymers can also present new macromolecular architectures with advanced properties (Vilela et al., 2014a). Among them, poly(hydroxyalkanoate)s (Pollet and Avérous, 2011), poly(lactic acid) (Avérous, 2004), poly(butylene succinate) (PBS) (Gigli et al., 2016a) have seen their interest and industrial productions growing for various fields e.g., on packaging, agriculture, biomedical applications or sanitary.

Till recently, biobased 1,3-propanediol (1,3-PDO) was not available in the market at low cost with sufficient purity for chemical purposes. These disadvantages have been lately overcome by the development of new bioprocesses permitting an increase of the industrial production using biochemical pathways, mainly from glycerol (Biebl et al., 1999; Drożdżyńska et al., 2011). The development of biorefineries around the world was a strong input on the production of biobased 1,3-PDO from different producers. Indeed, biorefineries permit the large bioproduction of a wide range of biobased building blocks, such as 1,4-butanediol (1,4-BDO), succinic acid (SA), adipic acid (AA)…(Becker et al., 2015; Bozell and Petersen, 2010) 1,4-BDO is a short diol which can now be industrially produced *via* a chemical process of hydrogenation from SA (Bechthold et al., 2008; Bozell and Petersen, 2010). However, recently Genomatica has genetically modified *E. Coli* to obtain the straight bioproduction of 1,4-BDO from sugars(Barton et al., 2014). Now industrially available, biobased 1,4-BDO can be largely used in polycondensation or polyaddition reactions for the synthesis of polyurethanes (Reulier and Avérous, 2015), polyesters (Debuissy et al., 2017a, 2016a) and polyamides (Debuissy et al., 2016a). Biobased SA, listed by the US-DoE as one of the strategic platform chemicals from renewable resources (Becker et al., 2015; Bechthold et al., 2008; Werpy et al., 2004), has seen its interest growing for the production of various polymers with different chemical structures such as polyesters, polyamides…(Becker et al., 2015; Debuissy et al., 2017b). AA is another aliphatic dicarboxylic acid which is also used for the synthesis of polyamides, polyurethanes and polyesters (Debuissy et al., 2017b, 2017a, 2016a). Recently, new biological pathways were discovered for the direct bioproduction of AA from different biomass (Polen et al., 2013).

Aliphatic polyesters based on these four different building blocks have been developed and especially SA-based (co)polyesters (Debuissy et al., 2017a, 2017b; Luo et al., 2010). PBS for instance, is one of the aliphatic polyesters with highest melting temperature (T_m of 113°C) and excellent mechanical properties, comparable with those of conventional petroleum-based polymers, such as polyolefins. PBS became, thus, a promising candidate to replace common polymers with a growing production level during the last decade (Xu and Guo, 2010).

Developed from both academic and industrial perspectives, aliphatic polyesters based on 1,3-PDO have also attracted increasing interest since two decades, due to their excellent properties. For instance, poly(1,3-propylene terephthalate) (PPT), one of the most studied 1,3-PDO-based polyesters, is commercially available (Sorona®, Dupont) since a decade

(Ho et al., 2000; Wang et al., 2001). Because of the odd number of methylene groups in 1,3-PDO, PPT chains have a more angular structure than the conventional poly(1,2-ethylene terephthalate) (PET) or poly(1,4-butylene terephthalate) (PBT) leading to PPT fibers showing a higher resilience and stress recovery than PET or PBT (Ward et al., 1976). Moreover, PPT as well as PET and PBT are not biodegradable due to the terephthalate moiety.

Recently, several renewable and biodegradable aliphatic polyesters based on 1,3-PDO such as poly(1,3-propylene succinate) (PPS), poly(1,3-propylene glutarate), poly(1,3-propylene adipate) (PPA) and poly(1,3-propylene azelate) have been studied (Soccio et al., 2007; Bikiaris et al., 2008; Umare et al., 2007; Papageorgiou and Bikiaris, 2005a). In addition, different copolyesters as a route to prepare tailor-made aliphatic copolyesters with improved properties were investigated, such as poly(caprolactone-*block*-1,3-propylene adipate) (Nanaki et al., 2011), poly(1,2-ethylene succinate-*co*-1,3-propylene succinate) (Papageorgiou and Bikiaris, 2009) and poly(1,3-propylene succinate-*co*-1,3-propylene adipate) (PPSA) (Debuissy et al., 2017c).

Besides, poly(1,3-propylene succinate-*co*-1,4-butylene succinate) (PPBS) copolyesters has been broadly studied in connection to the remarkable properties of both corresponding homopolyesters (*i.e.* PPS and PBS) (Papageorgiou and Bikiaris, 2007; Xu et al., 2007; Yongxiang Xu et al., 2008; Lu et al., 2010, 2012; Chen et al., 2010). Papageorgiou and Bikiaris showed that the addition of 1,3-PDO to PBS significantly decreased the T_m and the degree of crystallinity leading to an increase of the biodegradation rate (Papageorgiou and Bikiaris, 2007). Moreover, the T_g of PPBS non-linearly increased with the 1,3-PDO content (Yongxiang Xu et al., 2008) and a change of the crystalline structure of copolyesters was observed for high 1,3-PDO content (Papageorgiou and Bikiaris, 2007). Finally, the Young modulus increased with the 1,3-PDO content whereas the tensile strength decreased (Papageorgiou and Bikiaris, 2007). Nevertheless, none of previous studies paid attention to the possible isodimorphic co-crystallization behavior of PPBS as it was highlighted for other aliphatic copolyesters (Arandia et al., 2015; Díaz et al., 2014). For its part, the poly(1,3-propylene adipate-*co*-1,4-butylene adipate) (PPBA) copolyesters, which possesses a close structure to PPBS, had never been studied. The higher chain length of AA building blocks compared to SA could provide higher flexibility to the copolyester and, thus, counteract the poor crystallization rate of 1,3-PDO for example.

The aim of the study was, first, to synthesize high molar mass PPBS and PPBA copolyesters with various 1,3-PDO/1,4-BDO ratios using the transesterification polycondensation reaction process from the melt with an efficient titanium-based organometallic catalyst (Debuissy et al., 2017a; Soccio et al., 2007; Papageorgiou and Bikiaris, 2007). Then, in depth chemical and physico-chemical analyses of the different synthesized macromolecular architectures were performed. The molar mass and the chemical architectures of copolyesters were determined by SEC, ^{1}H-, ^{13}C-, ^{31}P-NMR and FTIR. The crystalline structure, thermal stability and thermal properties were analyzed by WAXS, TGA and DSC, respectively. The biodegradation rate in soil was investigated according to international standard test method (ISO 17556:2012). The effect of the 1,3-PDO/1,4-BDO molar composition and the diacid (SA or AA) used on copolyesters properties was particularly discussed.

3. Experimental part

3.1. Materials

Biobased succinic acid (SA) (99.5%) was kindly supplied by BioAmber (France). SA was bioproduced by fermentation of glucose (from wheat or corn) and obtained after a multistep process based on several purifications, evaporation and crystallization stages. 1,4-BDO (99%), methanol (≥99.6%), chloroform (99.0-99.4%), chromium(III) acetyl acetonate (97%), 2-chloro-4,4,5,5-tetramethyl-1,3,2-dioxaphospholane (Cl-TMDP, 95%) and cholesterol (> 99%) were purchased from Sigma-Aldrich. 1,3-propanediol (1,3-PDO) (98%) and pyridine HPLC grade (99.5+%) were purchased from Alfa Aesar. Adipic acid (AA) (99%), titanium (IV) isopropoxide (TTIP) (98+%) and extra dry toluene (99.85%) were supplied by Acros. All reactants were used without further purification. All solvents used for the analytical methods were of analytical grade.

3.2. Synthesis of copolyesters

Aliphatic copolyesters were synthesized by a two-stage melt polycondensation method (esterification and transesterification). Syntheses are performed in a 50 mL round bottom flask with a distillation device to remove by-

products of the reaction (mainly water). All reactions were performed with a diol/acid molar ratio of 1.1/1. For each reaction, 10.0 g of diacid (SA or AA) were used and the weight of diols was adjusted according to the composition. During the first step (esterification), the reaction mixture was maintained under a constant argon flux and magnetically stirred at 300 rpm. The reactor temperature was set to 190 °C for 3 h. After 3 h of oligomerization, the remaining by-products of the reaction was distilled off by reducing the pressure to 200 mbar for 5 min, and then the proper amount (0.1 mol.% of TTIP *vs.* the amount of diacid used) of a 5 wt.% solution of TTIP in extra dry toluene was introduced inside the reactor under a constant argon flux. The reaction mixture was heated to 210 °C for 45 min. In the second step (transesterification), the reactor temperature was slowly increased to 230 °C and the pressure was decreased stepwise over period of 5 min at 100, 50 and 25 mbar to avoid excessive foaming and to minimize oligomer sublimation (a potential problem during the melt polycondensation). The transesterification continued for 3-4 h. The global reaction procedure is summarized in Scheme 1. To end, the synthesized polyester was cooled down, dissolved in chloroform, and precipitated into a large volume of vigorously stirred dry ice-cold methanol. Thereafter, the precipitate was filtered with a fine filter (0.45 µm), washed with cold methanol and dried under reduced pressure in an oven at 40 °C, for 24 h. Lightly colored (ivory white or pale yellow) (co)polyesters were finally obtained.

Different poly(1,3-propylene succinate-*co*-1,4-butylene succinate) (PPBS) and poly(1,3-propylene adipate-*co*-1,4-butylene adipate) (PPBA) were synthesized with various 1,3-PDO/1,4-BDO molar ratios (100/0, 80/20, 60/40, 50/50, 40/60, 20/80 and 0/100). Samples are denoted "PPxByS" or "PPxByA" with x and y as the molar proportion of 1,3-PDO and 1,4-BDO (determined by ^{1}H-NMR), respectively. Then, the four basic homopolyesters ($PP_{100}B_0S$, $PP_0B_{100}S$, $PP_{100}B_0A$ and $PP_0B_{100}A$) can also be denoted as PPS, PBS, PPA and PBA, respectively.

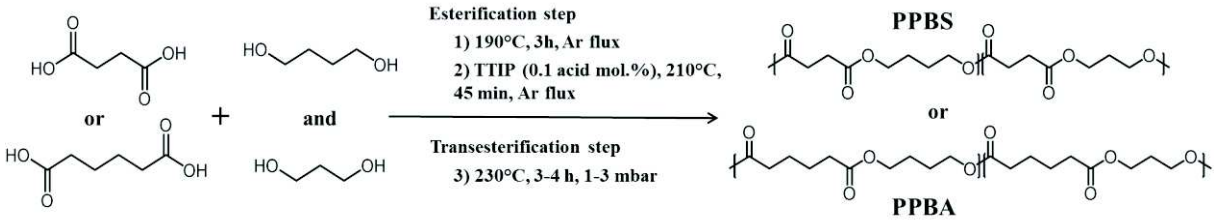

Scheme 2.3.1 : Reaction procedure of PPBS and PPBA copolyesters.

3.3. General methods and analysis

^{1}H- and ^{13}C-NMR spectra were obtained with a Bruker 400 MHz spectrometer. $CDCl_3$ was used as solvent to prepare solutions with concentrations of 8-10 and 30-50 mg/mL for ^{1}H-NMR and ^{13}C-NMR, respectively. The number of scans was set to 128 for ^{1}H-NMR and at least 4,000 for ^{13}C-NMR. Calibration of the spectra was performed using the specific $CDCl_3$ peak (δ_H = 7.26 ppm, δ_C = 77.16 ppm).

^{31}P-NMR was performed after phosphitylation of the samples, according to standard protocols (Debuissy et al., 2016a; Spyros et al., 1997). Spectra were obtained on a Bruker 400 MHz spectrometer (256 scans at 20 °C). All chemical shifts reported are relative to the reaction product of water with Cl-TMDP, which gives a sharp signal in pyridine/$CDCl_3$ at 132.2 ppm. The quantitative analysis of end-groups and the calculation of molar masses by ^{31}P-NMR were performed based on previous reports (Siotto et al., 2013; Spyros et al., 1997).

Size exclusion chromatography (SEC) was performed to determine the number-average molar mass (M_n), the mass-average molar mass (M_w) and the dispersity (Đ) of the samples. A Shimadzu liquid chromatograph was equipped with PLGel Mixed-C and PLGeL 100 Å columns and a refractive index detector. Chloroform was used as eluent at a flow rate of 0.8 ml/min. The apparatus was calibrated with linear polystyrene standards from 162 to 1,650,000 g/mol.

Infrared spectroscopy (IR) was performed with a Nicolet 380 Fourier transformed infrared spectrometer (Thermo Electron Corporation) used in reflection mode and equipped with an ATR diamond module (FTIR-ATR). The FTIR-ATR spectra were collected at a resolution of 4 cm^{-1} and with 64 scans per run.

Differential scanning calorimetry (DSC) was performed using a TA Instrument Q 200 apparatus under nitrogen (flow rate of 50 mL/min), calibrated with high purity standards. Samples of 2-3 mg were sealed in aluminum pans. A three-step procedure with a 10 °C/min ramp was applied that involved: (1) heating up from room temperature to 140 and 90 °C for PPBS and PPBA, respectively, and holding for 3 min to erase the thermal history, (2) cooling down to -80 °C

and holding for 3 min and (3) heating (second heating) from -80 °C to the same temperature as the first heating. To determine the glass transition temperature (T_g), (co)polyesters samples in pans were melted at 130 °C, quickly quenched in liquid nitrogen in order to obtain fully amorphous (co)polyesters and then heated from -80 to 0 °C at 10 °C/min. DSC analyses were repeated three times for each sample. The degree of crystallinity (X_c) is calculated according to Equation (2.3.1),

$$X_c(\%) = \frac{\Delta H_m}{\Delta H_m{}^0} \times 100 \qquad (2.3.1)$$

where ΔH_m is the melting enthalpy and $\Delta H_m{}^0$ is the melting enthalpy of a 100% pure crystalline polyester.

Thermal degradations were studied by thermogravimetric analyses (TGA). Measurements were conducted under helium atmosphere (flow rate of 25 mL/min) using a Hi-Res TGA Q5000 apparatus from TA Instruments. Samples (1-3 mg) were heated from room temperature up to 600 °C at a rate of 20 °C/min. Isothermal degradation was performed for 2 h at 230 °C under a helium atmosphere.

Wide angle X-ray Scattering (WAXS) data were recorded on a Siemens D5000 diffractometer using Cu K_α radiation (1.5406 Å) at 25-30 °C in the range of 2θ = 14-34° at 0.4 °.min^{-1}.

3.4. Ester function densisty

The ester function density of polyesters is defined by the number of ester function by repetitive unit on the number of carbons in the main chain by repetitive unit. The ester function density of PPBA copolyesters ($D_{ester,copo,PPBA}$) is given by Equation (2.3.2),

$$D_{ester,copo,PPBA} = \chi_{1,3-PDO} \times D_{ester,PPA} + \chi_{1,4-BDO} \times D_{ester,PBA} \qquad (2.3.2)$$

where: $\chi_{1,3\text{-PDO}}$ and $\chi_{1,4\text{-BDO}}$ are the 1,3-PDO and 1,4-BDO molar contents in the copolyester, $D_{ester,PPA}$ and $D_{ester,PBA}$ are the ester function density in PPA and PBA, respectively. The ester function density of PPBS copolyesters ($D_{ester,copo,PPBS}$) is defined by the same method.

3.5. Aerobic biodegradation study

Soil samples were collected from a biodynamic vineyard located in Mornington Peninsula (Victoria, Australia), and sieved using a screen size of 8 mm to obtain a homogeneous mix. Soil pH was 5.6 and moisture content approximately 38%.

Prior to the testing, the film samples were reduced in size to achieve approximately 2 cm × 2 cm maximum surface area of each individual piece of the test material. Each test material was tested in duplicate including the blank (the soil only) and positive reference (a mixture of cellulose and soil). The contents of all bioreactors were mixed and placed inside an in-house built respirometer unit (Way et al., 2010). The temperature was maintained at 30 ± 2 °C for a period of 180 days. Aerobic conditions were maintained by providing continuous supply of sufficient airflow to the vessels (70-80 ml/min). The amount of CO_2 generated in each bioreactor was measured (at least twice a day) using an infrared CO_2 analyzer and values were data logged into the computer. Theoretical amount of carbon dioxide ($THCO_2$), in grams per bioreactor, that the test and reference material can produce, was assessed and the degree of biodegradability (D_t), was calculated (for the test and reference materials) using Equation (2.3.3),

$$D_t = \frac{(CO_2)_T - (CO_2)_B}{THCO_2} \times 100 \qquad (2.3.3)$$

where $(CO_2)_T$ is the cumulative amount of carbon dioxide evolved in each bioreactor containing test material (in grams per bioreactor); $(CO_2)_B$ is the mean cumulative amount of carbon dioxide evolved in the blank vessel (in grams per bioreactor).

Following this step, the cumulative amount of carbon dioxide evolved as a function of time and a curve of percentage biodegradation as a function of time were plotted. Mean values were calculated from the replicate bioreactors and used for plotting the curves. The test was terminated after duration of 180 days.

4. Results

4.1. Characterization of the copolyesters macromolecular architectures

Several PPBS and PBBA copolyesters were synthesized following a two-step melt polycondensation pathway (Scheme 1). In the first one, the reaction led to the formation of oligomers (M_n of about 2-3 kg/mol after 3 h of esterification) necessary to avoid any removal phenomenon (*e.g.* monomer sublimation) during the next step. In the second one, the transesterification of previously synthesized oligomers using titanium isopropoxide (TTIP) resulted in a significant increase of molar masses as shown in Figure SI.4 (Annex 3). The molar masses of synthesized (co)polyesters determined by SEC are presented on Table 2.3.1. Synthesized polymers could be considered as high molar mass polyesters since these samples have $M_{n,SEC}$ higher than 20 kg/mol, with a dispersity (Đ) of about 1.6-1.9. Đ values were lower than the expected value of 2, surely due to a small loss of short oligomers during the precipitation step, even if this last process was performed with a maximum care (small filter and dry ice cold petroleum ether) to recover the maximum of short chains. Indeed, polymerization yields determined after precipitation were rather high and varied in a very narrow range, close to 90%.

The final chemical structure and microstructure of PPBS and PPBA copolyesters was verified by ^{1}H-, ^{13}C-, ^{31}P-NMR and FTIR. The ^{1}H-NMR spectra of $PP_{50}B_{50}A$ and $PP_{50}B_{50}S$ copolyesters, as an example, are presented in Figure 2.3.1-a and Figure SI.5-a, respectively. On the ^{1}H-NMR spectra of PPBA, the two close signals at δ = 4.14 and 4.18 ppm respectively assigned to O-C$\underline{H}_2$-CH_2- protons from 1,4-BDO and 1,3-PDO units confirmed the presence of ester functions. Other ^{1}H chemical signals at δ = 1.65, 1.70, 1.96 and 2.32 ppm were ascribed to CO-CH_2-C$\underline{H}_2$- protons from adipate units, to O-CH_2-C$\underline{H}_2$- protons from 1,4-BDO units, to O-CH_2-C$\underline{H}_2$- protons from 1,3-PDO units and to CO-CH_2-C$\underline{H}_2$- protons from adipate units, respectively. Interestingly, the hydroxyl (HO-C$\underline{H}_2$-) end-group signal was detected at tiny intensity at δ = 3.67 ppm, in compliance with the relatively high chain length of copolyesters. ^{1}H chemical shifts of succinate in PPBS were observed at δ = 1.70 and 2.62 ppm assigned to CO-CH_2-C$\underline{H}_2$- and CO-C$\underline{H}_2$-CH_2- protons, respectively. The molar composition (1,3-PDO/1,4-BDO) of copolyesters was determined from ^{1}H-NMR using propylene and butylene signals at δ = 4.14 and 4.18 ppm, respectively (more details in SI.3). Determined 1,3-PDO and 1,4-BDO contents in the chains are given in Table 2.3.1. All synthesized copolyesters presented 1,3-PDO/1,4-BDO molar ratio similar to the initial feed ones, because of (i) the close esterification rate of both diols with AA and SA for non-catalyzed systems (Kuo and Chen, 1989), (ii) our choice to perform the esterification step 20 °C below the 1,3-PDO boiling point (about 210 °C) to avoid monomer loss and (iii) the sufficient time of the first step to permit the synthesis of oligomers of enough length to avoid product loss.

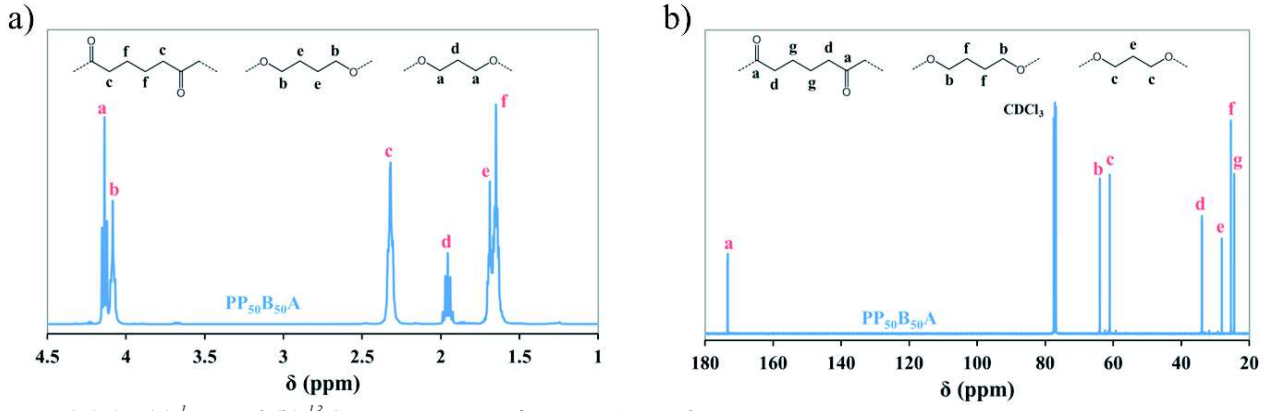

Figure 2.3.1 : (a) ^{1}H- and (b) ^{13}C-NMR spectra of $PP_{50}B_{50}A$ copolyester.

^{13}C-NMR was performed to investigate in detail the copolyester microstructure. ^{13}C-NMR spectra of $PP_{50}B_{50}A$ and $PP_{50}B_{50}S$ copolyesters are presented in Figure 2.3.1-b and Figure SI.5-b, respectively. The details of ^{13}C chemical shifts are presented in Annex 3. The copolyester microstructures (PAP, PAB and BAB triads for PPBA; PSP, PSB and BSB triads for PPBS), presented in Figure 2.3.2-a and Figure SI.6-a (with P, B, S and A as the 1,3-PDO, 1,4-BDO, SA and AA, respectively), were determined. For the PPBA copolyester, adipate units are present in all three triads and give distinctly different peaks with chemical shifts close to the ones of PPA or PBA for the CO-C$\underline{H}_2$-CH_2- carbons of adipate

at δ ~ 34 ppm. Such results, with the splitting of the two signals (carbon atoms d_1, d_2, d_3 and d_4 in Figure 2.3.2), enable the calculation of the average sequence length of PA and BA units (L_{PA} and L_{BA}, respectively) and the degree of randomness (R) using Equations (SI.7) to (SI.9). The same method was used in the case of PPBS, but the integration was performed using CO-CH_2- carbons of succinate at δ ~ 172 ppm (Figure SI.6-b). Main data are listed in Table 2.3.1. According to the 1,3-PDO/1,4-BDO ratio, L_{PA} and L_{BA} for PPBA copolyesters (or L_{PS} and L_{BS}) varied between 1.3 and 4.8. R is equal to 1 for fully random copolymers (Yamadera and Murano, 1967). R values in Table 2.3.1 show that we are precisely in this case for PPBA and PPBS copolyesters, composed of both diols, as it was expected by using a titanium-based organometallic catalyst (Chen et al., 2010; Debuissy et al., 2017a).

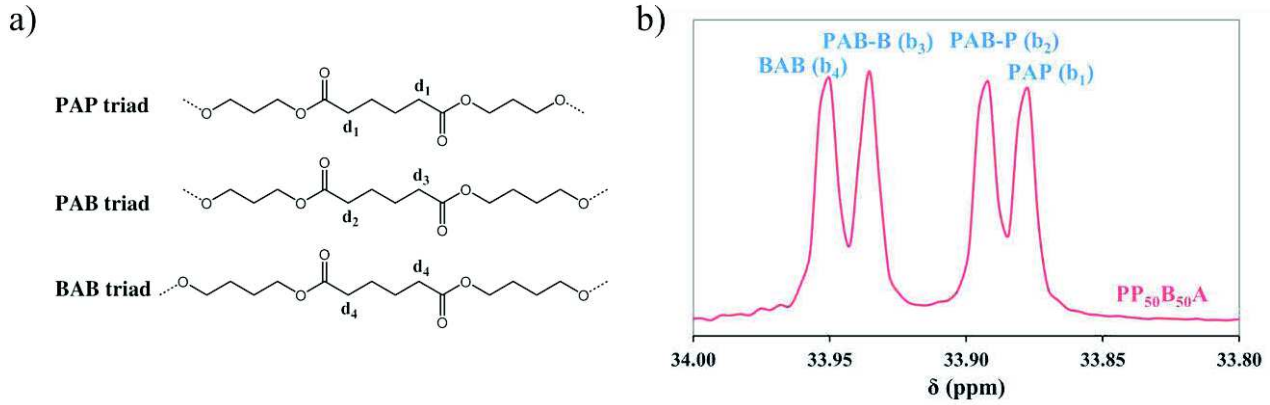

Figure 2.3.2 : (a) Possible triads for PPBA copolyesters, (b) ^{13}C-NMR spectra of PPBA centered at δ ~ 34 ppm.

^{31}P-NMR analysis of PPBA and PPBA copolyesters was performed in $CDCl_3$ with cholesterol as standard. ^{31}P-NMR spectra of copolyesters are presented in Figure SI.7 (in Annex 3). All copolyesters showed primary hydroxyl (OH) (147.2-147.4 ppm) and carboxylic acid (COOH) (134.9 ppm) end-groups. The large majority of end-groups were OH groups surely due to the excess of OH functions initially introduced in the reaction mixture. Interestingly, 1,3-PDO (147.38 ppm) and 1,4-BDO (147.25 ppm) OH end-groups signals were separated in ^{31}P-NMR spectra (Figure SI.8). The proportion of 1,3-PDO end-groups seemed to be slightly superior to the global 1,3-PDO content for all copolyesters (Table SI.4), which is quite surprising since the transesterification led to random structures. One can suppose that this small difference could come from measurement uncertainty and the possible difference of stability of both modified hydroxyl end-groups with the phosphorus reactant (Korntner et al., 2015). The molar masses of copolyesters determined by ^{31}P-NMR ($M_{n,NMR}$) were lower compared to the one obtained by SEC, the latter being overestimated partly due to the calibration based on PS standards. $M_{n,NMR}$ varied between 8 and 17 kg/mol. Moreover, for the PBS and PBA samples, by using the Mark-Houwink-Sakurada (MHS) equation and parameters (K and a) from Charlier *et al.* (Charlier, Q. et al., 2015) and Munari *et al.* (Munari et al., 1992), the calculated MHS-corrected M_n of PBS and PBA were 18.7 and 13.0 kg/mol, respectively. These results were close to the value determined by ^{31}P-NMR (*i.e.*, 17.3 and 13.6 kg/mol). In conclusion, as observed for poly(butylene succinate-*co*-butylene adipate) (PBSA) copolyesters (Debuissy et al., 2017a), $M_{n,NMR}$ gave a good estimation of a more accurate molar mass of copolyesters, even if this method based on the quantification of end-groups did not take into account the possible macrocycles that could have been produced during the polyester synthesis but which are not detectable by ^{31}P-NMR analysis (Charlier, Q. et al., 2015; Debuissy et al., 2017a).

FTIR spectra of homopolyesters are presented in Figure 2.3.3, whereas FTIR spectra of all PPBS and PPBA copolyesters are shown in Figures SI.9 (in Annex 3), respectively. First, strong signals at 1715-1725 cm^{-1} and 1150-1160 cm^{-1} respectively assigned to the C=O and -COO- asymmetric stretching vibrations demonstrated the presence of ester linkages. Then, the absence of broad signals around 3200-3500 cm^{-1} from COOH and OH end-groups confirmed the long chain length of (co)polyesters. Moreover, the presence of adipate segments instead of succinate segments shifted C=O stretching vibrations from 1715 to 1725 cm^{-1}, -CH_2- rocking vibrations from 805 to 735 cm^{-1} and -CO- stretching vibration from 1320 to 1255 cm^{-1}, respectively. Moreover, the intensity of the -CH_2- vibration signal at 2870-2970 cm^{-1} seemed to increase with the number of -CH_2- by repetitive units (for homopolyesters). Finally, few minor modifications of FTIR spectra were observed by increasing the 1,3-PDO content in PPBS and PPBA (more details in Annex 3).

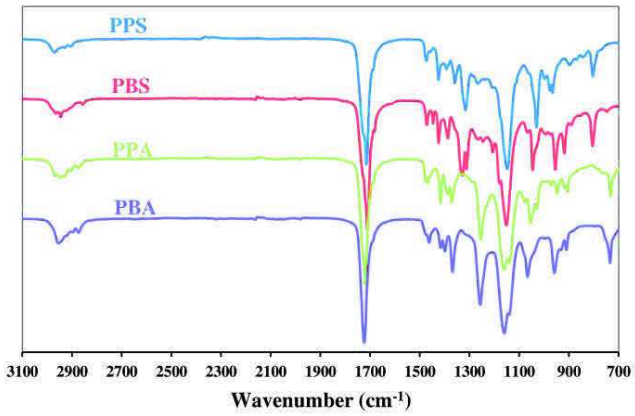

Figure 2.3.3 : FTIR spectra of PPS, PBS, PPA and PBA.

Table 2.3.1 : Molar composition and molar masses of PPBS samples.

Sample	Feed composition 1,3-PDO/1,4-BDO	^{1}H-NMR	SEC		^{13}C-NMR			^{31}P-NMR		
		Det. composition 1,3-PDO/1,4-BDO	M_n	Đ	L_{PS} (or L_{PA})	L_{BS} (or L_{BA})	R	M_n	OH end-groups	COOH end-groups
	mol.%	mol.%	kg/mol					kg/mol	%	%
PPS	100 / 0	100 / 0	35.1	1.7	-	-	-	15.5	88	12
$PP_{80}B_{20}S$	80 / 20	79.6 / 20.4	31.7	1.7	4.1	1.4	0.96	14.4	76	24
$PP_{60}B_{40}S$	60 / 40	60.3 / 39.7	32.9	1.9	2.6	1.7	0.98	16.0	81	19
$PP_{50}B_{50}S$	50 / 50	49.5 / 50.5	29.8	1.8	2.0	2.1	0.98	14.1	82	18
$PP_{41}B_{39}S$	40 / 60	40.8 / 59.2	23.7	1.6	1.7	2.4	1.00	8.6	87	13
$PP_{21}B_{79}S$	20 / 80	20.8 / 79.2	38.6	1.7	1.3	4.9	0.98	13.7	38	62
PBS	0 / 100	0 / 100	39.2	1.7	-	-	-	17.3	78	22
PPA	100 / 0	100 / 0	29.4	1.7	-	-	-	10.1	77	23
$PP_{79}B_{21}A$	80 / 20	78.9 / 21.1	29.4	1.7	4.3	1.3	1.01	10.8	94	6
$PP_{59}B_{41}A$	60 / 40	59.3 / 40.7	20.0	1.6	2.5	1.6	1.04	7.9	94	6
$PP_{50}B_{50}A$	50 / 50	49.5 / 50.5	29.7	1.6	2.0	2.1	0.98	11.0	66	34
$PP_{40}B_{60}A$	40 / 60	39.7 / 60.3	35.2	1.6	1.6	2.6	1.00	13.7	65	35
$PP_{21}B_{79}A$	20 / 80	21.0 / 79.0	34.9	1.8	1.3	4.5	1.02	12.2	63	37
PBA	0 / 100	0 / 100	33.3	1.8	-	-	-	13.6	79	21

4.2. Thermal degradation

Thermal stability of PPBS and PPBA copolyesters was determined from TGA analyses performed under helium. The mass loss curves of PPBS and PPBA samples with their derivatives (DTG) curves are plotted in Figure 2.3.4, whereas the corresponding data are reported in Table SI.5 (in Annex 3). At temperature below 260 °C, all samples appeared to be stable. All copolyesters degraded in two main steps involving competitive mechanisms. A small mass loss (< 5%) was first observed at 260-315 °C and 270-325 °C for PPBS and PPBA copolyesters, respectively. This mass loss was due to the degradation of the shortest polyester chains (Debuissy et al., 2016a). Then, a major degradation (90-95 wt.%) occurred at 315-415 °C or 325-400 °C corresponding to the main degradation of PPBS and PPBA copolyesters, respectively (Debuissy et al., 2016b). At the end, a small amount of ashes (1-2 wt.%) was recovered at 550 °C. The 2 wt.% degradation temperature ($T_{d,2\%}$) of all PPBS and PPBA copolyesters were about 275-300 °C and 295-310 °C, respectively (Figures 2.3.4-a,b). The 50 wt.% degradation temperature ($T_{d,50\%}$) and the maximal degradation rate temperature ($T_{deg,max}$) were equivalent for all PPBS compositions (around 385 and 395 °C, respectively), leading to a similar degradation profile for all PPBS samples which were perfectly superimposed. The same tendency was observed for PPBA with $T_{d,50\%}$ and $T_{deg,max}$ of about 375 and 380 °C, respectively.

Isothermal mass loss curves at 230 °C (*i.e.*, corresponding to the polymerization reaction temperature) of the four homopolyesters are presented in Figure 2.3.4-c. This isothermal degradation after 2 h was more important for succinate-

based (~ 18 wt.%) than adipate-based homopolyesters (~ 7-9 wt.%). Moreover, the degradation profile varied strongly according to the homopolyester. As an example, PPS showed an important linear degradation, whereas PBS exhibited a non-linear degradation with a reduction of the mass loss rate with time. Both degradations seemed to be driven by only one mechanism of degradation. Finally, both adipate-based homopolyesters (*i.e.*, PPA and PBA) presented isothermal degradation profiles composed of two linear segments with an increase of the degradation rate after 40-60 min. One can suppose the presence of two mechanisms for these adipate-based homopolyesters, the first one at the beginning of the thermal degradation and the second one after the thermal degradation initiation.

The comparison of thermal degradation profile between PBS and PBA homopolyesters (representative of PPBS and PPBA copolyesters) (Table SI.5), the isothermal degradation of the four homopolyesters and the use of $T_{d,2\%}$ as criterion for the thermal stability of polyesters all showed that adipate-based copolyesters possessed a higher thermal stability than succinate ones. As for the thermal stability, the degradation profile ($T_{d,50\%}$ and $T_{deg,max}$) depended exclusively on the carboxylic acid with a sharper degradation profile after the initiation for adipate-based copolyesters (Figure 2.3.4-a,b) (Debuissy et al., 2017a).

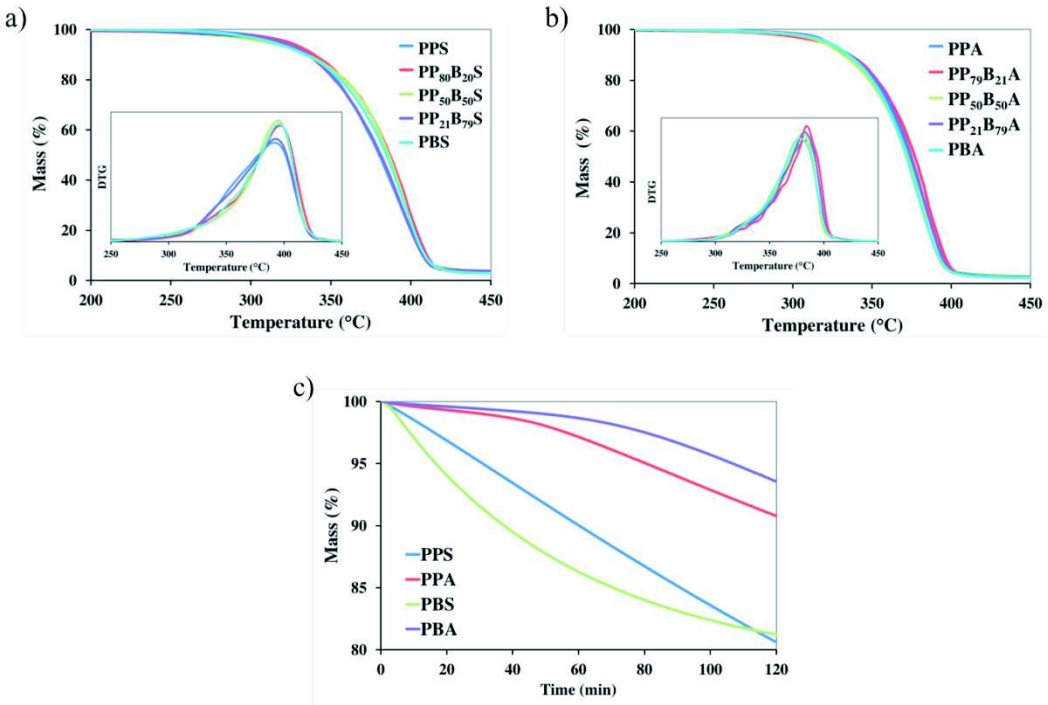

Figure 2.3.4 : Mass loss and DTG curves of (a) PPBS and (b) PPBA copolyesters under helium; (c) Isothermal mass loss curves of PPS, PPA, PBS and PBA at 230 °C under helium.

4.3. Crystalline structures

The crystalline structure of both copolyesters series was studied by WAXS. WAXS patterns of PPBS and PPBA copolyesters are shown in Figure 2.3.5. PPBS WAXS patterns highlighted that all samples were semi-crystalline at room temperature and presented only one type of crystals by composition. First, main diffraction peaks of PBS appeared at 2θ = 19.4, 21.7 and 22.4°, whereas ones of PPS appeared at 2θ = 17.9, 19.4, 20.3 and 22.3°, in agreement with previous reports (Debuissy et al., 2017a; Soccio et al., 2007; Papageorgiou and Bikiaris, 2007). Then, PPBS copolyesters could be split into two groups according to the 1,3-PDO content. Indeed, PPBS containing 60 mol.% or less of 1,3-PDO units are characterized by WAXS patterns very similar to PBS, indicating that these copolyesters crystallized according to the PBS lattice and the co-monomer (1,3-PDO in this case) incorporated in minor amount was excluded from the PBS crystals or only partially integrated in it. This led to the decrease of the crystal stability due to the presence of "defects" inside the chain and, thus, the degree of crystallinity decreased with the 1,3-PDO content. Moreover, one can observe that diffraction peaks broadened with the incorporation of the co-monomeric unit suggesting the decrease of the crystal size. On the contrary, samples containing 80 mol.% or more of 1,3-PDO units crystallized according to the PPS lattice.

Results from PPBA WAXS patterns indicated that, first, only some compositions were semi-crystalline at room temperature, since $PP_{50}B_{50}A$ and $PP_{59}B_{41}A$ were in molten state (see DSC analyses). On one side, PPA showed reflections at 2θ = 18.9, 20.2, 21.0, 22.1 and 24.3°. $PP_{79}B_{21}A$ with also BA units as minor component possessed only PPA type crystals but the diffraction peaks are less intense than for PPA due to the lower degree of crystallinity. On the other side, PPBA copolyesters with a 1,3-PDO content of 40 mol.% or lower exhibited WAXS patterns close to the one of PBA. PBA exhibited reflections at 2θ = 21.2 and 24.3° assigned to β-form crystals, but also reflections at 2θ = 21.5, 22.1 and 23.9° assigned to α-form crystals. The PBA homopolyester also exhibited α + β mixed crystals (Pan and Inoue, 2009). Such as for PBSA copolyesters, adipate-rich PPBA copolyesters (*i.e.*, $PP_{21}B_{79}A$ and $PP_{40}B_{60}A$) exhibited only β-form (kinetically favored) crystals of PBA, due to reduction of the crystallization rate by the inclusion of 1,3-PDO units (Debuissy et al., 2017a).

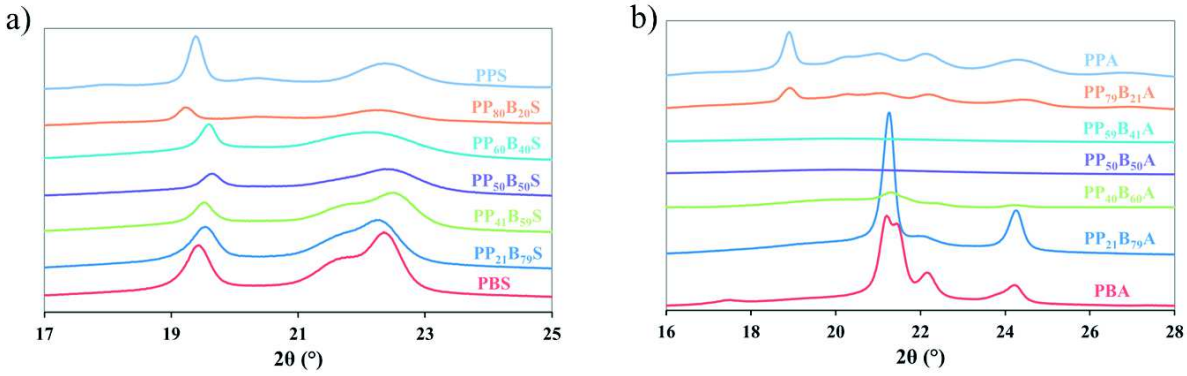

Figure 2.3.5 : WAXS patterns of (a) PPBS and (b) PPBA copolyesters.

4.4. Thermal behavior of copolyesters

Not only the thermal properties but also the crystalline structure of the copolyesters was studied by DSC, in complement to WAXS analysis. The cooling and second heating runs of (co)polyesters at 10 °C/min are presented in Figure 6, whereas corresponding data are summarized in Table 2.3.2. The variation of thermal properties is discussed as a function of the ester function density (D_{ester}) calculated according to Equation (2.3.2).

During the first heating run, all copolyesters except $PP_{80}B_{20}A$ and $PP_{60}B_{40}A$ exhibited an endothermic peak associated to the fusion. The evolution of melting temperatures (T_m) and enthalpies (ΔH_m) of PPBS as a function of the 1,3-PDO content during the first heating run is presented in Figure SI.10-a (in Annex 3). One can observe that T_m decreased from 116 to 32 °C with the 1,3-PDO content from PBS to $PP_{60}B_{40}S$, respectively, and then increased until 50 °C for PPS. Similarly, ΔH_m decreased with the inclusion of 1,3-PDO from 82 to 35 J/g for PBS to $PP_{80}B_{20}S$, respectively, and then increased until 46 J/g for PPS. T_m and ΔH_m exhibited, thus, a pseudo-eutectic behavior with minimal values for 1,3-PDO content around 60-80 mol.%. In the case of PPBA (Figure SI.10-b), a 1,3-PDO content around 50-60 mol.% led to molten state copolyesters at room temperature. Beyond these compositions, T_m and ΔH_m of PPBA copolyesters increased until having maximal values for 1,3-PDO content of 0 and 100 mol.% (*i.e.*, 58 °C and 80 J/g for PBA; 48 °C and 63 J/g for PPA). Since WAXS results evidenced only one crystal type by sample, the degree of crystallinity (X_c) of copolyesters was calculated according to Equation (2.3.1) using the homopolyesters $\Delta H_m°$ values determined from the groups contribution method of Van Krevelen (Van Krevelen, 1997) (124 and 135 J/g for PPA and PBA, respectively) or from experimental data (Papageorgiou and Bikiaris, 2005b) (140 and 210 J/g for PPS and PBS, respectively). Results are presented in Table 2.3.2. As observed by WAXS, the addition of a co-monomer to a homopolyester disrupted the symmetry of the chain and thus resulted in lower X_c for the copolyesters. Moreover, the increase of D_{ester} for homopolyesters resulted in a decrease of X_c from 59 (PBA) to 33% (PPS) due to the lower chain mobility. Indeed, D_{ester} increased with the amount of 1,3-PDO and SA unit in the copolyester.

During the cooling run, PPBS and PPBA copolyesters with 1,3-PDO content higher than 50 mol.% were not able to crystallize at 10 °C/min (Figure 2.3.6-a,b), surely due to the presence of a high 1,3-PDO content decreasing the crystallization rate. Moreover, one can observe that, surprisingly, $PP_{41}B_{59}S$ crystallized less than $PP_{50}B_{50}S$ during the cooling. However, by decreasing the cooling rate to 5 °C/min, PPA and $PP_{59}B_{41}A$ were able to crystallize partially contrary to their PPBS counterpart (Figures SI.11 and SI.12). This last result highlighted the higher crystallization rate

of copolyesters based on AA compared to those based on SA due to the increased chain mobility with the decrease of D_{ester}. $PP_{79}B_{21}A$ was also the only sample having an amorphous state after the cooling at 5 °C/min showing that the 79/21 (1,3-PDO/1,4-BDO) composition is the one with the lowest crystallization rate. Finally, for both copolyesters, the crystallization temperature (T_c) decreased significantly by increasing the 1,3-PDO content and T_c of PPBS copolyesters were globally higher than the one of PPBA.

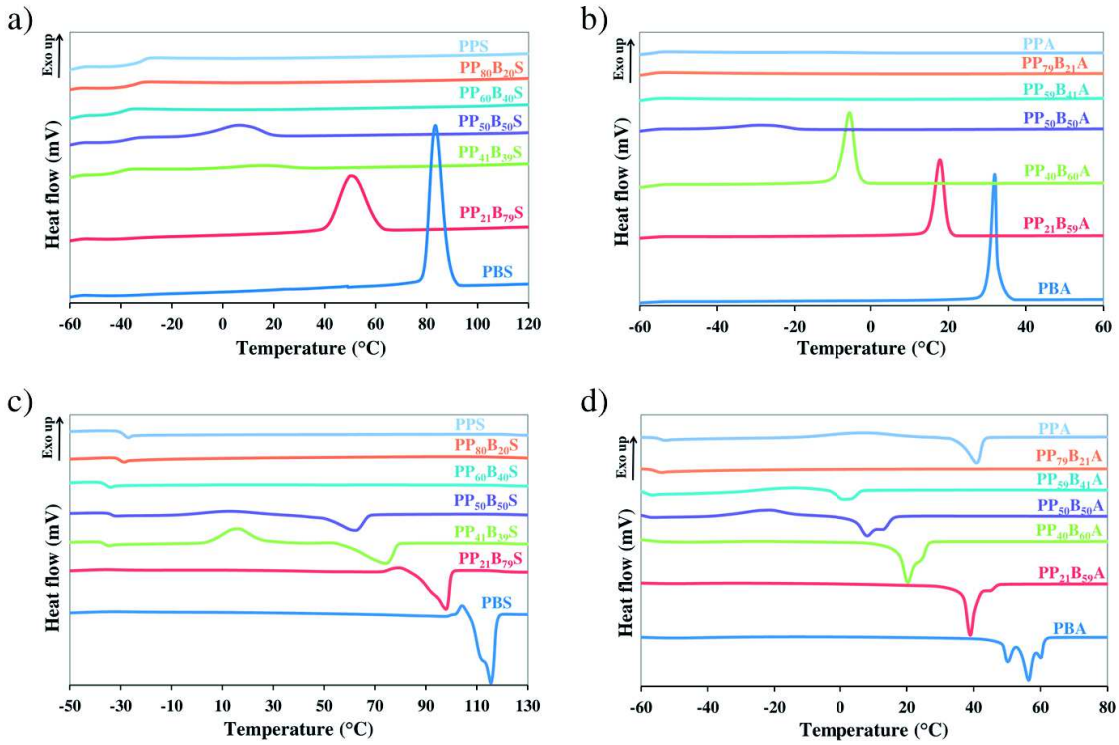

Figure 2.3.6 : DSC curves of the copolymers and the corresponding homopolymers. Cooling run curves of (a) PPBS and (b) PPBA; second heating run curves of (c) PPBS and (d) PPBA.

The second heating run was characterized by the presence of a glass-transition phenomenon and a melting phenomenon. Moreover, $PP_{50}B_{50}S$, $PP_{41}B_{59}S$, PPA, $PP_{59}B_{41}A$ and $PP_{50}B_{50}A$ exhibited, in addition to these two phenomena, a cold-crystallization phenomenon due to an incomplete or the absence of the crystallization during the cooling run. PPA, despite its high 1,3-PDO content, is able to crystallize due to the absence of "BA" units "defects" in the chain structure, contrary to $PP_{79}B_{21}A$ which is amorphous.

Glass transition temperatures (T_g) of copolyesters, summarized in Table 2.3.2, are plotted in Figure 2.3.7 as a function of the 1,3-PDO content. T_g of copolyesters increased with the 1,3-PDO content from -35 to -29 °C for PPBS and from -59 to -54 °C for PPBA. The decrease of the diol length of one carbon from 1,4-BDO to 1,3-PDO increases D_{ester}, which led to a higher amount of intra or inter-chain interactions between ester groups, hence the decrease of chain mobility leading to the increase of T_g. For the same reason, PPBA copolyesters containing "long" adipate segments had lower T_g than PPBS copolyesters. For random copolyesters, the variation of T_g with the composition often follows the Fox equation (Fox, 1956), defined by Equation (2.3.4),

$$\frac{1}{T_{g,copo}} = \frac{w_1}{T_{g,1}} + \frac{w_2}{T_{g,2}} \qquad (2.3.4)$$

where $T_{g,1}$ and $T_{g,2}$ are the glass transition temperature of homopolyesters, and w_1 and w_2 their respective mass fractions. One can observe, in Figure 2.3.7-a, that the Fox equation did not fit well with our experimental data for PPBS, which seems in contradiction with the study of Papageorgiou and Bikiaris (Papageorgiou and Bikiaris, 2007). Nevertheless, the Fox equation fitted quite correctly with experimental data for PPBA (except for $PP_{59}B_{41}A$). However, sometimes the Gordon-Taylor equation (Gordon and Taylor, 2007) permitted to describe better the T_g variation of random aliphatic copolyesters such as PBSA or PPSA (Debuissy et al., 2017a, 2017c; Pérez-Camargo et al., 2017), which is defined by Equation (2.3.5),

$$T_{g,copo} = \frac{w_1\, T_{g,1} + k(1-w_1)\, T_{g,2}}{w_1 + k(1-w_1)} \qquad (2.3.5)$$

where $T_{g,1}$ and $T_{g,2}$ are the glass transition temperature of homopolyesters, w_1 the respective mass fraction of the homopolyester 1 and k the Gordon-Taylor parameter. As observed in Figure 2.3.7-a, the Gordon-Taylor equation fitted correctly our PPBS experimental data with k = 2.33. Usually k is considered as a fitting parameter (Penzel et al., 1997), even if in the original version of volume additivity the parameter $k = \rho_1\Delta\alpha_2/\rho_2\Delta\alpha_1$ was well defined (ρ_i is the density and $\Delta\alpha_i = \alpha_{melt} - \alpha_{glass}$ is the increment at T_g of the expansion coefficient of the respective component i). Nonetheless, the low amplitude of T_g values of PPBS and PPBA copolyesters decreases the accuracy of the mixing law differentiation for each copolyesters series and, thus, results should be taken with care.

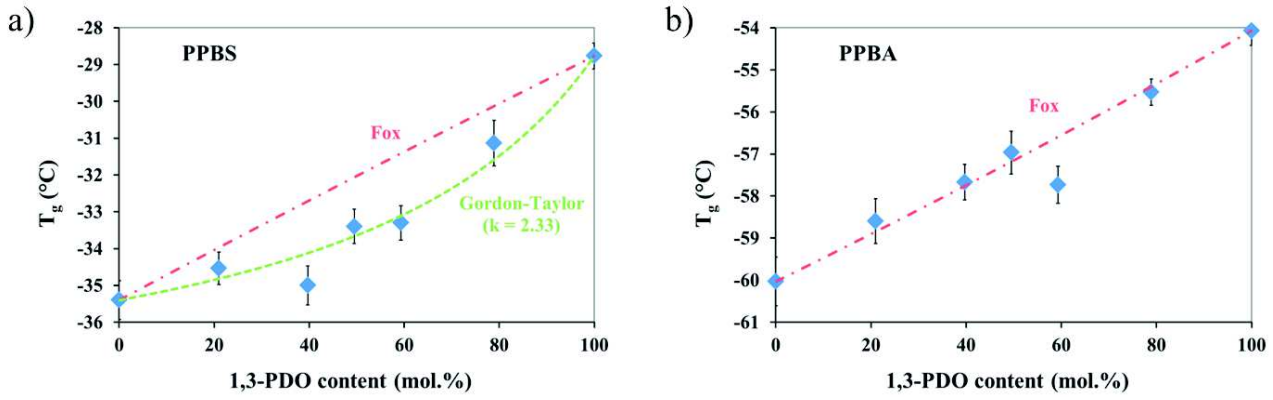

Figure 2.3.7 : Variation of the (a) PPBS and (b) PPBA T_g vs. 1,3-PDO content in copolyesters.

Figure 2.3.6-c,d highlighted that copolyesters exhibited crystallization-fusion phenomena composed of multiple peaks spread on large temperature ranges as commonly observed for aliphatic polyesters (Debuissy et al., 2017a, 2016a), due to the crystallite reorganization during the heating.

Plots of T_m and ΔH_m as a function of 1,3-PDO content of copolyesters during the second heating run are shown in Figure 2.3.8. T_m and ΔH_m of PPBS decreased continuously with the 1,3-PDO content from 116 °C and 65 J/g for PBS until having an amorphous state for 1,3-PDO content higher than 50 mol.%. The incorporated co-monomeric unit (1,3-PDO in this case) was included in the PBS crystal lattice, disrupting its symmetry and, thus, decreasing the PBS crystal size and strength. According to WAXS results, only BS units were able to crystallize. The chemical structure of 1,3-PDO which has an odd and small number of methylene carbons was responsible for the poor crystallization rate of PPBS copolyesters containing high 1,3-PDO content. However, by reducing the heating rate to 5 °C/min, PPS, showed a small cold-crystallization phenomenon, thanks to the homogeneity of it structure (Figure SI.11 in Annex 3). In the case of PPBA, only the composition with a 1,3-PDO content of 80 mol.% showed an amorphous behavior even at a heating rate of 5 °C/min (Figure SI.12 in Annex 3). Indeed, Figure 2.3.6-b,d showed that $PP_{59}B_{41}A$ and PPA, which are not able to crystallize at 10 °C/min during the cooling run, exhibited a small cold-crystallization phenomenon during the second heating run contrary to $PP_{60}B_{40}S$ and PPS confirming the better crystallization ability for copolyesters with AA compared to SA. As for PPBS, T_m and ΔH_m of PPBA decreased by increasing the 1,3-PDO content from 57 °C and 52 J/g for PBA until having an amorphous behavior for the composition with 80 mol.% of 1,3-PDO. However, PPA showed a semi-crystalline behavior with T_m at 41 °C and ΔH_m of 29 J/g, due to (i) the absence of "BA" units "defects" in the chain structure and (ii) the presence of AA segments (instead of SA segments) which increased the crystallization rate. X_c of copolyesters, determined from the second heating run, followed the trend of ΔH_m. However, one can observe that for an equivalent 1,3-PDO content, PPBA copolyesters had an higher X_c than PPBS proving the higher crystallization ability when increasing the diacid chain length from four to six carbons.

From DSC results showing (i) the presence of a pseudo-eutectic melting behavior for both copolyesters and (ii) that copolyester samples with low 1,3-PDO content are able to crystallize during the cooling run despite their randomness and from the WAXS results showing that (i) the minor co-monomeric units of one type are included in the crystal lattice of the other and vice versa, and (ii) crystalline unit cell parameters are composition dependent with only one crystal type by sample switching from one unit cell to the other one around the pseudo-eutectic , it can be concluded that PPBS

and PPBA showed isodimorphic co-crystallization behavior, in agreement with previous results on aliphatic copolyesters (Debuissy et al., 2017a, 2017c; Pérez-Camargo et al., 2017; Pérez–Camargo et al., 2015).

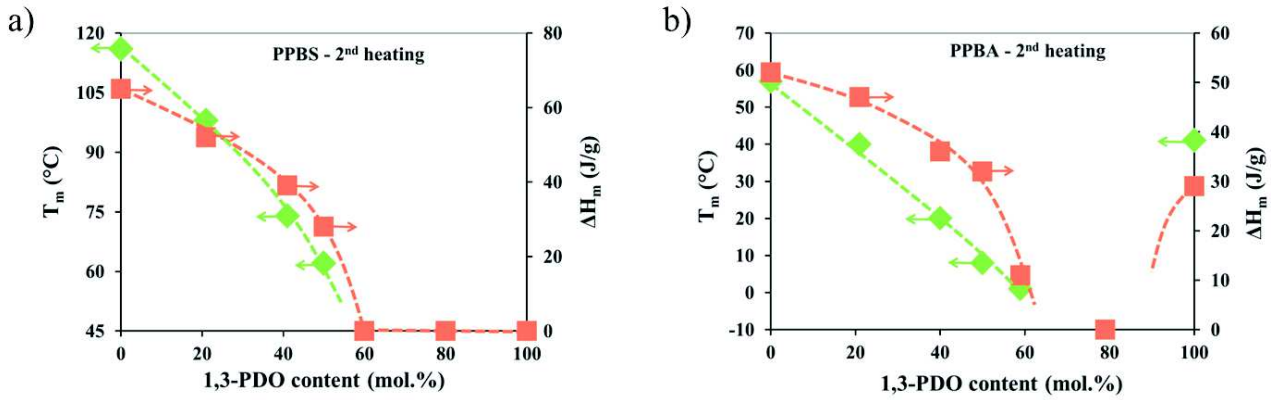

Figure 2.3.8 : Variation of T_m and ΔH_m vs. 1,3-PDO content for (a) PPBS and (b) PPBA during the second heating run.

Table 2.3.2 : DSC results of PPBS and PPBA copolyesters with heating and cooling rate of 10 °C/min.

Sample	D_{ester}	First heating			Cooling		T_g [a]	Second heating				
		T_m	ΔH_m	X_c	T_c	ΔH_c		T_{cc}	ΔH_{cc}	T_m	ΔH_m	X_c
	%	°C	J/g	%	°C	J/g	°C	°C	J/g	°C	J/g	%
PPS	28.6	50	46	33	-	-	-29	-	-	-	-	-
$PP_{80}B_{20}S$	27.8	42	35	25	-	-	-31	-	-	-	-	-
$PP_{60}B_{40}S$	27.1	32-48	40	29	-	-	-33	-	-	-	-	-
$PP_{50}B_{50}S$	26.8	51	42	20	6	14	-34	14	5	62	28	13
$PP_{41}B_{39}S$	26.5	75	49	24	24	4	-35	16	31	74	39	19
$PP_{21}B_{79}S$	25.8	98	65	31	50	52	-35	-	-	98	52	25
PBS	25.0	116	82	39	83	67	-35	-	-	116	65	31
PPA	22.2	48	63	51	-	-	-54	7	25	41	29	23
$PP_{79}B_{21}A$	21.7	40	35	28	-	-	-56	-	-	-	-	-
$PP_{59}B_{41}A$	21.3	-	-	-	-	-	-58	-15	12	1	11	-
$PP_{50}B_{50}A$	21.1	-	-	-	-29	11	-57	-27	19	7	35	-
$PP_{40}B_{60}A$	20.9	33	29	21	-5	36	-57	-	-	20	36	27
$PP_{21}B_{79}A$	20.5	48	53	39	18	48	-58	-	-	40	47	35
PBA	20.0	58	80	59	32	55	-59	-	-	57	52	39

[a] T_g values were determined after a quenching from the melt.

4.5. Aerobic biodegradation

An aerobic biodegradation of PPS, PBS, PPA, PBA and $PP_{50}B_{50}S$ samples was performed in soil to determine the influence of composition on the biodegradation rate. The cumulative CO_2 and percentage biodegradation profiles for each test sample are shown in Figure 2.3.9. A steady rate of carbon dioxide evolution from each test vessel, similar to cellulose reference, indicated that test materials were metabolized by soil microorganisms and did not have any residual ecotoxicity effect (Figure 2.3.9-a). Biodegradation of the reference material cellulose was initiated immediately after incubation in soil, without any lag phase, suggesting presence of actively metabolizing microbial population. Cellulose was 100% degraded within 60 days of incubation in soil (Figure 2.3.9-b). In comparison, most test specimens had an initial lag phase (~3 days) and thereafter their biodegradation progressed slowly. An exception was test material PBS that showed a lag of almost two weeks before its degradation commenced. It is likely that the higher molar mass of PBS may be responsible for the longer lag phase. After 90 days of incubation in soil, PBA and PBS showed slightly higher degree of degradation (44% and 40%, respectively) as compared to PPA and PPS (35% and 40% respectively). As the time progressed, PBA and PBS continued to biodegrade at almost similar rate and achieved maximum biodegradation of 61% and 71% respectively at the end of 180 days (Figure 2.3.9-b). In comparison, biodegradation profile of PPA and PPS plateaued, achieving a maximum biodegradation of 47% and 48%, respectively. $PP_{50}B_{50}S$ achieved a maximum

biodegradation of 50% at the end of 6 months (*i.e.* 180 days). It has been reported that the degree of crystallinity or melting temperatures of samples are important factors for the biodegradation rate (Rizzarelli et al., 2015; Šerá et al., 2016). However, results obtained in this study did not show any correlation between these two factors and rate of biodegradation of different samples. Test results suggested that chemical structure of polyesters influenced the biodegradation rate, which increased by increasing the length of the monomers. An increase in the diol chain length from 3 to 4 carbons led to a significant increase in the biodegradation rate, whereas the increase in the diacid chain length only had a minor effect on the biodegradation rate. These results suggested that lower ester function density of polyesters using AA instead of SA and 1,4-BDO instead of 1,3-PDO, allowing a higher chain flexibility attested by lower T_g values, permitted a higher degradation by microorganisms in soil. Nevertheless, the global ester function density is not the key parameter, strictly speaking, since calculated PPA ester function density was lower than the one of PBS. It is more likely that the key parameter that influenced degradation rate was rather the number of methylene carbons in monomers (*i.e.*, diacids and diols) between ester functions. Finally, since none of polyesters samples achieved a degree of biodegradation of 90% within 6 months, these samples cannot be considered as biocompostable according to the ISO 17556 regulation.

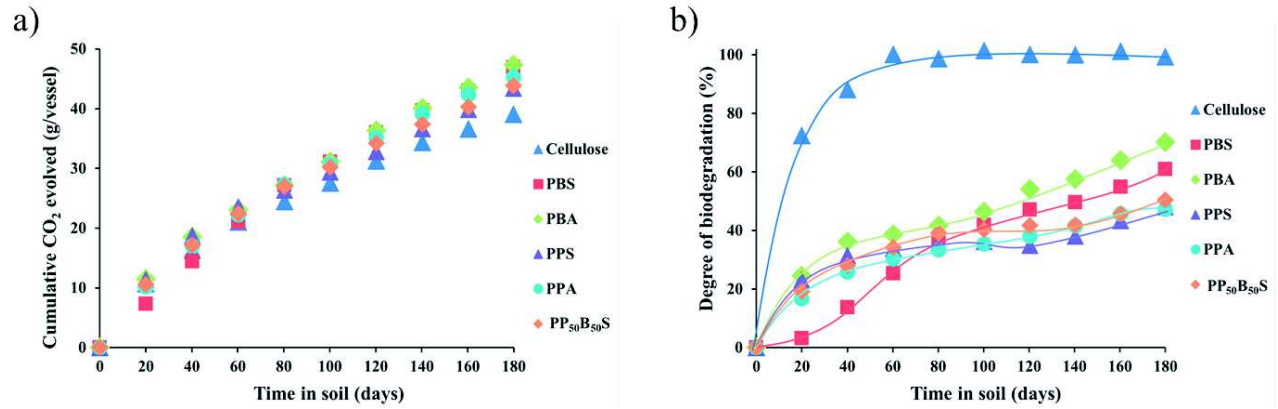

Figure 2.3.9 : Average values of (a) Cumulative CO2 data and (b) degrees of biodegradation of reference (cellulose) and test materials as a function of degradation in soil.

5. Conclusion

Two potentially biobased aliphatic copolyesters (PPBA and PPBS) based on renewable building blocks were successfully synthesized at different composition in melt with TTIP as catalyst. For both types of copolyesters, the synthetic pathway permitted to obtain (i) high molar masses, (ii) copolyesters with the same final molar composition than initial feed ratio and (iii) a random distribution between 1,3-PDO and 1,4-BDO segments along the (co)polyester chain.

PPBA and PPBS copolyesters exhibited both an excellent thermal stability without mass loss before 300 °C. Moreover, analysis of PPBS and PPBA copolyesters exhibited that the chemical nature and length of the diol had no effect on the thermal degradation profile unlike the diacid used.

Both copolyesters showed an isodimorphic co-crystallization behavior characterized by a pseudo-eutectic melting behavior and the presence of only one crystalline phase by sample, except for PPBA copolyesters with 1,3-PDO content of 50-59 mol.% which were in molten state at ambient temperature. The inclusion of the second co-monomer inside the crystal lattice altered significantly the crystal structures leading to a decrease of the degree of crystallinity with the co-monomer content. Moreover, the fact that some samples with high 1,3-PDO content did not crystallize during the cooling or the second heating run at a cooling/heating rate of 10 °C/min showed that 1,3-PDO decreased significantly the crystallization rate of the copolyesters. Finally, T_g of copolyesters increased with the 1,3-PDO content and by using SA instead of AA, due to the decrease of the chain mobility resulting from an increase of the ester function density.

One of the important features was that the aerobic biodegradation rate in soil increased slightly with the increase of the diol length from 3 to 4 carbons and especially with the diacid length from 4 to 6 carbons, without showing any residual ecotoxicity.

Finally, these two copolyesters seemed promising biobased and biodegradable materials, with the addition of 1,3-PDO units in the copolyesters being an interesting way to decrease their degree of crystallinity. These materials could thus have suitable properties for applications such as packaging, especially PPBS copolyesters with low 1,3-PDO content, since it has close properties to PBS and PBSA which are known for their packaging applications. Copolyesters with high 1,3-PDO content would be more suitable for applications such as adhesives due to their low crystallinity. To complete this study and confirm such potential applications, further investigations for instance on the climatic ageing (effect of humidity, temperature, UV) and the gas barrier properties of these materials could be performed.

6. References

Arandia, I., Mugica, A., Zubitur, M., Arbe, A., Liu, G., Wang, D., Mincheva, R., Dubois, P., Müller, A.J., 2015. Macromolecules 48, 43–57.

Avérous, L., 2004. J. Macromol. Sci. Part C 44, 231–274.

Barton, N.R., Burgard, A.P., Burk, M.J., Crater, J.S., Osterhout, R.E., Pharkya, P., Steer, B.A., Sun, J., Trawick, J.D., Dien, S.J.V., Yang, T.H., Yim, H., 2014. J. Ind. Microbiol. Biotechnol. 42, 349–360.

Bechthold, I., Bretz, K., Kabasci, S., Kopitzky, R., Springer, A., 2008. Chem. Eng. Technol. 31, 647–654.

Becker, J., Lange, A., Fabarius, J., Wittmann, C., 2015. Curr. Opin. Biotechnol. 36, 168–175.

Biebl, H., Menzel, K., Zeng, A.-P., Deckwer, W.-D., 1999. Appl. Microbiol. Biotechnol. 52, 289–297.

Bikiaris, D.N., Papageorgiou, G.Z., Giliopoulos, D.J., Stergiou, C.A., 2008. Macromol. Biosci. 8, 728–740.

Bozell, J.J., Petersen, G.R., 2010. Green Chem. 12, 539–554.

Charlier, Q., Girard, E., Freyermouth, F., Vandesteene, M, Jacquel, N., Ladavière, C., Rousseau, A., Fenouillot, F., 2015. Express Polym. Lett. 9, 424–434.

Chen, C.-H., Peng, J.-S., Chen, M., Lu, H.-Y., Tsai, C.-J., Yang, C.-S., 2010. Colloid Polym. Sci. 288, 731–738.

Debuissy, T., Pollet, E., Avérous, L., 2016a. Polymer 99, 204–213.

Debuissy, T., Pollet, E., Avérous, L., 2016b. Biomacromolecules 17, 4054–4063.

Debuissy, T., Pollet, E., Avérous, L., 2017a. Eur. Polym. J. 87, 84–98.

Debuissy, T., Pollet, E., Avérous, L., 2017b. Eur. Polym. J. 90, 92–104.

Debuissy, T., Pollet, E., Avérous, L., 2017c. J. Polym. Sci. Part Polym. Chem. n/a-n/a.

Díaz, A., Franco, L., Puiggalí, J., 2014. Thermochim. Acta 575, 45–54.

Drożdżyńska, A., Leja, K., Czaczyk, K., 2011. BioTechnologia 1, 92–100.

Fox, T., 1956. Bull. Am. Phys. Soc. 1, 123–132.

Gigli, M., Fabbri, M., Lotti, N., Gamberini, R., Rimini, B., Munari, A., 2016. Eur. Polym. J. 75, 431–460.

Gordon, M., Taylor, J.S., 2007. J. Appl. Chem. 2, 493–500.

Ho, R.-M., Ke, K.-Z., Chen, M., 2000. Macromolecules 33, 7529–7537.

Korntner, P., Sumerskii, I., Bacher, M., Rosenau, T., Potthast, A., 2015. Holzforschung 69, 807–814.

Kuo, C.-T., Chen, S.-A., 1989. J. Polym. Sci. Part Polym. Chem. 27, 2793–2803.

Lu, S.-F., Chen, M., Chen, C.H., 2012. J. Appl. Polym. Sci. 123, 3610–3619.

Lu, S.-F., Chen, M., Shih, Y.-C., Chen, C.H., 2010. J. Polym. Sci. Part B Polym. Phys. 48, 1299–1308.

Luo, S., Li, F., Yu, J., Cao, A., 2010. J. Appl. Polym. Sci. 115, 2203–2211.

Munari, A., Manaresi, P., Chiorboli, E., Chiolle, A., 1992. Eur. Polym. J. 28, 101–106.

Nanaki, S.G., Pantopoulos, K., Bikiaris, D.N., 2011. Int. J. Nanomedicine 6, 2981–2995.

Pan, P., Inoue, Y., 2009. Prog. Polym. Sci. 34, 605–640.

Papageorgiou, G.Z., Bikiaris, D.N., 2005a. Polymer 46, 12081–12092.

Papageorgiou, G.Z., Bikiaris, D.N., 2005b. Polymer 46, 12081–12092.

Papageorgiou, G.Z., Bikiaris, D.N., 2007. Biomacromolecules 8, 2437–2449.

Papageorgiou, G.Z., Bikiaris, D.N., 2009. Macromol. Chem. Phys. 210, 1408–1421.

Penzel, E., Rieger, J., Schneider, H.A., 1997. Polymer 38, 325–337.

Pérez-Camargo, R.A., Fernández-d'Arlas, B., Cavallo, D., Debuissy, T., Pollet, E., Avérous, L., Müller, A.J., 2017. Macromolecules 50, 597–608.

Pérez–Camargo, R.A., Saenz, G., Laurichesse, S., Casas, M.T., Puiggalí, J., Avérous, L., Müller, A.J., 2015. J. Polym. Sci. Part B Polym. Phys. 53, 1736–1750.

Polen, T., Spelberg, M., Bott, M., 2013. J. Biotechnol., Research on Industrial Biotechnology within the CLIB-Graduate Cluster - Part III 167, 75–84.

Pollet, E., Avérous, L., 2011. Production, Chemistry and Properties of Polyhydroxyalkanoates, in: Plackett, D. (Ed.), Biopolymers – New Materials for Sustainable Films and Coatings. John Wiley & Sons, Ltd, Chichester, pp. 65–86.

Reulier, M., Avérous, L., 2015. Eur. Polym. J. 67, 418–427.

Rizzarelli, P., Cirica, M., Pastorelli, G., Puglisi, C., Valenti, G., 2015. Polym. Degrad. Stab. 121, 90–99.

Šerá, J., Stloukal, P., Jančová, P., Verney, V., Pekařová, S., Koutný, M., 2016. J. Agric. Food Chem. 64, 5653–5661.

Soccio, M., Lotti, N., Finelli, L., Gazzano, M., Munari, A., 2007. Polymer 48, 3125–3136.

Spyros, A., Argyropoulos, D.S., Marchessault, R.H., 1997. Macromolecules 30, 327–329.

Umare, S.S., Chandure, A.S., Pandey, R.A., 2007. Polym. Degrad. Stab. 92, 464–479.

Van Krevelen, D.W., 1997. Chapter 5 - Calorimetric properties, in: Properties of Polymers (Third, Completely Revised Edition). Elsevier, Amsterdam, pp. 109–127.

Vilela, C., Sousa, A.F., Fonseca, A.C., Serra, A.C., Coelho, J.F.J., Freire, C.S.R., Silvestre, A.J.D., 2014. Polym. Chem. 5, 3119–3141.

Wang, B., Li, C.Y., Hanzlicek, J., Cheng, S.Z.D., Geil, P.H., Grebowicz, J., Ho, R.-M., 2001. Polymer 42, 7171–7180.

Ward, I.M., Wilding, M.A., Brody, H., 1976. J. Polym. Sci. Polym. Phys. Ed. 14, 263–274.

Way, C., Wu, D.Y., Dean, K., Palombo, E., 2010. Polym. Test. 29, 147–157.

Werpy, T.A., Holladay, J.E., White, J.F., 2004. Top Value Added Chemicals from Biomass: I. Results of Screening for Potential Candidates from Sugars and Synthesis Gas (No. PNNL-14808). Pacific Northwest National Laboratory (PNNL), Richland, WA (US).

Xu, J., Guo, B.-H., 2010. Biotechnol. J. 5, 1149–1163.

Xu, Y., Xu, J., Guo, B., Xie, X., 2007. J. Polym. Sci. Part B Polym. Phys. 45, 420–428.

Xu, Y., Xu, J., Liu, D., Guo, B., Xie, X., 2008. J. Appl. Polym. Sci. 109, 1881–1889.

Yamadera, R., Murano, M., 1967. J. Polym. Sci. [A1] 5, 2259–2268.

Sub-chapter 2.4. Synthesis of potentially biobased copolyesters based on adipic acid and butanediols: kinetic study between 1,4- and 2,3-butanediol and their influence on crystallization and thermal properties

Thibaud Debuissy, Eric Pollet and Luc Avérous*

BioTeam/ICPEES-ECPM, UMR CNRS 7515, Université de Strasbourg, 25 rue Becquerel, 67087 Strasbourg Cedex 2, France

*Corresponding author: luc.averous@unistra.fr

Published by Polymer, 2016, 99, 204-213

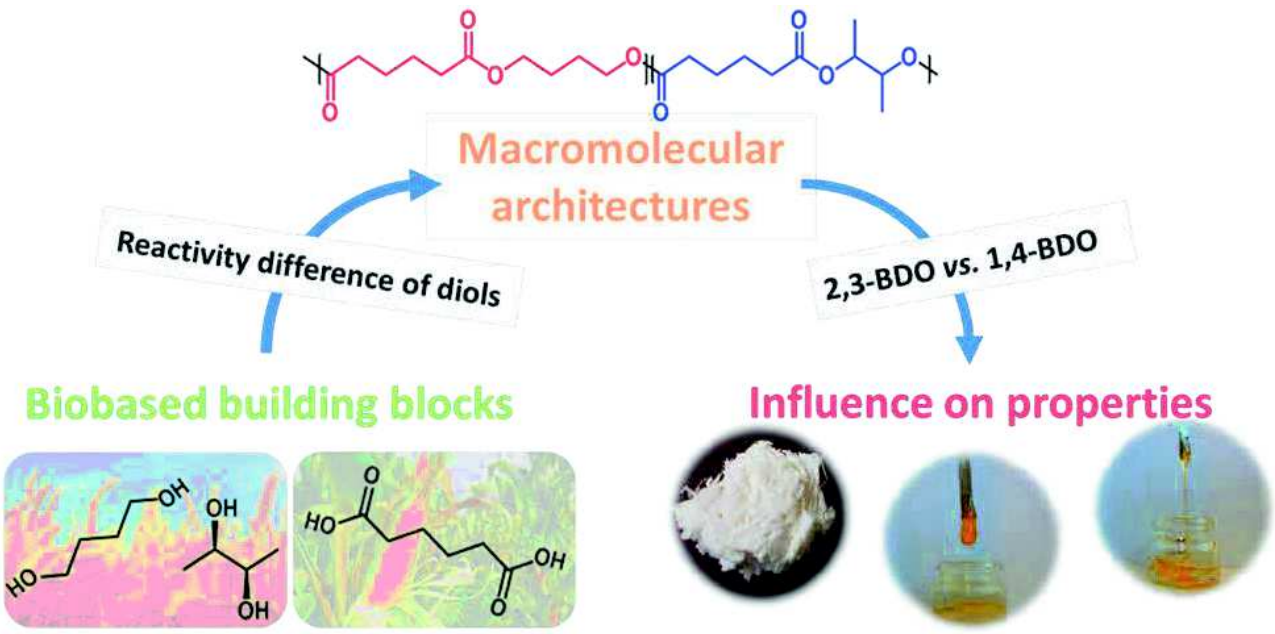

1. Abstract

Different potentially biobased copolyesters with specific macromolecular architectures are successfully synthesized from renewables diols and diacids, and characterized. The first part focuses on the study of the esterification kinetic of two equimolar systems, 1,4-butanediol (1,4-BDO)/adipic acid (AA) and 2,3-butanediol (2,3-BDO)/AA, with and without titanium isopropoxide (TTIP) as catalyst. The influence of the type of diol (primary vs. secondary hydroxyl groups) and the temperature is also investigated. The esterification rate with 2,3-BDO is slower than with 1,4-BDO leading to higher activation energy. In the second part, poly(1,4-butylene adipate) (PBA) and poly(2,3-butylene adipate) (PB'A) aliphatic polyesters and the corresponding copolyester [poly(1,4-butylene adipate-*co*-2,3-butylene adipate) (PBB'A)] are synthesized by transesterification in bulk using TTIP. According to our knowledge, the synthesis of PBB'A is reported here for the first time. All synthesized copolymers are characterized by NMR, SEC, FTIR, WAXS, MALDI-TOF, DSC, TGA and specific optical rotation. PBA with a mass-average molar mass around 60,000 g/mol is obtained, whereas molar mass of PB'A and PBB'A are significantly lower. The 2,3-BDO molar content in copolyesters is lower than the initial molar feed content. A linear evolution is observed between 2,3-BDO content and specific optical rotation of the polyesters allowing to use this relation as an additional method to determine PBB'A composition. PBA shows a semi-crystalline behavior, whereas PB'A is amorphous. An increase of the 2,3-BDO content in the copolyester raises the glass transition temperature and reduces the degree of crystallinity. All polyesters exhibit a good thermal stability, exceeding 280 °C, with a maximum rate of degradation around 380 °C.

2. Introduction

Over the last decades, renewable polymers have attracted considerable attention, as an alternative to petroleum-based materials. Some of the biobased polymers can also bring new macromolecular architectures with the corresponding advanced properties. Among them, poly(lactic acid) (PLA) (Avérous, 2004), poly(butylene succinate) (PBS) (Gigli et al., 2016b; Ojijo and Ray, 2012), poly(hydroxyalkanoates) (PHA) (Bordes et al., 2009b; Pollet and Avérous, 2011) have seen their interest growing on an industrial point of view. The development of biorefinery was necessary to produce the corresponding biobased monomers or building blocks, such as succinic acid, lactic acid, 1,4-butanediol (1,4-BDO), furans, glycerol and others (Becker et al., 2015; Bozell and Petersen, 2010).

Adipic acid (AA) is a very interesting aliphatic six-carbon diacid used as building block in the synthesis of nylon-6,6, polyurethanes and polyesters such as poly(butylene adipate-co-butylene terephthalate) (PBAT) (Avérous and Fringant, 2001; Chivrac et al., 2006) or poly(butylene succinate-co-butylene adipate) (Avérous and Fringant, 2001; Becker et al., 2015; Ojijo and Ray, 2012). New biological pathways were discovered for the bioproduction of AA from different biomass such as glucose (Polen et al., 2013), lignin (Vardon et al., 2015) and fatty acids (Picataggio et al., 1992). 1,4-BDO is a well-known short diol with primary hydroxyl (OH) functions used for example as chain extender in the polyurethane synthesis (Bueno-Ferrer et al., 2012; Reulier and Avérous, 2015) or as building block for the synthesis of PBS or polyamides. Biobased 1,4-BDO is obtained *via* a chemical process of hydrogenation from biobased succinic acid (Bozell and Petersen, 2010; Choi et al., 2015). 2,3-butanediol (2,3-BDO) is also a very interesting diol based on secondary OH functions, used as a precursor in the manufacture of a range of chemical products such as methyl ethyl ketone, gamma-butyrolactone and 1,3-butadiene (Köpke et al., 2011). Contrary to 1,3-propanediol and 1,4-BDO which are not natural metabolites, 2,3-BDO is a natural fermentation product of many species of bacteria and can be directly produced from different bio-resources such as xylose, sugar cane molasses, glucose and corn (Wang et al., 2016). Thus, 2,3-BDO is often easily obtained by fermentation but it still has a limited use as monomer.

Until now, only few researches have been focused on polyesters based on 2,3-BDO, even if the esterification of many diacids with 2,3-BDO were first published in 1950 by Watson et al (Watson, Ralph W., 1950; Watson et al., 1950). Earlier patents of low molar mass aromatic polyesters or resins containing 2,3-BDO as main diol, or co-diol for PBAT or other aliphatic-aromatic copolyesters synthesis, have been published (Alidedeoglu et al., 2013; Alidedeoglu and Kannan, 2013). Despite its expected lower reactivity, the properties induced from the use of 2,3-BDO such as a decrease in the degree of crystallinity or an increase of the glass transition can be of interest for some applications such as adhesives. The synthesis of low molar mass polyesters using 2,3-BDO for coating applications has been recently reported (E. Gubbels et al., 2013; Gubbels et al., 2014; Noordover et al., 2006). Recently, an unsaturated copolyesters

containing 2,3-BDO with more important molar mass has been synthesized (Hu et al., 2016). However, until now, no study has been reported on the synthesis of aliphatic biobased copolyesters containing 2,3-BDO and 1,4-BDO.

The transesterification polycondensation reaction from the melt with organometallic catalyst is the most used and a promising way to synthesize high molar mass polyesters. For instance, high molar masses PBA were synthesized with titanium (IV) n-butoxide or titanium (IV) isopropoxide (TTIP), as organometallic catalyst (Ahn et al., 2001; Nikolic and Djonlagic, 2001; Tserki et al., 2006b). Titanium-based catalysts are the most efficient organometallic catalysts for the transesterification reaction compared to catalysts based on zirconium, tin, hafnium or antinomy (Jacquel et al., 2011).

Most of the kinetic studies about polyester synthesis dealt with monomers containing only primary diols (Hakan Akat, 2006; Hu et al., 2010; Kuo and Chen, 1989; Vancsó-Szmercsányi et al., 1969). Few studies investigated the polyesterification kinetics between a diacid and a diol containing both primary and secondary OH functions such as 1,2-propanediol (Chang and Karalis, 1993; Vaidya and Nadkarni, 1989) or 1,3-BDO (Bacaloglu et al., 1998), but no comparison of the reactivity of these two types of OH functions was reported. To the best of our knowledge, the present study is the first to investigate the esterification rate between a diacid and a diol containing two secondary OH functions and to compare its reactivity with a diol having only primary OH functions.

The aim of this study is to investigate and compare, in a first step, the esterification kinetics between the non-catalyzed and TTIP-catalyzed esterification of two equimolar systems (1,4-BDO/AA and 2,3-BDO/AA) at different temperatures. For this purpose, the investigation is focused on: (i) the effect of BDOs (primary vs. secondary OH), (ii) the effect of the temperature and (iii) the effect of the TTIP catalyst. In the second part, esterification kinetic of non-equimolar systems containing 2 or 3 co-monomers is studied. The synthesis and the properties of high molar masses copolyesters (PBB'A) with varying 2,3-BDO contents are investigated and reported. For this purpose, the macromolecular structures of copolyesters, determined by NMR, SEC, FTIR, WAXS, MALDI-TOF and specific optical rotation, as well as their thermal behavior (DSC, TGA) are analyzed. The effect of the 2,3-BDO content for the copolyester properties is particularly discussed.

3. Experimental part

3.1. Materials

1,4-BDO (99%), chloroform (99.0-99.4%), chromium(III) acetyl acetonate (97%), tetramethyl-1,3,2-dioxaphospholane (Cl-TMDP, 95%) and cholesterol (> 99%) were purchased from Sigma-Aldrich. 2R,3R-(-)-2,3-BDO (98%, ee: 99%) and pyridine HPLC grade (99.5+%) were purchased from Alfa Aesar. AA (99%), titanium (IV) isopropoxide (TTIP) (98+%) and extra dry toluene (99.85%) were supplied by Acros. All reactants were used without further purification. All solvents used for the analytical methods were of analytical grade.

3.2. Kinetic study

Reactions were performed in a 50 mL round bottom flask with a micro-distillation device in order to recover the reaction by-product (water). A constant argon flux was supplied and the magnetic stirring was set to 400 rpm. All reactions were performed in stoichiometric conditions between OH functions (1,4-BDO or 2,3-BDO) and carboxylic acid functions (AA). For esterification with catalyst, TTIP was added with a ratio of 0.1 mol% of the amount of AA used. Kinetic studies were conducted at 140, 150 and 160 °C. Aliquots were withdrawn of the reaction mixture at predetermined reaction times (30, 60, 120, 180 and 240 min) and analyzed by ^{1}H-NMR.

3.3. Synthesis of copolyesters

3.3.1. Elaboration of the copolyesters

Aliphatic polyesters were synthesized by a two-stage melt polycondensation method (esterification and transesterification). Syntheses were performed in a 50 mL round bottom flask with a distillation device in order to recover the reaction by-product (mainly water). All reactions were performed with a diol/acid molar ratio of 1.25/1 at 150 °C. TTIP was added at a content of 0.1 mol% of the amount of AA used.

The round bottom flask was charged with AA and the proper amount of one diol or an equimolar mixture (50/50) of two diols (1,4-BDO/2,3-BDO). During the first step (esterification), the reaction mixture was maintained at 150 °C for 24 h under a constant argon flux and stirred at 300 rpm. After 24 h of oligomerization, the proper amount of a 5 wt% solution of TTIP in extra dry toluene was introduced in the reaction medium and the mixture was stirred for 1 h at 150 °C under an argon flux. After that, the reaction mixture was heated to 180 °C and the pressure was decreased stepwise over a period of 1 h in order to avoid uncontrolled foaming and to minimize oligomer sublimation. Finally, the pressure was decreased until 1-3 mbar and the transesterification step was allowed to proceed for 4 h. At the end, the crude synthesized polyester was recovered and dried under reduced pressure at 70 °C for 24 h in a ventilated oven.

3.3.2. Copolyester elaboration with improved 2,3-butanediol incorporation

A second procedure has been developed for the specific synthesis of the copolyester. In this case, the esterification time was increased to a total of 48 h with a global molar feed ratio of 50/50. The reaction mixture procedure is modified. At the beginning of the reaction, one equivalent of AA with 0.625 equivalent of 2,3-BDO were esterified at 150 °C under an argon flux for 24 h. After 24 h, 0.625 equivalent of 1,4-BDO were added into the reaction mixture and the esterification was continued for 24 h at 150 °C. The transesterification step was performed with the same procedure as before.

3.4. General methods and analysis

^{1}H- and ^{13}C-NMR spectra of polyesters were obtained with a Bruker 400 MHz spectrometer. DMSO-d_6 was used as solvent to prepare solutions with concentrations of 8-10 and 30-50 mg/mL for ^{1}H-NMR and ^{13}C-NMR, respectively. The number of scans was set to 128 for ^{1}H-NMR and at least 2048 for ^{13}C-NMR. Calibration of the spectra was performed using the DMSO peak (δ_H = 2.50 ppm, δ_C = 39.52 ppm).

^{31}P-NMR was performed after phosphitylation of the samples, according to standard protocols (Spyros et al., 1997). An accurately weighed amount of sample (about 50-100 mg) was dissolved in 500 µL of anhydrous $CDCl_3$. 100 µL of a standard solution of cholesterol (0.1 M in anhydrous $CDCl_3$/pyridine (1/1.6) solution) containing Cr(III) acetyl acetonate as relaxation agent was then added. Finally, 50 µL of 2-chloro-4,4,5,5-tetramethyl-1,3,2-dioxaphospholane (Cl-TMDP) were added and the mixture was stirred at room temperature for 2h. Spectra were measured on a Bruker 400 MHz spectrometer (128 scans at 20 °C). All chemical shifts reported are relative to the reaction product of water with Cl-TMDP, which gives a sharp signal in pyridine/$CDCl_3$ at 132.2 ppm. The quantitative analysis of end-groups and the calculation of molar masses by ^{31}P-NMR were performed based on previous reports (Siotto et al., 2013; Spyros et al., 1997).

The number-average molar mass (M_n), the mass-average molar mass (M_w) and the dispersity (Đ) of the polyesters samples were determined in chloroform by Size Exclusion Chromatography (SEC), using a Shimadzu liquid chromatograph. The columns used were PLGel Mixed-C and PLGeL 100 Å. A refractive index detector was used. Chloroform was used as eluent at a flow rate of 0.8 ml/min. The apparatus was calibrated with linear polystyrene standards from 162 to 1,650,000 g/mol.

MALDI-TOF MS analysis was performed using a MALDI-TOF-TOF Autoflex II TOF-TOF (Bruker Daltonics) equipped with a nitrogen laser (λ = 337 nm) and super DHB (9:1 mixture of DHB and 2-hydroxy-5-methoxybenzoic acid) as matrix. Scan accumulation and data processing were performed with FlexAnalysis 3.0 software.

Infrared spectroscopy (IR) was performed with a Fourier transformed infrared spectrometer Nicolet 380 (Thermo Electron Corporation) used in reflection mode and equipped with an ATR diamond module (FTIR-ATR). The FTIR-ATR spectra were collected at a resolution of 4 cm^{-1} and with 64 scans per run.

Differential scanning calorimetry (DSC) was performed using a TA Instrument Q 200 under nitrogen (flow rate of 50 mL/min), calibrated with high purity standards. Samples of 2-3 mg were sealed in aluminum pans. A three-step procedure was applied with a 10 °C min^{-1} ramp: (1) heating up to 30-40 °C above the melting temperature (minimum 90 °C) and holding for 5 min, to erase the thermal history; (2) cooling down to -80°C and holding for 5 min; (3) heating (second heating) from -80 °C to the same temperature as the first heating. The degree of crystallinity (X_c) is calculated according to Equation (2.4.1):

$$X_c(\%) = \frac{\Delta H_m}{\Delta H_m{}^0} \times 100 \qquad (2.4.1)$$

where the melting enthalpy (ΔH_m) is taken from the second heating run and $\Delta H_m{}^0$ is the melting enthalpy of a 100% pure crystalline polyester.

Thermal degradations were studied by thermogravimetric analyses (TGA). Measurements were conducted under helium atmosphere (flow rate of 25 mL/min) using a Hi-Res TGA Q5000 apparatus from TA Instruments. Samples (1-3 mg) were heated from room temperature up to 600 °C at a rate of 20 °C/min.

The specific optical rotation $[\alpha]^{20}_D$ was measured by a polarimeter MPC 200 thermostated at 20.0 °C, in a 100 mm long cell (diameter = 0.3 mm). Measured solution was prepared at a concentration between 1.5 and 2.5 g/100 mL in chloroform.

Wide angle X-ray Scattering (WAXS) data were recorded on a Siemens D5000 diffractometer using Cu K_α radiation (1.5406 Å) at 25-30°C in the range of 2θ = 5-40° at 1.7 °.min^{-1}.

3.5. Ester function density

The ester function density in copolyesters ($D_{ester,copo}$) is defined by Equation (2.4.2),

$$D_{ester,copo} = \omega_{1,4-butylene} \times D_{ester,PBA} + \omega_{2,3-butylene} \times D_{ester,PB'A} \qquad (2.4.2)$$

where: $\omega_{1,4\text{-butylene}}$ is the 1,4-butylene molar content in the copolyester, $\omega_{2,3\text{-butylene}}$ is the 2,3-butylene molar content in the copolyester, $D_{ester,PBA}$ is the ester function density in PBA and $D_{ester,PB'A}$ is the ester function density in PB'A.

4. Results and discussion

4.1. Kinetic study on esterification of equimolar systems based on 2 monomers

A kinety study of the esterification between two equimolar systems, 1,4-BDO/AA and 2,3-BDO/AA, both with and without catalyst (TTIP) was performed at different temperatures from 140 to 160°C. Kinetic studies are based on two main assumptions. First, all OH and COOH groups have the same activity regardless to the chain length of the corresponding molecule. Secondly, the hydrolysis is neglected due to (i) the important water removal (reaction temperature, argon flux, vigorous stirring), (ii) the conversion is lower than 0.95 (Bacaloglu et al., 1998; Kuo and Chen, 1989), and (iii) an ester group from a weak acid molecule (such as AA) can be less easily hydrolyzed than an ester group obtained from a strong acid (Vancsó-Szmercsányi et al., 1969).

Figure 2.4.1 presents the extent of esterification (p), calculated according to the method developed in Annex 4, at 140 and 160 °C of the four systems. As expected, the esterification rate increases with the temperature and the esterification reactions with 1,4-BDO proceed largely faster than with 2,3-BDO, due to the less reactive secondary OH groups for the latter. A temperature increase from 140 to 160 °C is profitable for the esterification with 2,3-BDO, with an extent almost doubled, whereas it has little effect on the one of 1,4-BDO. This could be due to the fact that, at 140 °C, the extent of esterification of the 2,3-BDO/AA system is very low, whereas the 1,4-BDO/AA already reached a significant extent of esterification. These results also show that TTIP has only a small effect on the esterification rate. This could be due, in our conditions (equimolar proportion of monomers, 140-160 °C), to the non-negligible contribution of auto-catalysis compared to the external catalyst contribution. Indeed, Garin et al. showed, for the synthesis of PBS from equimolar proportion of monomers, that the reaction rate constant of the auto-catalysis contribution is higher than the external-catalysis one (with a Ti-based catalyst) (Garin et al., 2014a). Finally, one can observe that the benefit of TTIP decreases with the temperature and depends on the diol used. The higher influence of TTIP at lower temperature (140 °C) can be explained by the reaction being mainly kinetically controlled whereas at higher temperature, the part of the thermodynamic control increases and so the catalyst has a much lower impact on the esterification rate.

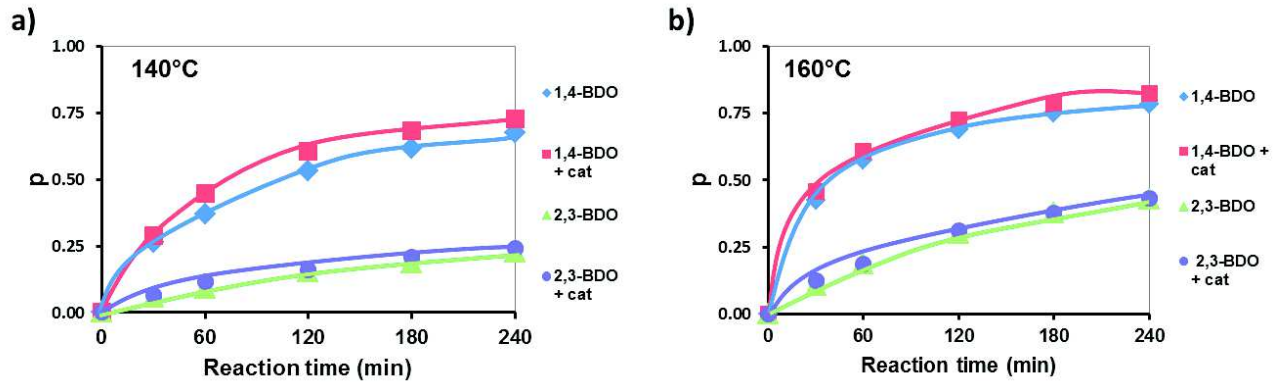

Figure 2.4.1 : Extent of the esterification vs. esterification time of four equimolar systems: 1,4-butanediol/AA, 1,4-BDO/AA+TTIP, 2,3-BDO/AA and 2,3-butanediol/AA+TTIP, at (a) 140 °C and (b) 160 °C.

For the two non-catalyzed equimolar systems (1,4-BDO/AA and 2,3-BDO/AA), plots of $1/(1-p)^{1,5}$ vs. esterification time show a linear relation proving that non-catalyzed esterifications verify an overall 2.5th order rate equation (Figure 2.4.2-a and Figure 2.4.2-b). According to Equation (SI.20) (in Annex 4), the corresponding esterification rate constants (k_2') are proportional to the slope. Plots of 1/(1-p) vs. esterification time of the two equimolar catalyzed systems show that titanium-based catalyzed esterifications verify an overall 2nd order rate equation (Figures 2.4.2-c,d). Catalyzed systems obey also to Equation (SI.13) (in Annex 4) and rate constants k_1' are proportional to the slope. All k_1' and k_2' values determined in this study are summarized in Table 2.4.1.

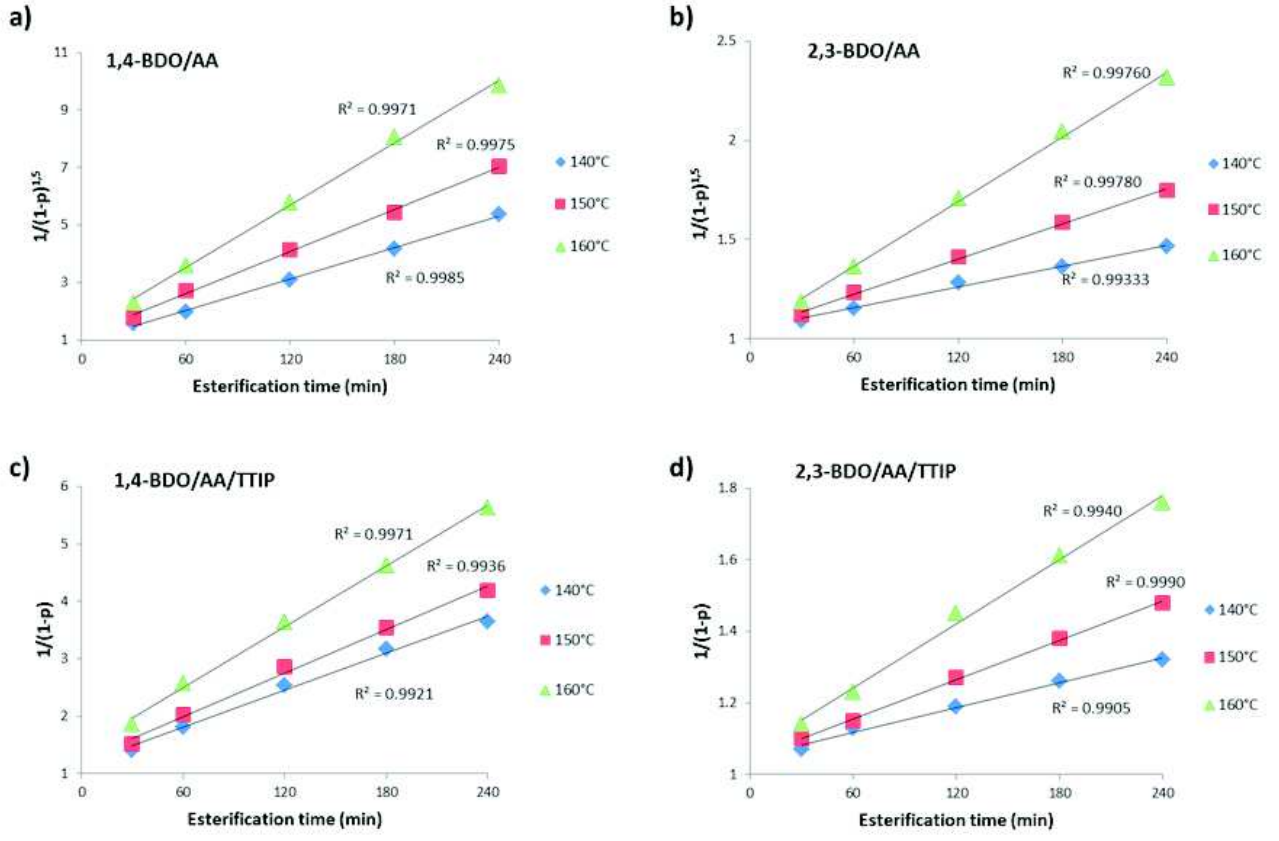

Figure 2.4.2 : Plots of $1/(1-p)^{1.5}$ vs. esterification time at different temperatures for equimolar non-catalyzed reactions of 1,4-BDO/AA (a) and 2,3-BDO/AA (b) systems; Plots of 1/(1-p) vs. esterification time at different temperatures for equimolar catalyzed reactions of 1,4-BDO/AA (c) and 2,3-BDO/AA (d) systems.

Kinetic constants (k_1' and k_2') increase with the temperature for all systems. Moreover, values obtained for 1,4-BDO are higher than for 2,3-BDO, confirming the higher reactivity of primary OH functions compared to secondary ones (Gallaher et al., 1996; Grecea et al., 2012). On the same way, rate constants with 1,4-BDO for non-catalyzed and catalyzed systems are about 10, 8 and 7 times higher than with 2,3-BDO at 140, 150 and 160 °C, respectively. By

increasing the temperature, the difference of k_1' (or k_2') decreases continuously between both systems. However, the relatively low boiling point of 2,3-BDO at around 175-180 °C does not allow to increase further the reaction temperature in order to reduce the reactivity gap between these two diols.

Plots of ln(k_1') vs. 1/T and ln(k_2') vs. 1/T (Figure 2.4.3) allow to calculate the activation energy (E_a) of the different systems. The Arrhenius equation (Equation SI.29 in Annex 4) is obeyed since straight lines are obtained for all systems. E_a of the non-catalyzed and catalyzed 1,4-BDO/AA systems are found to be 50.6 kJ.mol^{-1} and 37.3 kJ.mol^{-1}, respectively, whereas E_a of the non-catalyzed and catalyzed 2,3-BDO/AA systems are equal to 83.7 kJ.mol^{-1} and 70.7 kJ.mol^{-1}, respectively. As expected, E_a of systems containing 1,4-BDO are lower than E_a of systems with 2,3-BDO. The obtained value for non-catalyzed esterification of 1,4-BDO is in good agreement with previously reported data for non-catalyzed esterification (Kuo and Chen, 1989). Concerning the Ti-based catalyzed esterification of AA with 1,4-BDO, no data was found in the literature. However, our result is very close to the previously reported data for the *p*-toluenesulfonic acid-catalyzed esterification of 1,4-BDO/AA (Kuo and Chen, 1989). Lastly, E_a difference between non-catalyzed and catalyzed systems is similar (about 13 kJ.mol^{-1}) for both systems, showing that TTIP reduces by the same extent the energy barrier during the esterification with both diols.

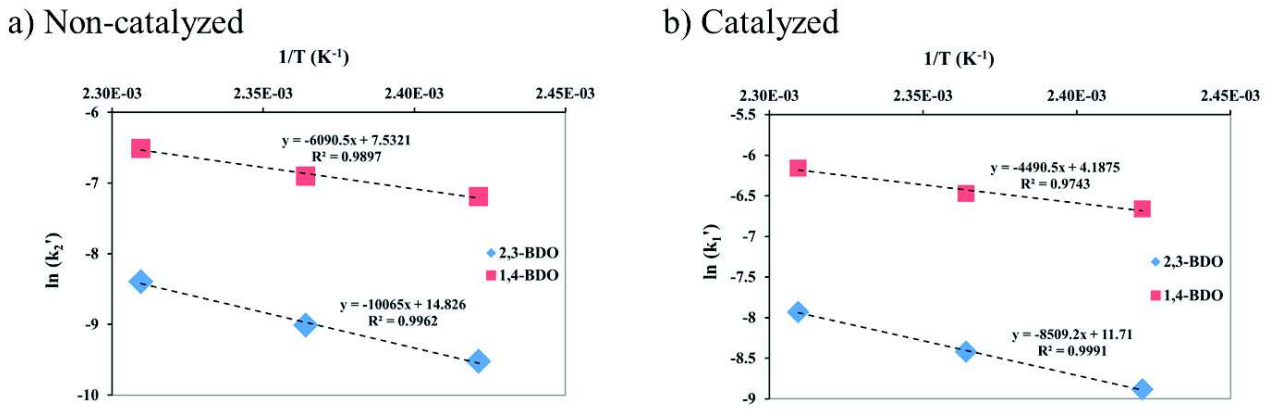

Figure 2.4.3 : (a) Plots of ln(k_2') vs. 1/T for equimolar non-catalyzed systems of 1,4-BDO/AA and 2,3-BDO/AA; (b) Plots of ln(k_1') vs. 1/T for equimolar catalyzed systems of 1,4-BDO/AA and 2,3-BDO/AA.

Table 2.4.1 : Kinetic constants and activation energies of PBA and PB'A esterification with and without TTIP.

	1,4-BDO / AA				2,3-BDO / AA			
	Non catalyzed		Catalyzed		Non catalyzed		Catalyzed	
Temperature °C	k_2' x 10^4 eq$^{1.5}$.kg$^{-1.5}$.min^{-1}	E_a kJ.mol^{-1}	k_1' x 10^3 eq.kg^{-1}.min^{-1}	E_a kJ.mol^{-1}	k_2' x 10^4 eq$^{1.5}$.kg$^{-1.5}$.min^{-1}	E_a kJ.mol^{-1}	k_1' x 10^4 eq.kg^{-1}.min^{-1}	E_a kJ.mol^{-1}
140	7.50		1.28		0.73		1.38	
150	10.0	50.6	1.54	37.3	1.22	83.7	2.20	70.7
160	14.8		2.11		2.25		3.59	

4.2. Synthesis of PBB'A copolyesters from non-equimolar systems and kinetic study

In the first step of the synthesis of copolyesters (Scheme 2.4.1), the non-catalyzed esterification at 150 °C for 24 h with 25 mol% excess of diol results in formation of oligomers with sufficient chain length to avoid any sublimation phenomenon during the next step. Reaction conditions were different from previous reports on 2,3-BDO-based polyesters which used higher temperature (E. Gubbels et al., 2013; Hu et al., 2016). In this study, a lower esterification temperature was used because of (i) the low boiling point of 2,3-butanediol ($T_b \approx 175$°C) and (ii) the use of a diol excess of only 25 mol%, whereas Koning *et al.* (E. Gubbels et al., 2013) used a 200 mol% excess of 2,3-butanediol, makes a 2,3-BDO loss not negligible for our syntheses.

Figure 2.4.4-a shows the monitoring of carboxylic acid (COOH) functions conversion during the esterification step of the synthesis of PBA, PB'A and PBB'A syntheses (molar feed ratio of 50/50 between 1,4-BDO/2,3-BDO). As observed for the equimolar esterification, all curves show an inverse-exponential shape and the rate of esterification is faster for PBA (based on 1,4-BDO) than for PB'A (based on 2,3-BDO). As expected, the copolyester PBB'A shows an intermediate reaction rate. After 24 h of esterification at 150 °C, extents of reaction are 0.75, 0.80 and 0.93 for PB'A, PBB'A and PBA, respectively. The higher reactivity of 1,4-BDO compared to 2,3-BDO in non-equimolar systems leads to higher molar masses after esterification for PBA than PB'A. After 24 h of esterification, SEC results show that the mass-average molar mass reaches 1,400, 2,500 and 6,500 g/mol for PB'A, PBB'A and PBA, respectively.

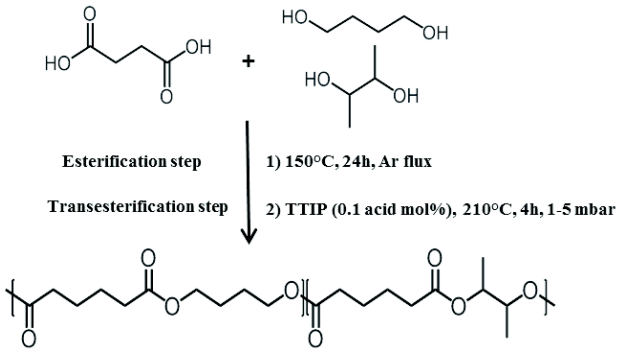

Scheme 2.4.1 : Reaction procedure of PBB'A copolyesters.

Using Equation (SI.26) (in Annex 4), relative to non-catalyzed esterification in non-equimolar proportions, kinetic constants of these reactions were determined. Figure 2.4.4-b shows the plot of (R-1)/(1-p) – ln [(R-p)/(1-p)] vs. esterification time for the three synthesized copolyesters. For each synthesis, the plot is a straight line with the rate constant (K_1) as slope. Figure 2.4.2-b points that K_1 values increase with the 1,4-BDO content. $K_{1,PBA}$ (9.9 x 10^{-2} h^{-1}) is about 9 times higher than $K_{1,PB'A}$ (1.1 x 10^{-2} h^{-1}). This result is in line with the difference of reactivity from the previous kinetic study on non-catalyzed equimolar systems, between the 1,4-BDO/AA and 2,3-BDO/AA system, at 150°C. In details, $K_{1,PBB'A}$ (2.2 x 10^{-2} h^{-1}) is the double of $K_{1,PB'A}$, whereas $K_{1,PBA}$ is more than four times higher than $K_{1,PBB'A}$. Even if the reaction mixture of the copolyester is charged with an equimolar proportion of 1,4-BDO and 2,3-BDO, the overall reaction rate (determined from the conversion of COOH functions) is not strictly on the average of the two $K_{1,PBA}$ and $K_{1,PB'A}$ values. It seems that 2,3-BDO acts as a "retardant" during the esterification. We assume that, at the beginning of the reaction, main consumed OH are primary OH groups from 1,4-BDO and then, as their content decreases, the proportion of secondary OH groups from 2,3-BDO consumed per unit of time increases.

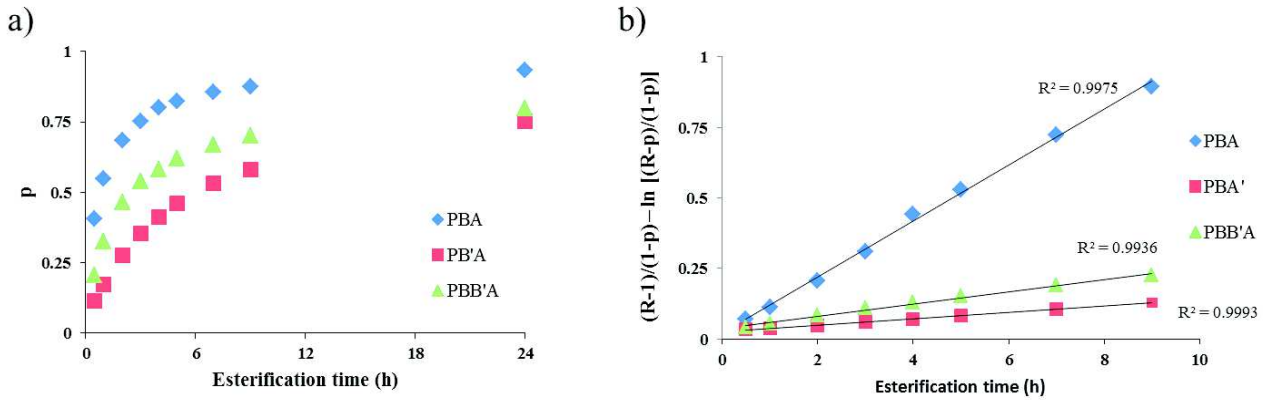

Figure 2.4.4 : (a) Plots of p vs. esterification time for the esterification step at 150°C of PBA, PB'A and PBB'A syntheses; (b) Plots of (R-1)/(1-p) – ln [(R-p)/(1-p)] vs. esterification time for the esterification step at 150°C of PBA, PB'A and PBB'A syntheses.

During the second step of the copolyesters synthesis, TTIP is added into the reaction mixture and transesterification under vacuum of the previously synthesized oligomers results in a significant increase of copolyesters molar masses. Figure SI.15 (in Annex 4) exhibits the chain growth of PBA, PB'A and PBB'A, determined by SEC, during the transesterification step. The chain extension is limited for PB'A and PBB'A with a rise of the mass-average molar mass

until 11,000-12,000 g/mol, whereas the chain extension of PBA is substantial with a final molar mass exceeding 60,000 g/mol after 5 h. This is due to the huge reactivity difference between the OH groups (secondary vs. primary). The same tendency was previously observed with the increase of the 2,3-BDO content (Hu et al., 2016). SEC results are summarized in Table 2.4.2. All samples have a dispersity of about 2.0.

The molar composition of synthesized copolyesters is determined from ^{1}H-NMR analyses (Equation (SI.31) in Annex 4). Results are summarized in Table 2.4.2. At the end of the reaction, the copolyester has a molar composition of 67/33 (1,4-butylene segments/2,3-butylene segments), whereas the feed molar ratio was 50/50. This result shows that not all the 2,3-BDO reacted during the synthesis and especially during the esterification step. This limited incorporation of 2,3-BDO could be due to (i) a very low reactivity with AA and, (ii) monomer loss by distillation because of it low boiling point.

In order to increase the 2,3-butylene content of the copolyester and also to reduce the difference between the feed and the final composition, the esterification procedure can be modified by increasing the esterification rate, promoting the esterification of 2,3-BDO. Then, the esterification protocol with 50/50 (1,4-BDO/2,3-BDO) has been modified by increasing the esterification time without changing the temperature (due to the low boiling point of 2,3-BDO) or the diol/diacid ratio. Previous study had shown that a higher esterification temperature or higher diol/diacid ratio lead to a higher reactivity of monomers, but with a strong increase of the monomers waste (E. Gubbels et al., 2013). With our new procedure, the reaction extent after the esterification step (48 h) increased up to 0.86. The corresponding final molar composition of the copolyester was 55/45, attesting for a strong increase in the final 2,3-butylene content in the PBB'A copolyester, from 33 to 45%. Since a longer reaction time allows to increase the 2,3-BDO content incorporated in the polymer closer to the feed value, then it could be concluded that the problem of limited 2,3-BDO incorporation observed on the previous procedure is more likely due to its low reactivity with AA and not to its potential loss by evaporation during the reaction. The final mass-average molar mass of the $PB_{55}B'_{45}A$ (12,400 g/mol) is also slightly superior to the one of $PB_{67}B'_{33}A$ (10,600 g/mol).

Table 2.4.2 : Molar composition and molar masses of synthesized polyesters.

Sample	Feed composition 1,4-BDO/2,3-BDO	Exp. composition [a] 1,4-BDO/2,3-BDO	M_n [b]	COOH end groups [b]	Primary OH end groups [b]	Secondary OH end groups [b]	M_n [c]	M_w [c]	Đ [c]	[α] [d]
	mol%	mol%	kg/mol	%	%	%	kg/mol	kg/mol		°
PBA	100 / 0	100 / 0	18.0	43.0	57.0	0	31.2	60.8	1.95	0
$PB_{67}B'_{33}A$	50 / 50	67.1 / 32.9	2.8	96.0	2.5	1.5	5.1	10.6	2.08	2.6
$PB_{55}B'_{45}A$	50 / 50	55.1 / 44.9	3.6	92.8	5.9	1.3	5.6	12.4	2.24	4.2
PB'A	0 / 100	0 / 100	3.8	90.8	4.2	5.0	5.9	11.8	2.01	10.2

[a] Experimental composition measured by ^{1}H-NMR in $CDCl_3$; [b] Measured in $CDCl_3$ by ^{31}P-NMR; [c] Determined in chloroform by SEC with PS standard; [d] Measured in chloroform at 20 °C with a polarimeter.

4.3. Analysis of the final architectures and properties of the synthesized copolyesters

Since 2R,3R-(-)-BDO monomer contains two asymmetric carbons, the corresponding synthesized copolyesters possess also asymmetric carbons. To investigate the optical behavior of copolyesters with 2,3-butylene segments, the specific optical rotation ([α]) of the different copolyesters are determined in chloroform at 20.0 °C and results are summarized in Table 2.4.2. PBA shows, as expected, [α] value of 0 due to the absence of asymmetric carbons in the 1,4-BDO and adipic acid monomers. However, $PB_{67}B'_{33}A$, $PB_{55}B'_{45}A$ and PB'A exhibit [α] values of +2.6, +4.2 and +10.2°, respectively. [α] of PBB'A follows a linear increase with the 2,3-butylene content (Figure 2.4.5). By using a line equation ($y = 0.104x - 0.363$), this analytical method could be used as a complement to ^{1}H-NMR to determine the molar composition of synthesized PBB'A copolyesters. However, due to the limited number of calculated values, this method should be fully validated on a greater numbers of tests.

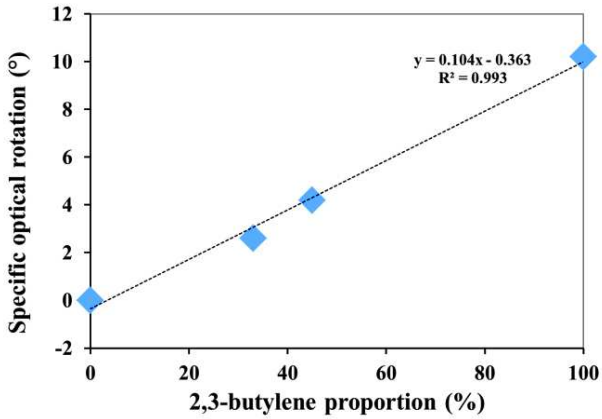

Figure 2.4.5 : Evolution of specific optical rotation of PBB'A copolyesters with the 2,3-butylene content.

^{1}H-NMR (Figure SI.14-a) and ^{13}C-NMR (Figure SI.14-b) spectra show characteristic signals of COOH end-groups attesting for the presence of a non-negligible amount of acid end-groups despite the fact that diols were introduced in excess in the reactor.

^{31}P-NMR analysis of PBA, PB'A, $PB_{67}B'_{33}A$ and $PB_{55}B'_{45}A$ are performed in $CDCl_3$ with cholesterol as standard (Figure 2.4.6-a). As expected, the ^{31}P-NMR spectrum of PBA shows COOH (134.9 ppm) and primary OH (147.2 ppm) end-groups. The calculated number-average molar mass of PBA by ^{31}P-NMR is 18,000 g/mol. This result is lower compared to the one obtained from SEC, which is overestimated due to the PS calibration. Surprisingly, the ^{31}P-NMR spectrum of PB'A shows COOH, secondary OH (146.1-146.4 ppm), but also primary OH end-groups. The majority of end-groups are COOH, whereas the amount of secondary and primary OH end-groups are low despite the higher introduced amount of OH functions compared to COOH groups. We suppose that the presence of primary OH end-groups in PB'A is due to the reduction of terminal COOH into primary OH, even if this assumption would need further investigations. The low amount of OH end-groups is more likely due to the chain extension by transesterification, which needs to consume at least one OH end-group, and thus decreases the OH end-groups content. We suppose that the limited extent of reaction after esterification (p = 0.80) is responsible for the large amount of COOH end-groups, which inhibit the chain extension, thus explaining why the number-average molar mass of PB'A reaches only 3,800 g/mol. The ^{31}P-NMR spectra of $PB_{67}B'_{33}A$ and $PB_{55}B'_{45}A$ are quite similar with a large majority of COOH end-groups (93-96%) and a low amount of primary and secondary OH end-groups. The number-average molar masses of $PB_{67}B'_{33}A$ and $PB_{55}B'_{45}A$ are 2,800 and 3,800 g/mol, respectively.

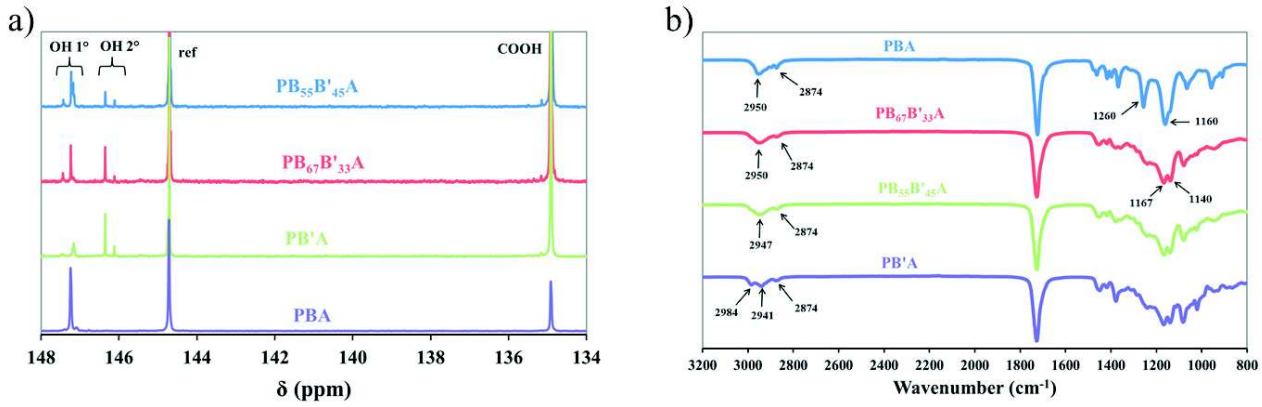

Figure 2.4.6 : (a) ^{31}P-NMR and (b) FTIR spectra of PBA, PB'A, $PB_{67}B_{33}'A$ and $PB_{55}B_{45}'A$.

MALDI-TOF analyses of copolyesters are presented in Figure SI.16 (in Annex 4). Results show that copolyesters have three different end-groups pairs: acid-acid, acid-alcohol or alcohol-alcohol. PBA chains display all three end-groups pairs but mostly have acid-alcohol end-groups and show lower amount of acid-acid and alcohol-alcohol pairs in equivalent proportion, which is in agreement with ^{31}P-NMR results (*i.e.*, 43% of COOH end-groups). The three copolyesters containing 2,3-BDO monomers (PB'A, $PBA_{67}B'_{33}A$ and $PBA_{55}B'_{45}A$) exhibit almost exclusively acid-acid

pairs, in perfect agreement with the high proportion (> 90%) of COOH end-groups determined by ^{31}P-NMR, due to the low reactivity of 2,3-BDO.

The FTIR analyses of PBA, PB'A and PBB'A are presented on Figure 2.4.6-b. FTIR spectra of $PB_{67}B'_{33}A$ and $PB_{55}B'_{44}A$ can be superimposed, whereas PBA and PB'A spectra present some differences. No broad resonance around 3400 cm^{-1} originating from OH end-groups are observed in all samples confirming the low amount of OH end-groups as previously stated by ^{31}P-NMR. As the 2,3-BDO content increases, the antisymmetric vibration of methylene carbons shifts to lower values from 2954 cm^{-1} (for PBA) to 2941 cm^{-1} for (PB'A) and it intensity decreases continuously. In the same time, the appearance of a signal at 2984 cm^{-1} assigned to the antisymmetric stretching vibration of methyl groups is observed by (i) the presence of a shoulder for $PB_{67}B'_{33}A$ and $PB_{55}B'_{44}A$, and (ii) the presence of a new signal at 2984 cm^{-1} for PB'A. A sharp signal is observed at 1727 cm^{-1} for the C=O stretching vibration from ester of all samples. Moreover, as the C-O stretching in the crystalline phase is composed of one strong signal at 1160 cm^{-1} in the PBA spectrum, two medium signals at 1167 and 1140 cm^{-1} are observed for PB'A, $PB_{67}B'_{33}A$ and $PB_{55}B'_{44}A$ samples, indicating the absence of crystalline phase in these three samples. Moreover, the CH_2 rocking vibration (725 cm^{-1}) are reduced in the PB'A spectrum compared to the PBA spectrum, probably due to the lower number of CH_2 in PB'A than in PBA.

TGA traces of PBA, PB'A and PBB'A samples are shown in Figure 2.4.7-a with their corresponding DTG curves. Under helium, all copolyesters degrade in three main steps which involve competitive mechanisms. First, a small mass loss is observed at 250-325 °C due to the degradation of low molar mass chains (Chrissafis et al., 2006a) along with the cyclization at the chain-ends and a back-biting reactions that are responsible for CO_2 and H_2O release, which are produced from the decomposition of COOH and OH chain-ends, respectively (Scheme SI.1 in Annex 1) (Persenaire et al., 2001). This degradation is more pronounced for PB'A and PBB'A than PBA, due to their lower molar masses. Secondly, a major degradation occurred between 325 and 425 °C, with a substantial mass loss of about 90-95 wt% corresponding to the thermal degradation, mostly by β- and α-hydrogen bond scissions. These reactions are responsible for the decomposition of polyesters into small compounds such as diacids, vinyl compounds, aldehydes and anhydrides (Bikiaris et al., 2007; Persenaire et al., 2001). After this decomposition step, mass residues of 3-4 wt% still remain. Then, a continuous low degradation rate is observed after 425 °C due to the decomposition of remaining material and finally only a small amount of ashes (1-2 wt%) is recovered at 550 °C. This multi-steps degradation is in agreement with previous reports (Bikiaris et al., 2007; Persenaire et al., 2001; Zorba et al., 2007).

The degradation temperature onset ($T_{d,2\%}$) of PBA, PB'A, $PBA_{67}B'_{33}A$ and $PBA_{55}B'_{45}A$ are 319, 280, 282 and 303 °C, respectively. By taking $T_{d,2\%}$ as criterion for the thermal stability of polyesters, PBA sample possess the highest thermal stability as a result of the highest molar mass. However, the 50 wt% degradation temperature and the maximal rate of thermal degradation are equivalent for all synthesized polyesters (around 373 and 380 °C, respectively), leading to a similar degradation profile for all samples.

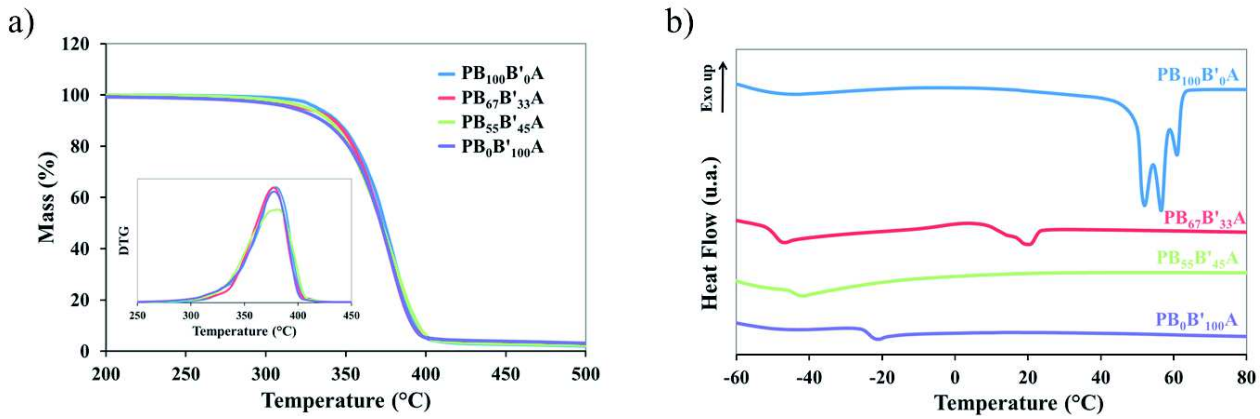

Figure 2.4.7 : (a) Mass loss and DTG, and (b) DSC curves of the second heating scan of PBA, $PB_{67}B'_{33}A$, $PB_{55}B'_{45}A$ and PB'A.

The WAXS analysis of copolyesters at 25 °C is presented in Figure 2.4.8. Results show that PB'A and $PB_{55}B'_{45}A$ are amorphous materials at room temperature, whereas PBA is a semi-crystalline polymer. Indeed, PBA shows diffraction

signals at 2θ = 21.4° and 24.4° assigned to β-form crystals but also reflections at 2θ = 21.6°, 22.4° and 24.0° assigned to α-form crystals. PBA thus exhibits (α + β) crystal mixture, as already reported by Yang *et al.* (Jinjun Yang et al., 2016). $PB_{67}B'_{33}A$ diffractogram exhibits very low degree of crystallinity with small diffraction peaks corresponding to crystal types similar to PBA ones.

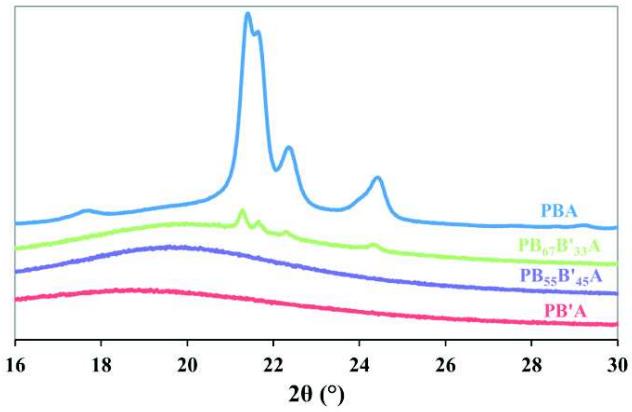

Figure 2.4.8 : WAXS curves of PBA, $PB_{67}B'_{33}A$, $PB_{55}B'_{45}A$ and PB'A at 25°C

From TGA results one can notice that no significant degradation occurs in the DSC analysis temperature range, *i.e.* from 20 to 100 °C. The DSC traces are presented in Figure 2.4.7-b and corresponding data are summarized in Table 2.4.3. The variation of polyester thermal properties is discussed in function of the ester function density (D_{ester}) calculated according to Equation (2.4.2). During the cooling from the melt (not shown here), PBA, which has the lowest D_{ester} due to 1,4-butylene segments, shows a sharp crystallization at around 29 °C. During the second heating scan of PBA, a large melting phenomenon between 45 and 65 °C, composed of three melting peaks (52, 57 and 61 °C) is observed. These multiple endothermic peaks are attributed to (a) fusion-recrystallization phenomena which are rather common for aliphatic polyesters (Nikolic and Djonlagic, 2001) and (b) to the polymorphism of PBA between α- and β-form crystals (Jinjun Yang et al., 2016), as observed by WAXS. The melting enthalpy value of 100% crystalline PBA ($\Delta H_{m,PBA}° = 135$ J/g) was taken from the literature and verified by calculation based on the groups contribution method proposed by Van Krevelen using Equation (1) (Tserki et al., 2006b; Van Krevelen, 1997). The calculated degree of crystallinity of PBA is 36%. The glass transition is not observed, however, previous data indicated that the T_g of PBA is between -60 and -76 °C (Ahn et al., 2001; Nikolic and Djonlagic, 2001; Zhao et al., 2010).

PB'A, which has the highest D_{ester} due to the shorter 2,3-butylene segments, shows an amorphous behavior with a T_g of -23 °C. Moreover, even by decreasing the cooling and heating rate until 2 °C/min, no crystallization or cold-crystallization peaks are observed (Figure SI.17 in Annex 4). Intra or inter-chains interactions between the ester groups are increased compared to PBA, the latter having a lower D_{ester}. This explains the higher T_g of PB'A and partly the absence of crystallinity. Moreover, the presence of the two methyl side groups in 2,3-butylene segments seem to prevent the crystallization. For instance, poly(ethylene adipate) is a semi-crystalline polyester (Jin et al., 2000b; Zorba et al., 2007), whereas PB'A is an amorphous polyester. The ability of 2,3-BDO to restrain crystallization has been employed previously to obtained amorphous copolyesters (Hu et al., 2016).

According to their 2,3-butylene content, PBB'A copolyesters have different D_{ester} which affect their thermal behavior. On one side, $PB_{67}B'_{33}A$, with a majority of 1,4-butylene segments, shows a semi-crystalline behavior with a T_g of -49 °C, a tiny cold-crystallization peak around 4°C and a small fusion around 20 °C with a melting enthalpy of 4 J/g. The low values for the cold-crystallization and melting enthalpies are due to the inclusion of rigid 2,3-butylene segments inside the PBA chain making difficult the crystallization. We suppose that only 1,4-butylene-adipate segments can crystallize. On the other side, $PB_{55}B'_{45}A$, which has almost the equivalent proportion of 1,4-butylene and 2,3-butylene segments and then a higher D_{ester} than $PB_{67}B'_{33}A$, exhibits an amorphous behavior with a T_g of -45 °C. A 2,3-butylene content of 45 mol% in the copolyester is sufficient to prevent its crystallization, even at a 2°C/min heating rate (Figure SI.17).

D_{ester} increases with the 2,3-BDO content and then the mobility of the chain decreases, leading to an increase of the T_g and a decrease of the degree of crystallinity. Furthermore, for copolyesters, only one T_g is observed between the one of

PB'A and PBA demonstrating that the copolyesters do not present a block structure, but rather a random distribution between 1,4-butylene and 2,3-butylene segments as expected for organometallic-catalyzed aliphatic–aromatic copolyesters (Chen et al., 1990; Gan et al., 2004; Wojtczak et al., 2014).

Table 2.4.3 : DSC results of polyesters with a cooling and heating ramp of 10°C/min.

Sample	D_{ester}	Cooling		Second heating					
		T_c	ΔH_c	T_g	T_{cc}	ΔH_{cc}	T_m	ΔH_m	X_c
		°C	J/g	°C	°C	J/g	°C	J/g	%
PBA	0.20	29	48	n.d.	-	-	45-65	48	36
$PB_{67}B'_{33}A$	0.217	-	-	-49	4	3	20	4	3
$PB_{55}B'_{45}A$	0.223	-	-	-45	-	-	-	-	-
PB'A	0.25	-	-	-23	-	-	-	-	-

5. Conclusion

New potentially fully biobased aliphatic copolyesters (PB'A and PBB'A) based on renewable building blocks were successfully synthesized in melt by using TTIP as catalyst, and characterized. The esterification of an equimolar 2,3-BDO/AA system was investigated at different temperature without and with TTIP and compared to an equimolar 1,4-BDO/AA system. For all systems, the esterification rate increased with the temperature, whereas the effect of TTIP addition on the extent of reaction was limited. Furthermore, the esterification rate was faster when using 1,4-BDO compared to 2,3-BDO. The esterification rate was between 6 and 10 times higher with 1,4-BDO than 2,3-BDO according to the temperature and the system studied.

PBA was obtained with a high mass-average molar mass, superior to 60,000 g/mol, whereas PB'A and PBB'A displayed mass-average molar masses around 11,000 g/mol. This study showed that by using 2,3-BDO as co-monomer the molar mass of copolyesters decreased. Moreover, due to the lower reactivity of 2,3-BDO compared to 1,4-BDO, PBB'A copolyesters exhibited a lower 2,3-BDO content than initially introduced, even if increasing the esterification time allowed to reduce the gap between the feed and the final composition. The end-group analysis showed that most of end-groups of copolyesters based on 2,3-BDO were COOH functions, thus limiting also the chain extension. Copolyesters containing 2,3-BDO exhibited a small positive specific optical rotation, which was found to be proportional to the 2,3-butylene content. Then, an additional method to determine the molar composition of PBB'A based on the specific optical rotation was proposed. From the thermal behavior of PBB'A, it has been noticed that the chain mobility of the copolyesters decreased as the 2,3-BDO content increased, leading to an increase of the T_g of PBB'A with the 2,3-BDO content and a decrease of the degree of crystallinity until having an amorphous copolyester for 2,3-BDO content higher than 45 mol%. All copolyesters showed an excellent thermal stability with an onset decomposition temperature above 280 °C and a temperature of maximum degradation rate around 380°C.

The 2,3-BDO, as a potentially biobased monomer and a product of biomass valorization, which is relatively simple to be biosynthesized, makes the PBB'A copolyester, with adjustable thermal properties and excellent thermal stability, a nice and promising sustainable material for some engineering applications such as adhesives, or for some biomedical applications. However, to fulfill the requirements of these fields, some additional tests must be carried out such as the study of the biodegradability, mechanical and ageing behaviors.

6. References

Ahn, B.D., Kim, S.H., Kim, Y.H., Yang, J.S., 2001. J. Appl. Polym. Sci. 82, 2808–2826.

Alidedeoglu, H.A., Deshpande, H.S., Duckworth, B., Gunale, T., Jayanna, D., Kannan, G., 2013. Method for the preparation of (polybutylene-co-adipate terephthalate) through the in situ phosphorus containing titanium based catalyst. US13/221,159.

Alidedeoglu, H.A., Kannan, G., 2013. Biodegradable aliphatic-aromatic copolyesters, methods of manufacture, and articles thereof. US13/435,865.

Avérous, L., 2004. J. Macromol. Sci. Part C 44, 231–274.

Avérous, L., Fringant, C., 2001. Polym. Eng. Sci. 41, 727–734.

Bacaloglu, R., Fisch, M., Biesiada, K., 1998. Polym. Eng. Sci. 38, 1014–1022.

Becker, J., Lange, A., Fabarius, J., Wittmann, C., 2015. Curr. Opin. Biotechnol. 36, 168–175.

Bikiaris, D.N., Chrissafis, K., Paraskevopoulos, K.M., Triantafyllidis, K.S., Antonakou, E.V., 2007. Polym. Degrad. Stab. 92, 525–536.

Bordes, P., Pollet, E., Avérous, L., 2009. Prog. Polym. Sci. 34, 125–155.

Bozell, J.J., Petersen, G.R., 2010. Green Chem. 12, 539.

Bueno-Ferrer, C., Hablot, E., Garrigós, M. del C., Bocchini, S., Averous, L., Jiménez, A., 2012. Polym. Degrad. Stab., 3rd International Conference on Biodegradable and Biobased Polymers (BIOPOL-2011) - Strasbourg 2011 97, 1964–1969.

Chang, W.L., Karalis, T., 1993. J. Polym. Sci. Part Polym. Chem. 31, 493–504.

Chen, M.S., Chang, S.J., Chang, R.S., Kuo, W.F., Tsai, H.B., 1990. J. Appl. Polym. Sci. 40, 1053–1057.

Chivrac, F., Kadlecová, Z., Pollet, E., Avérous, L., 2006. J. Polym. Environ. 14, 393–401.

Choi, S., Song, C.W., Shin, J.H., Lee, S.Y., 2015. Metab. Eng. 28, 223–239.

Chrissafis, K., Paraskevopoulos, K.M., Bikiaris, D.N., 2006. Thermochim. Acta 440, 166–175.

Gallaher, T.N., Gaul, D.A., Schreiner, S., 1996. J. Chem. Educ. 73, 465.

Gan, Z., Kuwabara, K., Yamamoto, M., Abe, H., Doi, Y., 2004. Polym. Degrad. Stab. 83, 289–300.

Garin, M., Tighzert, L., Vroman, I., Marinkovic, S., Estrine, B., 2014. J. Appl. Polym. Sci. 131, 40639/1-40639/10.

Gigli, M., Fabbri, M., Lotti, N., Gamberini, R., Rimini, B., Munari, A., 2016. Eur. Polym. J. 75, 431–460.

Grecea, M.L., Dimian, A.C., Tanase, S., Subbiah, V., Rothenberg, G., 2012. Catal. Sci. Technol. 2, 1500.

Gubbels, E., Drijfhout, J.P., Posthuma-van Tent, C., Jasinska-Walc, L., Noordover, B.A.J., Koning, C.E., 2014. Prog. Org. Coat. 77, 277–284.

Gubbels, E., Jasinska-Walc, L., Koning, C.E., 2013. J. Polym. Sci. Part Polym. Chem. 51, 890–898.

Hakan Akat, M.B., 2006. Iran. Polym. J. 15, 921–928.

Hu, L., Wu, L., Song, F., Li, B.-G., 2010. Macromol. React. Eng. 4, 621–632.

Hu, X., Shen, X., Huang, M., Liu, C., Geng, Y., Wang, R., Xu, R., Qiao, H., Zhang, L., 2016. Polymer 84, 343–354.

Jackson, W.J., Watkins, J.J., 1986. Aromatic polyesters derived from 2,3-butanediol. US4600768.

Jacquel, N., Freyermouth, F., Fenouillot, F., Rousseau, A., Pascault, J.P., Fuertes, P., Saint-Loup, R., 2011. J. Polym. Sci. Part Polym. Chem. 49, 5301–5312.

Jin, H.-J., Lee, B.-Y., Kim, M.-N., Yoon, J.-S., 2000. Eur. Polym. J. 36, 2693–2698.

Köpke, M., Mihalcea, C., Liew, F., Tizard, J.H., Ali, M.S., Conolly, J.J., Al-Sinawi, B., Simpson, S.D., 2011. Appl. Environ. Microbiol. 77, 5467–5475.

Kuo, C.-T., Chen, S.-A., 1989. J. Polym. Sci. Part Polym. Chem. 27, 2793–2803.

Nikolic, M.S., Djonlagic, J., 2001. Polym. Degrad. Stab. 74, 263–270.

Noordover, B.A.J., van Staalduinen, V.G., Duchateau, R., Koning, C.E., van Benthem, Mak, M., Heise, A., Frissen, A.E., van Haveren, J., 2006. Biomacromolecules 7, 3406–3416.

Ojijo, V., Ray, S.S., 2012. Poly(Butylene Succinate) and Poly[(Butylene Succinate)-co-Adipate] Nanocomposites, in: Avérous, L., Pollet, E. (Eds.), Environmental Silicate Nano-Biocomposites, Green Energy and Technology. Springer London, pp. 165–218.

Persenaire, O., Alexandre, M., Degée, P., Dubois, P., 2001. Biomacromolecules 2, 288–294.

Picataggio, S., Rohrer, T., Deanda, K., Lanning, D., Reynolds, R., Mielenz, J., Eirich, L.D., 1992. Nat. Biotechnol. 10, 894–898.

Polen, T., Spelberg, M., Bott, M., 2013. J. Biotechnol., Research on Industrial Biotechnology within the CLIB-Graduate Cluster - Part III 167, 75–84.

Pollet, E., Avérous, L., 2011. Production, Chemistry and Properties of Polyhydroxyalkanoates, in: Plackett, D. (Ed.), Biopolymers – New Materials for Sustainable Films and Coatings. John Wiley & Sons, Ltd, pp. 65–86.

Reulier, M., Avérous, L., 2015. Eur. Polym. J. 67, 418–427.

Siotto, M., Zoia, L., Tosin, M., Degli Innocenti, F., Orlandi, M., Mezzanotte, V., 2013. J. Environ. Manage. 116, 27–35.

Spyros, A., Argyropoulos, D.S., Marchessault, R.H., 1997. Macromolecules 30, 327–329.

Tserki, V., Matzinos, P., Pavlidou, E., Vachliotis, D., Panayiotou, C., 2006. Polym. Degrad. Stab. 91, 367–376.

Vaidya, U.R., Nadkarni, V.M., 1989. J. Appl. Polym. Sci. 38, 1179–1190.

Van Krevelen, D.W., 1997. Chapter 5 - Calorimetric properties, in: Properties of Polymers (Third, Completely Revised Edition). Elsevier, Amsterdam, pp. 109–127.

Vancsó-Szmercsányi, I., Maros-Gréger, K., Makay-Bödi, E., 1969. Eur. Polym. J. 5, 155–161.

Vardon, D.R., Franden, M.A., Johnson, C.W., Karp, E.M., Guarnieri, M.T., Linger, J.G., Salm, M.J., Strathmann, T.J., Beckham, G.T., 2015. Energy Env. Sci 8, 617–628.

Wang, X.-X., Hu, H.-Y., Liu, D.-H., Song, Y.-Q., 2016. New Biotechnol. 33, 16–22.

Watson, Ralph W., 1950. 2, 3-butanediyl phthalate resins. US2502686.

Watson, R.W., Grace, N.H., Barnwell, J.L., 1950. Can. J. Res. 28b, 652–659.

Wojtczak, M., Dutkiewicz, S., Galeski, A., Piorkowska, E., 2014. Eur. Polym. J. 55, 86–97.

Yang, J., Chen, Y., Hua, L., Liang, R., Zhu, D., 2016. J. Appl. Polym. Sci. 133, 42957.

Zhao, P., Liu, W., Wu, Q., Ren, J., Zhao, P., Liu, W., Wu, Q., Ren, J., 2010. J. Nanomater. J. Nanomater. 2010, 2010, Article ID 287082.

Zorba, T., Chrissafis, K., Paraskevopoulos, K.M., Bikiaris, D.N., 2007. Polym. Degrad. Stab. 92, 222–230.

Conclusion du chapitre 2

Le chapitre 2 a montré notre capacité à synthétiser des (co)polyesters biosourcés de structures macromoléculaires différentes à partir des synthons bifonctionnels (acide succinique, acide adipique, 1,3-propanediol, 1,4-butanediol et 2,3-butanediol) par catalyse organométallique à l'aide d'un catalyseur à base de titane. Les masses molaires importantes obtenues lors des synthèses par catalyse organométallique à partir des diols primaires sont du même ordre de grandeur et même parfois légèrement supérieures à celles rapportées jusqu'ici dans la littérature. Néanmoins, lorsque le 2,3-butanediol est utilisé comme synthon, les masses molaires des (co)polyesters obtenues sont beaucoup plus faibles dû à une plus faible réactivité des diols secondaires avec les diacides par rapport aux diols primaires. Il a été prouvé que les différents copolyesters synthétisés possèdent tous une microstructure présentant une distribution de séquence aléatoire, due aux très nombreuses réactions de transestérification provoquées par le catalyseur organométallique.

De plus, ce chapitre présente également des méthodes alternatives de détermination de la masse molaire des polyesters par RMN basées sur la quantification des bouts de chaînes et qui permettent d'obtenir des valeurs plus en adéquation avec la réalité que les valeurs obtenues par chromatographie d'exclusion stérique.

La stabilité thermique sous atmosphère inerte (hélium) des (co)polyesters obtenus est très bonne puisqu'aucune perte de masse n'est enregistrée avant 280 °C. Ces analyses montrent également que les (co)polyesters à base d'acide adipique présentent une stabilité thermique légèrement supérieure à celle des (co)polyesters à base d'acide succinique. Cette augmentation de la stabilité thermique avec l'acide adipique peut s'expliquer, en partie, par la diminution de la densité en fonction ester dans la chaîne diminuant ainsi le nombre possible de ruptures de chaîne. De même, bien que les structures macromoléculaires soient proches des unes des autres, les mécanismes de dégradation sont quelques peu différents les uns des autres avec une cinétique de dégradation plus importante pour les (co)polyesters à base d'unités adipates. Au final, il a été montré que le profil de dégradation thermique dépend fortement du diacide mais qu'il n'est pas influencé par la nature des diols contrairement à ce qui avait été avancé dans la littérature.

Les (co)polyesters obtenus présentent tous un phénomène de co-cristallisation isodimorphique caractérisé par la présence d'une seule structure cristalline par composition et par l'observation d'un pseudo-eutectique pour les températures et enthalpies de fusion et pour le taux de cristallinité. Cela signifie d'une part que les co-monomères en minorité dans une composition sont exclus ou alors seulement partiellement intégrés à la phase cristalline. D'autre part, les températures et les enthalpies de fusion ou de cristallisation diminuent fortement avec l'ajout d'un co-monomère à partir d'un homopolyester à cause de l'insertion de « défauts » dans la microstructure des copolyesters, diminuant ainsi la longueur moyenne des blocs ce qui réduit la taille et la résistance des cristaux.

De plus, ce chapitre a montré que seuls les copolyesters ayant une structure cristalline similaire à celle du PBS possèdent une température de fusion élevée (supérieure ou proche de 100 °C) tandis que les autres homopolyesters (PBA, PPS et PPA) ont des températures de fusion beaucoup plus faibles (40-60 °C) et proches de la température ambiante. Parmi les copolyesters étudiés, à part certaines compositions riches en

unités « butylène succinate » du PBSA et du PPBS, la plupart possèdent des températures de fusion encore plus faibles et sont même dans certains cas à l'état fondu à température ambiante.

Par ailleurs, il a démontré, au travers de ce travail d'ingénierie macromoléculaire et l'utilisation de ces différents synthons, que la présence de 1,3-propanediol ou de 2,3-butanediol dans la structure des (co)polyesters synthétisés diminue fortement leur vitesse de cristallisation et donc leur cristallinité jusqu'à obtenir des polymères amorphes pour des copolyesters à forte proportion en ces deux monomères. De même, l'utilisation d'acide adipique à la place de l'acide succinique diminue fortement la température de transition vitreuse d'une bonne vingtaine de degrés suite à l'augmentation de la flexibilité de chaîne provoquée par la diminution de la densité en fonction ester avec l'allongement de la structure carbonée des synthons utilisés. De même, l'utilisation de 1,4-butanediol à la place de 1,3-propanediol diminue également la température de transition vitreuse mais dans une plus faible mesure (~ 5-10 °C), tandis que le 2,3-butanediol l'augmente fortement. Ce chapitre a également montré que la variation des valeurs expérimentales de T_g des copolyesters varie non linéairement avec la composition selon la loi théorique de Fox, pour le PPBA, ou celle de Gordon-Taylor, pour les copolyesters PBSA, PPBS et PPSA.

CHAPITRE 3: SYNTHÈSE ENZYMATIQUE DE COPOLYESTERS ALIPHATIQUES BIOSOURCÉS PAR TRANSESTÉRIFICATION

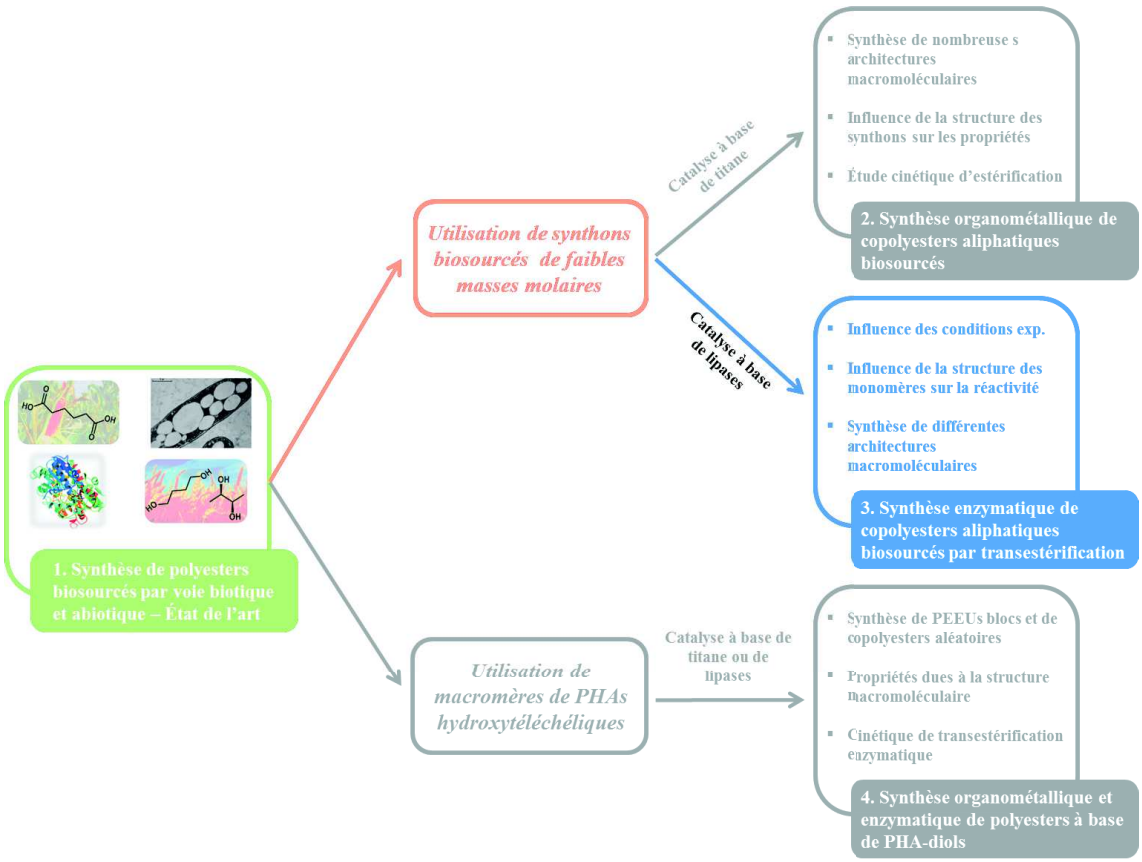

Introduction du chapitre 3

Le chapitre 2 a montré la possibilité de synthétiser des polyesters ou copolyesters biosourcés de structures macromoléculaires différentes à partir des synthons difonctionnels par catalyse organométallique à l'aide d'un catalyseur chimique à base de titane. Les différentes architectures macromoléculaires permettent d'obtenir des matériaux aux propriétés physiques très diverses : polymère cristallin ou amorphe avec une large gamme de températures de transition vitreuse ou de fusion. De plus, grâce à une collaboration internationale, la biodégradabilité partielle de nos matériaux dans un sol a été démontrée avec des vitesses de dégradation dépendant fortement de leurs structures macromoléculaires.

Dans le chapitre 3, nous nous intéresserons à la catalyse enzymatique pour la synthèse de polyesters ou de copolyesters à partir de synthons bifonctionnels à l'aide de la lipase B de *Candida antarctica*. Il s'agit tout d'abord d'étudier comment fonctionne cette voie biologique qui possède ses propres règles et qui est, à l'heure actuelle, en plein développement. Une première étape de développement est donc nécessaire afin d'optimiser nos systèmes réactionnels et d'étudier l'influence de la structure des synthons sur la réaction en elle-même. Suite au criblage des différents paramètres et à l'optimisation du meilleur procédé réactionnel, c'est le procédé en solution à 90 °C durant 72 h dans le diphényl éther sous vide qui a été choisi et utilisé pour la synthèse de nombreux (co)polyesters. La stabilité thermique, la structure cristalline ainsi que les propriétés thermiques et optiques des différents copolyesters ont été étudiées de la même manière que dans le chapitre 2.

Ce chapitre est découpé en trois sous-chapitres, les deux derniers sont présentés sous forme de publications :

- Le sous-chapitre 1 présentera le développement du procédé de synthèse de polyesters par catalyse enzymatique par transestérification à partir de synthons bifonctionnels. L'efficacité des procédés de synthèse, des conditions opératoires et l'influence de la longueur de chaîne des synthons seront, entre autres, étudiées afin d'optimiser la synthèse enzymatique de polyesters.
- Le sous-chapitre 2 présentera une étude tout d'abord sur la synthèse enzymatique de poly(1,4-butylène succinate-*ran*-2,3-butylène succinate) avec notamment l'influence de la proportion en 2,3-butanediol sur la masse molaire et son influence sur les propriétés thermiques et optiques de ce copolyester. Cette étude sera présentée sous la forme d'un article intitulé « Enzymatic synthesis and characterization of biobased poly(1,4-butylene succinate-*ran*-2,3-butylene succinate) copolyesters. Influence of 1,4- and 2,3-butanediol contents. » qui a été soumi récemment à *European Polymer Journal*.
- Le sous-chapitre 3 sera, quant à lui, dédié à l'étude à la synthèse enzymatique de PBSA et de PPBS en étudiant notamment l'influence de la longueur des monomères sur l'efficacité de la catalyse enzymatique, sur la structure macromoléculaire et sur les propriétés de ces copolyesters. Ce travail sera présenté sous la forme d'un article intitulé «Synthesis and characterization of biobased aliphatic copolyester: influence of monomer chain lengths on properties » qui sera soumis prochainement.

.

Sub-chapter 3.1. Introduction à la synthèse enzymatique de polyesters par transestérification à partir de synthons bifonctionnels– Développement de la méthode

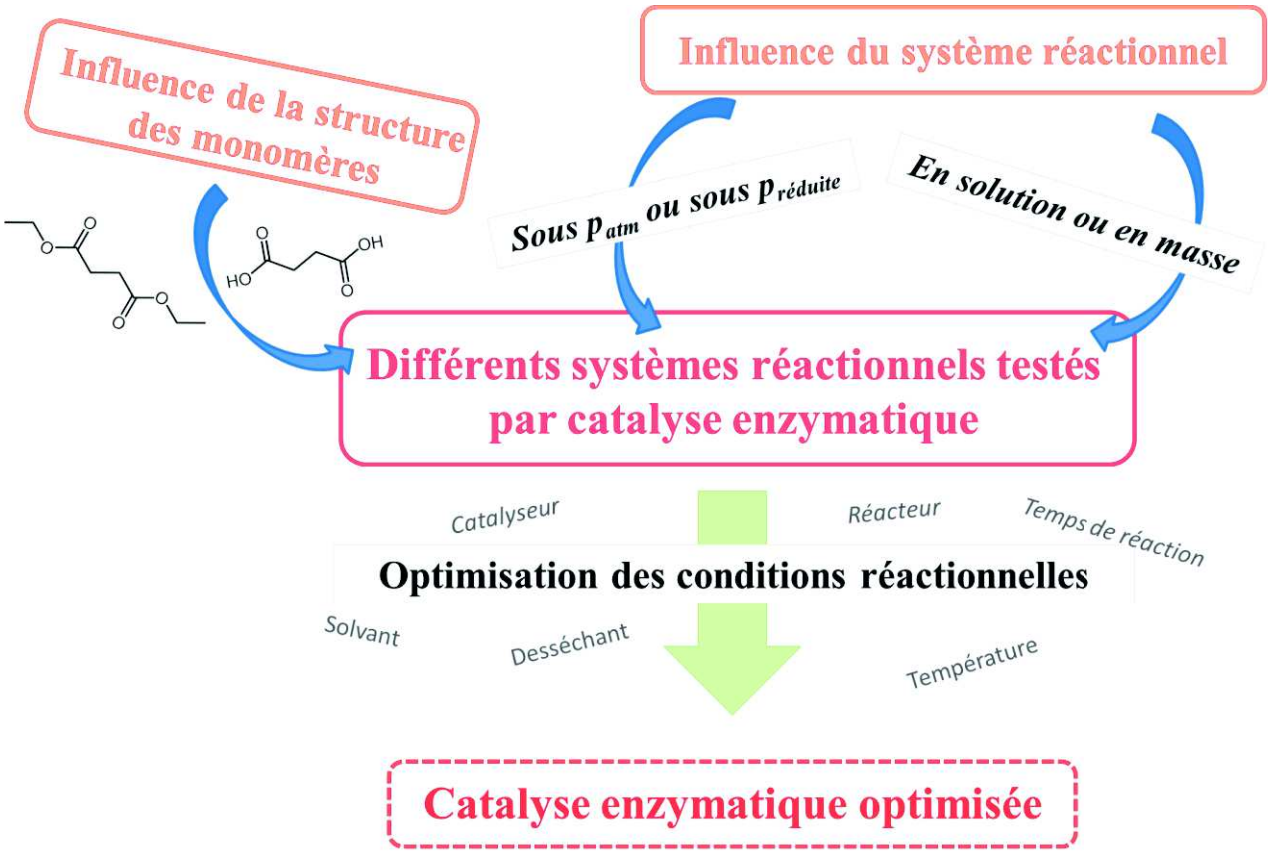

1. Introduction

La synthèse de polyesters par catalyse enzymatique est étudiée depuis une bonne vingtaine d'années et de nombreuses évolutions ont permis d'accroitre la diversité des substrats polymérisables ainsi que d'améliorer le procédé de synthèse. C'est dans cette optique que nous avons testé ici différents nouveaux systèmes avec également l'objectif d'en améliorer le procédé. Ainsi, différents tests de synthèse enzymatique des polyesters aliphatiques ont été effectués pour évaluer l'influence (i) de la structure des monomères (longueur de chaîne, état physique), (ii) du procédé de synthèse (en masse ou en solution), (iii) du solvant (nature, hydrophobicité, quantité), (iv) du système de « séchage » (tamis moléculaire *vs.* vide), (v) des paramètres réactionnels (température, temps) et (vi) du catalyseur.

Notre étude s'est évidemment focalisée sur les réactions d'estérification et/ou de transestérification des synthons biosourcés aliphatiques bifonctionnels que sont les diols primaires et les diacides étudiés dans le cadre de cette thèse. Le développement de la procédure de polymérisation enzymatique s'est axé sur la synthèse du poly(butylène succinate) (PBS) et du poly(butylène adipate (PBA) à partir de différents monomères et en utilisant différentes conditions expérimentales (température, solvant, pression…). Tous les monomères employés durant le développement du procédé de catalyse enzymatique avec la lipase B de *Candida antarctica* (CALB) sont présentés dans le Tableau 3.1.1.

Tableau 3.1.1 : Monomères utilisés lors la synthèse enzymatique de PBS et PBA.

Molécule		Structure	Masse molaire (g/mol)	Densité	T_f (°C)	$T_{ébu}$ (°C)	log P
1,3-propanediol	1,3-PDO		76,09	1,05	-26	213	-1,0
1,4-butanediol	1,4-BDO	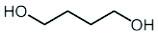	90,12	1,02	20	230	-0,8
Acide succinique	SA	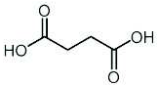	118,19	1,56	185	235	-0,6
Diméthyle succinate	DMS	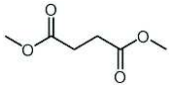	146,14	1,01	18	195	0,4
Diéthyle succinate	DES	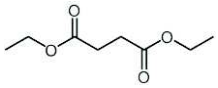	174,19	1,05	-20	218	1.2
Diméthyle adipate	DMA	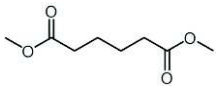	174,20	1,12	8	109 *	1.0
Diéthyle adipate	DEA	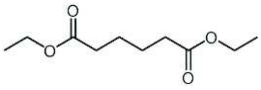	202,25	1,06	-20	245	2.4

* sous 14 mmHg de pression.

Les spectres de RMN ^{1}H et ^{13}C de certains monomères (*i.e.*, 1,4-BDO, DMS, DES, DEA) sont présentés dans les Figures 3.1.1-a et 3.1.1-b, respectivement.

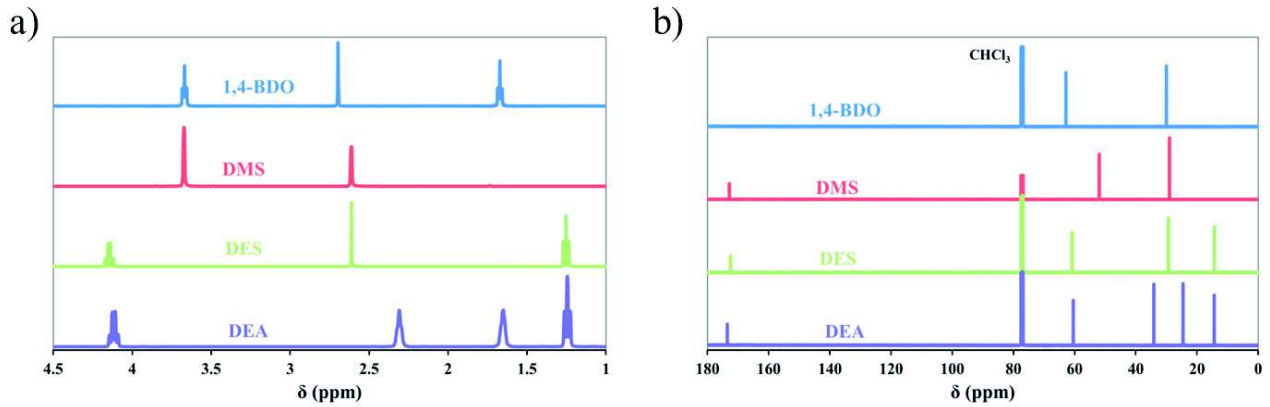

Figure 3.1.1 : Spectres de RMN (a) ^{1}H- et (b) ^{13}C des monomères 1,4-BDO, DMS, DES et DEA.

L'optimisation du procédé de catalyse enzymatique sera principalement discutée à partir des valeurs des masses molaires et des degrés de polymérisation (DP_n) des polyesters synthétisés.

2. Système réactionnel initial : réactions dans le toluène

2.1. Synthèses initiales de PBS

2.1.1. Protocole expérimental

Un premier système réactionnel, *i.e.* 200 pds.% de toluène anhydre, 10 pds.% de Novozym® 435 (N435) et 0,1 g/mL de tamis moléculaire, basé sur les résultats de Duchiron *et al.* (Duchiron et al., 2015), a été testé pour la synthèse de PBS. L'influence de différents paramètres (structure du monomère donneur d'acyle (le diacide), la quantité d'eau, le temps de réaction) a été étudiée. Les réactions ont été réalisées dans des tubes de Schlenk sous atmosphère d'argon selon le protocole expérimental décrit en détail ci-dessous et résumé dans le Schéma 3.1.1. Le montage réactionnel est présenté dans la Figure 3.1.2-a.

Un mélange équimolaire de SA (ou de DES) et de 1,4-BDO, 10 pds.% de N435 (*vs.* masse totale de monomères), toluène anhydre (200 pds.% *vs.* masse totale of monomères), tamis moléculaire sec (0,1 g/mL de solvant) sont introduits dans un tube de Schlenk sec, avec un barreau magnétique. Une colonne courte remplie de tamis moléculaire sec est placéée au-dessus du tube de Schlenk et le système est fermé par un septum. Le réacteur est immergé dans un bain d'huile chauffé à 90 °C et un flux d'argon est mis en place durant 2 h. Après 2 h, le flux d'argon est arrêté et la réaction se poursuit durant encore 70 h sous atmosphère d'argon statique. Après 72 h de réaction, 10 mL de chloroforme sont introduit dans le milieu réactionnel afin d'arrêter la réaction. Le milieu réactionnel est ensuite filtré et le filtrat est concentré à l'aide d'un évaporateur rotatif. Par la suite, le polyester synthétisé est précipité dans un large volume d'éther de pétrole (ou de méthanol) froid sous agitation vigoureuse, récupéré par filtration, lavé avec de l'éther de pétrole (ou du méthanol) froid et séché sous vide dans une étuve à 50 °C durant 24 h. A la fin de la réaction, le polymère est récupéré sous forme d'une poudre blanche.

Nota : Le SA a été séché à 60 °C sous vide dans une étuve durant 24 h avant d'être utilisé. Le N435 est utilisé soit "tel que reçu", soit il est séché à 25 °C sous vide dans une étuve durant 24 h en accord avec des travaux précédents (Loos et al. (Japu et al., 2015; Jiang et al., 2013, 2014a)*, Gross et al* .(Azim et al., 2006; Kumar and Gross, 2000a; Mahapatro et al., 2003)*). Le tamis moléculaire est utilisé soit tel quel ou après avoir été "activé" (séché) à 110 °C sous vide dans une étuve durant 24 h.*

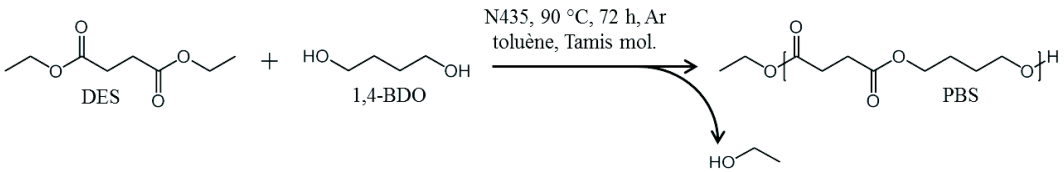

Schéma 3.1.1 : Schéma réactionnel de la synthèse enzymatique de PBS à partir de 1,4-BDO/DES dans le toluène.

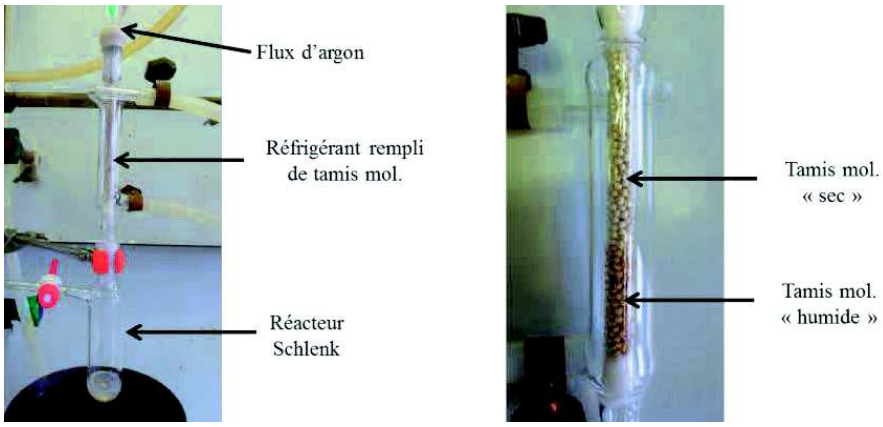

Figure 3.1.2 : Illustrations du (a) montage réactionnel du système dans le toluène sous argon, (b) colonne courte remplie de tamis moléculaire après 72 h de réaction.

2.1.2. Caractérisation des produits de réaction

Le produit synthétisé a été caractérisé par RMN ^{1}H dans le $CDCl_3$. Le spectre de RMN ^{1}H du polyester obtenu par catalyse enzymatique à partir de 1,4-BDO et de DES est présenté en Figure 3.1.3-a. Les pics à δ = 4,12, 2,62 et 1,70 ppm sont caractéristiques du PBS (voir chapitre précédent). Les deux petits signaux à δ = 3,67 et 1,25 ppm sont respectivement associés aux terminaisons 1,4-BDO (HO-C$\underline{H}_2$-) et ester (C$\underline{H}_3$-CH$_2$-O-). La masse molaire finale des polyesters est déterminée soit par CES, soit par RMN ^{1}H en utilisant les intensités relatives des pics caractéristiques du PBS et des terminaisons selon l'Equation (3.1.1). Contrairement à la formule développée par Jiang *et al.* (Jiang et al., 2013), notre méthode prend en compte la superposition de plusieurs signaux à δ = 4,12 ppm provenant du motif répétitif 1,4-butyle (O-C$\underline{H}_2$-CH$_2$-), de la terminaison 1,4-BDO (OH-CH$_2$-CH$_2$-CH$_2$-C$\underline{H}_2$-O-) et de la terminaison ester (CH$_3$-C$\underline{H}_2$-CO-). En utilisant la masse molaire déterminée par RMN ^{1}H ($M_{n,RMN}$) et la masse molaire du motif répétitif du PBS (172 g/mol), le degré de polymérisation (DP_n) est calculé. De plus, la proportion en terminaison ester ($\%_{terminaison\ ester}$) permettant de caractériser les terminaisons des polyesters synthétisés, est déterminée à partir des spectres de RMN ^{1}H en utilisant l'Equation (3.1.2).

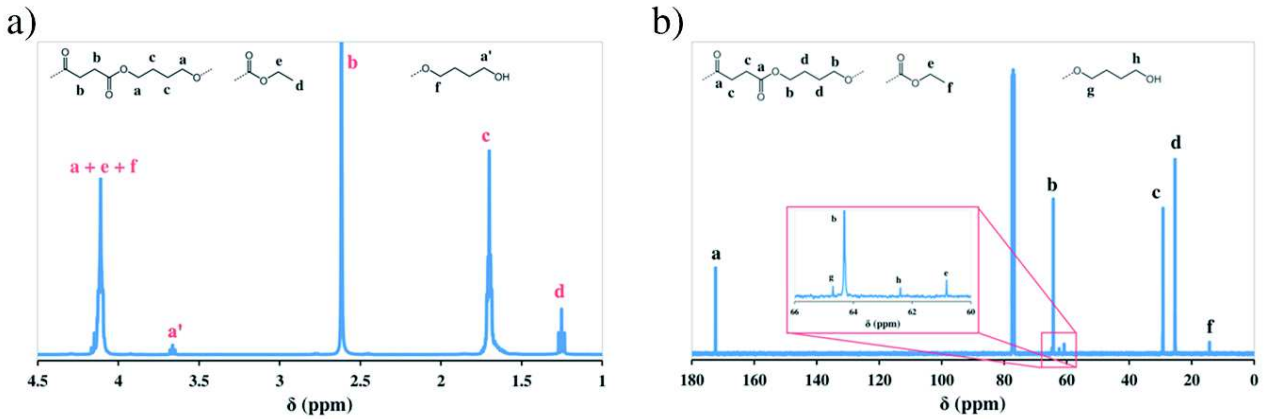

Figure 3.1.3 : Spectres de RMN (a) ^{1}H et (b) ^{13}C de PBS synthétisé à partir de 1,4-BDO/DES à l'aide de N435 analysé dans le $CDCl_3$.

$M_{n,RMN,PBS}$ est calculé à partir de l'Equation (3.1.1),

$$M_{n,RMN,PBS} = \frac{\frac{I_{4,12} - I_{3,67} - {}^{2}/_{3}\, I_{1,25}}{4} \times 88{,}10 + \frac{I_{2,62}}{4} \times 84{,}07 + \frac{I_{3,67}}{2} \times 89{,}11 + \frac{I_{1,25}}{3} \times 45{,}06}{0{,}5 \times \left(\frac{I_{3,67}}{2} + \frac{I_{1,25}}{3}\right)} \qquad (3.1.1)$$

où 88,10, 84,07, 89,11 et 45,06 sont les masses molaires respectives (en g/mol) des unités répétitives 1,4-butyl et succinate ainsi que des terminaisons 1,4-BDO et ester. De plus, la proportion en terminaison ester ($\%_{terminaison\ ester}$) peut être calculée selon l'Equation (3.1.2),

$$\%_{terminaison\ ester} = \frac{\frac{I_{1,25}}{3}}{\frac{I_{1,25}}{3} + \frac{I_{3,67}}{2}} \times 100 \qquad (3.1.2)$$

Toutefois, cette méthode de calcul présente des limites car elle dépend fortement des signaux des groupements terminaux qui deviennent de moins en moins intenses et visibles (par rapport à la ligne de base) lorsque la masse molaire du polyester augmente. La précision de cette méthode diminue donc avec l'augmentation de la masse molaire de ces polyesters.

Il est bien connu que la masse molaire des polyesters déterminée par CES est souvent surestimée de part notamment la calibration de la machine par des standards de PS. En utilisant la relation de Mark-Houwink-Sakurada (MHS) et les paramètres (K et a), une masse molaire plus pertinente peut être calculée, en appliquant une correction à la valeur obtenue par CES. La masse molaire corrigée ($M_{n,MHS}$ ou M_2) est calculée en utilisant l'Equation (3.1.3),

$$M_{n,MHS} = M_2 = exp\left[\frac{1}{1+a_2}\, ln\left(\frac{K_1}{K_2}\right) + \frac{1+a_1}{1+a_2}\, lnM_1\right] \qquad (3.1.3)$$

où les paramètres MHS (K_1 et a_1) du PS dans le $CHCl_3$ sont de $7{,}2.10^{-4}$ $dL.g^{-1}$ et 0,76 selon l'association américaine des standards de polymères (American Polymer Standards Corporation). Les paramètres MHS (K_2 et a_2) pour le PBS dans le $CHCl_3$ sont selon Garin *et al.* (Garin et al., 2014b) et Charlier *et al.* (Charlier, Q. et al., 2015) respectivement de K_2 = $4{,}0.10^{-4}$ et $6{,}4.10^{-4}$ $dL.g^{-1}$, tandis que a_2 = 0,71 et 0,67. Les résultats obtenus avec les paramètres MHS de Charlier *et al.* sont proches de ceux obtenus par Garin et *al*. Dans la suite et dans un but de simplification, seules les masses molaires corrigées avec les paramètres MHS de Garin *et al.* seront présentées.

Dans le but d'obtenir plus d'informations sur la structure de PBS obtenu par catalyse enzymatique à partir de DES, des analyses de RMN ^{13}C ont été réalisées. Le spectre de RMN ^{13}C est présenté dans la Figure 3.1.3-b. Les pics à δ = 172,4, 64,3, 29,1 et 25,4 ppm sont caractéristiques du PBS (voir chapitre précédent). De plus, la présence des faibles signaux à δ = 64,7, et 62,4 ppm est due aux carbones HO-CH_2-CH_2-CH_2-$\underline{C}H_2$-O et HO-$\underline{C}H_2$-CH_2-CH_2-CH_2-O des terminaisons hydroxyles (1,4-BDO), tandis que les faibles signaux à δ = 60,8 et 14,3 ppm sont dus aux carbones CH_3-$\underline{C}H_2$-O et $\underline{C}H_3$-CH_2-O des terminaisons esters (DES).

2.1.3. Résultats et discussions

Les caractéristiques des différents PBS synthétisés par catalyse enzymatique et analysés par RMN et CES, sont présentés dans le Tableau 3.1.2.

Ces résultats montrent tout d'abord que la présence de lipases (CALB) est nécessaire afin d'obtenir au moins des oligomères (entrées 1-2). De plus, l'utilisation de SA durant la synthèse enzymatique dans le toluène ne permet pas la synthèse d'oligomères même en présence de N435 (entrée 3), ce qui est dû à la séparation de phase observée dans le mélange réactionnel entre les deux monomères (SA et 1,4-BDO). En effet, le SA n'est pas ou très peu soluble dans le toluène à 90 °C et la réaction ne peut donc avoir lieu. Ce test préliminaire a donc mené à l'abandon du SA comme monomère pour les synthèses enzymatiques. Le DES, qui est liquide à température ambiante et à température de réaction (90 °C), est quant à lui miscible avec le 1,4-BDO et le toluène, permettant ainsi la réaction.

On peut observer que les différentes expériences impliquant le DES et le N435 permettent seulement la synthèse d'oligomères de PBS avec des $M_{n,RMN}$ d'approximativement 1,3-1,8 kg/mol (DP_n ~ 8-10) contrairement aux PBS synthétisés par catalyse organométallique qui présentent de hautes masses molaires. Par ailleurs, on peut observer que les différents oligomères de PBS synthétisés par voie enzymatique ont tous une proportion de terminaisons ester d'environ 60%. Ce résultat est en contradiction avec le mécanisme proposé par Binns *et al.* (Binns et al., 1998) qui repose sur une croissance de chaîne impliquant l'addition séquentielle d'un synthon AB (acide-diol) sur une structure BAB (diol-acide-diol). Les polyesters devraient donc avoir exclusivement des terminaisons hydroxyles (1,4-BDO). Toutefois, Nakaoki *et al.* (Nakaoki et al., 2003) ont observé lors de la polymérisation enzymatique d'acide adipique et de 1,6-hexanediol qu'au début de la réaction la majorité des chaînes polyesters présente des terminaisons hydroxyles, en accord avec le mécanisme proposé par Binns *et al.* (Binns et al., 1998). Mais ensuite, lorsque le temps de réaction augmente, les polyesters synthétisés ont plutôt des terminaisons carboxyles, à cause des réactions de transestérification (Nakaoki et al., 2003).

On observe que la masse molaire des oligomères synthétisés augmente légèrement lorsque le N435 est séché à l'étuve avant son utilisation (entrées 4-5). Le contrôle de la teneur en eau dans le système réactionnel lors d'une synthèse enzymatique est un paramètre clé de la catalyse enzymatique de polyesters. En effet, l'influence de la teneur en eau sur l'activité enzymatique a été étudiée pour les polymérisations par ouverture de cycle (eROP) (Dong et al., 1999; Henderson et al., 1996; MacDonald et al., 1995; Mei et al., 2002) et lors de la transestérification (Dong et al., 1999; Liu et al., 2015; Ma et al., 2002; Nordblad and Adlercreutz, 2013; Graber et al., 2003). Même si une teneur optimale en eau n'a pas pu être déterminée avec précision pour l'eROP, où elle intervient comme amorceur, Dong *et al.* ont montré que la vitesse de réaction augmente avec la teneur en eau mais entraine une forte baisse des masse molaire des polymères obtenus (Dong et al., 1999). Pour la transestérification, l'eau participe à la réaction inverse (hydrolyse) et donc son influence est différente. Liu *et al.* ont montré que la teneur en eau optimale dépend de la réaction étudiée mais également de l'enzyme utilisée (Liu et al., 2015). Par exemple, pour CALB sur N435, une teneur en eau optimale de 1% a été démontrée pour la synthèse de flavone C-glucosides, tandis qu'elle est de 2% pour la lipase de *Rhizumucor miehei* immobilisée et pour la lipase *Thermomyces lanuginosus* immobilisée. Néanmoins, Nordbald *et al.* ont montré que la vitesse de transestérification diminue avec la teneur en eau et suggèrent donc qu'une quantité nulle d'eau devrait être utilisée. De leur côté, Ma *et al.* ont montré qu'une teneur en eau minimale doit être présente dans le milieu dans le but de ne pas détruire la structure 3D de la lipase (Ma et al., 2002). En conclusion, une teneur en eau faible semble être préférable pour les réactions enzymatiques par transestérification. Dans le but de diminuer la teneur en eau dans le milieu réactionnel, du tamis moléculaire sec a été ajouté à une concentration de 0,1 g/mL de solvant. Les résultats montrent que la masse molaire des polyesters synthétisés diminue lorsque le tamis moléculaire n'est pas utilisé (entrées 5-6) et confirment donc l'intérêt de son ajout.

Pour les synthèses dans le toluène, nous avons créé un montage réactionnel avec du tamis moléculaire introduit dans une colonne courte placée au-dessus du réacteur dans le but de capter les molécules d'eau et d'éthanol distillées du milieu réactionnel par l'azéotrope formé avec le toluène (Figure 3.1.2-b). On observe alors que le tamis moléculaire emprisonné dans la colonne s'humidifie durant la réaction à cause des sous-produits de réaction volatiles issus du milieu réactionnel (Figure 3.1.2-b). L'élimination de l'éthanol issu de la réaction du mélange réactionnel par distillation azéotropique et son captage par le tamis moléculaire, permet de synthétiser préférentiellement des liaisons esters et d'obtenir ainsi des polyesters de hautes masses molaires. De plus, si une haute concentration en alcool demeure dans le système réactionnel, la vitesse de transestérification est fortement diminuée, comme observé précédemment (García-Alles and Gotor, 1998; Kulschewski et al., 2013; Sasso et al., 2015).

Par ailleurs, la répétabilité des synthèses a été étudiée en réalisant des triplicats des synthèses de PBS effectuées à partir de 1,4-BDO/DES, de tamis moléculaire sec et de N435 sans séchage. Les résultats montrent que les masses molaires varient d'approximativement 25%, tandis que la proportion en terminaisons esters reste constante à environ 60% (entrées 5, 7 et 8).

Un dernier test a été effectué avec du DES distillé (entrée 9) afin de réduire également la teneur en eau du système réactionnel. Les résultats montrent qu'il n'y a pas d'effet de la distillation du DES sur la masse molaire du polyester synthétisé. Par conséquent, suite à ce test, la purification préalable des monomères par distillation n'a plus été effectuée.

Pour conclure sur ces premiers tests de synthèses enzymatiques, les polyesters synthétisés ont des masses molaires peu élevées et, en réalité, les réactions ont conduit seulement à la synthèse d'oligomères (DP_n < 10). La procédure de synthèse enzymatique doit donc être améliorée afin d'obtenir des polyesters de plus hautes masses molaires.

Tableau 3.1.2 : Synthèse enzymatique de PBS dans le toluène anhydre à 90 °C.

	Conditions expérimentales				CES			RMN ^{1}H		
Entrée	Diacide	N435	Tamis mol.	Rendement	$M_{n,CES}$	Đ	$M_{n,MHS}$	$M_{n,RMN}$	DP_n	$\%_{terminaisons\ esters}$
				pds.%	kg/mol		kg/mol	kg/mol		%
1	SA	Non	Oui	0	0	-	0	0	0	-
2	DES	Non	Oui	0	0	-	0	0	0	-
3	SA	Sec	Oui	0	0	-	0	0	0	-
4	DES	Sec	Oui	88	4,5	1,7	2,1	1,8	10	64
5	DES	Comme reçu	Oui	86	3,6	1,7	1,7	1,5	9	59
6	DES	Comme reçu	Non	78	2,7	1,6	1,2	1,3	8	57
7	DES	Comme reçu	Oui	79	3,0	1,6	1,4	1,5	8	59
8	DES	Comme reçu	Oui	83	2,7	1,6	1,3	1,4	8	62
9	DES dist.	Comme reçu	Oui	88	2,6	1,6	1,2	1,3	7	56

2.2. Effet de la longueur de chaîne du monomère donneur d'acyle

L'influence de la structure des monomères et notamment la longueur de chaîne du monomère est étudiée et discutée sur base de la masse molaire des polyesters formés. Cette influence de la longueur de chaîne du monomère a déjà été étudiée dans la littérature. Ainsi, pour les réactions d'estérification et de transestérification, l'activité enzymatique et la masse molaire des polyesters augmentent, en général, avec la longueur initiale des diols et diacides (ou diesters carboxyliques) (Mahapatro et al., 2003; Jiang et al., 2014b; Feder and Gross, 2010; Hunsen et al., 2007; Linko et al., 1998; Wang et al., 1996). Dans le cadre de notre étude, des diesters carboxyliques de quatre à six carbones ont été utilisés et comparés.

La synthèse enzymatique de PBA à partir de 1,4-BDO et d'adipate de diéthyle (DEA) a été effectuée selon la procédure optimisée et développée pour le PBS (*i.e.*, 90 °C durant 72 h dans 200 pds.% de toluène anhydre avec du tamis moléculaire et du N435 sec). Les produits de synthèse ont été analysés par RMN ^{1}H et ^{13}C, ainsi que par CES. Le spectre de RMN ^{1}H du PBA synthétisé à partir de 1,4-BDO et de DEA est présenté en Figure 3.1.4-a. Les signaux à δ = 4,09, 2,32, 1,70 et 1,65 ppm sont caractéristiques du PBA (voir chapitre précédent). Tout comme avec le PBS, les terminaisons 1,4-BDO et esters sont visibles et se traduisent par des pics à respectivement δ = 3,67 et 1,25 ppm. La détermination de la masse molaire par RMN ^{1}H ($M_{n,RMN,PBA}$) est faite en utilisant l'Equation (3.1.4), tandis que la proportion en terminaisons esters s'effectue de la même manière que pour le PBS (Equation (3.1.3)). Le DP_n des PBA synthétisés est calculé en utilisant $M_{n,RMN,PBA}$ et la masse molaire du motif répétitif du PBA (200 g/mol). $M_{n,RMN,PBA}$ est calculé selon l'Equation (3.1.4),

$$M_{n,RMN,PBA} = \frac{\frac{I_{4,09} - I_{3,67} - {}^{2}/_{3}\, I_{1,25}}{4} \times 88{,}10 + \frac{I_{2,32}}{4} \times 112{,}13 + \frac{I_{3,67}}{2} \times 89{,}11 + \frac{I_{1,25}}{3} \times 45{,}06}{0{,}5 \times \left(\frac{I_{3,67}}{2} + \frac{I_{1,25}}{3}\right)} \qquad (3.1.4)$$

où 88,10, 89.11, 112,13 et 45,06 sont respectivement les masses molaires (en g/mol) des motifs répétitifs 1,4-butyle et adipate, ainsi que les masses molaires des terminaisons 1,4-BDO et esters.

Le spectre de RMN ^{13}C du PBA synthétisé est présenté en Figure 3.1.4-b. Les déplacements chimiques à δ = 173,4, 64,0, 34,0, 25,4 et 24,5 ppm sont caractéristiques du PBA (voir chapitre précédent). De plus, les signaux de faibles intensités à δ = 64,3, et 62,5 ppm sont dus aux carbones HO-CH_2-CH_2-CH_2-$\underline{C}H_2$-O et HO-$\underline{C}H_2$-CH_2-CH_2-CH_2-O des

terminaisons 1,4-BDO, tandis que les autres signaux de faible intensité à δ = 60,4, et 14,4 ppm sont dus aux carbones CH_3-$\underline{C}H_2$-O et $\underline{C}H_3$-CH_2-O des terminaisons esters.

Comme pour l'étude du PBS, la correction de la masse molaire déterminée par CES par la relation de MHS est possible en utilisant les paramètres MHS ($K = 7{,}31.10^{-4}$ $dL.g^{-1}$ et $a = 0.69$) du PBA dans le chloroforme déterminé par Munari (Munari et al., 1992). La masse molaire obtenue après correction par la relation MHS est similaire à celle calculée par RMN [1] nous faisant supposer une bonne corrélation des résultats.

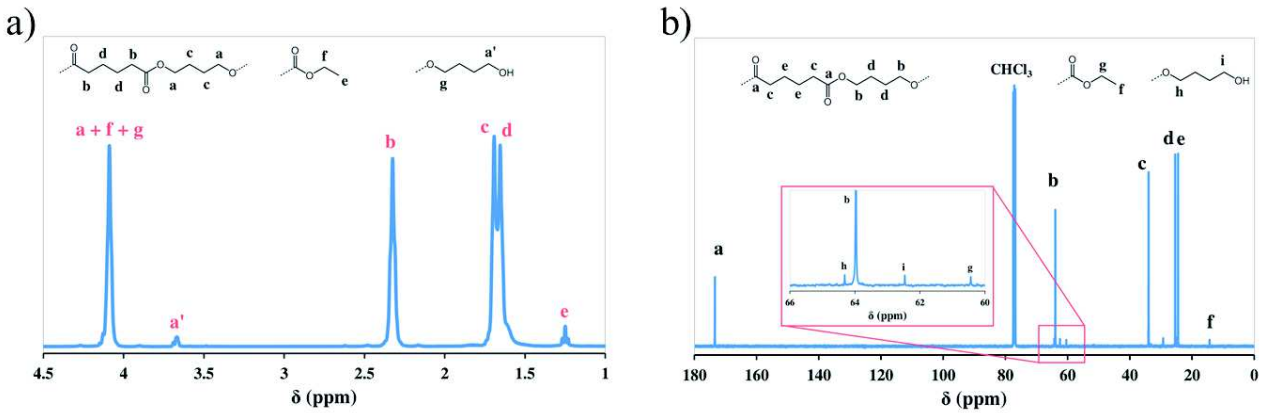

Figure 3.1.4 : Spectres de RMN (a) ^{1}H et (b) ^{13}C de PBA synthétisé par catalyse enzymatique à partir de 1,4-BDO/DEA analysé dans le $CDCl_3$.

Les données issues des synthèses de PBA sont présentées dans le Tableau 3.1.3. On observe, tout d'abord, une augmentation de la masse molaire des polyesters synthétisés (par rapport au PBS) en utilisant un monomère donneur d'acyle plus long (*i.e.*, DEA au lieu de DES). Néanmoins, les DP_n calculés des deux polyesters sont identiques (*i.e.* ~ 10) pour ce système réactionnel. Aussi, bien qu'on puisse généralement s'attendre à ce que des monomères plus longs, se rapprochant plus des acides gras qui sont les substrats naturels des lipases, donnent des chaînes plus longues, ce n'est pas le cas ici. Il est probable que de passer d'un monomère donneur d'acyle de 4 à 6 carbones seulement ne soit pas suffisant pour que celui-ci est une influence sur notre système.

Une synthèse supplémentaire de PBA à partir de 1,4-BDO et de DEA a été effectuée cette fois dans 150 pds.% de toluène anhydre. Le PBA ainsi obtenu possède des caractéristiques (masse molaire, proportion en terminaisons esters) identiques à celui synthétisé dans 200 pds.% de toluène anhydre. Cela signifie qu'il est possible de réduire la quantité de solvant et répondre ainsi également à l'un des « 12 principes de la Chimie Verte » énoncés par Anastas et Warner (Anastas and Warner, 2000).

2.3. Influence de la nature de l'ester monomère donneur d'acyle

L'influence de la nature de l'ester monomère donneur d'acyle a été étudiée en utilisant soit du diméthyle succinate/adipate soit du diéthyle succinate/adipate comme monomères. En utilisant du DMS à la place de DES, la réaction aura comme sous-produit de réaction du méthanol qui est plus volatile que l'éthanol car leurs températures d'ébullition sont respectivement de 65 et 78 °C. On peut donc supposer que le sous-produit de réaction sera d'autant plus facile à éliminer du milieu réactionnel, permettant ainsi la synthèse de polyesters de masses molaires plus importantes. A l'inverse, les diesters carboxyliques de méthyle sont plus hydrophiles que les diesters carboxyliques d'éthyle et peuvent donc éventuellement diminuer l'activité enzymatique des lipases. Afin d'étudier ce phénomène, les réactions ont été réalisées dans des réacteurs Schlenk à 90 °C durant 72 h dans 200 pds.% de toluène anhydre sous atmosphère d'argon, avec 10 pds.% de N435 et 0,1 g/mL de tamis moléculaire. Les résultats sont présentés dans le Tableau 3.1.3.

Tableau 3.1.3 : Influence de la structure du monomère donneur d'acyle sur la synthèse enzymatique de PBS et de PBA dans le toluène.

				CES			RMN ^{1}H		
Entrée	Polyester	Diester	Rendement (pds.%)	$M_{n,CES}$ (kg/mol)	Đ	$M_{n,MHS}$ (kg/mol)	$M_{n,RMN}$ (kg/mol)	DP_n	$\%_{terminaison\ ester}$ (%)
1	PBS	DMS	65	7,5	1,6	3,6	-	-	-
2		DES	88	4,5	1,7	2,1	1,8	10	64
3	PBA	DMA	84	6,9	1,5	2,5	-	-	-
4		DEA	74	5,9	1,4	2,1	2,0	10	57

Les structures des différents polyesters synthétisés sont analysées par RMN et CES. A cause de la structure des polyesters synthétisés à partir des diesters carboxyliques de diméthyle, le calcul de la masse molaire à partir des spectres de RMN ^{1}H n'est pas possible car le signal associé aux protons CO-O-C<u>H</u>$_3$ de la terminaison ester est superposé à celui de l'unité répétitive 1,4-butyle à δ = 4,12 ppm rendant impossible l'identification et la quantification des terminaisons esters (Figure 3.1.5).

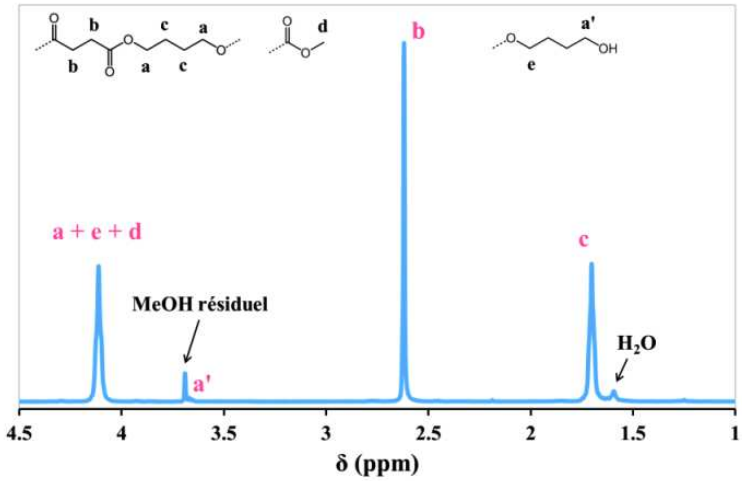

Figure 3.1.5 : Spectre de RMN ^{1}H de PBS synthétisé à partir de DMS et de 1,4-BDO.

Les résultats de CES indiquent que l'utilisation du DMS au lieu du DES comme monomère donneur d'acyle permet d'augmenter significativement (+67%) la masse molaire ($M_{n,CES}$) des PBS synthétisés. Comme évoqué précédemment, on peut supposer que l'évaporation plus aisée du méthanol (MeOH) est le principal facteur expliquant l'augmentation de la masse molaire. La Figure 3.1.6 montre l'évolution dans le temps de la masse molaire du PBS synthétisé durant 96 h à partir de 1,4-BDO/DMS ou de 1,4-BDO/DES. On observe que la masse molaire augmente continuellement au cours du temps mais que la différence de masses molaires entre 72 et 96 h devient négligeable, et c'est pourquoi un temps de réaction de 72 h a été choisi. On peut supposer l'existence d'un équilibre atteint après 72 h de réaction. L'influence de la structure de l'ester semble toutefois beaucoup moins importante dans le cas de l'adipate, avec une augmentation de $M_{n,CES}$ de seulement 17% entre le DEA et le DMA. Néanmoins, l'utilisation de diesters carboxyliques de diméthyle semble donc être la meilleure option pour augmenter sensiblement la longueur de chaîne des polyesters synthétisés dans le toluène anhydre.

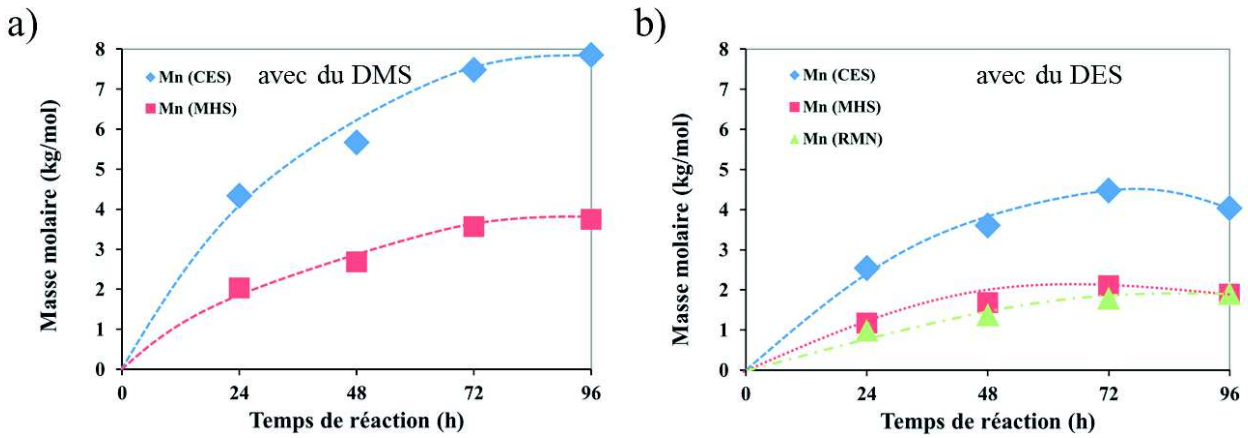

Figure 3.1.6 : Evolution dans le temps de $M_{n,CES}$, $M_{n,MHS}$ et $M_{n,RMN}$ pour la synthèse enzymatique de PBS dans le toluène à 90 °C à partir de 1,4-BDO et de (a) DMS ou (b) de DES.

Malgré les différents améliorations apportées à la synthèse enzymatique de PBS et de PBA dans le toluène sous atmosphère d'argon, les masses molaires obtenues après 72 h sont assez faibles (4 à 5 fois plus faibles que pour les polyesters synthétisés par catalyse organométallique) et un travail complémentaire d'optimisation doit donc être entrepris.

3. Optimisation de la catalyse enzymatique dans de nouveaux solvants

Un autre paramètre clé lors de la synthèse enzymatique de polyesters est le choix du solvant. En effet, de nombreux groupes de recherche ont déjà étudié l'influence du solvant sur la synthèse enzymatique de polyesters dans le but d'optimiser l'activité enzymatique et d'obtenir des polyesters de hautes masses molaires, mais les résultats ne sont pas pour le moment totalement compris. Kumar et Gross ont montré le rôle déterminant du solvant sur l'*e*ROP de l'ε-caprolactone avec N435 comme catalyseur et ont trouvé une relation expérimentale entre le coefficient de partition eau-octanol (log P) qui mesure l'hydrophobicité du milieu et la conversion en monomère (Kumar and Gross, 2000a). En effet, une haute activité enzymatique a été relevée pour les réactions de transestérification dans des solvants avec des log P > 1,9 et donc les solvants hydrophobes seront préférés (Yao et al., 2011). Lors de nos premiers tests, le toluène (log P = 2,7) était un solvant acceptable selon ce critère mais nous avons vu que les résultats obtenus n'étaient pas très satisfaisant et c'est pourquoi d'autres solvants hydrophobes ont été testés dans la suite de cette étude.

3.1. Réactions à pression atmosphérique

Comme le toluène ne permet pas la synthèse de polyesters de hautes masses molaires, d'autres solvants ont été testés tels que le cyclohexane, le mélange cyclohexane/toluène (6/1), le mélange toluène/triéthylamine (TEA) (4/1), le dodécane et le diphényl éther. Les réactions sont réalisées à partir de 1,4-BDO/DES à 80 °C durant 72 h dans 150 pds.% de solvant et 0,1 g/mL de tamis moléculaire sec. La température de réaction est abaissée à 80 °C à cause de la faible température d'ébullition du cyclohexane ($T_{ébu}$ = 81 °C) et de la TEA ($T_{ébu}$ = 89 °C). Les résultats des différentes synthèses sont présentés dans le Tableau 3.1.4.

La TEA est distillée avant utilisation et est utilisée comme un co-solvant nucléophile. En effet, Duchiron *et al.* ont montré une augmentation de l'activité enzymatique (vitesse de réaction 5 fois plus rapide) et de la masse molaire finale lors de l'ajout de TEA pour l'eROP de lactide, catalysée par N435 et par la lipase de *Burkholderia cepacia* (Duchiron et al., 2015). De même, Parker *et al.* ont démontré l'augmentation significative de l'activité enzymatique et de l'énantio-sélectivité en utilisant de la TEA (Parker et al., 1998). Le mélange cyclohexane/toluène (6/1) a déjà été testé avec succès par Jiang *et al.* et a montré des résultats similaires à ceux obtenus en polymérisation en masse (Jiang et al., 2014a). Néanmoins, contrairement à notre système réactionnel, ils ont effectué leur réaction dans le mélange cyclohexane/toluène (6/1) avec une quantité bien plus importante en solvant et en utilisant un système Dean-Stark.

Tableau 3.1.4 : Synthèses enzymatiques de PBS à partir de 1,4-BDO/DES catalysée par du N435 à 80 °C durant 72 h dans différents solvants avec 0,1 g/mL de tamis moléculaire.

Entrée	Solvant	Log P	Rendement	CES			RMN ^{1}H		
				$M_{n,CES}$	Đ	$M_{n,MHS}$	$M_{n,RMN}$	DP_n	$\%_{terminaisons\ esters}$
			pds.%	kg/mol		kg/mol	kg/mol		%
1	Toluène	2,7	83	1,9	1,4	0,9	1,0	6	59
2	Toluène/TEA (4/1)	2,7 / 1,4	84	2,9	1,5	1,3	1,2	7	64
3	Cyclohexane	3,4	93	3,2	1,3	1,5	1,3	8	62
4	Cyclohexane/toluène (6/1)	3,4 / 2,7	93	3,8	1,3	1,8	1,7	10	62
5	Dodécane	6,1	74	2,7	1,3	1,2	1,1	6	60
6	Diphényl éther	4,4	78	2,9	1,5	1,3	1,3	8	64

Les résultats obtenus montrent qu'aucun des systèmes ci-dessus ne permet une augmentation significative de la masse molaire des PBS synthétisés. La masse molaire du PBS synthétisé dans le toluène à 80 °C est plus faible que celle obtenue dans le toluène à 90 °C avec une diminution significative du DP_n de 10 à 6 (entrée 1). Cela est principalement dû au fait qu'à 80 °C l'azéotrope est beaucoup moins facilement atteint et donc la distillation de l'éthanol est beaucoup plus compliquée, limitant ainsi le déplacement de la réaction vers la synthèse du polyester. De plus, une température de réaction de 80 °C ne correspond peut-être pas à la température d'activité optimale de CALB pour cette réaction. Comme espéré, l'utilisation de TEA comme "solvant/co-catalyseur" permet d'augmenter légèrement la masse molaire. Toutefois, la masse molaire obtenue dans un système toluène/TEA à 80 °C n'a pas augmentée significativement (*i.e.*, augmentation du DP_n de 6 à 7) et reste plus faible que celle obtenue dans le toluène à 90 °C (entrée 2). Le PBS synthétisé dans le cyclohexane à 80 °C a une masse molaire légèrement plus haute que celui synthétisé dans le toluène à 80 °C (entrée 3). Mais les deux systèmes impliquant le cyclohexane (*i.e.*, le cyclohexane pur ou le mélange cyclohexane/toluène 6/1) deviennent solides après 24 h de réaction, à cause de la perte de solvant et/ou la faible solubilité du PBS dans ce solvant. Néanmoins, le mélange cyclohexane/toluène semble être le meilleur système à 80 °C avec une $M_{n,CES}$ finale d'environ 3,8 kg/mol (entrée 4), assez proche de la valeur obtenue dans le toluène anhydre à 90 °C (*i.e.*, 4,5 kg/mol). Cependant, à cause de la faible température d'ébullition du cyclohexane, la température de réaction ne peut pas être augmentée. Bien que le dodécane et le diphényl éther soient connus pour être de bons solvants pour la synthèse enzymatique de polyesters sous pression réduite (Jiang et al., 2013), les synthèses effectuées à pression atmosphérique et à 80 °C dans ces deux solvants n'ont pas permis la production de PBS hautes masses molaires (DP_n ~ 6-8). On observe par ailleurs que, quel que soit le solvant testé, tous les polyesters ont la même proportion en terminaisons esters (~ 60%) et donc que le solvant n'a pas d'influence sur ce paramètre.

Au final, même si certains solvants semblent légèrement meilleurs que le toluène à 80 °C, aucun des systèmes étudiés ne permet d'obtenir des masses molaires supérieures à celles obtenues dans le toluène à 90 °C (*i.e.*, $M_{n,CES}$ = 4,5 kg/mol).

3.2. Synthèses dans le dodécane et le diphényl éther sous pression réduite

Selon la littérature relative à la synthèse de polyesters par transestérification de monomères fonctionnels, des masses molaires importantes peuvent être obtenues par catalyse enzymatique en utilisant des solvants hydrophobes à haute température d'ébullition tels que le diphényl éther (Jiang et al., 2015a, 2013, Mahapatro et al., 2004, 2003). Dans le but d'augmenter la masse molaire des polyesters obtenus par catalyse enzymatique, nous avons choisi dans un premier temps de tester le dodécane et le diphényl éther comme solvant hydrophobe à haute température d'ébullition. Des synthèses de PBS ont alors été effectuées sous vide (pression minimale de 20 mbar) à 90 °C durant 72 h à partir de 1,4-BDO/DES dans 200 pds.% de diphényl éther (ou dodécane) avec 0,1 g/mL de tamis moléculaire et catalysée par 10 pds.% de N435.

Nota : Un mélange équimolaire de 1,4-BDO et de DES (5 mmol chacun), 10 pds.% de N435, 200 pds.% de diphényl éther et 0,1 g/mL de tamis moléculaire est introduit dans un réacteur Schlenk. Celui-ci est ensuite immergé dans un bain d'huile chauffé à 90 °C et la pression à l'intérieur du réacteur est diminuée petit à petit à 350, 100, 50 et 20 mbar

durant 4, 2, 2 et 64 h, respectivement. Après 72 h de réaction, 10 mL de chloroforme sont introduits dans le milieu réactionnel afin d'arrêter la réaction puis le milieu réactionnel est traité comme auparavant. Le protocole expérimental est résumé par le Schéma 3.1.2.

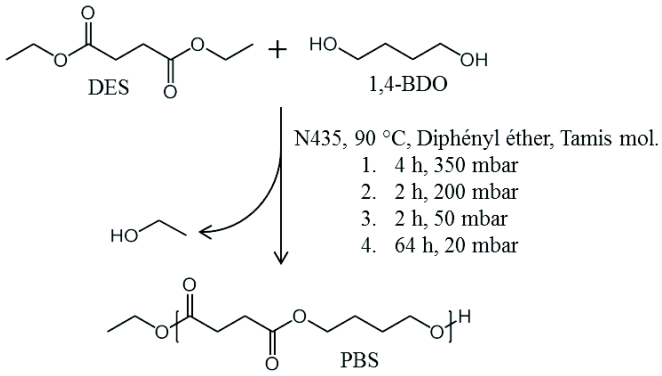

Schéma 3.1.2 : Synthèse enzymatique par transestérification dans le diphényl éther sous pression réduite.

Durant la réaction dans le dodécane, on observe que les billes de N435 se collent à la paroi du réacteur empêchant ainsi une bonne dispersion du catalyseur dans le milieu et diminuant l'efficacité de ce dernier. On suppose que cela est dû à une mauvaise affinité entre la matrice acrylique du N435 et le dodécane, ce qui réduit fortement l'attrait pour ce solvant.

Les résultats issus des synthèses de PBS sous pression réduite dans le dodécane et le diphényl éther sont comparés à ceux des synthèses réalisées à pression atmosphérique (décrites auparavant). Tous les résultats sont résumés dans le Tableau 3.1.5. A pression atmosphérique, ces solvants ne sont pas intéressants car les masses molaires sont faibles. Cependant sous pression réduite, pour des conditions expérimentales similaires, le diphényl éther semble bien plus avantageux que le dodécane. En effet, des polyesters de DP_n de seulement 14 sont synthétisés dans le dodécane à 90 °C, donc juste un peu plus long que ceux synthétisés dans le toluène (DP_n ~ 10). Par contre, dans le diphényl éther, des PBS de $M_{n,RMN}$ de presque 5 kg/mol (DP_n = 28) ont pu être obtenus, c'est-à-dire des chaînes trois fois plus longues que celles obtenues dans le toluène. Enfin, on observe que les polyesters synthétisés dans le diphényl éther sous pression réduite possèdent presque exclusivement des terminaisons esters ce qui est vraisemblablement dû au degré d'avancement élevé de réaction avec ce système catalytique.

Tableau 3.1.5 : Synthèse enzymatique de PBS à partir de 1,4-BDO/DES et de 10 pds.% de N435 dans différents milieux réactionnels.

	Conditions expérimentales					CES			RMN ^{1}H	
Entrée	Solvant	Temp. [a]	Pression	Qté de solvant [b]	Rendement	$M_{n,CES}$	Đ	$M_{n,MHS}$	$M_{n,RMN}$	$\%_{terminaisons\ esters}$
		°C	mbar	pds.%	pds.%	kg/mol		kg/mol	kg/mol	%
1	Dodécane	80	1000	150	74	2,7	1,3	1,2	1,1	60
2		90	1000	200	89	3,5	1,4	1,6	1,4	66
3		90	20	200	90	5,1	1,6	2,4	2,4	70
4	Diphényl éther	80	1000	150	78	2,9	1,5	1,3	1,3	64
5		90	1000	200	74	2,2	1,4	1,0	1,0	66
6		90	20	200	92	12,2	1,8	5,3	4,9	92

[a] Température de réaction. [b] Quantité de solvant introduit dans le réacteur.

Le suivi cinétique de la synthèse de PBS dans deux systèmes différents (dans le toluène sous pression atmosphérique et dans le diphényl éther sous pression réduite) à partir de DMS ou de DES a été réalisé durant 96 h avec prise d'échantillons toutes les 24 h. L'évolution de $M_{n,CES}$ en fonction du temps de réaction est présentée dans la Figure 3.1.7. Comme observé auparavant, les réactions réalisées dans le diphényl éther sous pression réduite ont permis d'obtenir des PBS de plus hautes masses molaires que dans le toluène sous pression atmosphérique. La masse molaire augmente durant 72 h et surtout durant les 24 premières heures. Ensuite, les masses molaires des PBS de certaines synthèses

diminuent légèrement entre 72 et 96 h ce qui tend à prouver l'existence d'un certain équilibre réactionnel. Un temps de réaction de 72 h est donc un bon compromis pour l'ensemble des synthèses (comme pour les réactions dans le toluène). De plus, tandis que l'utilisation de DMS est plus intéressante que celle du DES pour la synthèse dans le toluène, l'utilisation de DMS dans le diphényl éther sous pression réduite est moins intéressante. En effet, les résultats montrent que les masses molaires obtenues avec le DMS durant les premières 72 h de réaction sont plus faibles que celles obtenues avec le DES et c'est seulement après 96 h de réaction que les valeurs atteintes sont identiques. En effet, grâce au vide, l'élimination du méthanol et de l'éthanol est largement favorisée contrairement aux réactions menées dans le toluène. Donc la différence de température d'ébullition entre ces deux alcools n'est plus un paramètre pertinent dans le cas des synthèses dans le diphényl éther. De plus, le DES qui est plus hydrophobe que le DMS et qui possède une chaîne aliphatique plus longue peut présenter une meilleure affinité pour la lipase (CALB) et avoir ainsi une meilleure stabilisation dans le site actif de l'enzyme.

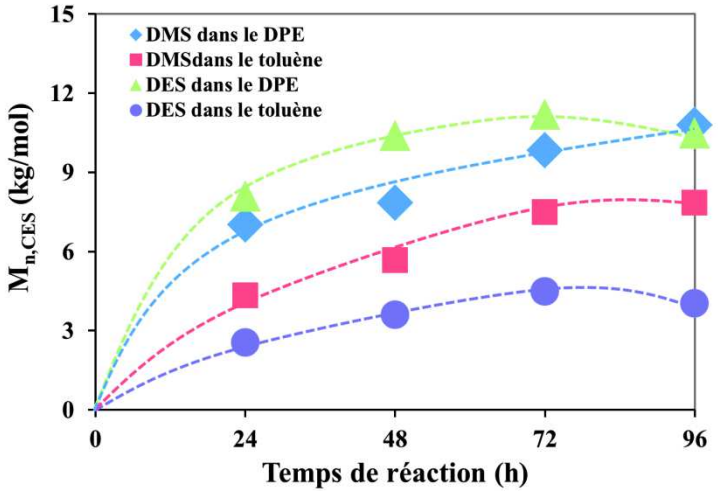

Figure 3.1.7 : (a) Evolution dans le temps de $M_{n,CES}$ pour la synthèse de PBS soit à partir de 1,4-BDO/DMS dans le diphényl éther (♦) ou le toluène (■), soit à partir de 1,4-BDO/DES dans le diphényl éther (▲) ou le toluène (●).

Les synthèses enzymatiques de PBA à partir de 1,4-BDO/DEA dans le dodécane et le diphényl éther ont été réalisées sous pression réduite dans les mêmes conditions expérimentales que les synthèses de PBS. Tout comme pour le PBS, la masse molaire du PBA synthétisé dans le dodécane sous pression réduite (DP_n = 19) est supérieure à celle du PBA synthétisé dans le toluène à pression atmosphérique (DP_n = 10). Comparé à la synthèse du PBS, la synthèse de PBA dans le dodécane semble plus efficace avec un DP_n un peu plus élevé. Par ailleurs, et comme pour le PBS, la réaction menée dans le diphényl éther sous pression réduite est celle permettant la synthèse de PBA avec le plus haut DP_n (environ 28, équivalent à celui du PBS). Donc, comme pour les synthèses dans le toluène, l'augmentation de la longueur du monomère donneur d'acyle de deux carbones méthylènes n'a pas d'influence sur le DP_n. De plus, on observe que la proportion en terminaisons esters augmente avec le DP_n et l'avancement de réaction comme montré par Nakaoki *et al.* (Nakaoki et al., 2003). Ainsi, tout comme pour le PBS, les PBA synthétisés dans le diphényl éther possèdent presque exclusivement des terminaisons esters.

Tableau 3.1.6 : Synthèses enzymatiques de PBA à partir de 1,4-BDO/DEA à 90 °C dans différents solvants à pression atmosphérique ou sous pression réduite.

	Conditions expérimentales					CES			RMN ^{1}H	
Entrée	Solvant	Temp. [a]	Pression	Qté de solvant [b]	Rendement	$M_{n,CES}$	Đ	$M_{n,MHS}$	$M_{n,RMN}$	$\%_{terminaisons\ esters}$
		°C	mbar	pds.%	pds.%	kg/mol		kg/mol	kg/mol	%
1	toluène	90	1000	200	74	5,9	1,4	2,1	2,0	57
2	dodécane	90	20	200	86	12,9	1,6	4,8	3,8	86
3	diphényl éther	90	20	200	91	16,7	1,7	6,3	5,7	91

[a] Température de réaction. [b] Quantité de solvant introduit dans le réacteur.

Le suivi cinétique de la synthèse de PBS et de PBA dans le diphényl éther sous pression réduite a été réalisé durant 96 h avec prises d'échantillons toutes les 24 h. L'évolution de $M_{n,CES}$ et de la proportion en terminaisons esters en fonction du temps de réaction sont présentées respectivement en Figures 3.1.8-a et 3.1.8-b. Dans les deux cas, les masses molaires augmentent sensiblement durant les premières 24 h puis cette augmentation ralentit jusqu'à même observer une réduction de M_n du PBS entre 72 et 96 h. Pour la synthèse dans le diphényl éther sous pression réduite, un temps de réaction de 72 h semble donc encore être un bon compromis. De plus, la proportion en terminaisons esters augmente de 60 à 90% en passant de 24 à 96 h de réaction pour le PBS synthétisé dans le diphényl éther.

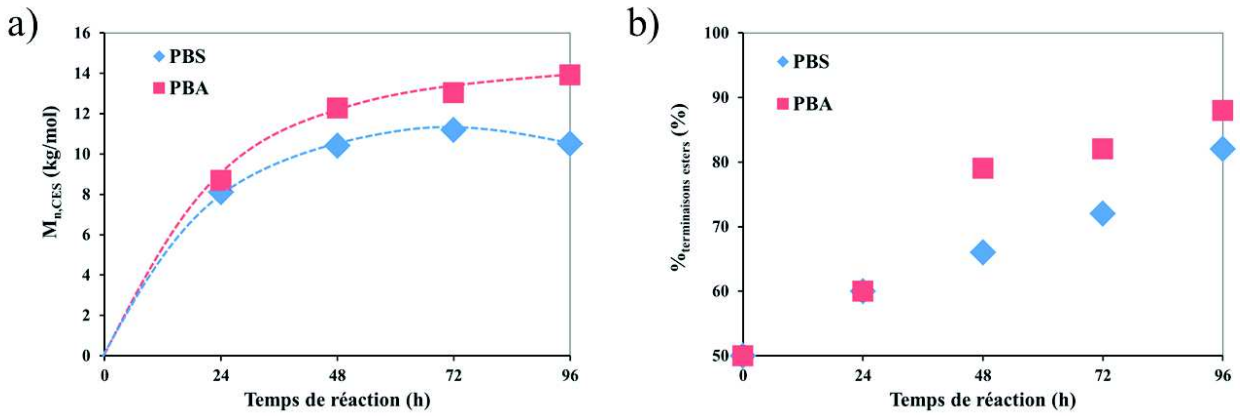

Figure 3.1.8 : Evolution (a) de $M_{n,CES}$ et (b) de la proportion en terminaisons esters pour la synthèse enzymatique de PBS (1,4-BDO/DES) et de PBA (1,4-BDO/DEA) réalisée à 90 °C durant 72 h dans le diphényl éther sous 20 mbar.

3.3. Nouveaux solvants pour les réactions enzymatiques sous pression réduite

La synthèse enzymatique sous pression réduite dans le diphényl éther a été jusqu'ici le meilleur système étudié. Nous avons vu que le dodécane ne semble, *a priori,* pas intéressant pour la synthèse de nos polyesters puisque les masses molaires sont faibles pour le PBS synthétisé dans ce solvant. Ceci peut s'expliquer par le fait que (i) le dodécane étant trop hydrophobe (log P = 6,1) il n'y a pas assez de molécules d'eau à la surface de la lipase ce qui modifie sa structure 3D opérationnelle et diminue son activité enzymatique, et/ou (ii) le dodécane a une mauvaise affinité avec la matrice acrylate du catalyseur ce qui entraîne l'agrégation des billes de catalyseur sur la paroi du réacteur limitant sa bonne dispersion dans le milieu.

Dans le but d'étudier plus en détail la réaction de transestérification, de nouveaux solvants éthers ont été testés puisqu'ils présentent en général de bons résultats pour la synthèse de polyesters. Azim *et al.* (Azim et al., 2006) et Mahapatro *et al.* (Mahapatro et al., 2003) ont montré que le diglyme (diméthoxyéthane) et le tetraglyme (tetraéthylène glycol diméthyléther), qui sont deux éthers aliphatiques, ne sont pas des solvants très intéressants puisque les masses molaires des polyesters obtenus dans ces deux solvants sont bien plus faibles que dans le diphényl éther. De leur côté, Uyama *et al*. ont obtenu des résultats intéressants dans l'éther d'isopropyle. Toutefois, la très faible température d'ébullition de ce solvant ($T_{ébu}$ = 69 °C) n'est pas adaptée à notre système réactionnel sous pression réduite. Pour leur part, Linko *et al.* ont montré que le système réactif constitué de la lipase de *Rhizomucor miehei* dans le vératrole (1,2-diméthyoxybenzène) sous pression réduite était également un système intéressant (Linko et al., 1995a, 1995b).

Pour poursuivre l'étude, un solvant éther aliphatique (éther dibutylique) et des solvants éthers aromatiques ayant des structures proches du vératrole (phénétole, anisole, benzyl méthyl éther et dibenzyl éther) ont donc été testés. A notre connaissance, c'est la première fois que certains de ces solvants ont été testés en synthèse enzymatique de polyesters. De plus, le xylène, qui a une structure chimique proche du toluène mais avec une température d'ébullition plus haute, a également été testé. Les propriétés de ces solvants sont résumées dans le Tableau 3.1.7.

Tableau 3.1.7 : Solvants utilisés lors des synthèses enzymatiques.

Solvant	Structure	log P	densité	T_f (°C)	$T_{ébu}$ (°C)
Ether dibutylique	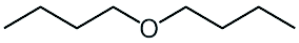	2,9	0,769	-98	142
Dodécane		6,1	0,746	-10	216
Toluène	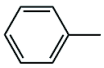	2,7	0,867	-95	111
Xylène	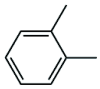	3,2	0,865	-34	138
Anisole	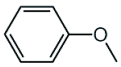	2,1	0,995	-37	154
Phénétole	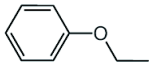	2,5	0,967	-30	170
Benzyl méthyl éther	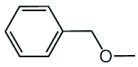	1,4	0,987	-52	174
Diphényl éther	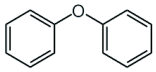	4,2	1,07	20	258
Dibenzyl éther	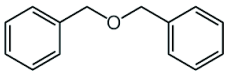	3,5	1,043	2	298

De nombreuses synthèses de PBS à partir de 1,4-BDO/DES ont été réalisées à 90 °C avec 10 pds.% de N435 dans différents solvants sous pression réduite. La pression est adaptée à la température d'ébullition des différents solvants. Les résultats des différentes synthèses sont présentés dans le Tableau 3.1.8. Tout d'abord, le xylène (qui a une structure proche du toluène) a été testé dans des réactions à différentes pressions (*i.e.*, 1000, 500 et 400 mbar). La masse molaire des polyesters synthétisés dans le xylène augmente avec la diminution de la pression en réacteur (entrées 2-4). Toutefois, la masse molaire des polyesters synthétisés dans le xylène sous 400 mbar (*i.e.*, la plus basse pression) est similaire à celle du PBS synthétisé dans le toluène à pression atmosphérique (*i.e.*, $M_{n,CES}$ ~ 4-5 kg/mol) (entrées 1 et 4). De même, le PBS synthétisé dans l'éther dibutylique sous 400 mbar a un M_n plus faible que celui synthétisé dans le toluène (entrée 5), à cause de la faible solubilité de ce polyester dans l'éther dibutylique (*i.e.*, précipitation après 24 h de réaction). Le xylène et l'éther dibutylique ne sont donc pas des solvants adaptés pour la synthèse enzymatique de PBS par transestérification. Pour l'anisole, le phénétole et le benzyl méthyl éther, qui sont des éthers contenant un cycle aromatique, les synthèses ont été réalisées sous une pression réduite de 150 mbar à cause de leur température d'ébullition située vers 155-175 °C. Les masses molaires (déterminées par CES) des PBS synthétisés dans l'anisole, le phénétole et le benzyl méthyl éther sont respectivement d'environ 14, 11 et 5 kg/mol, (entrées 6-8). Le benzyl méthyl éther n'est donc pas un solvant intéressant. En revanche, des masses molaires élevées ont été obtenues dans le phénétole (*i.e.*, 10,9 kg/mol) et surtout dans l'anisole (*i.e.*, 13,8 kg/mol) et celles-ci sont du même ordre de grandeur que celles du PBS synthétisé dans le diphényl éther sous 20 mbar (*i.e.*, 12,2 kg/mol). On observe également que lorsque la masse molaire augmente, la proportion en terminaisons esters tend à augmenter. Enfin, le dibenzyl éther, bien que composé de deux cycles aromatiques liés par une liaison éther comme le diphényl éther, ne permet pas de synthétiser des PBS de hautes masses molaires. Néanmoins, pour ces deux derniers solvants, la diminution de la pression permet d'augmenter la masse molaire (entrées 9-13). Bien que les structures du dibenzyl éther et du diphényl éther soient très proches avec des valeurs de log P voisines, les résultats obtenus sont très différents. Toutefois, comme c'est souvent le cas pour l'influence du solvant dans les synthèses enzymatiques, aucune explication particulière n'a pu être avancée pour expliquer cette différence. Ceci nécessiterait de plus amples investigations.

Tableau 3.1.8 : Synthèse enzymatique de PBS à 90 °C dans un réacteur Schlenk avec 10 pds.% de N435 dans 200 pds.% de différents solvants avec 0,1 g/mL de tamis moléculaire.

Entrée	Solvant	log P	Pression [a]	CES			RMN ^{1}H	
				$M_{n,CES}$	M_w	Đ	$M_{n,RMN}$	$\%_{terminaisons\ esters}$
			mbar	kg/mol	kg/mol		kg/mol	%
1	Toluène	2, 7	1000	4,5	7,7	1,7	1,8	59
2	Xylène	3, 2	1000	2,1	2,9	1,4	1,0	62
3	Xylène	3,2	500	4,1	6,4	1,6	1,8	77
4	Xylène	3,2	400	4,8	9,0	1,9	1,7	71
5	Ether dibutylique	2,9	400	2,6	4,0	1,6	1,2	52
6	Benzyl methyl ether	1,4	150	4,7	8,9	1,9	3,1	61
7	Phénetole	2,5	150	10,9	23,5	2,2	4,9	75
8	Anisole [b]	2,1	150	13,8	32,8	2,3	6,5	84
9	Diphényl éther	4,1	1000	2,2	3,1	1,4	1,0	66
10	Diphényl éther	4,1	150	6,8	15,6	2,3	4,1	78
11	Diphényl éther [b]	4,1	20	12,2	23,2	1,9	5,1	90
12	Dibenzyl éther	3,5	150	4,3	8,9	2,0	2,1	72
13	Dibenzyl éther	3,5	20	6,2	14,1	2,3	3,5	78

[a] Pression minimale dans le système, [b] Valeurs moyennes.

Tout comme pour le PBS, plusieurs synthèses de PBA à partir de 1,4-BDO/DEA ont été réalisées à 90 °C avec 10 pds.% de N435 dans différents solvants. Les résultats sont résumés dans le Tableau 3.1.9. La synthèse de PBA dans le dibenzyl éther, même à faible pression, et dans le toluène ne permet pas d'obtenir des PBA de hautes masses molaires, tandis que cela est possible dans le diphényl éther et dans l'anisole (*i.e.*, $M_{n,CES}$ ~ 18 kg/mol). Ces deux derniers solvants permettent la synthèse de PBA de masses molaires équivalentes, mais la Đ est plus importante dans l'anisole que le diphényl éther. De manière intéressante, la réaction dans le dodécane permet également d'obtenir des PBA de masses molaires importantes (*i.e.*, $M_{n,CES}$ ~ 12 kg/mol) alors que ce n'était pas le cas pour le PBS synthétisé dans ce solvant. Enfin, on observe que la proportion de terminaisons esters des PBA synthétisés sous pression réduite est importante (*i.e.*, 80-90%) quel que soit le solvant utilisé.

En conclusion, le diphényl éther (sous 20 mbar) et l'anisole (sous 150 mbar) semblent être les meilleurs systèmes réactionnels pour la synthèse de polyesters de hautes masses molaires par transestérification à partir de nos synthons bifonctionnels.

Tableau 3.1.9 : Synthèse enzymatique de PBA à 90 °C dans un réacteur Schlenk avec 10 pds.% de N435 dans 200 pds.% de différents solvants avec 0,1 g/mL de tamis moléculaire.

Entrée	Solvant	log P	Pression [a]	CES				RMN ^{1}H	
				$M_{n,CES}$	M_w	Đ	$M_{n,MHS}$	$M_{n,RMN}$	$\%_{terminaisons\ esters}$
			mbar	g/mol	g/mol		g/mol	g/mol	%
1	Toluène	2,7	1000	5,9	7,9	1,4	2,1	2,1	58
2	Dodécane	6,1	20	12,9	20,8	1,6	4,8	3,8	86
3	Diphényl éther [b]	4,1	20	17,7	29,4	1,7	6,7	5,7	83
4	Anisole	2,1	150	17,3	42,8	2,5	6,6	4,7	84
5	Dibenzyl éther	3,5	20	8,4	15,5	1,8	3,1	-	-

[a] Pression minimale dans le système, [b] Valeurs moyennes.

4. Optimisation du système réactionnel dans le diphényl éther sous vide

4.1. Optimisation des conditions expérimentales pour la synthèse de PBS

La recherche des conditions expérimentales optimales pour la synthèse enzymatique dans le diphényl éther sous vide nous a mené à devoir étudier l'influence de (i) la quantité de N435 introduite, (ii) la quantité de solvant, (iii) la température de réaction et (iv) la quantité de tamis moléculaire à introduire dans le réacteur pour la synthèse enzymatique de PBS à partir de 1,4-BDO/DES. Les résultats de l'étude sont présentés en Figure 3.1.9. La réaction de référence (sans enzyme) ne permet pas d'obtenir de polyester ce qui démontre que la polymérisation est bien catalysée par CALB (Figure 3.1.9-a). La masse molaire des PBS synthétisés augmente lorsque la quantité de N435 augmente de 1 à 10 pds.%, et diminue ensuite pour des quantités de N435 plus importantes. Le même comportement (avec un optimum) a été observé pour l'étude de la quantité de solvant optimale avec des masses molaires maximales obtenues pour 150 pds.% de solvant (Figure 3.1.9-b), et ceci en accord avec les travaux de Jiang *et al*. (Jiang et al., 2013). De même, la masse molaire des PBS augmente avec la température de réaction entre 70 et 90 °C, puis diminue pour de plus hautes températures à cause de la perte d'activité due à une possible dénaturation de la lipase à trop hautes températures. L'importante différence de masses molaires entre 80 et 90 °C est due au fait que le PBS, qui est un polyester à haute température de fusion (*i.e.*, 113°C), précipite après 32-48 h de réaction à 80 °C dans le diphényl éther (Figure 3.1.9-c). Enfin, la masse molaire des PBS synthétisés diminue avec l'augmentation de la quantité de tamis moléculaire introduite dans le milieu réactionnel (Figure 3.1.9-d). En conclusion, il est à retenir que pour les synthèses de PBS dans le diphényl éther sous pression réduite, les meilleurs résultats sont obtenus à 90 °C dans 150 pds.% de diphényl éther avec 10 pds.% de N435 et sans utilisation de tamis moléculaire.

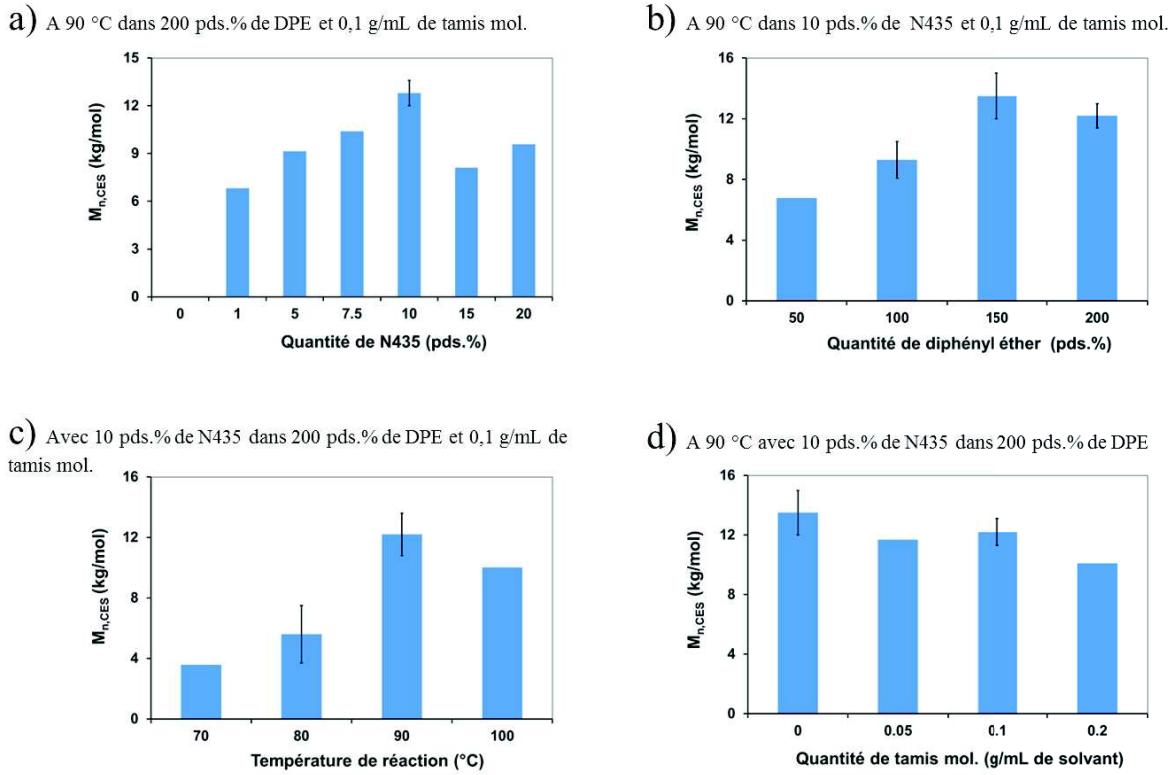

Figure 3.1.9 : Variation de $M_{n,CES}$ en fonction de (i) la quantité de N435, (ii) la quantité de diphényl éther, (iii) la température de réaction et (iv) la quantité de tamis moléculaire optimale pour la synthèse enzymatique de PBS à partir de 1,4-BDO/DES dans le diphényl éther sous 20 mbar.

4.2. Optimisation de la température pour la synthèse de PBA dans le diphényl éther

Tout comme pour le PBS, la température optimale pour la synthèse de PBA à partir de 1,4-BDO/DEA dans le diphényl éther sous vide a été recherchée. Les résultats de cette étude sont présentés dans la Figure 3.1.10. Contrairement au PBS, le PBA a une température de fusion plus faible (T_f ~ 60 °C) et ne présente donc pas l'inconvénient de précipiter dans le milieu réactionnel lorsque sa masse molaire est élevée. La masse molaire augmente avec la température entre

70 et 90 °C, puis diminue légèrement à 100 °C. De manière surprenante, la masse molaire du PBA obtenu à 60 °C est aussi élevée que celle à 80 °C sans que l'on puisse avancer une raison particulière. Au final, une température de réaction de 90 °C a été choisie pour la synthèse de PBA dans le diphényl éther.

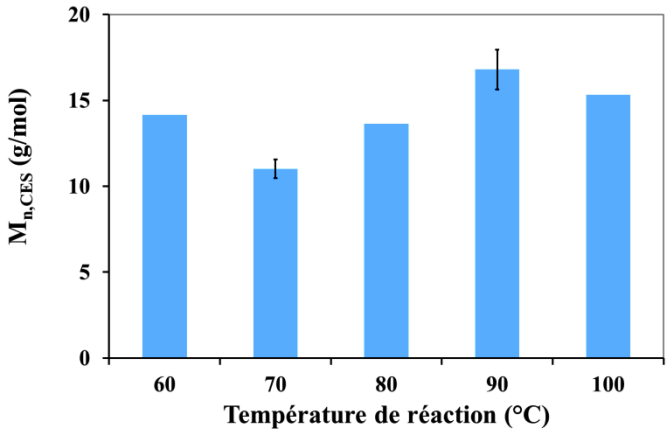

Figure 3.1.10 : Influence de la température sur la $M_{n,CES}$ de PBA synthétisé dans le diphényl éther sous 20 mbar.

4.3. Influence du montage réactionnel

L'influence de la présence ou non d'une colonne courte remplie de tamis moléculaire placé au-dessus du réacteur Schlenk (comme pour le système sous pression atmosphérique) durant la synthèse dans le diphényl éther sous pression réduite a également été étudiée. Quatre synthèses (*i.e.*, deux de PBS et deux de PBA) ont été réalisées à 90 °C durant 72 h avec 10 pds.% de N435, 200 pds.% de diphényl éther et 0,1 g/mL de tamis moléculaire avec une pression minimale de 10 mbar à partir de 1,4-BDO et de DES ou de DEA.

Les polyesters synthétisés sont analysés par RMN ^{1}H et CES, et les résultats sont présentés dans le Tableau 3.1.10. On observe que les masses molaires obtenues pour le PBS et le PBA sont plus élevées sans la colonne, ce qui signifie que l'utilisation d'une colonne courte remplie de tamis moléculaire n'est pas nécessaire pour les systèmes sous vide. En effet, les sous-produits de réaction (eau, éthanol) sont facilement éliminés du milieu réactionnel par le vide. De plus, l'usage d'une colonne remplie de tamis moléculaire peut amener certaines complications techniques (notamment lorsque le vide est coupé en fin de réaction ou durant des prélèvements). En conclusion, pour les systèmes sous vide, l'utilisation d'une colonne remplie de tamis moléculaire est désormais exclue.

De plus, ces réactions ont été réalisées sous une pression de 10 mbar. Aucune différence notable n'a été observée sur les polyesters synthétisés en diminuant la pression de 20 à 10 mbar. Des PBS de masses molaires ($M_{n,CES}$) maximales de 12-15 kg/mol peuvent être synthétisées dans ces conditions. La seule différence est le fait que lors de cette étude comparative, le PBS précipite au bout de 2 jours notamment du fait de la température de fusion élevée du PBS (T_f = 113 °C) et à l'insolubilité des PBS de hautes masses molaires dans le diphényl éther. En revanche, il est très peu probable que du solvant soit éliminé du milieu réactionnel lors de la réaction car la température d'ébullition du diphényl éther est très élevée ($T_{ébu}$ = 258 °C). De plus, des études précédentes ont rapporté l'utilisation du diphényl éther à des pressions encore plus basses (jusqu'à 2 mbar) (Jiang et al., 2014a, 2014b).

Tableau 3.1.10 : Synthèse enzymatique de PBS et de PBA dans le diphényl éther à 90 °C sous vide avec ou sans colonne remplie de tamis moléculaire placée au-dessus du réacteur Schlenk.

Entrée	Polyester	Colonne	Rendement	CES			RMN ^{1}H		
				$M_{n,CES}$	Đ	$M_{n,MHS}$	$M_{n,RMN}$	DP_n	$\%_{terminaisons\ esters}$
			pds.%	kg/mol		kg/mol	kg/mol		%
1	PBS	Oui	90	9,7	2,1	4,7	4,5	26	87
2		Non	93	12,3	2,1	5,9	5,6	32	92
3	PBA	Oui	85	15,4	1,6	5,8	6,0	30	100
4		Non	93	16,0	1,7	6,1	6,0	30	85

5. Synthèses enzymatiques en masse

Dans cette partie, la synthèse en masse de polyesters catalysée par N435 est étudiée afin de développer un procédé sans solvant, plus « vert » (Anastas and Warner, 2000). Pour cette étude, seule la synthèse de PBA a été considérée puisqu'il présente une température de fusion assez faible pour être à l'état fondu à la température de réaction.

5.1. Cinétique de la réaction enzymatique en masse en utilisant un évaporateur rotatif

L'étude cinétique de la synthèse en masse de PBA à partir de 1,4-BDO/DEA à 70 °C durant 10 h en utilisant un évaporateur rotatif avec une vitesse de rotation de 100 tr/min avec 10 pds.% de N435 sous 60-70 mbar a été réalisée avec des prises d'échantillons toutes les 2 h. Cette méthode est basée sur l'étude de Pellis *et al.* (Pellis et al., 2015b) qui ont montré que des masses molaires relativement élevées pouvaient être obtenues pour la synthèse enzymatique de poly(butylène itaconate) catalysée par N435 avec l'avantage d'une absence de relargage de lipase dans la matrice polymère. En effet, en milieu solvanté, une certaine fraction d'enzyme peut se désorber du support de N435 et se retrouver dans la matrice polyester aboutissant ainsi à une possible augmentation de la vitesse de dégradation/hydrolyse du polyester après la réaction (Pellis et al., 2015b). L'agitation du mélange réactionnel est assurée principalement par la rotation de l'évaporateur rotatif, tandis qu'une agitation diffusionnelle agit également sur le film polymère assez fin se formant sur la paroi lors de rotation.

Durant la réaction, on observe que la viscosité du milieu augmente rapidement au début de la réaction. Pour des temps de réaction longs, cela peut être un problème majeur. Les échantillons de polyesters et le polyester final sont analysés par RMN et CES. Les données de la cinétique sont résumées dans la Figure 3.1.11-a et présentées dans le Tableau 3.1.11. La masse molaire du PBA augmente continuellement lors de la réaction jusqu'à un $M_{n,RMN}$ de 2,6 kg/mol (ou un $M_{n,MHS}$ de 2,8 kg/mol). Après 10 h de réaction en masse, la masse molaire obtenue est presque la moitié de celle obtenue lors de la synthèse enzymatique dans le diphényl éther sous pression réduite après 72 h (*i.e.*, 6 kg/mol). Durant la réaction, la proportion en terminaisons esters augmente globalement avec le temps de réaction. Au final, un PBA d'un $M_{n,CES}$ de 7,8 kg/mol et de Đ = 1,6 est obtenu après 10 h de réaction.

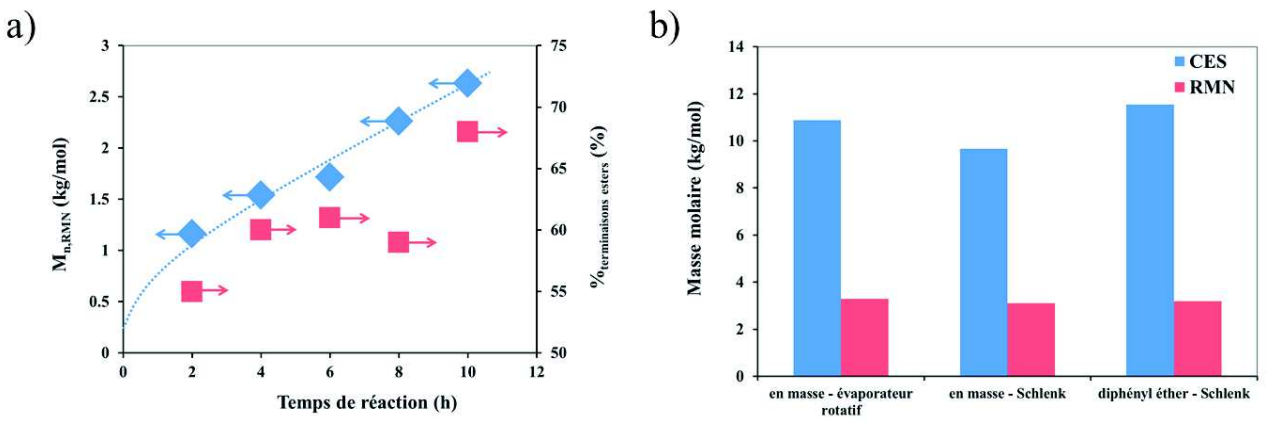

Figure 3.1.11 : (a) Evolution dans le temps de $M_{n,RMN}$ et de la proportion en terminaisons esters de PBA synthétisé en masse dans un évaporateur rotatif et (b) comparaison des différents systèmes catalytiques pour la synthèse en masse de PBA.

Tableau 3.1.11 : Suivi cinétique de la synthèse enzymatique de PBA dans un évaporateur rotatif à 70 °C.

	RMN ^{1}H			CES			
Temps de réaction	$M_{n,RMN}$	DP_n	$\%_{terminaisons\ esters}$	$M_{n,CES}$	M_w	Đ	$M_{n,MHS}$
h	kg/mol		%	kg/mol	kg/mol		kg/mol
2	1,2	6	55	-	-	-	-
4	1,5	8	60	-	-	-	-
6	1,7	9	61	-	-	-	-
8	2,3	11	59	-	-	-	-
10	2,6	13	68	7,8	12,4	1,6	2,8

5.2. Comparaison des différents systèmes réactionnels

Trois synthèses enzymatiques de PBA à partir de 1,4-BDO/DEA à 70 °C sous 80 mbar durant 24 h ont été effectuées avec trois systèmes différents (*i.e.,* réaction en masse dans un réacteur Schlenk avec une agitation magnétique, réaction en masse dans un évaporateur rotatif et réaction dans le diphényl éther). Les résultats sont présentés dans la Figure 3.1.11-b et le Tableau 3.1.12.

Durant la synthèse en masse dans le réacteur Schlenk, la viscosité du milieu augmente fortement. La vitesse de rotation d'agitation magnétique est donc réduite de 500 à 100 tr/min. Mais après 24 h de réaction, même à faible vitesse de rotation, l'agitation n'est plus possible.

On observe que les masses molaires obtenues (par RMN et CES) pour ces différents systèmes sont proches les unes des autres avec un DP_n final d'environ 16-17. De plus, toutes les synthèses de PBA ont des rendements massiques similaires (~ 80 pds.%) et une majorité de terminaisons esters (66-77%). La dispersité (Đ) des PBA synthétisés en masse est légèrement supérieure à celle du PBA synthétisé dans le diphényl éther. On peut supposer que l'augmentation de Đ est due à la plus haute viscosité des systèmes en masse diminuant ou limitant l'homogénéité du milieu réactionnel. En effet, sur des temps longs, sans efficacité d'agitation mécanique, la mobilité intermoléculaire des chaînes est due uniquement à la diffusion moléculaire qui est très limitée et qui diminue avec l'augmentation de la masse molaire. Ce problème est encore plus problématique pour la réaction en masse dans un réacteur Schlenk que dans un évaporateur rotatif. On observe que la plupart du polymère fondu est collé à la paroi du réacteur (même en utilisant l'évaporateur rotatif). Pour limiter ce problème, un petit ballon doit être utilisé afin d'avoir une épaisseur de polymère fondu suffisante sur la paroi du ballon.

La synthèse en masse en utilisant l'évaporateur rotatif est donc une bonne alternative à la réaction en masse dans un ballon ou un Schlenk. De plus, cela permet d'obtenir des résultats similaires après 24 h de réaction à ceux obtenus dans le diphényl éther. Cependant, cette méthode est limitée à la synthèse de polyesters avec une faible température de fusion. De plus, cette méthode exige un accès en continu à un évaporateur rotatif pour une longue durée ce qui n'est pas toujours simple dans le laboratoire. Au final, cette méthode est intéressante pour les 24 premières heures de réaction, mais des tests supplémentaires doivent être effectués pour étudier plus en détail les bénéfices de cette méthode de synthèse pour des temps de réaction plus longs.

Tableau 3.1.12 : Synthèse enzymatique de PBA à 70 °C sous 80 mbar durant 24 h dans différents systèmes réactionnels.

Entrée	Système	Rendement	SEC			RMN ^{1}H		
			$M_{n,CES}$	Đ	$M_{n,MHS}$	$M_{n,RMN}$	DP_n	$\%_{terminaisons\ esters}$
		pds.%	kg/mol		kg/mol	kg/mol		%
1	En masse – Evaporateur rotatif	83	10,9	1,8	4,1	3,3	17	70
2	En masse - Schlenk	77	9,7	1,7	3,6	3,1	16	66
3	Diphényl éther – Schlenk	83	11,5	1,5	4,3	3,2	16	77

6. Conclusions

Ce chapitre d'introduction à la synthèse enzymatique de polyesters à partir de synthons bifonctionnels diols et diesters carboxyliques (succinate et adipate) a permis de développer et d'optimiser le procédé de synthèse enzymatique de polyesters aliphatiques par estérification/transestérification.

Les différents systèmes testés à pression atmosphérique (sous argon) ne permettent la synthèse que d'oligomères (DP_n < 15-20). Néanmoins, le système utilisant du toluène anhydre à 90 °C avec du tamis moléculaire et des diesters carboxyliques de diméthyle est celui permettant d'obtenir les oligomères les plus longs. On peut supposer que l'augmentation significative de la masse molaire en utilisant des diesters carboxyliques de diméthyle à la place de diesters carboxyliques de diéthyle est notamment due à l'évaporation plus aisée et plus importante du méthanol produit lors de la synthèse par rapport à l'éthanol.

Une optimisation du procédé de synthèse a été réalisée en utilisant des systèmes sous vide afin d'éliminer efficacement l'alcool produit durant la transestérification et ainsi augmenter l'avancement de la réaction. De nombreux solvants de natures chimiques différentes (alcane, éther aliphatique, éther aromatique…) ont été testés. Les solvants « éther aromatique » tels que l'anisole, le phénétole et le diphényl éther permettent la synthèse de polyesters de hautes masses molaires et sont donc les plus intéressants. Nous avons choisi d'optimiser le procédé dans le diphényl éther pour en déterminer les meilleures conditions expérimentales, *i.e.* à 90 °C avec 10 pds.% de N435 dans 150 pds.% de diphényl éther sous 20 mbar et sans tamis moléculaire introduit dans le réacteur. A l'inverse du système sous pression atmosphérique, l'utilisation de diesters carboxyliques d'éthyle à la place de diesters carboxyliques de méthyle est légèrement plus intéressante pour les systèmes sous pression réduite.

Enfin, le procédé de synthèse en masse de PBA dans deux réacteurs différents (Schlenk et évaporateur rotatif) a été testé. Pour synthétiser des oligomères, la synthèse en masse est très intéressante. Le procédé en masse dans l'agitateur rotatif est même le système réactionnel le plus prometteur testé. Néanmoins, pour la synthèse de polyesters de hautes masses molaires, l'augmentation de la viscosité constitue un frein au développement de ce procédé. En effet, celle-ci limite l'agitation, et donc l'avancement de la réaction, dans l'évaporateur rotatif et empêche même toute agitation efficace dans le réacteur Schlenk.

Après avoir développé différents systèmes réactionnels, nous nous sommes concentrés, pour la suite de nos études sur la synthèse enzymatique de polyesters, au système réactionnel en solution dans des tubes de Schlenk. En utilisant ce système réactionnel, deux études ont pu être menées :

- Une portant sur la synthèse d'un copolyester à base de 2,3-butanediol et la différence de réactivité entre ce monomère (ayant exclusivement des groupements hydroxyles secondaires) et le 1,4-butanediol avec le diéthyle succinate.
- Une autre portant sur la synthèse de copolyesters à partir de soit deux diols de longueurs différentes pour un même monomère donneur d'acyle, soit de deux monomères donneur d'acyle pour un même diol.

7. Références

Anastas, P.T., Warner, J.C., 2000. Green chemistry: theory and practice. Oxford Univ. Press, Oxford.

Azim, H., Dekhterman, A., Jiang, Z., Gross, R.A., 2006. Biomacromolecules 7, 3093–3097.

Binns, F., Harffey, P., Roberts, S.M., Taylor, A., 1998. J. Polym. Sci. Part Polym. Chem. 36, 2069–2079.

Charlier, Q., Girard, E., Freyermouth, F., Vandesteene, M, Jacquel, N., Ladavière, C., Rousseau, A., Fenouillot, F., 2015. Express Polym. Lett. 9, 424–434.

Dong, H., Cao, S.-G., Li, Z.-Q., Han, S.-P., You, D.-L., Shen, J.-C., 1999. J. Polym. Sci. Part Polym. Chem. 37, 1265–1275.

Duchiron, S.W., Pollet, E., Givry, S., Avérous, L., 2015. RSC Adv. 5, 84627–84635.

Feder, D., Gross, R.A., 2010. Biomacromolecules 11, 690–697.

García-Alles, L.F., Gotor, V., 1998. Biotechnol. Bioeng. 59, 163–170.

Garin, M., Tighzert, L., Vroman, I., Marinkovic, S., Estrine, B., 2014. J. Appl. Polym. Sci. 131, 40887/1-40887/7.

Graber, M., Bousquet-Dubouch, M.-P., Lamare, S., Legoy, M.-D., 2003. Biochim. Biophys. Acta BBA - Proteins Proteomics 1648, 24–32.

Henderson, L.A., Svirkin, Y.Y., Gross, R.A., Kaplan, D.L., Swift, G., 1996. Macromolecules 29, 7759–7766.

Hunsen, M., Azim, A., Mang, H., Wallner, S.R., Ronkvist, A., Xie, W., Gross, R.A., 2007. Macromolecules 40, 148–150.

Japu, C., Martínez de Ilarduya, A., Alla, A., Jiang, Y., Loos, K., Muñoz-Guerra, S., 2015. Biomacromolecules 16, 868–879.

Jiang, Y., van Ekenstein, G.O.R.A., Woortman, A.J.J., Loos, K., 2014a. Macromol. Chem. Phys. 215, 2185–2197.

Jiang, Y., Woortman, A.J.J., Alberda van Ekenstein, G.O.R., Petrović, D.M., Loos, K., 2014b. Biomacromolecules 15, 2482–2493.

Jiang, Y., Woortman, A.J.J., van Ekenstein, G.O.R.A., Loos, K., 2013. Biomolecules 3, 461–480.

Jiang, Y., Woortman, A.J.J., Ekenstein, G.O.R.A. van, Loos, K., 2015. Polym. Chem. 6, 5451–5463.

Kulschewski, T., Sasso, F., Secundo, F., Lotti, M., Pleiss, J., 2013. J. Biotechnol. 168, 462–469.

Kumar, A., Gross, R.A., 2000. Biomacromolecules 1, 133–138.

Linko, Y.-Y., Lämsä, M., Wu, X., Uosukainen, E., Seppälä, J., Linko, P., 1998. J. Biotechnol., Biocatalysis 66, 41–50.

Linko, Y.-Y., Wang, Z.-L., Seppälä, J., 1995a. J. Biotechnol. 40, 133–138.

Linko, Y.-Y., Wang, Z.-L., Seppälä, J., 1995b. Enzyme Microb. Technol. 17, 506–511.

Liu, L., Pang, M., Zhang, Y., 2015. Eur. J. Lipid Sci. Technol. 117, 1636–1646.

Ma, L., Persson, M., Adlercreutz, P., 2002. Enzyme Microb. Technol. 31, 1024–1029.

MacDonald, R.T., Pulapura, S.K., Svirkin, Y.Y., Gross, R.A., Kaplan, D.L., Akkara, J., Swift, G., Wolk, S., 1995. Macromolecules 28, 73–78.

Mahapatro, A., Kalra, B., Kumar, A., Gross, R.A., 2003. Biomacromolecules 4, 544–551.

Mahapatro, A., Kumar, A., Kalra, B., Gross, R.A., 2004. Macromolecules 37, 35–40.

Mei, Y., Kumar, A., Gross, R.A., 2002. Macromolecules 35, 5444–5448.

Munari, A., Manaresi, P., Chiorboli, E., Chiolle, A., 1992. Eur. Polym. J. 28, 101–106.

Nakaoki, T., Danno, M., Kurokawa, K., 2003. Polym. J. 35, 791–797.

Nordblad, M., Adlercreutz, P., 2013. Biocatal. Biotransformation 31, 237–245.

Parker, M.-C., Brown, S.A., Robertson, L., Turner, N.J., 1998. Chem. Commun. 2247–2248.

Pellis, A., Corici, L., Sinigoi, L., D'Amelio, N., Fattor, D., Ferrario, V., Ebert, C., Gardossi, L., 2015. Green Chem. 17, 1756–1766.

Sasso, F., Kulschewski, T., Secundo, F., Lotti, M., Pleiss, J., 2015. J. Biotechnol. 214, 1–8.

Wang, Z.-L., Hiltunen, K., Orava, P., Seppälä, J., Linko, Y.-Y., 1996. J. Macromol. Sci. Part A 33, 599–612.

Yao, D., Li, G., Kuila, T., Li, P., Kim, N.H., Kim, S.-I., Lee, J.H., 2011. J. Appl. Polym. Sci. 120, 1114–1120
.

Sub-chapter 3.2. Enzymatic synthesis and characterization of biobased poly(1,4-butylene succinate-*ran*-2,3-butylene succinate) copolyesters. Influence of 1,4- and 2,3-butanediol contents.

Thibaud Debuissy, Eric Pollet and Luc Avérous*

BioTeam/ICPEES-ECPM, UMR CNRS 7515, Université de Strasbourg, 25 rue Becquerel, 67087 Strasbourg Cedex 2, France

*Corresponding author: luc.averous@unistra.fr

Published by European Polymer Journal, 2017, 93, 103-115

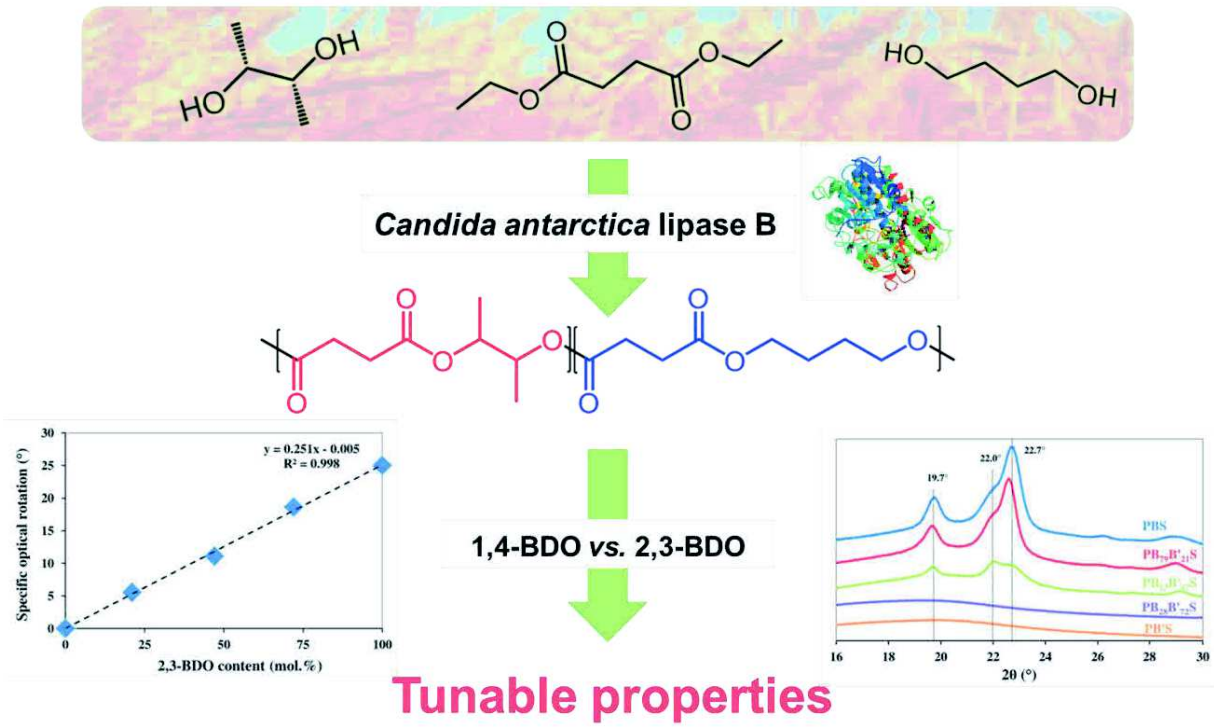

1. Abstract

Different (co)polyesters, poly(1,4-butylene succinate-*ran*-2,3-butylene succinate) (PBB'S), were enzymatically copolymerized at different 1,4-butanediol (1,4-BDO) / 2,3-butanediol (2,3-BDO) molar ratios, with immobilized *Candida antarctica* lipase B (CALB). The synthesized macromolecular architectures were characterized by NMR, SEC, FTIR, WAXS, MALDI-TOF MS, DSC, TGA and specific optical rotation. Based on an optimized process, PBB'S copolyesters were synthesized in high yield. A random distribution between both BDOs was obtained along the chain. M_w decreased with increasing 2,3-BDO content, from 26 to 6 kg/mol. The specific optical rotation decreased linearly with decreasing 2,3-BDO content, and can be used as a characterization technique to determine PBB'S composition. DSC results showed that an increase in 2,3-BDO content raised the Tg and reduced the degree of crystallinity, leading to amorphous materials for 2,3-BDO content higher than 47 mol.%. Synthesized copolyesters exhibited a good thermal stability, higher than 250 °C, with a degradation profile depending on the 1,4-BDO/2,3-BDO ratio.

.

2. Introduction

The research of renewable materials derived from biomass feedstocks is becoming an increasingly relevant topic in academic and industry fields, as such materials allow for the decrease of greenhouse gas emissions and permit the production of novel macromolecular architectures (Laurichesse and Avérous, 2014; Vilela et al., 2014b; Gandini, 2011; 2010). As an abundant carbon source, biomass stocks are produced from solar energy in a short cycle. The development of biorefinery throughout the world was a huge step in the production of a great number of monomers and macromers by biological pathways or chemical modifications (Bozell and Petersen, 2010; Werpy et al., 2004; Becker et al., 2015).

Biobased 1,4-butanediol (1,4-BDO) is a short diol principally obtained *via* a chemical hydrogenation of biobased succinic acid (Bozell and Petersen, 2010; Choi et al., 2015). However, recently Genomatica (USA) has genetically modified *E. Coli* for the direct bioproduction of 1,4-BDO from sugars (Barton et al., 2014). Produced at an industrial level by different companies (Novamont, BioAmber, Genomatica-BASF), biobased 1,4-BDO is largely used, for instance, as chain extender in the polyurethane synthesis (Bueno-Ferrer et al., 2012; Reulier and Avérous, 2015) or as building block for the synthesis of various polyesters and polyamides (Debuissy et al., 2016a; Jiang et al., 2013).

2,3-butanediol (2,3-BDO) is also a very interesting building block, with secondary hydroxyl functions, mainly used as a precursor in the synthesis of a wide range of chemical products (Köpke et al., 2011). 2,3-BDO is a very conventional fermentation product from many species of bacteria. It can be directly produced from different bio-resources such as xylose, sugar cane molasses, glucose and corn (Wang et al., 2016). However, it still has a limited use in macromolecular architectures as a monomer. Watson *et al.* (Watson, Ralph W., 1950; Watson et al., 1950), pioneered the work of 2,3-BDO-based polyesters by the esterification of many diacids with 2,3-BDO in 1950, followed by different studies on the synthesis of aliphatic-aromatic polyesters or resins containing 2,3-BDO as main or co-diol (Noordover et al., 2006; E. Gubbels et al., 2013; Erik Gubbels et al., 2013; Hu et al., 2016). In spite of its expected low reactivity, properties caused by the usage of 2,3-BDO such as a drop in crystallinity or a rise of the glass transition temperature can be interesting for some applications such as adhesives (Debuissy et al., 2016a; Noordover et al., 2006; E. Gubbels et al., 2013; Erik Gubbels et al., 2013; Hu et al., 2016).

The use of 2,3-BDO has monomer for polyester synthesis have been mainly studied using organometallic catalysts, in melt and under harsh reaction conditions (Debuissy et al., 2016a; Noordover et al., 2006; E. Gubbels et al., 2013; Erik Gubbels et al., 2013; Hu et al., 2016). For instance, our group has also recently investigated the kinetics and properties of the organometallic synthesis of copolyesters based on 1,4-BDO and 2,3-BDO (Debuissy et al., 2016a). However, conventional organometallic catalysts favored undesirable side reactions during the synthesis at temperatures above 200 °C, like decomposition and discoloration (Mahapatro et al., 2003). Besides, metal residues from the catalysts may induce some toxicity (which could be detrimental for *e.g.*, implants or tissue engineering) and environmental pollution (Tanzi et al., 1994). Therefore, it is necessary to develop a more eco-friendly pathway by replacing for instance, the metal catalyst with biocatalysts such as enzymes.

Lipases (E.C. 3.1.1.3) are non-toxic enzymes and more specifically serine hydrolases, which can be found in most organisms (Schmid and Verger, 1998b). In aqueous media, they catalyze ester bond cleavage, but are also able to catalyze the reverse reaction (*i.e.*, ester bonds formation) in organic media (Kobayashi, 2009). Enzymatic polymerization can thus be considered as an environment friendly process, and one of the best examples of "green polymer chemistry". Lipases have already been proven to be versatile in polyesters synthesis under mild conditions (Gustini et al., 2016), with a very good reaction control of enantio-, chemo-, regio-, and stereo-selectivity. Owing to these benefits, enzymatic processes could provide precise control of polymer architectures and increased energy savings (Kobayashi, 2009). Among lipases, *Candida antarctica* lipase B (CALB) and more particularly the immobilized form (Novozym 435 or N435) is the working horse in biocatalytic polyester synthesis, as it shows several advantages such as broad substrate specificity, high reaction yields, excellent thermal stability and commercial availability (Jiang and Loos, 2016). Moreover, CALB is able to form ester bonds with secondary hydroxyl (OH) groups even if their reactivity is much lower in comparison to primary OH groups (Gustini et al., 2015). CALB enantioselectivity towards secondary OH depends strongly on reactants, decreases by decreasing acyl donor chain length and decreases with the temperature (Ottosson and Hult, 2001; Raza et al., 2001; Rotticci et al., 1998). Rottici *et al.* showed that the CALB-catalyzed esterification of 3-methyl-2-butanol, (which has a close structure to 2,3-BDO) exhibited a higher preference for the *R* configuration of the secondary OH compared to the *S* configuration (Rotticci et al., 1998). By analogy, the *2R,3R* configuration of 2,3-BDO should be the most adequate stereoisomer of 2,3-BDO for CALB.

In recent years, enzymatic syntheses of sustainable polyesters from biobased building blocks have attracted much attention. Different biobased polyesters have been prepared *via* enzymatic polymerization, *e.g.* poly(lactic acid), succinate-, glycerol-, fatty acids-, sorbitol-, 1,4:3,6-dianhydrohexitol-, 2,5-furandicarboyxylate-based polyesters, etc (Kobayashi, 2009; Jiang and Loos, 2016; Duchiron et al., 2015; Öztürk et al., 2016; Öztürk Düşkünkorur et al., 2014; Düşkünkorur et al., 2015; Khan et al., 2014). Until now, to the best of our knowledge, only two researches mentioned the synthesis of enzyme-catalyzed polyesters based on 2,3-BDO. Jiang *et al.* reported the synthesis of small oligomers (500 g/mol) resulting from the CALB-catalyzed reaction between 2,3-BDO and dimethyl-2,5-furandicarboxylate (Jiang et al., 2015b), whereas Yoon *et al.* reported a CALB-catalyzed polycondensation between 2,3-BDO and sebacic acid without details on the achieved molar mass (Yoon et al., 2012).

The aim of this study was to investigate the CALB-catalyzed transesterification of 1,4-BDO, 2,3-BDO and diethyl succinate in solution after optimization of the reaction parameters (solvent type and amount, temperature, catalyst amount). To the best of our knowledge, the present study is the first to investigate in detail the lipase-catalyzed copolyesters synthesis with 2,3-BDO as a building block. Chemical and physicochemical properties of the different synthesized macromolecular architectures were fully investigated by ^{1}H-, ^{13}C-, HSQC 2D-NMR, SEC, FTIR, MALDI-TOF MS and specific optical rotation. The thermal stability, crystalline structure and thermal properties were analyzed by TGA, WAXS and DSC, respectively. The effect of the 1,4-BDO/2,3-BDO molar ratio on the physicochemical properties was particularly discussed.

3. Experimental part

3.1. Materials

Novozym® 435 (N435) (about 10 wt.% of immobilized *Candida antarctica* lipase B on an acrylic carrier (> 5,000 $U.g^{-1}$)), chloroform (99.0-99.4%) and deuterated chloroform ($CDCl_3$) were purchased from Sigma-Aldrich. 1,4-butanediol (1,4-BDO) (99%), 2*R*,3*R*-(-)-butanediol (2,3-BDO) and benzyl methyl ether (97%) were purchased from Alfa Aesar. Diethyl succinate (DES) (99%), diphenyl ether (99%), dibenzyl ether (99%), toluene (99.85%, extra dry, AcroSeal), n-dibutyl ether (99+%, extra dry, AcroSeal), phenetole (99%), dodecane (99%) and anhydrous anisole (99%, extra dry, AcroSeal) were supplied by Acros. Xylene (99.9%) was supplied by Fisher Chemicals. 4Å molecular sieves and petroleum ether were purchased from VWR. N435 and molecular sieves were dried at 25 and 120 °C, respectively, for 24 h under vacuum before use. All other reactants were used without further purification. All solvents used for the analytical methods were of analytical grade.

3.2. Enzymatic synthesis of PBB'S copolyesters

An equimolar proportion of DES and 1,4-BDO/2,3-BDO diol mixture, N435 (10 wt.% *vs.* total mass of monomers) and diphenyl ether (150 wt.% *vs.* total mass of monomers) were introduced in a Schlenk reactor. The schlenk reactor was immerged in a hot oil bath at 90 °C. The pressure inside the reactor was decreased stepwise at 350, 100, 50 and 20 mbar for 4, 4, 16 and 48 h, respectively. The global reaction scheme and conditions are summarized in Scheme 3.2.1. After 72 h of reaction, 10 mL of chloroform was introduced in the reaction mixture in order to quench the reaction. The diluted reaction mixture was filtered. The filtrate was concentrated in a rotavapor. Thereafter, the synthesized copolyester was precipitated into a large volume of vigorously stirred cold petroleum ether, recovered by filtration and dried under reduced pressure in an oven at 50 °C for 24 h.

Different poly(1,4-butylene succinate-*co*-2,3-butylene succinate) (PBB'S) copolyesters were synthesized varying the 1,4-BDO/2,3-BDO feed molar ratios (100/0, 75/25, 50/50, 25/75 and 0/100). The corresponding samples are named "PBxB'yS", with x and y as the molar proportion of 1,4-BDO and 2,3-BDO units determined by ^{1}H-NMR, respectively. Both homopolyesters ($PB_{100}B'_{0}S$ and $PB_{0}B'_{100}S$) are also named PBS and PB'S, respectively. Copolyesters syntheses were repeated at least three times.

In the case of PBS or PB'S syntheses in a solvent other than diphenyl ether, the vacuum was adapted to the boiling point of the solvents. For syntheses performed at atmospheric pressure, a short condenser filled with molecular sieves was placed on top of the Schlenk reactor and the reaction was performed under argon.

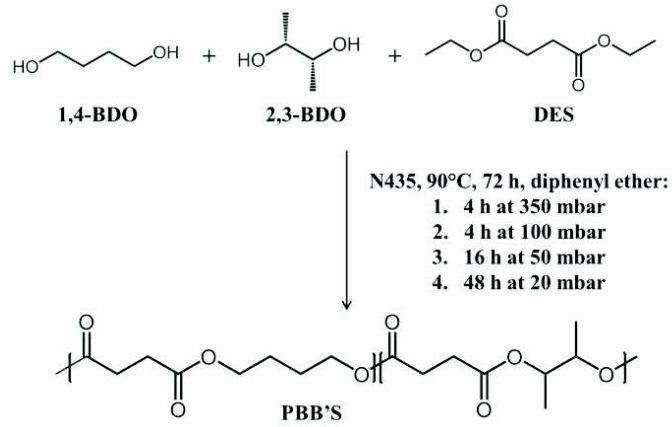

Scheme 3.2.1 : Reaction pathway for the CALB-catalyzed synthesis of PBB'S.

3.3. General methods and analysis

^{1}H- and ^{13}C-NMR spectra of polyesters were obtained on a Bruker 400 MHz spectrometer. $CDCl_3$ was used as solvent to prepare solutions with concentrations of 8-10 and 30-50 mg/mL for ^{1}H-NMR and ^{13}C-NMR, respectively. The number of scans was set to 128 for ^{1}H-NMR and at least 5,000 for ^{13}C-NMR. Calibration of the spectra was performed using the $CDCl_3$ peak (δ_H = 7.26 ppm, δ_C = 77.16 ppm).

Size exclusion chromatography (SEC) was performed to determine the number-average molar mass (M_n), the mass-average molar mass (M_w) and the dispersity (Đ) of the samples. A Shimadzu liquid chromatograph was equipped with PLGel Mixed-C and PLGeL 100 Å columns and a refractive index detector. Chloroform was used as eluent at a flow rate of 0.8 ml/min. The instrument was calibrated with linear PS standards from 162 to 1,650,000 g/mol.

Infrared spectroscopy (IR) was performed with a Nicolet 380 Fourier transformed infrared spectrometer (Thermo Electron Corporation) used in reflection mode and equipped with an ATR diamond module (FTIR-ATR). The FTIR-ATR spectra were collected at a resolution of 4 cm^{-1} and with 64 scans per run.

MALDI-TOF MS analysis was performed using a MALDI-TOF-TOF Autoflex II TOF/TOF (Bruker Daltonics) equipped with a nitrogen laser (λ = 337 nm) and super DHB (9:1 mixture of DHB and 2-hydroxy-5-methoxybenzoic acid) as matrix. Scan accumulation and data processing were performed with FlexAnalysis 3.0 software.

Differential scanning calorimetry (DSC) was performed using a TA Instrument Q 200 under nitrogen (flow rate of 50 mL/min), calibrated with high purity standards. Samples of 2-3 mg were sealed in aluminum pans. A three-step procedure with a 10 °C/min ramp was applied that involved: (1) heating up from room temperature to 130 °C and holding for 3 min to erase the thermal history, (2) cooling down to -80 °C and holding for 3 min and (3) heating (second heating) from -80 to 130 °C. The degree of crystallinity (X_c) was calculated according to Equation (3.2.1),

$$X_c(\%) = \frac{\Delta H_m}{\Delta H_m{}^0} \times 100 \qquad (3.2.1)$$

where ΔH_m is the melting enthalpy and $\Delta H_m{}^0$ is the melting enthalpy of a 100% crystalline polyester.

Thermal degradations were studied by thermogravimetric analyses (TGA). Measurements were conducted under helium atmosphere (flow rate of 25 mL/min) using a Hi-Res TGA Q5000 apparatus from TA Instruments. Samples (1-3 mg) were heated from room temperature up to 600 °C at a rate of 20 °C/min.

Wide angle X-ray Scattering (WAXS) data were recorded on a Siemens D5000 diffractometer using Cu K_α radiation (1.5406 Å) at 25-30 °C in the range of 2θ = 14-32° at 0.4 °.min^{-1}. Analyses are performed on compression-molded sheets.

The specific optical rotation $[\alpha]^{20}_D$ was measured by a polarimeter MPC 200 thermostated at 20.0°C at λ = 589 nm and in a 100 mm long cell (diameter = 0.3 mm). Measured solution was prepared at a concentration between 1.0 and 2.0 g/100 mL in chloroform.

3.4. Ester function density

The ester function density of polyesters is defined by the number of ester functions by repetitive unit on the number of carbons in the main chain by repetitive unit. The ester function density in PBB'S copolyesters ($D_{ester,PBB'S}$) is calculated by Equation (3.2.2),

$$D_{ester,PBB'S} = \chi_{1,4-BDO} \times D_{ester,PBS} + \chi_{2,3-BDO} \times D_{ester,PB'S} \qquad (3.2.2)$$

where $\chi_{1,4\text{-BDO}}$ and $\chi_{2,3\text{-BDO}}$ are the 1,4-butylene and 2,3-butylene molar contents, $D_{ester,PBS}$ and $D_{ester,PB'S}$ are the ester function densities in PBS and PB'S, respectively.

Table 3.2.1 : Copolyesters ester function density.

Copolyester	PBS	$PB_{79}B'_{21}S$	$PB_{53}B'_{47}S$	$PB_{28}B'_{72}S$	PB'S
D_{ester}	0.250	0.268	0.288	0.308	0.330

4. Results and discussion

4.1. Optimization of the CALB-catalyzed transesterification conditions

Succinic acid, a biobased and largely available building block for polyesters synthesis, is generally seen as a poor candidate for enzymatic polycondensation due to its low solubility in 1,4-BDO and in the most common solvents used in enzyme-catalyzed polyesters syntheses, leading to low polymerization efficiency (Azim et al., 2006). To avoid phase separation during polymerization, diethyl succinate (DES) was used as an acyl donor monomer. Moreover, DES is more hydrophobic than succinic acid and thus has a higher octanol-water partition coefficient (log *P*) value. Previous studies showed that the efficiency of the enzymatic polycondensation/transesterification had a tendency to increase when the hydrophobicity of the system had log *P* optimum values between 1.9 and 4.5 (Kumar and Gross, 2000a; Yao et al., 2011). Indeed, for lipase-catalyzed ester bond formation, systems should contain only traces of water for optimal enzymatic activity (Adlercreutz, 2013; Nordblad and Adlercreutz, 2013). Furthermore, with DES, ethanol is a by-product of the reaction and can be easily removed from the reaction mixture unlike water. Thus, products should be miscible in the solvent to avoid a phase separation. Finally, a favorable interaction is necessary between the N435

acrylic carrier matrix and the solvent; likewise a high enzyme-solvent affinity is required in order to have the optimal 3D shape of the binding site to allow for the site to be accessible to reactive groups.

In order to select the best solvent (*i.e.*, leading to polyester of higher molar mass), different CALB-catalyzed syntheses of poly(1,4-butylene succinate) (PBS) from 1,4-BDO and DES in various solvents and at different pressures were performed, and summarized in Table 3.2.2. The molar mass of synthesized PBS was determined by SEC ($M_{n,SEC}$) and ^{1}H-NMR ($M_{n,NMR}$) according to the method developed in the previous Sub-Chapter (Equation (3.1.1)) using the relative intensities of PBS and end-groups characteristic signals. Table 3.2.2 clearly shows that regardless of the solvent used, lowering the pressure led to increase polyesters molar masses. $M_{n,NMR}$ values were smaller than $M_{n,SEC}$ values, as the SEC calibration is based on PS standards. Only three solvents led to the synthesis of relatively high molar mass PBS (*i.e.*, > 10 kg/mol). $M_{n,SEC}$ of 10.9, 12.2 and 13.8 kg/mol were observed for syntheses in phenetole, diphenyl ether and anisole, respectively. All other tested solvents were deemed inadequate for this reaction as the synthesized polyesters had low molar masses (*i.e.*, $M_{n,SEC}$ < 5 kg/mol). PBS precipitated quickly (after 24-32 h) in n-dibutyl ether and xylene. The N435 acrylic carrier matrix showed poor affinity to dodecane. This led to the reduction of the extent of reaction as this solvent is too hydrophobic (*i.e.*, log *P* = 6.1); therefore, ultimately leading to a modification of the local water content which affected the enzyme 3D structure.

Anisole was determined as the most adequate solvent for the CALB-catalyzed synthesis of PBS. Moreover, this system was performed under a lower vacuum when compared to the reaction carried out in diphenyl ether (*i.e.*, 150 mbar instead of 20 mbar), as anisole has a lower boiling point. Nevertheless, as seen in Table 3.2.3, preliminary results of the CALB-catalyzed synthesis of poly(2,3-butylene succinate) (PB'S) from 2,3-BDO and DES had inferior molar mass in anisole compared to in diphenyl ether (presented below), thus the latter was chosen as the most adequate solvent for PBB'S synthesis. This results is in agreement with the literature as it has been previously reported that diphenyl ether is the preferred solvent to achieve high molar mass for lipase-catalyzed polyesters synthesis (Azim et al., 2006; Jiang et al., 2013; Mahapatro et al., 2003).

Table 3.2.2 : CALB-catalyzed synthesis of PBS at 90 °C with 10 wt.% of N435 and 0.1 g/mL of molecular sieves in 200 wt.% of various solvents and at different pressures.

	Experimental conditions			SEC		^{1}H-NMR
Entry	Solvent	log *P*	Pressure	$M_{n,SEC}$	Đ	$M_{n,NMR}$
			mbar	kg/mol		kg/mol
1	Benzyl methyl ether	1.4	150	4.7	1.9	3.1
2	Anisole	2.1	150	13.8	2.3	6.7
3	Phenetole	2.5	150	10.9	2.2	4.9
4	Toluene	2.7	1,000	4.0	1.7	1.7
5	n-dibutyl ether	2.9	400	2.6	1.6	1.2
6	Xylene	3.2	1,000	2.1	1.4	1.0
7	Xylene	3.2	500	4.1	1.6	1.8
8	Xylene	3.2	400	4.8	1.9	1.7
9	Dibenzyl ether	3.5	150	4.3	2.0	2.1
10	Diphenyl ether	4.1	1,000	2.2	1.4	1.0
11	Diphenyl ether	4.1	150	6.8	2.3	4.1
12	Diphenyl ether	4.1	20	12.2	2.1	5.1
13	Dodecane	6.1	1,000	3.5	1.4	1.4
14	Dodecane	6.1	20	5.1	1.6	2.4

The optimization of the reaction conditions in diphenyl ether was then investigated. The influence of (i) the N435 content, (ii) the solvent amount, (iii) the reaction temperature and (iv) the molecular sieve content on the CALB-catalyzed PBS synthesis in diphenyl ether will be discussed and main results are plotted in Figure 1. First, the control reaction (blank reaction without N435) did not allow for the synthesis of polyester, thus proving that the acylation between monomers observed for the other reactions was actually due to CALB (Figure 3.2.1-a). M_n of synthesized PBS

increased with increasing N435 content from 1 to 10 wt.% (*i.e.*, a CALB content between 0.1 and 1 wt.%), in agreement with previous data (Mahapatro et al., 2003), and then decreased for higher N435 amounts. The same tendency was observed for the solvent content with an optimal diphenyl ether amount at 150 wt.% (Figure 3.2.1-b), in agreement with Jiang *et al* (Jiang et al., 2013). Furthermore, M_n increased with the reaction temperature from 70 to 90 °C and then decreased due to a loss of activity resulting from CALB denaturation at high temperatures. The important M_n gap occurring between 80 and 90 °C was mainly due to the PBS which has a high melting temperature (*i.e.*, 113°C) and precipitated after 32-48 h at 80 °C in diphenyl ether (Figure 3.2.1-c). Finally, M_n decreased with the molecular sieve content (Figure 3.2.1-d). In conclusion, the optimal conditions for PBS synthesis were performed with 150 wt.% of diphenyl ether at 90 °C with 10 wt.% of N435 (*i.e.*, 1 wt.% of CALB) and without molecular sieves.

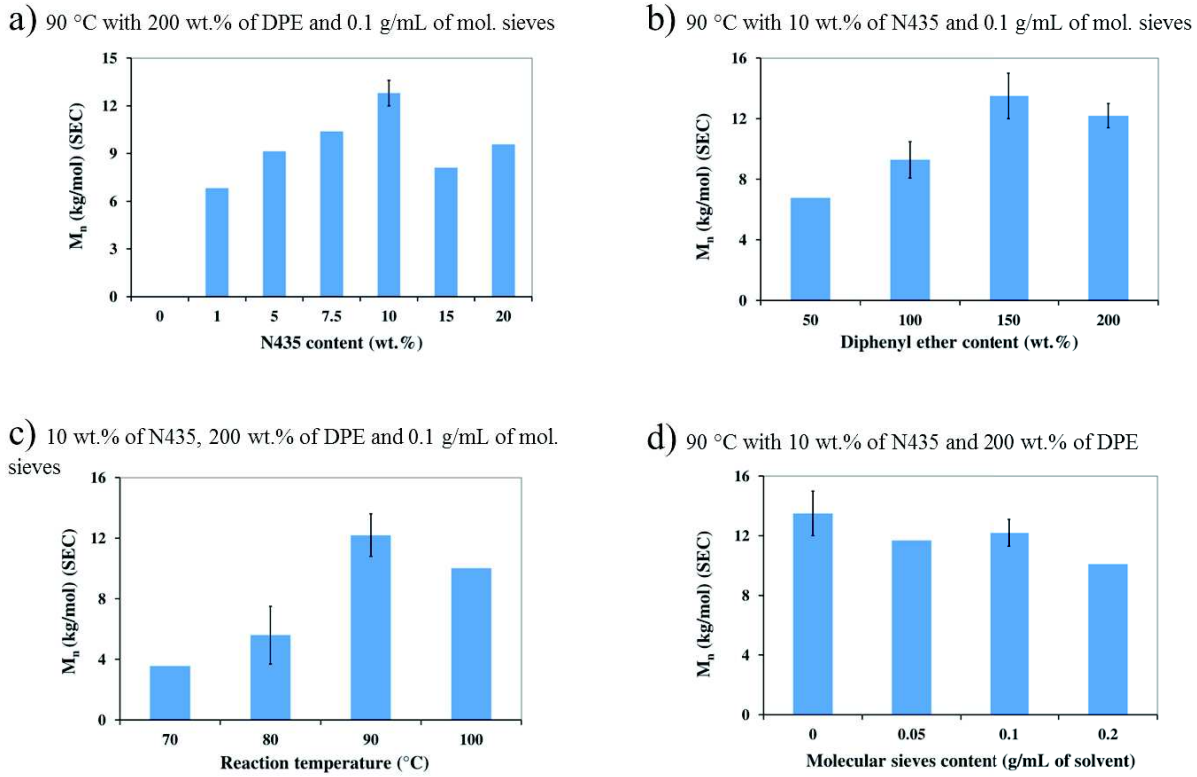

Figure 3.2.1 : Optimization of (a) the N435 content, (b) the diphenyl ether content, (c) the reaction temperature and (d) the molecular sieves content for the CALB-catalyzed PBS synthesis in diphenyl ether (DPE).

The optimization of the reaction conditions in diphenyl ether was then investigated. The influence of (i) the N435 content, (ii) the solvent amount, (iii) the reaction temperature and (iv) the molecular sieve content on the CALB-catalyzed PBS synthesis in diphenyl ether will be discussed and main results are plotted in Figure 1. First, the control reaction (blank reaction without N435) did not allow for the synthesis of polyester, thus proving that the acylation between monomers observed for the other reactions was actually due to CALB (Figure 1a). M_n of synthesized PBS increased with increasing N435 content from 1 to 10 wt.% (*i.e.*, a CALB content between 0.1 and 1 wt.%), in agreement with previous data (Mahapatro et al., 2003), and then decreased for higher N435 amounts. The same tendency was observed for the solvent content with an optimal diphenyl ether amount at 150 wt.% (Figure 1b), in agreement with Jiang *et al* (Jiang et al., 2013). Furthermore, M_n increased with the reaction temperature from 70 to 90 °C and then decreased due to a loss of activity resulting from CALB denaturation at high temperatures. The important Mn gap occurring between 80 and 90 °C was mainly due to the PBS which has a high melting temperature (*i.e.*, 113°C) and precipitated after 32-48 h at 80 °C in diphenyl ether (Figure 1c). Finally, M_n decreased with the molecular sieve content (Figure 1d). In conclusion, the optimal conditions for PBS synthesis were performed with 150 wt.% of diphenyl ether at 90 °C with 10 wt.% of N435 (*i.e.*, 1 wt.% of CALB) and without molecular sieves.

Table 3.2.3 : Enzymatic synthesis of PB'S at 90 °C catalyzed with 10 wt.% of N435 in 150 wt.% of solvent.

Entry	Experimental conditions			SEC		^{1}H-NMR
	Solvent	log *P*	Pressure mbar	$M_{n,SEC}$ kg/mol	Đ	$M_{n,NMR}$ kg/mol
1	Anisole	2.1	150	3.0	1.3	2.1
2	Phenetole	2.5	150	3.7	1.4	3.2
3	Toluene	2.7	1,000	0.9	1.5	0.7
4	Diphenyl ether	4.1	20	4.3	1.5	3.0
5	Dodecane	6.1	20	3.6	1.3	2.3

4.2. Enzymatic synthesis of PBB'S copolyesters

Different PBB'S copolyesters were synthesized from 1,4-BDO, 2,3-BDO and DES at different 1,4-BDO/2,3-BDO feed molar ratios according Scheme 3.2.1 using the optimized conditions previously determined, *i.e.* at 90 °C, in 150 wt.% diphenyl ether, under a 20 mbar vacuum and with 10 wt.% of N435. In order to avoid any monomer loss, the vacuum was decreased stepwise inside the system allowing for the synthesis of less volatile oligomers before significantly decreasing the pressure. Average and detailed results are given in this paper and in Annex 5 (Tables SI.6), respectively.

Table 3.2.4 : Enzymatic synthesis of PBB'S copolyesters of various compositions at 90 °C catalyzed by 10 wt.% of N435 in 150 wt.% of diphenyl ether.

Sample	Feed composition 1,4-BDO/2,3-BDO	^{1}H-NMR	Yield	SEC			^{1}H-NMR				^{13}C-NMR			[α]
		Exp. composition 1,4-BDO/2,3-BDO		$M_{n,SEC}$	M_w	Đ	$M_{n,NMR}$	1° OH	2° OH	ester	L_{BS}	$L_{B'S}$	R	
	mol.%	mol.%	%	kg/mol	kg/mol		kg/mol	%	%	%				°
PBS	100 / 0	100 / 0	87	13.5	26.2	2.0	4.6	15	0	85	-	-	-	0
$PB_{79}B'_{21}S$	75 / 25	79 / 21	82	7.9	15.5	2.0	3.4	7	5	88	4.7	1.2	1.02	5.6
$PB_{53}B'_{47}S$	50 / 50	53 / 47	65	7.0	12.7	1.8	2.9	7	10	83	2.2	1.7	1.03	11.1
$PB_{28}B'_{72}S$	25 / 75	28 / 72	69	5.4	8.8	1.6	2.6	2	16	82	1.6	2.7	1.00	18.6
PB'S	0 / 100	0 / 100	64	4.3	5.8	1.4	3.0	0	12	88	-	-	-	25.0

The final architectures of the synthesized copolyesters were verified by ^{1}H-, ^{13}C-NMR and FTIR. ^{1}H-NMR results of PBB'S copolyesters and their corresponding monomers are presented in Figure 3.2.2-a and Figure SI.18 (in Annex 5). In ^{1}H-NMR, the presence of esters functions was verified by the signal at δ = 4.12 and 4.98 ppm assigned to COO-C$\underline{H}_2$-CH_2- and COO-C$\underline{H}$(CH_3)- protons from 1,4-BDO and 2,3-BDO repeating units, respectively. ^{1}H chemical shifts at δ = 1.15, 1.70 and 2.62 ppm were ascribed to COO-CH(C$\underline{H}_3$)- protons from 2,3-BDO repeating units, COO-CH_2-C$\underline{H}_2$- protons from 1,4-BDO repeating units and CO-C$\underline{H}_2$- protons from succinate repeating units, respectively. Finally, the presence of 1,4-BDO, 2,3-BDO and ester (DES) end-groups were observed at δ = 3.67, 3.74 and 1.25 ppm, respectively. The ester end-group proportion is calculated according to Equation (3.2.3),

$$\%_{ester\ end-groups} = \frac{\frac{I_{1.25}}{3}}{\frac{I_{1.25}}{3} + \frac{I_{3.67}}{2} + I_{3.74}} \times 100 \qquad (3.2.3)$$

Copolyesters have mostly ester end-groups (*i.e.*, 80-90 mol.%), whereas the feed ratio between OH and ester function was 1/1. A first hypothesis could be that a small amount of diol was lost during the synthesis, even if a particular attention was paid to decrease stepwise the vacuum to prevent the evaporation of monomers. However, Nakaoki *et al.* (Nakaoki et al., 2003) observed that the enzyme-catalyzed polymerization of adipic acid and 1,6-hexanediol preferentially yielded hydroxyl terminated products, in agreement with the mechanism proposed by Binns *et al.* (Binns et al., 1998), at the early stage. Thus, when increasing the reaction time, the product is more likely to be carboxyl terminated by the transesterification reaction (Nakaoki et al., 2003). Furthermore, the 1,4-BDO/2,3-BDO molar

composition of synthesized copolyesters was determined from ^{1}H-NMR spectra using relative intensities of methine and methylene protons in α of ester functions in 1,4-BDO and 2,3BDO, respectively. The 2,3-BDO content was calculated according to Equation (3.2.4),

$$\chi_{2,3-BDO} = \frac{I_{4.98}}{I_{4.98} + \frac{I_{4.12} - I_{3.67} - {}^{2}/_{3} \times I_{1.25}}{2}} \qquad (3.2.4)$$

Calculations showed that the molar content of 1,4-BDO was slightly higher than the feed content for all copolyesters containing both diols. This discrepancy can be due to the difference of reactivity between both diols. However, even by increasing the reaction time before decreasing the pressure, no increase of the 2,3-BDO content was observed. Previously, our group synthesized copolyesters from 1,4-BDO and 2,3-BDO *via* an organometallic two-stage melt transesterification route, and the difference between the feed and the final 2,3-BDO content was higher (*i.e.*, 33-45 mol.% of 2,3-BDO in final copolyester from a 50 mol.% feed composition according to the method used) than by the enzymatic process (Debuissy et al., 2016a). Thus, less monomer loss was observed when compared to the present study. One can suppose that the difference of the experimental conditions (*i.e.*, equimolar amounts of monomer for the enzymatic process and a 25 mol.% excess of diol for the organometallic process), the difference of reaction type (*i.e.*, esterification in bulk *vs.* transesterification in solution) and the favorable reactivity of 2,3-BDO with CALB were the main reasons for the higher 2,3-BDO content by the enzymatic process. Indeed, during the organometallic process, a 25 mol.% excess of diol was used and thus a feed 0.67/0.67/1 (1,4-BDO/2,3-BDO/adipic acid) ratio was introduced and since 1,4-BDO was approximately 10 times more reactive than 2,3-BDO with adipic acid, some 2,3-BDO were not able to react and were removed from the reaction mixture (Debuissy et al., 2016a). Likewise, the esterification in bulk with an organometallic catalyst quickly reached an equilibrium prior to attaining 100% conversion, reducing the incorporation of less reactive species such as 2,3-BDO, causing significant raw material losses (Debuissy et al., 2016a).

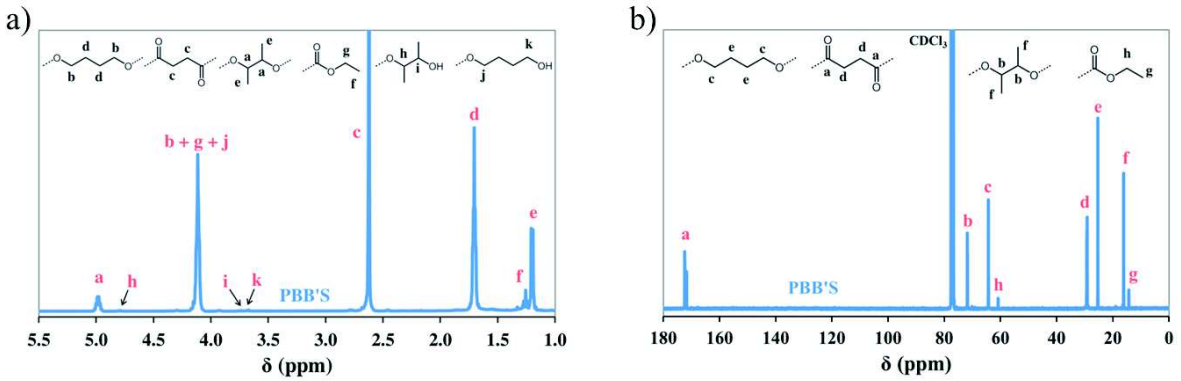

Figure 3.2.2 : [1]H- and (b) [13]C-NMR of PBB'S copolyesters in $CDCl_3$.

^{13}C-NMR was performed to obtain more detailed information about the PBB'S architecture. Corresponding results are presented in Figure 3.2.2-b. In addition, Distorsionless Enhancement Polarization Transfer (DEPT) 135 ^{13}C- and Heteronuclear Single Quantum correlation (HSQC) 2D-NMR spectra of PBB'S copolyesters are presented in Figure SI.19 and SI.20 (in Annex 5), respectively. ^{13}C chemical shifts at δ = 25.3 and 64.3 ppm were ascribed to COO-CH_2-CH_2- and COO-CH_2-CH_2- carbons from 1,4-BDO repeating units, whereas ones at δ = 16.1 and 71.8 ppm were ascribed to COO-CH(CH_3)-, and COO-CH(CH_3)- carbons from 2,3-BDO repeating units, respectively. Finally, ^{13}C chemical shifts at δ = 29.1-29.2 (multiple peaks), 171.7 (two peaks) and 172.4 (two peaks) ppm were ascribed to CO-CH_2-, CO-CH_2- next to a 2,3-butylene repetitive unit and CO-CH_2- next to a 1,4-butylene repetitive unit, respectively. The sensitivity of ^{13}C-NMR to small differences in the chemical environment enabled us to identify the different triads BSB, BSB', and B'SB' (with S, B and B' standing for succinate, 1,4-BDO and 2,3-BDO, respectively) presented in Figure 3.2.3-a. Succinate moieties are present in all three triads at distinctly different resonance absorptions close to chemical shifts of PBS ($PB_{100}B'_{0}S$) or PB'S ($PB_{0}B'_{100}S$). Such results, with the splitting of the two signals (carbon atoms a_1, a_2, a_3 and a_4 in Figure 3.2.3b), enable the calculation of the average sequence length of BS and B'S units (L_{BS} and $L_{B'S}$, respectively) and the degree of randomness (R) using Equations (3.2.5) to (3.2.7),

$$L_{BS} = 1 + \frac{2 \times I_{BSB}}{I_{BSB'-B} + I_{BSB'-B'}} \quad (3.2.5)$$

$$L_{B'S} = 1 + \frac{2 \times I_{B'SB'}}{I_{BSB'-B} + I_{BSB'-B'}} \quad (3.2.6)$$

$$R = \frac{1}{L_{BS}} + \frac{1}{L_{B'S}} \quad (3.2.7)$$

where I_{BSB}, $I_{BSB'-B}$, $I_{BSB'-B'}$ and $I_{B'SB'}$ are intensities of peaks assigned to carbonyl carbons of succinate segments (δ ~ 172 ppm) in BSB, BSB'-B side, BSB'-B' side and B'SB' triads of PBB'S copolyesters, respectively. The corresponding data are listed in Table 3.2.4.

According to the 1,4-BDO/2,3-BDO compositions, average block lengths of segments (L_{BS} and $L_{B'S}$) varied between 1.2 and 4.7. PBB'S copolyesters containing both diols all showed a randomness degree of approximately 1.0 meaning a random distribution sequence behavior between 1,4-butyl and 2,3-butyl segments along the polyester chain. Such a random distribution was expected since CALB is known to catalyze ester bond formation and also intermolecular transesterification leading to random structures (Kumar and Gross, 2000b; Kumar et al., 2000; Takamoto et al., 2001; Namekawa et al., 2000b, 2000a).

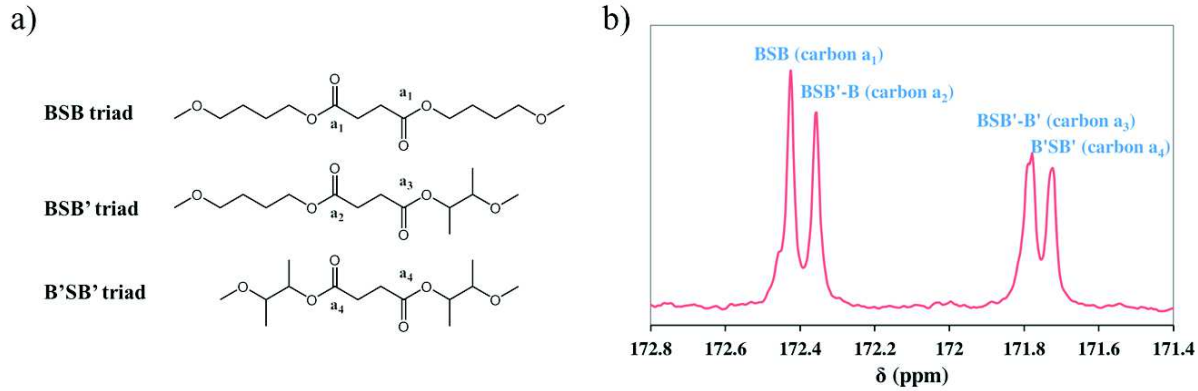

Figure 3.2.3 : ^{13}C-NMR spectra of PBB'S copolyester in $CDCl_3$ centered on carbonyl peaks and chemical structures corresponding to used abbreviations in the figure.

The molar masses and dispersities of synthesized copolyesters were analyzed by SEC in chloroform and are presented in Table 3.2.4. $M_{n,SEC}$ of copolyesters after 72 h varied with the 2,3-BDO content from 13.5 ± 1.5 to 4.3 ± 1.1 kg/mol for PBS and PB'S, respectively. Moreover, the evolution of the molar mass as a function of the reaction time of various PBB'S copolyesters is presented in Figure 3.2.4. For all compositions, the molar mass increased continuously for 72 h of reaction time, even if the increase was not significant between 48 and 72 h. This confirmed the initial choice to perform the syntheses over 72 h. However, the molar mass increase slowed down in the presence of 2,3-BDO. Likewise, Đ decreased with the 2,3-BDO content from 2.0 to 1.4. For PBS, a more accurate molar mass value using the Mark-Houwink-Sakurada (MHS) equation and parameters (K and a) from Garin *et al.* (Garin et al., 2014c) or Charlier *et al.* (Charlier, Q. et al., 2015) could be calculated from overestimated M_n values determined by SEC due to the calibration based on PS standards. The MHS-corrected M_n of PBS was approximately 6.0-6.5 kg/mol (DP_n ~ 35-38). The copolyester chain length decrease was also observed for molar mass obtained by ^{1}H-NMR (*i.e.*, from 4.6 to 2.6 kg/mol). $M_{n,NMR}$ was determined according to relative intensities of characteristics signals using Equation (3.2.8),

$$M_{n,NMR} = \frac{\left(\frac{I_{4.98}}{2} + \frac{I_{4.12} - I_{3.67} - {}^{2}/_{3}\, I_{1.25}}{4}\right) \times 88.10 + \frac{I_{2.62}}{4} \times 84.07 + \left(I_{3.74} + \frac{I_{3.67}}{2}\right) \times 89.11 + \frac{I_{1.25}}{3} \times 45.06}{0.5 \times \left(I_{3.74} + \frac{I_{3.67}}{2} + \frac{I_{1.25}}{3}\right)} \quad (3.2.8)$$

where 88.10, 84.07, 89.11 and 45.06 are the molar mass (in g/mol) of the diol unit, succinate unit, hydroxyl end-groups unit and ester end-groups unit , respectively.

$M_{n,NMR}$ of PBS (*i.e.*, 4.6 kg/mol) was lower than the one determined by the MHS equation. This difference could be due to the fact that, for high molar mass polyesters, ^{1}H-NMR signals of the end-groups were less prominent and were

difficult to differentiate from the baseline. Therefore, their intensities might be slightly overestimated leading to the underestimation of the calculated $M_{n,NMR}$. The decrease of the molar mass could be explained by the use of 2,3-BDO which is less reactive than 1,4-BDO. Nevertheless, to the best of your knowledge, this study is the first one to report the lipase-catalyzed polyesters from high 2,3-BDO content with molar mass higher than 1.0 kg/mol.

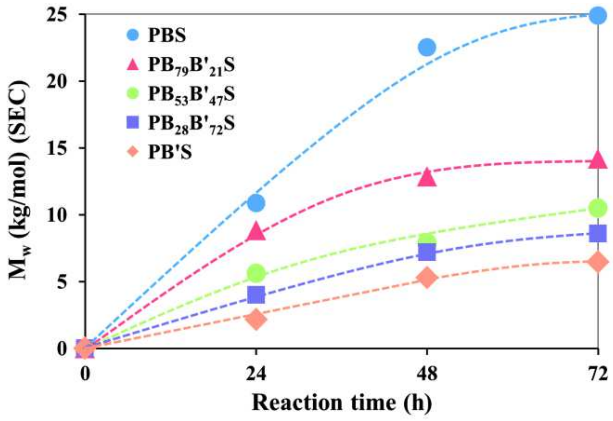

Figure 3.2.4 : Variation of M_w vs. reaction time during the CALB-catalyzed synthesis of PBB'S of different 1,4-BDO/2,3-BDO compositions.

Since the structure of *2R,3R*-(-)-butanediol contains two asymmetric carbons, synthesized copolyesters containing this monomer possess also asymmetric carbons. In order to study the optical properties of copolyesters with 2,3-BDO, their specific optical rotation ([α]) were determined in chloroform at 20 °C. Results are summarized in Table 3.2.3. Since PBS did not contain any asymmetric carbons, this copolyester showed, as expected, [α] value of 0. However, $PB_{79}B'_{21}S$, $PB_{53}B'_{47}S$, $PB_{28}B'_{72}S$ and PB'S exhibited [α] values of 5.9, 11.1, 18.6 and 25.0°, respectively. [α] of PBB'S copolyesters increased proportionately with increasing 2,3-butylene content (Figure 3.2.5-a). Using a line equation (y = 0.251x -0.005), this analytical method could be used as a complement to ^{1}H-NMR technique to determine the molar composition of synthesized PBB'S copolyesters, as it has already been used in a previous study on another copolyester architecture (Debuissy et al., 2016a).

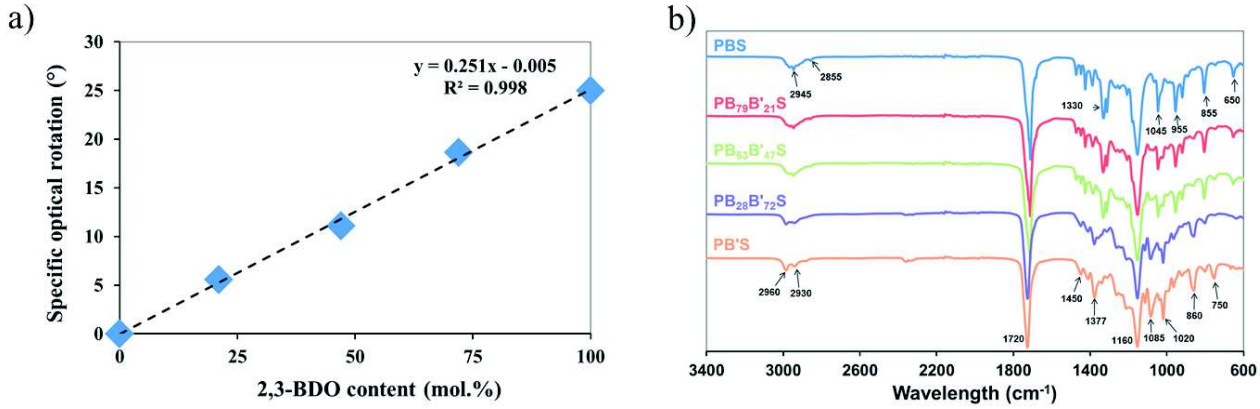

Figure 3.2.5 : (a) Variation of the specific optical rotation of PBB'S copolyesters in function of the 2,3-BDO content and (b) FTIR spectra of PBB'S copolyesters.

The FTIR analysis of different PBB'S copolyesters is presented in Figure 3.2.5-b. First, FTIR spectra of copolyesters showed two sharp signals at approximately 1715 and 1160 cm^{-1} assigned to the C=O and C-O-C stretching vibrations from ester confirming the presence of ester linkage in the polymer chemical structure. Moreover, no broad resonance around 3400 cm^{-1} originating from OH functions were observed in all samples confirming the low amount of OH end-groups as previously stated by NMR. Other signals in spectra depended highly on the 1,4-BDO/2,3-BDO molar composition of copolyesters. PB'S exhibited a signal at 2985 cm^{-1} assigned to the symmetrical C-H stretching vibrations of $-CH_3$ groups which decreased with the 1,4-BDO content until having a small shoulder for PBS due to the presence of ester end-groups. Likewise, signals at 2883, 1450 and 1377 cm^{-1} assigned to C-H stretching vibrations of methine, C-H asymmetrical and symmetrical bending vibration of methyl groups, respectively, were characteristic of

PB'S and their intensities decreased with increasing 1,4-BDO content. Conversely, signals at 2945, 2855 and 1330 cm^{-1} assigned to symmetrical C-H stretching vibrations, asymmetrical C-H stretching vibration and symmetric deformation of $-CH_2-$ groups, respectively, were characteristic of 1,4-BDO and their intensity decreased with increasing 2,3-BDO content. Finally, characteristic signals of PBS observed at 1046, 955, 805 and 653 cm^{-1} assigned to the O-C-C vibration in 1,4-BDO, the C-O symmetric stretching, the methylene in succinate in-plane bending and the –COO- bending shifted to 1085 (O-C-C vibration in 2,3-BDO), 1020, 860 and 750 cm^{-1} for PB'S, respectively (Cai et al., 2012; Muthuraj et al., 2015).

The MALDI-TOF MS spectrum of PB'S with peaks interpretation is shown in Figure 3.2.5, whereas PBS, $PB_{79}B'_{21}S$ and $PB_{28}B'_{72}S$ spectra are presented in Figure SI.21 (in Annex 5). First, all copolyesters exhibited mass peak patterns in the m/z region between 500 and 2500 (or 3500 for PBS). This analysis confirmed the decrease of the molar mass with increasing 2,3-BDO content. Different patterns were observed for PBB'S copolyesters, as listed in Table SI.7. First, the different patterns were separated by an m/z value of 172, in agreement with the molar mass of the PBB'S repetitive unit. Then, all copolyesters exhibited mostly ester/ester or acid/ester end-groups and ester/hydroxyl end-groups in low quantity, which was in agreement with NMR results and previous studies (Habeych et al., 2011; Jiang et al., 2015b, 2014b). Acid end-groups were produced from the hydrolysis of ester end-groups during or after the reaction (Chaudhary et al., 1997a). Moreover, in many samples, cyclic species were detected in tiny amount, in agreement with previous studies (Jiang et al., 2015b, 2014b). However, since cyclic species of PBB'S copolyesters have almost the same m/z signal than copolyesters with ester/ester end-groups, both signals were close to each other and these cyclic species were difficult to observe. Furthermore, PBS exhibited the presence of acid/hydroxyl end-groups and hydroxyl/hydroxyl end-groups, in tiny quantities. PBS seemed thus to have an increased hydrolysis sensitivity when compared to other copolyesters. This can be due to the local reduced ester function density of PBS, coming from longer 1,4-BDO units, which yields a polyester with higher chain mobility. Finally, $PB_{79}B'_{21}S$ exhibited a low intensity signal assigned to ester/vinyl end-groups. One can suppose the formation of vinyl end-groups from the hydroxyl dehydration. However, no extra resonance indicative of the presence of vinyl groups was observed in NMR spectra of PB'S and $PB_{79}B'_{21}S$.

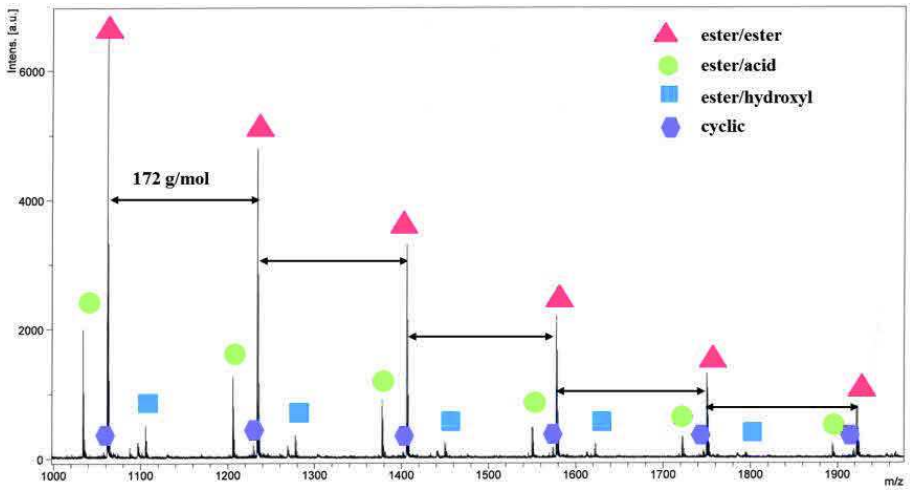

Figure 3.2.6 : MALDI-ToF MS spectrum of PB'S with peak assignment.

4.3. Influence of the reaction temperature on the PBB'S structure

The influences of the synthesis temperature on the PBB'S structure and on the presence of 2,3-BDO units inside the corresponding copolyesters were also investigated. Several copolyesters, with a 50/50 (1,4-BDO/2,3-BDO) ratio feed, were synthesized at different reaction temperatures (*i.e.*, 50, 60, 70, 80 and 90 °C). Results are summarized in Table 3.2.5. The temperature rise did not have a significant effect on the incorporation of 2,3-BDO units in the copolyesters (*i.e.*, 44-47 mol.%), even if a tiny increase trend seemed to be observed with the increase of the temperature. One can suppose that, by decreasing the temperature, the esterification rate of CALB decreased and thus less 2,3-BDO units reacted with DES to form oligomers (before the high vacuum step leading to 2,3-BDO loss by evaporation). All the copolyesters showed a random structure. Molar masses seemed to display an overall increase trend with increasing temperature, whereas Đ stayed globally constant (*i.e.,* 1.6-1.8). For example, $M_{n,SEC}$ rose from 4.1 to 6.2 kg/mol between 50 and 90 °C, respectively. However, this effect was less obvious between 60 and 80 °C. The temperature did

not affect the sequence distribution along the chain, whereas the end-groups proportion study showed no significant effect with mostly ester end-groups (75-87%). Moreover, it was noteworthy to observe that the proportion of 2,3-BDO end-groups was higher than 1,4-BDO end-groups for all samples confirming the lower reactivity of the secondary OH groups with acyl donor groups by CALB compared to primary OH groups.

Table 3.2.5 : Influence of the reaction temperature on the enzymatic PBB'S copolyester synthesis from a 50/50 (1,4-BDO/2,3-BDO) ratio in 150 wt.% of diphenyl ether with 10 wt.% of N435.

		SEC			^{1}H-NMR				^{13}C-NMR
Temperature	Exp. composition 1,4-BDO/2,3-BDO	M_n	M_w	Đ	M_n	Primary OH	Secondary OH	ester	R
°C	mol.%	kg/mol	kg/mol		g/mol	%	%	%	
50	56 /44	4.1	6.5	1.6	2.1	5	20	75	0.99
60	54 / 46	5.2	9.0	1.7	2.6	8	11	81	1.01
70	55 / 45	4.7	8.4	1.8	2.6	4	10	86	1.00
80	54 / 46	5.4	9.5	1.8	2.9	4	9	87	0.99
90	53 / 47	6.2	10.9	1.7	3.0	7	10	83	0.99

4.4. Thermal stability of PBB'S copolyesters

The TGA mass loss traces of PBB'S copolyesters and their derivatives curves (DTG) are shown in Figure 3.2.7 and results are summarized in Table 3.2.6. Under helium, all copolyesters degraded in three main steps, which involved competitive mechanisms. First, all samples were thermally stable until 250 °C and a small (< 3%) mass loss was observed at 250-300 °C due to the possible presence of residual solvent, the degradation of low molar mass chains along with the cyclization at the chain-ends and backbiting reactions (Chrissafis et al., 2006a; Persenaire et al., 2001). Furthermore, a major degradation occurred between 300 and 425 °C, with a substantial mass loss of approximately 85-90% corresponding to the thermal degradation, mostly by β- and α-hydrogen bond scissions (Scheme SI.1). These reactions are responsible for the decomposition of polyesters into small compounds such as diacids, vinyl compounds, aldehydes and anhydrides (Persenaire et al., 2001). After this decomposition step, mass residues of 3-7% still remained under non-oxidative atmosphere (helium). This multi-steps degradation was in agreement with previous reports (Debuissy et al., 2016a; Persenaire et al., 2001).

The 50% mass loss degradation temperature ($T_{d,50\%}$) and the maximal degradation temperature ($T_{deg,max}$) were approximately 350-385 and 360-390 °C, respectively, and both decreased with the 2,3-BDO content. The thermal degradation profile of "2,3-BDO rich" copolyesters was, thus, sharper compared to "1,4-BDO rich" copolyesters. To resume, the thermal degradation profile of PBB'S depended highly on the 1,4-BDO/2,3-BDO molar ratio. This result was in contradiction with a previous recent study performed on PBB'A in which no influence of the 1,4-BDO/2,3-BDO composition on the thermal degradation of poly(1,4-butylene adipate-*co*-2,3-butylene adipate) was observed (Debuissy et al., 2016a). On may suppose that the decrease of the molar mass linked to the 2,3-BDO units incorporation was responsible for the decrease of $T_{deg,max}$.

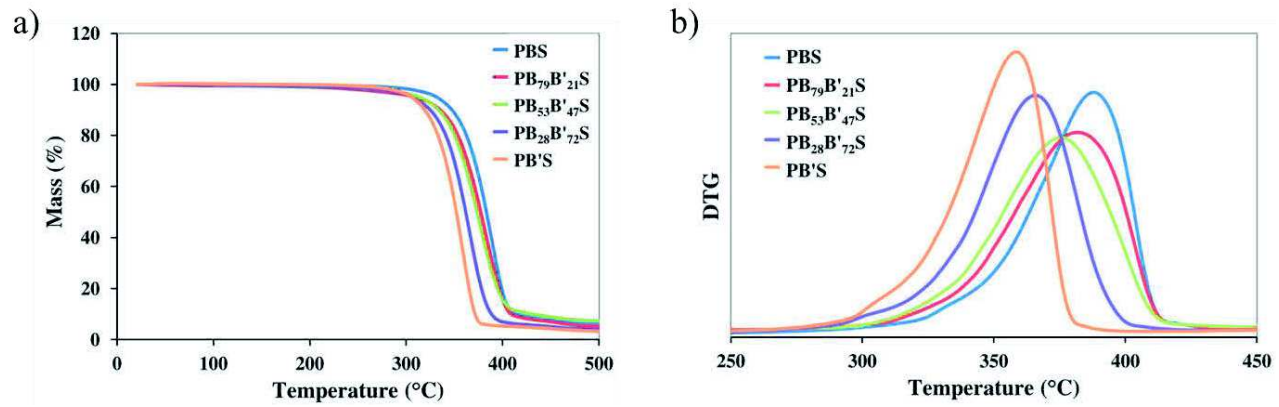

Figure 3.2.7 : (a) Mass loss and (b) DTG curves of PBB'S copolyesters under helium.

Table 3.2.6 : TGA data of PBB'S copolyesters in helium at 20 °C/min.

Copolyester	$T_{d,2\%}$ °C	$T_{d,50\%}$ °C	$T_{deg,max}$ °C	Residue at 550°C wt.%
PBS	306	383	388	6.0
$PB_{79}B'_{21}S$	249	377	382	4.9
$PB_{53}B'_{47}S$	268	373	375	6.9
$PB_{28}B'_{72}S$	271	362	366	3.9
PB'S	285	352	358	2.8

4.5. Crystalline structure and thermal properties of PBB'S copolyesters

The WAXS analyses of PBB'S copolyesters are presented in Figure 3.2.8-a. Results showed that PB'S and $PB_{28}B'_{72}S$ were amorphous at 25 °C. Contrary to the two aforementioned samples, PBS is a semi-crystalline polyester and its crystal structure has been already reported (Pan and Inoue, 2009). The main PBS diffraction peaks appeared at 2θ = 19.7, 22.0 and 22.7°. $PB_{79}B'_{21}S$ and $PB_{53}B'_{47}S$ copolyesters exhibited WAXS patterns similar to PBS, indicating that the crystal structure in these copolyesters has the same characteristics as the PBS lattice, but with lower intensities. The co-monomeric unit (2,3-BDO in this case) incorporated in minor amounts was found to be partially integrated or excluded from the PBS crystal lattice. This phenomenon decreased the crystal strength and lamellae sizes due to the presence of "2,3-BDO-based defects" in the copolyesters chains. Thus, the degree of crystallinity decreased with increasing 2,3-BDO content.

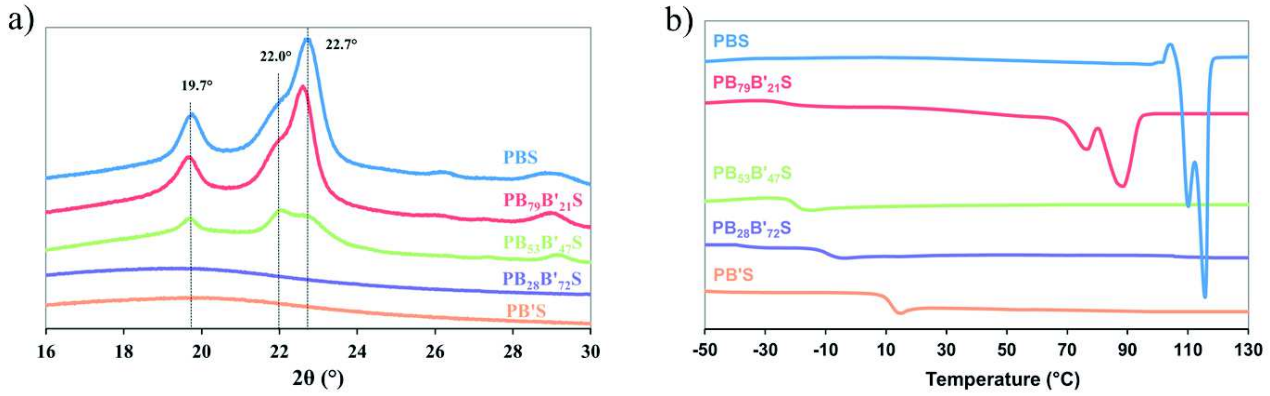

Figure 3.2.8 : (a) WAXS patterns of PBB'S copolyesters and (b) second heating run curves of PBB'S copolyesters at 10 °C/min.

In complement to WAXS analyses, the crystallinity and thermal properties of copolyesters were studied by DSC. Prior to this, it has been verified from TGA results that no significant degradation occurred in the samples amongst the DSC analysis temperature range. Second heating run curves are presented in Figure 3.2.8-b. The variation of thermal properties is discussed as a function of the ester function density (D_{ester}) calculated according to Equation (3.2.2). The degree of crystallinity (X_c) of copolyesters was calculated by Equation (3.2.1), taking into account the melting enthalpy value of 100 % crystalline phase of PBS ($\Delta H_{m,PBS}° = 210$ J/g) determined by Papageorgiou *et al.* (Papageorgiou and Bikiaris, 2005a), and WAXS results, which showed that samples exhibited only PBS crystals.

PBS, which has the lowest D_{ester} due to 1,4-butylene segments, is a semi-crystalline polyester with a sharp crystallization temperature (T_c) at 88 °C, a high melting temperature (T_m) of 115 °C and X_c = 37%. During the second heating run, a tiny cold-crystallization peak preceded a melting phenomenon decomposed on two peaks which was attributed to a fusion-recrystallization phenomenon which is rather common for aliphatic polyesters (Debuissy et al., 2016a, 2016b). $PB_{79}B'_{21}S$, similarly to PBS, is a semi-crystalline polyester, but with lower T_c, T_m and X_c of 48 °C, 88 °C and 23%, respectively. By increasing the 2,3-BDO content, PBB'S copolyesters exhibited an amorphous behavior. More specifically, $PB_{53}B'_{47}S$ exhibited a small endotherm at 45 °C with X_c = 15% during the first heating run but it did not crystallize during the cooling or the second heating run due to the high 2,3-BDO content. *A fortiori*, $PB_{28}B'_{72}S$ and PB'S were completely amorphous, in agreement with WAXS results.

Intra or inter-chains interactions between ester groups were more noticeable in PB'S than in PBS due to the increase of D_{ester} with the 2,3-BDO content from 25 to 33% for PBS and PB'S, respectively (Table 3.2.1). This led to the decrease of the chain mobility responsible for a global increase of the T_g from -37 to 12 °C for PBS and PB'S, respectively. Moreover, the presence of the two methyl side groups in 2,3-butylene segments seemed to prevent the crystallization. For instance, poly(ethylene succinate) is a semi-crystalline polyester (Papageorgiou and Bikiaris, 2005a), whereas PB'S is amorphous. The ability of 2,3-BDO to restrain crystallization has been employed previously to obtain amorphous copolyesters (Debuissy et al., 2016a; Hu et al., 2016).

5. Conclusion

An efficient approach for the green synthesis of fully biobased random poly(1,4-butylene succinate-*ran*-2,3-butylene succinate) (PBB'S) copolyesters by CALB-catalyzed enzymatic transesterification process from 1,4-butanediol (1,4-BDO), 2,3-butanediol (2,3-BDO) and diethyl succinate at 90 °C in diphenyl ether under vacuum was successfully demonstrated.

After the determination of the optimal CALB-catalyzed transesterification conditions on PBS synthesis, the procedure was applied for the PBB'S copolyesters elaboration. First, random copolyesters of relatively high molar masses and high 2,3-BDO contents were obtained. These copolyesters exhibited 2,3-BDO contents slightly lower than feed ones. M_w of copolyesters decreased from 26.2 to 5.8 kg/mol with the increase in the 2,3-BDO content from 0 to 100 mol.%, respectively. These results highlighted the lower reactivity of 2,3-BDO compared to 1,4-BDO, and confirmed that CALB prefers diols with longer chain lengths and primary OH functions. Moreover, we have shown with copolyesters with 50/50 (1,4-BDO/2,3-BDO) feed ratio that the reaction temperature did not have a significant influence on the 2,3-BDO final content (44-47 mol.%), contrary to the M_w that increased from 6.5 to 10.9 kg/mol, between 50 to 90 °C, respectively. CALB activity towards secondary alcohols seemed, thus, to increase with the temperature over the studied range. In addition, copolyesters containing 2,3-BDO exhibited a small positive specific optical rotation, which was found to be proportional to the 2,3-BDO content. This can be used as an additional technique to evaluate the molar composition. Furthermore, from the thermal behavior of PPB'S, it has been noticed that the chain mobility of the copolyester decreased as the 2,3-BDO content increased leading to a global increase of the T_g from -37 to 12 °C and a significant decreased of the degree of crystallinity. Amorphous copolyester are obtained for 2,3-BDO content higher than 47 mol.%. Finally, all copolyesters showed an excellent thermal stability with an onset decomposition temperature above 250 °C and the thermal degradation profile of PBB'S copolyesters was mainly driven by the 1,4-BDO/2,3-BDO composition, resulting in an acceleration of the degradation rate after the onset in copolyesters containing 2,3-BDO.

Conclusively, the possibility to use 2,3-BDO as a potentially biobased monomer and a product from biomass valorization, makes the PBB'S copolyester, with tunable thermal properties and excellent thermal stability, a promising sustainable material for some engineering applications such as adhesives, or for some biomedical applications. Moreover, the opportunity to use this monomer *via* an enzymatic process will increase the number of macromolecular engineering tools at our disposition and, thus, bring added value to the enzyme-catalyzed polymer technology.

6. References

Adlercreutz, P., 2013. Chem. Soc. Rev. 42, 6406.

Azim, H., Dekhterman, A., Jiang, Z., Gross, R.A., 2006. Biomacromolecules 7, 3093–3097.

Barton, N.R., Burgard, A.P., Burk, M.J., Crater, J.S., Osterhout, R.E., Pharkya, P., Steer, B.A., Sun, J., Trawick, J.D., Dien, S.J.V., Yang, T.H., Yim, H., 2014. J. Ind. Microbiol. Biotechnol. 42, 349–360.

Becker, J., Lange, A., Fabarius, J., Wittmann, C., 2015. Curr. Opin. Biotechnol. 36, 168–175.

Binns, F., Harffey, P., Roberts, S.M., Taylor, A., 1998. J. Polym. Sci. Part Polym. Chem. 36, 2069–2079.

Bozell, J.J., Petersen, G.R., 2010. Green Chem. 12, 539.

Bueno-Ferrer, C., Hablot, E., Garrigós, M. del C., Bocchini, S., Averous, L., Jiménez, A., 2012. Polym. Degrad. Stab., 3rd International Conference on Biodegradable and Biobased Polymers (BIOPOL-2011) - Strasbourg 2011 97, 1964–1969.

Cai, Y., Lv, J., Feng, J., 2012. J. Polym. Environ. 21, 108–114.

Charlier, Q., Girard, E., Freyermouth, F., Vandesteene, M, Jacquel, N., Ladavière, C., Rousseau, A., Fenouillot, F., 2015. Express Polym. Lett. 9, 424–434.

Chaudhary, A.K., Beckman, E.J., Russell, A.J., 1997. Biotechnol. Bioeng. 55, 227–239.

Choi, S., Song, C.W., Shin, J.H., Lee, S.Y., 2015. Metab. Eng. 28, 223–239.

Chrissafis, K., Paraskevopoulos, K.M., Bikiaris, D.N., 2006. Thermochim. Acta 440, 166–175.

Debuissy, T., Pollet, E., Avérous, L., 2016a. Polymer 99, 204–213.

Debuissy, T., Pollet, E., Avérous, L., 2016b. Biomacromolecules 17, 4054–4063.

Duchiron, S.W., Pollet, E., Givry, S., Avérous, L., 2015. RSC Adv. 5, 84627–84635.

Düşkünkorur, H.Ö., Bégué, A., Pollet, E., Phalip, V., Güvenilir, Y., Avérous, L., 2015. J. Mol. Catal. B Enzym. 115, 20–28.

Gandini, A., 2011. Green Chem. 13, 1061–1083.

Garin, M., Tighzert, L., Vroman, I., Marinkovic, S., Estrine, B., 2014. J. Appl. Polym. Sci. 131, 40887/1-40887/7.

Gubbels, E., Jasinska-Walc, L., Koning, C.E., 2013. J. Polym. Sci. Part Polym. Chem. 51, 890–898.

Gubbels, E., Jasinska-Walc, L., Noordover, B.A.J., Koning, C.E., 2013. Eur. Polym. J. 49, 3188–3198.

Gustini, L., Lavilla, C., Janssen, W.W.T.J., Martínez de Ilarduya, A., Muñoz-Guerra, S., Koning, C.E., 2016. ChemSusChem 9, 2250–2260.

Gustini, L., Noordover, B.A.J., Gehrels, C., Dietz, C., Koning, C.E., 2015. Eur. Polym. J. 67, 459–475.

Habeych, D.I., Juhl, P.B., Pleiss, J., Vanegas, D., Eggink, G., Boeriu, C.G., 2011. J. Mol. Catal. B Enzym. 71, 1–9.

Hu, X., Shen, X., Huang, M., Liu, C., Geng, Y., Wang, R., Xu, R., Qiao, H., Zhang, L., 2016. Polymer 84, 343–354.

Jiang, Y., Loos, K., 2016. Polymers 8, 243.

Jiang, Y., Woortman, A.J.J., Alberda van Ekenstein, G.O.R., Loos, K., 2015a. Polym Chem 6, 5198–5211.

Jiang, Y., Woortman, A.J.J., Alberda van Ekenstein, G.O.R., Petrović, D.M., Loos, K., 2014. Biomacromolecules 15, 2482–2493.

Jiang, Y., Woortman, A.J.J., van Ekenstein, G.O.R.A., Loos, K., 2013. Biomolecules 3, 461–480.

Jiang, Y., Woortman, A.J.J., Ekenstein, G.O.R.A. van, Loos, K., 2015b. Polym. Chem. 6, 5198–5211.

Khan, A., Sharma, S.K., Kumar, A., Watterson, A.C., Kumar, J., Parmar, V.S., 2014. ChemSusChem 7, 379–390.

Kobayashi, S., 2009. Macromol. Rapid Commun. 30, 237–266.

Köpke, M., Mihalcea, C., Liew, F., Tizard, J.H., Ali, M.S., Conolly, J.J., Al-Sinawi, B., Simpson, S.D., 2011. Appl. Environ. Microbiol. 77, 5467–5475.

Kumar, A., Gross, R.A., 2000a. Biomacromolecules 1, 133–138.

Kumar, A., Gross, R.A., 2000b. J. Am. Chem. Soc. 122, 11767–11770.

Kumar, A., Kalra, B., Dekhterman, A., Gross, R.A., 2000. Macromolecules 33, 6303–6309.

Laurichesse, S., Avérous, L., 2014. Prog. Polym. Sci., Topical Issue on Biomaterials 39, 1266–1290.

Linko, Y.-Y., Lämsä, M., Wu, X., Uosukainen, E., Seppälä, J., Linko, P., 1998. J. Biotechnol., Biocatalysis 66, 41–50.

Mahapatro, A., Kalra, B., Kumar, A., Gross, R.A., 2003. Biomacromolecules 4, 544–551.

Muthuraj, R., Misra, M., Mohanty, A.K., 2015. ACS Sustain. Chem. Eng. 3, 2767–2776.

Nakaoki, T., Danno, M., Kurokawa, K., 2003. Polym. J. 35, 791–797.

Namekawa, S., Uyama, H., Kobayashi, S., 2000a. Biomacromolecules 1, 335–338.

Namekawa, S., Uyama, H., Kobayashi, S., Kricheldorf, H.R., 2000b. Macromol. Chem. Phys. 201, 261–264.

Noordover, B.A.J., van Staalduinen, V.G., Duchateau, R., Koning, C.E., van Benthem, Mak, M., Heise, A., Frissen, A.E., van Haveren, J., 2006. Biomacromolecules 7, 3406–3416.

Nordblad, M., Adlercreutz, P., 2013. Biocatal. Biotransformation 31, 237–245.

Ottosson, J., Hult, K., 2001. J. Mol. Catal. B Enzym., Proceedings of the 4th International Symposium on Biocatalysis 11, 1025–1028.

Öztürk, H., Pollet, E., Phalip, V., Güvenilir, Y., Avérous, L., 2016. Polymers 8, 416.

Öztürk Düşkünkorur, H., Pollet, E., Phalip, V., Güvenilir, Y., Avérous, L., 2014. Polymer 55, 1648–1655.

Pan, P., Inoue, Y., 2009. Prog. Polym. Sci. 34, 605–640.

Papageorgiou, G.Z., Bikiaris, D.N., 2005. Polymer 46, 12081–12092.

Persenaire, O., Alexandre, M., Degée, P., Dubois, P., 2001. Biomacromolecules 2, 288–294.

Raza, S., Fransson, L., Hult, K., 2001. Protein Sci. 10, 329–338.

Reulier, M., Avérous, L., 2015. Eur. Polym. J. 67, 418–427.

Rotticci, D., Hæffner, F., Orrenius, C., Norin, T., Hult, K., 1998. J. Mol. Catal. B Enzym. 5, 267–272.

Schmid, R.D., Verger, R., 1998. Angew. Chem. Int. Ed. 37, 1608–1633.

Takamoto, T., Kerep, P., Uyama, H., Kobayashi, S., 2001. Macromol. Biosci. 1, 223–227.

Tanzi, M.C., Verderio, P., Lampugnani, M.G., Resnati, M., Dejana, E., Sturani, E., 1994. J. Mater. Sci. Mater. Med. 5, 393–396.

Uyama, H., Inada, K., Kobayashi, S., 2000. Polym. J. 32, 440–443.

Vilela, C., Sousa, A.F., Fonseca, A.C., Serra, A.C., Coelho, J.F.J., Freire, C.S.R., Silvestre, A.J.D., 2014. Polym. Chem. 5, 3119–3141.

Wang, X.-X., Hu, H.-Y., Liu, D.-H., Song, Y.-Q., 2016. New Biotechnol. 33, 16–22.

Wang, Z.-L., Hiltunen, K., Orava, P., Seppälä, J., Linko, Y.-Y., 1996. J. Macromol. Sci. Part A 33, 599–612.

Watson, R.W., Grace, N.H., Barnwell, J.L., 1950. Can. J. Res. 28b, 652–659.

Watson, Ralph W., 1950. 2, 3-butanediyl phthalate resins. US2502686.

Werpy, T.A., Holladay, J.E., White, J.F., 2004. Top Value Added Chemicals from Biomass: I. Results of Screening for Potential Candidates from Sugars and Synthesis Gas (No. PNNL-14808). Pacific Northwest National Laboratory (PNNL), Richland, WA (US).

Yao, D., Li, G., Kuila, T., Li, P., Kim, N.H., Kim, S.-I., Lee, J.H., 2011. J. Appl. Polym. Sci. 120, 1114–1120.

Yoon, K.R., Hong, S.-P., Kong, B., Choi, I.S., 2012. Synth. Commun. 42, 3504–3512.

Sub-chapter 3.3. Lipase-catalyzed synthesis of biobased and biodegradable aliphatic copolyesters from short building blocks. Effect of the monomer length on enzyme activity and on copolyesters properties.

Thibaud Debuissy, Eric Pollet and Luc Avérous*

BioTeam/ICPEES-ECPM, UMR CNRS 7515, Université de Strasbourg, 25 rue Becquerel, 67087 Strasbourg Cedex 2, France

*Corresponding author: luc.averous@unistra.fr

Submitted in European Polymer Journal

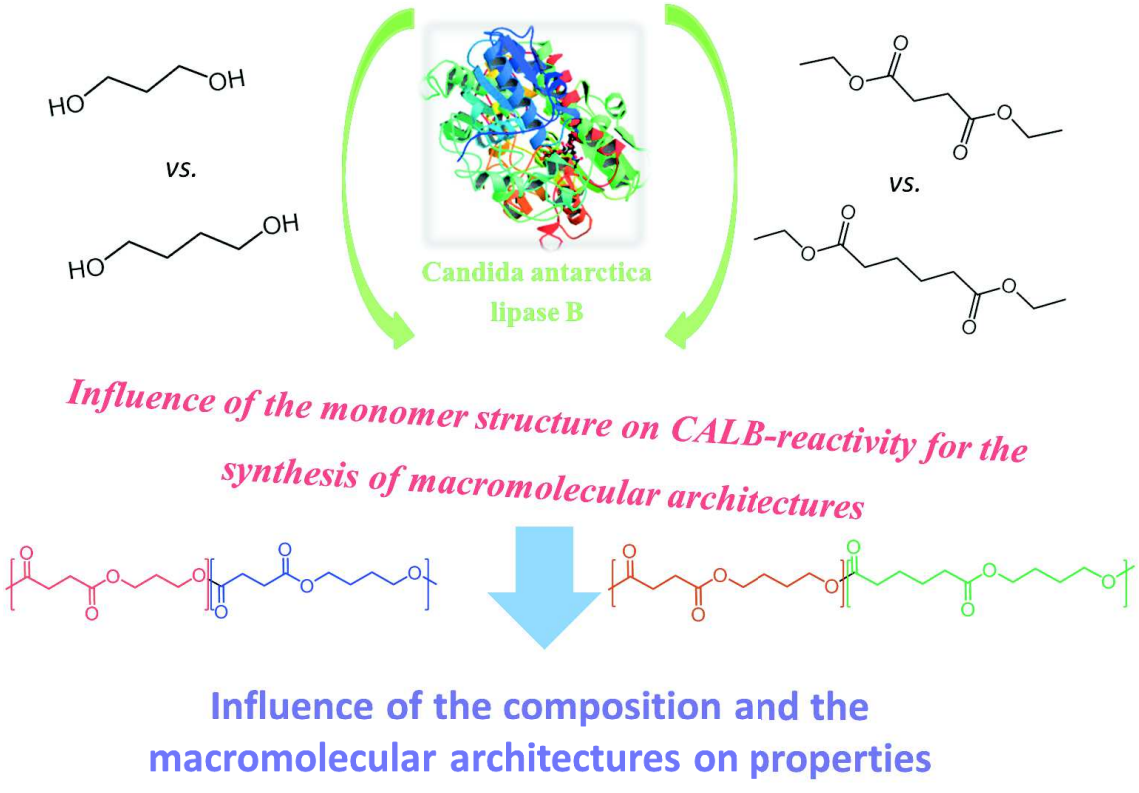

1. Abstract

Potentially biobased short aliphatic diols and diethyl carboxylates were enzymatically (co)polymerized in solution at mild temperature using the immobilized form of Candida antarctica lipase B (CALB) as biocatalyst. The influence of the monomer structure on the CALB activity was investigated. CALB showed a better affinity for 1,4-butanediol compared to 1,3-propanediol (1,3-PDO), whereas no preference was observed between diethyl succinate and diethyl adipate. In addition, two series of random copolyesters [poly(butylene succinate-ran-butylene adipate) (PBSA) and poly(propylene succinate-ran-butylene succinate) (PPBS)] were synthesized at different compositions to investigate the effect of the composition on copolyesters, which were fully characterized by various chemical and physico-chemical techniques including NMR, SEC, WAXS, DSC and TGA. Their compositions were similar to the feed ones, despite the activity difference of the monomers towards CALB. Nevertheless, this activity difference resulted in the decrease of the Mw of PPBS from 24 to 11 kg/mol for 1,3-PDO content varying from 0 to 100 mol.%. Moreover, 1,3-PDO induced an increase of Tg and a decrease of the crystallization rate until having an amorphous behavior for high 1,3-PDO content. On the other side, the reduction of the diethyl carboxylate chain length from diethyl adipate to diethyl succinate did not induce a clear tendency with Mn varying from 22 to 12 kg/mol with the succinate content. Furthermore, Tg increased with the succinate content and the good thermal stability of copolyesters were dependent on the diethyl carboxylates composition. Finally, both copolyesters exhibited an isodimorphic co-crystallization behavior.

2. Introduction

Biobased and biodegradable polymers have received extensive attention from both academia and industry point of views in the recent decades due to global increasing concern over the lasting behavior of plastics on the environment (Bozell and Petersen, 2010; Williams and Hillmyer, 2008). Since it can be synthesized from succinic acid (SA) and butanediol (1,4-BDO), which are building blocks currently industrially obtained by biotechnologies from renewable resources, poly(butylene succinate) (PBS) is nowadays considered as one of the most promising sustainable alternative to conventional fossil-based polymers (Bozell and Petersen, 2010). PBS is one of the most interesting aliphatic polyesters due to its very high melting point, excellent mechanical properties close to some polyolefins, biodegradability and easy processability (Tokiwa et al., 2009; Xu and Guo, 2010). All these properties make it suitable for short term applications such as disposable packaging, agriculture or biomedical products (Gigli et al., 2016a; Xu and Guo, 2010). PBS is nowadays also largely used for long term applications e.g., as a material for automotive or textile. These extensions are connected with the strong development of the production of biobased succinic acid from different companies through the world, such as BioAmber (Canada-USA), Succinity (Germany-Netherland), Reverdia (Netherland-France), Mitsubishi (Japan) or Myriant (USA). However, to broaden its range of application and properties, modification of PBS architecture can be performed. As a route to develop materials with improved properties, tailor-made aliphatic copolyesters were synthesized combining different biobased building blocks. To date, PBS derivatives to random copolyesters have been developed with various diacids, such as furan dicarboxylic acid, adipic acid (AA) and terephthalic acid (Deng et al., 2004; Debuissy et al., 2017a), or diols, such as ethylene glycol, propanediol (1,3-PDO) and isosorbide (Chen et al., 2009; Jasinska and Koning, 2010; Papageorgiou and Bikiaris, 2007). Poly(butylene succinate-*co*-butylene adipate) (PBSA), the most known succinate-based copolyester, has been developed at an industrial scale since 1990 by Showa Denko under tradename “Bionolle”. PBSA copolyester, which can be now fully biobased since new biological pathways were developed for the bioproduction of AA from different biomass (Polen et al., 2013; Vardon et al., 2015), has an excellent processability (Takiyama and Fujimaki, 1994) and also present lower melting temperature, lower degree of crystallinity and higher biodegradability than PBS (Debuissy et al., 2017a; Pérez-Camargo et al., 2017). Moreover, till recently, biobased 1,3-PDO was not largely available in the market at low cost with sufficient purity for chemical purposes. These limiting factors have been recently overcome by the development of new bioprocesses which permit an increase of the industrial production using biological pathways mainly from glycerol (Biebl et al., 1999; Drożdżyńska et al., 2011). Poly(propylene succinate-*co*-butylene succinate) (PPBS) copolyesters showed that the incorporation of 1,3-PDO decreased the crystallinity, tensile properties and melting point, whereas the enzymatic degradation rate was raised (Papageorgiou and Bikiaris, 2007).

Nevertheless, until now aliphatic (co)polyesters were mainly produced by melt polycondensation reaction process under vacuum at high temperature using an organometallic catalyst (Debuissy et al., 2017a, 2017b, 2016a; Papageorgiou and

Bikiaris, 2007). Nevertheless, conventional metal-based catalysts and temperatures above 200 °C promote unwanted side reactions such as discoloration and decomposition (Mahapatro et al., 2003). In addition, metal residues from catalysts might induce some environmental pollution (in the case of *e.g.*, compostability) and toxicity (which could be detrimental for medical applications and human health) (Tanzi et al., 1994). Consequently, an eco-friendlier pathway must be developed for the synthesis of polyesters. Interestingly, biocatalysts, such as esterases and more particularly lipases, can remedy to these drawbacks. Lipases (E.C. 3.1.1.3) are non-toxic enzymes that catalyze ester bond cleavage in aqueous media, but are also able to reverse their conventional behavior in organic media to catalyze ester bond formation. Lipases had already been reported to be versatile in polyesters synthesis under mild conditions with a high catalytic activity and a good control of stereo-, region, chemo- and enatio-selectivity (Jiang and Loos, 2016; Shoda et al., 2016). Then, lipase-catalyzed processes permit an excellent control of the synthesized macromolecular architecture with low energy costs and few by-products (Shoda et al., 2016).

Amongst lipases, *Candida antarctica* lipase B (CALB) and more particularly the commercial form, Novozym® 435 (N435), which is immobilized on macroporous acrylic polymer beads is the most used and one of the best biocatalysts for polyester synthesis. It shows several advantages such as high reaction yields, broad substrate specificity, excellent thermal stability and large commercial availability (Jiang and Loos, 2016). Then, recently lipase-catalyzed syntheses of sustainable polyesters from biobased monomers have attracted a considerable attention. Several biobased polyesters have been synthesized *via* enzymatic polycondensation and reported, *e.g.* poly(lactic acid), succinate-, glycerol-, fatty acids-, sorbitol-, 1,4:3,6-dianhydrohexitol-, 2,5-furanedicarboxylate-based polyesters…(Shoda et al., 2016; Debuissy et al., 2016b, 2017d; Düşkünkorur et al., 2015; Duchiron et al., 2015).

Since molar masses remain usually lower than with more conventional systems based on organometallic catalysis, many studies have been performed to optimize experimental conditions for lipase-catalyzed polyester synthesis, through the increase of the molar mass. Previous results showed that diphenyl ether is the preferred solvent to achieve high molar mass for lipase-catalyzed polyesters synthesis by esterification/transesterification (Mahapatro et al., 2003; Jiang et al., 2013; Debuissy et al., 2017d). Other studies investigated the influence of the monomer length or the monomer structure on the lipase-catalyzed synthesis of polyesters. It has been shown that the degree of polymerization (DP_n) of polyesters increased with the diol length (from 1,4-BDO to 1,10-hexanediol) and with the acyl donor monomer (diacid) length (from C4 to C6) for condensation reactions (Feder and Gross, 2010; Mahapatro et al., 2003). Moreover, Jiang et *al.* highlighted that the acyl donor functional group structure (*i.e.*, itaconic acid, dimethyl-, diethyl- or dibutyl itaconate) had a huge influence of the reaction yield and the incorporation of itaconate in the lipase-catalyzed synthesis of poly(butylene succinate-*co*-itaconate) (Jiang et al., 2013). However, to the best of our knowledge, the influence of the monomer length and structure has never been studied for the biosynthesis of copolyesters such as PBSA or PPBS.

The aim of this study was, thus, to investigate and compare the CALB affinity and efficiency towards different aliphatic biobased monomers. For that, CALB-catalyzed transesterification of 1,3-PDO and 1,4-BDO, diethyl succinate and diethyl adipate was performed, in solution, to synthesize PPBS and PBSA copolyesters at different compositions after optimization of the reaction parameters. The effect of the 1,3-PDO/1,4-BDO and succinate/adipate molar compositions on the CALB-catalyzed synthesis and copolyesters physicochemical properties was particularly discussed. Chemical and physicochemical properties of the synthesized macromolecular architectures were fully investigated by SEC and ^{1}H-, ^{13}C- NMR analyses. The thermal stability, crystalline structure and thermal properties were analyzed by TGA, WAXS and DSC, respectively.

3. Experimental part

3.1. Materials

1,4-butanediol (1,4-BDO) (99%) and 1,3-propanediol (1,3-PDO) (99%) were purchased from Alfa Aesar. Novozyme 435 (N435) (*Candida antarctica* lipase B immobilized on an acrylic carrier, > 5,000 $U.g^{-1}$, stored at 4°C), chloroform (99.0-99.4%) and deuterated chloroform ($CDCl_3$) were purchased from Sigma-Aldrich. Diethyl succinate (DES) (99%), diethyl adipate (DEA) (99%) and diphenyl ether (99%) were supplied by Acros. Petroleum ether 40-60°C was purchased from VWR. N435 was dried at 25 C for 24 h in an oven under vacuum before use. All other reactants were used without further purification. All solvents used for the analytical methods were of analytical grade.

3.2. Enzymatic synthesis of (co)polyesters

3.2.1. One-step process

An equimolar amount of diethyl carboxylates (DES and/or DEA) and diols (1,3-PDO and/or 1,4-BDO), N435 (10 wt.% *vs*. total mass of monomers) and diphenyl ether (200 wt.% *vs.* total mass of monomers) were introduced in a Schlenk reactor. The schlenk reactor was immerged in a hot oil bath at 90 °C and the pressure inside the reactor was decreased stepwise at 350, 100, 50 and 20 mbar for 4, 2, 2 and 64 h, respectively. The global reaction scheme and conditions are summarized in Scheme 3.3.1-a. After 72 h of reaction, 10 mL of chloroform were introduced in the reaction mixture in order to stop the reaction. The diluted reaction mixture was filtered. The filtrate was concentrated in a rotavapor. Thereafter, the synthesized copolyester was precipitated into a large volume of vigorously stirred cold petroleum ether, recovered by filtration, washed with petroleum ether and dried under reduced pressure in an oven at 40 °C for 24 h.

CALB-catalyzed homopolyesters syntheses in diphenyl ether were repeated three times. Average and detailed results are given in this paper and in Annex 6 (Table SI.8), respectively.

Copolyesters samples of different compositions (100:0, 75:25, 50:50, 25:75 and 0:100) are named PBS_wA_x and PP_yB_zS with "w", "x", "y" and "z" respectively the molar proportion of succinate (SA), adipate (AA), 1,3-propyl (1,3-PDO) and 1,4-butyl (1,4-BDO) moieties in the two different copolyesters, as determined by ^{1}H-NMR. The two homopolyesters PBS_0A_{100} and $PP_{100}B_0S$ are also named as PPS and PBA, respectively; whereas $PBS_{100}A_0$ and $PP_0B_{100}S$ refer to the same homopolyester, which is name as PBS.

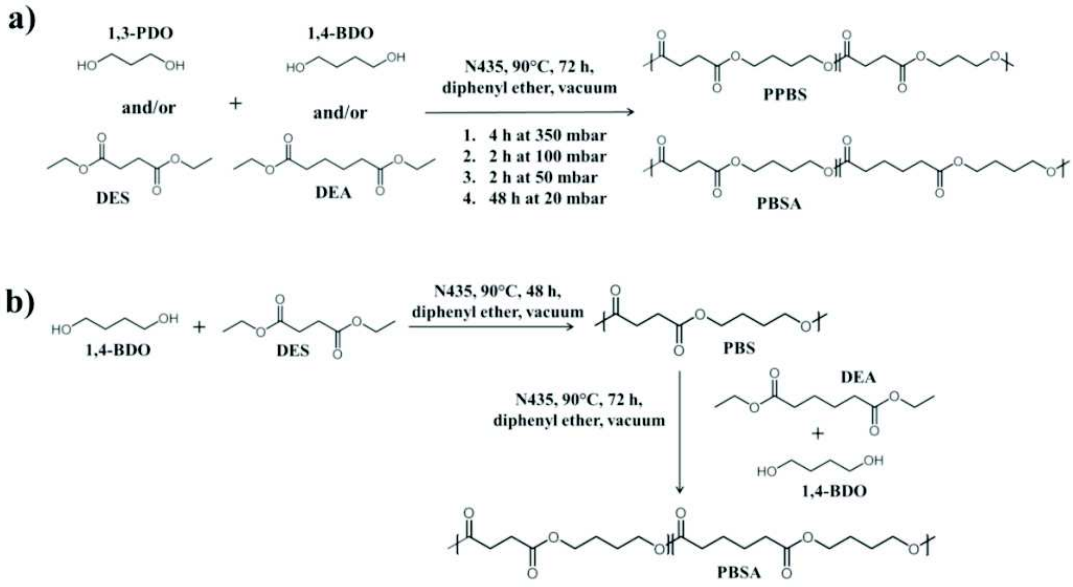

Scheme 3.3.1 : (a) PBSA and PPBS one-step and (b) PBSA two-step reaction procedure for the CALB-catalyzed synthesis.

3.2.2. Two-step process

To synthesize $PBS_{50}A_{50}$ according to a two-step process, an equimolar amount of DES and 1,4-BDO, N435 (20 wt.% *vs.* total mass of monomers) and diphenyl ether (400 wt.% *vs.* total mass of monomers) were introduced in a Schlenk reactor. The schlenk reactor was immerged in a hot oil bath at 90 °C and the pressure inside the reactor was decreased stepwise at 350, 100, 50 and 20 mbar for 4, 2, 2 and 16 h, respectively. After 24 h, the vacuum was broken and an equimolar amount similar to the first addition of DEA and 1,4-BDO was added into the reactor. Then, the pressure inside the reactor was decreased stepwise at 350, 100, 50 and 20 mbar for 4, 2, 2 and 40 h, respectively. The global reaction scheme and conditions involved are summarized in Scheme 3.3.1-b. After a total reaction time of 72 h, 10 mL of chloroform were introduced in the reaction mixture in order to stop the reaction and the copolyester recovery was performed as before.

3.3. Genereal methods and analysis

^{1}H- and ^{13}C-NMR spectra of polyesters were obtained with a Bruker 400 MHz spectrometer. $CDCl_3$ was used as solvent to prepare solutions with concentrations of 8-10 and 30-50 mg/mL for ^{1}H-NMR and ^{13}C-NMR, respectively. The number of scans was set to 128 for ^{1}H-NMR and at least 4,000 for ^{13}C-NMR. Calibration of the spectra was performed using the $CDCl_3$ peak (δ_H = 7.26 ppm, δ_C = 77.16 ppm).

Size Exclusion Chromatography (SEC) was performed to determine the number-average molar mass ($M_{n,SEC}$), the mass-average molar mass ($M_{w,SEC}$) and the dispersity (Đ) of the samples. A Shimadzu liquid chromatograph was equipped with PLGel Mixed-C and PLGeL 100 Å columns and a refractive index detector. Chloroform was used as eluent at a flow rate of 0.8 ml/min. The apparatus was calibrated with linear polystyrene standards ranging from 162 to 1,650,000 g/mol.

Differential scanning calorimetry (DSC) was performed using a TA Instrument Q 200 under nitrogen (flow rate of 50 mL/min), calibrated with high purity standards. Samples were stored at room temperature for at least two months prior to DSC analysis in order to let the polyester reach the crystallization equilibrium state.. Samples of 2-3 mg were sealed in aluminum pans. A three-step procedure with a 10 °C/min ramp was applied that involved: (1) heating up from room temperature to 130 °C and holding for 3 min to erase the thermal history, (2) cooling down to -80 °C and holding for 3 min, (3) heating (second heating) from -80 °C to 130 °C. The degree of crystallinity (X_c) of (co)polyesters is calculated according to Equation (3.1.1),

$$X_c(\%) = \frac{\Delta H_m}{\Delta H_m{}^0} \times 100 \qquad (3.3.1)$$

where ΔH_m is the melting enthalpy and $\Delta H_m{}^0$ is the melting enthalpy of a 100% crystalline polyester.

Thermal degradations were studied by thermogravimetric analyses (TGA). Measurements were conducted under helium atmosphere (flow rate of 25 mL/min) using a Hi-Res TGA Q5000 apparatus from TA Instruments. Samples (3-5 mg) were heated from room temperature up to 550 °C at a rate of 20 °C/min.

Wide angle X-ray Scattering (WAXS) data were recorded on a Siemens D5000 diffractometer using Cu K_α radiation (1.5406 Å) at 25-30 °C in the range of 2θ = 14-30° at 0.4 °.min^{-1}.

4. Results and discussion

4.1. CALB-catalyzed synthesis of homopolyesters

Poly(propylene succinate) (PPS), poly(butylene succinate) (PBS), poly(propylene adipate) (PPA) and poly(butylene adipate) (PBA) homopolyesters were synthesized by the CALB-catalyzed transesterification reaction at 90 °C in diphenyl ether under vacuum from 1,3-PDO, 1,4-BDO, DES and DEA according to the one-step process presented in Scheme 3.3.1-a. Results of these syntheses are presented in Table 3.3.1. The molar mass of polyesters was firstly determined by SEC ($M_{n,SEC}$). Since, polyester $M_{n,SEC}$ values are overestimated due to the calibration based on PS standards, a correction of the PBS and PBA molar masses has been performed using the Mark-Houwink-Sakurada (MHS) equation (Equation (3.1.3)) and parameter from Garin *et al.* (Garin et al., 2014c) and Munari (Munari et al., 1992). The MHS-corrected molar mass ($M_{n,MHS}$) of PBS and PBA samples was calculated and reported in Table 3.3.1. Unfortunately, MHS parameters in $CHCl_3$ are not known for PPS and PPA and thus the corrected molar mass values cannot be determined in these last cases.

The macromolecular architectures of the homopolyesters were verified by ^{1}H- and ^{13}C-NMR. ^{1}H-NMR spectra, presented in Figure SI.22 (in Annex 6), showed characteristic signals of succinate (at δ = 2.62 ppm), adipate (at δ = 2.32 and 1.65 ppm), 1,3-propyl (at δ ~ 4.15 and 1.97 ppm) and 1,4-butyl (at δ ~ 4.10 and 1.70 ppm) units (more details in Annex 6). In addition, ^{1}H-NMR characteristic signals of hydroxyl (OH-CH_2-) and ester end-groups (-O-CH_2-C$\underline{H}_3$) were observed at 3.67 and 1.25 ppm, respectively. These results allowed the calculation of molar mass of homopolyesters from ^{1}H-NMR spectra using relative intensities of the repeating units and end-groups signals according to Equations (3.3.1) and (SI.31)-(SI.33). The average degree of polymerization (DP_n) of homopolyesters was calculated from $M_{n,NMR}$. $M_{n,NMR}$ of homopolyesters were much lower than $M_{n,SEC}$ but close to $M_{n,MHS}$ values proving a good correlation between

both methods. Furthermore, the ester end-groups proportion ($\%_{DES\ end\text{-}groups}$) was calculated from ^{1}H-NMR spectra using relative intensities of both end-groups according to Equation (3.1.2).

$M_{n,NMR}$ and $M_{n,SEC}$ of homopolyesters increased with the lengths of the corresponding diethyl carboxylates. Interestingly, DP_n of 1,3-PDO-based homopolyesters (*i.e.*, PPS and PPA) slightly increased with diester carboxylates length, contrary to 1,4-BDO-based homopolyesters (*i.e.*, PBS and PBA). The increase of the CALB activity with DEA was expected since Garcia-Alles and Gotor showed that CALB had the highest activity for C6 acyl chain length (García-Alles and Gotor, 1998). Likewise, Jiang *et al.* showed that higher molar masses were obtained with DEA (M_n = 2.4 kg/mol) than with DES (M_n = 1.5 kg/mol) for the CALB-catalyzed reaction with 2,5-bis(hydroxymethyl)furan (Jiang et al., 2014b). On the other side, the shortening of the diol length from 1,4-BDO to 1,3-PDO decreased significantly the M_n and the DP_n, especially for succinate-based polyesters. The decrease of one single methylene carbon from 1,4-BDO to 1,3-PDO had, thus, a significant effect on the CALB activity. These observations were in contradiction with those of Linko and coworkers who showed that the increase of the diacid length from C4 to C6 had a significant effect on the DP_n, whereas the increase in DP_n was limited when the diol length rose from C3 to C4 (Linko et al., 1998; Wang et al., 1996). This discrepancy can be explained by the different reaction conditions between both studies. On their side, Jiang *et al.* showed the lower reactivity of 1,3-PDO compared to 1,4-BDO for the CALB-catalyzed reaction based on dimethyl-2,5-furanedicarboxylate (Jiang et al., 2015b). One can suppose that the higher hydrophobicity of the 1,4-BDO monomer was one of the main driver for the increase of the CALB activity. Higher hydrophobicity of the substrate eases the approach of the CALB reactive site, which is located at the bottom of an apolar funnel (in connection with the basic role of the lipase) (Pleiss et al., 1998). Finally, all homopolyesters exhibited a significant proportion of ester end-groups (*i.e.*, 86-91 mol.%), calculated from ^{1}H-NMR spectra, whereas the OH/ester ratio of the feed was 1:1. Such result has already been observed for the CALB-catalyzed synthesis of other polyesters by our group (Debuissy et al., 2017d). Nakaoki *et al.* observed that, even if at the early stage of the reaction the enzyme-catalyzed polymerization of diacid and diols yielded hydroxyl terminated chains in agreement with the mechanism proposed by Binns *et al.*, (Binns et al., 1998), carboxyl terminated ones were obtained at the end due to transesterification reactions.

Table 3.3.1 : CALB-catalyzed synthesis of homopolyesters at 90 °C for 72 h with 10 wt.% of N435 in diphenyl ether under vacuum.

Entry	Polyester	Yield	SEC			NMR		
			$M_{n,SEC}$	Đ	$M_{n,MHS}$	$M_{n,NMR}$	DP_n	$\%_{DES\ end\text{-}groups}$
		%	kg/mol		kg/mol	kg/mol		%
1	PBS	93 ± 1	12.8 ± 1.4	1.9 ± 0.1	5.9	4.8 ± 0.4	28 ± 2	90 ± 2
2	PBA	87 ± 4	16.8 ± 0.7	1.7 ± 0.1	6.4	5.6 ± 0.5	28 ± 2	86 ± 3
3	PPS	70 ± 4	6.5 ± 0.8	1.7 ± 0.2	-	2.8 ± 0.1	18 ± 1	91 ± 2
4	PPA	63 ± 2	9.3 ± 0.8	1.5 ± 0.1	-	4.2 ± 0.2	22 ± 1	90 ± 2

4.2. CALB-catalyzed synthesis of PBSA copolyesters

4.2.1. One-step synthesis using DES as acyl donor monomer

To study the evaluation of the reactivity difference between DES and DEA, several poly(butylene succinate-*co*-butylene adipate) (PBSA) copolyesters were synthesized from 1,4-BDO, DES and DEA with different DES/DEA feed ratio following the one-step CALB-catalyzed transesterification reaction under vacuum, developed in Scheme 3.3.1-a. The structure of CALB-catalyzed PBSA copolyesters was verified by ^{1}H-NMR. The ^{1}H-NMR spectrum of a typical PBSA copolyester is presented in Figure 3.3.1-a. Results are in agreement with a previous study on PBSA (Debuissy et al., 2017a). In addition to the characteristic PBSA signals, hydroxyl and ester end-groups signals were observed at 3.67 and 1.25 ppm, respectively. The molar content in succinate (χ_{SA}) and adipate (χ_{AA}) was determined using relative intensities of signals of methylene protons in α of the carbonyl in SA and AA repetitive units at δ = 2.62 and 2.32 ppm, respectively (see Equations (SI.1) and (SI.2), respectively). Results, presented in Table 3.3.2, showed that feed and final compositions were similar for all PBSA copolyesters attesting for the good reactivity of both monomers with CALB and the absence of monomer loss during the process.

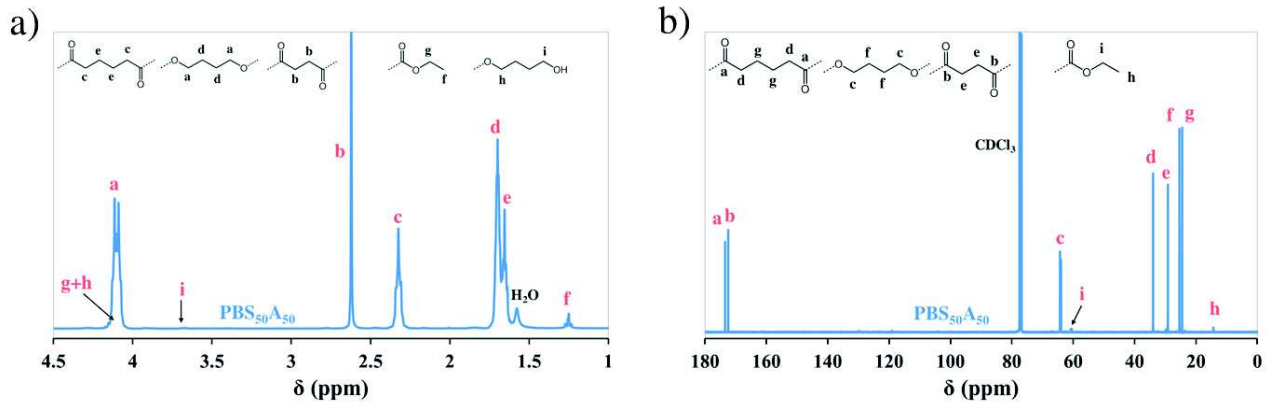

Figure 3.3.1 : (a) ^{1}H- and (b) ^{13}C-NMR spectrum of CALB-catalyzed $PBS_{50}A_{50}$ in $CDCl_3$.

To continue the investigation of the CALB-catalyzed PBSA structure, ^{13}C-NMR analysis was performed and a typical spectrum of PBSA copolyester is presented in Figure 3.3.1-b. Results are in agreement with PBSA ^{13}C-NMR spectrum with two additional signals at 10.4 and 60.4 ascribed to ester end-groups (Debuissy et al., 2017a). The presence of only ester end-groups confirmed the ^{1}H-NMR results which showed that ester end-groups are majority. Moreover, the PBSA microstructure, which is composed of different SBS, SBA and ABA triads as presented in Figure 2.1.2-a, was determined thanks to ^{13}C-NMR. 1,4-BDO units are present in all three triads and give distinctly different peaks with chemical shifts close to the ones of PBS or PBA. Indeed, chemical shifts at 64.0 (two peaks) and 64.3 (two peaks) ppm were assigned to O-$\underline{C}H_2$-CH_2- next to an adipate and a succinate repetitive units, respectively. Such results, with the splitting of the two signals (carbon atoms a_1, a_2, a_3 and a_4 in Figure 2.1.2), enable the calculation of the average sequence length of BS and BA units (L_{BS} and L_{BA}, respectively) and the degree of randomness (R) using Equations (2.1.3)-(2.1.5) according to the same method used in a previous study on PBSA (Debuissy et al., 2017a). Data are listed in Table 3.3.2. For fully random copolymers, R is equal to 1, whereas it is equal to 2 for strictly alternating and close to 0 for block copolymers. According to the SA/AA ratio, L_{BS} and L_{BA} varied between 1.4 and 4.0. PBSA copolyesters composed of both diacids all showed R values of approximately 1.0 meaning a random distribution sequence behavior between succinate and adipate segments along the chain. This result was quite expected since CALB is known to catalyze ester bond formation but also intermolecular transesterification leading to random structures (Kumar and Gross, 2000b; Takamoto et al., 2001; Debuissy et al., 2016b). $M_{n,SEC}$ of PBSA copolyesters varied between 10.8 and 22.0 kg/mol without a clear tendency with the adipate content, even if molar mass of copolyesters containing a high proportion of adipate units were higher than the one of PBS. Đ of PBSA varied between 1.5 and 1.9 in agreement with previous studies on lipase-catalyzed polyester synthesis (Mahapatro et al., 2003; Debuissy et al., 2017d). The PBSA molar mass was also determined by ^{1}H-NMR ($M_{n,NMR,PBSA}$) according to Equation (SI.34) using relative intensities of characteristics signals and data are reported in Table 3.3.2. PBSA copolyesters exhibited $M_{n,NMR,PBSA}$ values of approximately 4.5-7.3 kg/mol according to the composition together with a high ester end-group proportion of approximately 83-90%. Nevertheless, the DP_n of PBSA copolyesters varied between 25 and 38 without clear trend, attesting for the absence of a reactivity preference of CALB for DES or DEA, as already observed and stated for the homopolyesters.

Table 3.3.2 : CALB-catalyzed PBSA copolyesters of various compositions at 90°C with 10 wt.% of N435 in 200 wt.% of diphenyl ether.

Sample	Feed composition SA / AA	^{1}H NMR Exp. composition SA / AA	Yield	SEC $M_{n,SEC}$	SEC $M_{w,SEC}$	SEC Đ	^{1}H NMR $M_{n,NMR}$	^{1}H NMR Ester end-groups	^{1}H NMR DP_n	^{13}C NMR L_{BS}	^{13}C NMR L_{BA}	^{13}C NMR R
	mol.%	mol.%	%	kg/mol	kg/mol		kg/mol	%				
PBS	100 / 0	100 / 0	92	12.8	24.3	1.9	4.8	90	28	-	-	-
$PBS_{75}A_{25}$	75 / 25	74.9 / 25.1	83	10.8	18.3	1.7	4.5	83	25	4.0	1.4	0.96
$PBS_{50}A_{50}$	50 / 50	50.3 / 49.7	79	14.6	24.7	1.7	6.1	91	33	2.0	2.0	1.00
$PBS_{25}A_{75}$	25 / 75	25.4 / 74.6	81	22.0	33.6	1.5	7.3	84	38	1.4	3.7	0.99
PBA	0 / 100	0 / 100	88	16.8	27.0	1.7	5.6	86	28	-	-	-

4.2.2. Effect of the acyl donor monomer structure

In order to investigate the influence of the type of ester of the acyl donor monomer, an additional one-step synthesis of PBSA with a feed 50/50 (SA/AA) composition was performed under the same reaction conditions than previously, but using dimethyl succinate (DMS) as the acyl donor monomer for succinate derivatives instead of DES. Indeed, Jiang *et al.* showed that the nature of the ester from diester carboxylates (dimethyl or diethyl dicarboxylates) can play a significant role in the monomer incorporation into the chain (Jiang et al., 2013). The use of dimethyl carboxylates leads to the formation of methanol as by-product which has a lower boiling point than ethanol (65 and 78 °C, respectively), and is thus more easily removed from the reaction mixture. Nevertheless, the high vacuum used in this current study should significantly favor the removal of both alcohols and thus their difference of boiling point may not be relevant anymore. The characteristics of $PBS_{50}A_{50}$ obtained from DMS were compared to the ones of $PBS_{50}A_{50}$ previously synthesized with DES as acyl donor monomer. The reaction was followed by taking aliquots every 24 h. The kinetic data are presented in Table 3.3.3 and Figure SI.23 (Annex 6).

First, copolyesters synthesized from DMS did not exhibit a characteristic signal of ester end-groups due to the chemical structure of DMS, so the determinations of the ester end-groups proportion or the molar mass by ^{1}H-NMR is not possible. Results showed that the increase of the molar mass with the reaction time was similar for both diester carboxylates with final $M_{n,SEC}$ and Đ of approximately 14.5 kg/mol and 1.7, respectively. Likewise, after only 24 h of reaction, both copolyesters exhibited already a random structure with L_{BS} and L_{BA} of approximatively 2. However, one can observe that the SA content in the copolyesters synthesized from DMS was a bit lower than the targeted composition. This difference may be explained by the lower boiling point of DMS (200 °C) compared to the one of DES (216 °C) and thus to some DMS molecules being removed from the reaction mixture with the vacuum, even if a particular attention was paid to decrease stepwise the vacuum to prevent the evaporation of monomers. The use of DES as succinate derivative was, thus, the best choice for the CALB-catalyzed synthesis of PBSA copolyesters. This result leads us to not consider a comparative study between DEA and dimethyl adipate (DMA).

Table 3.3.3 : Kinetic study of CALB-catalyzed synthesis of $PBS_{50}A_{50}$ using DMS or DES as acyl donor monomer with DEA.

Acyl donor monomer	Reaction time	SEC			^{1}H-NMR		^{13}C-NMR		
		$M_{n,SEC}$	$M_{w,SEC}$	Đ	SA / AA	Ester end-group	L_{BS}	L_{BA}	R
	h	kg/mol	kg/mol		mol.%	%			
DMS	24	10.6	21.4	2.0	47.3 / 52.7	-	2.0	2.2	0.94
	48	11.5	24.1	2.1	47.1 / 52.9	-	2.0	2.2	0.95
	72	14.3	25.0	1.7	47.4 / 52.6	-	2.0	2.2	0.95
DES	24	9.3	15.7	1.7	50.2 / 49.8	69	2.1	2.1	0.96
	48	12.7	21.2	1.7	50.4 / 49.6	86	2.1	2.1	0.96
	72	14.6	24.7	1.7	50.5 / 49.5	91	2.1	2.1	0.97

4.2.3. PBSA synthesis via a two-step process

Another strategy of PBSA synthesis with a 50/50 (SA/AA) feed composition was performed at 90 °C in diphenyl ether, but this one was made using a two-step process according to the pathway presented in Scheme 3.3.1-b. Corresponding results are summarized in Table 3.3.4.

After the first step (48 h), a PBS homopolyester with a $M_{n,SEC}$ of approximately 6.3 kg/mol was obtained. Then, the introduction of the 1,4-BDO/DEA mixture permitted to synthesize a PBSA copolyester with a final content of 49 mol.% of adipate segments, so similar to the targeted molar composition. Moreover, one can observe that after the introduction of the second diester carboxylate monomer (*i.e.*, DEA), CALB directly incorporated adipate units inside the previously synthesized PBS chain and not at the end of synthesized chains. This is due to transesterification reactions which "homogenize" the copolyester structure. Indeed, 24 h after the introduction of DEA, the copolyester had already a random structure attested by the R value close to 1. Furthermore, $M_{n,SEC}$ of the copolyester increased significantly after the equimolar 1,4-BDO/DEA mixture introduction until reaching 13.7 kg/mol, likely due to the decrease of the dilution from 400 to 200 wt.%. Indeed, Jiang *et al*. proved that the molar mass of polyesters synthesized by transesterification in

diphenyl ether under vacuum decreased for diphenyl ether amount higher than 200 wt.% (Jiang et al., 2013). For longer reaction time *(i.e.*, > 24 h after the DEA introduction), the molar mass of the copolyester decreased due to transesterification reactions, whereas its molar composition and sequence distribution remained constant. Although a two-step pathway permitted to synthesize copolyesters directly from previously synthesized oligomers, the obtained results were similar to the one-step process, when the reaction was stopped after 72 h, contrary to what has been observed for other copolyesters (Debuissy et al., 2016b). Then, there was no direct benefit in this case to use the CALB-catalyzed two-step reaction instead of the one-step process.

Table 3.3.4 : CALB-catalyzed PBSA copolyesters with a 50/50 feed molar ratio via the two-step process.

		SEC			^{1}H-NMR		^{13}C-NMR		
Reaction time	Polyester	$M_{n,SEC}$	$M_{w,SEC}$	Đ	SA / AA	Ester end-group	L_{BS}	L_{BA}	R
h		kg/mol	kg/mol		mol.%	%			
48	PBS	6.3	12.3	2.0	100 / 0	85	∞	-	0
72		13.7	32.2	2.3	49.3 / 50.7	67	2.0	2.1	0.97
96	PBSA	11.0	21.6	2.0	48.7 / 51.3	i.d.	2.1	2.2	0.95
120		12.2	24.6	1.7	49.1 / 50.9	86	2.0	2.0	0.99

4.3. CALB-catalyzed synthesis of PPBS copolyesters

In a purpose to investigate in further details the influence of the diol length on the lipase activity, several CALB-catalyzed syntheses of poly(propylene succinate-*co*-butylene succinate) (PPBS) copolyesters from 1,3-PDO, 1,4-BDO and DES at different 1,3-PDO/1,4-BDO feed ratio (100:0, 75:25, 50:50, 25:75 and 0:100) were performed according to the one-step process.

The structure of CALB-catalyzed PPBS copolyesters was verified by ^{1}H-NMR and a typical spectrum is presented in Figure 3.3.2-a. The chemicals shifts at δ = 4.17 and 1.97 ppm were assigned to -O-C$\underline{H}_2$-CH$_2$- and -O-CH$_2$-C$\underline{H}_2$- protons from 1,3-PDO units, whereas shifts at δ = 4.12 and 1.70 ppm were assigned to -O-C$\underline{H}_2$-CH$_2$- and -O-CH$_2$-C$\underline{H}_2$- protons from 1,4-BDO units, respectively. The molar compositions in 1,3-PDO ($\chi_{1,3\text{-PDO}}$) and 1,4-BDO ($\chi_{1,4\text{-BDO}}$) segments were determined using relative intensities of signals at δ = 1.97 and 1.70 ppm, respectively and calculated according to Equations (SI.5) and (SI.6), respectively. Such as PBSA, the feed and final compositions were similar for all PPBS copolyesters. The lower boiling temperature of 1,3-PDO compared to 1,4-BDO had no importance using our reaction conditions with a stepwise pressure decrease to avoid monomers loss. Such as PBSA, PPBS copolyesters exhibited mainly ester end-groups attesting for a high extent of reaction.

It is noteworthy that the recovery yield of $PP_{74}B_{26}S$ was low, because the product contrary to other copolyesters was not solid but viscous during the precipitation process. A significant polymer loss was observed during the filtration step, whence the low yield observed for this composition. However, all other copolyesters were recovered at a correct yield (*i.e.*, 70-90%).

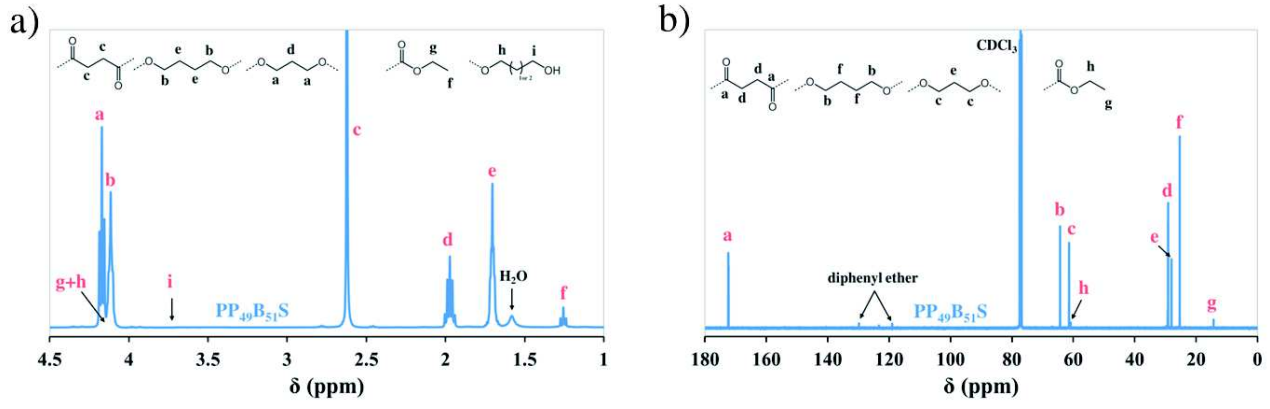

Figure 3.3.2 : (a) ^{1}H- and (b) ^{13}C-NMR spectrum of lipase-catalyzed $PP_{49}B_{51}S$ copolyester in $CDCl_3$.

To determine the sequence distribution of PPBS copolyesters, ^{13}C-NMR was performed and a typical spectrum of PPBS copolyester is presented in Figure 3.3.2-b. The chemical shifts at δ = 25.4 and 64.3 ppm were ascribed to -O-CH_2-$\underline{C}H_2$- and -O-$\underline{C}H_2$-CH_2- carbons from 1,4-BDO units, whereas ones at δ = 28.1 and 61.4 ppm were ascribed to -O-CH_2-$\underline{C}H_2$- and -O-$\underline{C}H_2$-CH_2- carbons from 1,3-PDO units, respectively. Finally, chemical shifts at δ = 29.2 (three peaks) and 172.3 (four peaks) ppm were assigned to -CO-$\underline{C}H_2$- and -$\underline{C}$O-CH_2- carbons in succinate units. Since, succinate moieties are present in all three triads at distinctly different peaks, carbonyl carbons of succinate units (δ ~ 172 ppm) were used as reference. The three different triad structures (PSP, PSB, and BSB) are presented in Figure 3.2.3, with P, S and B as the 1,3-PDO, SA and 1,4-BDO segments, respectively; while the calculation of the average sequence length of PS and BS units (L_{PS} and L_{BS}, respectively) and R was performed with the same method as for PBSA. Results are summarized in Table 3.3.5. Such as PBSA, all PPBS copolyesters exhibited a random structure.

$M_{w,SEC}$ of synthesized PPBS copolyesters increased continuously with the 1,4-BDO content from 11 to 24 kg/mol for PPS and PBS, respectively. Similarly, $M_{n,NMR,PPBS}$, calculated according to Equation (SI.35), increased with the 1,4-BDO content from 2.8 to 4.7 kg/mol for PPS and PBS, respectively. These results confirmed the higher affinity of the 1,4-BDO monomer with the CALB active site, as previously observed during the synthesis of homopolyesters.

Table 3.3.5 : CALB-catalyzed PPBS copolyesters of various compositions at 90°C with 10 wt.% of N435 in 200 wt.% of diphenyl ether.

Sample	^{1}H-NMR		SEC			^{1}H-NMR		^{13}C-NMR		
	Feed composition 1,3-PDO/1,4-BDO	Determined composition 1,3-PDO/1,4-BDO	Yield	$M_{n,SEC}$	$M_{w,SEC}$	Đ	$M_{n,NMR}$	Ester end-groups	L_{PS}	L_{BS}	R
	mol.%	mol.%	%	kg/mol	kg/mol		kg/mol	%			
$PP_{100}B_0S$	100 / 0	100 / 0	70	6.5	11.2	1.7	2.8	91	-	-	-
$PP_{74}B_{26}S$	75 / 25	74.4 / 25.6	46	8.4	14.5	1.7	3.2	90	4.1	1.4	0.97
$PP_{49}B_{51}S$	50 / 50	49.3 / 50.7	81	12.1	20.0	1.7	3.9	96	1.9	2.1	1.00
$PP_{26}B_{74}S$	25 / 75	25.9 / 74.1	90	11.8	23.3	2.0	4.9	93	1.4	3.9	0.98
$PP_0B_{100}S$	100 / 0	100 / 0	92	12.8	24.3	1.9	4.7	90	-	-	-

4.4. Thermal stability of (co)polyesters

Thermal stabilities of (co)polyesters under helium were determined from TGA. The mass loss curves of (co)polyesters are plotted in Figure 3.3.3 with their corresponding derivatives (DTG) curves. Data are reported in Table SI.9. At temperature below 240 °C, all samples appeared to be thermally stable. All (co)polyesters degraded into two main steps, but with different degradation rates and starting temperatures. First, a small mass loss (< 3%) was observed at 240-300 °C due to possible residual molecules and the degradation of the low molar mass chains (Debuissy et al., 2016a). In addition, a significant degradation happened at 280-410 °C with a substantial mass loss of approximately 90%, mostly by β- and α-hydrogen bond scissions (Debuissy et al., 2017a, 2016a). After this decomposition step, mass residues of approximately 3-7% were recovered.

For all (co)polyesters, the temperature corresponding to 2% mass loss ($T_{d,2\%}$) were about 255-285 °C. These temperatures were slightly lower than for these similar (co)polyesters synthesized by an organometallic process (Debuissy et al., 2017a), surely due to the lower molar mass obtained *via* the enzymatic process. For PBSA copolyesters, the 50% mass loss degradation temperature ($T_{d,50\%}$) and the maximal degradation temperature ($T_{deg,max}$) were approximately 350-385 and 355-390 °C, respectively. These two characteristic temperatures decreased with the adipate content, meaning an acceleration of the degradation rate with the adipate content (Figure 3.3.3-a). In summary, the thermal degradation profile of CALB-catalyzed PBSA depended highly on the SA/AA molar ratio, in good agreement with the results of a previous study on organometallic-catalyzed PBSA (Debuissy et al., 2017a). In the case of PPBS copolyesters, $T_{d,50\%}$ and $T_{deg,max}$ were approximately 380 and 388 °C, respectively, with similar degradation profile for all PPBS samples which were perfectly superimposed, showing the absence of influence of the diol on the degradation profile of PPBS copolyesters (Figure 3.3.3-b).

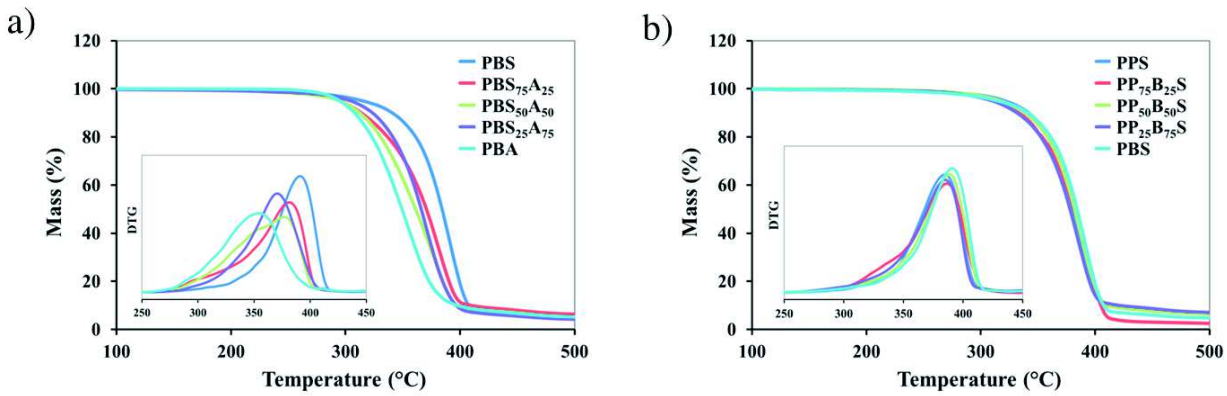

Figure 3.3.3 : Mass loss and DTG curses of lipase-catalyzed (a) PBSA and (b) PPBS copolyesters.

4.5. WAXS and DSC analysis

A WAXS analysis of both copolyesters was performed to determine the corresponding crystalline structures. PBSA and PPBS copolyesters patterns are plotted in Figure 3.3.4. WAXS patterns of copolyesters appeared to be characterized by well-defined diffraction peaks over the whole composition range. The patterns of PBSA and PPBS semi-crystalline copolyesters could be split into two groups according to the AA and 1,3-PDO contents, respectively.

PBSA copolyesters containing up to 50 mol.% of adipate units crystallized according to PBS crystalline structures. The co-monomer (adipate in this case) addition in minor content, which was partially integrated or excluded from the crystal lattice, decreased the chain homogeneity leading to the reduction of the crystal strength, lamellae sizes and crystallinity. PBSA copolyesters containing 75 mol.% or more of adipate units crystallized according to PBA crystals. However, whereas PBA exhibited α + β mixed crystals, $PBS_{25}A_{75}$ showed only β-form crystals of PBA (Pan and Inoue, 2009). One can suppose that the addition of succinate units, which disrupted the chain homogeneity, slowed down the crystallization rate leading to the formation of only kinetically-favored β-form crystals of PBA.

PPBS copolyesters containing 74 mol.% or more of 1,3-PDO units crystallized according to the PPS lattice, whereas samples containing up to 49 mol.% of 1,3-PDO units crystallized according to the PBS lattice (Papageorgiou and Bikiaris, 2007). Such as PBSA, the degree of crystallinity of PPBS copolyesters decreased with the inclusion of co-monomers.

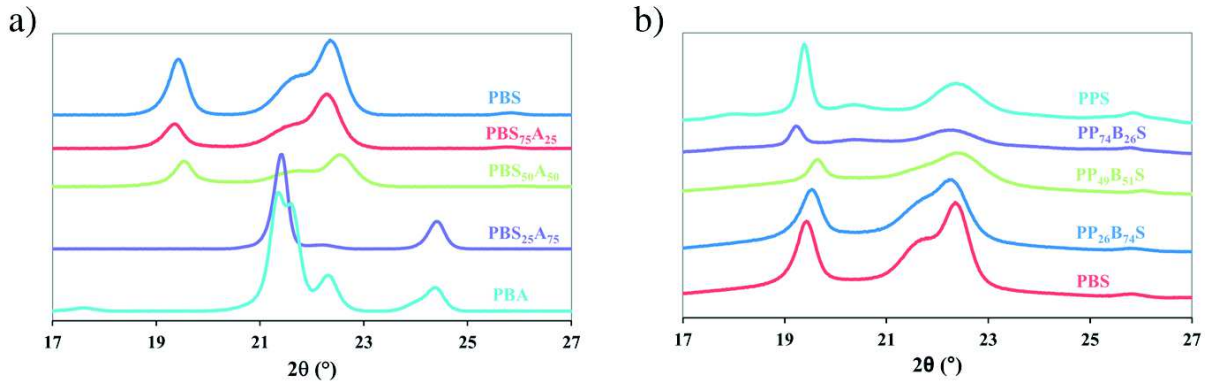

Figure 3.3.4 : WAXS patterns of lipase-catalyzed (a) PBSA and (b) PPBS copolyesters.

The thermal properties of CALB-catalyzed homo- and co-polyesters were studied by DSC. First, it has been verified from the TGA results that no significant degradation occurred for copolyesters in the DSC analyses temperature range. The DSC second heating run curves of copolyesters are presented in Figure 3.3.5 with corresponding data summarized in Table 3.3.6. Plots of T_m and ΔH_m of PBSA and PPBS copolyesters as a function of adipate or 1,3-PDO contents are shown in Figures 3.3.6 and 3.3.7, respectively. The variation of thermal properties is discussed as a function of the ester function density (D_{ester}).

During the cooling from the melt at a constant rate, most of samples were able to crystallize except for (co)polyesters having a high 1,3-PDO content, such as PPA, PPS and $PP_{74}B_{26}S$. In the case of PBSA copolyesters, T_c decreased with the adipate content starting from the PBS homopolyester until having a double crystallization phenomenon for $PBS_{50}A_{50}$ at -23 and 41 °C assigned to the PBA and PBS crystalline phase, respectively. Then, T_c of the PBA crystalline phase increased with higher adipate content until reaching 32 °C for the PBA homopolyester. For PPBS copolyesters, T_c and ΔH_c decreased with the 1,3-PDO content until the disappearance of the crystallization phenomena for 1,3-PDO content of 74 mol.% or more. "1,3-PDO rich" PPBS (co)polyester chains were not able anymore to crystallize due to the decrease of the crystallization rate caused by the low and odd number of methylene protons of this diol.

During the second heating run, glass transition and melting phenomena were observed. Moreover, $PP_{49}B_{51}S$ and PPA exhibited, in addition to these two phenomena, a cold-crystallization phenomenon at approximately -24 °C. For (co)polyesters, as the SA and 1,3-PDO content decreased, D_{ester} decreased, due to the higher content in "long" adipate and 1,4-butylene segments and, thus, the chain mobility increased. For all (co)polyesters, only one glass transition temperature (T_g) was observed demonstrating the absence of block structures in copolyesters as it was previously stated. T_g of polyesters increased with D_{ester} due to the reduction of the chain mobility induced by the use of 1,3-PDO and SA. Most (co)polyesters exhibited melting phenomena spread on a large temperature range and composed of multiple peaks. Moreover, a small cold-crystallization signal was sometimes observed just before the melting. These multiple peaks were attributed to both the crystallite reorganization occurring during the heating by a fusion-recrystallization phenomenon (Debuissy et al., 2017a, 2016a) and the polymorphism for PBA (Debuissy et al., 2016a; Pan and Inoue, 2009).

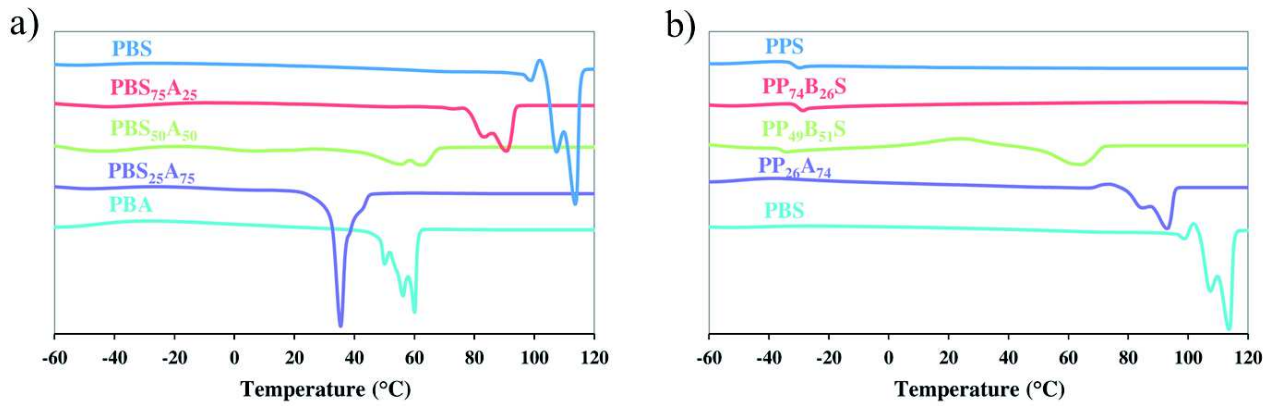

Figure 3.3.5 : DSC second heating run curves of lipase-catalyzed (a) PBSA and (b) PPBS copolyesters.

For lipase-catalyzed PBSA copolyesters, T_m and ΔH_m of PBS crystals decreased with the adipate content from 114 to 63 °C and 75 to 28 J/g for PBS and $PBS_{50}A_{50}$, respectively (Figure 3.3.6). Likewise, T_m and ΔH_m of PBA crystals decreased with the succinate content from 60 to 5 °C and 65 to 7 J/g for PBA and $PBS_{50}A_{50}$, respectively. Interestingly, $PBS_{50}A_{50}$ exhibited a mixture of both PBS and PBA crystalline phases such as for the titanium-catalyzed synthesis of $PBS_{50}A_{50}$ (Debuissy et al., 2017a). However, one can suppose that the presence of both crystalline phases spreads on a composition range around the 50:50 (SA:AA) composition. The PBA crystalline phase of $PBS_{50}A_{50}$ was not observed by WAXS due to its T_m lower than the WAXS experiment temperature. The variation of T_m and ΔH_m in function of the adipate content exhibited both pseudo-eutectic behaviors with minimal values near the 50:50 composition. The presence of both melting temperature and melting enthalpy pseudo-eutectic points, and the presence of different crystalline phases according to the molar composition highlighted the isodimorphic co-crystallization behavior of CALB-catalyzed PBSA, in agreement with a previous study on PBSA synthesized by organometallic catalysts (Debuissy et al., 2017a; Pérez-Camargo et al., 2017).

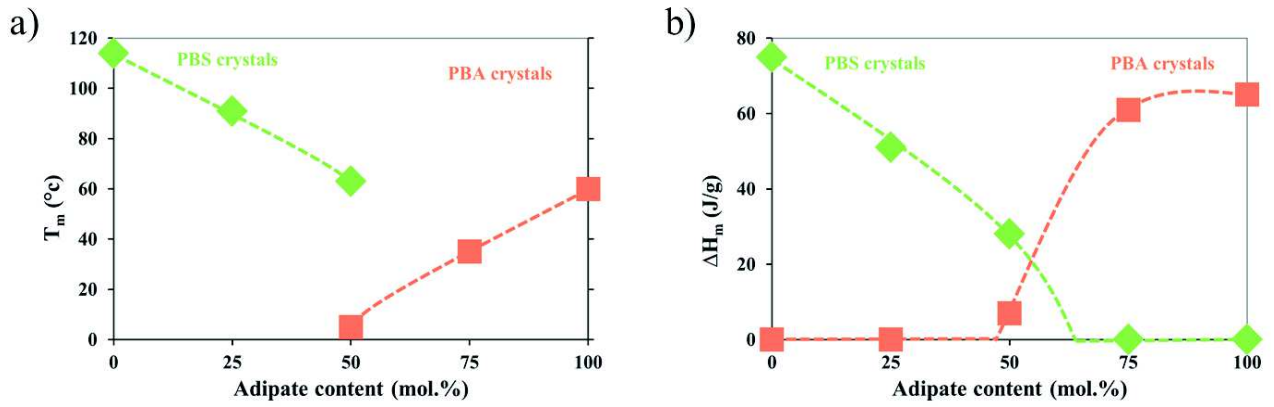

Figure 3.3.6 : Evolution of (a) T_m and (b) ΔH_m of CALB-catalyzed PBSA vs. adipate content measured during the second heating run.

For CALB-catalyzed PPBS copolyesters, T_m and ΔH_m decreased with the 1,3-PDO content from 114 °C and 75 J/g for PBS until having an amorphous behavior for 1,3-PDO content higher than 50 mol.% (Figure 3.3.7). As previously mentioned, the increase of D_{ester} and the 1,3-PDO structure prevented the formation of the crystalline phase during the cooling or the second heating run.

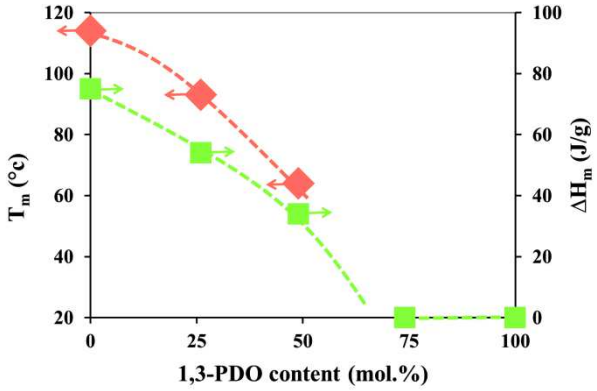

Figure 3.3.7 : Evolution of T_m and ΔH_m of CALB-catalyzed PPBS vs.1,3-PDO content measured during the second heating run.

Table 3.3.6 : DSC results of CALB-catalyzed PPBS and PPBA copolyesters.

Sample	D_{ester}	First heating			Cooling		Second heating					
		T_m	ΔH_m	X_c	T_c	ΔH_c	T_g	T_{cc}	ΔH_{cc}	T_m	ΔH_m	X_c
	%	°C	J/g	%	°C	J/g	°C	°C	J/g	°C	J/g	%
PBS	25.0	113	87	41	87	81	-37¤	-	-	114	75	36
PBA	20.0	56	103	76	32	64	-59¤	-	-	60	65	48
PPS	28.6	46	44	31	-	-	-30	-	-	-	-	0
PPA	22.2	41	61	49	-	-	-58	-12	39	39	47	38
$PBS_{75}A_{25}$	23.8	91	69	33	55	54	n.o.	-	-	91	51	24
$PBS_{50}A_{50}$	22.5	51	47	22	-23/41*	4/38*	-51¤	-	-	5/63*	7/28*	5/13*
$PBS_{25}A_{75}$	21.3	47	61	45	10	58	n.o.	-	-	35	61	45
$PP_{74}B_{26}S$	27.7	39	33	24	-	-	-32	-	-	-	-	0
$PP_{49}B_{51}S$	26.8	60	49	29	11	9	-35	24	24	64	34	16
$PP_{26}B_{74}S$	25.9	93	60	29	49	53	-36	-	-	93	54	26

n.o. not observed, ¤ T_g values were determined after a quenching from the melt, * presence of two crystalline phases (PBA phase / PBS phase).

The melting enthalpy value of 100% crystalline phase is determined from the groups contribution (Van Krevelen method) for PBA (135 J/g) and PPA (124 J/g) (Van Krevelen, 1997), and from experimental data for PBS (210 J/g) and PPS (140 J/g) (Papageorgiou and Bikiaris, 2005a). The degree of crystallinity (X_c) of CALB-catalyzed (co)polyesters was calculated by taking account that only one crystal structure was observed (except for $PBS_{50}A_{50}$) using Equation (3.3.1). Values are summarized in Table 3.3.6. For homopolyesters, higher X_c values are obtained with adipate as diacid and 1,4-BDO as diol. This can be explained by the lower D_{ester} of the corresponding polyesters allowing a higher flexibility of the chain and its ability to crystallize to a larger extent. X_c of CALB-catalyzed PBSA and PPBS was plotted as a function of the adipate and 1,3-PDO contents in Figure SI.24, respectively. Their curves followed the trend of ΔH_m with the decrease of (i) the PBS and PBA degrees of crystallinity with the insertion of the co-monomeric unit in PBSA and (ii) the PBS degree of crystallinity with the 1,3-PDO content for PPBS.

5. Conclusion

A green and efficient approach for the synthesis of biobased homopolyesters, random poly(1,4-butylene succinate-*ran*-1,4-butylene adipate) (PBSA) copolyesters and random poly(1,3-propylene succinate-*ran*-1,4-butylene succinate) (PPBS) copolyesters by the CALB-catalyzed polymerization process from 1,3-PDO, 1,4-BDO, diethyl succinate and diethyl adipate at 90 °C in diphenyl ether under vacuum was successfully demonstrated.

CALB exhibited a preference for diols in C4 compared to the one in C3, due to a probable better affinity of 1,4-BDO with the CALB active site than 1,3-PDO, leading to higher degrees of polymerization for 1,4-BDO-based polyesters compared to 1,3-PDO-based ones. This results into a continuous increase of the M_w with the 1,4-BDO content from 11 to 24 kg/mol for PPBS copolyesters. In the case of acyl donor monomers, CALB did not show any clear preference between diethyl carboxylates in C4 and C6. Although, molar masses of “adipate-rich” polyesters or copolyesters were higher than “succinate-rich” ones, their degrees of polymerization were similar. As an example, the PBSA M_w varied from 18-34 kg/mol without a clear trend with the composition.

Through the CALB reactivity and efficiency towards the different building blocks, the final architectures influenced highly material properties. Although all samples showed a remarkable thermal stability without significant mass loss before 250 °C, their thermal degradation curves were driven by the major diacid component with an acceleration of the degradation rate after the initiation for “adipate-rich” (co)polyesters. Moreover, the use of “longer” monomers, such as diethyl adipate and 1,4-BDO, permitted the decrease of the material T_g and an increase of the degree of crystalline for homopolyesters compared to “shorter” monomers. Then, 1,3-PDO, due to its low and odd number of methylene carbons in its backbone, induced a poor crystallization rate of (co)polyesters. This resulted to the amorphous behavior of PPBS compositions with 1,3-PDO content higher than 50 mol.%. On its side, succinate and adipate units showed a high ability to crystallize, which led to an isodimorphic co-crystallization behavior for PBSA.

Such as the organometallic-catalyzed synthesis of copolyesters using a two-step melt polycondensation process with a titanium-based catalyst that our group had previously used (Debuissy et al., 2017a, 2016a), the enzymatic process using lipases allows the synthesis of random copolyesters with the same feed and final compositions permitting to the materials to have similar thermal properties. However, contrary to the organometallic process, the enzymatic one (i) requires longer reaction time (*i.e.*, 48-72 h instead of few hours), (ii) depends highly on the monomer chain length, (iii) requires the use of solvent and (iv) lead to polyesters of lower molar mass (< 20 kg/mol) which decreased slightly the thermal stability of materials. Nevertheless, the enzymatic process permits (i) the reaction with a non-toxic catalyst which can be removed and reused contrary to the titanium-based one, (ii) the reaction at mild temperatures allowing the absence of discoloration, especially for 1,3-PDO-based copolyesters and (iii) energy savings.

The enzymatic process to synthesize PBSA and PPBS copolyesters instead of organometallic process, which is much more used, constitute an interesting way to obtain these sustainable and biodegradable materials without containing toxic residues. Nevertheless, some improvements on the molar mass especially for PPBS copolyesters with high 1,3-PDO content for these copolyesters in order to use these materials in industrial applications.

6. References

Biebl, H., Menzel, K., Zeng, A.-P., Deckwer, W.-D., 1999. Appl. Microbiol. Biotechnol. 52, 289–297.

Binns, F., Harffey, P., Roberts, S.M., Taylor, A., 1998. J. Polym. Sci. Part Polym. Chem. 36, 2069–2079.

Bozell, J.J., Petersen, G.R., 2010. Green Chem. 12, 539–554.

Chen, C.-H., Lu, H.-Y., Chen, M., Peng, J.-S., Tsai, C.-J., Yang, C.-S., 2009. J. Appl. Polym. Sci. 111, 1433–1439.

Debuissy, T., Pollet, E., Avérous, L., 2016a. Polymer 99, 204–213.

Debuissy, T., Pollet, E., Avérous, L., 2016b. Biomacromolecules 17, 4054–4063.

Debuissy, T., Pollet, E., Avérous, L., 2017a. Eur. Polym. J. 87, 84–98.

Debuissy, T., Pollet, E., Avérous, L., 2017b. Eur. Polym. J. 90, 92–104.

Debuissy, T., Pollet, E., Avérous, L., 2017c. Eur. Polym. J. 93, 103–115.

Deng, L.-M., Wang, Y.-Z., Yang, K.-K., Wang, X.-L., Zhou, Q., Ding, S.-D., 2004. Acta Mater. 52, 5871–5878.

Drożdżyńska, A., Leja, K., Czaczyk, K., 2011. BioTechnologia 1, 92–100.

Duchiron, S.W., Pollet, E., Givry, S., Avérous, L., 2015. RSC Adv. 5, 84627–84635.

Düşkünkorur, H.Ö., Bégué, A., Pollet, E., Phalip, V., Güvenilir, Y., Avérous, L., 2015. J. Mol. Catal. B Enzym. 115, 20–28.

Feder, D., Gross, R.A., 2010. Biomacromolecules 11, 690–697.

García-Alles, L.F., Gotor, V., 1998. Biotechnol. Bioeng. 59, 163–170.

Garin, M., Tighzert, L., Vroman, I., Marinkovic, S., Estrine, B., 2014. J. Appl. Polym. Sci. 131, 40887/1-40887/7.

Gigli, M., Fabbri, M., Lotti, N., Gamberini, R., Rimini, B., Munari, A., 2016. Eur. Polym. J. 75, 431–460.

Jasinska, L., Koning, C.E., 2010. J. Polym. Sci. Part Polym. Chem. 48, 2885–2895.

Jiang, Y., Loos, K., 2016. Polymers 8, 243.

Jiang, Y., Woortman, A.J.J., Alberda van Ekenstein, G.O.R., Petrović, D.M., Loos, K., 2014. Biomacromolecules 15, 2482–2493.

Jiang, Y., Woortman, A.J.J., van Ekenstein, G.O.R.A., Loos, K., 2013. Biomolecules 3, 461–480.

Jiang, Y., Woortman, A.J.J., Ekenstein, G.O.R.A. van, Loos, K., 2015. Polym. Chem. 6, 5198–5211.

Kumar, A., Gross, R.A., 2000. J. Am. Chem. Soc. 122, 11767–11770.

Linko, Y.-Y., Lämsä, M., Wu, X., Uosukainen, E., Seppälä, J., Linko, P., 1998. J. Biotechnol., Biocatalysis 66, 41–50.

Mahapatro, A., Kalra, B., Kumar, A., Gross, R.A., 2003. Biomacromolecules 4, 544–551.

Munari, A., Manaresi, P., Chiorboli, E., Chiolle, A., 1992. Eur. Polym. J. 28, 101–106.

Pan, P., Inoue, Y., 2009. Prog. Polym. Sci. 34, 605–640.

Papageorgiou, G.Z., Bikiaris, D.N., 2005. Polymer 46, 12081–12092.

Papageorgiou, G.Z., Bikiaris, D.N., 2007. Biomacromolecules 8, 2437–2449.

Pérez-Camargo, R.A., Fernández-d'Arlas, B., Cavallo, D., Debuissy, T., Pollet, E., Avérous, L., Müller, A.J., 2017. Macromolecules 50, 597–608.

Pleiss, J., Fischer, M., Schmid, R.D., 1998. Chem. Phys. Lipids 93, 67–80.

Polen, T., Spelberg, M., Bott, M., 2013. J. Biotechnol., Research on Industrial Biotechnology within the CLIB-Graduate Cluster - Part III 167, 75–84.

Shoda, S., Uyama, H., Kadokawa, J., Kimura, S., Kobayashi, S., 2016. Chem. Rev. 116, 2307–2413.

Takamoto, T., Kerep, P., Uyama, H., Kobayashi, S., 2001. Macromol. Biosci. 1, 223–227.

Takiyama, E., Fujimaki, T., 1994. Biodegradable plastics and polymers, in: Doi, Y., Fukuda, K. (Eds.), Biodegradable Plastics and Polymers. Elsevier Science, Burlington, p. 150.

Tanzi, M.C., Verderio, P., Lampugnani, M.G., Resnati, M., Dejana, E., Sturani, E., 1994. J. Mater. Sci. Mater. Med. 5, 393–396.

Tokiwa, Y., Calabia, B.P., Ugwu, C.U., Aiba, S., 2009. Int. J. Mol. Sci. 10, 3722–3742.

Van Krevelen, D.W., 1997. Chapter 5 - Calorimetric properties, in: Properties of Polymers (Third, Completely Revised Edition). Elsevier, Amsterdam, pp. 109–127.

Vardon, D.R., Franden, M.A., Johnson, C.W., Karp, E.M., Guarnieri, M.T., Linger, J.G., Salm, M.J., Strathmann, T.J., Beckham, G.T., 2015. Energy Env. Sci 8, 617–628.

Wang, Z.-L., Hiltunen, K., Orava, P., Seppälä, J., Linko, Y.-Y., 1996. J. Macromol. Sci. Part A 33, 599–612.

Williams, C.K., Hillmyer, M.A., 2008. Polym. Rev. 48, 1–10.

Xu, J., Guo, B.-H., 2010. Biotechnol. J. 5, 1149–1163.

Conclusion du chapitre 3

Le chapitre 3 a mis en avant le potentiel de la catalyse enzymatique à l'aide de la lipase B de *Candida antarctica* pour la synthèse de polyesters ou de copolyesters par transestérification. De plus, ce procédé de synthèse qui s'effectue sous conditions douces permet, comme pour la catalyse organométallique, d'obtenir des architectures macromoléculaires très variées.

Il a été démontré que les diacides utilisés dans le chapitre 2 ne sont pas de bons monomères pour les synthèses enzymatiques à cause de leur immiscibilité dans les solvants apolaires et dans les diols utilisés. L'usage de leurs équivalents estérifiés (diesters de méthyle ou d'éthyle) est donc beaucoup plus adapté du fait de leur état liquide et que le sous-produit de transestérification est un alcool volatile (méthanol ou éthanol). De même, l'utilisation de systèmes réactionnels sous vide a montré une bien meilleure réactivité des monomères que pour les synthèses effectuées à pression atmosphérique ce qui induit une forte augmentation de la masse molaire des polyesters synthétisés. Après avoir testé de nombreux solvants apolaires pour optimiser la synthèse enzymatique, il a été démontré que le diphényl éther, l'anisole et le phénétole (dans une moindre mesure), qui sont tous des éthers aromatiques, sont les trois solvants permettant d'obtenir les plus hautes masses molaires (*i.e.*, M_n > 10 000 g/mol) pour la synthèse du PBS et du PBA par catalyse enzymatique sous pression réduite. Bien que l'efficacité du système réactionnel dans le diphényl éther ait déjà été démontrée par de nombreux groupes de recherche, celle de l'anisole et du phénétole est une première. Cependant, même en utilisant ces trois meilleurs solvants, les masses molaires des (co)polyesters synthétisés par catalyse enzymatique sont plus faibles que celles obtenues par la catalyse organométallique de transestérification. Néanmoins, les masses molaires des PBS et PBA obtenues dans cette étude font partie des masses molaires les plus élevées rapportées jusqu'ici dans la littérature par catalyse enzymatique.

La synthèse enzymatique en masse de PBA a également été testée afin d'étudier un plus large spectre de systèmes réactionnels différents. Toutefois, bien que cette méthode, qualifiée de « plus verte », soit intéressante pour la synthèse rapide d'oligomères, nous ne sommes pas parvenus à obtenir des masses molaires finales élevées du fait de l'importante augmentation de la viscosité du milieu. Ce problème a toutefois pu être quelque peu atténué en utilisant un évaporateur rotatif comme réacteur ce qui permet une agitation plus efficace même à des viscosités élevées.

Par la suite, le système réactionnel sous vide dans le diphényl éther a été choisi comme système de référence pour les différentes synthèses enzymatiques de polyesters. Après une optimisation des différentes conditions expérimentales, il a été décidé d'effectuer les synthèses enzymatiques à 90 °C durant 72 h dans 150-200 pds.% de diphényl éther sous 20 mbar avec 10 pds.% de catalyseur enzymatique.

Afin d'étudier plus en détail l'influence de la longueur des monomères sur la réaction par voie enzymatique, deux copolyesters (PBSA et PPBS) ont été synthétisés avec succès avec plusieurs compositions en faisait varier soit le ratio des diols (pour le PPBS) soit le ratio des diacides estérifiés (pour le PBSA). Comme attendu, la masse molaire des copolyesters augmente en augmentant la proportion en monomère « les plus longs ». Néanmoins, les masses molaires obtenues pour ces deux copolyesters, même dans les conditions enzymatiques optimales, sont beaucoup plus faibles que celles obtenues par catalyse organométallique, cette

dernière n'étant pas impactée par la longueur des monomères. Les copolyesters montrent tous une distribution aléatoire des différentes unités les composant du fait des nombreuses réactions de transestérification induites par les lipases. Les propriétés (stabilité thermique, structure cristalline et propriétés thermiques) des copolyesters synthétisés par catalyse enzymatique sont similaires à celles observées dans le chapitre 2 pour ces deux mêmes copolyesters synthétisés par catalyse organométallique.

Pour finir, des poly(1,4-butylène succinate-*co*-2,3-butylène succinate)s de différentes compositions ont pu être synthétisés à partir de diéthyl succinate, de 1,4-butanediol et de 2,3-butanediol. De la même manière que pour la catalyse organométallique, la masse molaire des copolyesters diminue fortement avec la proportion en 2,3-butanediol mais de façon beaucoup plus linéaire. Cela montre bien que la structure du 2,3-butanediol n'est pas très adaptée à la forme du site actif de la lipase B de *Candida antarctica*. Malgré tout, et pour la première fois, des chaînes polyesters de masses molaires non négligeables ont pu être obtenus avec ce monomère. La détermination des propriétés du copolyester obtenu a ensuite démontré sa grande stabilité thermique similaire à celle des polyesters obtenus par voie organométallique. Comme pour le poly(1,4-butylène adipate-*co*-2,3-butylène adipate) étudié dans le chapitre 2 (sous-chapitre 4), la présence de deux carbones asymétriques dans le 2,3-butanediol permet de développer une nouvelle technique de détermination de la composition entre les deux diols dans le copolyester grâce aux propriétés optiques induites par la chiralité du 2,3-butanediol. De même, le 2,3-butanediol diminue fortement la cristallinité du copolyester et augmente de manière très significative sa température de transition vitreuse.

CHAPITRE 4: SYNTHÈSE ORGANOMÉTALLIQUE ET ENZYMATIQUE DE POLYESTERS À BASE D'OLIGOMÈRES DE PHA-DIOLS

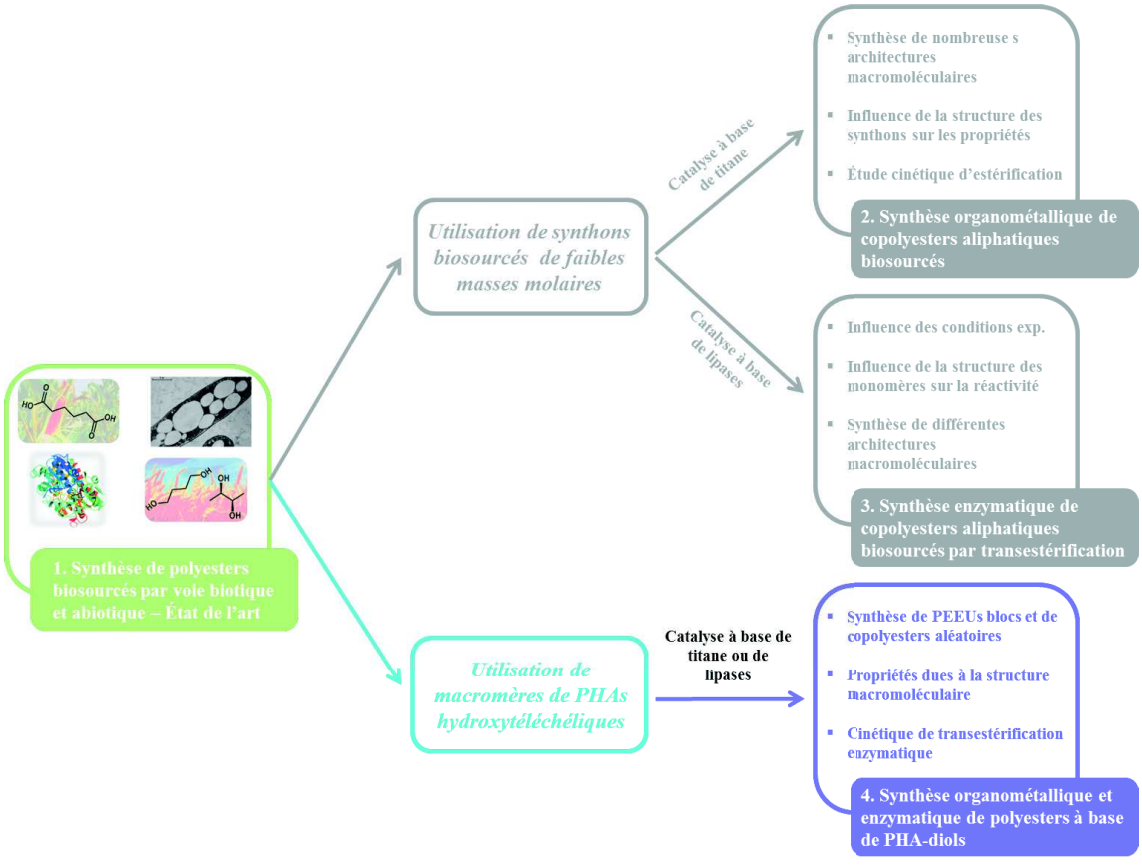

Introduction du chapitre 4

Dans deux précédents chapitres, nos études se sont principalement focalisées sur l'influence de la longueur du synthon (diacide et/ou diol) et/ou du type de diol (primaire et/ou secondaire) utilisé lors de la synthèse de différents copolyesters que ce soit par catalyse organométallique à l'aide d'un catalyseur chimique à base de titane (chapitre 2) ou alors d'un catalyseur biologique tel que la lipase B de *Candida antarctica* (chapitre 3).

Tandis que ces différentes études se sont faites à base uniquement des diols courts tels que le 1,3-propanediol, 1,4-butanediol et le le 2,3-butanediol, le chapitre 4 introduira, quant à lui, l'utilisation d'un macrodiol issu d'un polyester bactérien, le poly(3-hydroxybutyrate) (PHB) comme base d'une nouvelle étude. Le choix d'utiliser le PHB s'est fait en accord avec le projet européen auquel est rattachée cette thèse dans le but de valoriser ce PHA dans de nouveaux matériaux tels que des polyuréthanes ou des copolyesters synthétisés par différentes voies catalytiques. Pour cela, un oligomère de PHB (M_n ~ 1000-5000 g/mol) avec une fonctionnalisation exclusivement hydroxyle sera obtenu par alcoolyse organométallique en solution à partir d'un PHB bactérien de 180 000 g/mol. Notre choix d'obtenir ces macrodiols à partir d'un PHB bactérien et non par ouverture de cycle de lactones est dû à notre souhait de valoriser ce polymère biosourcé.

A partir de ce macrodiol, différents poly(ester-éther-uréthane)s ont pu être synthétisés en une seule étape en solution à l'aide d'un diisocyanate aromatique extrêmement réactif (le 4,4'-diisocyanate de diphénylméthane) et de différents polyéthers. De même, en utilisant ces macrodiols d'oligomères de PHB de différentes masses molaires, des copolyesters ont pu être synthétisés par transestérification organométallique ou enzymatique avec des poly(butylène dicarboxylate)s (PBS ou PBA) précédemment synthétisés. La cinétique de transestérification entre les deux polyesters de départ (PHB-diol et PBS (ou PBA)) sera particulièrement étudiée dans le cas de la transestérification par voie enzymatique.

Ce chapitre est découpé en trois sous-chapitres qui sont présentés sous forme de publications:

- Le sous-chapitre 1 présentera tout d'abord une étude sur la cinétique de la synthèse d'oligomères de PHB-diols par alcoolyse organométallique et l'influence de la masse molaire sur les propriétés de ces oligomères, puis une seconde étude sur la synthèse en solution de poly(ester-éther-uréthane)s à partir de ces oligomères de PHB-diols, de diols éthers et d'un diisocyanate aromatique sous la forme d'un article intitulé « Synthesis and characterization of block poly(ester-ether-urethane)s from poly(3-hydroxybutyrate) oligomers» publié dans *Journal of Polymer Science Part A : Polymer Chemistry*.
- Le sous-chapitre 2 présentera, pour sa part, une étude sur la catalyse organométallique par transestérification pour la synthèse de poly(3-hydroxybutyrate-*co*-butylene succinate) et de poly(3-hydroxybutyrate-*co*-butylene adipate) et leur caractérisation sous la forme d'un article intitulé « Titanium-catalyzed transesterification as a route to the synthesis of fully biobased poly(3-hydroxybutyrate-co-butylene dicarboxylate) copolyesters, from their homopolyesters» publié dans *European Polymer Journal.*
- Le sous-chapitre 3 présentera une étude sur la synthèse par catalyse enzymatique par transestérification de poly(3-hydroxybutyrate-*co*-butylene succinate) en insistant notamment sur l'influence des conditions opératoires sur la cinétique de la transestérification entre les deux homopolymères. Cette étude se présentera sous la forme d'un article intitulé « Enzymatic synthesis of a biobased copolyester from poly(butylene succinate) and poly((R)-3-hydroxybutyrate) – Study of reaction parameters on the transesterification rate » publié dans *Biomacromolecules.*

Sub-chapter 4.1. Synthesis and characterization of block poly(ester-ether-urethane)s from poly(3-hydroxybutyrate) oligomers.

Thibaud Debuissy, Eric Pollet and Luc Avérous*

BioTeam/ICPEES-ECPM, UMR CNRS 7515, Université de Strasbourg, 25 rue Becquerel, 67087 Strasbourg, Cedex 2, France

*Corresponding author: luc.averous@unistra.fr

Published by Journal of Polymer Science Part A: Polymer Chemistry, 2017, 55 (11), 1949-1961

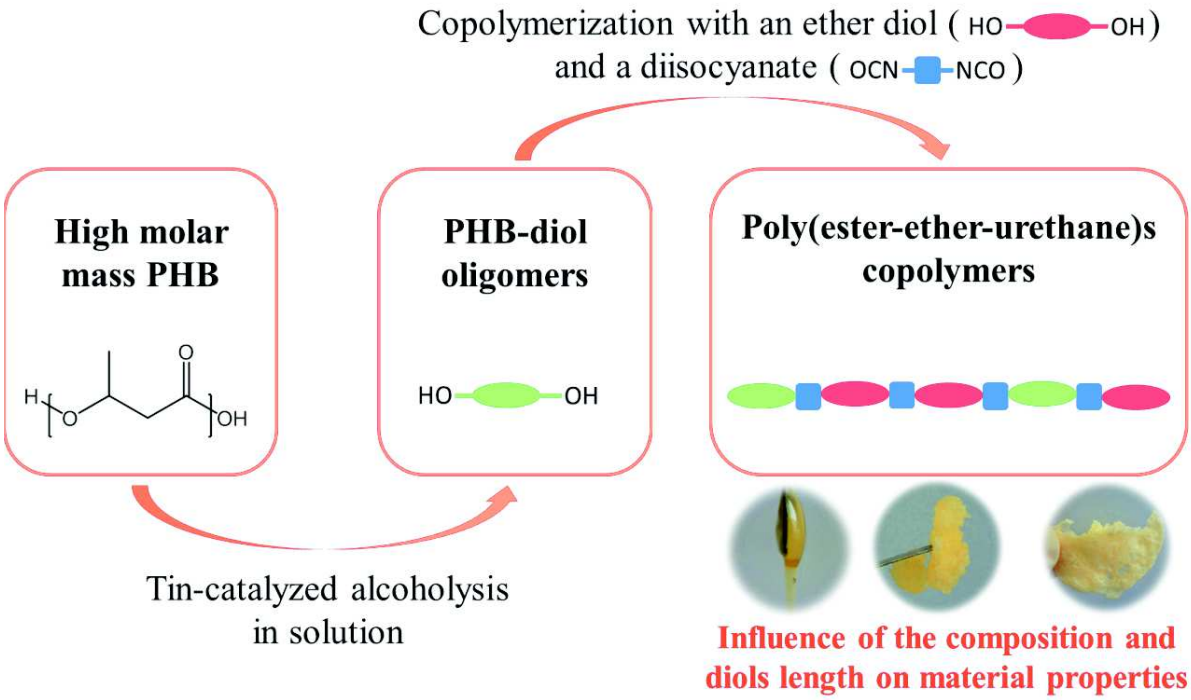

1. Abstract

Telechelic hydroxylated poly(3-hydroxybutyrate) (PHB-diol) oligomers have been successfully synthesized in 90-95% yield from high molar mass PHB by tin-catalyzed alcoholysis with different diols (mainly 1,4-butanediol) in diglyme. The PHB-diol oligomers structure was studied by NMR, FTIR MALDI-ToF MS and SEC, whereas their crystalline structures, thermal properties and thermal stability were analyzed by WAXS, DSC and TGA. The kinetic of the alcoholysis was studied and the influence of (i) the catalyst amount, (ii) the diol amount, (iii) the reaction temperature and (iv) the diol chain length on the molar mass was discussed. The influence of the PHB-diol molar mass on the thermal stability, the thermal properties and optical properties was investigated. Then, tin-catalyzed poly(ester-ether-urethane)s (PEEU) of M_n = 15 000-20 000 g/mol were synthesized in 1,2-dichloroethane from PHB-diol oligomers (Pester) with modified 4,4'-MDI and different polyether-diols (Pether) (PEG-2000, PEG-4000 and PPG-PEG-PPG). The influence of the PHB-diol chain length, the Pether/Pester ratio, the polyether segment nature and the PEG chain length on the thermal properties and crystalline structures of PEEUs was particularly discussed.

2. Introduction

Polyhydroxyalkanoates (PHA) are a family of biopolymers biosynthesized by several bacteria as intracellular carbon and energy storage granules. A wide variety of prokaryotic organisms accumulate PHA from 30 to 80% of their cellular dry weight, and from various renewable resources by fermentation, to develop environmentally friendly materials consistent with a more sustainable development. PHAs are biodegradable but exhibit also biocompatibility in contact with living tissues, suitable for biomedical applications, *e.g.*, tissue engineering (Pollet and Avérous, 2011; Bordes et al., 2009a). Poly(3-hydroxybutyrate) (PHB) is commercially available and it is one of the most prominent PHAs. However, its application as a thermoplastic material is rather limited, mainly due to its high melting temperature (T_m) of approximatively 175 °C, high glass transition temperature (T_g) of approximatively 4 °C, high degree of crystallinity (X_c) (approximatively 60%) and high thermal sensibility. Indeed, PHB possesses a low thermal stability with a degradation initiation close to the T_m (Pollet and Avérous, 2011), and decomposes easily by random *cis*-elimination chain scission producing crotonic groups, thus limiting PHB usage (Abe, 2006; Grassie et al., 1984a; Hablot et al., 2008).

Different approaches have been tested to try to overcome the above drawbacks and to obtain efficient PHB-based materials such as (i) the elaboration of multiphase systems, *e.g.*, by blending with other polymers (Qiu et al., 2003a) or plasticizers (Meszynska et al., 2015), or (ii) the bio- or chemosynthesis of HB-based copolymers. Bacterial syntheses with varying substrates and strains have allowed the biosynthesis of random copolyesters based on HB units (Cavalheiro et al., 2013; Gao et al., 2011; S. J. Park et al., 2012). Varying the amount and the chemical structures of the monomeric units afford copolyesters with a wide range of behaviors and properties. Copolyesters based on HB-blocks were successfully produced with improved properties over random copolyesters (Gao et al., 2011). However, despite their important and varied potential applications, studies of such macromolecular architectures generally still remain limited, mainly because of their lacks of availability in large quantities.

The production of controlled PHA oligomers is a first step for the elaboration of different biobased macromolecular architectures. It is also an elegant way to promote the development of PHA-based materials. Since the direct biosynthesis of PHA oligomers by bacteria is not an option till now, these oligomers must be chemically synthesized. The synthesis can be performed by either anionic- (Arslan et al., 1999; Lenz and Jedlinski, 1996), organometallic- (Guillaume et al., 2013; Jaffredo et al., 2013) and enzymatic- (Nobes et al., 1996; Xie et al., 1997) ring-opening polymerization (ROP) of lactones, or by the enzymatic (Shuai et al., 1999) and chemical (Lengweiler et al., 1996; Saad et al., 2001) esterification of hydroxyacids. Another way is the PHA molar mass reduction with controlled end-groups to obtain *e.g.*, hydroxyl-terminated PHA (PHA-diol) oligomers. This approach can be performed by either organometallic- (Andrade et al., 2002; Hirt et al., 1996) and acid-catalyzed (Deng and Hao, 2001) alcoholysis, or sodium borohydrate reduction (Baran et al., 2002; Bergamaschi et al., 2011).

From PHA oligomers, different tailored materials can be obtained including block poly(ester-urethanes), block poly(ester-ether-urethane)s (PEEU) and block or random copolyesters based on PHB blocks with others blocks, such as poly(ε-caprolactone) (PCL), poly(ethylene glycol) (PEG) or poly(butylene adipate) (PBA) (Ke, 2015; Ravenelle and

Marchessault, 2002). Micro-block and random poly(HB-*co*-CL) and poly(HB-*co*-BA) copolyesters with different compositions have also been synthesized by acid-catalyzed transesterification in solution (Impallomeni et al., 2013, 2002). Recently, micro-block and random poly(HB-*co*-butylene succinate) copolyesters have been synthesized in our group with different compositions by an enzymatic process in solution (Debuissy et al., 2016b). PHB-based block copolyesters were synthesized *via* the chemical (Reeve et al., 1993; Wu et al., 2010) or enzymatic (Dai and Li, 2008) ROP of ε-CL and lactide from PHB-diol oligomers. PEG-PHB-PEG triblock copolymers can be obtained by chain-end esterification (Li et al., 2003), whereas Ravenelle and Marchessault synthesized diblock copolyesters based on PHB and PEG by transesterification (Ravenelle and Marchessault, 2002).

PEEUs are high performance polymers obtained by the reaction of polyol-polyesters and polyisocyanate (Ke, 2015; Loh et al., 2007b). They are being increasingly used in different fields, even in the biomedical area. PEEU properties can be tuned by modifying the chemical nature of the initial compounds and then obtain different types of sequences between two urethane groups. They can be synthesized by either a one or a two-step process, in solution or in bulk (Ke, 2015). The advantage of segmented PEEUs over other kinds of materials is that their segments and domain structure can be easily controlled over a considerable range through the selection of materials, their relative proportions and the length of the blocks.

Contrary to 1,6-hexamethylene diisocyanate (HDI) which is widely used in academic research (Ke, 2015), 4,4'-diphenylmethylene diisocyanate (4,4'-MDI) has a much higher reactivity with hydroxyl functions than HDI (*i.e.*, 320 times) (Ionescu, 2005). Surprisingly, PHB-based PEEUs with 4,4'-MDI has been very rarely studied (Xue et al., 2010). Moreover, the presence of aromatic rings from 4,4'-MDI should permit the local stiffening of the macromolecular architecture.

The aim of this study was, first, to synthesize PHB-diol oligomers by tin-catalyzed alcoholysis from high molar mass PHB and 1,4-butanediol in diglyme. The influence of reaction conditions (catalyst amount, diol amount, temperature and diol chain length) on the alcoholysis rate has been particularly studied. Then, from PHB-diol oligomers (P_{ester}) with various chain lengths and different polyether (P_{ether}) segments (PPG-PEG-PPG or PEG), one-step tin-catalyzed PEEUs were synthesized in anhydrous 1,2-dichloroethane with 4,4'-MDI at different P_{ether}/P_{ester} molar ratios. Chemical and physicochemical properties of these different macromolecular architectures were fully investigated by NMR, SEC and FTIR. The thermal stability, crystalline structures and thermal properties were analyzed by TGA, WAXS and DSC, respectively. The influence of the PHB-diol molar mass, the P_{ether}/P_{ester} ratio and the P_{ether} chemical nature have been particularly discussed.

3. Experimental part

3.1. Materials

Poly(3-hydroxybutyrate) (PHB) (M_n = 180,000 g/mol and Đ = 2.3 (by SEC)), produced by microbial fermentation, was kindly supplied by Biocycle (Brazil). PHB was dried under vacuum in an oven at 60 °C for 24 h before use. 1,3-propanediol (1,3-PDO) (98%), 1,4-butanediol (1,4-BDO) (99%), poly(ethylene glycol) (M_n = 4,000 g/mol) (PEG-4000) and pyridine HPLC grade (99.5+%) were purchased from Alfa Aesar. Poly(ethylene glycol) (M_n = 2,000 g/mol) (PEG-2000), poly(propylene glycol)-*block*-poly(ethylene glycol)-*block*-poly(propylene glycol) (M_n = 2,700 g/mol) (PPG-PEG-PPG), dibutyltin (II) dilaurate (DBTL) (95%), 1,6-hexanediol (1,6-HDO) (97%), 1,10-decanediol (1,10-DCO) (98%), chromium (III) acetyl acetonate (97%), 2-chloro-4,4,5,5-tetramethyl-1,3,2-dioxaphospholane (Cl-TMDP, 95%), cholesterol (> 99%), deuterated chloroform ($CDCl_3$) and deuterated dimethyl sulfoxide (DMSO-d_6) were purchased from Sigma-Aldrich. Diglyme (99%) and 1,2-dichloroethane (99%+) were supplied by Acros Organics. Suprasec 2385 (uretonimine-modified 4,4'-diphenylmethylene diisocyanate (4,4'-MDI)) was supplied by Huntsman. Petroleum ether was purchased from VWR. All solvents used for the analytical methods were of analytical grade.

3.2. Organometallic synthesis of PHB-diol by alcoholysis

In a round-bottom reactor, a mixture of dried PHB, the appropriate amount of diol and diglyme (5 mL / g of PHB) was heated with an oil bath to 135 °C under an argon flux and magnetically stirred until PHB dissolution (≈ 15 min). Then, the temperature was adjusted to the reaction temperature (110-140 °C) and the proper amount of a 20 wt.% DBTL

solution in diglyme was added into the reaction mixture. Aliquots were withdrawn of the reaction mixture at predetermined reaction time in order to follow the reaction. The reaction was stopped by precipitated the reaction mixture into a large volume of vigorously stirred water. The precipitate was recovered by filtration, dissolved in a minimum of chloroform and precipitated again into a large volume of vigorously stirred petroleum ether. After recovery by filtration, the product was dried under reduced pressure in an oven at 50 °C for few hours.

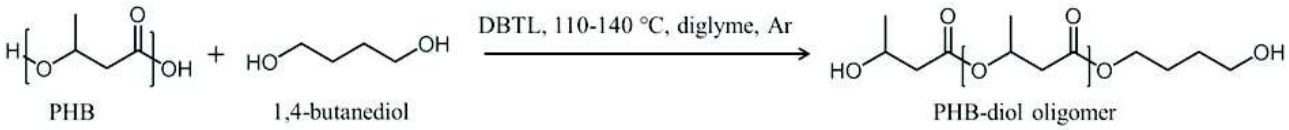

Scheme 4.1.1 : Reaction procedure for PHB-diol oligomers synthesis.

3.3. Poly(ester-ether-urethane)s synthesis

PEEUs were prepared with an isocyanate/hydroxyl (NCO/OH) equimolar ratio and different P_{ether}/P_{ester} molar ratio. In a round bottom flask of 50 mL, the appropriate amount of dried PHB-diol, PEG or PPG-PEG-PPG, modified 4,4'-MDI, 1,2-dichloroethane (~ 5 mL/g of monomer) and DBTL (2.5 mol.% *vs.* modified 4,4'-MDI molar amount) were introduced. The reaction mixture was heated with an oil bath at 75 °C under an argon flux for 4-8 h and magnetically stirred. At the end of the reaction (4-8 h according to the reaction mixture viscosity), PEEUs were dissolved in a minimum of chloroform, precipitated into a large volume of vigorously stirred petroleum ether, recovered by filtration and dried under reduced pressure in an oven at 50 °C for few hours.

3.4. General methods and analysis

^{1}H- and ^{13}C-NMR spectra of polyesters were obtained with a Bruker 400 MHz spectrometer. $CDCl_3$ and DMSO-d_6 were used as solvent to prepare solutions with concentrations of 8-10 and 30-50 mg/mL for ^{1}H-NMR and ^{13}C-NMR, respectively. The number of scans was set to 128 and 1024 for ^{1}H- and ^{13}C-NMR, respectively. Calibration of the spectra was performed using the $CDCl_3$ peak (δ_H = 7.26 ppm, δ_C = 77.16 ppm) or the DMSO-d_6 peak (δ_H = 2.50 ppm, δ_C = 39.52 ppm).

^{31}P-NMR was performed after phosphitylation of the samples, according to standard protocols (Spyros et al., 1997). An accurately weighed amount of sample (about 50-100 mg) was dissolved in 500 µL of anhydrous $CDCl_3$. 100 µL of a standard solution of cholesterol (0.1 M in anhydrous $CDCl_3$/pyridine (1/1.6) solution) containing Cr(III) acetyl acetonate as relaxation agent was then added. Finally, 50 µL of 2-chloro-4,4,5,5-tetramethyl-1,3,2-dioxaphospholane (Cl-TMDP) were added and the mixture was stirred at room temperature for 2 h. Spectra were obtained on a Bruker 400 MHz spectrometer (128 scans at 20 °C). All chemical shifts reported are relative to the reaction product of water with Cl-TMDP, which gives a sharp signal in pyridine/$CDCl_3$ at 132.2 ppm. The quantitative analysis of end-groups and the calculation of molar masses by ^{31}P-NMR were performed based on previous reports (Siotto et al., 2013; Spyros et al., 1997).

The number-average molar mass (M_n), the mass-average molar mass (M_w) and the dispersity (Đ) of the polyesters samples were determined in chloroform by size exclusion chromatography (SEC), using a Shimadzu liquid chromatograph. PLGel Mixed-C and PLGeL 100 Å columns and refractive index detector were used. Chloroform was used as eluent at a flow rate of 0.8 ml/min. The apparatus was calibrated with linear polystyrene standards from 162 to 1 650 000 g/mol. Indeed, it is common knowledge that molar masses of polyesters determined by SEC in chloroform are overestimated due to the calibration based on PS standards. By using the Mark-Houwink-Sakurada (MHS) relation and specific MHS parameters (K and a) previously determined, a more accurate molar mass was calculated. Three different MHS parameters for PHB were found in the literature (Mark, 1999), and MHS-corrected molar mass are named $M_{n,SEC-1}$ ($K = 7.7x10^{-3}$ ml.g^{-1} and a = 0.82), $M_{n,SEC-2}$ ($K = 11.8\ 10^{-3}$ ml.g^{-1} and a = 0.78) and $M_{n,SEC-3}$ ($K = 16.6x10^{-3}$ ml.g^{-1} and a = 0.76).

Infrared spectroscopy (IR) was performed with a Nicolet 380 Fourier transformed infrared spectrometer (Thermo Electron Corporation) used in reflection mode and equipped with an ATR diamond module (FTIR-ATR). The FTIR-ATR spectra were collected at a resolution of 4 cm^{-1} and with 64 scans per run.

MALDI-TOF MS analysis was performed using a MALDI-TOF-TOF Autoflex II TOF-TOF (Bruker Daltonics) equipped with a nitrogen laser (λ = 337 nm) and super DHB (9:1 mixture of DHB and 2-hydroxy-5-methoxybenzoic acid) as matrix. Scan accumulation and data processing were performed with FlexAnalysis 3.0 software.

Differential scanning calorimetry (DSC) was performed using a TA Instrument Q 200 under nitrogen (flow rate of 50 mL/min), calibrated with high purity standards. Samples of 2-3 mg were sealed in aluminum pans. A three-step procedure with a 10 °C/min ramp was applied that involved: (1) heating up from room temperature to 185 °C and holding for 3 min to erase the thermal history, (2) cooling down to -80 °C and holding for 3 min, (3) heating (second heating) from -80 °C to the same temperature as the first heating. The degree of crystallinity (X_c) is calculated according to Equation (4.1.1),

$$X_c(\%) = \frac{\Delta H_m}{\Delta H_m{}^0} \times 100 \qquad (4.1.1)$$

where ΔH_m is the melting enthalpy and $\Delta H_m{}^0$ is the melting enthalpy of a 100% pure crystalline polyester. The values of $\Delta H_m{}^0$ for PHB and PEG are 146 and 197 J/g, respectively (Barham et al., 1984; Wei et al., 2014). From TGA results one can notice that no significant degradation occurred in the DSC analysis temperature range.

Thermal degradations were studied by thermogravimetric analyses (TGA). Measurements were conducted under helium atmosphere (flow rate of 25 mL/min) using a Hi-Res TGA Q5000 apparatus from TA Instruments. Samples (1-3 mg) were heated from room temperature up to 600 °C at a rate of 20 °C/min.

Wide angle X-ray Scattering (WAXS) data were recorded on a Siemens D5000 diffractometer using Cu K_α radiation (1.5406 Å) at 25-30 °C in the range of 2θ = 10-32° at 0.4 °.min^{-1}.

4. Results and discussion

4.1. Synthesis of PHB-diols – Study of the transesterification conditions

In order to obtain fully hydroxyl-terminated PHB oligomers (PHB-diol) as diol macromer for further reactions, the alcoholysis reaction was performed on high molar mass PHB at different temperatures in diglyme with an exces of diol (mostly 1,4-butanediol) and catalyzed by DBTL. The reaction procedure is described in Scheme 4.4.1. The PHB-diol structure was verified by SEC, FTIR and NMR.

The molar mass reduction of PHB with increasing transesterification times was followed by SEC in chloroform (Figure 4.1.1-a), whereas the evolution of the dispersity (Đ) during the alcoholysis is plotted in Figure 4.4.1-b. SEC curves shifted to higher retention time with the reaction time due to the reduction of molar masses.

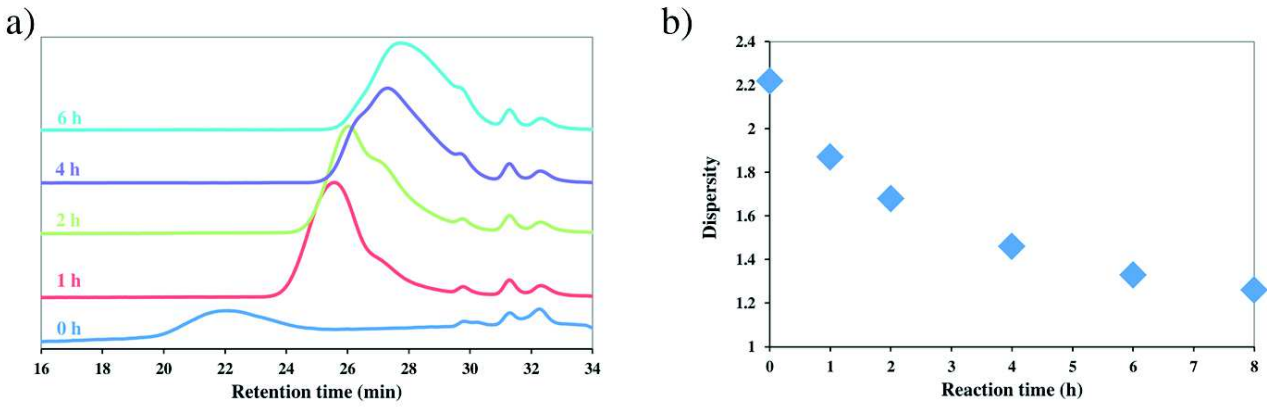

Figure 4.1.1 : (a) SEC profiles of PHB and PHB-diol samples from different reaction time of the tin-catalyzed molar mass reduction of PHB by 1000 eq. of 1,4-BDO and 2 eq. of DBTL at 130 °C; (b) Time evolution of the PHB-diol sample dispersity during the PHB molar mass reduction.

The FTIR analysis of PHB and PHB-diol oligomers (from 1,000 to 10,000 g/mol) is presented in Figure SI.25 (in Annex 7) and showed almost superimposed curves characterized by signals at 3000-2850, 1720, 1380, 1275, 1055 and

975 cm^{-1} assigned to the symmetric and antisymmetric C-H stretching vibration, the -C=O stretching vibration from ester groups, the CH_3 symmetric deformation, the symmetric C-C-O stretching vibration, the C-O stretching vibration and CH_3 rocking vibrations, respectively (Mark, 1999). However, as the molar mass of PHB-diol decreased, a large and low intensity peak appeared around 3300-3500 cm^{-1} assigned to the presence of hydroxyl or carboxylic acid end-groups, which were more abundant as the molar mass decreased (Figure 4.1.2-a).

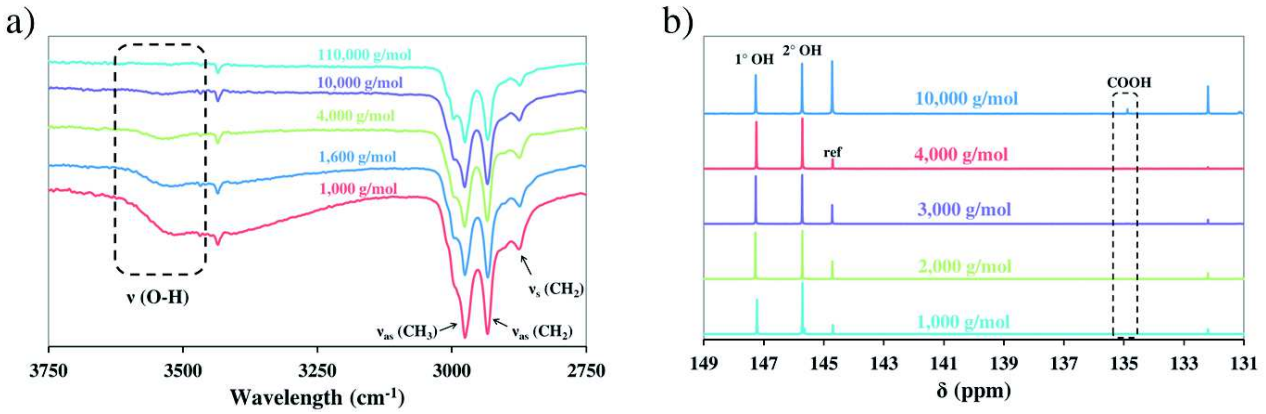

Figure 4.1.2 : (a) FTIR spectra mass focused on 2750-3750 cm^{-1} and (b) ^{31}P-NMR spectra of PHB-diol of various molar mass.

^{1}H-NMR of PHB-diol copolyesters was performed in $CDCl_3$ and results are presented in Figure 4.1.3-a. In ^{1}H-NMR, characteritics HB repetitive units were observed at δ = 5.26, 2.45-2.65 and 1.27 ppm for -C<u>H</u>(CH_3)-CH_2-CO-, -CH(CH_3)-C<u>H</u>$_2$-CO- and -CH(C<u>H</u>$_3$)-CH_2-CO- protons, respectively. The presence of hydroxyl end-groups on PHB-diol was confirmed by the presence of additional peaks signals at δ = 3.67 and 4.22 ppm ascribed to HO-C<u>H</u>$_2$-CH_2- and HO-C<u>H</u>(CH_3)-CH_2- protons from primary and secondary OH end-groups, respectively (more details in Annex 7).

To obtain more detailed information about the structure, ^{13}C-NMR, DEPT 135 and 2D-HSQC NMR in $CDCl_3$ were also performed and presented in Figure 4.1.3-b, Figure SI.26-a (in Annex 7) and Figure SI.26-b, respectively. ^{13}C chemical shifts at δ = 169.3, 67.7, 40.9 and 19.9 ppm were ascribed to -CH(CH_3)-CH_2-<u>C</u>O-, -<u>C</u>H(CH_3)-CH_2-CO-, -CH(CH_3)-<u>C</u>H_2-CO- and -CH(<u>C</u>H$_3$)-CH_2-CO- carbons from HB repetitive units, respectively. The presence of primary OH end-groups from 1,4-BDO units was confirmed by signals at δ = 172.1, 64.7, 62.3, 29.2 and 25.2 ppm, whereas the presence of scondary OH end-groups was confirmed by ^{13}C chemical shifts at δ = 170.3, 64.5, 43.4 and 22.6 ppm.

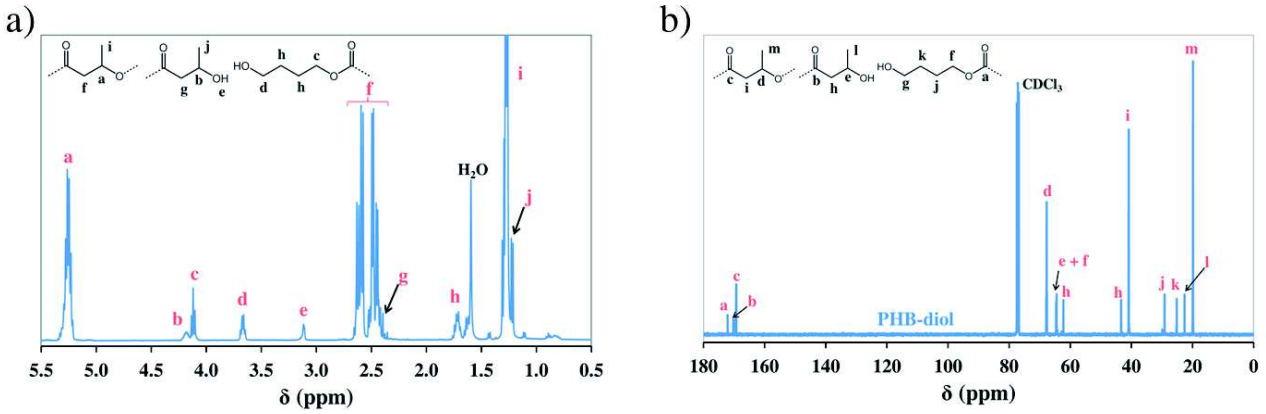

Figure 4.1.3 : (a) ^{1}H- and (b) ^{13}C-NMR spectra of PHB-diol oligomers in $CDCl_3$.

^{31}P-NMR analyses of PHB-diol were performed in $CDCl_3$ with cholesterol as standard and ^{31}P-NMR spectra are presented in Figure 4.1.2-b. Results proved the presence of primary and secondary OH ending groups at δ = 145.8 and 147.1 ppm, respectively. Moreover, the absence of carboxylic ending groups (δ = 134.9 ppm) in PHB-diol oligomers for molar mass lower or equal to 4,000 g/mol was verified.

Finally, a PHB-diol sample of a molar mass of approx. 2,100 g/mol (determined by SEC) was analyzed by MALDI-ToF MS. The MALDI-ToF MS spectrum with peak interpretation is presented in Figure 4.1.4. Three oligomeric species with different end-groups were identified. Oligomers are terminated either by hydroxyl/hydroxyl, acid/hydroxyl or vinyl/hydroxyl end-groups. The majority of species were hydroxyl/hydroxyl which is in agreement with ^{31}P-NMR results. However, contrary to the ^{31}P-NMR analysis, the presence of acid end-groups was observed, at tiny intensity, since structures with acid/hydroxyl end-groups were identified. Finally, the presence of vinyl end-groups from the PHB thermal degradation was observed for low molar mass oligomers (M_n < 750 g/mol) (Abe, 2006; Grassie et al., 1984a; Hablot et al., 2008).

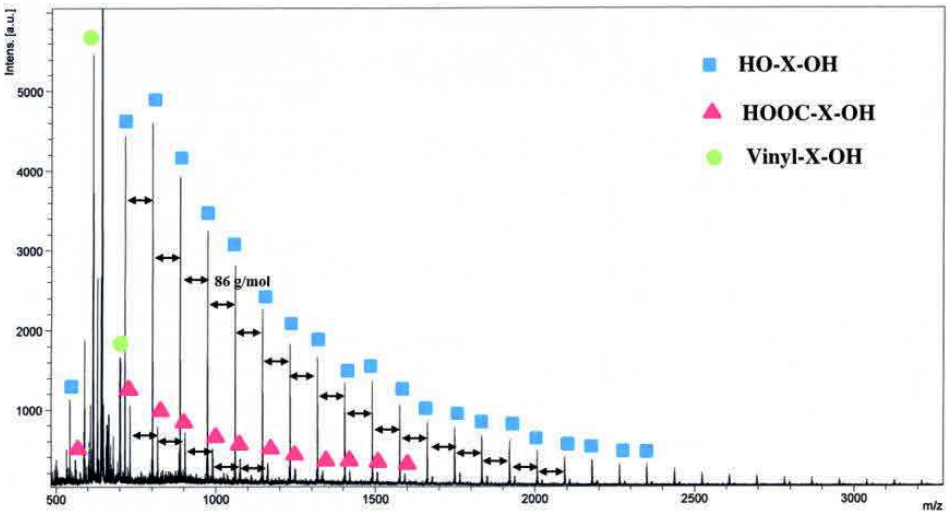

Figure 4.1.4 : MALDI-ToF MS spectrum of PHB-diol with peak interpretation.

The influence of the reaction temperature (*i.e.,* 110, 120, 130 and 140 °C), the PHB/DBTL molar ratio (1/1, 1/2, 1/4 and 1/8), the PHB/alcohol molar ratio (1/100, 1/500, 1/1000 and 1/3000) and the diol chain length (1,3-PDO, 1,4-BDO, 1,6-HDO and 1,10-DCO) was discussed according to the alcoholysis rate, the end-group analysis and the product aspect. The alcoholysis rate was determined following the molar mass of synthesized PHB-diol oligomers obtained by SEC. Moreover, at a constant temperature, the variation of the average number of bond cleavages per original polymer molecule (N_t) with the reaction time could be calculated according to Equation (4.1.2) (Abe, 2006; Aoyagi et al., 2002; Grassie et al., 1984c),

$$N_t = \frac{M_{n,0}}{M_{n,t}} - 1 = K \times t \qquad (4.1.2)$$

where $M_{n,0}$ and $M_{n,t}$ represent the number-average molar mass at time 0 and t, respectively, and K is the rate constant of PHB alcoholysis.

Plots of M_n *vs.* reaction time for the different studies are presented in Figure 4.1.5, whereas K values, summarized in Table 4.1.1, were obtained from the slope of linear plots of N_t *vs.* reaction time (Figure SI.29 in Annex 7). The plot of $M_{n,t}$ *vs.* reaction time showed that all curves exhibited an inverse-exponential shape with a high reduction of the molar mass at the beginning of the reaction and the presence of a plateau after few hours of reaction, whereas plots of N_t. *vs.* reaction time at the beginning of reaction (*i.e.,* from 0 to 4 h) showed a linear relation with good correlation coefficients. One can observe that by increasing the time range until 8 h, the relation was no more verified. Finally, it was interesting to remark that in each case the dispersity of PHB oligomers decreased with the reaction time due to the randomness of the alcoholysis reaction and permitting the synthesis of PHB-diol oligomers with narrow dispersity of approx. 1.5 (Figure 4.1.1-b).

As expected, the molar mass reduction increased with (i) the amount of catalyst, (ii) the reaction temperature and (iii) the diol amount. However, even if a high amount of DBTL (*i.e.,* 8 molar equivalent (eq.)) permited the increase of the alcoholysis rate and then achieved targeted low molar mass and hydroxyl end-groups quickly (*i.e.*, 4 h instead of 8 h for the PHB alcoholysis with 1,000 eq. of 1,4-BDO at 120 °C) (Figure 4.1.5-a), the synthesized PHB-diol oligomers tend to yellowish, after few hours of reaction. Moreover, the alcoholysis rate (K) increased of only 36% by double the DBTL amount from 4 to 8 eq. (Table 4.1.1). The use of 4 eq. of DBTL seemed, thus, as a good compromise.

On one side, the low amount of diol (*i.e.,* ratios 1/100 and 1/500) decreased drastically the alcoholysis rate (*i.e.,* K equal to 1.5 and 4.2, respectively) and, thus, did not permit the synthesis of low molar mass PHB oligomers only based on hydroxyl ending groups. For example, after 8 h of reaction at 120 °C with 2 eq. of DBTL, PHB oligomers still possessed 28 and 5% of acid end-groups for PHB/alcohol molar ratio of 1/100 and 1/500, respectively. On the other side, a very high excess of diol (*i.e.*, ratio 1/3000) as it was used in previous studies did not increase significantly the alcoholysis rate compared to the diol excess used (Figure 4.1.5-b) (Hirt et al., 1996; Andrade et al., 2002). Indeed, when the diol amount triples, K increased only from 10.6 to 19.9 h^{-1}. The 1/1000 (PHB/alcohol) ratio seemed, thus, a good comprise between the alcoholysis rate and the limitation of monomer waste.

The low thermal stability of PHB (Abe, 2006), in which secondary hydroxyl end-groups can form crotonyl end-groups by dehydration (Scheme SI.2), limits the reaction temperature below 145 °C (Hirt et al., 1996). This study showed that a reaction temperature of 110 °C did not permit to obtain low molar mass oligomers (Figure 4.1.5-c) due to the low alcoholysis rate (K = 4.4 h^{-1}) and the limited solubility of PHB in diglyme at the studied concentration (0.2 g of PHB/mL). At the opposite site, a reaction temperature of 140 °C permitted the high alcoholysis rate (K = 21.2 h^{-1}) leading to low molar mass oligomers, but synthesiszed oligomers were slightly yellowish. However, ^{1}H-NMR did not exhibit the presence of crotonyl end-groups (generally observed at ^{1}H chemical shifts near 6-7 ppm) (Hablot et al., 2008).

The alcoholysis rate of PHB by different chain length of aliphatic diol was partially studied. Previous study showed for instance, that aliphatic diols were more reactive than glycerol (Špitalský et al., 2006). However, the investigation of the effect of the aliphatic diol chain length on the reaction rate has never been investigated. Figure 4.1.5-d and Table 4.1.1 exhibited that the diol chain length have no influence on the alcoholysis rate of PHB and only modified the primary hydroxyl end-group structure. Anyway, due to the higher T_m of 1,6-HDO and 1,10-DCO, which are solid at room tempertaure and have a low solubility in precipitation solvents (water and petroleum ether), the purification of PHB-diol with these two diols were complicate and, thus, 1,6-HDO and 1,10-DCO were not suitable.

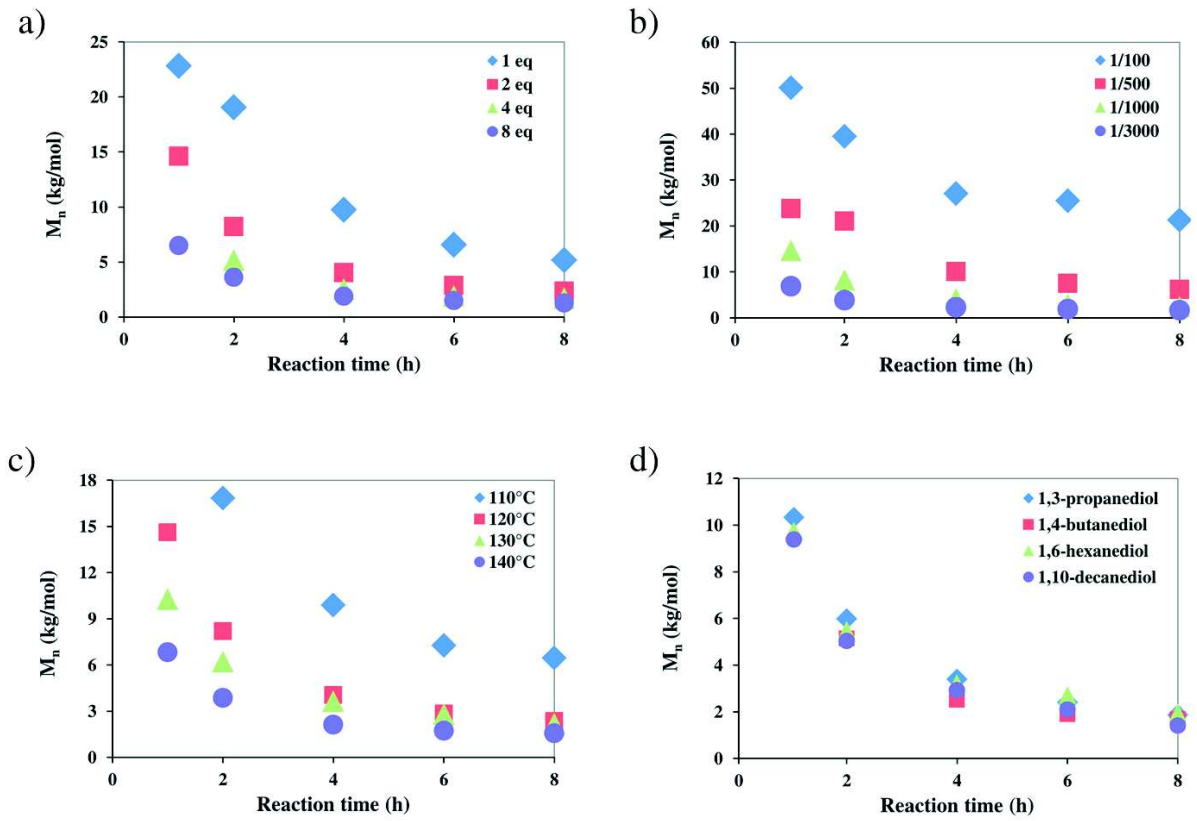

Figure 4.1.5 : Plots of M_n vs. reaction time for the PHB molar mass reduction at (a) different DBTL amounts, (b) different 1,4-BDO amounts, (c) different reaction temperature and (d) with different aliphatic diols.

Table 4.1.1 : Alcoholysis rate constants of different systems.

Influence of the diol amount [a]		Influence of the DBTL amount [b]		Influence of the temperature [c]		Influence of the diol [d]	
PHB/1,4-BDO ratio	K (h^{-1})	PHB/DBTL ratio	K (h^{-1})	Temperature (°C)	K (h^{-1})	Diol type	K (h^{-1})
1 / 100	1.5	1 / 1	4.4	110	4.4	1,3-PDO	13.2
1 / 500	4.2	1 / 2	10.6	120	10.6	1,4-BDO	17.3
1 / 1,000	10.6	1 / 4	17.3	130	12.5	1,6-HDO	14.1
1 / 3,000	19.9	1 / 8	23.6	140	21.2	1,10-DCO	15.5

[a] PHB alcoholysis with 1,4-BDO at 120 °C with 2 eq. of DBTL. [b] PHB alcoholysis with 1,000 eq. of 1,4-BDO at 120 °C. [c] PHB alcoholysis with 1,000 eq. of 1,4-BDO and 2 eq. of DBTL. [d] PHB alcoholysis at 120 °C with 1,000 eq.of diol and 4 eq. of DBTL.

4.2. Comparison of different methods to determine the PHB-diol molar mass

In order to obtain more accurate molar masses of the synthesized PHB-diols, four different methods were used and compared such as SEC in chloroform with Mark-Houwink-Sakurada (MHS) correction, ^{31}P-NMR in $CDCl_3$, ^{1}H-NMR in $CDCl_3$ and ^{1}H-NMR in DMSO-d_6. The $M_{n,1H\text{-}NMR,CDCl3}$ and $M_{n,1H\text{-}NMR,DMSO}$ determinations were based on relative intensities of characteristic signals of (i) methine protons in HB units, (ii) methylene protons in α of primary hydroxyl end-groups and (iii) methine protons in α of secondary hydroxyl end-groups. $M_{n,1H\text{-}NMR,CDCl3}$ and $M_{n,1H\text{-}NMR,DMSO}$ were calculated according to Equations (SI.37) and (SI.39), respectively. The $M_{n,1H\text{-}NMR,DMSO}$ determination can be used only for PHB-diol oligomers lower than 2,000 g/mol because of the insolubility of longer PHB-diol oligomers in DMSO. The $M_{n,31P\text{-}NMR}$ determination was based on the quantification of hydroxyl and carboxylic end-groups according to previous studies (Spyros et al., 1997). Moreover, ^{1}H-NMR in $CDCl_3$ and DMSO-d_6 permitted to determine the primary/secondary OH end-groups ratio according to Equations (SI.38) and (SI.40), respectively, such as with ^{31}P-NMR. Results showed that PHB-diol oligomers exhibited a slight excess of secondary hydroxyl end-groups *vs.* primary hydroxyl end-groups (ratio ~ 1/0.9) likely arising from the initial presence of secondary hydroxyl end-groups in PHB. $M_{n,SEC}$ determination was based on SEC analysis with MHS correction.

Plots of $M_{n,1H\text{-}NMR,CDCl3}$ *vs.* $M_{n,31P\text{-}NMR}$, $M_{n,1H\text{-}NMR,DMSO}$ *vs.* $M_{n,31P\text{-}NMR}$ and $M_{n,1H\text{-}NMR,DMSO}$ *vs.* $M_{n,1H\text{-}NMR,CDCl3}$ are presented in Figures 4.1.6-a,b,c and data are summarized in Table SI.10. Results showed that molar masses obtained from these three methods are in good agreement. However, due to the limitation of the PHB solubility in DMSO, NMR analysis in this solvent was not the most adapted technique. Plots of $M_{n,31P\text{-}NMR}$ *vs.* $M_{n,SEC\text{-}1}$ ($K = 7.7x10^{-3}$ ml.g^{-1} and $a = 0.82$), $M_{n,31P\text{-}NMR}$ *vs.* $M_{n,SEC\text{-}2}$ ($K = 11.8\ 10^{-3}$ ml.g^{-1} and $a = 0.78$) and $M_{n,31P\text{-}NMR}$ *vs.* $M_{n,SEC\text{-}3}$ ($K = 16.6x10^{-3}$ ml.g^{-1} and $a = 0.76$) are presented in Figure 4.1.6-d and Figure SI.30. Results exhibited that the MHS correction with $K = 16.6x10^{-3}$ ml.g^{-1} and $a = 0.76$ (SEC-3) was more appropriate for PHB-diol oligomers even if the correlation became lower at high molar mass and, thus, these MHS parameters (*i.e.,* $K = 16.6x10^{-3}$ ml.g^{-1} and $a = 0.76$) were selected for the rest of the study.

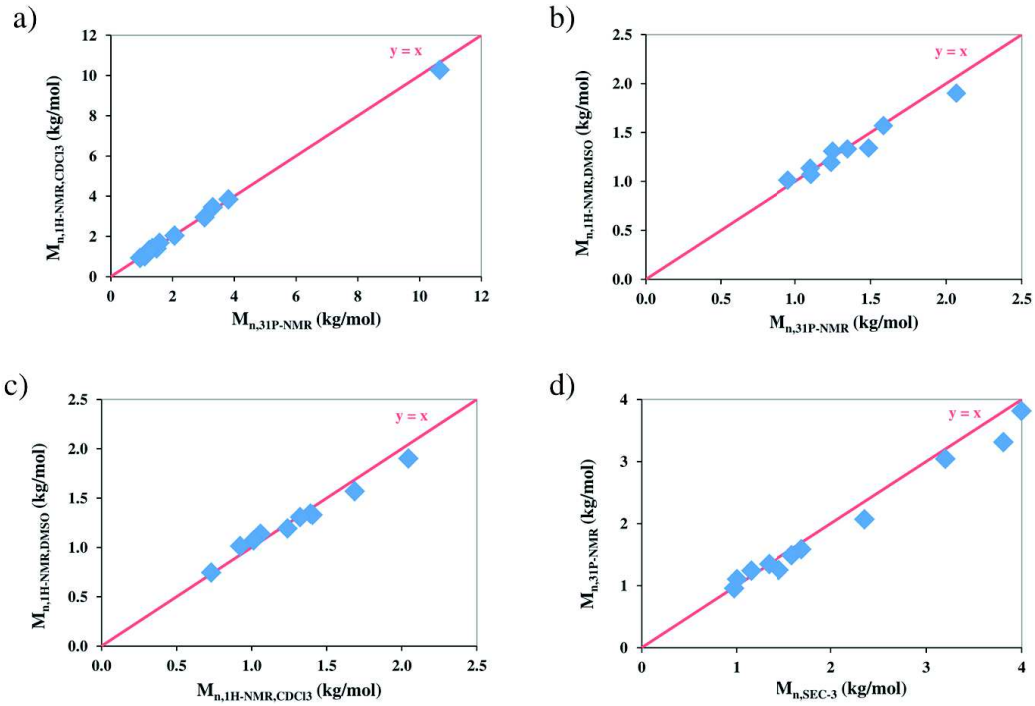

Figure 4.1.6 : Plots of (a) $M_{n,1H\text{-}NMR,CDCl3}$ vs. $M_{n,31P\text{-}NMR}$, (b) $M_{n,1H\text{-}NMR,DMSO}$ vs. $M_{n,31P\text{-}NMR}$, (c) $M_{n,1H\text{-}NMR,DMSO}$ vs. $M_{n,1H\text{-}NMR,CDCl3}$ and (d) $M_{n,31P\text{-}NMR}$ vs. $M_{n,SEC\text{-}3}$.

4.3. Influence of PHB-diol molar mass on thermal properties and the crystalline structure

TGA traces of PHB and PHB-diol oligomers are presented in Figure 4.1.7-a with their derivatives (DTG) curves and data are summarized in Table SI.11. Results showed that all samples had a good thermal stability under helium since no mass loss was recorded before 225 °C. By taking the 2% mass loss degradation temperature ($T_{d,2\%}$) as criterion for the thermal stability, $PHB_{110,000}$, which is the corrected molar mass of initial PHB by the MHS relation, possessed the highest thermal stability, since no mass loss was reported before 260 °C, as a result of it high molar mass. Contrary to $PHB_{110,000}$ which degraded in one step, PHB-diols degraded in two steps. First, a small mass loss was observed at 225-250 °C due to the cyclization of chains-ends and back-biting reactions (Persenaire et al., 2001). Secondly, a major degradation occurred between 250 and 310 °C, with a maximum degradation rate temperature ($T_{deg,max}$) at approximatively 280 °C, with a substantial mass loss of 90-95% mostly by *cis*-elimination responsible for the formation of oligomers with crotonic acid end-groups (Abe, 2006). This multi-steps degradation was in agreement with previous reports (Debuissy et al., 2017a, 2016a, 2016b). PHB-diol samples did not show any difference of stability or thermal degradation profile with M_n varying between 1,000 and 10,000 g/mol.

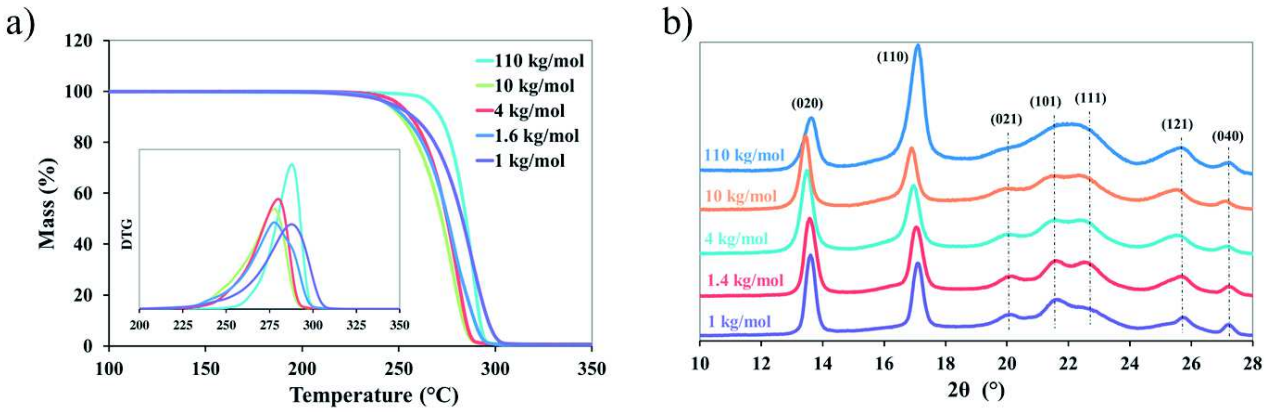

Figure 4.1.7 : (a) Mass loss and DTG curves of PHB and PHB-diol of various molar mass under helium at 20 °C/min, and (b) WAXS pattern of high molar mass PHB and PHB-diol oligomers.

Figure 4.1.7-b exhibits the WAXS analysis of PHB and PHB-diol oligomers. Results showed that PHB-diol oligomers presented quasi similar diffraction signals to PHB with two intense diffraction signals at 2θ = 13.6 and 17.1° (Khasanah et al., 2015). However, the intensity of the diffraction peak at 2θ = 20.1° decreased with the molar mass, whereas the one at 2θ = 22.5° increased leading to the formation of a single broad peak centered at 2θ = 21.7° corresponding to (101) plane. This modification can be due to the decrease of the degree of crystallinity observed by DSC.

The thermal behavior of PHB and PHB-diol oligomers monitored by DSC is presented in Figure 4.1.8 and data are summarized in Table SI.11. The crystallization temperature (T_c) of PHB-diol decreased (except for PHB) as the PHB-diol M_n decreased until the disappearance of the crystallization for PHB-diol$_{1000}$. During the heating run, PHB-diol$_{1000}$ was the only sample to exhibit a glass transition phenomenon at approximatively -24 °C, whereas high molar mass PHB should have a T_g around -2 °C (Barham et al., 1984). The glass transition phenomenon of PHB-diol with M_n > 1000 g/mol was not observed due to the high degree of crystallinity of samples. The reduction of the PHB-diol chain length thus lowered the chain rigidity and T_m decreased from 175 to 105 °C for high molar mass PHB and PHB-diol$_{1000}$, respectively. X_c of PHB-diols did not show significant variation for molar mass higher than 1600 g/mol, but decreased significantly for lower molar masses. The drop of (i) T_m, (ii) the chain rigidity and (iii) X_c with the decrease of the PHB-diol chain length could, thus, improve the solubility of PHB samples in solvent as observed with DMSO-d_6.

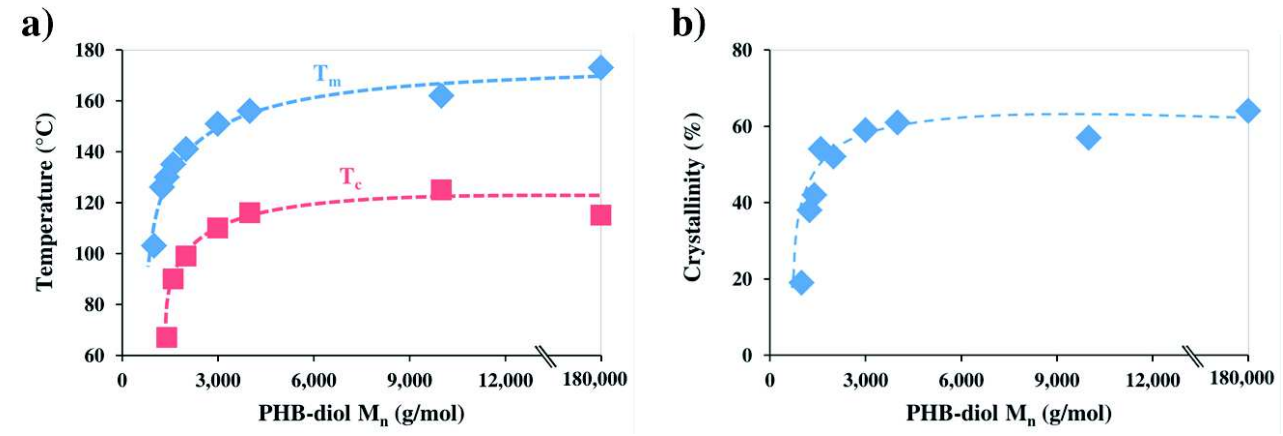

Figure 4.1.8 : Plots of (a) T_m and T_c and (b) the crystallinity in function of the PHB-diol M_n.

4.4. Synthesis of PHB-based poly(ester-ether-urethane)s

Few series of PHB-based poly(ester-ether-urethane)s (PEEUs) were synthesized in high yields *via* a one-step process in 1,2-dichlorethane at 75 °C catalyzed by DBTL using PHB-diol oligomers of different chain lengths, three different polyether segment diols (P_{ether}) (PEG-2000, PEG-4000 or PPG-PEG-PPG) at different P_{ether}/P_{ester} ratios and modified 4,4'-MDI. The increase of the reaction temperature was not possible due to the chosen solvent (boiling point of 1,2-dichlorethane at 85 °C). The PEEUs molar masses determined by SEC are presented in Table 4.1.2. M_n values of approximately 15,400-22,000 g/mol were obtained with a large dispersity (Đ) ranging from 5 to 12. This last result is not on agreement with a previous study which used HDI as coupling agent and obtained PEEUs with Đ around 1.5 (Loh et al., 2007a). One can suppose that, in our case, the high Đ was due to the higher reactivity of 4,4'-MDI compared to HDI and the higher concentration of reactants during the PEEU synthesis leading to a faster but more heterogeneous reaction. After the synthesis, PEEUs physical aspects varied according to (i) the PHB-diol M_n, (ii) the P_{ether}/P_{ester} ratio and (iii) the nature of the P_{ether}. Indeed, PEEUs were viscous or soft using PPG-PEG-PPG whereas they were solid using PEG as polyether. Likewise, PPG-PEG-PPG-based PEEUs became less fluid as the PHB-diol M_n and the HB content increased.

Table 4.1.2 : Molecular characteristics of the synthesized PEEUs.

Sample	P_{ether} structure	M_n of PHB-diol	P_{ether}/P_{ester} ratio	PHB content [a]	M_n	M_w	Đ	Aspect
		g/mol	mol.%	wt.%	kg/mol	kg/mol		
PU-A1	PPG-PEG-PPG	2,350	80 / 20	16.2	15.5	101	6.5	Soft
PU-A2	PPG-PEG-PPG	1,600	80 / 20	11.6	19.8	201	10.1	Soft
PU-A3	PPG-PEG-PPG	950	80 / 20	7.2	17.4	167	9.6	Viscous
PU-A4	PPG-PEG-PPG	950	65 / 35	14.1	14.5	102	7.0	Viscous
PU-A5	PPG-PEG-PPG	950	50 / 50	22.7	14.8	73	4.9	Soft
PU-B1	PEG-2000	950	50 / 50	23.8	22.4	257	11.5	Solid
PU-B2	PEG-2000	1,600	50 / 50	34.5	16.4	148	9.0	Solid
PU-B3	PEG-2000	2,350	50 / 50	43.6	15.5	144	9.3	Solid
PU-B4	PEG-2000	2,350	65 / 35	30.2	15.4	108	7.0	Solid
PU-B5	PEG-2000	2,350	80 / 20	17.1	14.0	94	6.7	Solid
PU-C1	PEG-4000	2,350	50 / 50	36.5	13.7	67	4.9	Solid

[a] Feed HB content introduced in the reactor for the synthesis of PEEUs.

The chemical structures of PEEUs with polyester and polyether segments were verified by FTIR, ^{1}H- and ^{13}C-NMR. FTIR spectra are presented in Figure 4.1.9 and Figure SI.31, respectively. Results showed that the O-H vibration of PHB-diol oligomers and NCO functions at respectively 3500 and 2300 cm^{-1} disappeared. Distinctive absorption bands of the urethane group are observed at 3300-3400 and 1535 cm^{-1} belonging to the N-H unit in the urethane linkage. The absorption bands at 2940 and 2870 cm^{-1} are associated to the asymmetric and symmetric stretching $–CH_2$- groups, while other vibration modes of $-CH_2$- are observed at 1460, 1370 and 1240 cm^{-1}. The methyl $-CH_3$ stretching vibration of HB and PPG units appeared at 2980 cm^{-1} and was intense for PU-A series (Figure 4.1.9-a). The characteristic absorption at 1720 cm^{-1} corresponds to the carbonyl stretching of the ester group in PHB overlapped with the carbonyl of the urethane function. The intensity of this band increased with the HB content (Figure 4.1.9-b). The signal at 1100 cm^{-1}, assigned to the C-O-C stretching vibration of ether and ester functions from both diols, increased with the P_{ether} amount. Finally, contrary to PU-A series, PU-B series exhibited strong $-CH_2$- rocking vibrations at 960 and 840 cm^{-1} which increased with the PEG content (Figure 4.1.9-b).

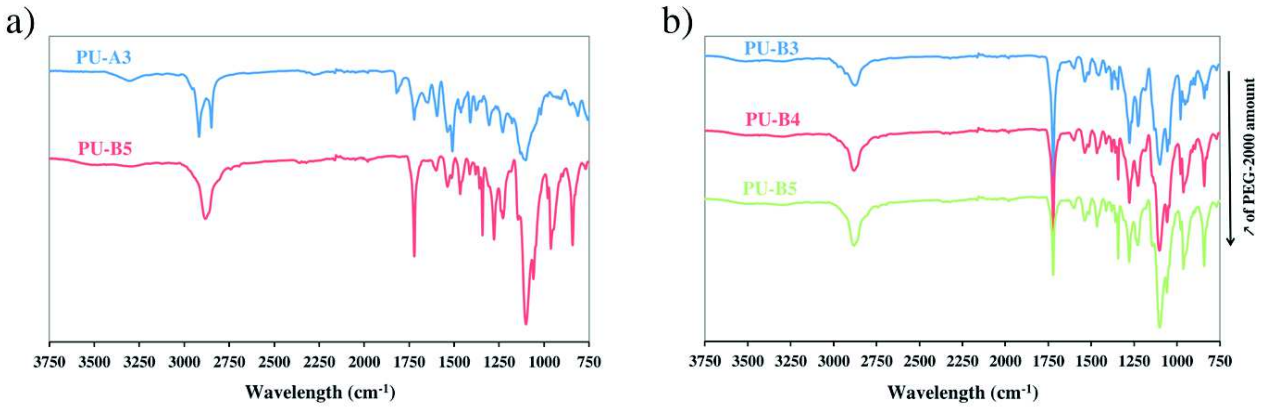

Figure 4.1.9 : FTIR spectra of (a) typical samples from PU-A and PU-B series and (b) PU-B PEEUs with various P_{ether}/P_{ester} ratios.

Figure 4.1.10-a shows, as a typical example, the ^{1}H-NMR spectrum of PU-A5 in $CDCl_3$, in which all proton signals belonging to PHB, PPG-PEG-PPG and modified 4,4'-MDI were confirmed. The peak assignment of PEEU was performed by comparison with ^{1}H-NMR spectra of the precursors (see Figure 4.1.3-a and Figure SI.32-a). The signal corresponding to methylene protons in PEG repetitive units was observed at 3.64 ppm. ^{1}H chemical shifts at δ = 3.54, 3.41 and 1.12 ppm were assigned to O-CH_2-C<u>H</u>(CH_3)-, O-C<u>H_2</u>-CH(CH_3)- and O-CH_2-CH(C<u>H_3</u>)-protons of PPG repetitive units, respectively. The presence of HB segments was confirmed by the signal at δ = 5.25 and 2.56 ppm assigned to methine and methylene protons of PHB, respectively. Finally, the presence of 4,4'-MDI was confirmed by

the presence of signals at δ = 7.30-7.10 and 3.87 ppm assigned to aromatic and methylene protons, respectively. ^{13}C-NMR was used to ascertain the chemical composition of PEEU. Figure 4.1.10-b shows the ^{13}C-NMR spectrum of PEEU-4 in $CDCl_3$. The peak assignments of PEEU were performed by comparison with ^{13}C-NMR spectra of the precursors (see Figure 4.1.3-b and Figure SI.32-b). Briefly, ^{13}C chemical shifts at δ = 17.5, 73.5 and 75.4 ppm were ascribed to O-CH_2-CH($\underline{C}H_3$)-, O-$\underline{C}H_2$-CH(CH_3)- and O-CH_2-$\underline{C}$H(CH_3)- carbons of PPG segments, whereas the one at δ = 70.7 ppm was assigned to methylene carbons of the PEG segment. Signals at δ = 19.9, 40.9, 67.7 and 169.3 ppm were assigned to methyl, methylene, methine and carbonyl carbons of PHB segment. Finally, peaks attributed to the 4,4'-MDI junction unit could be observed at δ = 40.8 and 115-140 ppm for methylene and aromatic carbons, respectively.

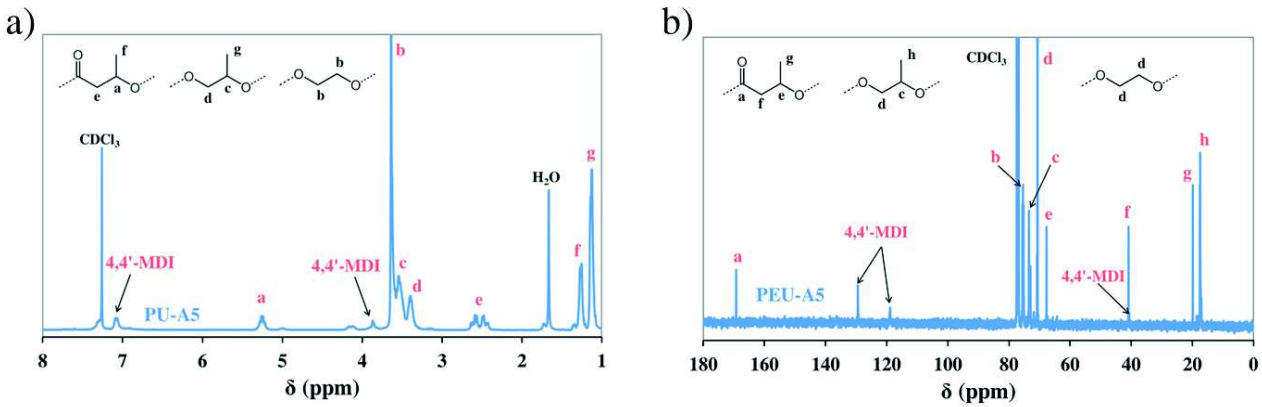

Figure 4.1.10 : (a) ^{1}H and (b) ^{13}C-NMR spectra of PU-A5 (typical example from PU-A samples) in $CDCl_3$.

Typical TGA traces of PEEUs and their derivatives curves (DTG) are presented in Figure 4.1.11. Main data are summarized in Table 4.1.3. Under helium, all samples exhibited a good thermal stability since no mass loss was recorded before 200 °C and $T_{d,2\%}$ of all PEEUs were at approximatively 220-240 °C. All samples degraded in two steps with first a degradation at 220-325 °C assigned to the PHB degradation with a $T_{deg,max}$ at approximatively 270 °C and followed by a major degradation at 350-425 °C assigned to the P_{ether} thermal degradation with a $T_{deg,max}$ at approximatively 380 and 395 °C for PPG-PEG-PPG- and PEG-based PEEUs, respectively. The first degradation mass loss increased with the HB content and calculated mass losses were similar to the HB content. At the end, mass residues of 1-3% still remained at 500 °C.

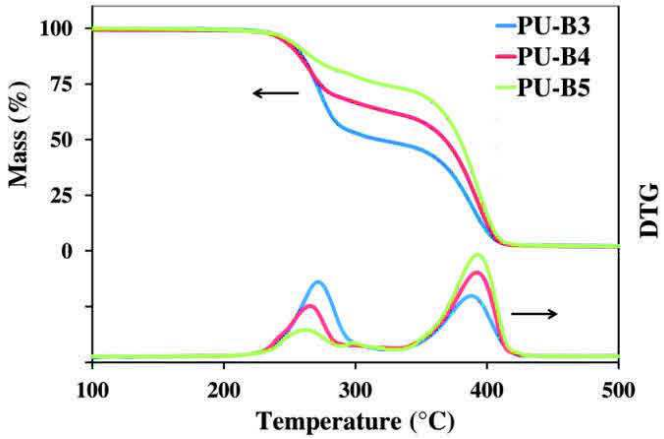

Figure 4.1.11 : Mass loss and DTG curves of PEUs with PEG-2000 as polyether under helium at 20 °C/min.

Table 4.1.3 : TGA results of PEEUs samples under helium at 20 °C/min.

Sample	PHB content	$T_{d,2\%}$	1st degradation		2nd degradation		Residue at 500 °C
			$T_{deg,max,PHB}$	Mass loss	$T_{deg,max,Pether}$	Mass loss	
	wt.%	°C	°C	wt.%	°C	wt.%	wt.%
PU-A1	25.1	237	278	25	382	73	1.5
PU-A2	21.5	238	270	22	379	75	1.6
PU-A3	17.6	247	280	18	375	79	1.4
PU-A4	25.6	242	289	26	379	71	1.8
PU-A5	35.6	239	288	36	380	61	1.7
PU-B1	42.8	227	255	37	394	58	3.4
PU-B2	46.2	235	271	42	405	55	2.1
PU-B3	52.8	235	273	50	390	47	2.2
PU-B4	39.5	230	265	37	392	60	2.0
PU-B5	26.5	233	262	26	393	71	2.1
PU-C1	44.9	220	251	41	392	56	1.8

The thermal behavior of PEEUs was analyzed by DSC and the corresponding data are summarized in Table 4.1.4. The degree of crystallinity of both segments was determined from the second heating scan using Equation (4.1.1) and the melting enthalpy value of 100% crystalline phase of PEG and PHB determined in previous studies (Barham et al., 1984; Wei et al., 2014). The corresponding X_c values are summarized in Table 4.1.4.

PPG-PEG-PPG-based PEEUs (PU-A) exhibited a T_g at approximatively -50 °C with small crystallization and melting phenomena. During the cooling run, contrary to neat PPG-PEG-PPG, none of the PU-A samples exhibited crystallization from PPG-PEG-PPG segments, confirming the decrease of the P_{ether} mobility in PEEUs and the lack of rearrangement. $T_{c,PHB}$ and $\Delta H_{c,PHB}$ assigned to PHB crystals increased with the PHB-diol M_n and the HB content. Even PU-A4 and PU-A5, which are PU-A samples with low PHB-diol M_n (*i.e.,* 950 g/mol) but high HB content (*i.e.,* 35-50 mol.%), were able to crystallize, to a small extent, at approximatively 40 °C. During the second heating run, T_g of PU-A samples did not vary with the PHB-diol chain length, but increased with the HB content to reach values ranging from -55 to -45 °C for HB content of 20 to 50 mol.%, respectively. One can suppose that the T_g was ascribed to the P_{ether} blocks and the rigidity of this block increased with the HB content. Moreover, PU-A with high proportion of PPG-PEG-PPG (*i.e.,* 80/20) showed a cold-crystallization (T_{cc}) phenomenon from -25 to -10 °C assigned to the PPG-PEG-PPG crystallization. However, the formed crystals subsequently melted at approximatively 5 °C and so did not bring any crystallinity to PU-A samples at room temperature. The enthalpy of the PPG-PEG-PPG cold-crystallization ($\Delta H_{cc,PPG-PEG-PPG}$) increased with the PHB-diol M_n, whereas T_{cc} decreased. One can suppose that this is due to the higher $X_{c,PHB}$ of PU-A samples with long PHB-diol segments after the cooling run. This results in an amorphous phase richer in PPG-PEG-PPG improving, thus, the corresponding cold-crystallization. For lower PPG-PEG-PPG content, no cold-crystallization was observed. PPG-PEG-PPG had difficulties to crystallize, even at high molar mass (*i.e.,* 2,700 g/mol), due to the triblock structure and the PPG unit structure. Finally, $T_{m,PHB}$ of small PHB crystalline phases slightly increased with the PHB-diol M_n and the HB content due to the higher crystal strength.

Compared to PU-A samples, PEG-2000-based PEEUs (PU-B) exhibited a higher degree of crystallinity and a higher T_g at approximatively -10 °C. Contrary to PU-A samples, both segments in PU-B samples melted at temperature higher than 25 °C, whence the solid physical aspect of these PEEUs at room temperature. During the cooling run, both PHB and PEG segments crystallized except for PU-B1 as a result of its low PHB-diol molar mass. $T_{c,PHB}$ and $\Delta H_{c,PHB}$ increased with the PHB-diol M_n and HB content, whereas the opposite trend was observed for the PEG phase. Surprisingly, the PEG phase was not able to crystallize in PU-B1 likely because of the absence of a PHB crystalline phase leading to a rich PHB amorphous phase preventing the PEG crystallization. During the second heating run, the observed T_g, at respectively -9 and -12 °C for PU-B4 and PU-B5, were assigned to the PHB phase and seemed to increase with the HB content. An intense cold-crystallization phenomenon linked to PEG was observed for PU-B samples with high HB content. Furthermore, T_m and X_c of the PEG crystalline phase increased with the PEG content from 39 to 48 °C and from 19 to 45% for P_{ether}/P_{ester} ratio of 50/50 and 80/20, respectively, without a significant influence of the PHB-diol M_n. On the other side, T_m and especially X_c of the PHB crystalline phase increased with the PHB-diol M_n and the HB content, as observed for PU-A.

Finally, the influence of the PEG chain length on thermal properties was studied. PU-C1 was synthesized with the same PHB-diol M_n and P_{ether}/P_{ester} ratio than PU-B3 but with a two times longer PEG segment. Due to the use of a longer PEG segment for an identical molar P_{ether}/P_{ester} ratio, the HB mass content of PU-C1 was lower than the one of PU-B3. That is why, $\Delta H_{c,PHB}$ was lower for PU-C1 than PU-B3, whereas $\Delta H_{c,PEG}$ was higher. Moreover, longer PEG segments had enough mobility to crystallize to their maximum level during the cooling run and, thus, no cold-crystallization phenomena were observed. As expected, $T_{m,PEG}$ and $X_{c,PEG}$ with PEG-4000 was higher than with PEG-2000 due to the stronger crystals obtained with PEG-4000. This result was in agreement with the study of Loh *et al* (Loh et al., 2007b).

Table 4.1.4 : Thermal properties of the synthesized PEEUs.

Sample	Cooling				Second heating								
	PHB phase		P_{ether} phase			P_{ether} phase					PHB phase		
	T_c	ΔH_c	T_c	ΔH_c	T_g	T_{cc}	ΔH_{cc}	T_m	ΔH_m	X_c	T_m	ΔH_m	X_c
	°C	J/g	°C	J/g	°C	°C	J/g	°C	J/g	%	°C	J/g	%
PPG-PEG-PPG	-	-	-25	44	-65	-	-	13	47	24	-	-	0
PEG-2000	-	-	21	163	n.o.	-	-	52	179	91	-	-	0
PEG-4000	-	-	34	176	n.o.	-	-	57	180	91	-	-	0
PU-A1	98	9	-	-	-56	-24	15	5	15	8	144	7	5
PU-A2	95	3	-	-	-55	-12	6	5	7	4	139	2	1
PU-A3	-	-	-	-	-55	-9	3	5	3	2	-	-	0
PU-A4	36	1	-	-	-51	-	-	-	-	0	84	3	2
PU-A5	46	3	-	-	-45	-	-	-	-	0	88	7	5
PU-B1	-	-	-	-	n.o.	13	33	34	34	17	-	-	0
PU-B2	89	21	-13	17	n.o.	-27	28	37	47	24	138	18	12
PU-B3	103	27	-11	2	n.o.	-26	32	39	38	19	146	23	16
PU-B4	102	15	6	52	-9*	-	-	42	58	29	144	11	8
PU-B5	93	8	-5	75	-12*	-	-	48	88	45	141	6	4
PU-C1	104	20	18	54	-11*	-	-	53	54	27	146	18	12

n.o. not observed. * T_g assigned to the PHB segment.

WAXS patterns of PEEUs are presented in Figure 4.1.12. For PU-A samples (Figure 4.1.12-a), WAXS patterns confirmed DSC results on the absence of a crystalline phase assigned to the PPG-PEG-PPG segment at room temperature and $X_{c,PHB}$ decreased with the PHB-diol M_n and the HB content. All PU-A samples had at least a small PHB crystalline phase. The difference of results between DSC and WAXS analyses was due to the slow PHB crystallization rate of PU-A3 at the DSC cooling/heating rate, hence the absence of a PHB crystalline phase during the second heating run. PU-B series WAXS patterns (Figure 4.1.13-b) exhibited the presence of both PHB and PEG crystalline phases in all samples. The PEG crystalline phase is defined by a monoclinic unit cell with two strong diffraction patterns at 19.2 and 23.3° assigned to (110) and (200) planes, respectively (Meng et al., 2013). As expected, the PHB degree of crystallinity increased with the PHB-diol M_n and the HB content. Moreover, for PU-B3 to PU-B5, the degree of crystallinity difference between PEG and PHB crystalline phases increased markedly with the PEG content.

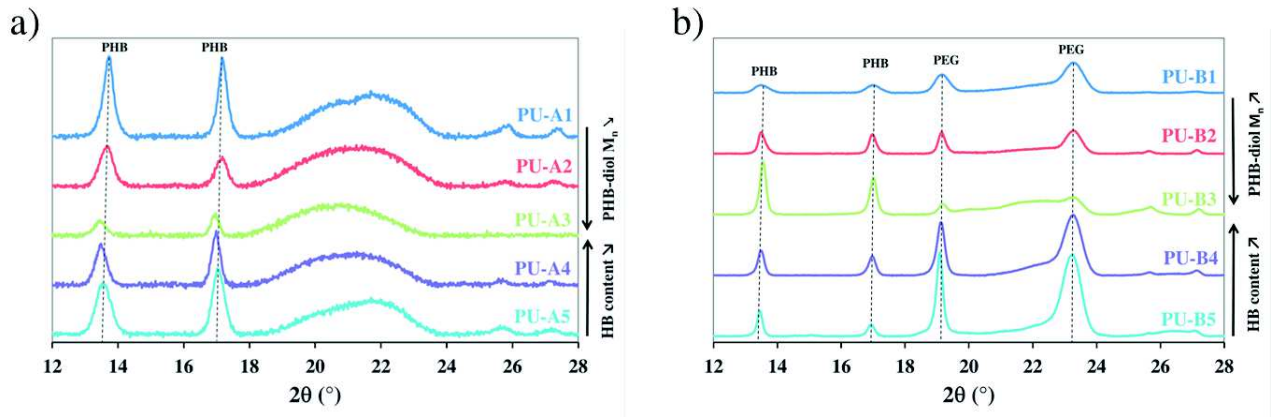

Figure 4.1.12 : WAXS patterns of (a) PU-A and (b) PU-B samples.

5. Conclusion

This study demonstrated the efficiency and versatility of the tin-catalyzed alcoholysis of high molar mass PHB in diglyme as an easy route to synthesize well-defined telechelic hydroxylated PHB (PHB-diol) oligomers. The obtained PHB-diol exhibited a good thermal stability without mass loss before 230 °C. Thermal properties of PHB-diol oligomers were highly dependent on their molar mass. Besides, the degree of crystallinity, T_m, T_c and T_g of PHB-diol decreased highly with the reduction of molar mass, for M_n < 3,000 g/mol.

Different PEEUs were successfully synthesized from PHB-diol oligomers as macrodiol with tin-catalyzed copolymerization reactions with different polyether (P_{ether}) segments (PEG or PPG-PEG-PEG). 4,4'-MDI has been used as a coupling agent in order to synthesize high molar mass PEEUs in high yield. PEEUs exhibited a good thermal stability higher than 200 °C and showed tunable physical and thermal properties according to the P_{ether}/P_{ester} ratio, the PHB-diol M_n and the chemical nature and structure of the polyether segments. The PHB crystalline phase of PEEUs increased with the PHB-diol chain length and the HB content. Moreover, despite PPG-PEG-PPG did not contribute to the PHB crystallinity, PEG segments increased highly the degree of crystallinity in PEEUs. PEG degree of crystallinity and melting temperature increased with the PEG chain length and the PEG content.

PEEUs thus represent an excellent opportunity (i) to expend the development of the bioproduction of PHAs, (ii) to obtain high performance polymers, and (iii) to go beyond the well-known drawbacks of most of the conventional PHAs (thermal sensitivity, low performance). PEEUs are nice and promising materials for some applications such as biomedical devices since the biocompatibility is still one of the most essential properties of PHAs. Nevertheless, additional analyses must be carried out to increase the known properties of the materials such as an investigation of hydrophilicity, biodegradability and mechanical behaviors.

6. References

Abe, H., 2006. Macromol. Biosci. 6, 469–486.

Andrade, A.P., Witholt, B., Hany, R., Egli, T., Li, Z., 2002. Macromolecules 35, 684–689.

Aoyagi, Y., Yamashita, K., Doi, Y., 2002. Polym. Degrad. Stab. 76, 53–59.

Arslan, H., Adamus, G., Hazer, B., Kowalczuk, M., 1999. Rapid Commun. Mass Spectrom. 13, 2433–2438.

Baran, E.T., Özer, N., Hasirci, V., 2002. J. Microencapsul. 19, 363–376.

Barham, P.J., Keller, A., Otun, E.L., Holmes, P.A., 1984. J. Mater. Sci. 19, 2781–2794.

Bergamaschi, J.M., Pilau, E.J., Gozzo, F.C., Felisberti, M.I., 2011. Macromol. Symp. 299–300, 10–19.

Cavalheiro, J.M.B.T., Pollet, E., Diogo, H.P., Cesário, M.T., Avérous, L., de Almeida, M.C.M.D., da Fonseca, M.M.R., 2013. Bioresour. Technol. 147, 434–441.

Dai, S., Li, Z., 2008. Biomacromolecules 9, 1883–1893.

Debuissy, T., Pollet, E., Avérous, L., 2016a. Biomacromolecules 17, 4054–4063.

Debuissy, T., Pollet, E., Avérous, L., 2016b. Polymer 99, 204–213.

Debuissy, T., Pollet, E., Avérous, L., 2017. Eur. Polym. J. 87, 84–98.

Deng, X.M., Hao, J.Y., 2001. Eur. Polym. J. 37, 211–214.

Gao, X., Chen, J.-C., Wu, Q., Chen, G.-Q., 2011. Curr. Opin. Biotechnol., 22/6 Chemical biotechnology and Pharmaceutical biotechnology 22, 768–774.

Grassie, N., Murray, E.J., Holmes, P.A., 1984a. Polym. Degrad. Stab. 6, 47–61.

Grassie, N., Murray, E.J., Holmes, P.A., 1984b. Polym. Degrad. Stab. 6, 95–103.

Guillaume, S.M., Annunziata, L., Rosal, I. del, Iftner, C., Maron, L., Roesky, P.W., Schmid, M., 2013. Polym. Chem. 4, 3077–3087.

Hablot, E., Bordes, P., Pollet, E., Avérous, L., 2008. Polym. Degrad. Stab. 93, 413–421.

Hirt, T.D., Neuenschwander, P., Suter, U.W., 1996. Macromol. Chem. Phys. 197, 1609–1614.

Impallomeni, G., Carnemolla, G.M., Puzzo, G., Ballistreri, A., Martino, L., Scandola, M., 2013. Polymer 54, 65–74.

Impallomeni, G., Giuffrida, M., Barbuzzi, T., Musumarra, G., Ballistreri, A., 2002. Biomacromolecules 3, 835–840.

Ionescu, M., 2005. Chemistry and technology of polyols for polyurethanes. Rapra Technology, Shawbury, Shrewsbury, Shropshire, U.K.

Jaffredo, C.G., Carpentier, J.-F., Guillaume, S.M., 2013. Macromolecules 46, 6765–6776.

Ke, Y., 2015. Express Polym. Lett. 10, 36–53.

Khasanah, Reddy, K.R., Sato, H., Takahashi, I., Ozaki, Y., 2015. Polymer 75, 141–150.

Lengweiler, U.D., Fritz, M.G., Seebach, D., 1996. Helv. Chim. Acta 79, 670–701.

Lenz, R.W., Jedlinski, Z., 1996. Macromol. Symp. 107, 149–161.

Li, J., Li, X., Ni, X., Leong, K.W., 2003. Macromolecules 36, 2661–2667.

Loh, X.J., Goh, S.H., Li, J., 2007a. Biomacromolecules 8, 585–593.

Loh, X.J., Wang, X., Li, H., Li, X., Li, J., 2007b. Mater. Sci. Eng. C, Symposium A: Advanced Biomaterials International Conference on Materials for Advanced Technologies (ICMAT 2005) 27, 267–273.

Mark, J.E., 1999. Polymer Data Handbook. Oxford University Press.

Meng, J., Tang, X., Li, W., Shi, H., Zhang, X., 2013. Thermochim. Acta 558, 83–86.

Meszynska, A., Pollet, E., Odelius, K., Hakkarainen, M., Avérous, L., 2015. Macromol. Mater. Eng. 300, 661–666.

Nobes, G.A.R., Kazlauskas, R.J., Marchessault, R.H., 1996. Macromolecules 29, 4829–4833.

Park, S.J., Kim, T.W., Kim, M.K., Lee, S.Y., Lim, S.-C., 2012. Biotechnol. Adv., Special issue on ACB 2011 30, 1196–1206.

Perrine Bordes, Eric Pollet, Luc Avérous, 2009. Potential Use of Polyhydroxyalkanoate (PHA) for Biocomposite Development, in: Nano- and Biocomposites. CRC Press, pp. 193–226.

Persenaire, O., Alexandre, M., Degée, P., Dubois, P., 2001. Biomacromolecules 2, 288–294.

Pollet, E., Avérous, L., 2011. Production, Chemistry and Properties of Polyhydroxyalkanoates, in: Plackett, D. (Ed.), Biopolymers – New Materials for Sustainable Films and Coatings. John Wiley & Sons, Ltd, pp. 65–86.

Qiu, Z., Ikehara, T., Nishi, T., 2003. Polymer 44, 2503–2508.

Ravenelle, F., Marchessault, R.H., 2002. Biomacromolecules 3, 1057–1064.

Reeve, M.S., McCarthy, S.P., Gross, R.A., 1993. Macromolecules 26, 888–894.

Saad, G.R., Lee, Y.J., Seliger, H., 2001. Macromol. Biosci. 1, 91–99.

Shuai, X., Jedlinski, Z., Kowalczuk, M., Rydz, J., Tan, H., 1999. Eur. Polym. J. 35, 721–725.

Siotto, M., Zoia, L., Tosin, M., Degli Innocenti, F., Orlandi, M., Mezzanotte, V., 2013. J. Environ. Manage. 116, 27–35.

Špitalský, Z., Lacík, I., Lathová, E., Janigová, I., Chodák, I., 2006. Polym. Degrad. Stab. 91, 856–861.

Spyros, A., Argyropoulos, D.S., Marchessault, R.H., 1997. Macromolecules 30, 327–329.

Wei, T., Zheng, B., Yi, H., Gao, Y., Guo, W., 2014. Polym. Eng. Sci. 54, 2872–2876.

Wu, L., Wang, L., Wang, X., Xu, K., 2010. Acta Biomater. 6, 1079–1089.

Xie, W., Li, J., Chen, D., Wang, P.G., 1997. Macromolecules 30, 6997–6998.

Xue, L., Dai, S., Li, Z., 2010. Biomaterials 31, 8132–8140.

Sub-chapter 4.2. Enzymatic synthesis of a biobased copolyester from poly(butylene succinate) and poly((R)-3-hydroxybutyrate) – Study of reaction parameters on the transesterification rate

Thibaud Debuissy, Eric Pollet and Luc Avérous*

BioTeam/ICPEES-ECPM, UMR CNRS 7515, Université de Strasbourg, 25 rue Becquerel, 67087 Strasbourg Cedex 2, France

*Corresponding author: luc.averous@unistra.fr

Published by Biomacromolecules, 2016, 17 (12), 4054-4063

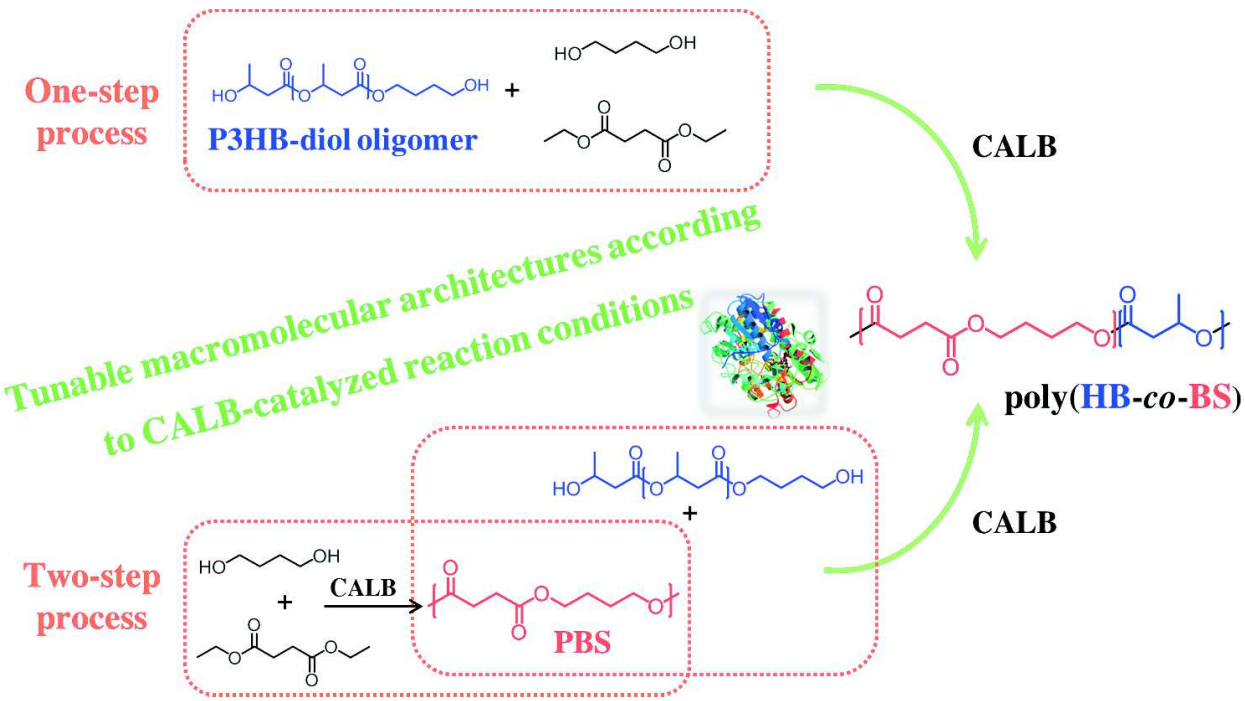

1. Abstract

The enzyme-catalyzed synthesis of fully biobased poly(3-hydroxybutyrate-co-butylene succinate) (poly(HB-co-BS)) copolyesters is reported for the first time. Different Candida antarctica lipase B (CALB)-catalyzed copolyesters were produced in solution, *via* a one-step or a two-step process from 1,4-butanediol, diethyl succinate and synthesized telechelic hydroxylated poly(3-hydroxybutyrate) oligomers (PHB-diol). The influence of the ester/hydroxyl functionality ratio, catalyst amount, PHB-diol oligomer chain length, hydroxybutyrate (HB) and butylene succinate (BS) contents and the nature of the solvent were investigated. The two-step process allowed the synthesis of copolyesters of high molar masses (Mn up to 18,000 g/mol), compared to the one-step process (Mn ~ 8,000 g/mol), without thermal degradation. The highest molar masses were obtained with diphenyl ether as solvent, compared with dibenzyl ether or anisole. During the two-step process, the transesterification rate between the HB and BS segments (i) increased with increasing amount of catalyst and decreasing molar mass of the PHB-diol oligomer, (ii) decreased when anisole was used as the solvent and (iii) was not influenced by the HB/BS ratio. Tendencies toward block or random macromolecular architectures were observed as a function of the reaction time, the PHB-diol oligomer chain length and the chosen solvent. Immobilized CALB-catalyzed copolyesters were thermally stable up to 200 °C. The crystalline structure of the poly(HB-co-BS) copolyesters depended on the HB/BS ratio and the average sequence length of the segments. The crystalline content, T_m and T_c decreased with increasing HB content and the randomness of the copolymer structure.

2. Introduction

Polyhydroxyalkanoates (PHA) are a family of polyesters produced from a wide variety of micro-organisms by fermentation of different renewable resources (microbial polymers), to develop environmentally friendly materials consistent with sustainable development. PHAs are biodegradable but exhibit biocompatibility in contact with living tissues making them suitable for biomedical applications, *e.g.*, tissue engineering (Pollet and Avérous, 2011; Bordes et al., 2009a). Microbial poly[(R)-3-hydroxybutyrate] (PHB) is one of the most prominent PHAs, as it is commercially available. However, its application as a thermoplastic material is rather limited, partly due to its high melting point (T_m) of approx. 175 °C, high glass transition temperature (T_g) of approx. 4 °C, high degree of crystallinity (X_c) (*ca.* 60%) and fast thermal degradation initiation close to the T_m (Pollet and Avérous, 2011). PHB possesses low thermal stability and decomposes easily by random *cis*-elimination chain scission at temperatures above 150 °C producing a crotonic group, thus limiting PHB usage (Abe, 2006; Grassie et al., 1984a; Hablot et al., 2008). Many approaches have been developed to try to solve these issues, such as PHA copolymers. Bacterial syntheses with varying substrates and strains have allowed the preparation of random copolyesters based on HB units (Gao et al., 2011; S. J. Park et al., 2012). Recently PHA block copolyesters based on HB were successfully produced with improved properties over random copolyesters (Gao et al., 2011). Oligomers can be used for the synthesis of new tailored block-copolymers. PHA molar mass reduction and functionalization can, for instance, give hydroxyl-terminated PHA oligomers by organometallic- (Andrade et al., 2002; Hirt et al., 1996; Lorenzini et al., 2013) or acid-catalyzed (Deng and Hao, 2001) alcoholysis. Examples of tailored materials include block poly(ester-urethanes) or block copolyesters based on rigid PHB blocks and soft blocks, which can be based on poly(ε-caprolactone) (PCL), poly(ethylene glycol), poly(butylene adipate) (PBA) and poly[(R)-3-hydroxyoctanoate] (Ke, 2015; Ravenelle and Marchessault, 2002). Random poly(HB-*co*-CL) and poly(HB-*co*-BA) copolyesters with different compositions have also been synthesized by acid-catalyzed transesterification in solution (Impallomeni et al., 2013, 2002). Some of these copolymers demonstrate good thermoplastic properties. However, such chemical modifications involve the use of toxic catalysts and chemicals.

Enzymatic catalysis shows great potential as a substitute for toxic metal-based catalysts or organocatalysts to limit the toxicity of the end-product and negative environmental impacts, in perfect agreement with the concepts of green chemistry. By enzymatic catalysis, reactions can be performed under mild conditions (low temperature and pressure), limiting the chain degradation and the generation of by-products often observed with traditional catalysts. Systems with high catalytic activity and excellent control of enantio-, chemo-, regio-, and stereo-selectivity can be also expected. Owing to these advantages, enzymatic processes could provide precise control of the final polymer architectures with clean processes and low energy consumption. Enzymatic catalysis is considered as one of the best examples of “green polymer chemistry”.

Interest in the enzymatic modification of microbial polyesters to prepare thermoplastic copolyesters has grown in recent years. Avoiding high temperatures is a key-point for these thermally sensitive polymers. The mild conditions used during enzymatic reactions (< 100 °C) are a great advantage. Different enzymes have been used for such polyester syntheses. *Candida antarctica* lipase B (CALB) appears to be one of the most promising enzymatic catalysts for this kind of reaction. While both CALB and *Pseudomonas fluorescens* lipase are known to be excellent transesterification enzymatic catalysts leading to copolyesters, with a mainly random architecture, from mixtures of two homopolyesters (Kumar and Gross, 2000b; Kumar et al., 2000; Takamoto et al., 2001; Namekawa et al., 2000b, 2000a), the enzymatic syntheses of PHA-based polymers are rarely reported. Some notable exceptions based on PHB-diol oligomers are as (i) initiator for the CALB-catalyzed ring-opening polymerization of trimethylene carbonate or ε-CL, or (ii) as a building block for the CALB-catalyzed polycondensation of PHO-diol oligomers and divinyl adipate with mercaptoalkanoic acids (Dai et al., 2011; Dai and Li, 2008; Dai et al., 2009; Iwata et al., 2003).

Until now, no enzymatic transesterification between poly(butylene succinate) (PBS), a well-known biobased, biodegradable and biocompatible aliphatic polyester suitable for packaging and biomedical applications (Gigli et al., 2016a; Hwang et al., 2012; Rhim et al., 2013), and PHB-diol oligomers was reported and none of these previous publications investigated the kinetics of transesterification.

The aim of this study was to synthesize poly(HB-*co*-BS) copolyesters by two different CALB-catalyzed pathways (one- and two-step processes) with PHB-diol oligomers, 1,4 butanediol (1,4-BDO) and diethyl succinate (DES), Scheme 4.3.1. The effect of (i) the enzymatic process, (ii) the hydroxyl/ester molar ratio, (iii) the catalyst amount, (iv) the PHB-diol molar mass, (v) the hydroxybutyrate (HB) / butylene succinate (BS) molar ratio and (vi) the nature of the solvent on the resulting copolyester architectures, molar masses, and the transesterification rate were specifically analyzed and discussed. The macromolecular architectures (composition and sequence distribution) of the resulting copolyesters were determined by NMR. The thermal stability, the crystalline structure and thermal properties of the corresponding architectures were studied by TGA, WAXS and DSC, respectively.

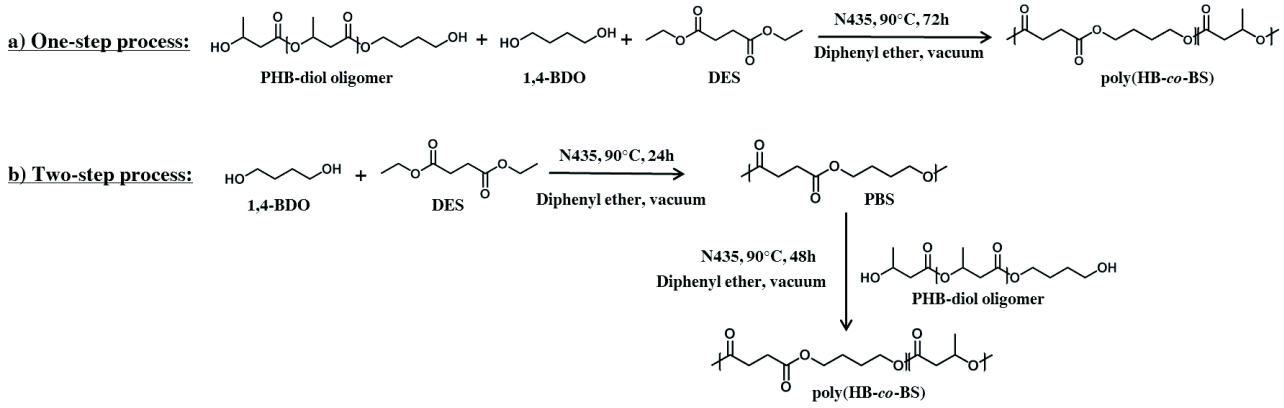

Scheme 4.2.1 : Enzymatic synthesis of poly(HB-co-BS) with immobilized CALB (N435) by (a) a one-step, or (b) a two-step process.

3. Experimental part

3.1. Materials

Telechelic hydroxylated poly[(*R*)-3-hydroxybutyrate] (PHB-diol) of different molar masses ($M_{n,1H\text{-}NMR}$: 900, 975, 1,400, 2,000 and 3,000 g/mol) were synthesized according to a protocol given in previous reports (Andrade et al., 2002; Hirt et al., 1996). The experimental protocol is detailed in the sub-chapter 4.1. 1,4-BDO was purchased from Alfa Aesar. Immobilized *Candida antarctica* lipase B on an acrylic carrier (> 5,000 $U.g^{-1}$) under the trade-name Novozym®435 (N435), chloroform (99.0-99.4%) and deuterated chloroform ($CDCl_3$) were purchased from Sigma-Aldrich. DES, diphenyl ether (99%), dibenzyl ether (99%) and anhydrous anisole (99%, extra dry, AcroSeal) were supplied by Acros. 4Å molecular sieves and petroleum ether were purchased from VWR. Molecular sieves were activated at 120 °C under vacuum for 24 h before use. N435 and PHB-diols were dried at 25 and 60 °C, respectively,

for 24 h under vacuum before use. All other reactants were used without further purification. All solvents used for the analytical methods were of analytical grade.

3.2. Kinetic study

PHB-diol oligomers were introduced as a solid powder. After preliminary optimization experiments, all further reactions were performed at 90 °C. At lower temperatures PHB-diol oligomers were not soluble in the mixture; in fact the reactive systems became solid. By contrast, higher temperature can denaturate the enzymes (Figure 3.1.9).

3.2.1. One-Step process

To start the one-step process (Scheme 4.2.1-a), PHB-diol, 1,4-BDO, an appropriate amount of DES (1/1 molar ratio of hydroxyl (from PHB-diol and 1,4-BDO) to ester functionality), N435 (10 wt.% *vs.* the total mass of monomers), diphenyl ether (200 wt.% *vs.* the total mass of monomers) and 4Å molecular sieves (0.1 g/mL) were introduced into a dry Schlenk reactor containing a magnetic stirring bar. The Schlenk reactor was immersed in a hot oil bath at 90 °C. The pressure inside the reactor was decreased stepwise to (i) 300 mbar for 4 h, (ii) 100 mbar for 4 h, (iii) 50 mbar for 16 h and (iv) 20 mbar for 48 h. After 72 h of reaction, 10 mL of chloroform were introduced into the reaction mixture to quench the reaction. The diluted reaction mixture was filtered and the filtrate was concentrated in a rotary evaporator. Thereafter, the synthesized copolyester was precipitated in petroleum ether, recovered by filtration, washed with petroleum ether and dried under reduced pressure in an oven at 50 °C for several hours.

For the kinetic study, small aliquots were withdrawn from the Schlenk reactor at predetermined reaction times (24 and 48 h). The polyester was precipitated in petroleum ether, recovered by filtration and dried under reduced pressure in an oven at 50 °C for several hours.

3.2.2. Two-Step process

In the two-step procedure (Scheme 4.2.1-b), the enzymatic synthesis of PBS was carried out over the first 24 h and the PHB-diol was subsequently introduced into the reaction mixture. Briefly, an equimolar amount of DES and 1,4-BDO, N435 (10 wt.% *vs.* the total mass of monomers), diphenyl ether (200 wt.% *vs.* the total mass of monomers) and 4 Å molecular sieves (0.1 g/mL) were introduced into a dry Schlenk reactor containing a magnetic stirring bar. The Schlenk reactor was immersed in a hot oil bath at 90 °C. The pressure inside the reactor was decreased stepwise to 300 mbar for 4 h, then to 100 mbar for 4 h and, finally to 50 mbar for 16 h. After 24 h of reaction (CALB-catalyzed synthesis of PBS), an appropriate amount of the PHB-diol oligomer was added and the pressure was finally decreased to 20 mbar until the end of the reaction. After 72 h of reaction, the reaction was quenched with 10 mL of chloroform. The diluted reaction mixture was filtered and the filtrate was concentrated with a rotary evaporator. Subsequently, the synthesized copolyester was precipitated into petroleum ether, recovered by filtration, washed with petroleum ether and dried under reduced pressure in an oven at 50 °C for several hours. For the kinetic study, small aliquots were withdrawn from the Schlenk reactor at predetermined reaction times (26, 28, 32 and 48 h) and treated as previously described.

3.3. General methods and analysis

^{1}H- and ^{13}C-NMR spectra were obtained on a Bruker 400 MHz spectrometer. $CDCl_3$ and DMSO-d_6 were used as solvents to prepare solutions with concentrations of 8-10 mg/mL and 30-50 mg/mL for ^{1}H-NMR and ^{13}C-NMR, respectively. The number of scans was set to 128 for ^{1}H-NMR and at least 4,000 for ^{13}C-NMR. Calibration of the spectra was performed using the $CDCl_3$ peak (δ_H = 7.26 ppm, δ_C = 77.16 ppm).

The number-average molar mass (M_n), the mass-average molar mass (M_w) and the dispersity (Đ) were determined in chloroform by size exclusion chromatography (SEC), using a Shimadzu liquid chromatograph with PLGel Mixed-C and PLGeL 100 Å columns and a refractive index detector. Chloroform was used as eluent at a flow rate of 0.8 ml/min. The instrument was calibrated with linear polystyrene standards from 162 to 1,650,000 g/mol.

Infrared spectroscopy (IR) was performed with a Nicolet 380 Fourier transform infrared spectrometer (Thermo Electron Corporation) used in reflection mode and equipped with an ATR diamond module (FTIR-ATR). The FTIR-ATR spectra were collected at a resolution of 4 cm^{-1} with 64 scans per run.

Differential scanning calorimetry (DSC) was performed using a TA Instrument Q200 under nitrogen (flow rate of 50 mL/min), calibrated with high purity standards. Samples of 2-3 mg were sealed in aluminum pans. A three-step procedure with a 10 °C/min ramp was applied that involved: (1) heating from room temperature to 170 °C and holding for 3 min to erase the thermal history, (2) cooling to -80 °C and holding for 3 min and (3) heating (second heating) from -80 to 180 °C. The degree of crystallinity (X_c) was calculated according to Equation (4.2.1):

$$X_c(\%) = \frac{\Delta H_m}{\Delta H_m{}^0} \times 100 \qquad (4.2.1)$$

where the melting enthalpy (ΔH_m) is taken from the second heating run and $\Delta H_m{}^0$ is the melting enthalpy of a 100% pure crystalline polyester. The value of $\Delta H_m{}^0$ of pure PHB and PBS are 146 and 210 J/g, respectively (Barham et al., 1984; Papageorgiou and Bikiaris, 2005a).

Thermal degradation was studied by thermogravimetric analysis (TGA). Measurements were conducted under helium atmosphere (flow rate of 25 mL/min) using a Hi-Res TGA Q5000 apparatus from TA Instruments. Samples (1-3 mg) were heated from room temperature to 600 °C at a rate of 20 °C/min.

Wide angle X-ray scattering (WAXS) data were recorded on a Siemens D5000 diffractometer using Cu K_α radiation (1.5406 Å) at 25-30 °C in the range 2θ = 10-35 ° at 0.5 °.min^{-1}.

4. Results and discussion

4.1. Enzymatic synthesis of poly(HB-co-BS) copolyesters by a one-step process

The one-step CALB-catalyzed synthesis of poly(3-hydroxybutyrate-*co*-butylene succinate) (poly(HB-*co*-BS)) was investigated and the main results are summarized in Table 4.2.1 (entries 1-3).

The structures of the poly(HB-*co*-BS) copolyesters were determined and confirmed by FTIR, ^{1}H-, ^{13}C- and HSQC 2D-NMR (Figures SI.33, 4.2.1-a, 4.2.2-b and SI.34, respectively). The FTIR spectra of poly(HB-*co*-BS) copolyesters and PBS can almost be superimposed. The main difference between the PBS and poly(HB-*co*-BS) spectra was the lower intensities of vibration bands in the copolyester spectrum, with the exception of the ester bands at 1715 cm^{-1}. Moreover, the higher intensity of the signal at 2965 cm^{-1} assigned to the symmetrical C-H stretching vibrations of the –CH_3 groups of ester end-groups and HB segments also confirmed the presence of HB segments in the copolyesters. Nevertheless, this signal appears to be the only one that confirms the presence of HB segments in the copolyesters due to the low HB content. Moreover, the copolyester molar composition was determined by ^{1}H-NMR using Equations (SI.41)-(SI.42) and the characteristic signals of the BS and HB segments at δ = 4.10 and 1.25 ppm, respectively. The final molar composition of the copolyesters was close to the feed composition, meaning an absence of monomer loss during the one-step enzymatic reaction. This result validated the initial choice to decrease stepwise the pressure during the reaction to avoid loss of 1,4-BDO and DES by evaporation. The presence of primary hydroxyl end-groups was observed at δ = 3.67 and 62.3 ppm in ^{1}H- and ^{13}C-NMR spectra, respectively. The presence of secondary hydroxyl end-groups at δ = 4.15 and 1.10 ppm (presence of a shoulder) was also observed in the ^{1}H-NMR and HSQC 2D-NMR spectra. Ester end-groups from DES could be seen at δ = 14.3 ppm in the ^{13}C-NMR spectra. Signal intensities of characteristic end-groups were low, attesting to a significant poly(HB-*co*-BS) molar mass. However, small intensity signals assigned to crotonyl end-groups were observed in the ^{1}H-NMR spectra at δ = 1.87 ppm for methyl protons, with δ = 5.83 and 6.9 ppm for olefinic protons resulting from some random PHB chain scissions (Hablot et al., 2008). ^{1}H-NMR results showed that the amount of crotonyl end-groups increased with the reaction time, the PHB content and the decrease of the PHB-diol molar mass (Figure SI.31 in Annex 8).

The number-average molar mass (M_n), the mass-average molar mass (M_w) and dispersity (Đ) of poly (HB-*co*-BS) copolyesters were determined by SEC in chloroform. M_n between 6,000 and 9,000 g/mol were obtained after 72 h of reaction with Đ approx. 2.0-2.3. M_n seems to slightly increase when the amount of PHB-diol oligomer introduced into the reaction mixture decreases, whereas the PHB-diol chain length has no influence on the final M_n of the copolyester. When this reaction was performed without catalyst (control experiment), no polymerization occurred and the initial compounds (PHB-diol, DES and 1,4-BDO) remained unmodified.

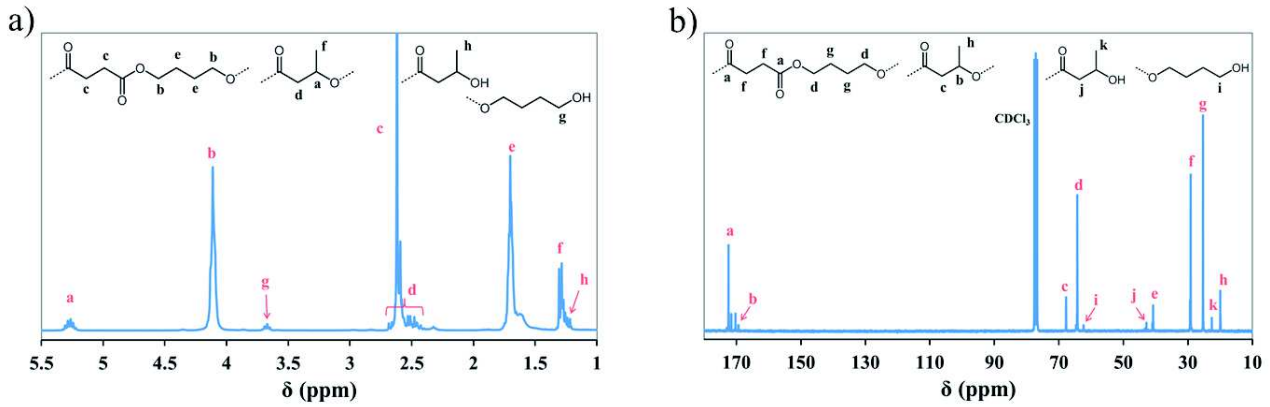

Figure 4.2.1 : (a) ^{1}H- and ^{13}C-NMR of poly(HB-co-BS) in $CDCl_3$.

The sequence distribution was investigated by ^{13}C-NMR according to the method applied by Impallomeni *et al.* (detailed in the Annex 8) (Impallomeni et al., 2013). Copolyesters synthesized from a short PHB-diol (900-975 g/mol) had a random distribution of sequences (R ~ 1) between HB and BS segments, whereas the use of a 2,000 g/mol PHB-diol led to a less random copolyester (R = 0.73). It seems that the use of a longer PHB-diol, which has a dense and rigid structure, decreases its capacity of insertion inside the specific conical CALB active site, thus hindering the transesterification. The same tendency was also observed for the transesterification of PCL and PPDL (Kumar and Gross, 2000b). Nevertheless, according to the kinetics of the one-step reactions (Table 4.3.1, entries 2-3, for further details see Table SI.12), R did not vary too much between 24 and 72 h of reaction, whereas M_n reached its maximum after 48 h and then decreased. One can conclude that the optimal reaction time with diphenyl ether is, thus, 48 h. It is surprising that R did not vary between 24 and 72 h when R < 1. This could be due to (i) the reaching of a specific equilibrium (different than for R ~ 1) or (ii) the low affinity of long PHB-diol oligomers in the system preventing optimal transesterification.

Table 4.2.1 : Syntheses of poly(HB-co-BS) copolyesters by N435-catalyzed polycondensation at 90 °C after 72 h of reaction via one-step and two-step reactions in different solvents.

Entry	Experimental conditions					SEC			^{1}H-NMR	^{13}C-NMR		
	Process	Solvent	$M_{n,PHB\text{-}diol}$ (g/mol) [a]	HB/BS [b]	PHB/BDO/DES [c]	M_n (g/mol)	M_w (g/mol)	Đ	HB/BS [d]	L_{BS}	L_{HB}	R
1	One-step	DPE [e]	900	1 / 0.96	0.5 / 5.0 / 5.5	6,000	13,500	2.3	1 / 1.16	3.4	1.4	0.99
2	One-step	DPE	975	1 / 2.4	0.2 / 5.0 / 5.2	8,300	17,600	2.1	1 / 2.50	6.4	1.2	1.01
3	One-step	DPE	2,000	1 / 2.4	0.1 / 5.0 / 5.1	8,800	17,600	2.0	1 / 2.33	7.7	1.7	0.73
4	Two-step	DPE	900	1 / 0.96	0.5 / 5.0 / 5.0	6,100	13,000	2.1	1/ 1.09	3.6	1.5	0.97
5	Two-step	DPE	975	1 / 2.4	0.2 / 5.0 / 5.0	15,100	27,700	1.8	1 / 2.10	6.4	1.2	0.99
6	Two-step	DPE	1,400	1 / 2.4	0.14 / 5.0 / 5.0	17,900	34,600	1.9	1 / 2.13	6.2	1.4	0.88
7	Two-step	DPE	2,000	1 / 2.4	0.1 / 5.0 / 5.0	11,200	31,300	2.8	1 / 1.93	9.9	2.4	0.51
8	Two-step	DPE	3,000	1 / 2.4	0.07 / 5.0 / 5.0	11,700	32,900	2.8	1 / 2.10	19.6	4.7	0.27
9	Two-step	DPE	975	1 / 1.5	0.33 / 5.0 / 5.0	6,700	13,200	2.0	1 / 1.38	4.7	1.3	0.98
10	Two-step	DPE	975	1 / 4.4	0.1 / 5.0 / 5.0	17,600	38,400	2.2	1 / 4.10	11.3	1.1	0.99
11	Two-step	DPE	975	1 / 2.4	0.2 / 5.0 / 5.2	11,400	23,300	2.0	1 / 2.35	6.4	1.2	1.00
12	Two-step	DBE [f]	975	1 / 2.4	0.2 / 5.0 / 5.0	5,900	10,800	1.8	1 / 2.30	6.5	1.2	1.00
13	Two-step	Anisole	975	1 / 1.5	0.33 / 5.0 / 5.0	6,600	12,800	1.9	1 / 1.39	5.0	1.5	0.88
14	Two-step	Anisole	975	1 / 2.4	0.2 / 5.0 / 5.0	10,000	19,500	1.9	1 / 2.23	6.9	1.4	0.87
15	Two-step	Anisole	1,400	1 / 2.4	0.14 / 5.0 / 5.0	10,300	22,400	2.2	1 / 2.11	7.1	1.4	0.85
16	Two-step	Anisole	2,000	1 / 2.4	0.1 / 5.0 / 5.0	11,400	24,800	2.2	1 / 2.00	7.6	1.6	0.76

[a] PHB-diol molar mass determined by ^{1}H-NMR. [b] Feed molar ratio between HB and BS segments. [c] Feed molar ratio between PHB-diol, 1,4-BDO and DES. [d] Experimental molar ratio after 72 h of reaction between HB and BS segments. [e] Diphenyl ether. [f] Dibenzyl ether.

4.2. Enzymatic synthesis of poly(HB-co-BS) copolyesters by a two-step process

4.2.1. Influence of the ester/hydroxyl functionality ratio

To obtain greater control of the copolyester architecture, different two-step CALB-catalyzed syntheses of poly(HB-*co*-BS) were performed. This process is based on the following steps:

(i) the enzymatic synthesis of PBS from 1,4-BDO and DES at 90 °C in different solvents (diphenyl ether, dibenzyl ether or anisole) under reduced pressure with N435 and molecular sieves for 24 h,

(ii) the subsequent addition of PHB-diol oligomers of various molar masses (*i.e,.* from 975 to 3,000 g/mol) into the same reactive system. As with the one-step reaction, this procedure, summarized in Scheme 4.3.1-b, had a total reaction time of 72 h.

On can observe that, contrary to the one-step process, no or only a negligible amount of degradation occurred during the two-step process since no or a small amount of crotonyl end-groups were observed in ^{1}H NMR spectra (Figure SI.32).

The two-step CALB-catalyzed transesterification was mainly performed with equimolar contents of reactive functionalities for the PBS synthesis from 1,4-BDO and DES in order to obtain the highest M_n for PBS after the first reaction step. Nevertheless, the overall proportion of reactive functionalities was not equimolar, with an excess of hydroxyl groups introduced by the addition of PHB-diol oligomers. The reaction with an overall equimolar proportion of hydroxyl to ester moieties (Table 4.2.1, entry 11) achieved a lower M_n for PBS after the first step (M_n of PBS was 2 times smaller) and a lower M_n for the final copolyester after the second step compared to an equivalent reaction performed without equimolar ratios (Table 4.2.1, entry 5). Taking into account this last result, the following studies were only based on equimolar 1,4-BDO/DES proportions for the two-step process.

4.2.2. Influence of the catalyst amount

Figure 4.2.2 shows the evolution of M_w and R *vs.* time for the two-step reaction of PHB-diol oligomers (M_n = 975 g/mol) and PBS, at 90 °C in 200 wt.% diphenyl ether under 20 mbar for two catalyst amounts (*i.e.,* 5 and 10 wt.% N435). The kinetic data for these reactions are presented in Table SI.13 (in Annex 8). In both syntheses, the introduction of "short" PHB-diol oligomers significantly decreased the M_w of the copolyesters. The molar mass then increased again until M_w > 22,000 g/mol. The highest catalyst content (*i.e.,* 10 wt.%) permitted the synthesis of copolyesters with higher molar masses (M_w of 27,700 g/mol after 72 h). This result was in agreement with a previous study performed on the N435-catalyzed PBS synthesis at 90 °C in diphenyl ether, which showed that the M_n of PBS increased with N435 content from 1 to 10 wt.% (Figure 3.1.9-a). The influence of N435 content on the evolution of R is also discussed. As expected, R increased more slowly with lower amounts of catalyst and, thus, the copolyester had a greater tendency toward block structure without negatively affecting the corresponding molar mass. For example, at 5 wt.% catalyst, 8 h after the introduction of the PHB-diol, the average sequence length of BS segments (L_{BS}) was almost double that with 10 wt.% catalyst (*i.e.,* L_{BS} = 14 instead of 8 for a 1/2.4 HB/BS ratio). After 72 h of reaction, the difference in sequence distribution between the two syntheses became almost negligible (R = 0.93 and 0.99 for 5 and 10 wt.% N435, respectively), and thus the macromolecular architectures of the copolyesters are assumed to be quite similar. Nevertheless, by stopping the reaction earlier, the variation of R should not be negligible and poly(HB-*co*-BS) copolyesters with the same composition are likely to have different macromolecular architectures.

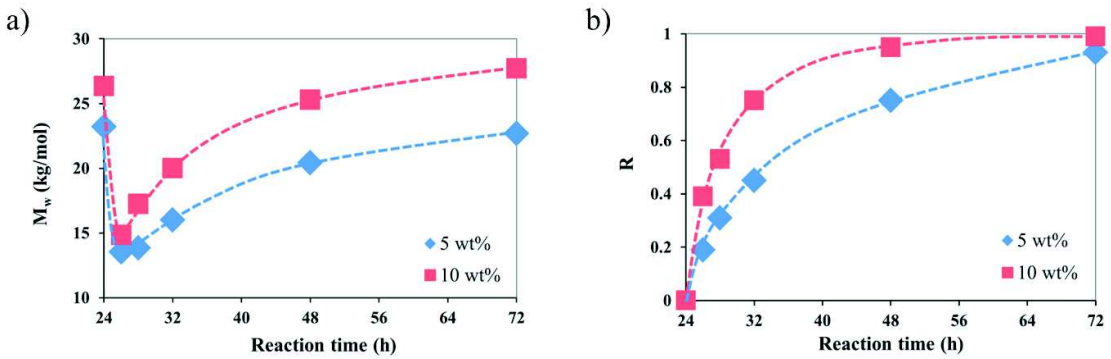

Figure 4.2.2 : Plots of M_w (a) and R (b) vs. reaction time for two-step syntheses of poly(HB-co-BS) at 90 °C in 200 wt.% diphenyl ether at a 1/2.4 HB/BS feed ratio with a PHB-diol of 975 g/mol and 5 or 10 wt.% N435.

4.2.3. Influence of the PHB-diol chain length

Figure 4.2.3 shows the evolution of M_w and R *vs.* time for the two-step reaction between PHB-diol oligomers of different molar masses (*i.e.*, from 975 to 3,000 g/mol) and PBS at 90 °C in 200 wt.% diphenyl ether under 20 mbar with 10 wt.% N435 at the same HB/BS molar ratio (*i.e.,* 1/2.4). These reactions are summarized in Table 4.2.1 (entries 5-8) and the kinetic data are detailed in Table SI.14. The use of longer PHB-diols permitted the limitation of the M_w decrease after the PHB-diol addition, resulting in higher molar mass copolyesters only a few hours after the PHB-diol addition. Indeed, the addition of longer PHB-diols for an equivalent HB/BS composition limited the number of hydroxyl end-groups inside the reactive system, which could reduce the M_w of the synthesized copolyesters, as mentioned previously. The evolution of R as a function of the reaction time depended strongly on the molar mass of PHB-diol oligomers. R increased faster when the PHB-diol molar mass was low. For example, in diphenyl ether, the transesterification with small PHB-diol oligomers (975 g/mol) allowed the production of random copolyesters (R = 0.95) after 24 h, whereas R reached values of just 0.84, 0.46 and 0.21 with PHB-diol oligomers of 1,400, 2,000 and 3,000 g/mol, respectively. This drop in R can be explained by (i) the greater rigidity of the PHB-diol chains with increasing molar mass, decreasing the potential of migration of the PHB-diols to the active site of the enzyme, (ii) the use of longer PHB-diol oligomers, which greatly increased L_{BS}, thus, decreasing R, and (iii) the lower solvent affinity of "longer" PHB-diol oligomers in the reaction mixture. Indeed, even if long PHB-diol oligomers were soluble in the system on a macroscopic scale, at the molecular scale the affinity of the polyester varies according to the M_n. For instance, during the addition, longer PHB-diols were more difficult to solubilize and reaction mixtures were more turbid than with shorter PHB-diol oligomers. The same study was performed in anisole with PHB-diols from 975 to 2,000 g/mol. The same tendency was observed, *e.g.* a decrease in the esterification rate and increase of M_w with increasing PHB-diol chain length, in anisole as in diphenyl ether (see Table SI.14 in Annex 8). However, the difference in the esterification rate between PHB-diol chain lengths was less significant in anisole compared to diphenyl ether. This could be due to a lower difference in affinity between PHB-diols of different molar masses and CALB, in anisole compared to diphenyl ether.

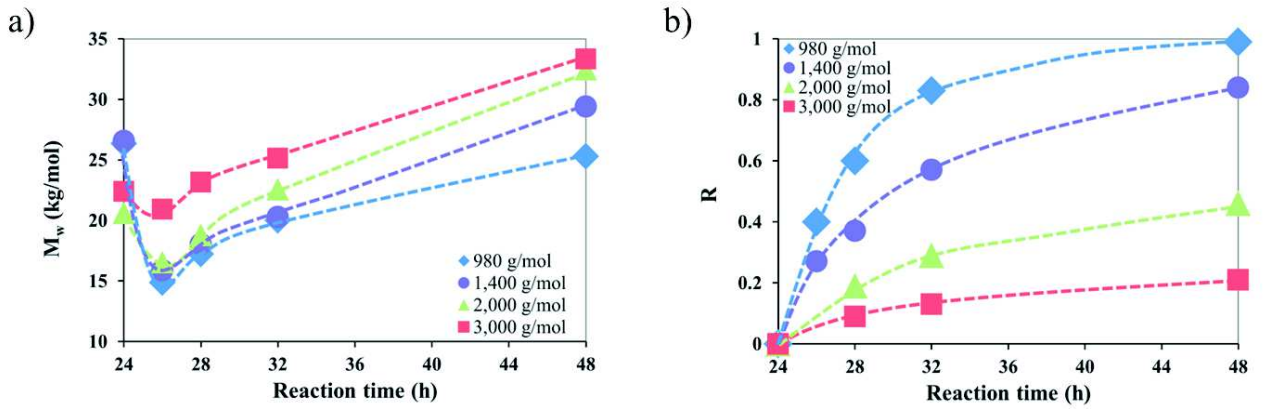

Figure 4.2.3 : Plots of M_w (a) and R (b) vs. reaction time for two-step syntheses of poly(HB-co-BS) at 90 °C in 200 wt.% diphenyl ether at a 1/2.4 HB/BS feed ratio with 10 wt.% N435 and PHB-diols of various molar masses.

4.2.4. Influence of the HB/BS composition

Figure 4.2.4 shows the evolution of M_w and R *vs.* time for the two-step reaction between PHB-diol oligomers (M_n = 975 g/mol) and PBS at 90 °C in 200 wt.% diphenyl ether under reduced pressure with 10 wt.% N435 at different HB/BS molar ratios. The results of these syntheses are presented in Table 4.2.1 (entries 5, 9 and 10). The kinetic data are detailed in Table SI.15 (in Annex 8). After the addition of PHB-diol oligomers, M_w decreased as the HB/BS composition increased due to the lower M_w of the PHB-diol oligomers (2,250 g/mol) compared to the PBS chains. M_w did not evolve greatly during the second step when a high content of PHB-diol was added. Results showed that the M_w of the copolyesters increased with a decrease in the amount of PHB-diol added, as previously observed with the one-step reaction. This was likely due to the fact that, for the synthesis of PBS, an equimolar amount of 1,4-BDO and DES was selected leading to PBS chains with 65-75% ester end-groups (from DES, determined by ^{1}H-NMR according to Equation (3.1.2)). The addition of a high content of short PHB-diol oligomers greatly modified the hydroxyl/ester end-group ratio and led to a significant excess of hydroxyl groups in the system, resulting in a decrease of M_w. The evolution of R as a function of the reaction time seemed to be equivalent for all compositions. Thus, the PHB-diol

amount had no influence on the transesterification rate. L_{BS} decreased with the transesterification time until a minimal value at R = 1 was reached. However, due to variations in composition and for the same R value, L_{BS} decreased with the HB content leading to smaller BS blocks in the copolyester structure.

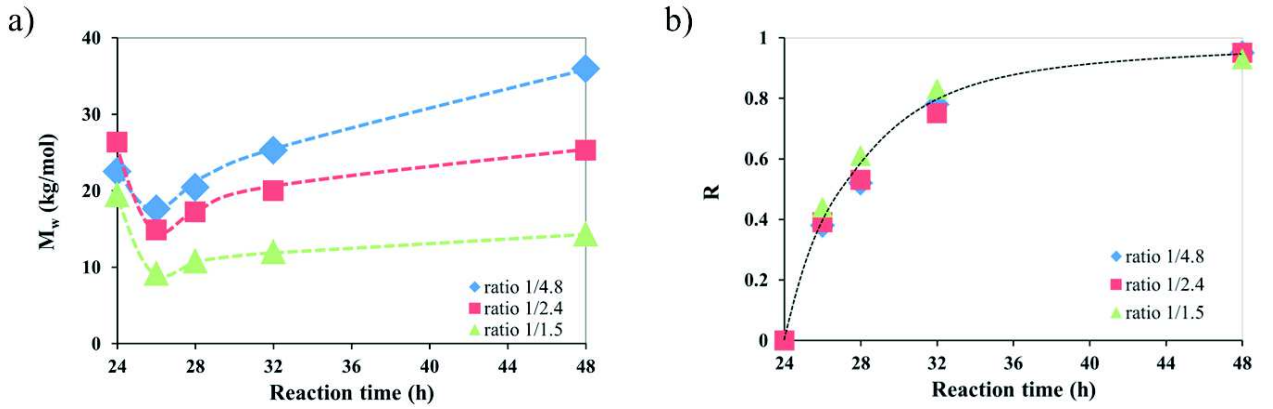

Figure 4.2.4 : Plots of M_w (a) and R (b) vs. reaction time for the two-step syntheses of poly(HB-co-BS) at 90 °C in 200 wt.% diphenyl ether at different HB/BS feed ratios with PHB-diol (975 g/mol) and 10 wt.% N435.

4.2.5. Influence of the solvent

Figure 4.2.5 shows the evolution of M_w and R *vs.* time for the two-step reaction between the PHB-diol oligomers (M_n = 975 g/mol) and PBS at 90 °C with 10 wt.% N435 in 200 wt.% of solvent (diphenyl ether, dibenzyl ether or anisole) under reduced pressure (20 mbar for diphenyl ether and dibenzyl ether, and 175 mbar for anisole). The results of these syntheses are summarized in Table 4.2.1 (entries 5, 12 and 14). The kinetic data are detailed in Table SI.16 (in Annex 8). Firstly, the influence of the solvent on M_w is discussed. Results showed that the M_w of the synthesized PBS after 24 h of reaction were higher with diphenyl ether (M_w = 26,300 g/mol) compared to anisole (M_w = 15,700 g/mol) or dibenzyl ether (M_w = 12,100 g/mol). Moreover, after the addition of the PHB-diol, the M_w increase was higher with diphenyl ether (from 15,000 to 25,000 g/mol between 26 and 72 h of reaction, respectively) than with other solvents. Diphenyl ether was also the only solvent that permitted the synthesis of copolyesters with M_w higher than 20,000 g/mol, using a small chain length PHB-diol. However, using longer PHB-diols, the M_w of the synthesized copolyesters increased as seen previously and the copolyester synthesized in anisole with the longer PHB-diol had a M_w > 20,000 g/mol (Table SI.14, entries 6 and 7). Diphenyl ether seems to be the best solvent to obtain high molar mass copolyesters although anisole can also be used with longer PHB-diols. However, we have seen previously that using longer PHB-diols significantly decreased the transesterification rate.

An influence of the solvent on the transesterification rate can be also observed. The evolutions of R with diphenyl ether and dibenzyl ether were equivalent and one can conclude that the esterification rate was the same. As the synthesized copolyesters have the same macromolecular structure with dibenzyl ether as with diphenyl ether but with a lower M_w, this solvent is not optimum. Contrary to both previous solvents, the rise of R was much lower with anisole over the first 24 h after PHB-diol introduction and, subsequently, less random structures were preferentially obtained (R = 0.63). It is, however, noteworthy that, as observed in the one-step process with long PHB-diols (Table 4.2.1, entry 3), no clear evolution of R was recorded for the two-step reaction in diphenyl ether with longer PHB-diols, 24 h or more after the PHB-diol introduction, whereas the increase in anisole was significant (Figure 4.2.6). Even if the esterification rate in anisole immediately after the introduction of long PHB-diol oligomers was slower than in diphenyl ether, the global esterification rate was faster because no activity decrease was recorded in anisole, leading to a higher tendency toward random copolyesters for reaction times greater than 48 h.

The reasoning behind the evolution of M_w and R as a function of the solvent for these enzymatic syntheses is not obvious. Diphenyl and dibenzyl ethers are both high boiling point solvents composed of two aromatic rings linked together with an ether bond, whereas anisole is composed of only one aromatic ring and has a lower boiling point, generating a lower vacuum during the reaction. Even when the use of dibenzyl ether resulted in the same transesterification rate as with diphenyl ether, the M_w of the synthesized copolyesters were much lower. This could be

due to a lower solubility of the copolyesters in dibenzyl ether compared to diphenyl ether. The effect of the solvent on enzymatic reaction has been difficult to anticipate. Some previous studies showed that hydrophobic solvents with a log *P* (*P* is the partition coefficient between 1-octanol and water) value > 1.5 are good candidates for transesterification (Kumar and Gross, 2000a; Laane et al., 2009; Yao et al., 2011). Anisole, dibenzyl ether and diphenyl ether have log *P* values of 2.1, 3.5 and 4.1, respectively. Here, it seems that the transesterification rate increases with log *P*. However, some differences cannot be explained considering log *P* values alone. A better understanding of how geometry, dipole moment, solubilization of substrates, substrate polarity and other factors influence the physicochemical and catalytic properties of enzymes is needed (Laane et al., 2009). The choice of solvent is, thus, an important factor for the macromolecular engineering of enzymatic syntheses. Until now, the choice of solvent in enzyme-catalyzed polyester syntheses was based only on the molar mass or yields achieved at the end of the reaction, but this study has demonstrated the necessity to also consider the transesterification rate.

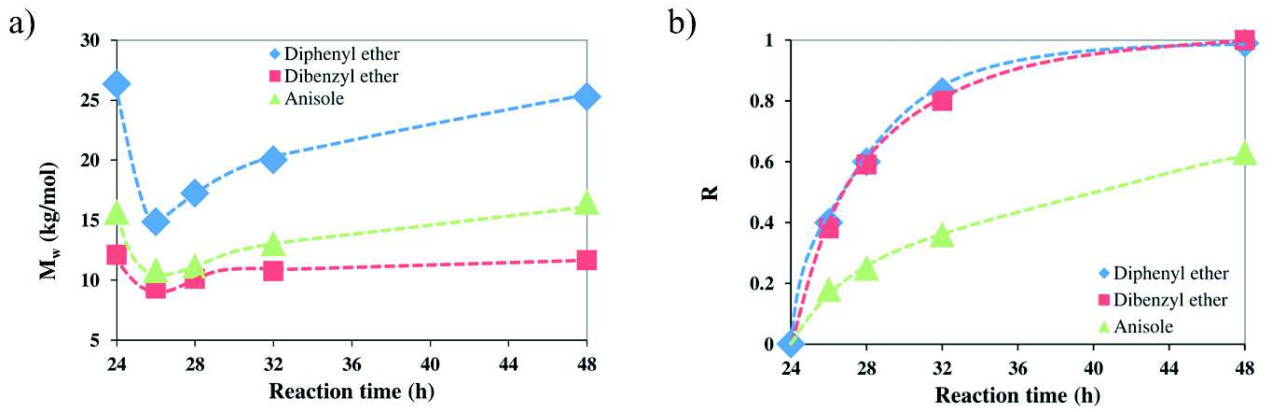

Figure 4.2.5 : Plots of M_w (a) and R (b) vs. reaction time for the two-step syntheses of poly(HB-co-BS) at 90 °C in 200 wt.% of various solvents at a 1/2.4 HB/BS feed ratio with PHB-diol of 975 g/mol and 10 wt.% N435.

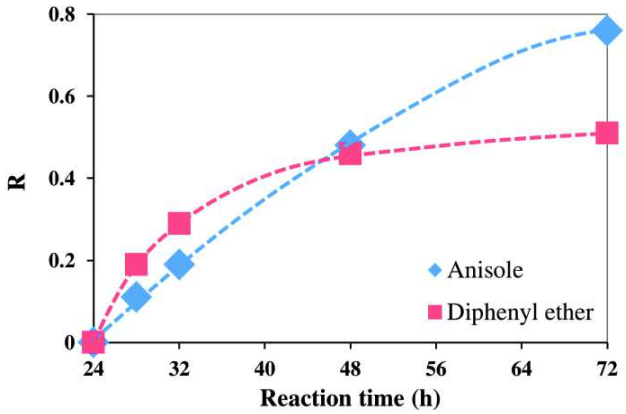

Figure 4.2.6 : Influence of the solvent on R vs. reaction time for the two-step syntheses of poly(HB-co-BS) at 90 °C in 200 wt.% of solvent at a 1/2.4 HB/BS feed ratio with PHB-diol of 2,000 g/mol and 10 wt.% N435.

4.3. Thermal stability of poly(HB-*co*-BS) copolyesters

TGA traces of three poly(HB-*co*-BS) copolyesters of different HB/BS ratios are shown in Figure 4.2.7. Under helium, all copolyesters degraded in a minimum of three main steps, which involve competitive mechanisms. All samples were thermally stable until at least 170 °C. A small mass loss was observed at 170-200 °C only for copolyesters with a high proportion of HB and, thus, a low M_n (Table 4.2.1, entry 9) due to the degradation of low molar mass chains along with the cyclization at the chain-ends and backbiting reactions (Chrissafis et al., 2006a; Persenaire et al., 2001). Longer copolyesters were thermally stable until 225 °C, after which, a major mass loss occurred at 225-325 °C ($T_{deg,max,PHB}$ ~ 270 °C) assigned to the PHB degradation, followed by another loss at 325-425 °C ($T_{deg,max,PBS}$ ~ 385 °C) assigned to the PBS degradation (Figure SI.38). The thermal degradation of the two blocks of the copolyesters was in agreement with the thermal degradation of their respective homopolymers. The intensity of these mass losses depended on the HB/BS

ratio in the copolymer structure. One can notice that the observed mass loss corresponding to PHB was approx. 10% lower than the theoretical one. In total, both degradations led to a substantial mass loss of approx. 90-94 wt.% mostly by β-(*cis*-elimination) and α-hydrogen bond scissions (Grassie et al., 1984b; Hablot et al., 2008), which are responsible for decomposition with the generation of small molecules such as diacids, vinyl compounds (*e.g.*, crotonic acid), aldehydes and anhydrides (Abe, 2006; Grassie et al., 1984a; Persenaire et al., 2001). After these main mass losses, copolyester masses of 7-10 wt.% still remained. Subsequently, a small mass loss was observed at 425-500 °C. After 500 °C, no mass loss was observed and a small amount of ash (~ 4 wt.%) was recovered at 550 °C.

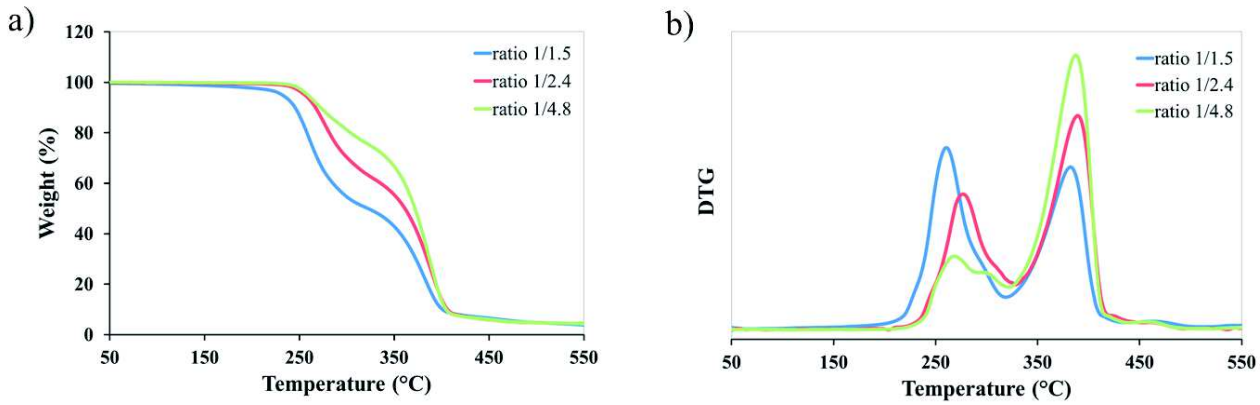

Figure 4.2.7 : (a) Mass loss and (b) derivative mass loss (DTG) curves of poly(HB-co-BS) copolyesters of various HB/BS molar ratios (Table 4.2.1; entries 5, 9 and 10) under helium.

4.4. Influence of the sequence length on the crystallinity and thermal properties of poly(HB-*co*-BS)

The thermal analysis of PBS, PHB-diol and several poly(HB-*co*-BS) copolyesters were investigated by DSC. From the TGA results one can notice that no significant degradation occurred for the copolyesters within the DSC analysis temperature range. PBS exhibits a semi-crystalline thermal behavior with a high T_m around 115 °C and a degree of crystallinity (X_c) of 34% determined according to Equation (4.2.1).

In comparison, PHB-diol is a semi-crystalline polyester with a high T_m decreasing with the molar mass reduction from 150 to 105 °C (at M_n = 3,000 and 975 g/mol, respectively) (see Sub-chapter 4.1) and X_c is approx. 50-60%. The decrease of $T_{m,PHB\text{-}diol}$ is interesting in order to more easily solubilize PHB-diol oligomers into enzymatic reaction mixtures. The synthesized P(HB-*co*-BS) copolyesters with different HB/BS molar compositions all exhibited a semi-crystalline behavior with T_g and T_m depending on the HB/BS composition and R. Syntheses in this study were performed with an excess of BS segments compared to HB, thus, the PHB crystalline phase was of very low intensity compared to the PBS crystalline phase and appeared only for copolyesters with L_{HB} values greater than 6 (Table 4.2.1, entry 15 after 26 and 28 h of reaction). Small $T_{m,PHB}$ and $T_{c,PHB}$ signals were recorded at approx. 135-140 °C and 90-95 °C, respectively. The presence of PHB crystals in copolyesters was verified by WAXS (Figure 4.2.8). Small signals at 2θ = 13.6 and 17.1° assigned to the (020) and (110) planes in the WAXS patterns are characteristic of PHB crystals (Khasanah et al., 2015). Other PHB signals overlapped with intense PBS signals confirming the much higher degree of crystallinity in the PBS crystalline phase. All other samples exhibited exclusively a PBS crystalline phase.

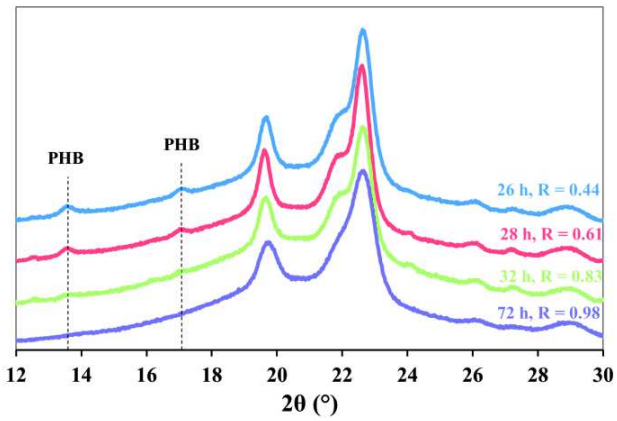

Figure 4.2.8 : WAXS patterns of poly(HB-co-BS) copolyester at different reaction times (different R values).

In a copolyester with a given composition, L_{BS} and L_{HB} decreased with the reaction time leading to a reduction of $T_{m,PBS}$ and the melting enthalpy ($\Delta H_{m,PBS}$) of the PBS crystal phase due to the presence of "defects" along the PBS chain (Figure 4.2.9-b,c). PBS-like crystals in copolyesters were smaller and less homogeneous than in pure PBS, which implied that melting peaks were larger. Some melting phenomena were composed of two peaks. These multiple endothermic peaks were attributed to fusion-recrystallization phenomena, which are rather common for aliphatic polyesters (Debuissy et al., 2016a). In the same way, the crystallization temperature ($T_{c,PBS}$) and the crystallization enthalpy ($\Delta H_{c,PBS}$) decreased with the reaction time (Figure 4.2.8-a,c) until complete disappearance when $L_{BS} < 5$ (see Table SI.17, entry 6). However, for copolyesters in which no crystallization or partial crystallization phenomena were observed during the cooling scan, a cold-crystallization phenomenon appeared during the second heating scan. Thus, the degree of crystallinity of copolyesters decreased as the L_{BS} decreased. DSC results exhibited that the T_g of the amorphous phase was approx. -30 to -37 °C and seemed to decrease with the HB content (Table SI.17). This result was surprising because PHB has a higher T_g than PBS of approx. +2 compared to -35 °C (Barham et al., 1984; Gigli et al., 2016a). This could be due to the higher insertion of short HB units in the BS amorphous segments with their methyl side group that increased the free volume and thus slightly decreased the T_g. The low T_g (*i.e.,* -37 °C) value of the copolyester with a high HB content can also be explained by the much lower M_n (*i.e.,* 6,700 g/mol) of this copolyester compared to the two others (> 15,000 g/mol).

Finally, for a given R value, L_{BS} decreased as the molar content of HB increased leading to a decrease in $T_{m,PBS}$ and $\Delta H_{m,PBS}$ as before (see Table SI.18). For example, $T_{m,PBS}$ decreased from 113 °C to 66, 79 and 96 °C for the 1/1.35, the 1/2.4 and the 1/4.4 HB/BS ratios, respectively, when R ~ 1. Likewise, $\Delta H_{m,PBS}$ decreased from 71 J/g to 6, 41 and 57 J/g for the 1/1.35, the 1/2.4 and the 1/4.4 HB/BS ratios, respectively.

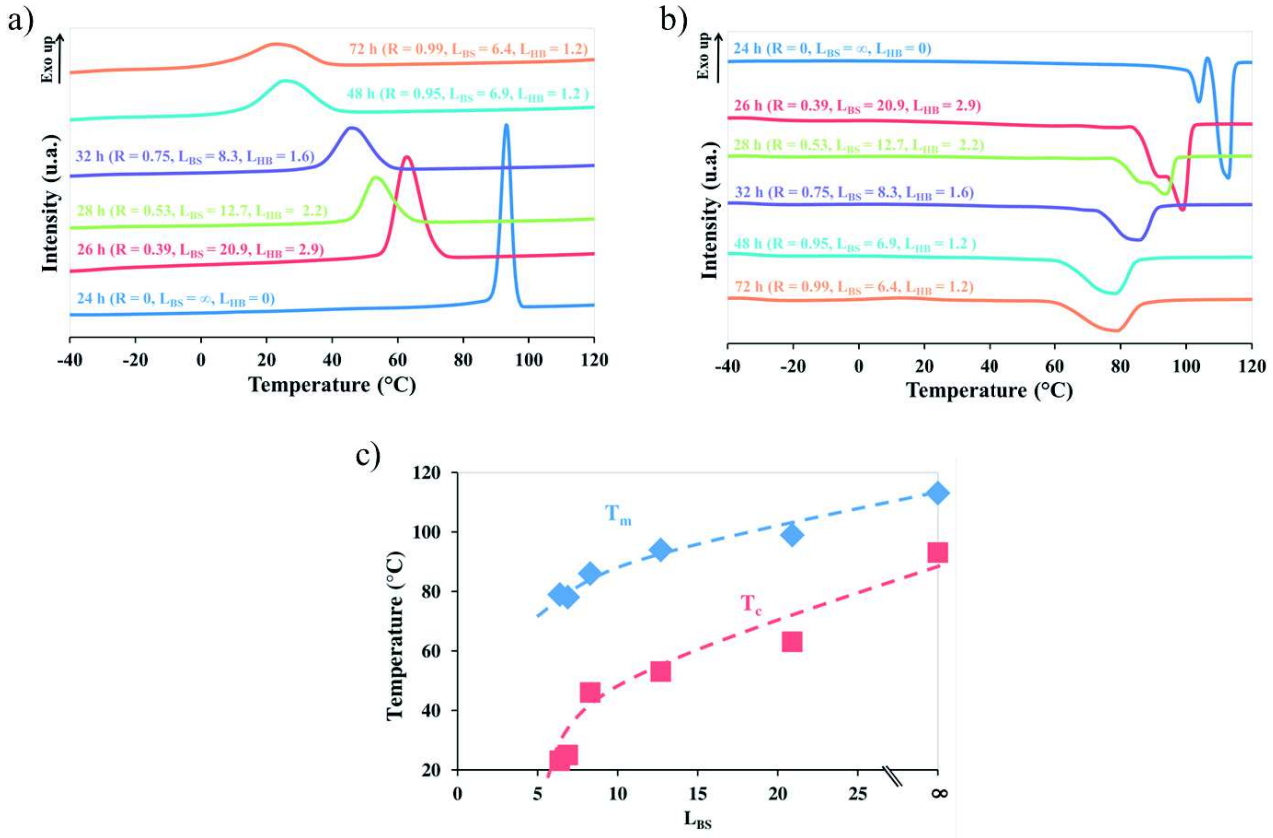

Figure 4.2.9 : DSC cooling (a) and second heating (b) curves of poly(HB-co-BS) copolyesters synthesized in diphenyl ether with 10 wt.% N435, PHB-diols of 975 g/mol and a HB/BS molar ratio of 1/2.4 taken at varying reaction times. (c) Variation of T_m and T_c as a function of the L_{BS} of previous samples.

5. Conclusion

An efficient method for the preparation of fully biobased poly(3-hydroxybutyrate-*co*-butylene succinate) copolyesters by CALB-catalyzed enzymatic polymerization from 1,4-BDO, DES and PHB-diol oligomers *via* a one-step and a two-step process at 90 °C in different solvents was successfully demonstrated.

For both processes, the HB/BS composition in the synthesized copolyesters was almost equal to the feed ratio. The one-step process in diphenyl ether allowed the synthesis of copolyesters with lower molar masses and showed evidence of PHB thermal degradation, in comparison to the two-step process. In the one-step process, M_n decreased with increasing HB content and random copolyesters were obtained with low molar mass PHB-diols, whereas less random copolyesters were obtained with longer PHB-diol oligomers (M_n > 2,000 g/mol).

The two-step process was performed by first synthesizing the PBS homopolyester and then introducing the PHB-diol oligomer into the system. Higher M_w were obtained using the two-step process as compared to the one-step process. The two-step process is, thus, a better process for this reaction. An increase in the PHB-diol chain length greatly decreased the transesterification rate between the PHB-diol oligomer and the PBS chain in diphenyl ether, whereas the decrease was less pronounced in anisole. In both solvents, the copolyester M_w increased relative to HB content and PHB-diol chain length due to the reduced amount of hydroxyl groups introduced by the PHB-diol into the system. The transesterification rate was the same in dibenzyl ether as in diphenyl ether, and both were higher than in anisole. Higher M_w values were achieved using diphenyl ether, whereas dibenzyl ether produced copolyesters with very low molar masses, thus, the latter seems much less interesting for these reactions.

All synthesized copolyesters had good thermal stabilities with no mass loss before 200 °C. Synthesized thermoplastic copolyesters have thermal properties depending on the macromolecular structures and, more precisely, their sequence lengths. For random copolyesters, no crystalline phase assigned to PHB was observed. $T_{m,PBS}$ and $\Delta H_{m,PBS}$ also

decreased relative to HB content and increasing randomness. Only copolyesters with a significant block tendency and a non-negligible amount of HB segments exhibited a small PHB crystalline phase.

A two-step process for enzyme-catalyzed copolyesters is very interesting and permits the synthesis of many different structures according to experimental conditions, resulting in different properties. The biobased poly(HB-*co*-BS) copolyester is a good example of this process, while future work should investigate the mechanical properties of the different structures of these materials in order to determine their interest for applications such as food packaging.

6. References

Abe, H., 2006. Macromol. Biosci. 6, 469–486.

Andrade, A.P., Witholt, B., Hany, R., Egli, T., Li, Z., 2002. Macromolecules 35, 684–689.

Barham, P.J., Keller, A., Otun, E.L., Holmes, P.A., 1984. J. Mater. Sci. 19, 2781–2794.

Chrissafis, K., Paraskevopoulos, K.M., Bikiaris, D.N., 2006. Thermochim. Acta 440, 166–175.

Dai, S., Li, Z., 2008. Biomacromolecules 9, 1883–1893.

Dai, S., Xue, L., Li, Z., 2011. ACS Catal. 1, 1421–1429.

Dai, S., Xue, L., Zinn, M., Li, Z., 2009. Biomacromolecules 10, 3176–3181.

Debuissy, T., Pollet, E., Avérous, L., 2016. Polymer 99, 204–213.

Deng, X.M., Hao, J.Y., 2001. Eur. Polym. J. 37, 211–214.

Gao, X., Chen, J.-C., Wu, Q., Chen, G.-Q., 2011. Curr. Opin. Biotechnol., 22/6 Chemical biotechnology and Pharmaceutical biotechnology 22, 768–774.

Gigli, M., Fabbri, M., Lotti, N., Gamberini, R., Rimini, B., Munari, A., 2016. Eur. Polym. J. 75, 431–460.

Grassie, N., Murray, E.J., Holmes, P.A., 1984a. Polym. Degrad. Stab. 6, 47–61.

Grassie, N., Murray, E.J., Holmes, P.A., 1984b. Polym. Degrad. Stab. 6, 127–134.

Hablot, E., Bordes, P., Pollet, E., Avérous, L., 2008. Polym. Degrad. Stab. 93, 413–421.

Hirt, T.D., Neuenschwander, P., Suter, U.W., 1996. Macromol. Chem. Phys. 197, 1609–1614.

Hwang, S.Y., Yoo, E.S., Im, S.S., 2012. Polym. J. 44, 1179–1190.

Impallomeni, G., Carnemolla, G.M., Puzzo, G., Ballistreri, A., Martino, L., Scandola, M., 2013. Polymer 54, 65–74.

Impallomeni, G., Giuffrida, M., Barbuzzi, T., Musumarra, G., Ballistreri, A., 2002. Biomacromolecules 3, 835–840.

Iwata, S., Toshima, K., Matsumura, S., 2003. Macromol. Rapid Commun. 24, 467–471.

Ke, Y., 2015. Express Polym. Lett. 10, 36–53.

Khasanah, Reddy, K.R., Sato, H., Takahashi, I., Ozaki, Y., 2015. Polymer 75, 141–150.

Kumar, A., Gross, R.A., 2000a. J. Am. Chem. Soc. 122, 11767–11770.

Kumar, A., Gross, R.A., 2000b. Biomacromolecules 1, 133–138.

Kumar, A., Kalra, B., Dekhterman, A., Gross, R.A., 2000. Macromolecules 33, 6303–6309.

Laane, C., Boeren, S., Vos, K., Veeger, C., 2009. Biotechnol. Bioeng. 102, 1–8.

Lorenzini, C., Renard, E., Bensemhoun, J., Babinot, J., Versace, D.-L., Langlois, V., 2013. React. Funct. Polym. 73, 1656–1661.

Namekawa, S., Uyama, H., Kobayashi, S., 2000a. Biomacromolecules 1, 335–338.

Namekawa, S., Uyama, H., Kobayashi, S., Kricheldorf, H.R., 2000b. Macromol. Chem. Phys. 201, 261–264.

Papageorgiou, G.Z., Bikiaris, D.N., 2005. Polymer 46, 12081–12092.

Park, S.J., Kim, T.W., Kim, M.K., Lee, S.Y., Lim, S.-C., 2012. Biotechnol. Adv., Special issue on ACB 2011 30, 1196–1206.

Perrine Bordes, Eric Pollet, Luc Avérous, 2009. Potential Use of Polyhydroxyalkanoate (PHA) for Biocomposite Development, in: Nano- and Biocomposites. CRC Press, pp. 193–226.

Persenaire, O., Alexandre, M., Degée, P., Dubois, P., 2001. Biomacromolecules 2, 288–294.

Pollet, E., Avérous, L., 2011. Production, Chemistry and Properties of Polyhydroxyalkanoates, in: Plackett, D. (Ed.), Biopolymers – New Materials for Sustainable Films and Coatings. John Wiley & Sons, Ltd, pp. 65–86.

Ravenelle, F., Marchessault, R.H., 2002. Biomacromolecules 3, 1057–1064.

Rhim, J.-W., Park, H.-M., Ha, C.-S., 2013. Prog. Polym. Sci., Progress in Bionanocomposites: from green plastics to biomedical applications 38, 1629–1652.

Takamoto, T., Kerep, P., Uyama, H., Kobayashi, S., 2001. Macromol. Biosci. 1, 223–227.

Yao, D., Li, G., Kuila, T., Li, P., Kim, N.H., Kim, S.-I., Lee, J.H., 2011. J. Appl. Polym. Sci. 120, 1114–1120.

Sub-chapter 4.3. Titanium-catalyzed transesterification as a route to the synthesis of fully biobased poly(3-hydroxybutyurate-*co*-butylene dicarboxylate) copolyesters, from their homopolyesters

Thibaud Debuissy, Eric Pollet and Luc Avérous*

BioTeam/ICPEES-ECPM, UMR CNRS 7515, Université de Strasbourg, 25 rue Becquerel, 67087 Strasbourg Cedex 2, France

*Corresponding author: luc.averous@unistra.fr

Published by European Polymer Journal, 2017, 90, 92-104

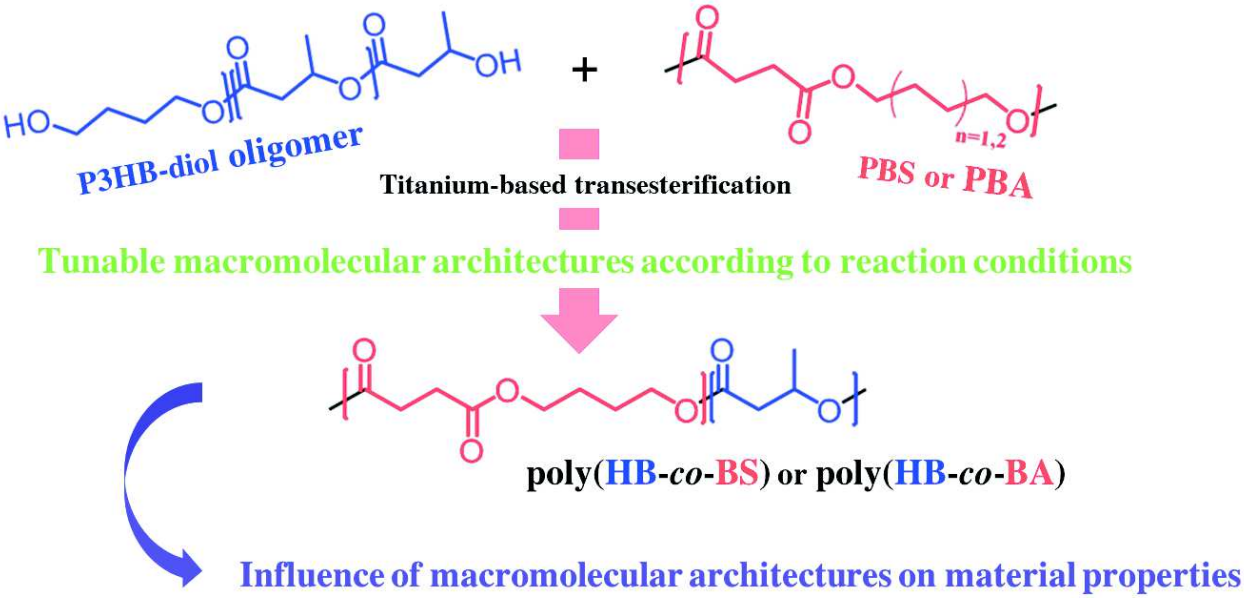

1. Abstract

Fully biobased poly(3-hydroxybutyrate-*co*-butylene adipate) (poly(HB-*co*-BA)) and poly(3-hydroxybutyrate-*co*-butylene succinate) (poly(HB-*co*-BS)) copolyesters were synthesized by transesterification between small chain length PHB and poly(butylene dicarboxylate)s (PBS or PBA) with different molar masses, different HB/BA (or HB/BS) molar ratios, in solution or in bulk, using titanium (IV) isopropoxide (TTIP) as an effective catalyst. All synthesized copolyesters were fully characterized by different chemical and physicochemical techniques including NMR, SEC, FTIR, WAXS, DSC and TGA. The influence of (i) the reaction process (ii) the nature of poly(butylene dicarboxylate) used, (iii) the molar masses of the starting homopolymers, (iv) the reaction temperature, (v) the catalyst amount and (vi) the HB/BS (or HB/BA) molar ratio on the transesterification reaction and copolyester properties were investigated. The transesterification in bulk with 1 mol.% of TTIP at 175 °C from low molar mass starting homopolyesters permitted to quickly obtain random copolyesters with final composition similar to the feeds and without thermal degradation. Random poly(HB-co-BA) copolyesters were amorphous at room temperature, whereas poly(HB-*co*-BS) copolyesters melted at temperatures higher than 40 °C. Poly(HB-*co*-BS) copolyesters exhibited only a PBS crystalline phase, except for copolyesters with a low degree of randomness and a significant HB content. The melting and crystallization temperatures as well as their respective enthalpies decreased with the randomization and the HB content.

2. Introduction

Polyhydroxyalkanoates (PHA) are a family of biopolymers synthesized by several bacteria as intracellular carbon and energy storage granules. A wide variety of prokaryotic organisms can accumulate PHA from 30 to 80% of their cellular dry weight. PHAs can be produced from various renewable resources by fermentation, to develop environmentally friendly materials consistent with a more sustainable development. PHAs are biodegradable but exhibit also biocompatibility in contact with living tissues, suitable for biomedical applications, *e.g.*, tissue engineering (Pollet and Avérous, 2011; Bordes et al., 2009a). Poly[3-hydroxybutyrate] (PHB) is commercially available and it is one of the most prominent PHAs. However, its application as a thermoplastic material is rather limited, mainly due to its high melting temperature (T_m) of approx. 175 °C, high glass transition temperature (T_g) of approx. 4 °C, high degree of crystallinity (X_c) (approx. 60%) and high thermal sensitivity (Bordes et al., 2009a). Indeed, PHB possesses a low thermal stability with a degradation initiation close to the T_m (Pollet and Avérous, 2011) and decomposes easily by random *cis*-elimination chain scission at temperatures above 150 °C, thus limiting its usage (Abe, 2006; Grassie et al., 1984a; Hablot et al., 2008).

Different approaches have been tested to overcome the above drawbacks and then obtain efficient PHB-based materials such as (i) the elaboration of multiphase systems, *e.g.*, by blending with other polymers (Qiu et al., 2003a, 2003b; Ma et al., 2014) or plasticizers (Meszynska et al., 2015), or (ii) the bio- or chemo-synthesis of 3-hydroxybutyrate (HB)-based copolymers. Bacterial syntheses with varying substrates and strains have allowed the (bio)synthesis of random copolyesters based on HB units (Cavalheiro et al., 2013; Gao et al., 2011; S. J. Park et al., 2012). Varying the chemical structure of the co-monomeric unit and its amount in the copolymer afford copolyesters with a wide range of T_m, X_c and behaviors. Moreover, block copolyesters based on HB segments were successfully bioproduced with improved properties over random copolyesters (Gao et al., 2011). However, despite their important and varied potential applications, studies of such macromolecular architectures still remain limited, mainly because of their lacks of availability in large quantities and their costs.

The chemosynthesis of PHA-based copolymers required first the production of controlled PHA oligomers. These oligomers can be synthesized by anionic- (Arslan et al., 1999; Lenz and Jedlinski, 1996), chemical- (Guillaume et al., 2013; Jaffredo et al., 2013) and enzymatic (Nobes et al., 1996; Xie et al., 1997) ring-opening polymerization (ROP) of lactones, or by the enzymatic (Shuai et al., 1999) and chemical (Lengweiler et al., 1996; Saad et al., 2001) esterification of hydroxyacids. PHA molar mass reduction with functionalization to obtain hydroxyl-terminated PHA (PHA-diol) oligomers can be performed by either organometallic- (Hirt et al., 1996) and acid-catalyzed (Deng and Hao, 2001) alcoholysis or sodium borohydrate reduction (Baran et al., 2002; Bergamaschi et al., 2011). From PHA oligomers, different tailored materials can be obtained including block poly(ester-urethane)s, block poly(ester-ether)s and block or random copolyesters based on PHB blocks with others blocks, such as poly(ε-caprolactone) (PCL), poly(ethylene

glycol) (PEG) or poly(butylene adipate) (PBA) (Ke, 2015; Ravenelle and Marchessault, 2002). PHB-based block copolyesters were synthesized *via* the chemical (Reeve et al., 1993; Wu et al., 2010) or enzymatic (Dai and Li, 2008) ROP of ε-CL and lactide initiated from PHB-diol oligomers. PEG-PHB-PEG triblock copolymers can be obtained by chain-end esterification (Li et al., 2003). Micro-block and random poly(HB-*co*-CL) and poly(HB-*co*-BA) copolyesters with different compositions have also been synthesized by acid-catalyzed transesterification in solution (Impallomeni et al., 2013, 2002).

In a recent study (Debuissy et al., 2016b), lipase-catalyzed synthesis of biobased micro-block and random copolyesters from PHB-diol oligomers and poly(butylene succinate) (PBS), a well-known biobased, biodegradable and biocompatible aliphatic polyester suitable for packaging and biomedical applications (Gigli et al., 2016a; Hwang et al., 2012; Rhim et al., 2013), has been investigated. More than lipases, organometallic catalysts have been widely used to synthesize high molar mass aliphatic (co)polyesters from diacid and diol building blocks (Debuissy et al., 2016a; Chrissafis et al., 2006a; Papageorgiou and Bikiaris, 2005a). Recently, poly(lactic acid) and poly(3-hydroxybutyrate-*co*-3-hydroxyvalerate) have been slightly transesterified by zinc acetate to improve the compatibility of the blend (Jian Yang et al., 2016). However, the efficiency of the transesterification was not analyzed. Whilst these metal-based catalysts showed a remarkable transesterification capacity, especially for titanium-based catalysts (Jacquel et al., 2011), to the best of our knowledge, no organometallic transesterification between PHB and PBS or PBA has been reported so far.

The aim of this study was, thus, to synthesize poly(HB-*co*-BA) and poly(HB-*co*-BS) copolyesters by two different transesterification processes (solution or bulk) from PHB and PBA or PBS with titanium (IV) isopropoxide (TTIP) as an effective catalyst. Impallomeni *et al*. demonstrated that the transesterification between two homopolyesters occurred at a correct rate only when homopolyesters molar mass are not too high (Impallomeni et al., 2002, 2013). Then, small chain length PHB, and PBA or PBS with limited molar masses, were used. The effect of (i) the catalytic process, (ii) the temperature, (iii) the catalyst amount, (iv) the starting homopolyesters molar masses, (v) the HB/BS molar ratio and others factors on the architecture of the synthesized copolyesters were studied. The macromolecular architectures (*e.g.*, composition and sequence distribution) of the resulting copolyesters were determined by NMR, FTIR and SEC. The crystalline structure, thermal stability and thermal properties of the corresponding architectures were studied by WAXS, TGA and DSC, respectively. Finally, the bulk transesterification pathway has been compared to the enzymatic one which had been previously described (Debuissy et al., 2016b).

3. Experimental part

3.1. Materials

Small chain length poly[3-hydroxybutyrate] (PHB) of different molar masses (M_n: 4,000, 7,000 and 15,000 g/mol, as determined by SEC) were synthesized by tin-catalyzed alcoholysis of high molar mass PHB with 1,4-butanediol, according to a protocol based on previous reports (Hirt et al., 1996) and detailed in the Sub-chapter 4.1. Poly(butylene adipate) (PBA) and poly(butylene succinate) (PBS) with different molar masses were synthesized according to a protocol based on previous reports (Debuissy et al., 2016a; Chrissafis et al., 2006a; Papageorgiou and Bikiaris, 2005a) and also detailed in the Sub-Chapter 2.1. PBA of M_n = 8,000 and 20,000 g/mol and PBS of 10,800 and 28,000 g/mol (from SEC determinations) were used. Before the reaction, small chain length PHB, PBA and PBS were dried at 40 °C under vacuum in an oven for 16 h. Titanium (IV) isopropoxide (TTIP) (98+%) was supplied by Acros. Anhydrous 1,2-dichlorobenzene (99%) and chloroform were supplied by Sigma-Aldrich. Petroleum ether was supplied from Fisher. All solvents for the analytical methods were of analytical grade, and used without further purifications.

3.2. Titanium-catalyzed transesterification in solution

In a round-bottom reactor, dried small chain length PHB and PBA (or PBS) were dissolved in a small amount of anhydrous 1,2-dichlorobenzene (~ 1.5 mL / g of homopolyester) at 150-175 °C under an argon atmosphere. After 15 min, the proper amount of TTIP (from a 20 wt.% solution of TTIP in 1,2-dichlorobenzene) was added into the reaction mixture. The reaction continued for 4 h at atmospheric pressure under argon. At the end of the reaction, the mixture was precipitated into a large volume of vigorously stirred cold petroleum ether and the copolyester was recovered by

filtration. The copolyester was then purified by first a dissolution step in a minimum of chloroform, and then a second precipitation step into a large volume of vigorously stirred cold petroleum ether followed by a filtration. The recovered final product was dried under reduced pressure in an oven at 50 °C for 24 h.

3.3. Titanium-catalyzed transesterification in bulk

After a first step leading to the homogenization of dried PHB and PBA (or PBS) in anhydrous 1,2-dichlorobenzene (~ 1 mL / g of homopolyester) at 150-175 °C under an argon atmosphere, two possibilities have been studied to add the catalyst: before the solvent removal ("distillation after TTIP introduction") and after the solvent removal ("distillation before TTIP introduction).

In the case of bulk transesterifications with distillation after TTIP introduction (Scheme 4.3.1-a), after 1 h of reaction with TTIP under an argon flux, the solvent (~ 1 mL / g of homopolyester) was distilled off the reaction mixture by vacuum and the transesterification proceeded under reduced pressure (~ 3 mbar) for 2 h. At the end of the reaction, the reaction mixture was dissolved in $CHCl_3$, precipitated into a large volume of stirred cold petroleum ether and recovered by filtration. The final product was dried under reduced pressure in an oven at 50 °C for 24 h.

In the case of Scheme 4.3.1-b (distillation before TTIP introduction), after an homogenization step of 15 min, the solvent was distilled off the reaction mixture and the proper amount of TTIP (from a 20 wt.% solution of TTIP in 1,2-dichlorobenzene) was added into the reaction mixture. The reaction mixture was then stirred for 1 h under an argon atmosphere. After 1 h, the pressure was decreased, resulting in the removal of the residual solvent. The transesterification was performed under reduced pressure (~ 3 mbar) for 2 h. The copolyester recovery was performed as previously stated.

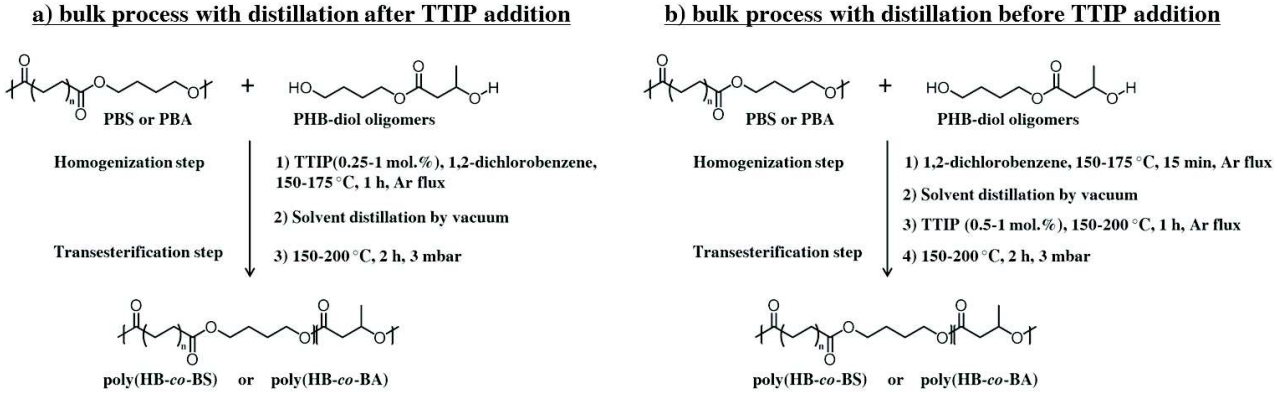

Scheme *4.3.1 : Bulk transesterification process with distillation (a) after and (b) before TTIP addition in the reaction mixture.*

3.4. General methods and analysis

^{1}H- and ^{13}C-NMR spectra of polyesters were obtained with a Bruker 400 MHz spectrometer. $CDCl_3$ was used as solvent to prepare solutions with concentrations of 8-10 and 30-50 mg/mL for ^{1}H-NMR and ^{13}C-NMR, respectively. The number of scans was set to 128 for ^{1}H-NMR and at least 4,000 for ^{13}C-NMR. Calibration of the spectra was performed using the $CDCl_3$ peak (δ_H = 7.26 ppm, δ_C = 77.16 ppm).

The number-average molar mass (M_n), the mass-average molar mass (M_w) and the dispersity (Đ) of the polyesters samples were determined in chloroform by size exclusion chromatography (SEC), using a Shimadzu liquid chromatograph. PLGel Mixed-C and PLGeL 100 Å columns and refractive index detector were used. Chloroform was used as eluent at a flow rate of 0.8 ml/min. The apparatus was calibrated with linear polystyrene standards from 162 to 1,650,000 g/mol.

Infrared spectroscopy (IR) was performed with a Nicolet 380 Fourier transformed infrared spectrometer (Thermo Electron Corporation) used in reflection mode and equipped with an ATR diamond module (FTIR-ATR). The FTIR-ATR spectra were collected at a resolution of 4 cm^{-1} and with 64 scans per run.

Differential scanning calorimetry (DSC) was performed using a TA Instrument Q200 under nitrogen (flow rate of 50 mL/min), calibrated with high purity standards. Samples of 2-3 mg were sealed in aluminum pans. A three-step procedure with a 10 °C/min ramp was applied that involved: (i) heating from room temperature to 180 °C and holding for 3 min to erase the thermal history, (ii) cooling to -80 °C and holding for 3 min and (iii) heating (second heating) from -80 to 180 °C. The degree of crystallinity (X_c) was calculated according to Equation (4.3.1),

$$X_c(\%) = \frac{\Delta H_m}{\Delta H_m{}^0} \times 100 \qquad (4.3.1)$$

where ΔH_m is the melting enthalpy and $\Delta H_m{}^0$ is the melting enthalpy of a 100% pure crystalline polyester.

Thermal degradations were studied by thermogravimetric analyses (TGA). Measurements were conducted under helium atmosphere (flow rate of 25 mL/min) using a Hi-Res TGA Q5000 apparatus from TA Instruments. Samples (1-3 mg) were heated from room temperature up to 600 °C at a rate of 20 °C/min.

Wide angle X-ray Scattering (WAXS) data were recorded on a Siemens D5000 diffractometer using Cu K_α radiation (1.5406 Å) at 25-30 °C in the range of 2θ = 14-34° at 0.4 °.min^{-1}.

4. Results and discussion

4.1. Organometallic synthesis of poly(HB-*co*-BA) copolyesters in bulk and solution

Titanium-catalyzed syntheses of poly(3-hydroxybutyrate-*co*-butylene adipate) (poly(HB-*co*-BA)) copolyesters with different HB/BA molar ratios were carried out in bulk (with "distillation before TTIP addition") or in solution, from PBA of two different molar masses (M_n = 8,000 or 20,000 g/mol) and from small chain length PHB of two different molar masses (M_n of 4,000 or 7,000 g/mol). M_n and Đ of the corresponding copolyesters were determined by SEC and presented in Table 4.3.1. M_n between 2,600 and 8,700 g/mol were obtained with Đ of approx. 1.5-2.0. Copolyesters were recovered with a high yield (~ 75-90 wt.%).

Reactions in solution led to the synthesis of copolyesters with lower M_n than ones synthesized *via* the reaction in bulk. The decrease of M_n for reactions in solution was higher when the reaction was performed at higher temperature, with a higher catalyst amount and using initial homopolyesters of lower molar mass as observed for Copo-BA-4 compared to Copo-BA-1. One can suppose that the decrease of M_n for Copo-BA-4 was due to the PHB thermal degradation by random β-scissions, creating crotonyl end-groups which are non-reactive end-groups (Abe, 2006; Grassie et al., 1984a; Hablot et al., 2008). On the other side, the reaction in bulk permitted to obtain copolyesters with higher molar masses. Moreover, one can observe that M_n values seemed not influenced by the feed HB/BA ratio. This latest result was very interesting to synthesize copolyesters with high HB content since Impallomeni *et al.* reported a decrease of M_w with the HB content for the acid-catalyzed transesterification in solution (Impallomeni et al., 2013). However, since the previous statement was based on only two samples, it should be taken with caution.

Table 4.3.1 : Copolyesters obtained from organometallic transesterification of PHB and PBA.

Sample	Experimental conditions								Yield	^{1}H-NMR		SEC		^{13}C-NMR		
	Feed HB/BA	$M_{n,PBA}$	$M_{n,PHB}$	Reaction type	Temp. [a]	Time	Pressure	TTIP amount		Exp. HB/BA [b]	Therm. degrad. [c]	M_n	Đ	L_{BA}	L_{HB}	R
	mol.%	kg/mol	kg/mol		°C	h	mbar	mol.%	wt.%	mol.%	mol.%	kg/mol				
Copo-BA-1	1 / 1	20.0	7.0	Solution	150	4	1,000	1	91	0.92 / 1	0	6.1	1.7	43	19	0.07
Copo-BA-2	1 / 1	8.0	4.0	Bulk	210	2	3	1	79	0.89 / 1	8	8.7	2.0	3.3	1.4	0.99
Copo-BA-3	2 / 1	8.0	4.0	Bulk	175	2	3	1	81	1.89 / 1	1	8.5	1.9	2.1	2.0	0.96
Copo-BA-4	2 / 1	8.0	4.0	Solution	175	4	1,000	10	74	1.84 / 1	6	2.6	1.5	2.2	1.9	0.98

[a] Reaction temperature, [b] Experimental HB/BS molar ratio determined by ^{1}H-NMR, [c] Percentage of PHB thermal degradation calculated using ^{1}H-NMR.

The chemical structures of poly(HB-*co*-BA) copolyesters and their corresponding homopolyesters (PBA and PHB-diol) were verified by ^{1}H-, ^{13}C-NMR and FTIR. The ^{1}H-NMR spectrum of poly(HB-*co*-BA) is presented in Figure 4.3.1-a. ^{1}H chemical shifts at δ = 1.28, 2.45-2.65 and 5.25 ppm were assigned to -O-CH(C$\underline{H}_3$)-CH$_2$-CO-, -O-CH(CH$_3$)-C$\underline{H}_2$-CO- and -O-C$\underline{H}$(CH$_3$)-CH$_2$-CO- protons from HB repetitive units, respectively. ^{1}H chemical shifts at δ = 1.69 and 4.09 ppm were ascribed to -O-CH$_2$-C$\underline{H}_2$- and -O-C$\underline{H}_2$-CH$_2$- protons from 1,4-BDO repetitive units, whereas the ones at δ = 1.65 and 2.32 ppm were ascribed to –CO-CH$_2$-C$\underline{H}_2$- and -CO-C$\underline{H}_2$-CH$_2$- protons from adipate repetitive units, respectively. Moreover, the primary (HO-C$\underline{H}_2$-CH$_2$-) and secondary (HO-CH(C$\underline{H}_3$)-CH$_2$-) hydroxyl terminal groups signals were observed at respectively δ = 3.67 and 1.20 ppm, at tiny intensities, in agreement with the relatively high molar mass of the samples. Furthermore, the presence of crotonyl end-groups from PHB degradation was verified by ^{1}H chemical shifts at δ = 1.87, 5.82 and 6.96 ppm ascribed to C$\underline{H}_3$-CH=CH-CO-, CH$_3$-C$\underline{H}$=CH-CO- and CH$_3$-CH=C$\underline{H}$-CO- protons, respectively (Hablot et al., 2008). The intensity of crotonyl, end-groups was calculated using relative intensities of protons at δ = 6.96 and 5.25 ppm assigned to crotonyl and HB groups, respectively. The presence of PHB thermal degradation was observed at different intensities in copolyesters, except for Copo-BA-1. Whereas the thermal degradation of Copo-BA-3 was very low (*i.e.*, 1 mol.%), Copo-BA-2 and Copo-BA-4 exhibited significant amount of crotonyl end-groups. The high amount of PHB thermal degradation in Copo-BA-2 was due to the high reaction temperature, whereas the one in Copo-BA-4 was surely due to the too high amount of catalyst.

The final molar composition in BA (χ_{BA}) and HB (χ_{HB}) segments in poly(HB-*co*-BA) copolyesters was calculated from ^{1}H-NMR spectra using relative intensities of protons in α of ester functions in 1,4-BDO (δ = 4.12 ppm) and HB (δ = 5.25 ppm) segments, respectively. In this calculation, since the primary hydroxyl end-groups (OH-CH$_2$-CH$_2$-CH$_2$-C$\underline{H}_2$-O) exhibited also a signal at 4.12 ppm and was, thus, overlapped with the one of the 1,4-BDO repetitive unit, the contribution of the primary hydroxyl end-groups in the intensity of the signal at 4.12 ppm assigned mainly to the 1,4-BDO repetitive unit should be removed. χ_{HB} was determined according to Equation (4.3.2),

$$\chi_{HB} = \frac{I_{5.25}}{\frac{I_{4.12} - I_{3.67}}{4} + I_{5.25}} \times 100 \qquad (4.3.2)$$

Final HB and BA contents in the chains are presented in Table 4.3.1. All synthesized copolyesters presented a HB/BA molar ratio close to the initial feed one.

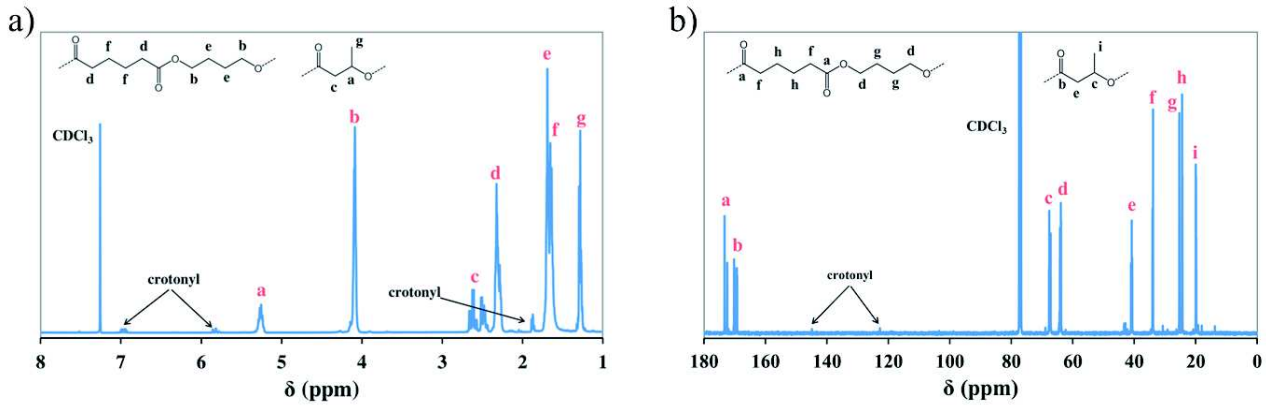

Figure 4.3.1 : (a) ^{1}H- and (b) ^{13}C-NMR spectra of poly(HB-co-BA) copolyesters in $CDCl_3$.

To investigate further the structure of poly(HB-*co*-BA) copolyesters, ^{13}C-NMR was performed. The ^{13}C-NMR spectrum of poly(HB-*co*-BA) is presented in Figure 4.3.1-b. ^{13}C chemical shifts at δ = 24.4 and 33.9 ppm were ascribed to CO-CH$_2$-C$\underline{H}_2$- and CO-C$\underline{H}_2$-CH$_2$ - carbons from adipate repeating units, whereas ones at δ = 25.3 and 64.0 ppm were ascribed to O-CH$_2$-C$\underline{H}_2$- and O-C$\underline{H}_2$-CH$_2$- carbons from 1,4-BDO repeating units, respectively. ^{13}C chemical shifts at δ = 20.0, 40.8 and 67.2-67.8 ppm were assigned to -O-CH(C$\underline{H}_3$)-CH$_2$-CO-, -O-CH(CH$_3$)-C$\underline{H}_2$-CO- and -O-C$\underline{H}$(CH$_3$)-CH$_2$-CO- carbons from HB repeating units, respectively. Finally, four doublets of ^{13}C chemical shifts were observed at δ = 169-173 ppm assigned to carbonyl carbons from HB and adipate repetitive units. Characteristics signals of PHB thermal degradation were observed at δ = 120-150 ppm. Moreover, due to the high sensibility of ^{13}C-NMR to small differences in the chemical environment, the different triad structures (B-A-B, HB-A-B, B-A-HB, HB-A-HB, A-HB-B, HB-HB-B, A-HB-HB and HB-HB-HB) were observed on the ^{13}C-NMR spectra presented in Figure 4.3.2, with HB, B

and A as the HB, 1,4-BDO and adipate segments, respectively. The splitting of signals assigned to PHB (δ = 169 ppm) or PBA (δ = 173.3 ppm) permitted the determination of the average sequence length of HB and BA units (L_{HB} and L_{BA}, respectively) and the degree of randomness (R) using Equations (4.3.3) to (4.3.5) (Impallomeni et al., 2013),

$$L_{BA} = 1 + \frac{2 \times (I_{B-A-B} + (I_{HB-A-B})}{I_{A-HB-B} + I_{HB-HB-B} + I_{B-A-HB} + I_{HB-A-HB}} \quad (4.3.3)$$

$$L_{HB} = 1 + \frac{2 \times (I_{A-HB-HB} + (I_{HB-HB-HB})}{I_{A-HB-B} + I_{HB-HB-B} + I_{B-A-HB} + I_{HB-A-HB}} \quad (4.3.4)$$

$$R = \frac{1}{L_{HB}} + \frac{1}{L_{BA}} \quad (4.3.5)$$

where $I_{B\text{-}A\text{-}B}$, $I_{HB\text{-}A\text{-}B}$, $I_{B\text{-}A\text{-}HB}$, $I_{HB\text{-}A\text{-}HB}$, $I_{A\text{-}HB\text{-}B}$, $I_{HB\text{-}HB\text{-}B}$, $I_{A\text{-}HB\text{-}HB}$ and $I_{HB\text{-}HB\text{-}HB}$ are integration of peaks assigned to carbonyl carbons (δ ~ 169-173 ppm).

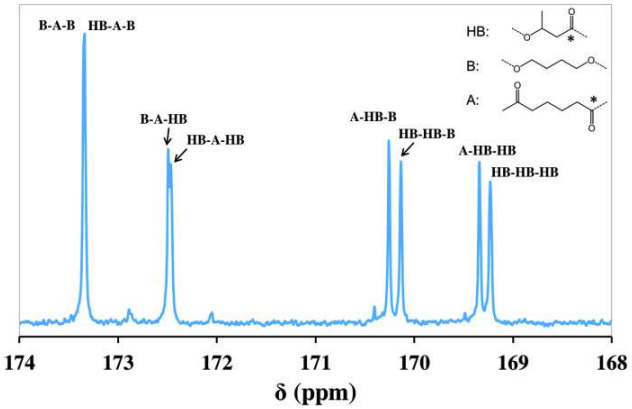

Figure 4.3.2 : ^{13}C-NMR spectra of poly(HB-co-BA) copolyester in $CDCl_3$ centered on carbonyl peaks and chemical structures corresponding to abbreviations.

Results are listed in Table 4.3.1. For a mixture of homopolymers R is equal to 0, the values between 0 and 1 are obtained for block copolymers, whereas R is equal to 1 for fully random copolymers and R = 2 for strictly alternating distribution. According to the copolyester, L_{HB} and L_{BA} varied between 1.4 and 43. The transesterification in solution of Copo-BA-1 was not performed at a significant extent (*i.e.* L_{BA} = 43, L_{HB} = 19 and R = 0.07) contrary to Copo-BA-4 which had a random structure (*i.e.,* L_{BA} = 2, L_{HB} = 2 and R = 0.98). This result can be due to (i) the lower amount of catalyst used, (ii) the lower reaction temperature and (iii) the use of starting materials with higher molar masses, which has been reported to prevent the transesterification reaction (Impallomeni et al., 2013). The two copolyesters synthesized in bulk exhibited a random distribution sequence, between HB and BA segments, as it was expected using a titanium-based organometallic catalyst (Chen et al., 2010; Debuissy et al., 2016a).

FTIR spectra of poly(HB-*co*-BA) copolyesters are presented in Figure 4.3.3. Characteristic vibration bands were observed in the poly(HB-*co*-BA) spectrum at 2955 (C-H asymmetrical stretching), 2855 (C-H symmetrical stretching), 1720 (C=O stretching of ester moieties), 1370 (symmetric deformation of the $–CH_2$- groups), 1160 (C-O-C stretching of ester moities), 1055 (O-C-C vibration in 1,4-BDO), 955 (C-O symmetric stretching) and 735 cm^{-1} ($–CH_2$- of the adipate in-plane bending) (Cai et al., 2012; Debuissy et al., 2016a).

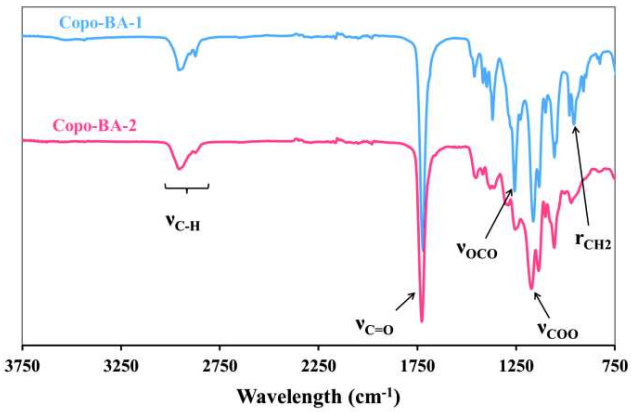

Figure 4.3.3 : FTIR spectra of Copo-BA-1 and Copo-BA-2.

TGA traces of poly(HB-*co*-BA) copolyesters are shown in Figure 4.3.4 with their corresponding derivatives (DTG) curves. Main data are summarized in Table SI.19 (in Annex 9). Under helium, all copolyesters degraded in two or three main steps which involve competitive mechanisms. First, Copo-BA-1, Copo-BA-2 and Copo-BA-3 showed a good thermal stability without mass losses before 180-200 °C. For its part, Copo-BA-4 showed a mass loss starting at already 150 °C due to its lower molar mass, as demonstrated by Chrissafis *et al.* (Chrissafis et al., 2006a), and maybe some residual solvent. First, a small mass loss was recorded at approx. 200-230 °C for Copo-BA-1 to 3 and 150-220 °C for Copo-BA-4 attributed to the degradation of low molar mass chains along with the cyclization at the chain-ends and backbiting reactions (Scheme SI.1) (Chrissafis et al., 2006a; Persenaire et al., 2001). Copo-BA-1 exhibited a two-step degradation profile with DTG maximums at 245 and 345 °C corresponding to HB and BA segments thermal degradation, respectively. The thermal degradation temperatures of the two blocks were in agreement with the thermal degradation temperatures of their respective homopolyesters (Figure SI.39 in Annex 9). All three other copolyesters with random structures (Copo-BA-2 to 4) exhibited a three-step degradation profile between 200 and 400 °C with three maximum degradation rates ($T_{deg,max}$) determined from the DTG curves at approx. 265, 315 and 355 °C. The first temperature was assigned to HB segments, whereas the two others were ascribed to the BA thermal degradation. In total, degradations led to a substantial mass loss of approx. 90-94% mostly by β-(*cis*-elimination) and α-hydrogen bond scissions (Grassie et al., 1984b; Hablot et al., 2008). After 450 °C, no mass loss was observed and a small amount of ash (~ 4 wt.%) was recovered at 500 °C.

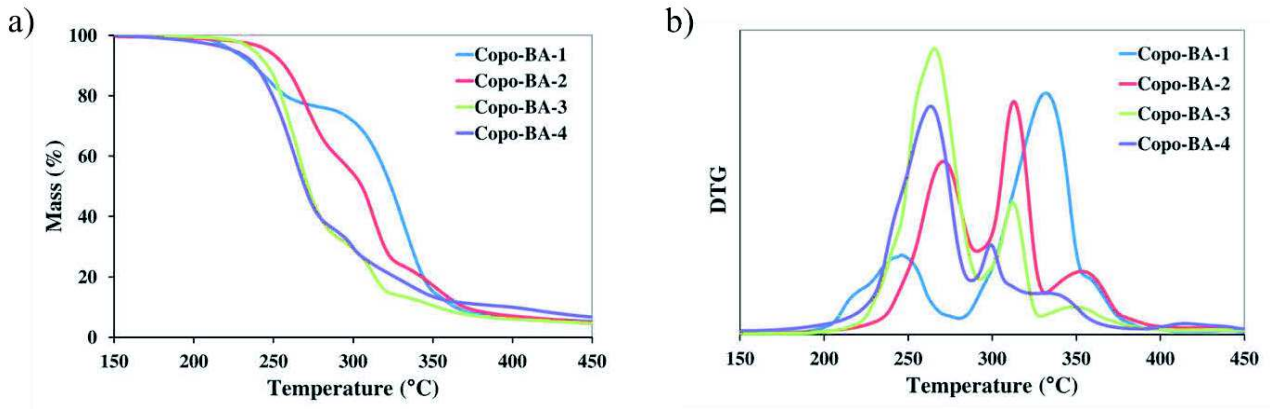

Figure 4.3.4 : (a) Mass loss and (b) their DTG curves of poly(HB-co-BA) copolyesters degradation under helium.

The crystalline structure of poly(HB-*co*-BA) copolyesters was studied by WAXS. WAXS patterns of Copo-BA-1 and Copo-BA-2 are presented in Figure 4.3.5 and compared to PHB and PBA patterns. Copo-BA-2 exhibited similar patterns as Copo-BA-3 and Copo-BA-4 (data not shown). No crystalline structures were observed in these three copolyesters. However, Copo-BA-1 exhibited a mixture of both PHB and PBA crystalline phases. Small diffraction signals at 2θ = 13.6 and 17.1° assigned to the (020) and (110) planes in the WAXS patterns, were attributed to PHB crystals (Khasanah et al., 2015), whereas signals at 2θ = 21.7, 22.5 and 24.1° were assigned to the PBA β-form crystals which are formed when T_c < 28 °C (Pan and Inoue, 2009).

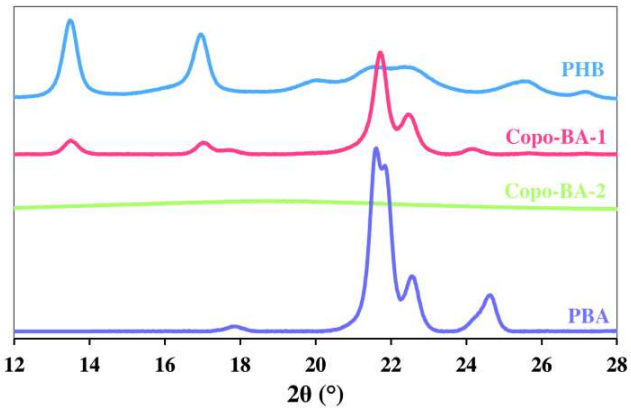

Figure 4.3.5 : WAXS patterns of PHB, Copo-BA-1, Copo-BA-2 and PBA.

The thermal properties of copolyesters were studied by DSC. Prior to this, it has been verified, from TGA results, that no significant degradation occurred in the DSC analyses temperature range. DSC curves of cooling and second heating runs of copolyesters are presented in Figure 4.3.6, whereas data are summarized in Table 4.3.2. During the first heating run, only Copo-BA-1 showed melting phenomena at 51 and 142 °C assigned to the PBA and PHB crystalline phase, respectively. During the cooling run, Copo-BA-1 exhibited a significant exothermic phenomenon at 23 °C assigned to the crystallization, whereas Copo-BA-2 and Copo-BA-3 showed no crystallization. Copo-BA-1 showed easier crystallization, resulting from its block structure, contrary to the two other random copolyesters. During the second heating run, two small endothermal baseline deviations associated to the glass-transition (T_g) phenomenon were observed for Copo-BA-1 at approx. -59 and 1 °C, and were ascribed to BA and HB blocks since they were close to the T_g of their corresponding homopolyesters (*i.e.,* approx. -60 and 4 °C for PBA (Ahn et al., 2001) and PHB (Pollet and Avérous, 2011), respectively). After that, a small cold-crystallization peak followed by a double melting phenomenon at approx. 50 °C were observed for Copo-BA-1 and were ascribed to the PBA crystalline phase. This complex phenomenon was probably due to the fusion-recrystallization process commonly observed for aliphatic polyesters such as PBA and PBS (Debuissy et al., 2016a, 2016b; Pan and Inoue, 2009). A second melting phenomenon assigned to the PHB crystalline phase was observed at 131 °C. The crystallization rate of both segments was, thus, sufficient for the co-crystallization of Copo-BA-1. For their part, Copo-BA-2 and Copo-BA-3 exhibited an amorphous thermal behavior with the presence of a unique T_g between the ones of both homopolyesters. As expected, T_g increased with the HB content. The degree of crystallinity (X_c) of the two copolyester phases in Copo-BA-1 was calculated from the second heating run with the help of Equation (4.3.1) using the melting enthalpy value of 100% crystalline phase ($\Delta H_m°$) of PBA (determined from the groups contribution method as proposed by Van Krevelen) and PHB (experimentally determined). $\Delta H_{m,PBA}^{\circ}$ and $\Delta H_{m,PHB}^{\circ}$ are 135 and 146 J/g, respectively (Barham et al., 1984; Van Krevelen, 1997). X_c of 35 and 8% for PBA and PHB crystals were calculated and reported in Table 4.3.1.

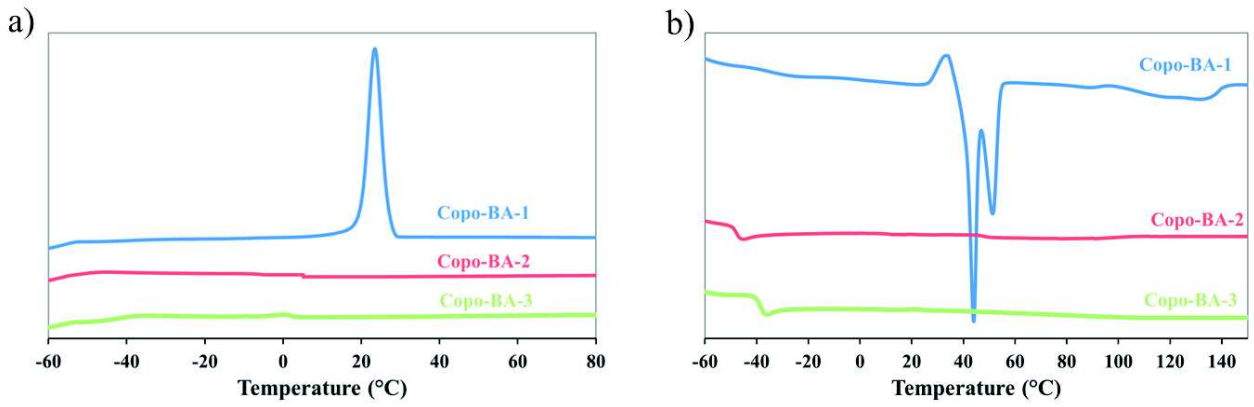

Figure 4.3.6 : DSC (a) cooling and (b) second heating runs of poly(HB-co-BA) copolyesters.

Table 4.3.2 : Thermal properties of poly(HB-co-BA) copolyesters at 10°C/min.

Sample	Cooling		Second heating									
	T_c	ΔH_c	$T_{g,1}$	$T_{g,2}$	T_{cc}	ΔH_{cc}	$T_{m,1}$	$\Delta H_{m,1}$	$X_{c,1}$	$T_{m,2}$	$\Delta H_{m,2}$	$X_{c,2}$
	°C	J/g		°C	°C	J/g	°C	J/g	%	°C	J/g	%
Copo-BA-1	23	52	-59	1	27	5	50	47	35	131	12	8
Copo-BA-2	1	1	-48	-	-	-	15	1	i.d.	-	-	-
Copo-BA-3	0	1	-38	-	-	-	15	1	i.d.	-	-	-

n.o. : not observed, i.d. : impossible to determine.

Based on the study of the poly(HB-*co*-BA) synthesis, the titanium-catalyzed transesterification in bulk was more interesting than the process in solution. However, due to the low average sequence length of BA units (L_{BA}), synthesized random poly(HB-*co*-BA) copolyesters were amorphous at room temperature. For its part, PBS, which has a higher T_m than PBA and a significant degree of crystallinity (Gigli et al., 2016a; Hwang et al., 2012; Rhim et al., 2013), could be a suitable starting homopolyester for the synthesis of a solid HB-based copolyester at room temperature.

4.2. Study of the titanium-catalyzed bulk transesterification process during the synthesis of poly(HB-co-BS) copolyesters

Several poly(HB-*co*-BS) copolyesters were synthesized in high yields (~ 85-90 wt.%) in bulk under vacuum at high temperature with TTIP as catalyst. To homogenize the reaction mixture, a small amount of anhydrous 1,2-dichlorobenzene was added at the beginning of the reaction in order to solubilize both copolyesters, then this solvent was removed under vacuum.

The final chemical structure of poly(HB-*co*-BS) copolyesters was verified by ^{1}H-, ^{13}C-NMR and FTIR. ^{1}H-, ^{13}C-NMR and FTIR spectra of poly(HB-*co*-BS) copolyesters are presented in Figures 4.3.7-a, 4.3.7-b and SI.40 (in Annex 9), respectively. All the spectra of poly(HB-*co*-BA) and poly(HB-*co*-BS) copolyesters look alike due to the similar structure between PBS and PBA homopolyesters. Nevertheless, the complete ^{1}H- and ^{13}C-NMR peaks assignements of poly(HB-*co*-BS) copolyester are presented in the Annex 9. The HB/BS composition of poly(HB-*co*-BS) copolyesters was calculated using Equation (4.3.2) and relative intensities of protons in 1,4-BDO (δ = 4.12 ppm) and HB (δ = 5.25 ppm) repetitive units. All synthesized copolyesters presented HB/BS molar ratio close to the initial feed ones.

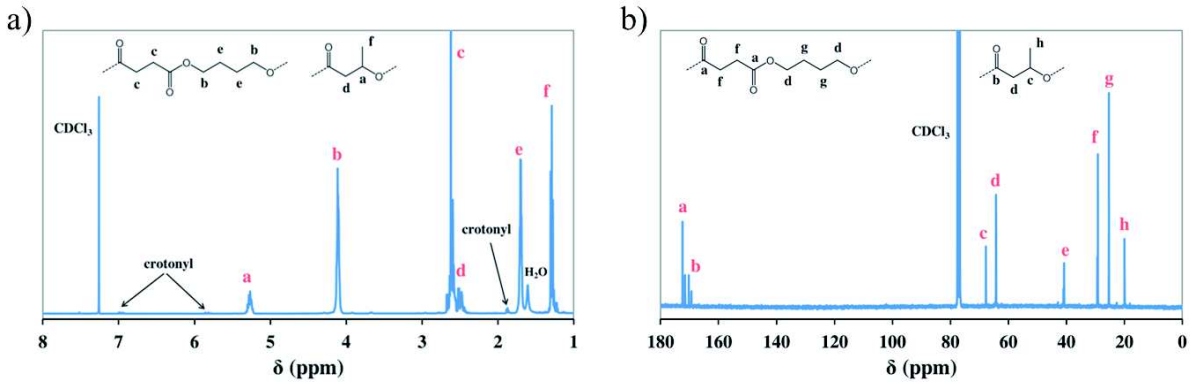

Figure 4.3.7 : (a) ^{1}H- and (b) ^{13}C-NMR of poly(HB-co-BS) copolyesters.

Likewise, ^{13}C-NMR spectra were used to determine the average sequence length of HB and BS units (L_{HB} and L_{BS}, respectively) and R using Equations (SI.43) to (SI.45) and intensities of carbonyl carbons of the different triads at δ = 169-172 ppm (Figure SI.35 in Annex 9). Determined HB and BS contents in the chains, L_{HB}, L_{BS} and R values are presented in Table 4.3.3 together with the SEC results. The transesterification rate and final molar masses were particularly discussed in function of (i) initial homopolyesters molar masses, (ii) the reaction temperature, (iii) the time of introduction of the catalyst and (iv) the HB/BS molar ratio.

As previously stated, no significant transesterification (R = 0, L = ∞) occurred when starting from high molar mass homopolyesters (Table 4.3.3, Copo-BS-1 to 3), leading to a mixture of two homopolyesters. However, decreasing the molar mass of only one of the two homopolyesters led to improved transesterification rate (Table 4.3.3, Copo-BS-7) but only a block copolyester is obtained (R = 0.11, L_{BS} = 29, L_{HB} = 13). Likewise, the absence of TTIP as catalyst prevented any transesterification leading to a blend of homopolyesters (Table 4.3.3, Copo-BS-5).As expected, the transesterification rate and copolyesters molar mass increased with the TTIP amount (Table 4.3.3, Copo-BS-5, 6 and 8) and the reaction temperature (Table 4.3.3, Copo-BS-4, 8 and 9). However, increasing the temperature to 200 °C, for Copo-BS-8, led to PHB thermal degradation as previously observed during the poly(HB-*co*-BA) copolyester synthesis. Reaction temperature higher than 175 °C was, thus, avoided. Likewise, due to the high T_m of small chain length PHB and even if T_m decreased with the molar mass (Figure 4.1.8 in Sub-chapter 4.1), small chain length PHB did not melt very well at 150 °C and reactive systems became solid quickly after the solvent distillation preventing an efficient transesterification. As a result, only blocky copolyesters of low molar mass were obtained for such low temperature (Copo-BS-4).

The crucial point of the catalyst efficiency was the presence or not of the "homogenization solvent" during the TTIP addition in the reaction mixture. Indeed, for copolyesters with the "distillation after TTIP addition" process (Scheme 4.3.1), the transesterification was null (mixture of two homopolyesters) using both high molar mass homopolyesters and partial (block copolyesters) using lower molar masses. However, random copolyesters were obtained only *via* the "distillation before TTIP addition" process (Table 4.3.3, Copo-BS-10 to 12), as it was also the case in the poly(HB-*co*-BA) copolyester study. To explain the difference between the two processes, as observed when comparing Copo-BS-8 and Copo-BS-11, one can suppose a partial deactivation of the catalyst during the homogenization step or some catalyst removal during the distillation of the large amount of solvent Indeed, titanium alkoxides catalysts can be hydrolyzed by water to form TiO_2 and R'OH molecules, which show no catalytic effect (Otera, 1993). Even if an anhydrous solvent was used to minimize this risk, when TTIP was added before the removal of the "homogenization solvent", TTIP was then diluted in a much larger amount of solvent and the risk of titanium hydrolysis was, thus, increased. Otherwise, one can suppose that during the "distillation after TTIP addition" process, a non-negligible amount of catalyst was pulled away by the high amount of solvent during the distillation and thus removed from the reaction mixture.

Finally, the HB/BS molar ratio seemed to have no effect on the transesterification rate since Copo-BS-10 to 12 exhibited a random structure. Nevertheless, the molar mass seemed to slightly decrease with the HB content in agreement with the study of Impallomeni *et al* (Impallomeni et al., 2013). Likewise, the PHB thermal degradation increased with the HB content and the temperature.

Table 4.3.3 : Copolyesters obtained from organometallic transesterification of PHB and PBS.

Sample	Experimental conditions						Yield	^{1}H-NMR		SEC		^{13}C-NMR		
	Feed HB/BS	$M_{n,PBS}$	$M_{n,PHB}$	Temp. [a]	TTIP amount	Distillation before TTIP addition		Exp. HB/BS [b]	Thermal. degrad. [c]	M_n	Đ	L_{BS}	L_{HB}	R
	mol.%	kg/mol	kg/mol	°C	mol.%	a	wt.%	mol.%	%	kg/mol				
Copo-BS-1	1 / 1	28.0	15.0	175	0.25	No	89	1 / 0.86	0	12.1	2.2	∞	∞	0
Copo-BS-2	1 / 1	28.0	15.0	175	0.5	No	87	1 / 1.08	0	28.4	1.7	∞	∞	0
Copo-BS-3	1 / 1	28.0	15.0	175	1	No	92	1 / 1.13	0	22.4	1.9	∞	∞	0
Copo-BS-4	1 / 1	10.8	4.0	150	1	No	88	1 / 1.12	0	6.7	2.0	21.0	17.7	0.10
Copo-BS-5	1 / 1	10.8	4.0	175	0	No	81	1 / 1.10	0	6.6	1.9	∞	∞	0
Copo-BS-6	1 / 1	10.8	4.0	175	0.5	No	84	1 / 1.16	0	8.4	2.2	17.2	7.3	0.19
Copo-BS-7	1 / 1	10.8	15.0	175	0.5	No	88	1 / 1.07	0	13.8	2.0	29.3	12.9	0.11
Copo-BS-8	1 / 1	10.8	4.0	175	1	No	87	1 / 1.16	0	10.2	2.4	8.7	4.4	0.34
Copo-BS-9	1 / 1	10.8	4.0	200	1	No	85	1 / 1.17	3	14.9	1.9	4.5	2.1	0.70
Copo-BS-10	1 / 1	10.8	4.0	175	1	Yes	89	1 / 1.09	2	12.6	1.8	3.0	1.5	1.01
Copo-BS-11	1 / 3	10.8	4.0	175	1	Yes	90	1 / 2.90	2	15.1	1.7	6.8	1.3	0.93
Copo-BS-12	1 / 5	10.8	4.0	175	1	Yes	90	1 / 5.16	0	15.5	1.8	17.5	1.2	0.95

[a] Reaction temperature, [b] Presence of thermal degradation observed in NMR spectra (~ : negligible amount, + : medium amount).

The poly(HB-*co*-BS) copolyesters thermal stability was investigated by TGA. TGA curves are presented in Figure 4.3.8, with corresponding data summarized in Table SI.19, and compared to their homopolyesters (Figure SI.39 in Annex 9). All copolyesters were thermally stable until 220 °C. Poly(HB-*co*-BS) copolyesters degradation profiles were almost similar to the one of poly(HB-co-BA) copolyesters previously presented, with a two-step degradation in which the first degradation was assigned to PHB degradation ($T_{deg,max}$ ~ 280 °C) with its intensity increasing with the HB content and the second one was ascribed to PBS degradation ($T_{deg,max}$ ~ 385 °C).

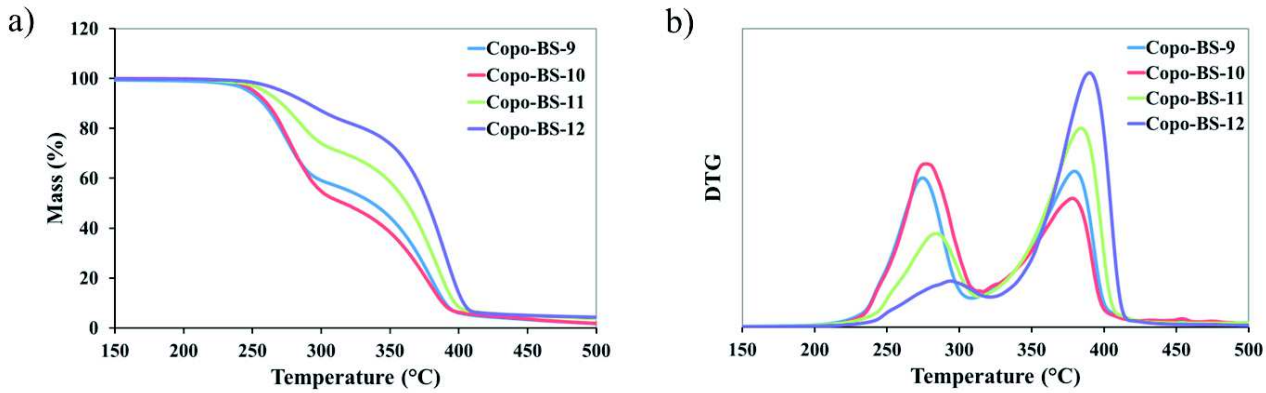

Figure 4.3.8 : (a) Mass loss and (b) DTG curves of different poly(HB-co-BS) copolyesters.

The crystalline structure and thermal properties of copolyesters according to their structure were studied by WAXS and DSC. The WAXS patterns of different poly(HB-co-BS) copolyesters with the same composition but different randomness degree is presented in Figure 4.3.9. All these copolyesters exhibited signals at 2θ = 19.5, 21.7 and 22.4° assigned to the PBS crystalline phase, even for random structures, contrary to poly(HB-*co*-BA) (Pan and Inoue, 2009). The intensity of these signals decreased with the randomization and, thus, decreased with L_{BS}. The two peaks at 2θ = 13.5 and 17.0° were ascribed to the PHB crystalline phase. As for poly(HB-co-BA), only copolyesters with $L_{HB} \geq 7$ and, thus, a marked blocky structure were able to show a PHB crystalline phase.

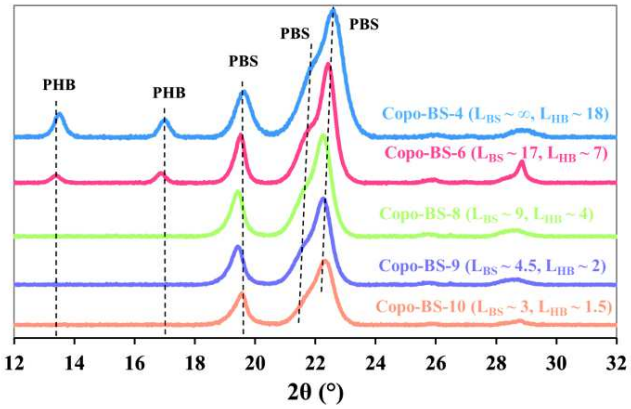

Figure 4.3.9 : WAXS patterns of different poly(HB-co-BS) copolyesters.

DSC traces of some poly(HB-*co*-BS) copolyesters are presented in Figure 4.3.10 and data are summarized in Table 4.3.4. Copo-BS-1, which is composed of a mixture of two homopolyesters, was the only sample showing the presence of two melting phenomena at 112 and 140 °C assigned to the PBS and PHB crystalline phases, respectively. All other copolyesters exhibited only one melting phenomenon during the first heating run, even for random structures (Copo-BS-10 to 12), contrary to poly(HB-*co*-BA) copolyesters. For poly(HB-*co*-BS) copolyesters of a given composition with nearly equimolar HB and BS contents (Table 4.3.3, Copo-BS-1 and Copo-BS-8 to 10), as L_{BS} and L_{HB} decreased due to the randomization, T_m, T_c, ΔH_c and ΔH_m of the PBS crystal phase decreased too, due to the disruption of the symmetry in the chain. Likewise, after the first heating run, Copo-BS-9 and Copo-BS-10 were not able to crystallize during the cooling or the second heating run leading to amorphous materials. The randomization decreased drastically the crystallization ability and, thus, the crystallinity. X_c for poly(HB-*co*-BS) copolyesters was calculated from the second

heating run using Equation (4.3.1) and the experimentally determined $\Delta H_m°$ value of PBS (210 J/g) (Papageorgiou and Bikiaris, 2005a). Moreover, as for poly(HB-*co*-BA) copolyesters, T_g of poly(HB-*co*-BS) copolyesters determined during the second heating run was comprised between the T_g of both homopolyesters and tended to decrease with the randomization. One can suppose that, due to the decrease of the BS crystallization ability with the randomization, the degree of crystallinity after the cooling run decreased and, thus, the amorphous phase of copolyesters was more concentrate in BS repetitive units, hence the decrease of T_g. Finally, for a given R value, L_{BS} increased as the molar content of HB decreased leading to an increase of T_m and ΔH_m (see Table 4.3.4, Copo-BS-10 to 12).

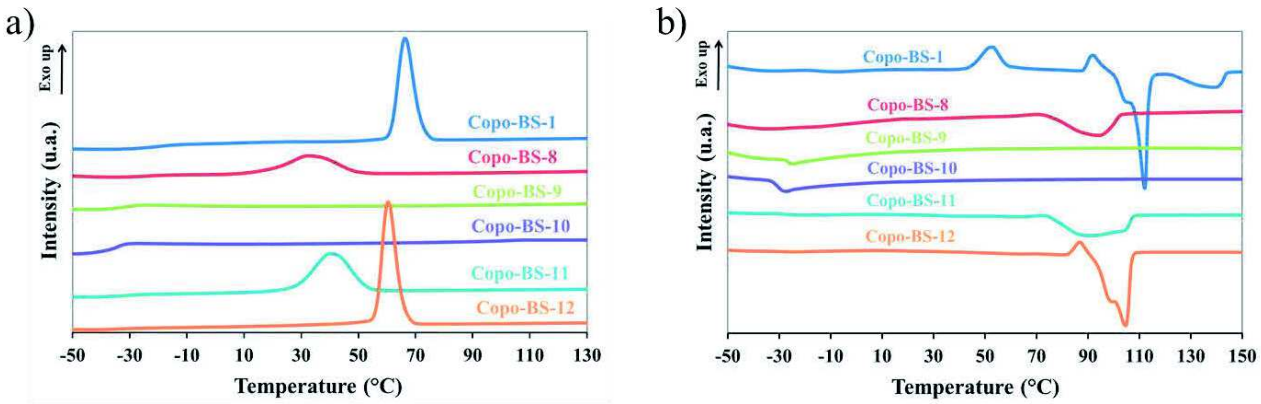

Figure 4.3.10 : DSC (a) cooling and (b) second heating scans of poly(HB-co-BS) copolyesters.

Table 4.3.4 : Thermal properties of poly(HB-co-BS) copolyesters.

Samples	First heating		Cooling		Second heating					
	T_m	ΔH_m	T_c	ΔH_c	T_g	T_{cc}	ΔH_{cc}	T_m	ΔH_m	X_c
	°C	J/g	°C	J/g	°C	°C	J/g	°C	J/g	%
PBS	115	83	84	67	-35	104	4	115	67	32
PHB	176	90	115	84	2	-	-	173	93	64
Copo-BS-1	112 / 141*	43 / 13*	66	40	-14	53	14	112 / 139*	46 / 14*	22 / 10*
Copo-BS-8	94	43	32	35	-25	-	-	94	41	20
Copo-BS-9	65	21	-	-	-26	-	-	-	-	0
Copo-BS-10	41	17	-	-	-30	-	-	-	-	0
Copo-BS-11	93	46	40	45	-28	-	-	91	42	20
Copo-BS-12	106	62	61	58	-30	87	4	105	60	29

n.o. : not observed. * Presence of two crystalline phases: PBS phase / PHB phase.

4.3. Comparison between enzymatic and organometallic transesterification on the synthesis of poly(HB-*co*-BS) copolyesters

The synthesis of poly(HB-*co*-BS) copolyesters by lipase-catalyzed transesterification from PBS and PHB-diol oligomers ("two-step reaction") in solution under vacuum using the immobilized form of *Candida antartica* lipase B (CALB) on acrylic beads (Novozym® 435) as catalyst has been previously reported (Debuissy et al., 2016b). This two-step enzymatic transesterification procedure is summarized in Scheme 4.3.2. Then, similarities and differences between the results of titanium- and CALB-catalyzed transesterification on the synthesis of poly(HB-*co*-BS) copolyesters are discussed.

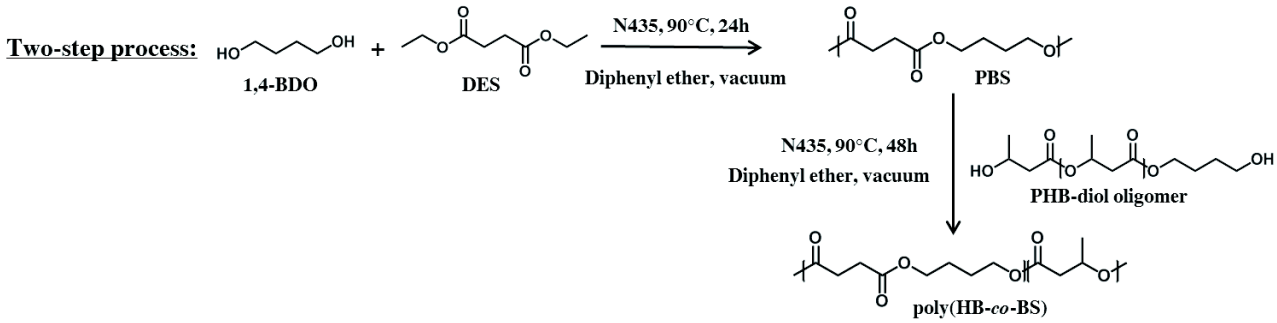

Scheme 4.3.2 : Enzymatic synthesis of poly(HB-co-BS) copolyesters catalyzed by CALB according to a two-step process.

As for the titanium-catalyzed transesterification in bulk, the PHB thermal degradation could be avoided in the enzymatic process by controlling the reaction process. Both processes performed under vacuum permitted to obtained copolyesters with (i) similar feed and final compositions, (ii) micro-block or random structures according to the reaction conditions and (iii) molar mass of ~ 15-20 kg/mol for copolyesters with low HB content. By increasing the HB content, the titanium process was more suitable since no significant molar mass decrease was reported contrary to the enzymatic process.

The main advantage of the organometallic process was the much lower reaction time to obtain random copolyesters (2 h maximum), even if titanium-catalyzed transesterification required much higher reaction temperatures (175 °C) and vacuum (1-3 mbar) compared to the enzymatic process (72 h, 90 °C and 20 mbar, respectively). Likewise, contrary to the enzymatic process, the titanium one permitted to start with homopolyesters of higher molar mass, particularly for PHB. Indeed, PHB oligomers higher than 2 kg/mol had to be avoided for the enzymatic process due to the insolubility of long PHB-diols in reaction solvents and the low reactivity of long PHB oligomers with CALB. The previous reaction (PHB alcoholysis to obtain small chain length PHB) was thus faster since PHB homopolyesters > 5,000 g/mol can be used for the organometallic transesterification. Moreover, the titanium-catalyzed transesterification in bulk permit to synthesize copolyesters using directly diacids and not diacid derivatives such as diesters dicarboxylic acid used for the enzymatic transesterification. Furthermore, the titanium-catalyzed process in bulk permitted to use three times less solvent than the enzymatic one, which is one of the key point of the green chemistry (Anastas and Warner, 2000).

On the other side, the enzymatic catalysis permitted to perform the reaction with a non-toxic catalyst which can be removed and reused after the reaction contrary to the titanium catalyst. This allowed the synthesized material to may be biocompatible permitting it use in additional applications which are not possible for the same material synthesized *via* the titanium-catalyzed process. Moreover, provided that PHB-diol oligomers were small enough, high molar mass random copolyesters were synthesized under mild conditions with a great control of the macromolecular architectures and without PHB thermal degradation.

5. Conclusion

A family of biobased copolyesters was obtained by titanium-catalyzed transesterification of PHB and PBS or PBA homopolyesters performed in bulk or in solution. Both processes permitted the synthesis of final copolyesters with the same molar composition than the initial feed ratio. The titanium-catalyzed transesterification in bulk was the most appropriate way for the synthesis of copolyesters. Its main advantages are (i) higher molar masses for the copolyesters, (ii) a fast transesterification rate with a negligible PHB thermal degradation and (iii) a low amount of catalyst.

On one side, random poly(HB-*co*-BA) copolyesters were amorphous at room temperature with a T_g increasing with the HB content. They possessed a good thermal stability until 220 °C. On the other side, poly(HB-*co*-BS) copolyesters were solid at room temperature and exhibited crystalline phase due to the PBS part. The melting temperatures and the degree of crystallinity of these copolyesters decreased with (i) the randomization of the structure due to the decrease of the average sequence length of the BS segment and (ii) the HB content. These copolyesters also exhibited a good thermal stability with an absence of mass loss until 230 °C.

Contrary to the enzymatic process, the titanium-catalyzed transesterification process in bulk permitted to quickly obtain random structures with a similar range of molar mass (~15 kg/mol) to the enzymatic process and using small chain length PHB with higher molar mass. The titanium-catalyzed transesterification process was particularly interesting to synthesize copolyesters with high HB contents due to the low influence of the HB contents on the final copolyester molar mass contrary to the enzyme-catalyzed process. Nevertheless, since the titanium catalyst is complicate to remove from the copolyester matrix, only biomedical and tissue engineering applications that do not require metal-free catalysts can be envisaged for such titanium-catalyzed HB-based copolyesters.

Finally, these copolyesters could be also used as compatibilizers in blends based on two non-miscible matrixes, such as PHB with PBS (or PBA) to improve the miscibility, the final properties and the range of applications of these blends (Qiu et al., 2003b, 2003a; Ma et al., 2014). More specifically, the use of oligomers or small chain length of PHB may contribute to a greater industrial development of PHAs in terms of applications. Besides, poly(HB-*co*-BS) and poly(HB-*co*-BA) copolyesters could be interesting for thermoplastic applications where a high biobased content and biodegradable or biocompatible properties are targeted, such as short term packaging, agriculture, or in biomedical area. Nevertheless, to complete the investigation of these materials, some additional tests must be fulfilled such as the study of the reaction time during the bulk transesterification, biodegradability or biocompatibility, mechanical, processing and ageing behaviors.

6. References

Abe, H., 2006. Macromol. Biosci. 6, 469–486.

Ahn, B.D., Kim, S.H., Kim, Y.H., Yang, J.S., 2001. J. Appl. Polym. Sci. 82, 2808–2826.

Anastas, P.T., Warner, J.C., 2000. Green chemistry: theory and practice. Oxford Univ. Press, Oxford.

Arslan, H., Adamus, G., Hazer, B., Kowalczuk, M., 1999. Rapid Commun. Mass Spectrom. 13, 2433–2438.

Baran, E.T., Özer, N., Hasirci, V., 2002. J. Microencapsul. 19, 363–376.

Barham, P.J., Keller, A., Otun, E.L., Holmes, P.A., 1984. J. Mater. Sci. 19, 2781–2794.

Bergamaschi, J.M., Pilau, E.J., Gozzo, F.C., Felisberti, M.I., 2011. Macromol. Symp. 299–300, 10–19.

Cai, Y., Lv, J., Feng, J., 2012. J. Polym. Environ. 21, 108–114.

Cavalheiro, J.M.B.T., Pollet, E., Diogo, H.P., Cesário, M.T., Avérous, L., de Almeida, M.C.M.D., da Fonseca, M.M.R., 2013. Bioresour. Technol. 147, 434–441.

Chen, C.-H., Peng, J.-S., Chen, M., Lu, H.-Y., Tsai, C.-J., Yang, C.-S., 2010. Colloid Polym. Sci. 288, 731–738.

Chrissafis, K., Paraskevopoulos, K.M., Bikiaris, D.N., 2006. Thermochim. Acta 440, 166–175.

Dai, S., Li, Z., 2008. Biomacromolecules 9, 1883–1893.

Debuissy, T., Pollet, E., Averous, L., 2016a. Biomacromolecules.

Debuissy, T., Pollet, E., Avérous, L., 2016b. Polymer 99, 204–213.

Deng, X.M., Hao, J.Y., 2001. Eur. Polym. J. 37, 211–214.

Gao, X., Chen, J.-C., Wu, Q., Chen, G.-Q., 2011. Curr. Opin. Biotechnol., 22/6 Chemical biotechnology and Pharmaceutical biotechnology 22, 768–774.

Gigli, M., Fabbri, M., Lotti, N., Gamberini, R., Rimini, B., Munari, A., 2016. Eur. Polym. J. 75, 431–460.

Grassie, N., Murray, E.J., Holmes, P.A., 1984a. Polym. Degrad. Stab. 6, 47–61.

Grassie, N., Murray, E.J., Holmes, P.A., 1984b. Polym. Degrad. Stab. 6, 127–134.

Guillaume, S.M., Annunziata, L., Rosal, I. del, Iftner, C., Maron, L., Roesky, P.W., Schmid, M., 2013. Polym. Chem. 4, 3077–3087.

Hablot, E., Bordes, P., Pollet, E., Avérous, L., 2008. Polym. Degrad. Stab. 93, 413–421.

Hirt, T.D., Neuenschwander, P., Suter, U.W., 1996. Macromol. Chem. Phys. 197, 1609–1614.

Hwang, S.Y., Yoo, E.S., Im, S.S., 2012. Polym. J. 44, 1179–1190.

Impallomeni, G., Carnemolla, G.M., Puzzo, G., Ballistreri, A., Martino, L., Scandola, M., 2013. Polymer 54, 65–74.

Impallomeni, G., Giuffrida, M., Barbuzzi, T., Musumarra, G., Ballistreri, A., 2002. Biomacromolecules 3, 835–840.

Jacquel, N., Freyermouth, F., Fenouillot, F., Rousseau, A., Pascault, J.P., Fuertes, P., Saint-Loup, R., 2011. J. Polym. Sci. Part Polym. Chem. 49, 5301–5312.

Jaffredo, C.G., Carpentier, J.-F., Guillaume, S.M., 2013. Macromolecules 46, 6765–6776.

Ke, Y., 2015. Express Polym. Lett. 10, 36–53.

Khasanah, Reddy, K.R., Sato, H., Takahashi, I., Ozaki, Y., 2015. Polymer 75, 141–150.

Lengweiler, U.D., Fritz, M.G., Seebach, D., 1996. Helv. Chim. Acta 79, 670–701.

Lenz, R.W., Jedlinski, Z., 1996. Macromol. Symp. 107, 149–161.

Li, J., Li, X., Ni, X., Leong, K.W., 2003. Macromolecules 36, 2661–2667.

Ma, P., Hristova-Bogaerds, D.G., Zhang, Y., Lemstra, P.J., 2014. Polym. Bull. 71, 907–923.

Meszynska, A., Pollet, E., Odelius, K., Hakkarainen, M., Avérous, L., 2015. Macromol. Mater. Eng. 300, 661–666.

Nobes, G.A.R., Kazlauskas, R.J., Marchessault, R.H., 1996. Macromolecules 29, 4829–4833.

Otera, J., 1993. Chem. Rev. 93, 1449–1470.

Pan, P., Inoue, Y., 2009. Prog. Polym. Sci. 34, 605–640.

Papageorgiou, G.Z., Bikiaris, D.N., 2005. Polymer 46, 12081–12092.

Park, S.J., Kim, T.W., Kim, M.K., Lee, S.Y., Lim, S.-C., 2012. Biotechnol. Adv., Special issue on ACB 2011 30, 1196–1206.

Perrine Bordes, Eric Pollet, Luc Avérous, 2009. Potential Use of Polyhydroxyalkanoate (PHA) for Biocomposite Development, in: Nano- and Biocomposites. CRC Press, pp. 193–226.

Persenaire, O., Alexandre, M., Degée, P., Dubois, P., 2001. Biomacromolecules 2, 288–294.

Pollet, E., Avérous, L., 2011. Production, Chemistry and Properties of Polyhydroxyalkanoates, in: Plackett, D. (Ed.), Biopolymers – New Materials for Sustainable Films and Coatings. John Wiley & Sons, Ltd, pp. 65–86.

Qiu, Z., Ikehara, T., Nishi, T., 2003a. Polymer 44, 2503–2508.

Qiu, Z., Ikehara, T., Nishi, T., 2003b. Polymer 44, 7519–7527.

Ravenelle, F., Marchessault, R.H., 2002. Biomacromolecules 3, 1057–1064.

Reeve, M.S., McCarthy, S.P., Gross, R.A., 1993. Macromolecules 26, 888–894.

Rhim, J.-W., Park, H.-M., Ha, C.-S., 2013. Prog. Polym. Sci., Progress in Bionanocomposites: from green plastics to biomedical applications 38, 1629–1652.

Saad, G.R., Lee, Y.J., Seliger, H., 2001. Macromol. Biosci. 1, 91–99.

Shuai, X., Jedlinski, Z., Kowalczuk, M., Rydz, J., Tan, H., 1999. Eur. Polym. J. 35, 721–725.

Van Krevelen, D.W., 1997. Chapter 5 - Calorimetric properties, in: Properties of Polymers (Third, Completely Revised Edition). Elsevier, Amsterdam, pp. 109–127.

Wu, L., Wang, L., Wang, X., Xu, K., 2010. Acta Biomater. 6, 1079–1089.

Xie, W., Li, J., Chen, D., Wang, P.G., 1997. Macromolecules 30, 6997–6998.

Yang, J., Zhu, H., Zhang, C., Jiang, Q., Zhao, Y., Chen, P., Wang, D., 2016. Polymer 83, 230–238.

Conclusion du chapitre 4

Dans le chapitre 4, quelques utilisations possibles du poly[(*R*)-3-hydroxubutyrate] (PHB) comme macrodiols ou homopolyesters pour l'élaboration de nouveaux polyuréthanes ou de nouveaux copolyesters ont été démontrées afin de modifier les propriétés intrinsèques du PHB de ce polyester bactérien, d'améliorer sa faible stabilité thermique et d'ainsi d'augmenter son attractivité pour de futures applications.

Tout d'abord, le PHB a dû être fonctionnalisé et voir sa masse molaire fortement réduite afin de pouvoir synthétiser des polyuréthanes thermoplastiques. L'alcoolyse en solution, par catalyse organométallique, du PHB par des diols aliphatiques courts tel que le 1,4-butanediol permet d'obtenir des oligomères de PHB à terminaisons exclusivement hydroxyles (PHB-diol) en quelque heures sans dégradation thermique. La cinétique de cette réaction a montré que les conditions d'alcoolyse de PHB sont optimales pour une température de 125-130 °C avec 4 eq. de dilaurate de dibutylétain et 1000 eq. de 1,4-butanediol. De plus, pour des PHB-diols avec une masse molaire inférieure à 3000 g/mol il a été montré que leurs propriétés thermiques évoluent fortement en fonction de la masse molaire.

Ensuite, en utilisant les PHB-diols de différentes masses molaires, plusieurs poly(ester-éther-uréthane)s (PEEU) ont pu être synthétisés en solution par couplage de chaînes à l'aide de 4,4'-diphénylméthylène diisocyanate et de différents polyéthers [poly(éthylène glycol) et poly(propylène glycol)-*block*-poly(éthylène glycol)-*block*-poly(propylène glycol) (PPG-PEG-PPG)] avec différents ratios entre les PHB-diols et les polyéthers. Contrairement au PHB bactérien d'origine, les PEEUs montrent une bonne stabilité thermique avec aucune perte de masse enregistrée avant 220 °C. De plus, leurs propriétés physiques et thermiques peuvent être contrôlées et ajustées car elles dépendent du ratio entre le PHB et les polyéthers, de la longueur des segments PHB et polyéther, ainsi que de la nature chimique des polyéthers. En effet, la présence d'une phase cristalline de PHB est conditionnée au fait d'utiliser des PHB-diols suffisamment longs (M_n > 1600 g/mol) et en proportion non négligeable. Ensuite, seul le PEG comme polyéther permet d'obtenir une phase cristalline « éther » à cause de la nature physique du PPG-PEG-PPG qui est liquide à température ambiante. Les températures de fusion et la cristallinité de chaque domaine cristallin augmentent avec la masse molaire des segments utilisés et leur proportion relative.

Par la suite, des poly(HB-*co*-BS)s de différentes structures macromoléculaires ont été synthétisés par transestérification enzymatique en solution soit en une seule étape à partir de PHB-diol, de 1,4-butanediol et de diéthyl succinate, soit en deux étapes à partir de PHB-diol et de chaînes de PBS préalablement synthétisées. Ces deux procédés enzymatiques permettent la synthèse de copolyesters de la même composition que celle introduite dans le milieu réactionnel avec des architectures macromoléculaires que l'on peut façonner en fonction des conditions réactionnelles. A cause des conditions douces requises pour la synthèse enzymatique et des solvants apolaires utilisés, seuls des PHB-diols courts (M_n < 3 000 g/mol) peuvent être utilisés par ce procédé afin qu'ils soient solubles dans le milieu réactionnel. Même si la synthèse enzymatique en une seule étape à l'aide de la lipase B de *Candida antarctica* est plus facile à mettre en œuvre que le procédé en deux étapes, elle ne permet pas d'obtenir des masses molaires très importantes (M_n < 8 000 g/mol) et semble favoriser la dégradation thermique des PHB-diols. De son côté, le procédé en deux étapes permet un meilleur contrôle de l'architecture macromoléculaire et des masses molaires plus

importantes (M_n > 15 000 g/mol). En augmentant la longueur de chaîne des PHB-diols, la réactivité des lipases est fortement diminuée à cause de la grande rigidité de chaîne et cela engendre alors des copolyesters présentant une tendance bloc plutôt qu'une distribution aléatoire des monomères. Ce phénomène est plus prononcé lorsque les synthèses s'effectuent dans le diphényl éther que l'anisole. Toutefois, les masses molaires des copolyesters obtenus sont plus importantes dans le diphényl éther que dans l'anisole. De plus, la masse molaire des copolyesters diminue avec l'augmentation de la proportion en unité HB dans le copolyester. Au final, les copolyesters synthétisés possèdent une meilleure stabilité thermique que les PHB bactérien. Leurs structures cristallines et leurs propriétés mécaniques dépendent exclusivement de la longueur des blocs HB et BS composant les copolyesters. La cristallinité de chaque phase cristalline augmente avec la longueur et la proportion des blocs respectifs même si la présence d'une phase cristalline de PHB est plus difficile à obtenir de par la plus faible cinétique de cristallisation du PHB par rapport à celle du PBS et à une plus faible composition en unité HB dans les copolyesters synthétisés.

Pour finir, deux copolyesters [poly(HB-*co*-BS) et poly(HB-*co*-BA)] à base de PHB-diols et de PBS ou de PBA ont été synthétisés par transestérification en masse et en solution à l'aide d'un catalyseur organométallique à base de titane. L'utilisation d'homopolyesters (PHB, PBS ou PBA) de masses molaires trop élevées ne permet pas d'avoir, ou alors peu, de réaction de transestérification ce qui implique soit un mélange d'homopolyesters à la fin de la réaction, soit un copolyester à tendance bloc. En effet, des copolyesters aléatoires ne sont obtenus qu'en utilisant des PHB-diols relativement courts (M_n ~ 5 000 g/mol). La structure macromoléculaire souhaitée peut donc être « façonnée » en fonction des conditions réactionnelles. Au final, la transestérification organométallique en masse est bien plus intéressante que le procédé en solution car ce dernier engendre une diminution de la masse molaire finale des copolyesters synthétisés et favorise la dégradation thermique du PHB. Ensuite, alors que les poly(HB-*co*-BA)s synthétisés ayant une structure aléatoire sont amorphe, les poly(HB-*co*-BS)s aléatoires sont semi-cristallins à température ambiante. La stabilité thermique et leurs propriétés thermiques sont similaires aux poly(HB-*co*-BS)s synthétisés par voie enzymatique. Au final, la comparaison des deux méthodes (enzymatique et organométallique) de synthèses des copolyesters à base d'oligomère de PHB et de poly(butylène dicarboxylate) (PBS ou PBA) montre que, contrairement à la catalyse enzymatique, la transestérification par catalyse organométallique est un procédé plus rapide, qui nécessite moins de solvant et qui permet d'utiliser des PHB-diols plus longs. De plus, l'effet de diminution de la masse molaire des copolyesters avec la proportion en unités HB est bien moins marqué pour la catalyse organométallique que pour le procédé enzymatique. Toutefois, du fait que ce type de catalyseur à base de titane est très difficile à extraire de la matrice copolyester, certaines applications biomédicales ne pourront pas être envisagées pour les copolyesters synthétisés par transestérification organométallique.

CONCLUSION GÉNÉRALE ET PERSPECTIVES

Ce travail de doctorat s'inscrit dans le cadre d'un Projet Européen multipartenaire FP7 intitulé « SYNPOL » qui a pour finalité la création d'une plateforme technologique intégrant la pyrolyse de bio-déchets complexes et la synthèse de polymères/matériaux biosourcés par des procédés technologiques avancés, notamment par fermentation à partir de syngas comme source de carbone.

Ce projet de thèse, associant la chimie des polymères et leurs caractérisations physico-chimiques, avait pour objectif d'élaborer de nouveaux polyesters aliphatiques thermoplastiques dans une approche de chimie verte à partir de composés plus ou moins directement issus de la biomasse par bioproduction (biotechnologie blanche), tels que :

(i) Différent synthons courts tels que l'acide succinique, l'acide adipique, le 1,3-propanediol, le 1,4- et 2,3-butanediol,

(ii) Oligomères issus d'un polyester bactérien, le poly((*R*)-3-hydroxybutyrate) (PHB).

Différentes voies catalytiques (*i.e.*, organométallique et enzymatique) ont été appliquées pour la synthèse de nouvelles architectures macromoléculaires. Les relations « structure-propriété » de ces systèmes ont été plus particulièrement étudiées.

L'étude bibliographique présentée dans le **chapitre 1** de ce manuscrit dresse un état de l'art des différents polyesters thermoplastiques issus de la biomasse et leurs principales voies de synthèses (biotique et abiotique). L'analyse de la bibliographie a permis d'appréhender les principales problématiques de ces voies de synthèse, notamment celles relatives à la catalyse enzymatique, plus récente dans le domaine de la chimie et qui ne présente pas encore une maturité et antériorité comparable à celle de la catalyse organométallique, et requière donc encore d'importants efforts de recherche. Mais, la catalyse enzymatique s'inscrit très clairement dans une démarche de chimie verte. Cet état de l'art a également montré la richesse des différentes architectures macromoléculaires synthétisées durant ces dernières décennies à partir de diacides et de diols issus de la biomasse, généralement par catalyse organométallique en masse. De plus, il a montré que pour la synthèse de polyesters par catalyse enzymatique, les lipases, et plus particulièrement la lipase B de *Candida antarctica*, montrent la meilleure activité catalytique permettant d'obtenir des polyesters aliphatiques de masses molaires non négligeables (M_n > 10 000 g/mol) pour des conditions optimisées. Toutefois, il a été démontré que de nombreux paramètres réactionnels doivent être pris en compte lors de cette voie de synthèse comme la nature du solvant, la quantité de lipase, la température ou encore la structure des monomères afin de travailler dans des conditions opératoires optimales pour la synthèse des polyesters. Enfin, cet état de l'art a montré que les polyhydroxyalcanoates (PHAs), des polyesters bactériens biodégradables et biocompatibles, présentent une grande variété de structures. Ils peuvent être utilisés après une étape contrôlée de dépolymérisation, comme macrodiols (oligomères) pour la synthèse de nouvelles architectures macromoléculaires tels que des poly(ester-éther-uréthane)s (PEEU) ou des copolyesters. Cette voie de valorisation des PHAs permet (i) de pallier la faible stabilité thermique de certains PHAs (*e.g.*, PHB) qui limite leurs valorisations, et (ii) d'obtenir de nouveaux matériaux dont les propriétés peuvent être ajustées au en fonction de l'application souhaitée.

La présentation des résultats issus de ce travail de thèse a été découpée en trois parties distinctes (chapitres 2 à 4), et divisée en plusieurs sous chapitres comme présenté dans la Figure C.1.

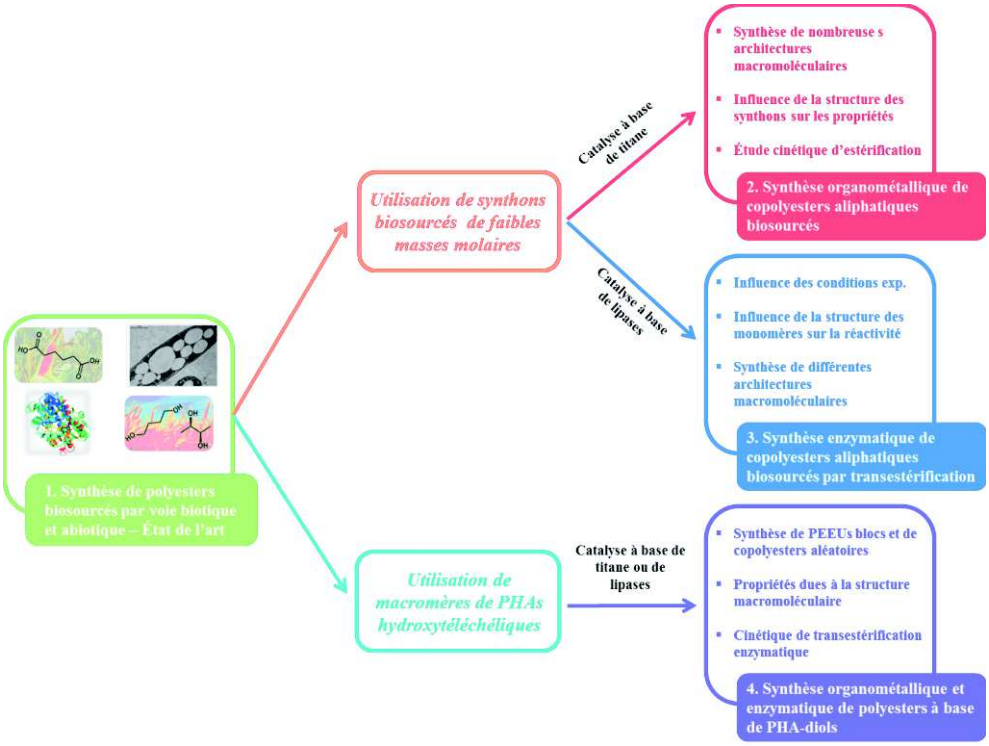

Figure C.1 : Récapitulatif de la stratégie développée au cours de la thèse.

Les relations « structure-propriété » des nombreux copolyesters (PBSA, PPSA, PPBS, PPBA et PBB'A), de hautes masses molaires (M_n > 20 000 g/mol), synthétisés à partir de diacides et diols courts à l'aide d'un catalyseur à base de titane (titanium (IV) isopropoxide) ont été largement étudiées dans le **chapitre 2**. Il a été notamment démontré que la longueur des synthons étudiés (par exemple acide succinique *vs.* acide adipique) n'influe pas sur la synthèse ou la réactivité des monomères, alors que le type de diol (primaire (*i.e.*, 1,4-butanediol) *vs.* secondaire (*i.e.*, 2,3-butanediol)) impacte fortement les masses molaires finales obtenues pour des conditions réactives similaires. En effet, il a été déterminé que la réactivité du 2,3-butanediol avec l'acide adipique était environ dix fois inférieure à celle du 1,4-butanediol ce qui conduit à la synthèse d'oligomères, contenant au minimum 33 mol.% de 2,3-butanediol, avec un M_n de seulement 6 000 g/mol. D'autre part, après une étude minutieuse de chaque structure macromoléculaire obtenue, il a été montré que les différents copolyesters présentent une excellente stabilité thermique jusqu'à des températures supérieures à 250 °C ce qui indique que ces copolyesters présentent une bonne résistance dégradation thermique ce qui est un atout pour la mise en œuvre de ces matériaux. Au regard des différents synthons étudiés (*i.e.*, acide succinique, acide adipique, 1,3-propanediol, 1,4-butanediol et 2,3-butanediol), il s'avère que la structure de ces monomères n'a que peu d'influence sur la stabilité thermique bien qu'une légère amélioration (d'environ 10-20 °C) ait été observée avec l'acide adipique par rapport à l'acide succinique. Ceci peut s'expliquer par une plus faible densité en fonctions ester où se produisent préférentiellement les réactions de scission de chaînes lors de la dégradation thermique. Par ailleurs, il est à noter que les différents copolyesters synthétisés, qui appartiennent à la même famille et qui possèdent des architectures

macromoléculaires assez proches, présentent tous un phénomène de co-cristallisation isodimorphique. Il est caractérisé par la présence d'une seule phase cristalline et d'un pseudo-eutectique concernant les variations de la température et de l'enthalpie de fusion de cette phase cristalline en fonction de la composition. Toutefois, leurs propriétés thermiques et leurs structures cristallines varient de manière significative avec la structure des synthons biosourcés. En effet, il a été démontré que la diminution de la longueur de la chaîne alkyle, même d'un seul carbone, réduit de manière significative la vitesse de cristallisation et la cristallinité du polymère. Par exemple, les copolyesters à forte teneur en 1,3-propanediol (un diol court avec 3 atomes de carbones) possèdent des vitesses de cristallisation si faibles que lors des analyses de DSC, ceux-ci ne cristallisent pas lors du refroidissement, même pour de faibles vitesses de refroidissement, ni au cours du seconde cycle de chauffe. De la même manière, la cristallinité de ces matériaux est fortement réduite par l'utilisation de 2,3-butanediol, qui ne possède que 2 carbones entre les fonctions hydroxyles avec des groupements méthyles latéraux diminuant ainsi la mobilité de chaîne, ce qui limite l'organisation des chaînes vers la cristallisation. On obtient par exemple, un copolyester PBB'A amorphe pour une composition en 2,3-butanediol supérieure à 45 mol.%. La structure des synthons incorporés impacte la mobilité de chaîne et influe donc grandement sur la température de transition vitreuse. Celle-ci diminue avec la réduction de la densité en fonction ester, le long de la chaîne. Cette étude montre donc très clairement des relations nettes entre la structure des synthons et le comportement thermique et en cristallisation des polyesters correspondants. Par ailleurs, la biodégradabilité en compost de certains matériaux a pu être étudiée et il a été démontré d'une part qu'aucun de ces matériaux ne présente d'écotoxicité et d'autre part, qu'en règle générale, la vitesse de biodégradation augmente avec l'augmentation de la longueur du diol (entre le 1,3-propanediol et le 1,4-butanediol) et du diacide (entre l'acide succinique et l'acide adipique). Toutefois, comme aucun des échantillons n'a montré une perte de masse d'au minimum 90% après six mois en milieu compost contrôlé, nos matériaux ne peuvent pas prétendre à la qualification de « compostable » au titre de la norme de référence EN 13432. Cette première partie de l'étude a donc permis d'établir tout un ensemble de relations « structures-propriétés » relatives à ces copolyesters.

Dans le **chapitre 3**, la synthèse de différents polyesters aliphatiques par catalyse enzymatique à l'aide de la lipase B de *Candida antarctica* et l'influence de la structure du monomère sur sa réactivité vis-à-vis de cette estérase ont été largement étudiées. Afin notamment d'avoir une miscibilité de phase entre les substrats et la lipase, et contrairement à la catalyse organométallique en masse, la synthèse enzymatique nécessite l'utilisation de diesters (méthyle ou éthyle) à la place des diacides carboxyliques. Comme cela avait été évoqué dans la partie bibliographique, nous avons pu vérifier que la réactivité de la lipase augmente avec la longueur de la chaîne alkyle du monomère, au moins pour notre gamme de monomères étudiés, ce qui se traduit par une augmentation de la masse molaire finale des polyesters. Afin de développer et améliorer cette voie de synthèse, une optimisation des conditions réactionnelles a été nécessaire. Il a ainsi été démontré que la réalisation de la réaction dans 150-200 pds.% de diphényl éther comme solvant à 90 °C durant 2-3 jours à l'aide de 10 pds.% de la lipase B de *Candida antarctica* immobilisée permet d'obtenir les meilleurs résultats. Ces conditions opératoires ont pu alors être adoptées pour synthétiser et caractériser différents copolyesters (PBSA, PPBS et PBB'S). Suivant l'augmentation de la réactivité des substrats avec la longueur de leurs chaînes alkyles, les masses molaires du PBSA et du PPBS augmentent avec la proportion en unité adipate et

1,4-butyle, respectivement. Toutefois, malgré les différences de réactivité, les différents copolyesters présentent tous une composition finale similaire à celle des monomères introduits dans le milieu réactionnel avec une distribution aléatoire des séquences, comme cela avait été aussi observé pour la catalyse organométallique. De la même manière, la réactivité du 2,3-butanediol porteur de fonctions hydroxyles secondaires est bien moindre que celle du 1,4-butanediol ou même du 1,3-propanediol, mais elle est quand même suffisante pour obtenir des oligomères de poly(2,3-butylène succinate) ayant un M_n d'environ 4 300 g/mol. Enfin, la remarquable activité enzymatique de la lipase B de *Candida antarctica* dans des éthers aromatiques tels que l'anisole et le phénétole a été démontrée. L'anisole, par exemple, a permis la synthèse de polyesters de masses molaires similaires ou supérieures à celles obtenues dans le diphényl éther (M_n > 16 kg/mol à comparer à 10-14 kg/mol dans le diphényl éther). L'étude liée à ce chapitre 3 a permis de développer la catalyse enzymatique pour la synthèse de polyesters par transestérification dans des conditions optimisées. La synthèse de copolyesters avec des architectures différentes a permis de comparer la réactivité de différents monomères vis-à-vis de la lipase B de *Candida antarctica*.

Le **chapitre 4** s'est focalisé sur la synthèse et la caractérisation de différentes architectures à partir oligomères hydroxytéléchéliques de PHB en utilisant les deux voies catalytiques précédemment citées, dans l'optique de valorisation des PHAs avec une approche de déconstruction partielle de ces polymères bactériens et de reconstruction de nouvelles architectures macromoléculaires avec des propriétés largement améliorées. En premier lieu, la fonctionnalisation hydroxyle et la réduction de masse molaire du PHB a été nécessaire afin d'obtenir des oligomères hydroxytéléchéliques de PHB pouvant être utilisés comme macrodiols dans la synthèse de nouveaux poly(ester-éther-uréthane)s (PEEU). La synthèse des oligo-PHB diols s'est effectuée, dans le diglyme avec 1 000 équivalents molaire d'un diol (*i.e.*, 1,3-propanediol ou 1,4-butanediol) à l'aide de 4 équivalents molaire de dilaurate de dibutylétain comme catalyseur organométallique à 125 °C, qui sont les conditions optimales alliant une bonne cinétique de réaction et une absence totale de dégradation thermique. En utilisant ces conditions réactionnelles, la masse molaire des oligomères des PHB hydroxylés (PHB-diol) peut être totalement ajustée *via* le temps de réaction. En couplant chimiquement ces PHB-diols, de masses molaires variables, avec différents polyéthers (poly(éthylène glycol) ou poly(propylène glycol)-*b*-poly(éthylène glycol)-*b*-poly(propylène glycol)) à l'aide de 4,4'-diphénylméthylène diisocyanate avec différents ratios PHB/polyéther, de nouveaux copolymères à tendance bloc, ayant des propriétés physico-chimiques ajustables en fonction de la composition et la longueur des blocs la composant, ont ainsi pu être synthétisés. Il a été démontré que la présence d'une phase cristalline de PHB dans ces matériaux PEEU est conditionnée au fait que la masse molaire du bloc PHB soit d'au moins 1 600 g/mol ou que celui-ci soit en proportion assez importante (> 20 mol.%). Par ailleurs, les oligo-PHB diols ont également été utilisés pour l'élaboration de copolyesters par transestérification avec d'autres polyesters tels que le PBS ou le PBA. D'une part, des copolyesters issus de PHB-diol et de PBS ont été synthétisés par transestérification enzymatique à l'aide de la lipase B de *Candida antarctica* dans des conditions douces limitant grandement la présence de dégradation thermique. Il a été montré que ce procédé permet la synthèse de copolyesters de masses molaires supérieures à 12 000 g/mol ayant la même composition que celle introduite dans le milieu réactionnel avec des architectures macromoléculaires (bloc, micro-bloc ou aléatoire) que l'on peut contrôler en fonction des paramètres de réaction (nature du solvant,

longueur du PHB-diol, composition en PHB-diol). D'autre part, ces mêmes copolyesters ont été obtenus par catalyse organométallique de transestérification à l'aide d'un catalyseur à base de titane. Contrairement à la voie enzymatique, cette voie catalytique présente de nombreux inconvénients lorsqu'elle est effectuée en solution telle qu'une forte sensibilité à la dégradation thermique et l'obtention uniquement de polyesters de faibles masses molaires (M_n < 8 000 g/mol). Le procédé par catalyse organométallique en masse permet quant à lui d'obtenir, tout comme le procédé enzymatique, des copolyesters de masses molaires supérieures à 10 000 g/mol, sans présence de dégradation thermique majeure, avec différentes architectures macromoléculaires selon l'importance des réactions de transestérification, de la nature du second homopolyester sélectionné et la proportion relative en unité HB. À la différence du procédé enzymatique, celui-ci est bien plus rapide, permet d'utiliser des PHB-diols plus longs et souffre moins d'une diminution de la masse molaire du copolyester avec la proportion en unité HB. Toutefois, du fait de l'utilisation du catalyseur à base de titane, très difficile à extraire de la matrice polyester, certaines applications biomédicales ne pourront pas être envisagées pour les copolyesters synthétisés par cette voie. Les divers copolyesters obtenus présentent tous une meilleure stabilité thermique que le PHB initial, ce qui permet de remédier à cet inconvénient majeur et d'envisager leur utilisation dans des procédés de mise en œuvre. La cristallinité de chaque phase cristalline diminue fortement avec la réduction de la longueur des blocs respectifs, jusqu'à avoir des vitesses de cristallisation si lentes, notamment pour la phase PHB, que lors des analyses de DSC, ceux-ci ne cristallisent pas lors du refroidissement, même pour de faibles vitesses de refroidissement, ni au cours du seconde cycle de chauffe.

Au final, au cours de ces différentes études, l'intérêt de synthétiser ces différentes architectures de copolyesters issus de synthons biosourcés par catalyse organométallique et enzymatique a été largement montré. Ceci permettra de mieux valoriser certains synthons obtenus par fermentation de biomasse (2,3-butanediol, PHA,). De nombreuses connaissances scientifiques ont pu être collectées quant à la nature des relations « structures-propriétés » sur un grand nombre d'architectures macromoléculaires synthétisées, plus ou moins proches. De plus, bien que le procédé par catalyse organométallique permette la synthèse rapide de polyesters de hautes masses molaires (M_n > 20 000 g/mol), la catalyse enzymatique a montré un excellent potentiel pour la synthèse de polyesters avec une masse molaire finale supérieure à 10,000 g/mol en utilisant des conditions douces et avec un excellent contrôle de l'architecture obtenue. L'amélioration de l'activité enzymatique pour la synthèse de polyesters par transestérification dans l'anisole par rapport à celle observée jusqu'ici dans le diphényl éther a été démontrée, et ouvre la voie à des développements futurs.

Huit articles sont actuellement publiés dans divers journaux scientifiques, tels que *Polymer* (*2016, 99, 204-213 & 2017, 122, 105-116*), *European Polymer Journal* (*2017, 87, 84-98* ; *2017, 90, 92-104 et 2017,* 93, 103-115), *Journal of Polymer Science Part A : Polymer Chemistry* (*2017, 55 (11), 1949-1961 et 2017, DOI:10.1002/pola.28668*) et *Biomacromolecules* (*2016, 17 (12), 4054–4063*). Un article supplémentaire a été publié dans *Macromolécules (2017, 50 (2), 597–608)* dans le cadre d'une collaboration internationale (hors consortium SYNPOL) avec le Pr. Alejandro Müller de l'université du Pays Basque (Espagne). Avec cette équipe, un autre article collaboratif est en cours d'écriture. De plus, un article (Polymer, 2017, 122, 105-116) a été récemment accepté dans le cadre d'une autre collaboration scientifique internationale avec le

CSIRO (Commonwealth Scientific and Industrial Research Organisation) à Clayton (Australie) et le Dr. Parween Sangwan. Il porte en partie sur l'étude de la compostabilité de ces copolyesters. Par ailleurs et pour finaliser cette étape de valorisation du travail de doctorat une review va être prochainement soumise.

****

Les résultats très intéressants et prometteurs obtenus dans le cadre de cette étude permettent d'ouvrir de nombreuses perspectives pour la synthèse par catalyse organométallique et enzymatique avec de nouvelles structures macromoléculaires issues de synthons biosourcés.

Tout d'abord, un travail important reste à mener afin d'acquérir des connaissances plus fines sur les différents matériaux que nous avons synthétisés. Ainsi, des tests mécaniques en statique et dynamique et des analyses de vieillissements climatiques (UV, température, humidité) sont nécessaires afin de compléter nos études sur les différents copolyesters synthétisés par catalyse organométallique et préparer un transfert vers le monde industriel. De même, nous n'avons pu analyser que six de nos polyesters (PBS, PBS, PPS, PPA, $PBS_{50}A_{50}$ et $PP_{50}B_{50}S$) par biodégradation dans un compost. En associant ces tests (en compost) avec des tests respirométriques de type Sturm en milieu liquide, il serait très intéressant de compléter ce travail et d'analyser divers d'échantillons, notamment avec une gamme de compositions plus large et complète pour un même copolyester afin d'avoir une meilleure compréhension des nombreux mécanismes pouvant être impliqués dans la biodégradation de ces matériaux (par exemple : masse molaire, cristallinité…). De même, l'analyse de biodégradabilité de nos architectures macromoléculaires à base d'oligomères de PHB constituerait un bon complément au travail effectué dans le cadre de cette thèse en portant notamment une attention plus particulière à l'analyse de de la phytotoxicité et l'écotoxicité de nos PEEUS contenant du 4,4'-diphénylméthylène diisocyanate, en relation notamment avec la norme EN 13432.

Ensuite, nous avons observé que sur l'ensemble des copolyesters étudiés, seul le PBS et les copolyesters à forte proportion en unité butylène-succinate présentent une température de fusion supérieure à 90 °C. Il serait donc intéressant d'envisager l'utilisation de synthons biosourcés aromatiques permettant d'apporter plus de rigidité à la structure macromoléculaire tels que l'acide 2,5-furandicarboxylique, les dérivés de l'acide vanillique et férulique, ou encore le résorcinol (Figure C.2). L'aromaticité apporte d'autres propriétés spécifiques telles qu'une amélioration de la tenue à la chaleur, au feu et aux produits chimiques. L'utilisation de dianhydrohexitols (*i.e.*, isosorbide, isomannide et isoidide) qui sont des diols aliphatiques rigides issus de sucres pourrait être envisagée. Ces différents synthons apporteraient globalement une augmentation de la température de fusion, la température de transition vitreuse et le module d'Young des matériaux ce qui pourrait ouvrir des usages et applications pour ces copolyesters biosourcés.

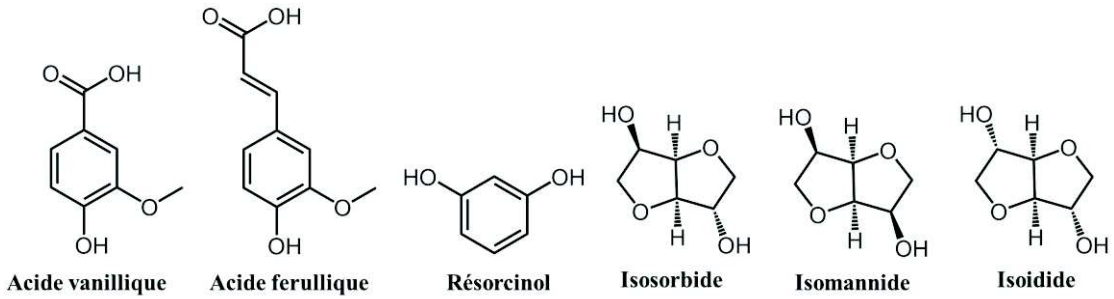

Figure C.2 : Structures chimiques de synthons biosourcés potentiellment intéressants.

En ce qui concerne la synthèse de polyesters par catalyse enzymatique, un travail important reste encore à mener dans la compréhension des mécanismes réactionnels. Cela ouvre notamment la porte à de nombreux travaux à conduire dans le domaine de la modélisation moléculaire afin de mieux appréhender les différents phénomènes mis en jeu au niveau du site actif en fonction du solvant, de la structure 3D de l'enzyme et de celle des monomères. De même, nous avons pu observer que la lipase B de *Candida antarctica* immobilisée permet la réaction de transestérification entre de nombreuses structures différentes (*e.g.*, 1,3-propanediol, 1,4-butanediol, diéthyle succinate) y compris le 2,3-butanediol. Toutefois, il serait intéressant de tester d'autres hydrolases afin de déterminer si certaines d'entre elles pourraient montrer une activité catalytique particulière par rapport notamment à des diols secondaires. Par ailleurs, nous avons pu observer que les masses molaires des copolyesters obtenus par catalyse enzymatique semblent atteindre une sorte de « plafond de verre » qui pourrait être lié à un manque de stabilité de l'enzyme avec une perte d'activité dans le temps. On peut donc penser qu'un important travail d'ingénierie génétique pourrait être mené par des spécialistes du domaine, afin d'améliorer la stabilité et la réactivité des enzymes. Ceci pourrait être associé à de la biologie synthétique afin d'élaborer des enzymes optimisées et à façon.

Enfin, de par la très grande variété des PHAs existant, l'élaboration et l'étude de nouvelles architectures macromoléculaires à base d'oligomères hydroxytéléchéliques pourrait connaître un fort développement et permet d'envisager des applications notamment dans le domaine biomédical. L'obtention d'architectures macromoléculaires nouvelles par fermentation permettrait de sortir des trop classiques PHB et PHBV, et d'élaborer des PHA à base de chaînes moyennes ou longues. Cela passera par un effort de recherche en biotechnologie afin d'identifier ou de créer de nouvelles souches bactériennes capables de produire des PHAs peu conventionnels en utilisant des substrats carbonés peu chers tels que des déchets de biomasse.

LISTE COMPLÈTE DES RÉFÉRENCES BIBLIOGRAPHIQUES

Abe, H., 2006. Macromol. Biosci. 6, 469–486.

Adlercreutz, P., 2013. Chem. Soc. Rev. 42, 6406.

Aeschelmann, F., Carus, 2016. Bio-based Building Blocks and Polymers - Global Capacities and Trends 2016 – 2021. Nova-Institute, Germany.

Agarwal, S., Mast, C., Dehnicke, K., Greiner, A., 2000. Macromol. Rapid Commun. 21, 195–212.

Aharoni, S.M., 2002. Industrial-Scale Production of Polyesters, Especially Poly(Ethylene Terephthalate), in: DSc, S.F. (Ed.), Handbook of Thermoplastic Polyesters. Wiley-VCH Verlag GmbH & Co. KGaA, pp. 59–103.

Ahn, B.D., Kim, S.H., Kim, Y.H., Yang, J.S., 2001. J. Appl. Polym. Sci. 82, 2808–2826.

Albertsson, A.-C., Srivastava, R.K., 2008. Adv. Drug Deliv. Rev., Design and Development Strategies of Polymer Materials for Drug and Gene Delivery Applications 60, 1077–1093.

Albertsson, A.-C., Varma, I.K., 2003. Biomacromolecules 4, 1466–1486.

Aldor, I.S., Kim, S.-W., Prather, K.L.J., Keasling, J.D., 2002. Appl. Environ. Microbiol. 68, 3848–3854.

Alidedeoglu, H.A., Deshpande, H.S., Duckworth, B., Gunale, T., Jayanna, D., Kannan, G., 2013. Method for the preparation of (polybutylene-co-adipate terephthalate) through the in situ phosphorus containing titanium based catalyst. US13/221,159.

Alidedeoglu, H.A., Kannan, G., 2013. Biodegradable aliphatic-aromatic copolyesters, methods of manufacture, and articles thereof. US13/435,865.

Amass, A.J., 1979. Polymer 20, 515–516.

Anastas, P.T., Warner, J.C., 2000. Green chemistry: theory and practice. Oxford Univ. Press, Oxford.

Andrade, A.P., Witholt, B., Hany, R., Egli, T., Li, Z., 2002. Macromolecules 35, 684–689.

Anis, S.N.S., Nurhezreen, M.I., Sudesh, K., Amirul, A.A., 2012. Appl. Biochem. Biotechnol. 167, 524–535.

Aoyagi, Y., Yamashita, K., Doi, Y., 2002. Polym. Degrad. Stab. 76, 53–59.

Arandia, I., Mugica, A., Zubitur, M., Arbe, A., Liu, G., Wang, D., Mincheva, R., Dubois, P., Müller, A.J., 2015. Macromolecules 48, 43–57.

Arslan, H., Adamus, G., Hazer, B., Kowalczuk, M., 1999. Rapid Commun. Mass Spectrom. 13, 2433–2438.

Avérous, L., 2004. J. Macromol. Sci. Part C 44, 231–274.

Avérous, L., Fringant, C., 2001. Polym. Eng. Sci. 41, 727–734.

Avérous, L., Pollet, E., 2012. Biodegradable Polymers, in: Avérous, L., Pollet, E. (Eds.), Environmental Silicate Nano-Biocomposites, Green Energy and Technology. Springer London, pp. 13–39.

Azim, H., Dekhterman, A., Jiang, Z., Gross, R.A., 2006. Biomacromolecules 7, 3093–3097.

Bacaloglu, R., Fisch, M., Biesiada, K., 1998. Polym. Eng. Sci. 38, 1014–1022.

Badenes, S.M., Lemos, F., Cabral, J.M.S., 2011. Biotechnol. Bioeng. 108, 1279–1289.

Baran, E.T., Özer, N., Hasirci, V., 2002. J. Microencapsul. 19, 363–376.

Barham, P.J., Keller, A., Otun, E.L., Holmes, P.A., 1984. J. Mater. Sci. 19, 2781–2794.

de Barros, D.P.C., Fonseca, L.P., Cabral, J.M.S., Weiss, C.K., Landfester, K., 2009a. Biotechnol. J. 4, 674–683.

de Barros, D.P.C., Fonseca, L.P., Fernandes, P., Cabral, J.M.S., Mojovic, L., 2009b. J. Mol. Catal. B Enzym. 60, 178–185.

de Barros, D.P.C., Lemos, F., Fonseca, L.P., Cabral, J.M.S., 2010. J. Mol. Catal. B Enzym. 66, 285–293.

Bart, J.C.J., Cavallaro, S., 2015. Ind. Eng. Chem. Res. 54, 1–46.

Barton, N.R., Burgard, A.P., Burk, M.J., Crater, J.S., Osterhout, R.E., Pharkya, P., Steer, B.A., Sun, J., Trawick, J.D., Dien, S.J.V., Yang, T.H., Yim, H., 2014. J. Ind. Microbiol. Biotechnol. 42, 349–360.

Bates, F.S., 1991. Science 251, 898–905.

Bechthold, I., Bretz, K., Kabasci, S., Kopitzky, R., Springer, A., 2008. Chem. Eng. Technol. 31, 647–654.

Becker, J., Lange, A., Fabarius, J., Wittmann, C., 2015. Curr. Opin. Biotechnol. 36, 168–175.

Beerthuis, R., Rothenberg, G., Shiju, N.R., 2015. Green Chem. 17, 1341–1361.

Belgacem, M.N., Gandini, A. (Eds.), 2008. Monomers, polymers and composites from renewable resources, 1st ed. ed. Elsevier, Amsterdam ; Boston.

Bergamaschi, J.M., Pilau, E.J., Gozzo, F.C., Felisberti, M.I., 2011. Macromol. Symp. 299–300, 10–19.

Bersot, J.C., Jacquel, N., Saint-Loup, R., Fuertes, P., Rousseau, A., Pascault, J.P., Spitz, R., Fenouillot, F., Monteil, V., 2011. Macromol. Chem. Phys. 212, 2114–2120.

Beun, J.J., Dircks, K., Van Loosdrecht, M.C.M., Heijnen, J.J., 2002. Water Res. 36, 1167–1180.

Biebl, H., Menzel, K., Zeng, A.-P., Deckwer, W.-D., 1999. Appl. Microbiol. Biotechnol. 52, 289–297.

Bikiaris, D.N., Achilias, D.S., 2006. Polymer 47, 4851–4860.

Bikiaris, D.N., Chrissafis, K., Paraskevopoulos, K.M., Triantafyllidis, K.S., Antonakou, E.V., 2007. Polym. Degrad. Stab. 92, 525–536.

Bikiaris, D.N., Papageorgiou, G.Z., Achilias, D.S., 2006. Polym. Degrad. Stab. 91, 31–43.

Bikiaris, D.N., Papageorgiou, G.Z., Giliopoulos, D.J., Stergiou, C.A., 2008. Macromol. Biosci. 8, 728–740.

Binns, F., Harffey, P., Roberts, S.M., Taylor, A., 1998. J. Polym. Sci. Part Polym. Chem. 36, 2069–2079.

Bordes, P., Pollet, E., Avérous, L., 2009a. Potential Use of Polyhydroxyalkanoate (PHA) for Biocomposite Development, in: Nano- and Biocomposites. CRC Press, Boca Raton, pp. 193–226.

Bordes, P., Pollet, E., Avérous, L., 2009b. Prog. Polym. Sci. 34, 125–155.

Borman, S., 2004. Chem. Eng. News 82, 35–39.

Bozell, J.J., 2008. CLEAN – Soil Air Water 36, 641–647.

Bozell, J.J., Petersen, G.R., 2010. Green Chem. 12, 539–554.

Brandl, H., Gross, R.A., Lenz, R.W., Fuller, R.C., 1988. Appl. Environ. Microbiol. 54, 1977–1982.

Bueno-Ferrer, C., Hablot, E., Garrigós, M. del C., Bocchini, S., Averous, L., Jiménez, A., 2012. Polym. Degrad. Stab., 3rd International Conference on Biodegradable and Biobased Polymers (BIOPOL-2011) - Strasbourg 2011 97, 1964–1969.

Bukhari, A., Idris, A., Atta, M., Loong, T.C., 2014. Chin. J. Catal. 35, 1555–1564.

Buzin, P., Lahcini, M., Schwarz, G., Kricheldorf, H.R., 2008. Macromolecules 41, 8491–8495.

Cai, Y., Lv, J., Feng, J., 2012. J. Polym. Environ. 21, 108–114.

Campistron, I., Reyx, D., Hamza, M., Oulmidi, A., 1997. Macromol. Symp. 122, 329–334.

Cao, A., Okamura, T., Nakayama, K., Inoue, Y., Masuda, T., 2002. Polym. Degrad. Stab. 78, 107–117.

Carothers, W.H., 1929. J. Am. Chem. Soc. 51, 2548–2559.

Carothers, W.H., 1931. Chem. Rev. 8, 353–426.

Carothers, W.H., 1936. Trans Faraday Soc 32, 39–49.

Carothers, W.H., Arvin, J.A., 1929. J. Am. Chem. Soc. 51, 2560–2570.

Carré, C., Bonnet, L., Avérous, L., 2014. RSC Adv 4, 54018–54025.

Carvalho, C.M.L., Aires-Barros, M.R., Cabral, J.M.S., 1998. Electron. J. Biotechnol. 1, 160–173.

Carvalho, C.M.L., Aires-Barros, M.R., Cabral, J.M.S., 1999. Biotechnol. Bioeng. 66, 17–34.

Cavalheiro, J.M.B.T., Pollet, E., Diogo, H.P., Cesário, M.T., Avérous, L., de Almeida, M.C.M.D., da Fonseca, M.M.R., 2013. Bioresour. Technol. 147, 434–441.

Celińska, E., Grajek, W., 2009. Biotechnol. Adv. 27, 715–725.

Celli, A., Marchese, P., Sisti, L., Dumand, D., Sullalti, S., Totaro, G., 2013. Polym. Int. 62, 1210–1217.

Champagne, É., Lévaray, N., Zhu, X.X., 2017. ACS Sustain. Chem. Eng. 5, 689–695.

Chandure, A.S., Umare, S.S., 2007. Int. J. Polym. Mater. Polym. Biomater. 56, 339–353.

Chanfreau, S., Mena, M., Porras-Domínguez, J.R., Ramírez-Gilly, M., Gimeno, M., Roquero, P., Tecante, A., Bárzana, E., 2010. Bioprocess Biosyst. Eng. 33, 629–638.

Chang, W.L., Karalis, T., 1993. J. Polym. Sci. Part Polym. Chem. 31, 493–504.

Charlier, Q., Girard, E., Freyermouth, F., Vandesteene, M, Jacquel, N., Ladavière, C., Rousseau, A., Fenouillot, F., 2015. Express Polym. Lett. 9, 424–434.

Chaudhary, A., Beckman, E.J., Russell, A.J., 1995. J. Am. Chem. Soc. 117, 3728–3733.

Chaudhary, A.K., Beckman, E.J., Russell, A.J., 1997a. Biotechnol. Bioeng. 55, 227–239.

Chaudhary, A.K., Lopez, J., Beckman, E.J., Russell, A.J., 1997b. Biotechnol. Prog. 13, 318–325.

Chen, C.-H., Lu, H.-Y., Chen, M., Peng, J.-S., Tsai, C.-J., Yang, C.-S., 2009. J. Appl. Polym. Sci. 111, 1433–1439.

Chen, C.-H., Peng, J.-S., Chen, M., Lu, H.-Y., Tsai, C.-J., Yang, C.-S., 2010. Colloid Polym. Sci. 288, 731–738.

Chen, G.-Q., 2009. Chem. Soc. Rev. 38, 2434–2446.

Chen, G.-Q. (Ed.), 2010. Plastics from bacteria: natural functions and applications, Microbiology monographs. Springer, Berlin.

Chen, G.-Q., Hajnal, I., Wu, H., Lv, L., Ye, J., 2015. Trends Biotechnol. 33, 565–574.

Chen, M.S., Chang, S.J., Chang, R.S., Kuo, W.F., Tsai, H.B., 1990. J. Appl. Polym. Sci. 40, 1053–1057.

Chen, Y., Chen, J., Yu, C., Du, G., Lun, S., 1999. Process Biochem. 34, 153–157.

Chen, Y., Li, M., Meng, F., Yang, W., Chen, L., Huo, M., 2014. Environ. Technol. 35, 1791–1801.

Chen, Y., Yang, H., Zhou, Q., Chen, J., Gu, G., 2001. Process Biochem. 36, 501–506.

Chisti, Y., 2003. Trends Biotechnol. 21, 89–93.

Chivrac, F., Kadlecová, Z., Pollet, E., Avérous, L., 2006. J. Polym. Environ. 14, 393–401.

Chivrac, F., Pollet, E., Avérous, L., 2007. J. Polym. Sci. Part B Polym. Phys. 45, 1503–1510.

Choi, J., Lee, S.Y., 1999a. Biotechnol. Bioeng. 62, 546–553.

Choi, J., Lee, S.Y., 1999b. Appl. Environ. Microbiol. 65, 4363–4368.

Choi, S., Song, C.W., Shin, J.H., Lee, S.Y., 2015. Metab. Eng. 28, 223–239.

Chrissafis, K., Paraskevopoulos, K.M., Bikiaris, D.N., 2006a. Thermochim. Acta 440, 166–175.

Chrissafis, K., Paraskevopoulos, K.M., Bikiaris, D.N., 2006b. Polym. Degrad. Stab. 91, 60–68.

Comim Rosso, S.R., Bianchin, E., de Oliveira, D., Oliveira, J.V., Ferreira, S.R.S., 2013. J. Supercrit. Fluids, Special Issue – 10th International Symposium on Supercritical FluidsSpecial Issue – 10th International Symposium on Supercritical Fluids 79, 133–141.

Corma, A., Iborra, S., Velty, A., 2007. Chem. Rev. 107, 2411–2502.

Cui, Z., Qiu, Z., 2015. Polymer 67, 12–19.

Dai, J., Ma, S., Wu, Y., Han, L., Zhang, L., Zhu, J., Liu, X., 2015. Green Chem. 17, 2383–2392.

Dai, J.-Y., Zhao, P., Cheng, X.-L., Xiu, Z.-L., 2015. Appl. Biochem. Biotechnol. 175, 3014–3024.

Dai, S., Li, Z., 2008. Biomacromolecules 9, 1883–1893.

Dai, S., Xue, L., Li, Z., 2011. ACS Catal. 1, 1421–1429.

Dai, S., Xue, L., Zinn, M., Li, Z., 2009. Biomacromolecules 10, 3176–3181.

Debuissy, T., Pollet, E., Avérous, L., 2016a. Polymer 99, 204–213.

Debuissy, T., Pollet, E., Avérous, L., 2016b. Biomacromolecules 17, 4054–4063.

Debuissy, T., Pollet, E., Avérous, L., 2017a. Eur. Polym. J. 87, 84–98.

Debuissy, T., Pollet, E., Avérous, L., 2017b. Eur. Polym. J. 90, 92–104.

Debuissy, T., Pollet, E., Avérous, L., 2017c. J. Polym. Sci. Part Polym. Chem. n/a-n/a.

Debuissy, T., Pollet, E., Avérous, L., 2017d. Eur. Polym. J. 93, 103–115.

Deng, L.-M., Wang, Y.-Z., Yang, K.-K., Wang, X.-L., Zhou, Q., Ding, S.-D., 2004. Acta Mater. 52, 5871–5878.

Deng, X.M., Hao, J.Y., 2001. Eur. Polym. J. 37, 211–214.

Deng, X.M., Yuan, M.L., Xiong, C.D., Li, X.H., 1999. J. Appl. Polym. Sci. 71, 1941–1948.

Deng, Y., Ma, L., Mao, Y., 2016. Biochem. Eng. J. 105, Part A, 16–26.

Díaz, A., Franco, L., Puiggalí, J., 2014. Thermochim. Acta 575, 45–54.

Doi, Y., 1990. Microbial polyesters, John Wiley & Sons, Inc. ed. VCH, New York.

Dong, H., Cao, S.-G., Li, Z.-Q., Han, S.-P., You, D.-L., Shen, J.-C., 1999. J. Polym. Sci. Part Polym. Chem. 37, 1265–1275.

Drożdżyńska, A., Leja, K., Czaczyk, K., 2011. BioTechnologia 1, 92–100.

Du, G.C., Chen, J., Yu, J., Lun, S., 2001. Biochem. Eng. J. 8, 103–110.

Duchiron, S.W., Pollet, E., Givry, S., Avérous, L., 2015. RSC Adv. 5, 84627–84635.

Duh, B., 2001. J. Appl. Polym. Sci. 81, 1748–1761.

Duh, B., 2002. Polymer 43, 3147–3154.

Düşkünkorur, H.Ö., Bégué, A., Pollet, E., Phalip, V., Güvenilir, Y., Avérous, L., 2015. J. Mol. Catal. B Enzym. 115, 20–28.

Egmond, M.R., de Vlieg, J., 2000. Biochimie, Lipase 2000 82, 1015–1021.

El-Imam, A.A., Du, C., 2014. J. Biodivers. Bioprospecting Dev.

Feder, D., Gross, R.A., 2010. Biomacromolecules 11, 690–697.

Fidler, S., Dennis, D., 1992. FEMS Microbiol. Rev. 9, 231–235.

Flory, Paul J., 1939. J. Am. Chem. Soc. 61, 3334–3340.

Fortunati, E., Gigli, M., Luzi, F., Dominici, F., Lotti, N., Gazzano, M., Cano, A., Chiralt, A., Munari, A., Kenny, J.M., Armentano, I., Torre, L., 2017. Carbohydr. Polym. 165, 51–60.

Fox, T., 1956. Bull. Am. Phys. Soc. 1, 123–132.

Fradet, A., Maréchal, E., 1982. Kinetics and mechanisms of polyesterifications, in: Polymerizations and Polymer Properties. Springer, Berlin, Heidelberg, pp. 51–142.

Fradet, A., Tessier, M., 2003. Polyesters, in: Rogers, rtin E., Long, T.E. (Eds.), Synthetic Methods in Step-Growth Polymers. John Wiley & Sons, Inc., pp. 17–134.

Fu, H., Kulshrestha, A.S., Gao, W., Gross, R.A., Baiardo, M., Scandola, M., 2003. Macromolecules 36, 9804–9808.

Fukui, T., Doi, Y., 1998. Appl. Microbiol. Biotechnol. 49, 333–336.

Gallaher, T.N., Gaul, D.A., Schreiner, S., 1996. J. Chem. Educ. 73, 465.

Gamerith, C., Zartl, B., Pellis, A., Guillamot, F., Marty, A., Acero, E.H., Guebitz, G.M., 2017. Process Biochem.

Gan, Z., Abe, H., Doi, Y., 2002. Macromol. Chem. Phys. 203, 2369–2374.

Gan, Z., Kuwabara, K., Yamamoto, M., Abe, H., Doi, Y., 2004. Polym. Degrad. Stab. 83, 289–300.

Gandini, A., 2011. Green Chem. 13, 1061–1083.

Gao, X., Chen, J.-C., Wu, Q., Chen, G.-Q., 2011. Curr. Opin. Biotechnol., 22/6 Chemical biotechnology and Pharmaceutical biotechnology 22, 768–774.

Garaleh, M., Lahcini, M., Kricheldorf, H.R., Weidner, S.M., 2009. J. Polym. Sci. Part Polym. Chem. 47, 170–177.

García-Alles, L.F., Gotor, V., 1998. Biotechnol. Bioeng. 59, 163–170.

Garin, M., Tighzert, L., Vroman, I., Marinkovic, S., Estrine, B., 2014a. J. Appl. Polym. Sci. 131, 40639/1-40639/10.

Garin, M., Tighzert, L., Vroman, I., Marinkovic, S., Estrine, B., 2014b. J. Appl. Polym. Sci. 131, 40887/1-40887/7.

Garin, M., Tighzert, L., Vroman, I., Marinkovic, S., Estrine, B., 2014c. J. Appl. Polym. Sci. 131, 40887/1-40887/7.

Geciova, J., Bury, D., Jelen, P., 2002. Int. Dairy J. 12, 541–553.

Ghassemi, H., Schiraldi, D.A., 2014. J. Appl. Polym. Sci. 131, n/a-n/a.

Gigli, M., Fabbri, M., Lotti, N., Gamberini, R., Rimini, B., Munari, A., 2016a. Eur. Polym. J. 75, 431–460.

Gigli, M., Fabbri, M., Lotti, N., Gamberini, R., Rimini, B., Munari, A., 2016b. Eur. Polym. J. 75, 431–460.

Gigli, M., Lotti, N., Gazzano, M., Finelli, L., Munari, A., 2013. Polym. Eng. Sci. 53, 491–501.

Gordon, M., Taylor, J.S., 2007. J. Appl. Chem. 2, 493–500.

Gotor-Fernández, V., Vicente, G., 2007. Use of Lipases in Organic Synthesis, in: Polaina, J., MacCabe, A.P. (Eds.), Industrial Enzymes. Springer Netherlands, pp. 301–315.

Graber, M., Bousquet-Dubouch, M.-P., Lamare, S., Legoy, M.-D., 2003. Biochim. Biophys. Acta BBA - Proteins Proteomics 1648, 24–32.

Grassie, N., Murray, E.J., Holmes, P.A., 1984a. Polym. Degrad. Stab. 6, 47–61.

Grassie, N., Murray, E.J., Holmes, P.A., 1984b. Polym. Degrad. Stab. 6, 127–134.

Grassie, N., Murray, E.J., Holmes, P.A., 1984c. Polym. Degrad. Stab. 6, 95–103.

Grecea, M.L., Dimian, A.C., Tanase, S., Subbiah, V., Rothenberg, G., 2012. Catal. Sci. Technol. 2, 1500.

Griffin, G.J.L. (Ed.), 1994. Chemistry and technology of biodegradable polymers, 1st ed. ed. Blackie Academic & Professional, London ; New York.

Gross, S.M., Flowers, D., Roberts, G., Kiserow, D.J., DeSimone, J.M., 1999. Macromolecules 32, 3167–3169.

Gross, S.M., Roberts, G.W., Kiserow, D.J., DeSimone, J.M., 2000. Macromolecules 33, 40–45.

Gubbels, E., Drijfhout, J.P., Posthuma-van Tent, C., Jasinska-Walc, L., Noordover, B.A.J., Koning, C.E., 2014. Prog. Org. Coat. 77, 277–284.

Gubbels, E., Jasinska-Walc, L., Koning, C.E., 2013. J. Polym. Sci. Part Polym. Chem. 51, 890–898.

Gubbels, Erik, Jasinska-Walc, L., Noordover, B.A.J., Koning, C.E., 2013. Eur. Polym. J. 49, 3188–3198.

Guillaume, S.M., Annunziata, L., Rosal, I. del, Iftner, C., Maron, L., Roesky, P.W., Schmid, M., 2013. Polym. Chem. 4, 3077–3087.

Guisan, J.M., Betancor, L., Fernandez-Lorente, G., Flickinger, M.C., 2009. Immobilized Enzymes, in: Encyclopedia of Industrial Biotechnology. John Wiley & Sons, Inc.

Gumel, A.M., Annuar, M.S.M., Chisti, Y., 2013. Ultrason. Sonochem. 20, 937–947.

Gumel, A.M., Annuar, M.S.M., Chisti, Y., Heidelberg, T., 2012. Ultrason. Sonochem. 19, 659–667.

Gustini, L., Lavilla, C., Janssen, W.W.T.J., Martínez de Ilarduya, A., Muñoz-Guerra, S., Koning, C.E., 2016. ChemSusChem 9, 2250–2260.

Gustini, L., Noordover, B.A.J., Gehrels, C., Dietz, C., Koning, C.E., 2015. Eur. Polym. J. 67, 459–475.

Guzmán-Lagunes, F., López-Luna, A., Gimeno, M., Bárzana, E., 2012. J. Supercrit. Fluids 72, 186–190.

Habeych, D.I., Juhl, P.B., Pleiss, J., Vanegas, D., Eggink, G., Boeriu, C.G., 2011. J. Mol. Catal. B Enzym. 71, 1–9.

Hablot, E., Bordes, P., Pollet, E., Avérous, L., 2008. Polym. Degrad. Stab. 93, 413–421.

Hakan Akat, M.B., 2006. Iran. Polym. J. 15, 921–928.

Harmsen, P.F.H., Hackmann, M.M., Bos, H.L., 2014. Biofuels Bioprod. Biorefining 8, 306–324.

Harrison, S.T.L., 1991. Biotechnol. Adv. 9, 217–240.

Hedstrom, L., 2001. An Overview of Serine Proteases, in: Current Protocols in Protein Science. John Wiley & Sons, Inc.

Hedstrom, L., 2002. Chem. Rev. 102, 4501–4524.

Hejazi, P., Vasheghani-Farahani, E., Yamini, Y., 2003. Biotechnol. Prog. 19, 1519–1523.

Henderson, L.A., Svirkin, Y.Y., Gross, R.A., Kaplan, D.L., Swift, G., 1996. Macromolecules 29, 7759–7766.

Hernández, J.J., Rueda, D.R., García-Gutiérrez, M.C., Nogales, A., Ezquerra, T.A., Soccio, M., Lotti, N., Munari, A., 2010. Langmuir 26, 10731–10737.

Hirt, T.D., Neuenschwander, P., Suter, U.W., 1996. Macromol. Chem. Phys. 197, 1609–1614.

Ho, R.-M., Ke, K.-Z., Chen, M., 2000. Macromolecules 33, 7529–7537.

Høegh, I., Patkar, S., Halkier, T., Hansen, M.T., 1995. Can. J. Bot. 73, 869–875.

Hoekman, S.K., Broch, A., Robbins, C., Ceniceros, E., Natarajan, M., 2012. Renew. Sustain. Energy Rev. 16, 143–169.

Hoffmann, A., Kreuzberger, S., Hinrichsen, G., 1994. Polym. Bull. 33, 355–359.

Holden, G., Adams, R.K. (Eds.), 1996. Thermoplastic elastomers, 2. ed. ed. Hanser [u.a.], Munich.

Holmberg, A.L., Reno, K.H., Wool, R.P., Thomas H. Epps, I.I.I., 2014. Soft Matter 10, 7405–7424.

Holmes, P.A., 1985. Phys. Technol. 16, 32.

Hori, H., Takahashi, H., Yamaguchi, A., Hagiwara, T., 1995. Can. J. Microbiol. 41, 282–288.

Hori, Y., Suzuki, M., Yamaguchi, A., Nishishita, T., 1993a. Macromolecules 26, 5533–5534.

Hori, Y., Takahashi, Y., Yamaguchi, A., Nishishita, T., 1993b. Macromolecules 26, 4388–4390.

Hotelier, T., Renault, L., Cousin, X., Negre, V., Marchot, P., Chatonnet, A., 2004. Nucleic Acids Res. 32, D145–D147.

Hu, D., Chung, A.-L., Wu, L.-P., Zhang, X., Wu, Q., Chen, J.-C., Chen, G.-Q., 2011. Biomacromolecules 12, 3166–3173.

Hu, L., Wu, L., Song, F., Li, B.-G., 2010. Macromol. React. Eng. 4, 621–632.

Hu, X., Shen, X., Huang, M., Liu, C., Geng, Y., Wang, R., Xu, R., Qiao, H., Zhang, L., 2016. Polymer 84, 343–354.

Huang, C.Q., Luo, S.Y., Xu, S.Y., Zhao, J.B., Jiang, S.L., Yang, W.T., 2010. J. Appl. Polym. Sci. 115, 1555–1565.

Hunsen, M., Abul, A., Xie, W., Gross, R., 2008. Biomacromolecules 9, 518–522.

Hunsen, M., Azim, A., Mang, H., Wallner, S.R., Ronkvist, A., Xie, W., Gross, R.A., 2007. Macromolecules 40, 148–150.

Hwang, S.Y., Yoo, E.S., Im, S.S., 2012. Polym. J. 44, 1179–1190.

Impallomeni, G., Carnemolla, G.M., Puzzo, G., Ballistreri, A., Martino, L., Scandola, M., 2013. Polymer 54, 65–74.

Impallomeni, G., Giuffrida, M., Barbuzzi, T., Musumarra, G., Ballistreri, A., 2002. Biomacromolecules 3, 835–840.

Ionescu, M., 2005. Chemistry and technology of polyols for polyurethanes. Rapra Technology, Shawbury, Shrewsbury, Shropshire, U.K.

Ishihara, K., Ohara, S., Yamamoto, H., 2000. Science 290, 1140–1142.

Ishii, M., Okazaki, M., Shibasaki, Y., Ueda, M., Teranishi, T., 2001. Biomacromolecules 2, 1267–1270.

Isikgor, F.H., Becer, C.R., 2015. Polym. Chem., Polymer Chemistry 6, 4497–4559.

Iwata, S., Toshima, K., Matsumura, S., 2003. Macromol. Rapid Commun. 24, 467–471.

Jackson, W.J., Watkins, J.J., 1986. Aromatic polyesters derived from 2,3-butanediol. US4600768.

Jacquel, N., Freyermouth, F., Fenouillot, F., Rousseau, A., Pascault, J.P., Fuertes, P., Saint-Loup, R., 2011. J. Polym. Sci. Part Polym. Chem. 49, 5301–5312.

Jaffredo, C.G., Carpentier, J.-F., Guillaume, S.M., 2013. Macromolecules 46, 6765–6776.

Jansen, M.L., van Gulik, W.M., 2014. Curr. Opin. Biotechnol., Chemical biotechnology • Pharmaceutical biotechnology 30, 190–197.

Japu, C., Martínez de Ilarduya, A., Alla, A., Jiang, Y., Loos, K., Muñoz-Guerra, S., 2015. Biomacromolecules 16, 868–879.

Jasinska, L., Koning, C.E., 2010. J. Polym. Sci. Part Polym. Chem. 48, 2885–2895.

Jbilou, F., Dole, P., Degraeve, P., Ladavière, C., Joly, C., 2015. Eur. Polym. J. 68, 207–215.

Jesionowski, T., Zdarta, J., Krajewska, B., 2014. Adsorption 20, 801–821.

Ji, X.-J., Huang, H., Ouyang, P.-K., 2011. Biotechnol. Adv. 29, 351–364.

Jiang, W., Wang, S., Wang, Y., Fang, B., 2016. Biotechnol. Biofuels 9, 57.

Jiang, Y., van Ekenstein, G.O.R.A., Woortman, A.J.J., Loos, K., 2014a. Macromol. Chem. Phys. 215, 2185–2197.

Jiang, Y., Loos, K., 2016. Polymers 8, 243.

Jiang, Y., Woortman, A.J.J., Alberda van Ekenstein, G.O.R., Petrović, D.M., Loos, K., 2014b. Biomacromolecules 15, 2482–2493.

Jiang, Y., Woortman, A.J.J., van Ekenstein, G.O.R.A., Loos, K., 2013. Biomolecules 3, 461–480.

Jiang, Y., Woortman, A.J.J., Ekenstein, G.O.R.A. van, Loos, K., 2015a. Polym. Chem. 6, 5451–5463.

Jiang, Y., Woortman, A.J.J., Ekenstein, G.O.R.A. van, Loos, K., 2015b. Polym. Chem. 6, 5198–5211.

Jiménez-Quero, A., Pollet, E., Zhao, M., Marchioni, E., Avérous, L., Phalip, V., 2016a. J. Microbiol. Biotechnol. 26, 1557–1565.

Jiménez-Quero, A., Pollet, E., Zhao, M., Marchioni, E., Averous, L., Phalip, V., 2016b. J. Microbiol. Biotechnol.

Jin, H.-J., Lee, B.-Y., Kim, M.-N., Yoon, J.-S., 2000a. Eur. Polym. J. 36, 2693–2698.

Jin, H.-J., Lee, B.-Y., Kim, M.-N., Yoon, J.-S., 2000b. Eur. Polym. J. 36, 2693–2698.

Johnson, K., Jiang, Y., Kleerebezem, R., Muyzer, G., van Loosdrecht, M.C.M., 2009. Biomacromolecules 10, 670–676.

Jourdan, N., Deguire, S., Brisse, F., 1995. Macromolecules 28, 8086–8091.

Jung, I.L., Phyo, K.H., Kim, K.C., Park, H.K., Kim, I.G., 2005. Res. Microbiol. 156, 865–873.

Kahar, P., Agus, J., Kikkawa, Y., Taguchi, K., Doi, Y., Tsuge, T., 2005. Polym. Degrad. Stab. 87, 161–169.

Kahar, P., Tsuge, T., Taguchi, K., Doi, Y., 2004. Polym. Degrad. Stab. 83, 79–86.

Kampouris, E.M., Papaspyrides, C.D., 1985. Polymer 26, 413–417.

Kapoor, M., Gupta, M.N., 2012. Process Biochem. 47, 555–569.

Kapritchkoff, F.M., Viotti, A.P., Alli, R.C.P., Zuccolo, M., Pradella, J.G.C., Maiorano, A.E., Miranda, E.A., Bonomi, A., 2006. J. Biotechnol. 122, 453–462.

Kathiraser, Y., Aroua, M.K., Ramachandran, K.B., Tan, I.K.P., 2007. J. Chem. Technol. Biotechnol. 82, 847–855.

Kaur, G., Srivastava, A.K., Chand, S., 2012. Biochem. Eng. J. 64, 106–118.

Kawai, F., Nakadai, K., Nishioka, E., Nakajima, H., Ohara, H., Masaki, K., Iefuji, H., 2011. Polym. Degrad. Stab. 96, 1342–1348.

Kawai, R., Miura, M., Takakuwa, K., Isahaya, Y., Fujimori, T., Suito, J., Nakamura, M., Kawai, R., Miura, M., Takakuwa, K., Isahaya, Y., Fujimori, T., Suito, J., Nakamura, M., 1995. Aliphatic polyester carbonate and process for producing the same.

EP0684270 (A2).

Ke, Y., 2015. Express Polym. Lett. 10, 36–53.

Kerep, P., Ritter, H., 2006. Macromol. Rapid Commun. 27, 707–710.

Kerep, P., Ritter, H., 2007. Macromol. Rapid Commun. 28, 759–766.

Khan, A., Sharma, S.K., Kumar, A., Watterson, A.C., Kumar, J., Parmar, V.S., 2014. ChemSusChem 7, 379–390.

Khasanah, Reddy, K.R., Sato, H., Takahashi, I., Ozaki, Y., 2015. Polymer 75, 141–150.

Kim, M., Cho, K.-S., Ryu, H.W., Lee, E.G., Chang, Y.K., 2003. Biotechnol. Lett. 25, 55–59.

Kint, D.P.R., Alla, A., Deloret, E., Campos, J.L., Muñoz-Guerra, S., 2003. Polymer 44, 1321–1330.

Kobayashi, S., 2009. Macromol. Rapid Commun. 30, 237–266.

Kobayashi, S., 2015. Polym. Adv. Technol. 26, 677–686.

Kobayashi, S., Uyama, H., Namekawa, S., 1998. Polym. Degrad. Stab., Biodegradable Polymers and Macromolecules 59, 195–201.

Kong, X., Qi, H., Curtis, J.M., 2014. J. Appl. Polym. Sci. 131, n/a-n/a.

Koning, G.J.M. de, Witholt, B., 1997. Bioprocess Eng. 17, 7–13.

Köpke, M., Mihalcea, C., Liew, F., Tizard, J.H., Ali, M.S., Conolly, J.J., Al-Sinawi, B., Simpson, S.D., 2011. Appl. Environ. Microbiol. 77, 5467–5475.

Korntner, P., Sumerskii, I., Bacher, M., Rosenau, T., Potthast, A., 2015. Holzforschung 69, 807–814.

Kraus, G.A., 2008. CLEAN – Soil Air Water 36, 648–651.

Kricheldorf, H.R., Behnken, G., Schwarz, G., 2005. Polymer 46, 11219–11224.

Kulschewski, T., Sasso, F., Secundo, F., Lotti, M., Pleiss, J., 2013. J. Biotechnol. 168, 462–469.

Kumar, A., Gross, R.A., 2000a. Biomacromolecules 1, 133–138.

Kumar, A., Gross, R.A., 2000b. J. Am. Chem. Soc. 122, 11767–11770.

Kumar, A., Kalra, B., Dekhterman, A., Gross, R.A., 2000. Macromolecules 33, 6303–6309.

Kunioka, M., Wang, Y., Onozawa, S., 2005. Macromol. Symp. 224, 167–180.

Kuo, C.-T., Chen, S.-A., 1989. J. Polym. Sci. Part Polym. Chem. 27, 2793–2803.

Kwolek, S.L., Morgan, P.W., 1964. J. Polym. Sci. A 2, 2693–2703.

Laane, C., Boeren, S., Vos, K., Veeger, C., 2009. Biotechnol. Bioeng. 102, 1–8.

Laurichesse, S., Avérous, L., 2014. Prog. Polym. Sci., Topical Issue on Biomaterials 39, 1266–1290.

Laycock, B., Halley, P., Pratt, S., Werker, A., Lant, P., 2013. Prog. Polym. Sci., Topical Issue on Biorelevant Polymers 38, 536–583.

Le Nôtre, J., Witte-van Dijk, S.C.M., van Haveren, J., Scott, E.L., Sanders, J.P.M., 2014. ChemSusChem 7, 2712–2720.

Lee, S.Y., 1996. Trends Biotechnol. 14, 431–438.

Lee, S.Y., Lee, Y., Wang, F., 1999. Biotechnol. Bioeng. 65, 363–368.

Lee, W.-H., Loo, C.-Y., Nomura, C.T., Sudesh, K., 2008. Bioresour. Technol. 99, 6844–6851.

Lemoigne, M., 1926. Bull Soc Chim Bio 8, 770–782.

Lengweiler, U.D., Fritz, M.G., Seebach, D., 1996. Helv. Chim. Acta 79, 670–701.

Lenz, R.W., Jedlinski, Z., 1996. Macromol. Symp. 107, 149–161.

Li, G., Yao, D., Zong, M., 2008. Eur. Polym. J. 44, 1123–1129.

Li, J., Li, X., Ni, X., Leong, K.W., 2003. Macromolecules 36, 2661–2667.

Li, S.Y., Dong, C.L., Wang, S.Y., Ye, H.M., Chen, G.-Q., 2011. Appl. Microbiol. Biotechnol. 90, 659–669.

Li, Z.-J., Shi, Z.-Y., Jian, J., Guo, Y.-Y., Wu, Q., Chen, G.-Q., 2010. Metab. Eng. 12, 352–359.

Liaw, D.-J., Liaw, B.-Y., Hsu, J.-J., Cheng, Y.-C., 2000. J. Polym. Sci. Part Polym. Chem. 38, 4451–4456.

Lin, C.C., Hsieh, K.H., 1977. J. Appl. Polym. Sci. 21, 2711–2719.

Lindström, A., Albertsson, A.-C., Hakkarainen, M., 2004. Polym. Degrad. Stab. 83, 487–493.

Linko, Y.-Y., Lämsä, M., Wu, X., Uosukainen, E., Seppälä, J., Linko, P., 1998. J. Biotechnol., Biocatalysis 66, 41–50.

Linko, Y.-Y., Wang, Z.-L., Seppälä, J., 1995a. J. Biotechnol. 40, 133–138.

Linko, Y.-Y., Wang, Z.-L., Seppälä, J., 1995b. Enzyme Microb. Technol. 17, 506–511.

Liu, L., Pang, M., Zhang, Y., 2015. Eur. J. Lipid Sci. Technol. 117, 1636–1646.

Lo, C.-W., Wu, H.-S., Wei, Y.-H., 2011. J. Taiwan Inst. Chem. Eng. 42, 240–246.

Loeker, F.C., Duxbury, C.J., Kumar, R., Gao, W., Gross, R.A., Howdle, S.M., 2004. Macromolecules 37, 2450–2453.

Loh, X.J., Goh, S.H., Li, J., 2007a. Biomacromolecules 8, 585–593.

Loh, X.J., Karim, A.A., Owh, C., 2015. J. Mater. Chem. B Mater. Biol. Med. 3, 7641–7652.

Loh, X.J., Wang, X., Li, H., Li, X., Li, J., 2007b. Mater. Sci. Eng. C, Symposium A: Advanced Biomaterials International Conference on Materials for Advanced Technologies (ICMAT 2005) 27, 267–273.

Longhi, S., Nicolas, A., Creveld, L., Egmond, M., Verrips, C.T., de Vlieg, J., Martinez, C., Cambillau, C., 1996. Proteins Struct. Funct. Bioinforma. 26, 442–458.

Loos, K. (Ed.), 2010. Front Matter, in: Biocatalysis in Polymer Chemistry. Wiley-VCH Verlag GmbH & Co. KGaA.

Lorenzini, C., Renard, E., Bensemhoun, J., Babinot, J., Versace, D.-L., Langlois, V., 2013. React. Funct. Polym. 73, 1656–1661.

Lu, S.-F., Chen, M., Chen, C.H., 2012. J. Appl. Polym. Sci. 123, 3610–3619.

Lu, S.-F., Chen, M., Shih, Y.-C., Chen, C.H., 2010. J. Polym. Sci. Part B Polym. Phys. 48, 1299–1308.

Luo, S., Li, F., Yu, J., Cao, A., 2010. J. Appl. Polym. Sci. 115, 2203–2211.

Luo, S.Y., Zhang, Y., Zhao, J.B., 2006. Adv. Mater. Res. 11–12, 387–390.

Ma, L., Persson, M., Adlercreutz, P., 2002. Enzyme Microb. Technol. 31, 1024–1029.

Ma, P., Hristova-Bogaerds, D.G., Zhang, Y., Lemstra, P.J., 2014. Polym. Bull. 71, 907–923.

MacDonald, R.T., Pulapura, S.K., Svirkin, Y.Y., Gross, R.A., Kaplan, D.L., Akkara, J., Swift, G., Wolk, S., 1995. Macromolecules 28, 73–78.

Madison, L.L., Huisman, G.W., 1999. Microbiol. Mol. Biol. Rev. MMBR 63, 21–53.

Mahapatro, A., Kalra, B., Kumar, A., Gross, R.A., 2003. Biomacromolecules 4, 544–551.

Mahapatro, A., Kumar, A., Kalra, B., Gross, R.A., 2004. Macromolecules 37, 35–40.

Makay-Bödi, E., Vancso-Szercsanyi, I., 1969. Eur. Polym. J. 5, 145.

Mallon, F., Beers, K., Ives, A., Ray, W.H., 1998. J. Appl. Polym. Sci. 69, 1789–1791.

Mani, R., Bhattacharya, M., Leriche, C., Nie, L., Bassi, S., 2002. J. Polym. Sci. Part Polym. Chem. 40, 3232–3239.

Marcilla, R., de Geus, M., Mecerreyes, D., Duxbury, C.J., Koning, C.E., Heise, A., 2006. Eur. Polym. J. 42, 1215–1221.

Mark, J.E., 1999. Polymer Data Handbook. Oxford University Press, New York.

Martinez, C., De Geus, P., Lauwereys, M., Matthyssens, G., Cambillau, C., 1992. Nature 356, 615–618.

Martinez, C., Nicolas, A., van Tilbeurgh, H., Egloff, M.P., Cudrey, C., Verger, R., Cambillau, C., 1994. Biochemistry (Mosc.) 33, 83–89.

Matos, T.D., King, N., Simmons, L., Walker, C., McClain, A.R., Mahapatro, A., Rispoli, F.J., McDonnell, K.T., Shah, V., 2011. Green Chem. Lett. Rev. 4, 73–79.

McChalicher, C.W.J., Srienc, F., 2007. J. Biotechnol. 132, 296–302.

Medway, A.M., Sperry, J., 2014. Green Chem. 16, 2084–2101.

Mei, Y., Kumar, A., Gross, R.A., 2002. Macromolecules 35, 5444–5448.

Mei, Y., Miller, L., Gao, W., Gross, R.A., 2003. Biomacromolecules 4, 70–74.

Mena, M., Chanfreau, S., Gimeno, M., Bárzana, E., 2010. Bioprocess Biosyst. Eng. 33, 1095–1101.

Mena, M., López-Luna, A., Shirai, K., Tecante, A., Gimeno, M., Bárzana, E., 2013. Bioprocess Biosyst. Eng. 36, 383–387.

Meng, J., Tang, X., Li, W., Shi, H., Zhang, X., 2013. Thermochim. Acta 558, 83–86.

Meszynska, A., Pollet, E., Odelius, K., Hakkarainen, M., Avérous, L., 2015. Macromol. Mater. Eng. 300, 661–666.

Mezoul, G., Lalot, T., Brigodiot, M., Maréchal, E., 1995. J. Polym. Sci. Part Polym. Chem. 33, 2691–2698.

Miletić, N., Loos, K., Gross, R.A., 2010. Enzymatic Polymerization of Polyester, in: Loos, K. (Ed.), Biocatalysis in Polymer Chemistry. Wiley-VCH Verlag GmbH & Co. KGaA, pp. 83–129.

Mincheva, R., Delangre, A., Raquez, J.-M., Narayan, R., Dubois, P., 2013. Biomacromolecules 14, 890–899.

Miura, M., Takakuwa, K., Fujimori, S., Ito, M., 1998. Aliphatic Polyestercarbonate and Its Production. JPH1045884 (A).

Mochizuki, M., Mukai, K., Yamada, K., Ichise, N., Murase, S., Iwaya, Y., 1997. Macromolecules 30, 7403–7407.

Mohamad, N.R., Marzuki, N.H.C., Buang, N.A., Huyop, F., Wahab, R.A., 2015. Biotechnol. Biotechnol. Equip. 29, 205–220.

Mohsen-Nia, M., Memarzadeh, M.R., 2013. Polym. Bull. 70, 2471–2491.

Montaudo, G., Rizzarelli, P., 2000. Polym. Degrad. Stab. 70, 305–314.

Munari, A., Manaresi, P., Chiorboli, E., Chiolle, A., 1992. Eur. Polym. J. 28, 101–106.

Murphy, C.A., Cameron, J.A., Huang, S.J., Vinopal, R.T., 1996. Appl. Environ. Microbiol. 62, 456–460.

Muthuraj, R., Misra, M., Mohanty, A.K., 2015. ACS Sustain. Chem. Eng. 3, 2767–2776.

Nakaoki, T., Danno, M., Kurokawa, K., 2003. Polym. J. 35, 791–797.

Nakaoki, T., Kitoh, M., Gross, R.A., 2005. Enzymatic Ring Opening Polymerization of ε-Caprolactone in Supercritical CO2, in: Polymer Biocatalysis and Biomaterials, ACS Symposium Series. American Chemical Society, pp. 393–404.

Namekawa, S., Uyama, H., Kobayashi, S., 2000a. Biomacromolecules 1, 335–338.

Namekawa, S., Uyama, H., Kobayashi, S., Kricheldorf, H.R., 2000b. Macromol. Chem. Phys. 201, 261–264.

Nanaki, S.G., Pantopoulos, K., Bikiaris, D.N., 2011. Int. J. Nanomedicine 6, 2981–2995.

Nardini, M., Dijkstra, B.W., 1999. Curr. Opin. Struct. Biol. 9, 732–737.

Neves, A., Müller, J., 2012. Biotechnol. Prog. 28, 1575–1580.

Niaounakis, M., 2014. Biopolymers: Processing and Products. William Andrew.

Nikolic, M.S., Djonlagic, J., 2001. Polym. Degrad. Stab. 74, 263–270.

Nobes, G.A.R., Kazlauskas, R.J., Marchessault, R.H., 1996. Macromolecules 29, 4829–4833.

Noordover, B.A.J., van Staalduinen, V.G., Duchateau, R., Koning, C.E., van Benthem, Mak, M., Heise, A., Frissen, A.E., van Haveren, J., 2006. Biomacromolecules 7, 3406–3416.

Nordblad, M., Adlercreutz, P., 2013. Biocatal. Biotransformation 31, 237–245.

Ohara, H., Nishioka, E., Yamaguchi, S., Kawai, F., Kobayashi, S., 2011. Biomacromolecules 12, 3833–3837.

Ohara, H., Onogi, A., Yamamoto, M., Kobayashi, S., 2010. Biomacromolecules 11, 2008–2015.

Ojijo, V., Ray, S.S., 2012. Poly(Butylene Succinate) and Poly[(Butylene Succinate)-co-Adipate] Nanocomposites, in: Avérous, L., Pollet, E. (Eds.), Environmental Silicate Nano-Biocomposites, Green Energy and Technology. Springer London, pp. 165–218.

Okabe, M., Lies, D., Kanamasa, S., Park, E.Y., 2009. Appl. Microbiol. Biotechnol. 84, 597–606.

Ollis, D.L., Cheah, E., Cygler, M., Dijkstra, B., Frolow, F., Franken, S.M., Harel, M., Remington, S.J., Silman, I., Schrag, J., 1992. Protein Eng. 5, 197–211.

Ortner, A., Pellis, A., Gamerith, C., Yebra, A.O., Scaini, D., Kaluzna, I., Mink, D., Wildeman, S. de, Acero, E.H., Guebitz, G.M., 2017. Green Chem. 19, 816–822.

Otera, J., 1993. Chem. Rev. 93, 1449–1470.

Otera, J., Danoh, N., Nozaki, H., 1991. J. Org. Chem. 56, 5307–5311.

Otton, J., Ratton, S., Vasnev, V.A., Markova, G.D., Nametov, K.M., Bakhmutov, V.I., Komarova, L.I., Vinogradova, S.V., Korshak, V.V., 1988. J. Polym. Sci. Part Polym. Chem. 26, 2199–2224.

Ottosson, J., Hult, K., 2001. J. Mol. Catal. B Enzym., Proceedings of the 4th International Symposium on Biocatalysis 11, 1025–1028.

Öztürk Düşkünkorur, H., Pollet, E., Phalip, V., Güvenilir, Y., Avérous, L., 2014. Polymer 55, 1648–1655.

Öztürk, H., Pollet, E., Phalip, V., Güvenilir, Y., Avérous, L., 2016. Polymers 8, 416.

Pan, P., Inoue, Y., 2009. Prog. Polym. Sci. 34, 605–640.

Papageorgiou, G.Z., Bikiaris, D.N., 2005a. Polymer 46, 12081–12092.

Papageorgiou, G.Z., Bikiaris, D.N., 2005b. Polymer 46, 12081–12092.

Papageorgiou, G.Z., Bikiaris, D.N., 2007. Biomacromolecules 8, 2437–2449.

Papageorgiou, G.Z., Bikiaris, D.N., 2009. Macromol. Chem. Phys. 210, 1408–1421.

Papageorgiou, G.Z., Bikiaris, D.N., Achilias, D.S., Papastergiadis, E., Docoslis, A., 2011. Thermochim. Acta 515, 13–23.

Papageorgiou, G.Z., Vassiliou, A.A., Karavelidis, V.D., Koumbis, A., Bikiaris, D.N., 2008. Macromolecules 41, 1675–1684.

Papaspyrides, C.D., Vouyiouka, S.N. (Eds.), 2009. Solid state polymerization. Wiley, Hoboken, N.J.

Park, H., Seo, J., Lee, H.-Y., Kim, H.-W., Wall, I.B., Gong, M.-S., Knowles, J.C., 2012. Acta Biomater. 8, 2911–2918.

Park, H.G., Chang, H.N., Dordick, J.S., 1994. Biocatalysis 11, 263–271.

Park, S.J., Kim, T.W., Kim, M.K., Lee, S.Y., Lim, S.-C., 2012. Biotechnol. Adv., Special issue on ACB 2011 30, 1196–1206.

Parker, M.-C., Brown, S.A., Robertson, L., Turner, N.J., 1998. Chem. Commun. 2247–2248.

Patel, R.N., 2008. Expert Opin. Drug Discov. 3, 187–245.

Patil, D.R., Rethwisch, D.G., Dordick, J.S., 1991. Biotechnol. Bioeng. 37, 639–646.

Pederson, E.N., McChalicher, C.W.J., Srienc, F., 2006. Biomacromolecules 7, 1904–1911.

Pellis, A., Acero, E.H., Weber, H., Obersriebnig, M., Breinbauer, R., Srebotnik, E., Guebitz, G.M., 2015a. Biotechnol. J. 10, 1739–1749.

Pellis, A., Corici, L., Sinigoi, L., D'Amelio, N., Fattor, D., Ferrario, V., Ebert, C., Gardossi, L., 2015b. Green Chem. 17, 1756–1766.

Pellis, A., Ferrario, V., Zartl, B., Brandauer, M., Gamerith, C., Acero, E.H., Ebert, C., Gardossi, L., Guebitz, G.M., 2016. Catal. Sci. Technol. 6, 3430–3442.

Pellis, Alessandro, Guebitz, G.M., Farmer, T.J., 2016a. Molecules 21, 1245.

Pellis, Alessandro, Haernvall, K., Pichler, C.M., Ghazaryan, G., Breinbauer, R., Guebitz, G.M., 2016b. J. Biotechnol., Special Issue on ACIB, Dedicated to the Occasion of Prof. Dr. Helmut Schwab's 65th Birthday 235, 47–53.

Pellis, Alessandro, Herrero Acero, E., Gardossi, L., Ferrario, V., Guebitz, G.M., 2016c. Polym. Int. 65, 861–871.

Penco, M., Ranucci, E., Ferruti, P., 1998. Polym. Int. 46, 203–216.

Penzel, E., Rieger, J., Schneider, H.A., 1997. Polymer 38, 325–337.

Peoples, O.P., Sinskey, A.J., 1989a. J. Biol. Chem. 264, 15293–15297.

Peoples, O.P., Sinskey, A.J., 1989b. J. Biol. Chem. 264, 15298–15303.

Pérez-Camargo, R.A., Fernández-d'Arlas, B., Cavallo, D., Debuissy, T., Pollet, E., Avérous, L., Müller, A.J., 2017. Macromolecules 50, 597–608.

Pérez–Camargo, R.A., Saenz, G., Laurichesse, S., Casas, M.T., Puiggalí, J., Avérous, L., Müller, A.J., 2015. J. Polym. Sci. Part B Polym. Phys. 53, 1736–1750.

Persenaire, O., Alexandre, M., Degée, P., Dubois, P., 2001. Biomacromolecules 2, 288–294.

Philip, S., Keshavarz, T., Roy, I., 2007. J. Chem. Technol. Biotechnol. 82, 233–247.

Picataggio, S., Rohrer, T., Deanda, K., Lanning, D., Reynolds, R., Mielenz, J., Eirich, L.D., 1992. Nat. Biotechnol. 10, 894–898.

Pio, T.F., Macedo, G.A., 2009. Chapter 4 Cutinases:: Properties and Industrial Applications, in: Microbiology, B.-A. in A. (Ed.), . Academic Press, pp. 77–95.

Pion, F., Reano, A.F., Oulame, M.Z., Barbara, I., Flourat, A.L., Ducrot, P.-H., Allais, F., 2015. Chemo-enzymatic Synthesis, Derivatizations, and Polymerizations of Renewable Phenolic Monomers Derived from Ferulic Acid and Biobased Polyols: An Access to Sustainable Copolyesters, Poly(ester-urethane)s, and Poly(ester-alkenamer)s, in: Green Polymer Chemistry: Biobased Materials and Biocatalysis, ACS Symposium Series. American Chemical Society, pp. 41–68.

Piotrowska, U., Sobczak, M., 2014. Molecules 20, 1–23.

Plage, B., Schulten, H.R., 1990. Macromolecules 23, 2642–2648.

Pleiss, J., Fischer, M., Schmid, R.D., 1998. Chem. Phys. Lipids 93, 67–80.

Polen, T., Spelberg, M., Bott, M., 2013. J. Biotechnol., Research on Industrial Biotechnology within the CLIB-Graduate Cluster - Part III 167, 75–84.

Pollet, E., Avérous, L., 2011. Production, Chemistry and Properties of Polyhydroxyalkanoates, in: Plackett, D. (Ed.), Biopolymers – New Materials for Sustainable Films and Coatings. John Wiley & Sons, Ltd, Chichester, pp. 65–86.

Poojari, Y., Clarson, S.J., 2013. Biocatal. Agric. Biotechnol. 2, 7–11.

Przystałowska, H., Lipiński, D., Słomski, R., 2015. Acta Biochim. Pol. 62, 23–34.

Qi, P., Chen, H.-L., Nguyen, H.T.H., Lin, C.-C., Miller, S.A., 2016. Green Chem. 18, 4170–4175.

Qiu, S., Qiu, Z., 2016. J. Appl. Polym. Sci. 133, n/a-n/a.

Qiu, Z., Ikehara, T., Nishi, T., 2003a. Polymer 44, 2503–2508.

Qiu, Z., Ikehara, T., Nishi, T., 2003b. Polymer 44, 7519–7527.

Ranucci, E., Liu, Y., Söderqvist Lindblad, M., Albertsson, A.-C., 2000. Macromol. Rapid Commun. 21, 680–684.

Ravenelle, F., Marchessault, R.H., 2002. Biomacromolecules 3, 1057–1064.

Raza, S., Fransson, L., Hult, K., 2001. Protein Sci. 10, 329–338.

Reeve, M.S., McCarthy, S.P., Gross, R.A., 1993. Macromolecules 26, 888–894.

Rehm, S., Trodler, P., Pleiss, J., 2010. Protein Sci. 19, 2122–2130.

Rejasse, B., Lamare, S., Legoy, M.-D., Besson, T., 2007. J. Enzyme Inhib. Med. Chem. 22, 519–527.

Ren, M., Song, J., Song, C., Zhang, Huiliang, Sun, X., Chen, Q., Zhang, Hongfang, Mo, Z., 2005. J. Polym. Sci. Part B Polym. Phys. 43, 3231–3241.

Reulier, M., Avérous, L., 2015. Eur. Polym. J. 67, 418–427.

Reulier, M., Perrin, R., Avérous, L., 2016. J. Appl. Polym. Sci. 133, n/a-n/a.

Rhim, J.-W., Park, H.-M., Ha, C.-S., 2013. Prog. Polym. Sci., Progress in Bionanocomposites: from green plastics to biomedical applications 38, 1629–1652.

Risso, M., Mazzini, M., Kröger, S., Saenz-Méndez, P., Seoane, G., Gamenara, D., 2012. Green Chem. Lett. Rev. 5, 539–543.

Rizzarelli, P., Cirica, M., Pastorelli, G., Puglisi, C., Valenti, G., 2015. Polym. Degrad. Stab. 121, 90–99.

Roa Engel, C.A., Straathof, A.J.J., Zijlmans, T.W., van Gulik, W.M., van der Wielen, L.A.M., 2008. Appl. Microbiol. Biotechnol. 78, 379–389.

Rotticci, D., Hæffner, F., Orrenius, C., Norin, T., Hult, K., 1998. J. Mol. Catal. B Enzym. 5, 267–272.

Roy, I., Visakh, P.M. (Eds.), 2014. Polyhydroxyalkanoate (PHA) Based Blends, Composites and Nanocomposites, RSC Green Chemistry. Royal Society of Chemistry, Cambridge.

Rudnik, E., 2010. Compostable Polymer Materials. Elsevier.

Rydz, J., Sikorska, W., Kyulavska, M., Christova, D., 2014. Int. J. Mol. Sci. 16, 564–596.

Saad, G.R., Lee, Y.J., Seliger, H., 2001. Macromol. Biosci. 1, 91–99.

Saam, J.C., 1998. J. Polym. Sci. Part Polym. Chem. 36, 341–356.

Santos, M., Gangoiti, J., Llama, M.J., Serra, J.L., Keul, H., Möller, M., 2012. J. Mol. Catal. B Enzym. 77, 81–86.

Sasso, F., Kulschewski, T., Secundo, F., Lotti, M., Pleiss, J., 2015. J. Biotechnol. 214, 1–8.

Schmid, R.D., Verger, R., 1998a. Angew. Chem. Int. Ed. 37, 1608–1633.

Schmid, R.D., Verger, R., 1998b. Angew. Chem. Int. Ed. 37, 1608–1633.

Schrag, J.D., Cygler, M., 1997. [4] Lipases and αβ hydrolase fold, in: Enzymology, B.-M. in (Ed.), Lipases, Part A: Biotechnology. Academic Press, pp. 85–107.

Šerá, J., Stloukal, P., Jančová, P., Verney, V., Pekařová, S., Koutný, M., 2016. J. Agric. Food Chem. 64, 5653–5661.

Shah, M.V., van Mastrigt, O., Heijnen, J.J., van Gulik, W.M., 2016. Yeast Chichester Engl. 33, 145–161.

Sheldon, R.A., 2014. Green Chem. 16, 950–963.

Sheldon, R.A., Arends, I., Hanefeld, U., 2008. Green chemistry and catalysis, Repr. ed, Green chemistry. Wiley-VCH, Weinheim.

Shi, C., DeSimone, J.M., Kiserow, D.J., Roberts, G.W., 2001a. Macromolecules 34, 7744–7750.

Shi, C., Gross, S.M., DeSimone, J.M., Kiserow, D.J., Roberts, G.W., 2001b. Macromolecules 34, 2060–2064.

Shirahama, H., Kawaguchi, Y., Aludin, M.S., Yasuda, H., 2001. J. Appl. Polym. Sci. 80, 340–347.

Shoda, S., Uyama, H., Kadokawa, J., Kimura, S., Kobayashi, S., 2016. Chem. Rev. 116, 2307–2413.

Shuai, X., Jedlinski, Z., Kowalczuk, M., Rydz, J., Tan, H., 1999. Eur. Polym. J. 35, 721–725.

Silva, C.M., Carneiro, F., O'Neill, A., Fonseca, L.P., Cabral, J.S.M., Guebitz, G., Cavaco-Paulo, A., 2005. J. Polym. Sci. Part Polym. Chem. 43, 2448–2450.

Silva, G.P. da, Contiero, J., Neto, Á., Marcelo, P., Lima, C.J.B. de, 2014. Quím. Nova 37, 527–534.

Siotto, M., Zoia, L., Tosin, M., Degli Innocenti, F., Orlandi, M., Mezzanotte, V., 2013. J. Environ. Manage. 116, 27–35.

Smith, R. (Ed.), 2005. Biodegradable polymers for industrial applications. Woodhead ; CRC Press, Cambridge : Boca Raton.

Smitthipong, W., Chollakup, R., Nardin, M., 2014. Bio-Based Composites for High-Performance Materials: From Strategy to Industrial Application. CRC Press.

Soccio, M., Lotti, N., Finelli, L., Gazzano, M., Munari, A., 2007. Polymer 48, 3125–3136.

Soccio, M., Lotti, N., Finelli, L., Gazzano, M., Munari, A., 2009. Eur. Polym. J. 45, 3236–3248.

Solaiman, D.K.Y., Ashby, R.D., Foglia, T.A., Marmer, W.N., 2006a. Appl. Microbiol. Biotechnol. 71, 783–789.

Solaiman, D.K.Y., Ashby, R.D., Hotchkiss, A.T., Foglia, T.A., 2006b. Biotechnol. Lett. 28, 157–162.

Song, C.W., Lee, S.Y., 2015. Appl. Microbiol. Biotechnol. 99, 8455–8464.

Spinella, S., Ganesh, M., Re, G.L., Zhang, S., Raquez, J.-M., Dubois, P., Gross, R.A., 2015. Green Chem. 17, 4146–4150.

Špitalský, Z., Lacík, I., Lathová, E., Janigová, I., Chodák, I., 2006. Polym. Degrad. Stab. 91, 856–861.

Spyros, A., Argyropoulos, D.S., Marchessault, R.H., 1997. Macromolecules 30, 327–329.

Srinivasan, R., Desai, P., Abhiraman, A.S., Knorr, R.S., 1994. J. Appl. Polym. Sci. 53, 1731–1743.

Stegmann, P., 2014. The environmental performance of biobased 1,3-propanediol production from glycerol compared to conventional production pathways - A Life Cycle Assessment (Master's Thesis). University of Utrecht, Utrecht, Netherlands.

Steinbüchel, A., Hofrichter, M. (Eds.), 2001. Biopolymers, Polyesters III - Applications and Commercial Products. Wiley-VCH, Weinheim ; Chichester.

Steinbüchel, A., Valentin, H.E., 1995. FEMS Microbiol. Lett. 128, 219–228.

Stempfle, F., Ortmann, P., Mecking, S., 2016. Chem. Rev. 116, 4597–4641.

Sudesh, K., Abe, H., Doi, Y., 2000. Prog. Polym. Sci. 25, 1503–1555.

Sugihara, S., Toshima, K., Matsumura, S., 2006. Macromol. Rapid Commun. 27, 203–207.

Sun, X., Shen, X., Jain, R., Lin, Y., Wang, Jian, Sun, J., Wang, Jia, Yan, Y., Yuan, Q., 2015. Chem. Soc. Rev. 44, 3760–3785.

Suzuki, Y., Ohura, T., Kasuya, K., Toshima, K., Doi, Y., Matsumura, S., 2000. Chem. Lett. 29, 318–319.

Suzuki, Y., Taguchi, S., Hisano, T., Toshima, K., Matsumura, S., Doi, Y., 2003. Biomacromolecules 4, 537–543.

Suzuki, Y., Taguchi, S., Saito, T., Toshima, K., Matsumura, S., Doi, Y., 2001. Biomacromolecules 2, 541–544.

Tachibana, Y., Masuda, T., Funabashi, M., Kunioka, M., 2010. Biomacromolecules 11, 2760–2765.

Takahashi, H., Hayakawa, T., Ueda, M., 2000. Chem. Lett. 29, 684–685.

Takamoto, T., Kerep, P., Uyama, H., Kobayashi, S., 2001. Macromol. Biosci. 1, 223–227.

Takamoto, T., Uyama, H., Kobayashi, S., 2013. E-Polym. 1, 19–24.

Takasu, A., Iio, Y., Mimura, T., Hirabayashi, T., 2005a. Polym. J. 37, 946–953.

Takasu, A., Iio, Y., Oishi, Y., Narukawa, Y., Hirabayashi, T., 2005b. Macromolecules 38, 1048–1050.

Takasu, A., Makino, T., Yamada, S., 2009. Macromolecules 43, 144–149.

Takasu, A., Oishi, Y., Iio, Y., Inai, Y., Hirabayashi, T., 2003. Macromolecules 36, 1772–1774.

Takiyama, E., Fujimaki, T., 1994. Biodegradable plastics and polymers, in: Doi, Y., Fukuda, K. (Eds.), Biodegradable Plastics and Polymers. Elsevier Science, Burlington, p. 150.

Tang, T., Moyori, T., Takasu, A., 2013. Macromolecules 46, 5464–5472.

Tanzi, M.C., Verderio, P., Lampugnani, M.G., Resnati, M., Dejana, E., Sturani, E., 1994. J. Mater. Sci. Mater. Med. 5, 393–396.

Taresco, V., Creasey, R.G., Kennon, J., Mantovani, G., Alexander, C., Burley, J.C., Garnett, M.C., 2016. Polymer 89, 41–49.

Thurecht, K.J., Heise, A., deGeus, M., Villarroya, S., Zhou, J., Wyatt, M.F., Howdle, S.M., 2006. Macromolecules 39, 7967–7972.

Tokiwa, Y., Calabia, B.P., Ugwu, C.U., Aiba, S., 2009. Int. J. Mol. Sci. 10, 3722–3742.

Tripathi, L., Wu, L.-P., Chen, J., Chen, G.-Q., 2012. Microb. Cell Factories 11, 44.

Tripathi, L., Wu, L.-P., Meng, D., Chen, J., Chen, G.-Q., 2013. Biomacromolecules 14, 862–870.

Tsai, C.-J., Chang, W.-C., Chen, C.-H., Lu, H.-Y., Chen, M., 2008. Eur. Polym. J. 44, 2339–2347.

Tserki, V., Matzinos, P., Pavlidou, E., Panayiotou, C., 2006a. Polym. Degrad. Stab. 91, 377–384.

Tserki, V., Matzinos, P., Pavlidou, E., Vachliotis, D., Panayiotou, C., 2006b. Polym. Degrad. Stab. 91, 367–376.

Tsuge, T., 2002. J. Biosci. Bioeng. 94, 579–584.

Umare, S.S., Chandure, A.S., Pandey, R.A., 2007. Polym. Degrad. Stab. 92, 464–479.

United States Department of Agriculture, 2011. Biobased Economy Indicators - A report to the U.S. Congress. Washington DC.

Uppenberg, J., Hansen, M.T., Patkar, S., Jones, T.A., 1994. Structure 2, 293–308.

Uppenberg, J., Oehrner, N., Norin, M., Hult, K., Kleywegt, G.J., Patkar, S., Waagen, V., Anthonsen, T., Jones, T.A., 1995. Biochemistry (Mosc.) 34, 16838–16851.

Uyama, H., Inada, K., Kobayashi, S., 2001. Macromol. Biosci. 1, 40–44.

Uyama, H., Kobayashi, S., 1994. Chem. Lett. 23, 1687–1690.

Uyama, H., Kobayashi, S., 2006. Enzymatic Synthesis of Polyesters via Polycondensation, in: Kobayashi, S., Ritter, H., Kaplan, D. (Eds.), Enzyme-Catalyzed Synthesis of Polymers, Advances in Polymer Science. Springer Berlin Heidelberg, pp. 133–158.

Uyama, H., Takamoto, T., Kobayashi, S., 2002. Polym. J. 34, 94–96.

Uyama, H., Yaguchi, S., Kobayashi, S., 1999. J. Polym. Sci. Part Polym. Chem. 37, 2737–2745.

Vaidya, U.R., Nadkarni, V.M., 1989. J. Appl. Polym. Sci. 38, 1179–1190.

Valappil, S.P., Misra, S.K., Boccaccini, A.R., Roy, I., 2006. Expert Rev. Med. Devices 3, 853–868.

Valappil, S.P., Rai, R., Bucke, C., Roy, I., 2008. J. Appl. Microbiol. 104, 1624–1635.

Van Krevelen, D.W., 1997. Chapter 5 - Calorimetric properties, in: Properties of Polymers (Third, Completely Revised Edition). Elsevier, Amsterdam, pp. 109–127.

Vancsó-Szmercsányi, I., Maros-Gréger, K., Makay-Bödi, E., 1969. Eur. Polym. J. 5, 155–161.

Vardon, D.R., Franden, M.A., Johnson, C.W., Karp, E.M., Guarnieri, M.T., Linger, J.G., Salm, M.J., Strathmann, T.J., Beckham, G.T., 2015. Energy Env. Sci 8, 617–628.

Vasnes, V.A., Ignatov, V.N., Vinogradova, S.V., Tseitlin, H.M., 1990. Makromol. Chem. 191, 1759–1763.

Verlinden, R.A., Hill, D.J., Kenward, M.A., Williams, C.D., Piotrowska-Seget, Z., Radecka, I.K., 2011. AMB Express 1, 11.

Vilela, C., Sousa, A.F., Fonseca, A.C., Serra, A.C., Coelho, J.F.J., Freire, C.S.R., Silvestre, A.J.D., 2014a. Polym. Chem. 5, 3119–3141.

Vilela, C., Sousa, A.F., Fonseca, A.C., Serra, A.C., Coelho, J.F.J., Freire, C.S.R., Silvestre, A.J.D., 2014b. Polym. Chem. 5, 3119–3141.

Villano, M., Valentino, F., Barbetta, A., Martino, L., Scandola, M., Majone, M., 2014. New Biotechnol., Polyhydroxyalkanoate (PHA) by Mixed Microbial Cultures: Fermentation, Control and Downstream Processing 31, 289–296.

Vinogradova, S.V., Korshak, V.V., 1965. , in: Polyesters, Chapt. 6. Pergamon Press, Oxford.

Vouyiouka, S.N., Karakatsani, E.K., Papaspyrides, C.D., 2005. Prog. Polym. Sci. 30, 10–37.

Wang, B., Li, C.Y., Hanzlicek, J., Cheng, S.Z.D., Geil, P.H., Grebowicz, J., Ho, R.-M., 2001. Polymer 42, 7171–7180.

Wang, X.-X., Hu, H.-Y., Liu, D.-H., Song, Y.-Q., 2016. New Biotechnol. 33, 16–22.

Wang, Y., Kunioka, M., 2005. Macromol. Symp. 224, 193–206.

Wang, Y., Onozawa, S., Kunioka, M., 2003. Green Chem. 5, 571–574.

Wang, Z.-L., Hiltunen, K., Orava, P., Seppälä, J., Linko, Y.-Y., 1996. J. Macromol. Sci. Part A 33, 599–612.

Ward, I.M., Wilding, M.A., Brody, H., 1976. J. Polym. Sci. Polym. Phys. Ed. 14, 263–274.

Watson, Ralph W., 1950. 2, 3-butanediyl phthalate resins. US2502686.

Watson, R.W., Grace, N.H., Barnwell, J.L., 1950. Can. J. Res. 28b, 652–659.

Way, C., Wu, D.Y., Dean, K., Palombo, E., 2010. Polym. Test. 29, 147–157.

Wei, T., Zheng, B., Yi, H., Gao, Y., Guo, W., 2014. Polym. Eng. Sci. 54, 2872–2876.

Werpy, T.A., Holladay, J.E., White, J.F., 2004. Top Value Added Chemicals from Biomass: I. Results of Screening for Potential Candidates from Sugars and Synthesis Gas (No. PNNL-14808). Pacific Northwest National Laboratory (PNNL), Richland, WA (US).

Wibowo, A.H., Crysandi, R., Verdina, A., Makhnunah, N., Wijayanta, A.T., Storz, H., 2017. Mater. Chem. Phys. 186, 552–560.

Williams, C.K., Hillmyer, M.A., 2008. Polym. Rev. 48, 1–10.

Witt, U., Müller, R.-J., Augusta, J., Widdecke, H., Deckwer, W.-D., 1994. Macromol. Chem. Phys. 195, 793–802.

Wojcieszak, R., Santarelli, F., Paul, S., Dumeignil, F., Cavani, F., Gonçalves, R.V., 2015. Sustain. Chem. Process. 3, 9.

Wojtczak, M., Dutkiewicz, S., Galeski, A., Piorkowska, E., 2014. Eur. Polym. J. 55, 86–97.

Wu, B., Xu, Y., Bu, Z., Wu, L., Li, B.-G., Dubois, P., 2014. Polymer 55, 3648–3655.

Wu, L., Wang, L., Wang, X., Xu, K., 2010. Acta Biomater. 6, 1079–1089.

Wu, X.Y., Seppäl↠, J., Linko, Y.-Y., 1996. Biotechnol. Tech. 10, 793–798.

Xie, W., Li, J., Chen, D., Wang, P.G., 1997. Macromolecules 30, 6997–6998.

Xu, J., Guo, B.-H., 2010. Biotechnol. J. 5, 1149–1163.

Xu, S.Y., Shi, Y.H., Zhao, J.B., Jiang, S.L., Yang, W.T., 2011. Polym. Adv. Technol. 22, 2360–2367.

Xu, Yixiang, Hanna, M.A., Isom, L., 2008. Open Agric. J. 2, 54–61.

Xu, Y., Xu, J., Guo, B., Xie, X., 2007. J. Polym. Sci. Part B Polym. Phys. 45, 420–428.

Xu, Yongxiang, Xu, J., Liu, D., Guo, B., Xie, X., 2008. J. Appl. Polym. Sci. 109, 1881–1889.

Xue, L., Dai, S., Li, Z., 2010. Biomaterials 31, 8132–8140.

Yagihara, T., Matsumura, S., 2012. Polymers 4, 1259–1277.

Yamadera, R., Murano, M., 1967. J. Polym. Sci. [A1] 5, 2259–2268.

Yang, Jinjun, Chen, Y., Hua, L., Liang, R., Zhu, D., 2016. J. Appl. Polym. Sci. 133, 42957.

Yang, Jian, Zhu, H., Zhang, C., Jiang, Q., Zhao, Y., Chen, P., Wang, D., 2016. Polymer 83, 230–238.

Yang, S.-T., El Enshasy, H., Thongchul, N. (Eds.), 2013. Bioprocessing technologies in biorefinery for sustainable production of fuels, chemicals, and polymers. AIChE : John Wiley & Sons, Inc, Hoboken, New Jersey.

Yang, Y., Yu, Y., Zhang, Y., Liu, C., Shi, W., Li, Q., 2011. Process Biochem. 46, 1900–1908.

Yang, Y.-H., Brigham, C., Willis, L., Rha, C., Sinskey, A., 2011. Biotechnol. Lett. 33, 937–942.

Yao, D., Li, G., Kuila, T., Li, P., Kim, N.H., Kim, S.-I., Lee, J.H., 2011. J. Appl. Polym. Sci. 120, 1114–1120.

Yashiro, T., Kricheldorf, H.R., Huijser, S., 2009a. Macromol. Chem. Phys. 210, 1607–1616.

Yashiro, T., Kricheldorf, H.R., Huijser, S., 2009b. Macromol. Chem. Phys. 210, 1607–1616.

Yasuda, M., Ebata, H., Matsumura, S., 2010. Enzymatic Synthesis and Properties of Novel Biobased Elastomers Consisting of 12-Hydroxystearate, Itaconate and Butane-1,4-diol, in: Green Polymer Chemistry: Biocatalysis and Biomaterials, ACS Symposium Series. American Chemical Society, pp. 237–251.

Yim, H., Haselbeck, R., Niu, W., Pujol-Baxley, C., Burgard, A., Boldt, J., Khandurina, J., Trawick, J.D., Osterhout, R.E., Stephen, R., Estadilla, J., Teisan, S., Schreyer, H.B., Andrae, S., Yang, T.H., Lee, S.Y., Burk, M.J., Van Dien, S., 2011. Nat. Chem. Biol. 7, 445–452.

Yoon, K.R., Hong, S.-P., Kong, B., Choi, I.S., 2012. Synth. Commun. 42, 3504–3512.

Yu, J., Chen, L.X.L., 2006. Biotechnol. Prog. 22, 547–553.

Yu, J.-L., Xia, X.-X., Zhong, J.-J., Qian, Z.-G., 2014. Biotechnol. Bioeng. 111, 2580–2586.

Zhang, H., Grinstaff, M.W., 2014. Macromol. Rapid Commun. 35, 1906–1924.

Zhang, L., Shi, Z.-Y., Wu, Q., Chen, G.-Q., 2009. Appl. Microbiol. Biotechnol. 84, 909–916.

Zhao, P., Liu, W., Wu, Q., Ren, J., Zhao, P., Liu, W., Wu, Q., Ren, J., 2010. J. Nanomater. J. Nanomater. 2010, 2010, Article ID 287082.

Zhao, X., Bansode, S.R., Ribeiro, A., Abreu, A.S., Oliveira, C., Parpot, P., Gogate, P.R., Rathod, V.K., Cavaco-Paulo, A., 2016. Ultrason. Sonochem. 31, 506–511.

Zheng, L., Li, C., Zhang, D., Guan, G., Xiao, Y., Wang, D., 2011. Polym. Int. 60, 666–675.

Zhu, C., Zhang, Z., Liu, Q., Wang, Z., Jin, J., 2003. J. Appl. Polym. Sci. 90, 982–990.

Zhu, K., Zhu, W.-P., Gu, Y.-B., Shen, Z.-Q., Chen, W., Zhu, G.-X., 2007. Chin. J. Chem. 25, 1581–1583.

Zinn, M., Witholt, B., Egli, T., 2001. Adv. Drug Deliv. Rev., Polymeric Materials for Advanced Drug Delivery 53, 5–21.

Zorba, T., Chrissafis, K., Paraskevopoulos, K.M., Bikiaris, D.N., 2007. Polym. Degrad. Stab. 92, 222–230.

ANNEXES

Annexe 1 : Supporting information du sous-chapitre 2.1

➢ *SA/AA molar ratio determination by ^{1}H-NMR*

The molar composition in succinate (χ_{SA}) and adipate (χ_{AA}) segments in the copolyesters can be calculated using copolyesters ^{1}H-NMR spectra. The determination of χ_{SA} and χ_{AA} is based on the integration of the succinate and adipate signals from BS and BA segments at 2.62 and 2.32 ppm, respectively. χ_{SA} and χ_{AA} are calculated according to Equation (SI.1) and Equation (SI.2), respectively.

$$\chi_{SA} = \frac{I_{2.62}}{I_{2.62} + I_{2.32}} \times 100 \qquad (SI.1)$$

$$\chi_{AA} = \frac{I_{2.32}}{I_{2.62} + I_{2.32}} \times 100 \qquad (SI.2)$$

^{31}P-NMR analysis of the (co)polyesters

Table SI.1 : End-group analysis of PBS, PBSA copolyesters and PBA by ^{31}P-NMR.

Sample	^{1}H-NMR	^{31}P-NMR				
	Exp. composition SA/AA	M_n	OH end-groups	COOH end-groups	SA end-groups proportion *vs.* total COOH end-groups	AA end-groups proportion *vs.* total COOH end-groups
	mol.%	kg/mol	%	%	mol.%	mol.%
PBS ($PBS_{100}A_0$)	100 / 0	17.3	78	22	100	0
$PBS_{79}A_{21}$	79.2 / 20.8	16.4	65	35	71	29
$PBS_{59}A_{41}$	58.6 / 41.4	9.5	42	58	42	58
$PBS_{50}A_{50}$	49.7 / 50.3	13.7	60	40	43	57
$PBS_{39}A_{61}$	39.1 / 60.9	12.0	55	45	34	66
$PBS_{21}A_{79}$	20.9 / 79.1	10.7	94	6	31	69
PBA (PBS_0A_{100})	0 / 100	13.6	79	21	0	100

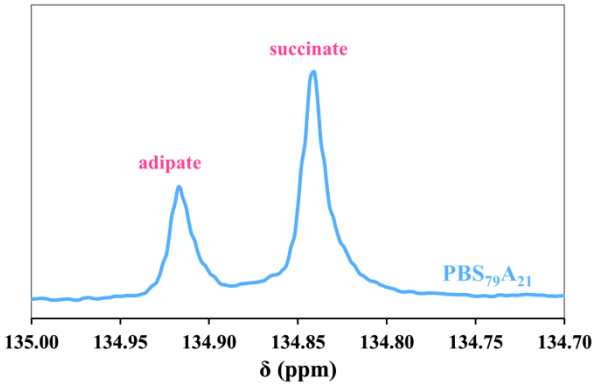

Figure SI.1 : ^{31}P-NMR spectra of $PBS_{79}A_{21}$ centered on the COOH end-group signal.

➢ ***Main possible reactions during thermal degradation of aliphatic polyesters***

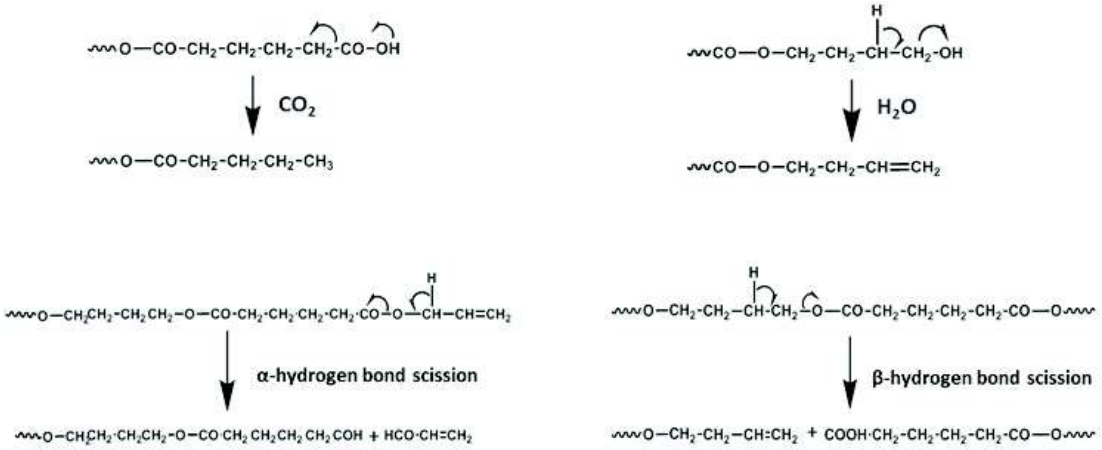

Scheme SI.1 : Main possible reactions during thermal decomposition of the polyesters.

➢ ***Pseudo-eutectic melting behavior of copolyesters***

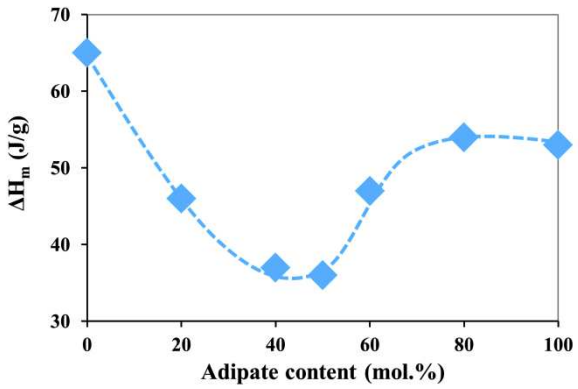

Figure SI.2 : Variation of H_m of PBSA copolyesters vs. adipate content by combining both crystalline phases.

Annexe 2 : Supporting information du sous-chapitre 2.2

➢ *SA/AA molar ratio determination by ^{1}H-NMR*

The molar composition in succinate (χ_{SA}) and adipate (χ_{AA}) segments in PPSA copolyesters can be calculated ^{1}H-NMR spectra. The determination of χ_{SA} and χ_{AA} is based on the integration of the succinate and adipate signals from PS and PA segments at 2.62 and 2.32 ppm, respectively. χ_{SA} and χ_{AA} are calculated according to Equation (SI.3) and Equation (SI.4), respectively.

$$\chi_{SA} = \frac{I_{2.62}}{I_{2.62} + I_{2.32}} \times 100 \qquad (SI.3)$$

$$\chi_{AA} = \frac{I_{2.32}}{I_{2.62} + I_{2.32}} \times 100 \qquad (SI.4)$$

^{31}P-NMR analysis of PPSA

Table SI.2 : End-group analysis of PPSA copolyesters by ^{31}P-NMR.

Sample	^{1}H-NMR	^{31}P-NMR				
	Exp. composition SA/AA	M_n	OH end-groups	COOH end-groups	SA end-groups proportion *vs.* total COOH end-groups	AA end-groups proportion *vs.* total COOH end-groups
	mol.%	kg/mol	%	%	mol.%	mol.%
PPS ($PPS_{100}A_0$)	100 / 0	15.5	88	12	100	0
$PPS_{79}A_{21}$	79.4 / 20.6	14.4	82	18	70	30
$PPS_{49}A_{51}$	49.2 / 50.8	11.8	67	33	43	57
$PPS_{20}A_{80}$	20.4 / 79.6	8.5	44	56	17	83
PPA (PPS_0A_{100})	0 / 100	10.1	77	23	0	100

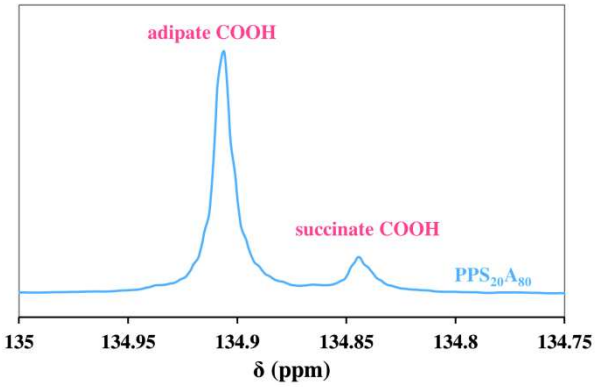

Figure SI.3 : ^{31}P-NMR spectra of $PPS_{20}A_{80}$ centered on the COOH end-group signal.

➢ *DSC analysis of PPSA copolyesters at cooling/heating rate of 5 °C/min*

Table SI.3 : DSC results of PPSA copolyesters at 5 °C/min.

Sample	D_{ester}	1st heating			cooling		2nd heating					
		T_m	ΔH_m	χ	T_c	ΔH_c	T_g	T_{cc}	ΔH_{cc}	T_m	ΔH_m	χ
	%	°C	J/g	%	°C	J/g	°C	°C	J/g	°C	J/g	%
PPS ($PPS_{100}A_0$)	28.6	51	42	30	-	-	-30	22	1	47	1	1
$PPS_{79}A_{21}$	27.3	41	21	15	-	-	-37	-	-	-	-	0
$PPS_{49}A_{51}$	25.4	-	-	-	-	-	-47	-	-	-	-	0
$PPS_{20}A_{80}$	23.5	38	35	28	-	-	-51	-	-	-	-	0
PPA (PPS_0A_{100})	22.2	47	58	46	-9	17	-54	-7	23	42	40	32

Annexe 3 : Supporting information du sous-chapitre 2.3

➢ *Evolution of the molar mass during the synthesis*

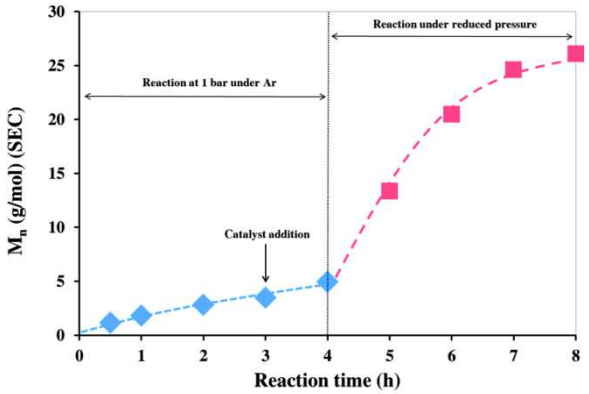

Figure SI.4 : Evolution of the $PP_{50}B_{50}S$ molar mass during the melt polycondensation reaction.

➢ *^{1}H- and ^{13}C-NMR analysis*

Poly(propylene succinate-*co*-butylene succinate) (PPBS) (^{1}H-NMR, $CDCl_3$, δ): 4.17 ppm (4H, -O-C**H**$_2$-CH_2-, from propyl), 4.11 ppm (4H, -O-C**H**$_2$-CH_2-, from butyl), 2.62 ppm (4H, -CO-C**H**$_2$-, from succinate), 1.97 ppm (2H, -O-CH_2-C**H**$_2$-, from propyl) and 1.70 ppm (4H, -O-CH_2-C**H**$_2$-, from butyl); low intensity resonances ascribed to 1,3-PDO and 1,4-BDO end groups at 3.67 ppm (2H, HO-C**H**$_2$-CH_2-CH_2-O-).

Poly(propylene adipate-*co*-butylene adipate) (PPBA) (^{1}H-NMR, $CDCl_3$, δ): 4.14 ppm (4H, -O-C**H**$_2$-CH_2-, from propyl), 4.09 ppm (4H, -O-C**H**$_2$-CH_2-, from butyl), 2.32 ppm (4H, -CO-C**H**$_2$-CH_2-, from adipate), 1.96 ppm (2H, -O-CH_2-C**H**$_2$-, from propyl), 1.69 ppm (4H, -O-CH_2-C**H**$_2$-, from butyl) and 1.65 ppm (4H, -CO-CH_2-C**H**$_2$-, from adipate); low intensity resonances ascribed to 1,3-PDO and 1,4-BDO end groups at 3.67 ppm (2H, HO-C**H**$_2$-CH_2-CH_2-O-).

PPBS (^{13}C-NMR, $CDCl_3$, δ): 172.3-172.4 ppm (4 peaks, -**C**O-CH_2-, from succinate), 64.3 ppm (-O-**C**H$_2$-CH_2-, from butyl), 61.4 ppm (-O-**C**H$_2$-CH_2-, from propyl), 29.2 ppm (-CO-**C**H$_2$-, from succinate), 28.1 ppm (-O-CH_2-**C**H$_2$-, from propyl) and 25.4 ppm (-O-CH_2-**C**H$_2$-, from butyl).

PPBA (^{13}C-NMR, $CDCl_3$, δ): 173.3-173.4 ppm (4 peaks, -**C**O-CH_2-CH_2-, from adipate), 64.0 ppm (-O-**C**H$_2$-CH_2-, from butyl), 61.0 ppm (-O-**C**H$_2$-CH_2-, from propyl), 33.9-34.0 ppm (4 peaks, -CO-**C**H$_2$-CH_2-, from adipate), 28.1 ppm (-O-CH_2-**C**H$_2$-, from propyl), 25.4 ppm (-O-CH_2-**C**H$_2$-, from butyl) and 24.4 ppm (-CO-CH_2-**C**H$_2$-, from adipate).

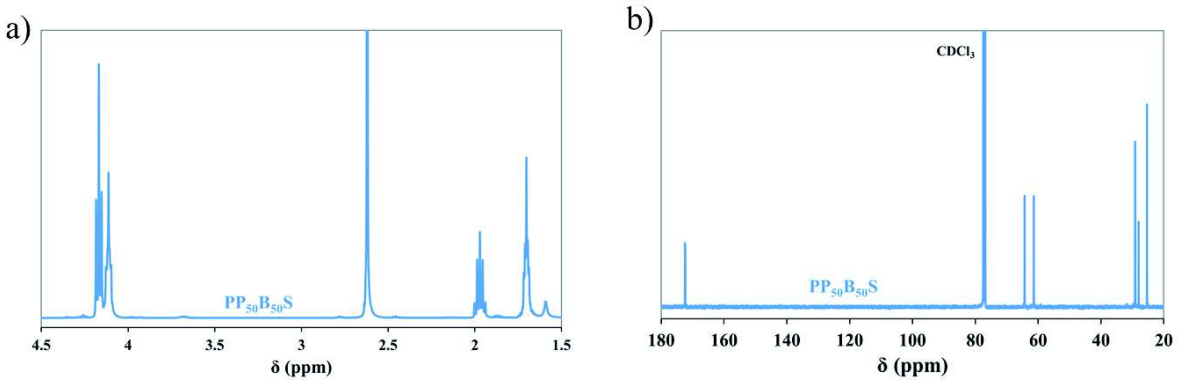

Figure SI.5 : (a) ^{1}H- and (b) ^{13}C-NMR spectra of $PP_{50}B_{50}S$ in $CDCl_3$.

➢ *1,3-PDO/1,4-BDO molar ratio determination by ^{1}H-NMR*

The molar composition in 1,3-propyl ($\chi_{1,3\text{-PDO}}$) and 1,4-butyl ($\chi_{1,4\text{-BDO}}$) segments in PPBS and PPBA copolyesters can be calculated using PPBS and PPBA copolyesters ^{1}H-NMR spectra. The determination of χ_{PDO} and χ_{BDO} is based on the integration of the 1,3-propylene and 1,4-butylene signals from PS and BS segments at 4.16 and 4.12 ppm, respectively. χ_{PDO} and χ_{BDO} are calculated according to Equation (SI.5) and Equation (SI.6), respectively.

$$\chi_{1,3-PDO} = \frac{I_{4.16}}{I_{4.16} + I_{4.12}} \times 100 \quad (SI.5)$$

$$\chi_{1,4-BDO} = \frac{I_{4.12}}{I_{4.16} + I_{4.12}} \times 100 \quad (SI.6)$$

➢ *Sequence distribution study*

The average block length (L) and the randomness degree (R) of copolyesters allowing the sequence distribution study are calculated from ^{13}C-NMR spectra of PPBS and PPBA with high number of scans. In the case of PPBA copolyesters, the average block length of propylene-adipate (PA) segments (L_{PA}), the average block length of butylene-adipate (BA) segments (L_{BA}) and R are calculated according to Equation (SI.7)-(SI.9),

$$L_{PA} = 1 + \frac{2 \times I_{PAP}}{I_{PAB-P} + I_{PAB-B}} \quad (SI.7)$$

$$L_{BA} = 1 + \frac{2 \times I_{BAB}}{I_{PAB-P} + I_{PAB-B}} \quad (SI.8)$$

$$R = \frac{1}{L_{PA}} + \frac{1}{L_{BA}} \quad (SI.9)$$

where I_{PAP}, I_{PAB-P}, I_{PAB-B} and I_{BAB} are integration of peaks assigned to methylene carbons in α of the carbonyl (δ ~ 34 ppm) in adipate segment of PAP, PAB-P side, PAB-B side and BAB triads for PPBA copolyesters. In the case of PPBS copolyesters, the study is based on the integration of carbonyl carbons in (δ ~ 172 ppm) in succinate segment.

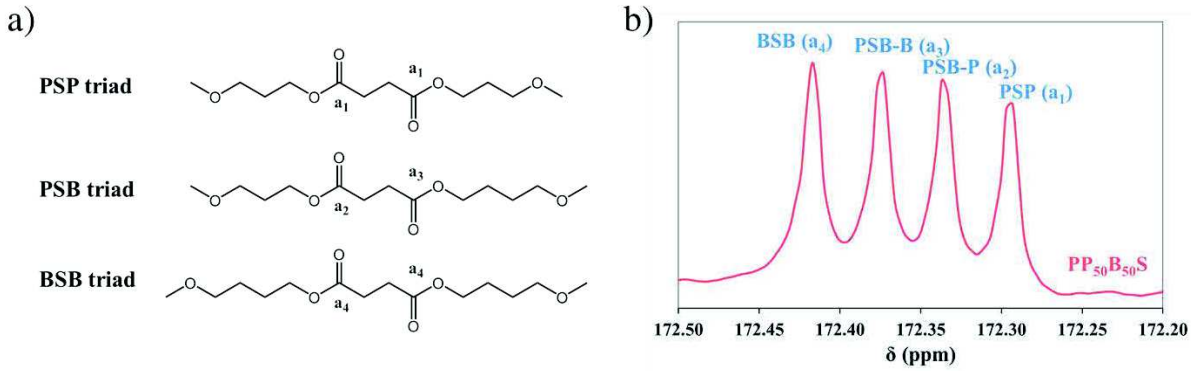

Figure SI.6 : (a) Possible triads and (b) ^{13}C-NMR spectra of PPBS centered at δ ~ 172.4 ppm.

➢ *^{31}P-NMR analysis of PPBS and PPBA copolyesters*

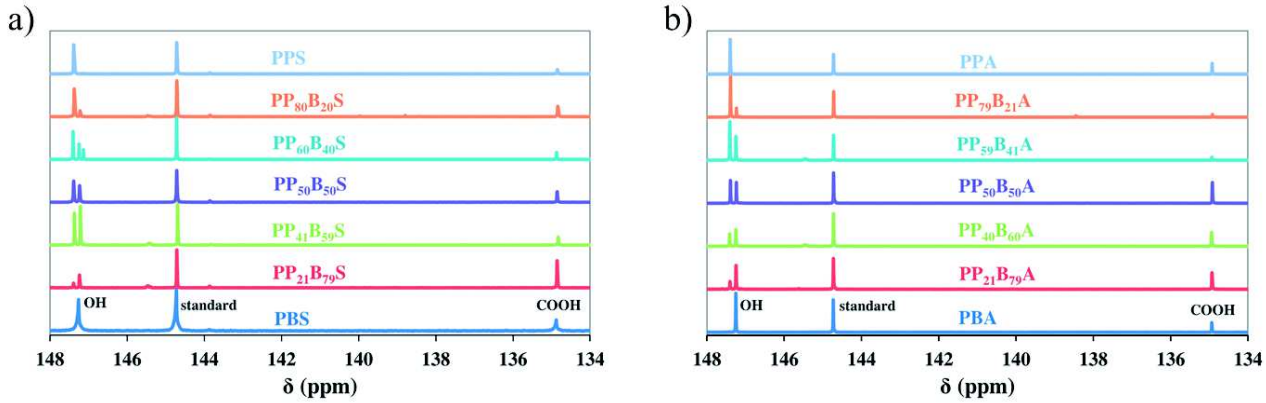

Figure SI.7 : ^{31}P-NMR spectra of (a) PPBS and (b) PPBA copolyesters in $CDCl_3$.

Table SI.4 : End-group analysis of PPBS and PPBA copolyesters by ^{31}P-NMR.

Sample	^{1}H-NMR	^{31}P-NMR			
	Determined composition 1,3-PDO/1,4-BDO	M_n	OH end-groups	COOH end-groups	1,3-PDO end-groups proportion vs total OH end-groups
	mol.%	kg/mol	%	%	mol.%
PPS	100 / 0	15.5	88	12	100
$PP_{80}B_{20}S$	79.6 / 20.4	14.4	76	24	82
$PP_{60}B_{40}S$	60.3 / 39.7	16.0	81	19	65
$PP_{50}B_{50}S$	49.5 / 50.5	14.1	82	18	56
$PP_{41}B_{59}S$	40.8 / 59.2	8.6	87	13	46
$PP_{21}B_{79}S$	20.8 / 79.2	13.7	38	62	29
PBS	0 / 100	17.3	78	22	0
PPA	100 / 0	10.1	77	23	100
$PP_{79}B_{21}A$	78.9 / 21.1	10.8	94	6	84
$PP_{59}B_{41}A$	59.3 / 40.7	7.5	94	6	64
$PP_{50}B_{50}A$	49.5 / 50.5	11.0	66	34	55
$PP_{40}B_{60}A$	39.7 / 60.3	13.7	65	35	45
$PP_{21}B_{79}A$	21.0 / 79.0	12.2	63	37	29
PBA	0 / 100	13.6	79	21	0

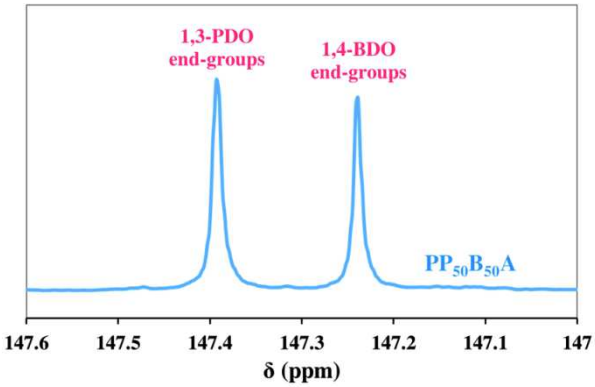

Figure SI.8 : ^{31}P-NMR spectra of $PP_{50}B_{50}A$ centered on the hydroxyl end-group signal.

➢ *FTIR analysis of PPBS and PPBA copolyesters*

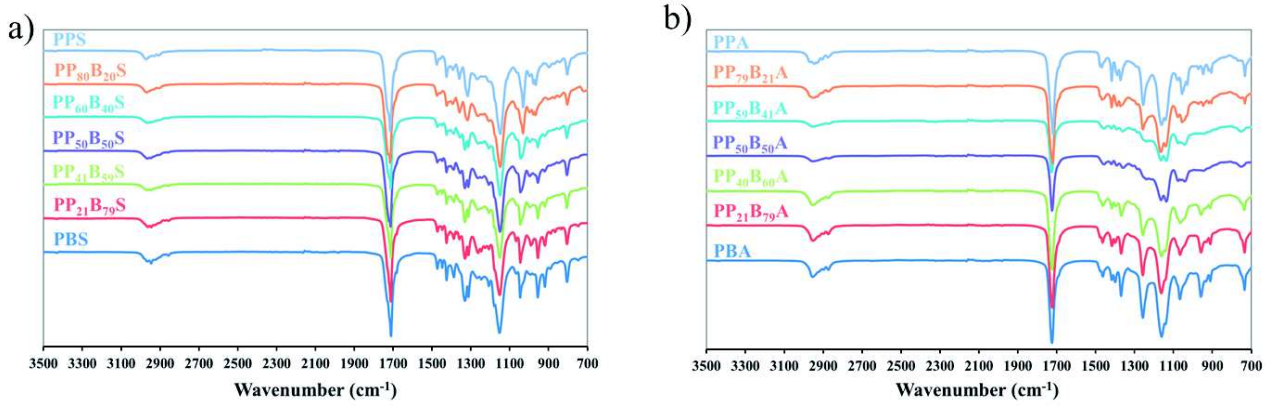

Figure SI.9 : FTIR spectra of (a) PPBS and (b) PPBA copolyester of various 1,3-PDO/1,4-BDO compositions.

In PPBS copolyesters (Figure SI.9-a), signals at 1447, 1330 and 920 cm^{-1} disappeared progressively by increasing the 1,3-PDO content from PBS to PPS. Moreover, the strong C-O symmetric stretching vibration at 955 cm^{-1} in PPBS copolyesters with 1,3-PDO content lower than 60 mol.% was replaced by two medium signals at 966 and 978 cm^{-1} in PPBS copolyesters with high 1,3-PDO content. In PPBA copolyesters (Figure SI.9-b), only the signal at 959 cm^{-1} disappeared by increasing the 1,3-PDO content from PBA to PPA.

➢ *Thermal stability of PPBS and PPBA copolyesters*

Table SI.5 : TGA results of PBBS and PPBA copolyesters at a heating rate of 20 °C/min in helium.

Sample	$T_{deg,2\%}$ °C	$T_{deg\ 50\%}$ °C	$T_{deg,max}$ °C	Residue at 550 °C wt.%
PPS	299	381	394	1.7
$PP_{80}B_{20}S$	291	387	397	1.7
$PP_{50}B_{50}S$	274	386	396	1.8
$PP_{21}B_{79}S$	281	381	392	1.8
PBS	300	386	397	1.0
PPA	299	374	383	1.5
$PP_{79}B_{21}A$	293	379	387	1.6
$PP_{50}B_{50}A$	299	372	380	1.3
$PP_{21}B_{79}A$	306	374	382	1.3
PBA	301	372	377	0.6

➢ *DSC analysis of PPBS and PPBA copolyesters*

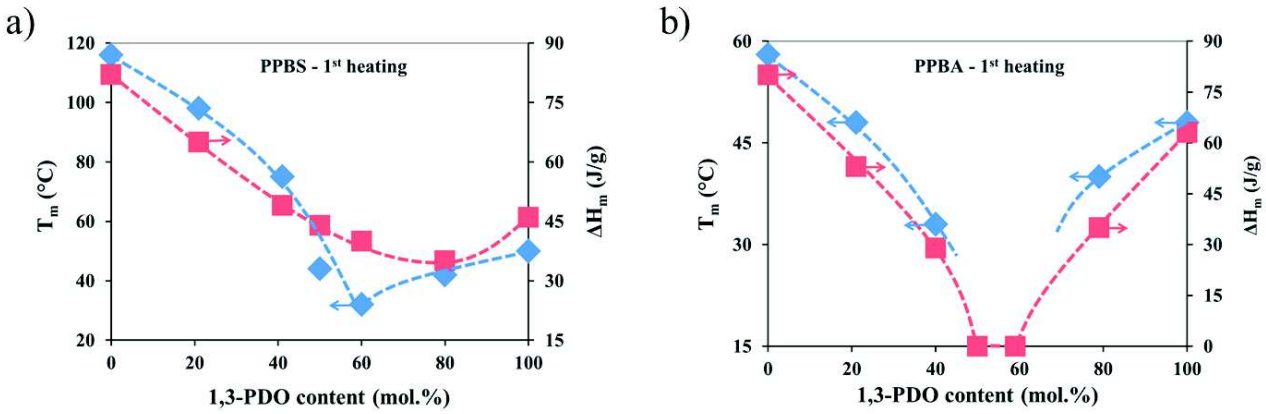

Figure SI.10 : Variation of T_m and ΔH_m vs. 1,3-PDO content for (a) PPBS and (b) PPBA during the first heating run.

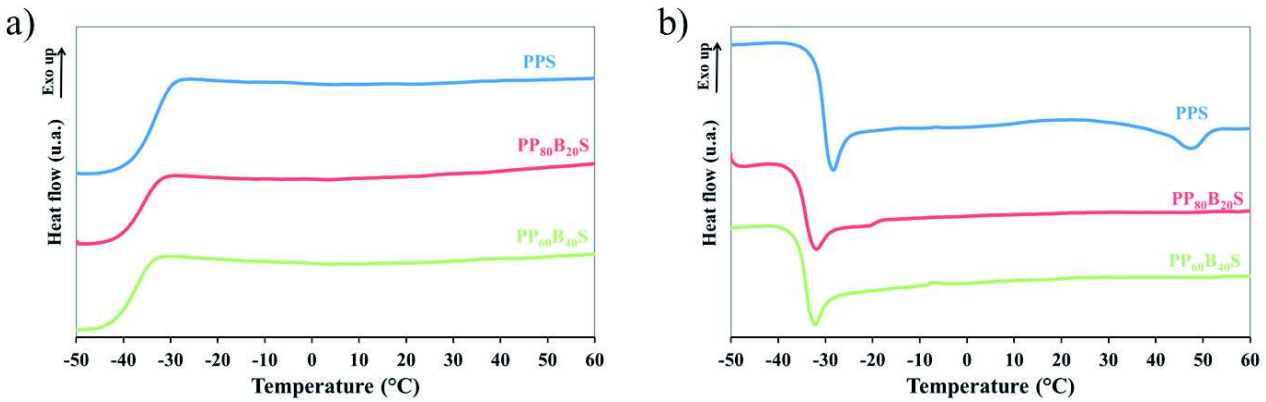

Figure SI.11 : DSC cooling scan (a) and 2nd heating scan (b) of PPS, $PP_{80}B_{20}S$ and $PP_{60}B_{40}S$ at 5 °C/min.

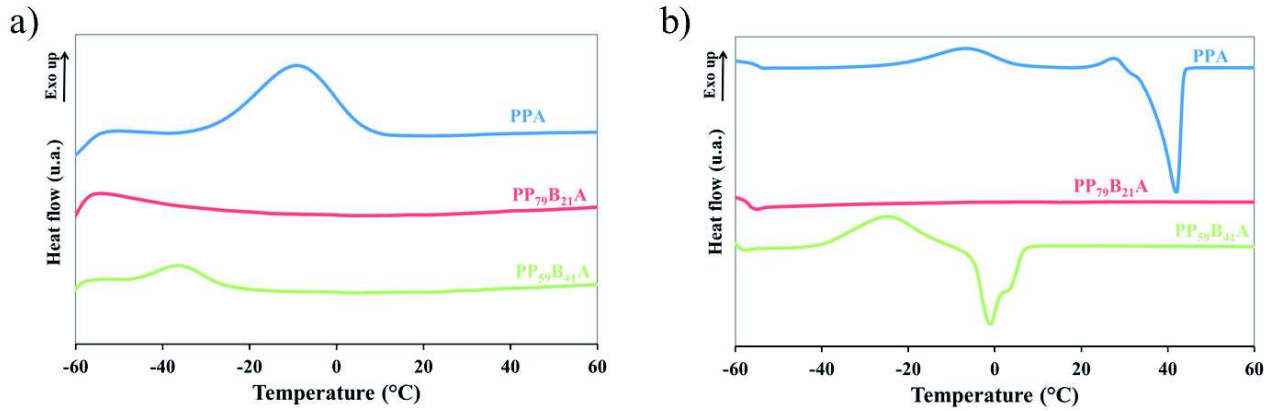

Figure SI.12 : DSC cooling scan (a) and 2nd heating scan (b) of PPA, $PP_{79}B_{21}A$ and $PP_{59}B_{41}A$ at 5 °C/min.

Annexe 4 : Supporting information du sous-chapitre 2.4

- ***Esterification kinetic study***

Case of equimolar proportion of monomers with an external catalysis

The rate of polycondensation with an external catalyst can be defined as the rate at which the reactive function concentration diminishes. Flory (Flory, Paul J., 1939) expressed this rate by Equation (SI.11),

$$v = -\frac{d[COOH]}{dt} = k_1[COOH][OH][cat] \qquad (SI.10)$$

where [COOH] is the concentration of carboxyl functions, [OH] is the concentration of OH functions and [cat] is the concentration of the catalyst. For stoichiometric proportion of monomers, at all time: [COOH] = [OH] and then Equation (SI.11) becomes Equation (SI.12),

$$v = -\frac{d[COOH]}{dt} = k_1[cat]\,[COOH]^2 \qquad (SI.11)$$

After the integration and in terms of the extent of reaction, p, Equation (SI.12) may be written as Equation (SI.13),

$$\frac{1}{1-p} = k_1'[COOH]_0 t + 1 \qquad (SI.12)$$

where:

$$[COOH] = [COOH]_0(1-p) \qquad (SI.13)$$

$$k_1' = k_1[cat] \qquad (SI.14)$$

The plot of 1/(1-p) vs. esterification time should be a straight line with k_1' as rate constant.

Case of equimolar proportion of monomers without catalyst

Without external catalyst, the diacid itself acts as a catalyst and then Equation (SI.11) may be represented by Equation (SI.16),

$$v = -\frac{d[COOH]}{dt} = k_2[COOH][OH][H^+] \qquad (SI.15)$$

Flory (Flory, Paul J., 1939) proposed initially to substitute [H^+] for [COOH] and, because of the stoichiometric proportion, the equation should be third order. This substitution would lead to the well-known Equation (SI.17),

$$\frac{1}{(1-p)^2} = 2\,k_2[COOH]_0^2 t + 1 \qquad (SI.16)$$

However, the plot of $1/(1-p)^2$ vs. reaction time is not perfectly linear for low extent of reaction ($p < 0.8$). The deviation from linearity was attributed to the change in dielectric constant during the reaction. Moreover, this relation could be exact only if all acidic protons are dissociated from carbonyl functions. However, in the case of polyester synthesis, weak acids are used. The dissociation constant (K_a) of the weak acid should be taken in consideration (Amass, 1979) and it is defined by Equation (SI.18),

$$K_a = \frac{[RCOO^-]\,[H^+]}{[RCOOH]} \qquad (SI.17)$$

However, [H^+] equals [$RCOO^-$] at all time. By using Equation (SI.18) and according to the fact that stoichiometric proportions of monomers are used, Equation (SI.16) can be written as Equation (SI.19),

$$v = -\frac{d[COOH]}{dt} = k_2 K_a^{1/2}[COOH]^{5/2} \qquad (SI.18)$$

After the integration and in terms of the extent of reaction (p), Equation (SI.19) may be written as Equation (SI.20),

$$\frac{1}{(1-p)^{3/2}} = k_2'[COOH]_0^{3/2} t + 1 \qquad (SI.19)$$

where:

$$k_2' = \frac{3}{2} k_2 {K_a}^{1/2} \quad (SI.20)$$

According to Equation (SI.20), a plot of $1/(1-p)^{3/2}$ vs. reaction time should be a straight line with k_2' as rate constant.

Case of non-equimolar proportion of monomers without catalyst

In the case of a non-catalyzed esterification with non-stoichiometric proportion of reactive functions due to an excess of OH functions, Equation (SI.16) was modified into Equation (SI.22) (Lin and Hsieh, 1977):

$$v = -\frac{d[COOH]}{dt} = k_2[COOH][COOH + a][H^+] \quad (SI.21)$$

where:

$$[OH] = [COOH] + a \quad (SI.22)$$

$$a = (R-1)[COOH]_0 \quad (SI.23)$$

$$R = \frac{[OH]_0}{[COOH]_0} > 1 \quad (SI.24)$$

By integrating Equation (SI.22), we obtain Equation (SI.26):

$$\frac{R-1}{1-p} - \ln\left(\frac{R-p}{1-p}\right) = K_1 t + K_2 \quad (SI.25)$$

where:

$$K_2 = \frac{a}{[COOH]_0} - \ln(R) = R - 1 - ln(R) \quad (SI.26)$$

According to Equation (SI.26), a plot of (R-1)/(1-p) – ln [(R-p)/(1-p)] vs. reaction time should be a straight line with K_1 as rate constant.

Energy of activation

The activation energy of a reaction is defined by Equation (SI.28):

$$k = Ae^{\frac{-E_a}{RT}} \quad (SI.27)$$

where k is the reaction rate constant, A is the frequency factor, E_a is the energy of activation (in $kJ.mol^{-1}$), R is the universal gas constant (R = 8,314 $J.mol^{-1}.K^{-1}$) and T is the reaction temperature (in K). Equation (SI.28) can be transformed into Equation (SI.29):

$$\ln k = \ln A - \frac{E_a}{RT} \quad (SI.28)$$

This equation allows to graphically determine the activation energy of a reaction by plotting ln(k) vs. 1/T. The slope of the line is equal to ($-E_a/R$) and so the activation energy of a system can be calculated.

- ***Determination of the extent of reaction (p) by ^{1}H-NMR in DMSO-d_6***

During the esterification kinetic, the extent of reaction was calculated by comparing the integration of two signals in ^{1}H-NMR spectra (Figure SI.13). The first one at 2.20 ppm is attributed to methylene protons in α of the acid function (corresponding to unreacted functions), whereas the second signal at 2.30 ppm corresponds to methylene protons in α of the ester function (corresponding to reacted functions). The extent of reaction (p) is calculated according to Equation (SI.30);

$$p = \frac{I_{2.30}}{I_{2.20} + I_{2.30}} \quad (SI.29)$$

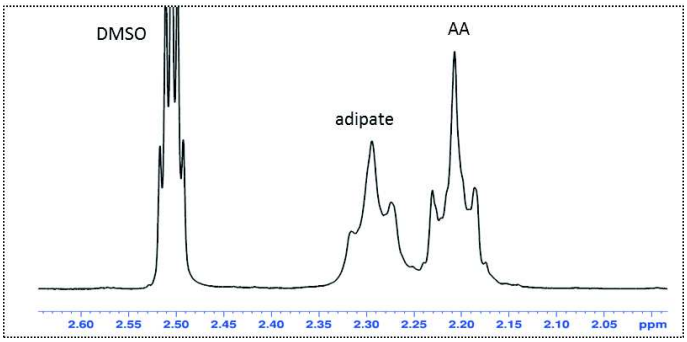

Figure SI.13 : [1]H-NMR spectrum of an aliquot of the 1,4-BDO/AA system in DMSO-d_6 centered on methylene protons in α of the carbonyl.

➢ *NMR analysis of PBB'A copolyesters*

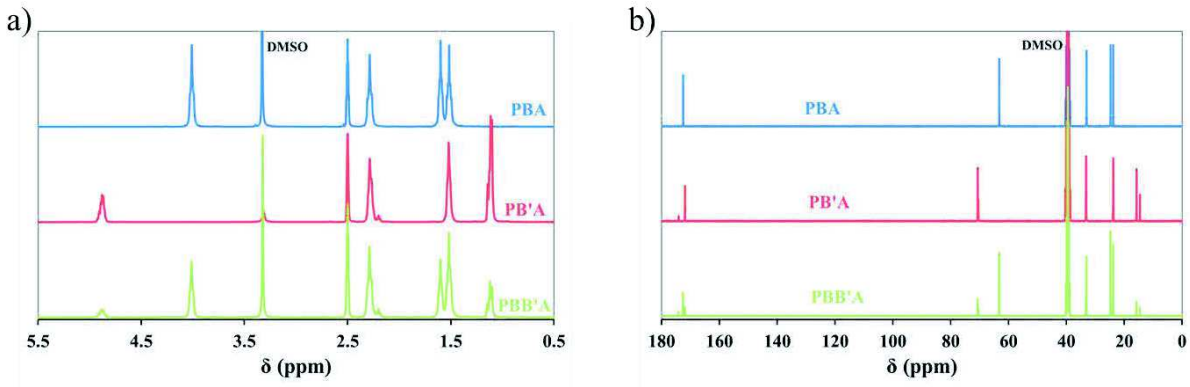

Figure SI.14 : (a) [1]H- and (b) [13]C-NMR of PBA, PB'A and PBB'A.

PBB'A ([1]H-NMR, 400 MHz, DMSO-d_6, δ): 4.87 ppm (2H, -O-C**H**(CH_3)-CH-, from 2;3-BDO), 4.01 ppm (4H, -O-C**H**$_2$-CH_2-, from 1,4-BDO), 2.29 ppm (4H, -CO-C**H**$_2$-CH_2-, from adipate), 1.60 ppm (4H, -O-CH_2-C**H**$_2$-, from 1,4-BDO), 1.52 ppm (4H, -CO-CH_2-C**H**$_2$-, from adipate), 1.11 ppm (6H, -O-CH(C**H**$_3$)-CH-, from 2,3-BDO); low intensity resonances ascribed to the proton from carboxylic end-groups: 2.20 ppm (4H, HOOC-C**H**$_2$-CH_2-, from AA).

PBB'A ([13]C-NMR, 400 MHz, DMSO-d_6, δ): 172.6 ppm (-**C**O-CH_2-CH_2-, from adipate next to 1,4-BDO), 171.9 ppm (-**C**O-CH_2-CH_2-, from adipate next to 2,3-BDO), 70.7-70.5 ppm (2 signals, -O-**C**H(CH_3)-CH-, from 2,3-BDO), 63.2 ppm (-O-**C**H$_2$-CH_2-, from 1,4-BDO), 33.2 ppm (-CO-**C**H$_2$-CH_2-, from adipate next to 2,3-BDO), 33.1 ppm (-CO-**C**H$_2$-CH_2-, from adipate next to 1,4-BDO), 24.8 ppm (-O-CH_2-**C**H$_2$-, from 1,4-BDO), 23.8 ppm (-CO-CH_2-**C**H$_2$-, from adipate), 15.7-14.6 ppm (2 signals, -O-CH(**C**H$_3$)-CH-, from 2,3-BDO); low intensity resonances ascribed to the carbon from carboxylic end-groups: 174.1 ppm (HOO**C**-CH_2-CH_2-CH_2-CH_2-CO-, from AA).

In the [13]C-NMR spectra of PB'A and PBB'A, carbons assigned to 2,3-BDO have both two signals 70.7-70.5 ppm for methine carbons and 15.8-14.6 ppm for methyl carbons. Each time, these two closed signals are linked as it is confirmed by the heteronuclear single quantum correlation (HSQC) NMR. The presence of two signals for methine and methyl carbons in 2,3-butyl segments are probably due to the 3D conformation of the polyester chain. Indeed, according to the orientation of the C-O-C angle between the adipate and the 2,3-butylene segment, the methine carbon can be more or less far away from the oxygen of the carbonyl function, hence explaining the two signals recorded by [13]C-NMR.

➢ *Determination of the 2,3-butylene content in copolyesters*

By using [1]H-NMR spectra of PBB'A, the copolyester molar composition in 1,4-butylene and 2,3-butylene segments is determined. The method consists in comparing the integration of the two signals at 4.87 ppm and 4.01 ppm respectively assigned to methine protons in α of ester functions in 2,3-butyl segments and to methylene protons in α of ester

functions in 1,4-butyl segments. The proportion of 2,3-butyl segment inside the copolyester is calculated according to Equation (SI.31),

$$\chi_{2,3-butyl} = \frac{\frac{I_{4.87}}{1}}{\frac{I_{4.87}}{1} + \frac{I_{4.01}}{2}} \qquad (SI.30)$$

➢ ***Determination of the 2,3-butylene content in copolyesters***

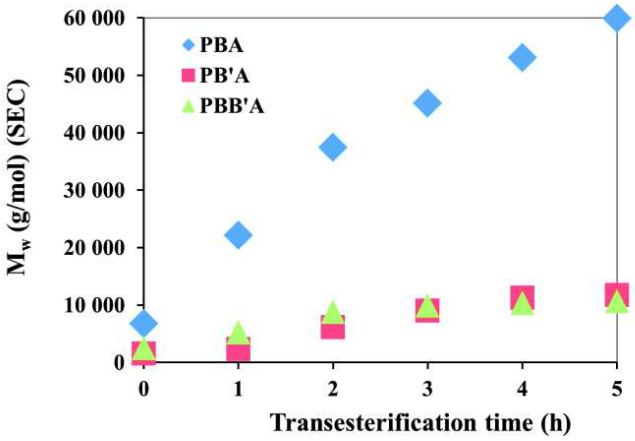

Figure SI.15 : Chain growth of PBA, PB'A and $PB_{67}B'_{33}A$ during the transesterification at 210°C under vacuum in the presence of TTIP catalyst.

➢ ***Mass spectroscopy (MALDI-TOF) of copolyesters***

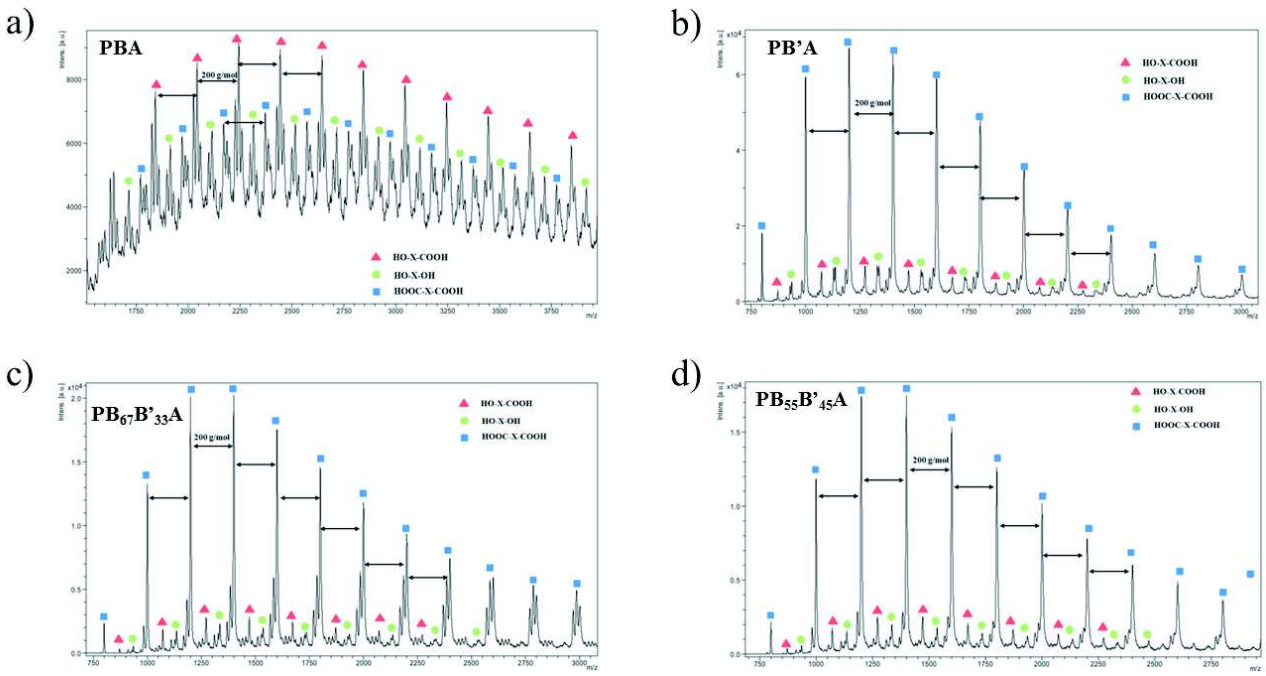

Figure SI.16 : MALDI-TOF spectra of (a) PBA, (b) PB'A, (c) $PB_{67}B'_{33}A$ and (d) $PB_{55}B'_{45}A$.

➢ ***DSC analysis of PB'A, $PB_{55}B'_{45}A$ and $PB_{67}B'_{33}A$***

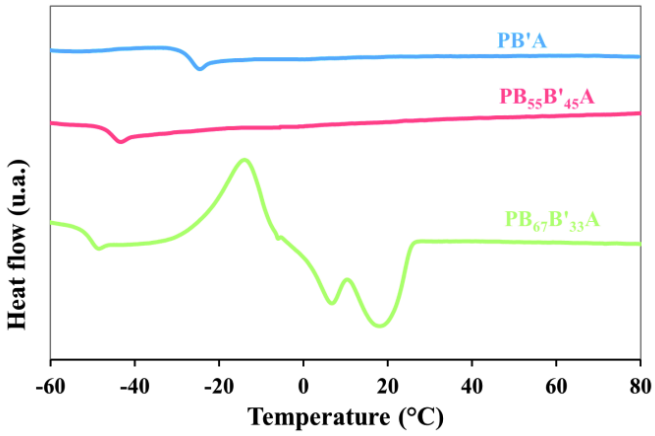

Figure SI.17 : DSC curves of the 2nd heating scan of PB'A, $PB_{55}B'_{45}A$ and $PB_{67}B'_{33}A$ at 2 °C/min.

Annexe 5 : Supporting information du sous-chapitre 3.2

➢ ***NMR analysis***

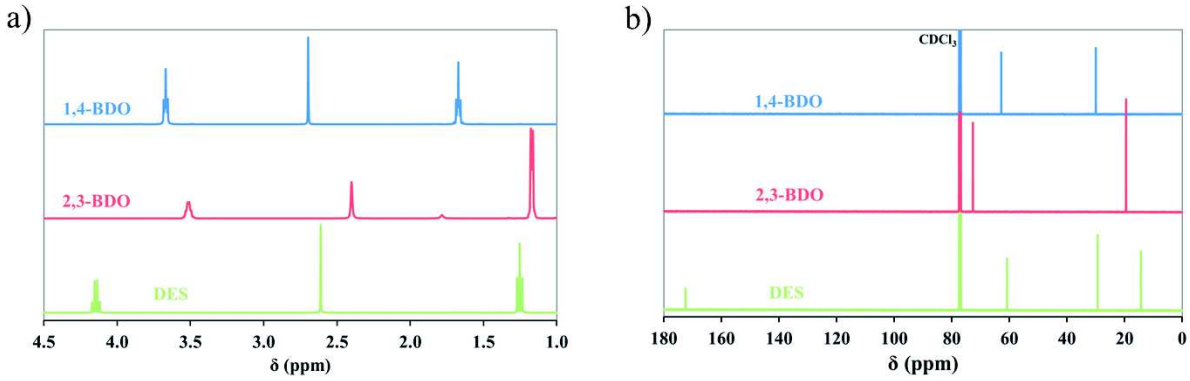

Figure SI.18 : (a) ^{1}H- and (b) ^{13}C-NMR spectra of 1,4-BDO, 2,3-BDO and DES in $CDCl_3$.

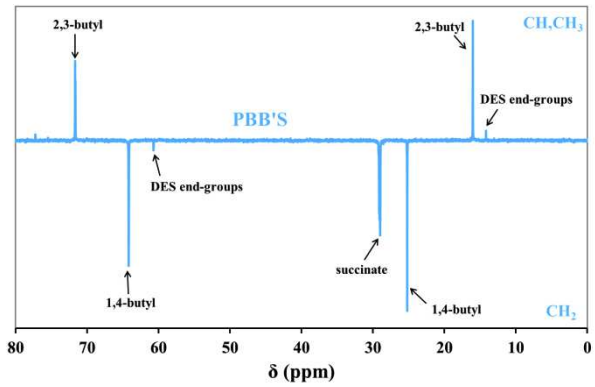

Figure SI.19 : DEPT 135 spectrum of a PBB'S copolyester in $CDCl_3$.

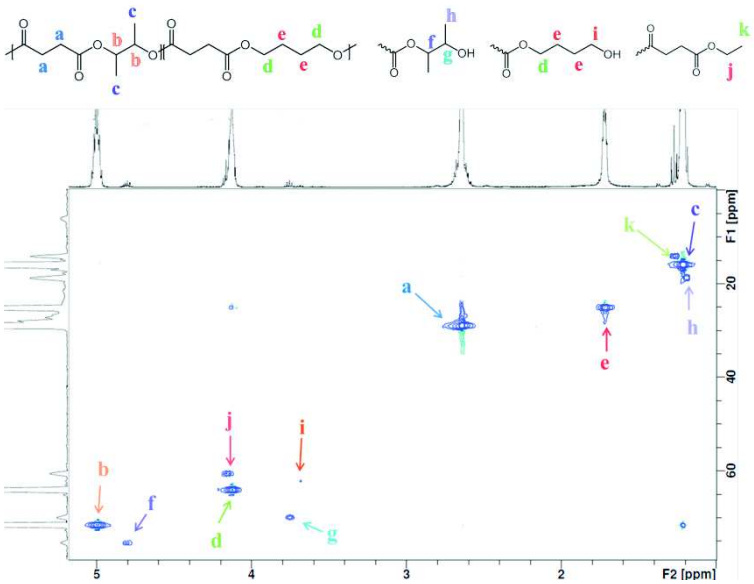

Figure SI.20 : HSQC 2D-NMR spectrum of a PBB'S copolyester.

➢ *CALB-catalyzed copolyesters synthesis*

Table SI.6 : Data collection of all replicates of CALB-catalyzed synthesis of PBB'S copolyesters of various compositions at 90 °C in 150 wt.% of diphenyl ether and catalyzed by 10 wt.% of N435.

Composition		SEC			^{1}H-NMR	
Feed composition 1,4-BDO/2,3-BDO	Exp. composition 1,4-BDO/2,3-BDO	M_n	M_w	Đ	M_n	Ester end-groups
mol.%	mol.%	kg/mol	kg/mol		kg/mol	%
100 / 0	100 / 0	14.4	29.2	1.96	5.0	81
	100 / 0	14.4	25.1	1.75	4.6	87
	100 / 0	11.2	24.2	2.16	4.1	87
75 / 25	79.2 / 20.8	8.7	16.6	1.91	2.6	84
	78.4 / 21.6	8.2	16.6	2.02	4.1	91
	79.5 / 20.5	6.7	13.2	1.98	3.4	90
50 / 50	53.5 / 46.5	9.0	17.3	1.93	2.5	76
	52.7 / 47.3	6.0	11.8	1.97	2.8	89
	52.6 / 47.4	6.2	10.7	1.72	3.0	83
	52.7 / 47.3	6.7	10.8	1.69	3.1	90
25 / 75	28.1 / 71.9	5.3	8.2	1.56	2.2	82
	28.4 / 71.6	6.0	10.9	1.81	2.8	65
	27.3 / 72.7	5.0	7.7	1.56	2.7	90
	27.3 / 72.7	5.4	8.2	1.52	2.6	90
0 / 100	0 / 100	5.7	7.2	1.27	3.6	87
	0 / 100	3.7	5.2	1.42	2.1	95
	0 / 100	4.3	6.4	1.51	3.0	77
	0 / 100	3.4	4.2	1.26	3.4	93

➢ *MALDI-ToF MS analysis of copolyesters*

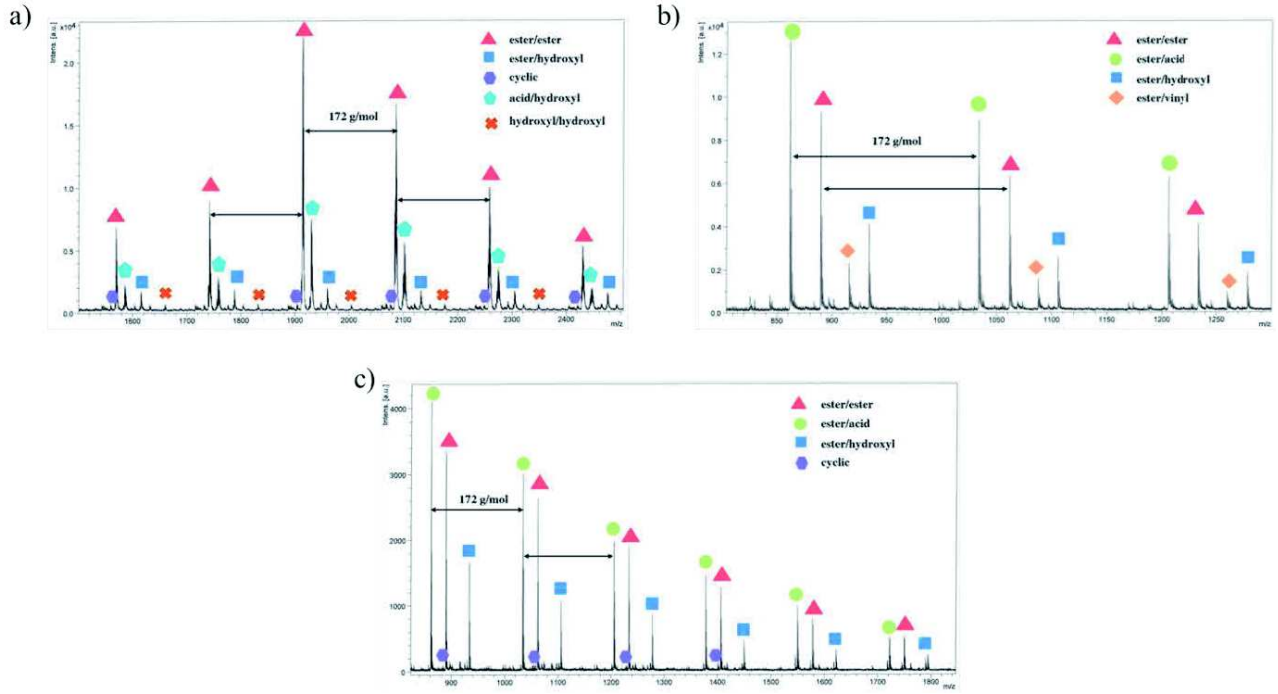

Figure SI.21 : MALDI-ToF MS spectra of (a) PBS, (b) $PB_{79}B'_{21}S$ and (c) $PB_{28}B'_{72}S$.

Table SI.7 : Different microstructures and end-groups of CALB-catalyzed PBB'S copolyesters.

End-groups	Symbol	Microstructure	Remaining mass (g/mol)
ester/vinyl		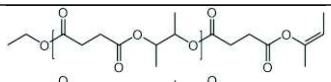	220.23
ester/ester		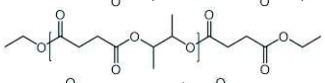	174.20
ester/acid		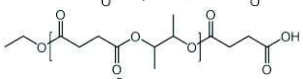	146.14
hydroxyl/hydroxyl		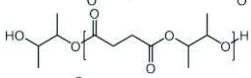	90.12
ester/hydroxyl		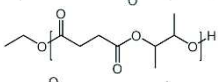	46.07
acid/hydroxyl		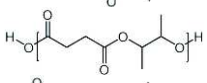	18.02
cyclic		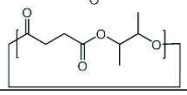	0

Annexe 6 : Supporting information du sous-chapitre 3.3

➢ *^{1}H- and ^{13}C-NMR analysis of monomers and homopolyesters*

Poly(butylene succinate) (PBS) (^{1}H-NMR, $CDCl_3$, δ): 4.12 ppm (4H, -O-C**H**$_2$-CH$_2$-, from butyl segments), 2.62 ppm (4H, -CO-C**H**$_2$-, from succinate segments) and 1.71 ppm (4H, -O-CH$_2$-C**H**$_2$-, from butyl segments); low intensity resonances ascribed to 1,4-BDO end-groups at 3.67 ppm (2H, HO-C**H**$_2$-CH$_2$-CH$_2$-CH$_2$-O) and to ester end-groups at 1.25 ppm (3H, C**H**$_3$-CH$_2$-O-CO-).

Poly(butylene adipate) (PBA) (^{1}H-NMR, $CDCl_3$, δ): 4.09 ppm (4H, -O-C**H**$_2$-CH$_2$-, from butyl segments), 2.32 ppm (4H, -CO-C**H**$_2$-CH$_2$-, from adipate segments), 1.70 ppm (4H, -O-CH$_2$-C**H**$_2$-, from butyl segments) and 1.65 ppm (4H, -CO-CH$_2$-C**H**$_2$-, from adipate segments); low intensity resonances ascribed to 1,4-BDO end-groups at 3.67 ppm (2H, HO-C**H**$_2$-CH$_2$-CH$_2$-CH$_2$-O) and to ester end-groups at 1.25 ppm (3H, C**H**$_3$-CH$_2$-O-CO-).

Poly(propylene succinate) (PPS) (^{1}H-NMR, $CDCl_3$, δ): 4.17 ppm (4H, -O-C**H**$_2$-CH$_2$-, from propyl segments), 2.62 ppm (4H, -CO-C**H**$_2$-, from succinate segments) and 1.97 ppm (2H, -O-CH$_2$-C**H**$_2$-, from propyl segments); low intensity resonances ascribed to 1,3-PDO end-groups at 3.67 ppm (2H, HO-C**H**$_2$-CH$_2$-CH$_2$-O) and to ester end-groups at 1.25 ppm (3H, C**H**$_3$-CH$_2$-O-CO-).

Poly(propylene adipate) (PPA) (^{1}H-NMR, $CDCl_3$, δ): 4.14 ppm (4H, -O-C**H**$_2$-CH$_2$-, from propyl segments), 2.32 ppm (4H, -CO-C**H**$_2$-CH$_2$-, from adipate segments), 1.97 ppm (2H, -O-CH$_2$-C**H**$_2$-, from propyl segments) and 1.65 ppm (4H, -CO-CH$_2$-C**H**$_2$-, from adipate segments); low intensity resonances ascribed to 1,3-PDO end-groups at 3.67 ppm (2H, HO-C**H**$_2$-CH$_2$-CH$_2$-O) and to ester end-groups at 1.25 ppm (3H, C**H**$_3$-CH$_2$-O-CO-).

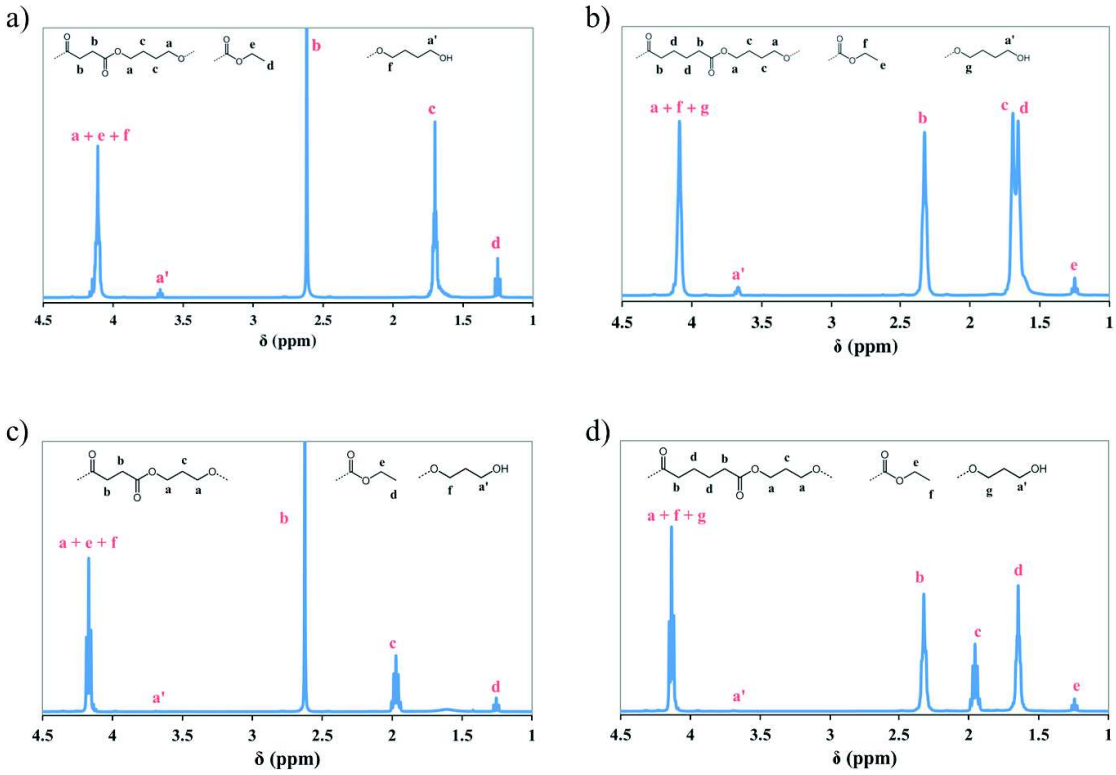

Figure SI.22 : ^{1}H-NMR spectra of CALB-catalyzed (a) PBS, (b) PBA, (c) PPS and (d) PPA homopolyesters.

➢ *Determination of homopolyesters M_n and end-groups proportion by ^{1}H-NMR*

Using ^{1}H-NMR spectra of CALB-catalyzed PBA, PPS and PPA homopolyesters, the molar mass ($M_{n,NMR,PBA}$, $M_{n,NMR,PPS}$ and $M_{n,NMR,PPA}$) can be calculated using characteristic signals of repetitive units and ester groups. It is important to take count that the hydroxyl end-group and the ester end-group both give a signal at approx. 4.1 ppm overlapped with the main 1,4-butylene or 1,3-propylene signal. $M_{n,NMR,PBA}$, $M_{n,NMR,PPS}$ and $M_{n,NMR,PPA}$, are calculated according to Equations (SI.32)-(SI.34), respectively,

$$M_{n,NMR,PBA} = \frac{\frac{I_{4.09} - I_{3.67} - 2/3\, I_{1.25}}{4} \times 88.10 + \frac{I_{2.32}}{4} \times 112.13 + \frac{I_{3.67}}{2} \times 89.11 + \frac{I_{1.25}}{3} \times 45.06}{0.5 \times \left(\frac{I_{3.67}}{2} + \frac{I_{1.25}}{3}\right)} \quad (SI.31)$$

$$M_{n,NMR,PPS} = \frac{\frac{I_{4.17} - I_{3.67} - 2/3\, I_{1.25}}{4} \times 74.08 + \frac{I_{2.62}}{4} \times 84.07 + \frac{I_{3.67}}{2} \times 75.09 + \frac{I_{1.25}}{3} \times 45.06}{0.5 \times \left(\frac{I_{3.67}}{2} + \frac{I_{1.25}}{3}\right)} \quad (SI.32)$$

$$M_{n,NMR,PPA} = \frac{\frac{I_{4.14} - I_{3.67} - 2/3\, I_{1.25}}{4} \times 74.08 + \frac{I_{2.32}}{4} \times 112.13 + \frac{I_{3.67}}{2} \times 75.09 + \frac{I_{1.25}}{3} \times 45.06}{0.5 \times \left(\frac{I_{3.67}}{2} + \frac{I_{1.25}}{3}\right)} \quad (SI.33)$$

where 74.08, 88.10, 84.07, 112.13, 75.09, 89.11 and 45.06 are the molar mass (in g/mol) of the propyl unit, butyl unit, succinate unit, adipate unit, 1,3-PDO end-groups, 1,4-BDO end-groups and ester end-groups, respectively.

➢ *CALB-catalyzed synthesis of homopolyesters*

Table SI.8 : Data collection of all replicates of CALB-catalyzed synthesis of homopolyesters at 90 °C in 200 wt.% of diphenyl ether under vacuum and catalyzed by 10 wt.% of N435.

			SEC		^{1}H-NMR		
Entry	Polyester	Yield (%)	$M_{n,SEC}$ (kg/mol)	Đ	$M_{n,NMR}$ (g/mol)	DP_n	$\%_{DES\ end\text{-}groups}$(%)
1		93	14.9	1.9	5.1	30	90
2	PBS	92	11.2	1.8	4.8	28	87
3		93	12.2	2.1	4.5	27	94
4		81	16.6	1.7	5.5	28	91
5	PBA	93	16.0	1.6	6.1	30	85
6		87	17.8	1.7	5.1	26	83
7		64	5.6	1.5	2.8	18	94
8	PPS	69	6.1	1.6	2.9	19	88
9		76	7.7	2.1	2.7	18	92
10		64	8.2	1.6	n.d.	-	n.d.
11	PPA	65	10.2	1.4	4.2	23	88
12		59	9.6	1.6	4.1	22	92

n.d. not determined

➢ *Molar mass determination of PBSA and PPBS copolyesters by ^{1}H-NMR*

Using ^{1}H-NMR spectra of a CALB-catalyzed PBSA and PPBS copolyesters, the molar mass ($M_{n,NMR,PBSA}$ and $M_{n,NMR,PPBS}$) can be calculated using characteristic signals of repetitive units and ester groups. In PBSA, it is important to take count that the hydroxyl end-group and the ester end-group has both a signal at approx. 4.1 ppm overlapped with the main 1,4-butylene signal.

$M_{n,NMR,PBSA}$ and $M_{n,NMR,PPBS}$ are calculated according to Equations (SI.35) and (SI.36), respectively,

$$M_{n,NMR,PBSA} = \frac{\frac{I_{4.12} - I_{3.67} - 2/3\, I_{1.25}}{4} \times 88.10 + \frac{I_{2.62}}{4} \times 84.07 + \frac{I_{2.32}}{4} \times 112.13 + \frac{I_{3.67}}{2} \times 89.11 + \frac{I_{1.25}}{3} \times 45.06}{0.5 \times \left(\frac{I_{3.67}}{2} + \frac{I_{1.25}}{3}\right)} \quad (SI.34)$$

$$M_{n,NMR,PPBS} = \frac{\frac{I_{1.97}}{2} \times 74.08 + \frac{I_{1.70}}{4} \times 88.10 + \frac{I_{2.62}}{4} \times 84.07 + \frac{I_{3.67}}{2} \times \left(75.09 \times \chi_{1,3-PDO} + 89.11 \times \chi_{1,4-BDO}\right) + \frac{I_{1.25}}{3} \times 45.06}{0.5 \times \left(\frac{I_{3.67}}{2} + \frac{I_{1.25}}{3}\right)} \quad (SI.35)$$

where 74.08, 88.10, 84.07, 112.13, 75.09, 89.11 and 45.06 are the molar mass (in g/mol) of the propyl unit, butyl unit, succinate unit, adipate unit, 1,3-PDO end-groups, 1,4-BDO end-groups and ester end-groups, respectively, and $\chi_{1,3\text{-PDO}}$ and $\chi_{1,4\text{-BDO}}$ are the propyl and butyl content in PPBS copolyesters, respectively.

➢ ***Kinetics of CALB-catalyzed synthesis of $PBS_{50}A_{50}$***

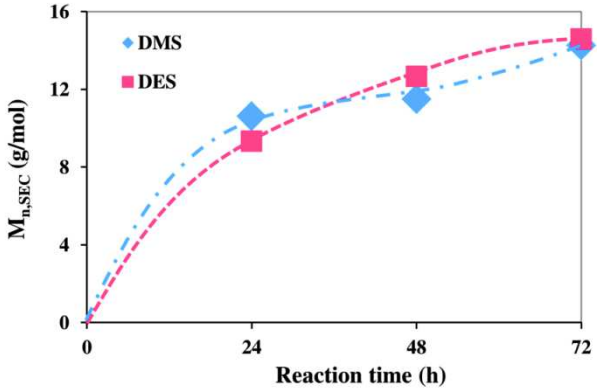

Figure SI.23 : Plots of $M_{n,SEC}$ vs. reaction time for the CALB-catalyzed synthesis of $PBS_{50}A_{50}$ using 1,4-BDO, DEA and DMS/DES as monomer at 90 °C in 200 wt.% of diphenyl ether and with 10 wt.% of N435.

➢ ***Thermal stability of (co)polyesters***

Table SI.9 : TGA results of (co)polyesters under helium with a heating rate of 20 °C/min.

Sample	D_{ester}	$T_{d,2\%}$	$T_{d,50\%}$	$T_{deg,max}$	Residue at 500 °C
	%	°C	°C	°C	wt.%
PBS	25.0	276	384	391	4.8
PBA	20.0	280	350	355	5.3
PPS	28.6	287	379	385	7.0
PPA	22.2	255	334	340	7.3
$PBS_{75}A_{25}$	24.0	270	371	382	6.3
$PBS_{50}A_{50}$	23.0	259	361	377	5.2
$PBS_{25}A_{75}$	22.5	270	366	371	4.3
$PP_{74}B_{26}S$	27.6	286	380	387	3.1
$PP_{49}B_{51}S$	26.8	286	382	389	6.4
$PP_{26}B_{74}S$	25.9	279	378	385	7.1

➢ ***Variation of the crystallinity of PBSA and PPBS copolyesters***

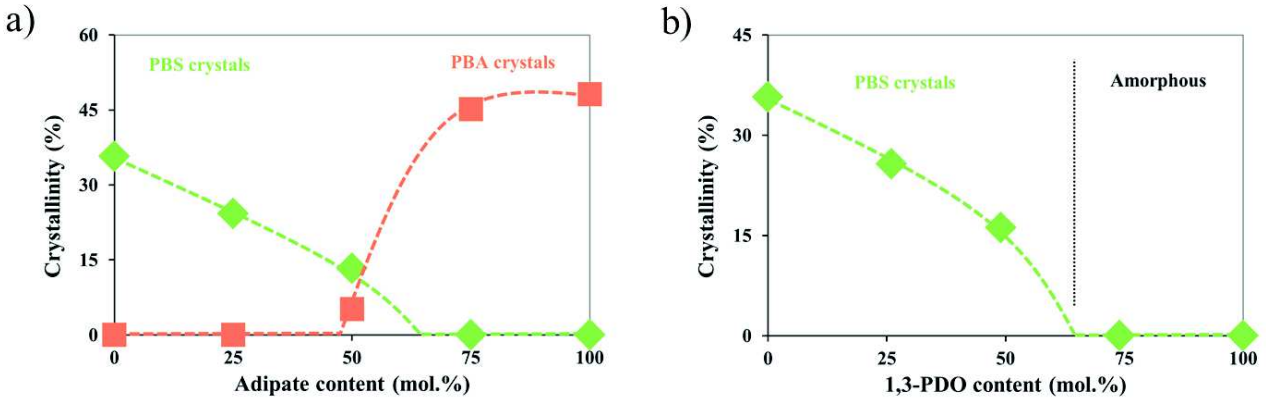

Figure SI.24 : (a) Crystallinity vs. adipate content in CALB-catalyzed PBSA copolyesters, (b) crystallinity vs. 1,3-PDO content in CALB-catalyzed PPBS copolyesters.

Annexe 7 : Supporting information du sous-chapitre 4.1

➢ *FTIR analysis of PHB-diols*

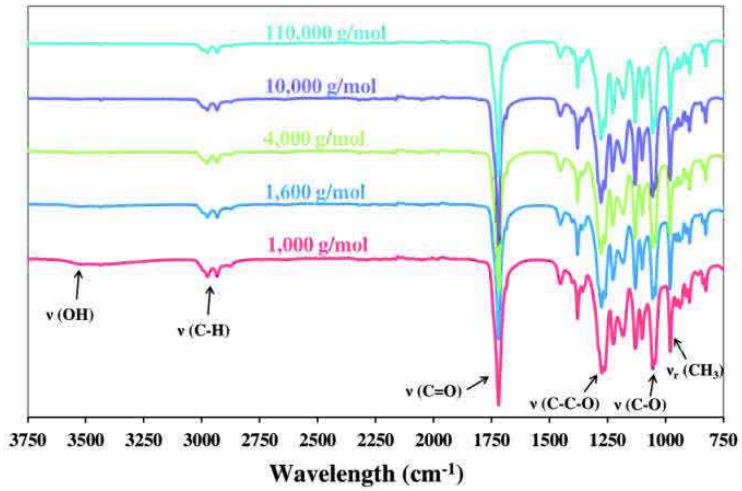

Figure SI.25 : FTIR spectra of PHB and PHB-diol of various molar mass.

➢ *^{1}H-, ^{13}C-, DEPT 135 and HSQC 2D-NMR analysis of PHB-diol in $CDCl_3$*

PHB-diol (^{1}H-NMR, $CDCl_3$, *δ*): 5.26 ppm (1H, -O-C**H**(CH_3)-CH_2-CO-, from PHB), 4.22 ppm (1H, HO-C**H**(CH_3)-CH_2-CO-, 2° OH end-groups), 4.15 ppm (2H, HO-CH_2-CH_2-CH_2-C**H**$_2$-O-, 1° OH end-groups), 3.67 ppm (2H, HO-C**H**$_2$-CH_2-CH_2-CH_2-O-, 1° OH end-groups), 3.12 ppm (1H, **H**O-CH(CH_3)-CH_2-CO-, 2° OH end-groups), 2.45-2.65 ppm (2H, -O-CH(CH_3)-C**H**$_2$-CO-, from PHB and 2° OH end-groups), 1.6-1.7 ppm (4H, HO-CH_2-C**H**$_2$-C**H**$_2$-CH_2-O-, 1° OH end-groups), 1.27 ppm (3H, -O-CH(C**H**$_3$)-CH_2-CO-, from PHB) and 1.20 ppm (3H, HO-CH(C**H**$_3$)-CH_2-CO-, 2° OH end-groups).

By using ^{1}H-NMR spectra of PHB-diol, the molar mass of PHB-diol oligomers can be calculated by making the hypothesis that there are only hydroxyl (primary or secondary) end-groups. For ^{1}H-NMR spectra in $CDCl_3$, the molar mass determination is based on relative intensities of the PHB signal at 5.26 ppm, the primary hydroxyl end-groups at 3.67 ppm and the secondary hydroxyl end-groups at 4.22 ppm according to Equation (SI.37),

$$M_{n,1H-NMR,CDCl3} = \frac{I_{5.26} \times 86.09 + \frac{I_{3.67}}{2} \times 89.11 + I_{4.22} \times 87.10}{0.5 \times \left(\frac{I_{3.67}}{2} + I_{4.22}\right)} \qquad (SI.36)$$

where 86.09, 89.11 and 87.10 are the molar mass (in g/mol) of HB repetitive units, primary and secondary hydroxyl end-groups, respectively. Moreover, the molar ratio (r_{OH}) between primary and secondary hydroxyl end-groups is calculated, from ^{1}H-NMR spectra in $CDCl_3$, according to Equation (SI.38,

$$r_{OH} = \frac{\frac{I_{3.67}}{2}}{I_{4.22}} \qquad (SI.37)$$

PHB-diol (^{13}C-NMR, $CDCl_3$, 1,4-BDO, *δ*): 172.1 ppm (HO-CH_2-CH_2-CH_2-CH_2-**C**O-, 1° OH end-groups), 170.3 ppm (HO-CH(CH_3)-CH_2-**C**O-, 2° OH end-groups), 169.3 ppm (-O-CH(CH_3)-CH_2-**C**O-, from PHB), 67.7 ppm (-O-**C**H(CH_3)-CH_2-CO-, from PHB), 64.7 ppm (HO-CH_2-CH_2-CH_2-**C**H_2-O-, 1° OH end-groups), 64.5 ppm (HO-**C**H(CH_3)-CH_2-CO-, 2° OH end-groups), 62.3 ppm (HO-**C**H_2-CH_2-CH_2-CH_2-O-, 1° OH end-groups), 43.4 ppm (HO-CH(CH_3)-**C**H_2-CO-, 2° OH end-groups), 40.9 ppm (-O-CH(CH_3)-**C**H_2-CO-, from PHB), 29.2 ppm (HO-CH_2-CH_2-**C**H_2-CH_2-O-, 1° OH end-groups), 25.2 ppm (HO-CH_2-**C**H_2-CH_2-CH_2-O-, 1° OH end-groups), 22.6 ppm (HO-CH(**C**H_3)-CH_2-CO-, 2° OH end-groups) and 19.9 ppm (-O-CH(**C**H_3)-CH_2-CO-, from PHB).

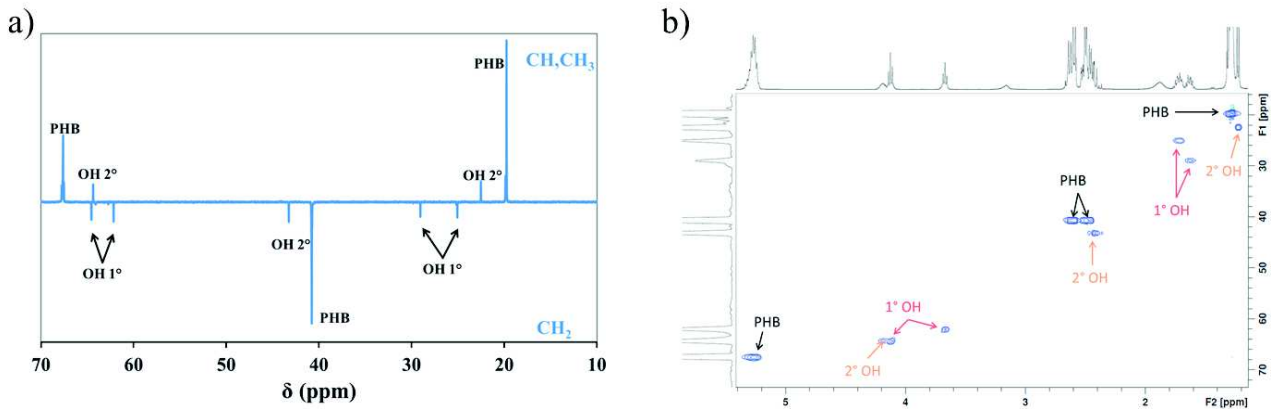

Figure SI.26 : (a) DEPT 135 and (b) HSQC spectra of PHB-diol oligomers in $CDCl_3$.

➢ *^{1}H-, ^{13}C-, DEPT 135 and HSQC 2D-NMR analysis of PHB-diol in DMSO-d_6*

PHB-diol (1,4-BDO) (^{1}H-NMR, DMSO-d_6, δ): 5.10 ppm (1H, -O-C**H**(CH_3)-CH_2-CO-, from PHB), 4.68 ppm (1H, **H**O-CH(CH_3)-CH_2-CO-, 2° OH end-groups), 4.42 ppm (1H, **H**O-CH_2-, 1° OH end-groups), 4.02 ppm (2H, HO-CH_2-CH_2-CH_2-C**H**$_2$-O-, 1° OH end-groups), 3.95 ppm (1H, HO-C**H**(CH_3)-CH_2-CO-, 2° OH end-groups), 3.38 ppm (2H, HO-C**H**$_2$-CH_2-CH_2-CH_2-O-, 1° OH end-groups), 2.45-2.65 ppm (2H, -O-CH(CH_3)-C**H**$_2$-CO-, from PHB), 2.29 ppm (2H, HO-CH(CH_3)-C**H**$_2$-CO-, 2° OH end-groups), 1.4-1.6 ppm (4H, HO-CH_2-C**H**$_2$- CH_2-CH_2-O-, 1° OH end-groups), 1.19 ppm (3H, -O-CH(C**H**$_3$)-CH_2-CO-, from PHB) and 1.08 ppm (3H, HO-CH(C**H**$_3$)-CH_2-CO-, 2° OH end-groups).

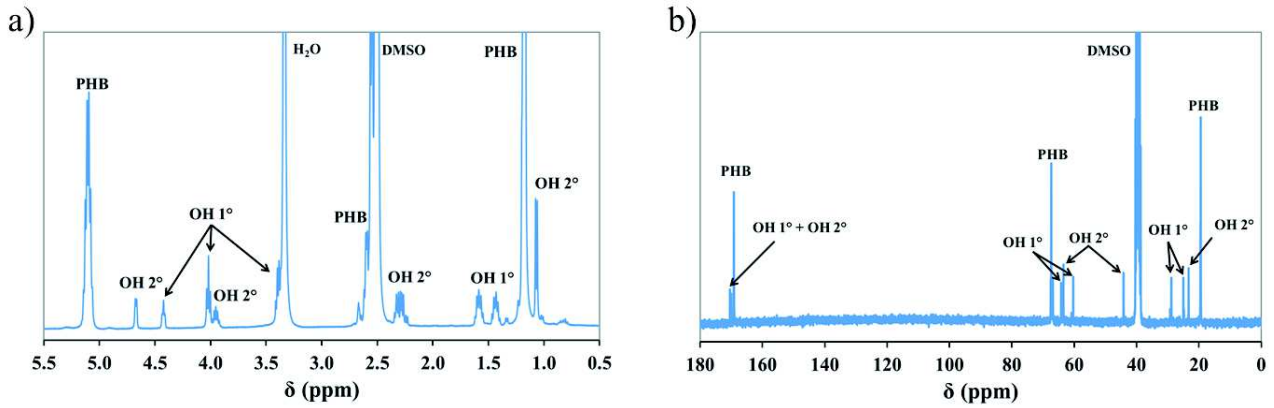

Figure SI.27 : (a) ^{1}H-and (b) ^{13}C- NMR spectra of PHB-diol in DMSO-d6.

For ^{1}H-NMR spectra in DMSO-d_6, the molar mass determination is based on relative intensities of the PHB signal at 5.10 ppm, the primary hydroxyl end-groups at 4.22 ppm and the secondary hydroxyl end-groups at 4.68 ppm according to Equation (SI.39),

$$M_{n,1H-NMR,DMSO} = \frac{I_{5.10} \times 86.09 + I_{4.42} \times 89.11 + I_{4.68} \times 87.10}{0.5 \times (I_{4.42} + I_{4.68})} \qquad (SI.38)$$

where 86.09, 89.11 and 87.10 are the molar mass (in g/mol) of HB repetitive units, primary and secondary hydroxyl end-groups, respectively. Moreover, from ^{1}H-NMR spectra in DMSO-d_6, the molar ratio (r_{OH}') between primaryand secondary hydroxyl end-groups is calculated according to Equation (SI.40),

$$r_{OH}{}' = \frac{I_{4.42}}{I_{4.68}} \qquad (SI.39)$$

PHB-diol (^{13}C-NMR, DMSO-d_6, 1,4-BDO, δ): 170.4 ppm (HO-CH_2-CH_2-CH_2-**C**O-, 1° OH end-groups), 170.1 ppm (HO-CH(CH_3)-CH_2-**C**O-, 2° OH end-groups), 169.2 ppm (-O-CH(CH_3)-CH_2-**C**O-, from PHB), 67.3 ppm (-O-**C**H(CH_3)-CH_2-CO-, from PHB), 64.2 ppm (HO-CH_2-CH_2-CH_2-**C**H_2-O-, 1° OH end-groups), 63.4 ppm (HO-**C**H(CH_3)-CH_2-CO-, 2° OH end-groups), 60.3 ppm

(HO-**C**H_2-CH_2-CH_2-CH_2-O-, 1° OH end-groups), 44.2 ppm (HO-CH(CH_3)-**C**H_2-CO-, 2° OH end-groups), 40.0 ppm (-O-CH(CH_3)-**C**H_2-CO-, from PHB), 28.8 ppm (HO-CH_2-CH_2-**C**H_2-CH_2-O-, 1° OH end-groups), 25.0 ppm (HO-CH_2-**C**H_2-CH_2-CH_2-O-, 1° OH end-groups), 23.3 ppm (HO-CH(**C**H_3)-CH_2-CO-, 2° OH end-groups) and 19.4 ppm (-O-CH(**C**H_3)-CH_2-CO-, from PHB).

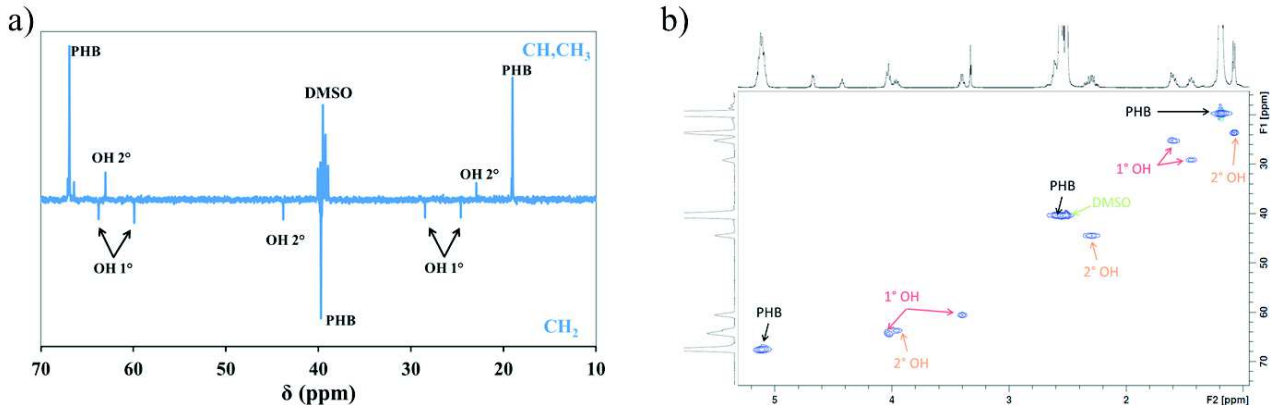

Figure SI.28 : (a) DEPT 135 and (b) HSQC spectra of PHB-diol oligomers in DMSO-d_6.

➢ ***PHB alcoholysis kinetic***

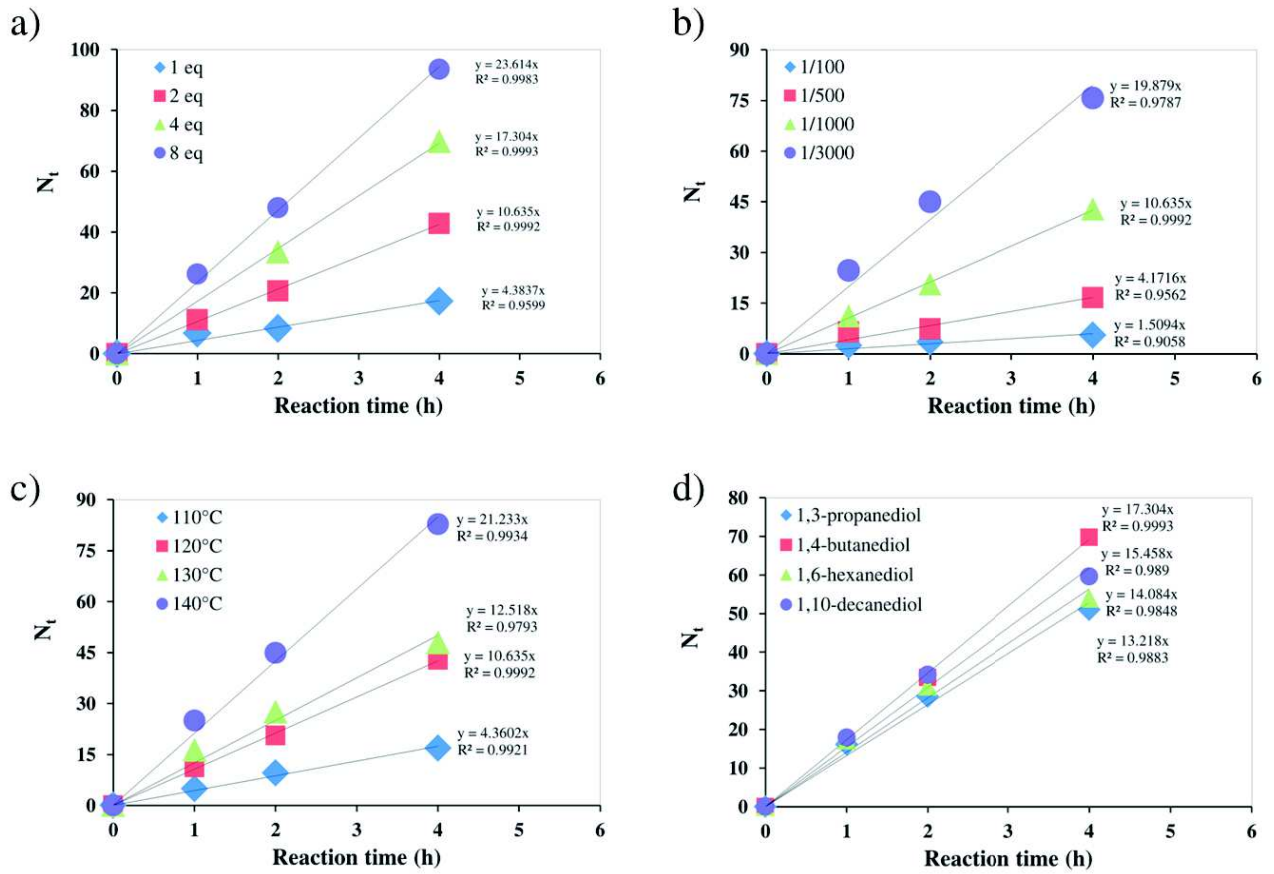

Figure SI.29 : Plots of N_t vs. reaction time for the PHB alcoholysis at (a) different DBTL amounts, (b) different 1,4-BDO amounts, (c) different reaction temperatures and (d) with different aliphatic diols.

➢ *PHB-diol molar masses comparison*

Table SI.10 : Molar mass of PHB-diols determined by different methods.

Entry	SEC with MHS correction			^{31}P-NMR	^{1}H-NMR	
	K = 7.7x10^{-3} a = 0.82	K = 11.8 x10^{-3} a = 0.78	K = 16.6 x10^{-3} a = 0.76		$CDCl_3$	DMSO-d_6
1	14 700	14 350	13 180	10 650	10 270	not. sol.
2	4 640	4 410	4 000	3 810	3 840	not. sol.
3	4 430	4 210	3 810	3 310	3 450	not. sol.
4	3 740	3 540	3 200	3 040	2 960	not. sol.
5	2 780	2 610	2 360	2 070	2 040	1 900
6	2 020	1 890	1 700	1 590	1 690	1 570
7	1 910	1 780	1 590	1 490	1 390	1 340
8	1 620	1 500	1 340	1 350	1 410	1 330
9	1 750	1 630	1 460	1 250	1 320	1 310
10	1 400	1 290	1 160	1 240	1 240	1 190
11	1 210	1 130	1 000	1 100	1 020	1 070
12	1 180	1 090	970	965	920	1 010

not.sol.: sample not soluble; MHS correction with polystyrene parameters: K = 7.16 x10^{-3} ml.g^{-1} and a = 0.76

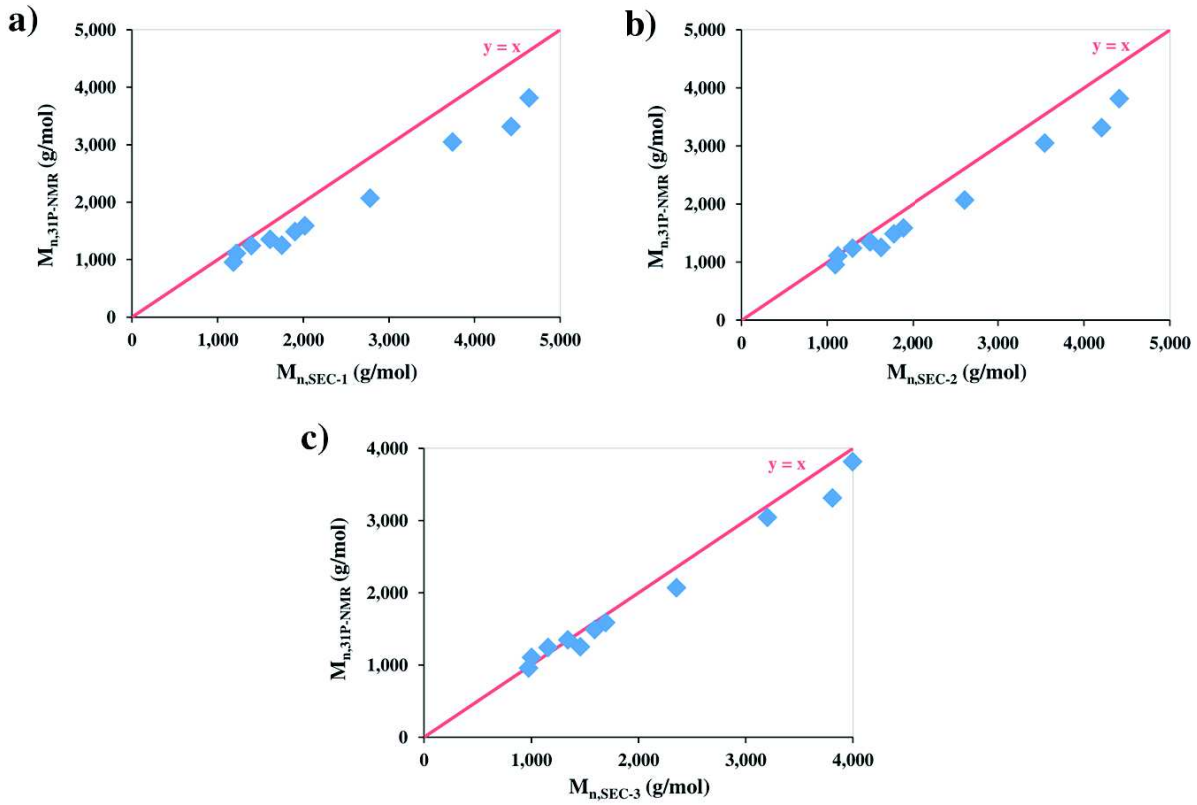

Figure SI.30 : Plots of (a) $M_{n,31P\text{-}NMR}$ vs. $M_{n,SEC\text{-}1}$, (b) $M_{n,31P\text{-}NMR}$ vs. $M_{n,SEC\text{-}2}$ and (c) $M_{n,31P\text{-}NMR}$ vs. $M_{n,SEC\text{-}3}$ of few PHB-diols oligomers.

➢ *Thermal analysis of PHB-diol oligomers by DSC and TGA*

Table SI.11 : DSC (heating and cooling rate of 10 °C/min) and TGA (20 °C/min under helium) results of PHB and PHB-diol samples.

		DSC								TGA		
		cooling		2nd heating								
Sample	M_n	T_c	ΔH_c	T_g	T_{cc}	ΔH_{cc}	T_m	ΔH_m	χ	$T_{d,2\%}$	$T_{d,50\%}$	$T_{deg,max}$
	g/mol	°C	J/g	°C	°C	J/g	°C	J/g	%	°C	°C	°C
PHB	110 000	115	84	n.o.	-	-	173	93	64	260	285	288
PHB-diol$_{10000}$	10 000	125	82	n.o.	-	-	160	83	57	236	272	288
PHB-diol$_{4000}$	4 000	116	85	n.o.	-	-	156	89	61	242	275	278
PHB-diol$_{3000}$	3 000	110	83	n.o.	-	-	151	86	59	n.a.	n.a.	n.a.
PHB-diol$_{2000}$	2 000	99	73	n.o.	-	-	141	76	52	n.a.	n.a.	n.a.
PHB-diol$_{1600}$	1 600	90	79	n.o.	-	-	135	80	54	236	275	280
PHB-diol$_{1400}$	1 400	67	63	-18*	-	-	130	62	42	n.a.	n.a.	n.a.
PHB-diol$_{1000}$	1 000	-	-	-24	51	28	103	28	19	233	283	277

n.o.: not observed; n.a.: not analyzed; * glass transition temperature determined only after a fast cooling run

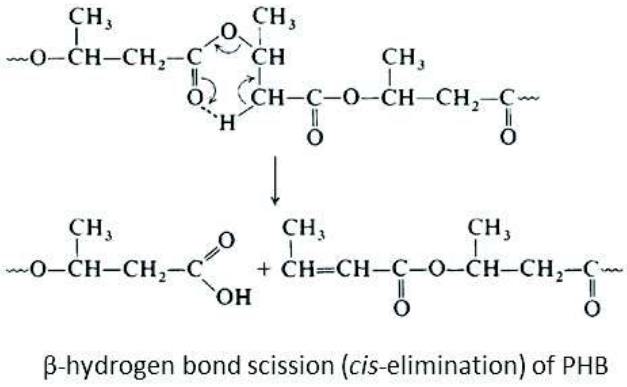

Scheme SI.2 : Thermal degradation mechanism of PHB.

➢ *FTIR spectra of polyether diols*

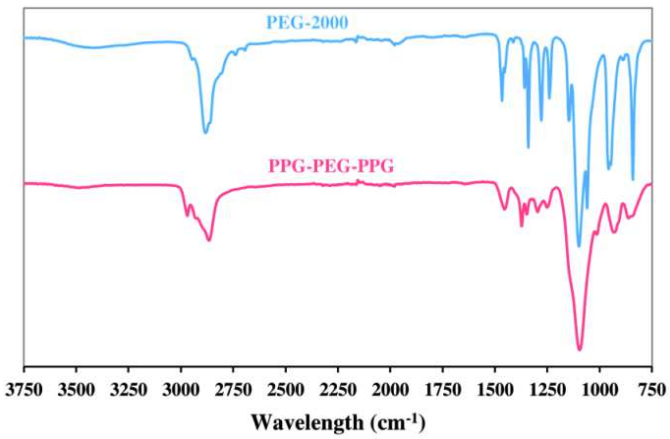

Figure SI.31 : FTIR spectra of PEG-2000 and PPG-PEG-PPG polyethers.

➢ *^{1}H- and ^{13}C-NMR study of PEEU precursors*

PPG-PEG-PPG (^{1}H-NMR, $CDCl_3$, *δ*): 3.64 ppm (4H, -O-C**H**$_2$-C**H**$_2$-O-, from PEG segment), 3.54 ppm (2H, -O-CH(CH_3)-C**H**$_2$-O-, from PPG segment), 3.39 ppm (1H, -O-C**H**(CH_3)-CH_2-O-, from PPG segment) and 1.13 ppm (3H, -O-CH(C**H**$_3$)-CH_2-O-, from PPG segment).

PEG-2000 (^{1}H-NMR, $CDCl_3$, *δ*): 3.64 ppm (4H, -O-C**H**$_2$-C**H**$_2$-O-).

Modified 4,4'-MDI (^{1}H-NMR, $CDCl_3$, *δ*): 7.20-7.00 ppm (8H, aromatic protons), 3.54 ppm (2H, -Ring-C**H**$_2$-Ring-) and 1.54 ppm.

PPG-PEG-PPG (^{13}C-NMR, $CDCl_3$, *δ*): 75.4 ppm (3 signals, -O-**C**H(CH_3)-CH_2-O-, from PPG segment), 73.5 ppm (2 signals, -O-CH(CH_3)-**C**H_2-O-, from PPG segment), 70.7 ppm (-O-**C**H_2-**C**H_2-O-, from PEG segment) and 17.6 ppm (-O-CH(**C**H_3)-CH_2-O-, from PPG segment).

PEG-2000 (^{13}C-NMR, $CDCl_3$, *δ*): 70.7 ppm (-O-**C**H_2-**C**H_2-O-).

Modified 4,4'-MDI (^{13}C-NMR, $CDCl_3$, *δ*): 138.5-125.0 ppm (aromatic carbons) and 40.9 ppm (-Ring-**C**H_2-Ring-).

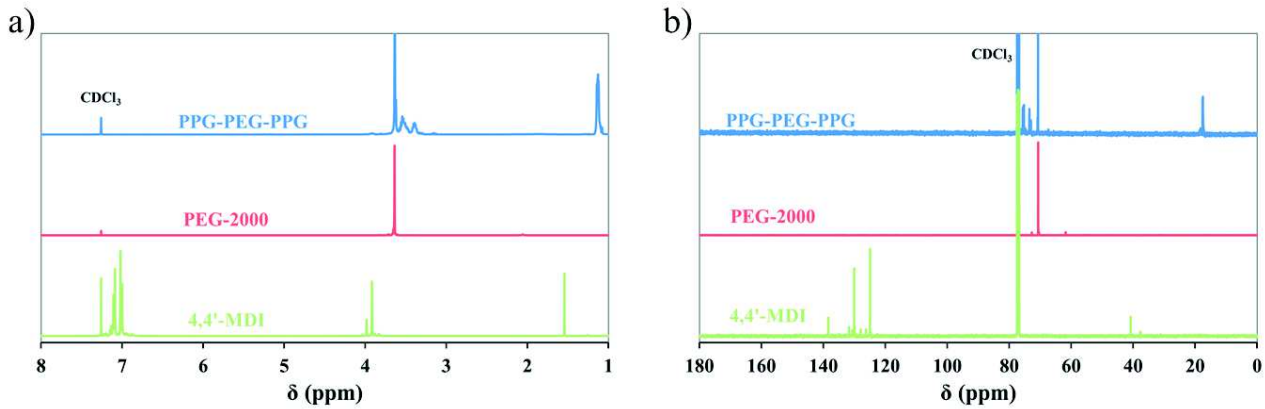

Figure SI.32 : (a) ^{1}H- and (b) ^{13}-NMR spectra of PPG-PEG-PPG, PEG-2000 and 4,4'-MDI in $CDCl_3$.

Annexe 8 : Supporting information du sous-chapitre 4.2

➢ *FTIR analysis*

Characteristic vibration bands of PBS were observed in the poly(HB-co-BS) spectra at 2945, 2855, 1715, 1330, 1155, 1045, 955 and 805 cm-1 assigned to the C-H asymmetrical and symmetrical bending vibrations of the methyl groups, the C=O stretching vibrations from ester moieties, the symmetric deformation of the –CH2- groups, the C-O-C stretching vibrations from the ester groups, the O-C-C vibration in 1,4-BDO, the C-O symmetric stretching and the –CH2- of the succinate in-plane bending, respectively.

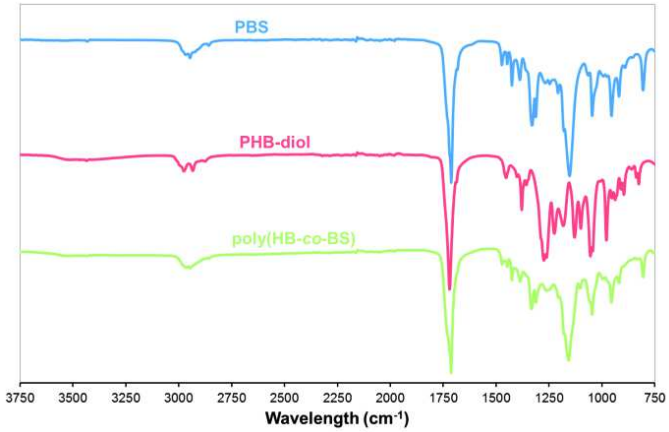

Figure SI.33 : FTIR spectra of PBS, PHB-diol and poly(HB-co-BS) copolyester.

➢ *HSQC 2D NMR analysis*

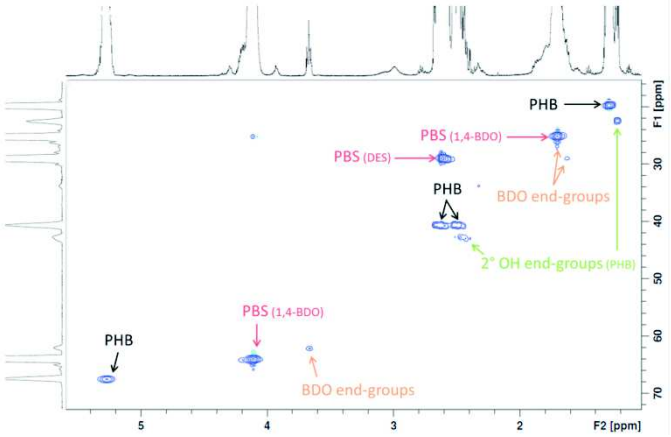

Figure SI.34 : HSQC spectrum of the poly(HB-co-BS) copolyester in $CDCl_3$.

➢ *HB/BS molar ratio determination by ^{1}H-NMR*

The molar mass determination of N435-catalyzed poly(HB-*co*-BS) copolyesters is not possible because the characteristic signal of ester end-groups (methyl proton) at 1.25 ppm is completely overlapped with methyl protons signal from HB segments. However, the molar composition in BS (χ_{BS}) and HB (χ_{HB}) segments in poly(HB-*co*-BS) can be calculated using the poly(HB-*co*-BS) ^{1}H-NMR spectrum. The determination of χ_{BS} and χ_{HB} is based on the integration of the 1,4-butylene signal from BS segments at 4.12 ppm and of the HB signal at 1.25 ppm. In this calculation, secondary hydroxyl and ester end-groups are neglected due to the relatively high molar masses of poly(HB-

co-BS) obtained during N435-catalyzed syntheses. χ_{BS} and χ_{HB} are calculated according to Equations (SI.41) and (SI.42), respectively,

$$\chi_{BS} = \frac{\frac{I_{4.12} - I_{3.67}}{4}}{\frac{I_{4.12} - I_{3.67}}{4} + \frac{I_{1.25}}{3}} \times 100 \qquad (SI.40)$$

$$\chi_{HB} = \frac{\frac{I_{1.25}}{3}}{\frac{I_{4.12} - I_{3.67}}{4} + \frac{I_{1.25}}{3}} \times 100 \qquad (SI.41)$$

➢ *Sequence distribution study for poly(HB-co-BS) copolyesters*

The average sequence length (L) and the randomness degree (R) of copolyesters allowing the sequence distribution study are calculated from ^{13}C-NMR spectra of poly(HB-*co*-BS) copolyesters with high number of scans according to these relations:

$$L_{BS} = 1 + \frac{2 \times (I_{B-S-B} + (I_{HB-S-B})}{I_{S-HB-B} + I_{HB-HB-B} + I_{B-S-HB} + I_{HB-S-HB}} \qquad (SI.42)$$

$$L_{HB} = 1 + \frac{2 \times (I_{S-HB-HB} + (I_{HB-HB-HB})}{I_{S-HB-B} + I_{HB-HB-B} + I_{B-S-HB} + I_{HB-S-HB}} \qquad (SI.43)$$

$$R = \frac{1}{L_{HB}} + \frac{1}{L_{BS}} \qquad (SI.44)$$

where $I_{B\text{-}S\text{-}B}$, $I_{HB\text{-}S\text{-}B}$, $I_{B\text{-}S\text{-}HB}$, $I_{HB\text{-}S\text{-}HB}$, $I_{S\text{-}HB\text{-}B}$, $I_{HB\text{-}HB\text{-}B}$, $I_{S\text{-}HB\text{-}HB}$ and $I_{HB\text{-}HB\text{-}HB}$ are integration of peaks assigned to carbonyl carbons (δ ~ 169-172 ppm).

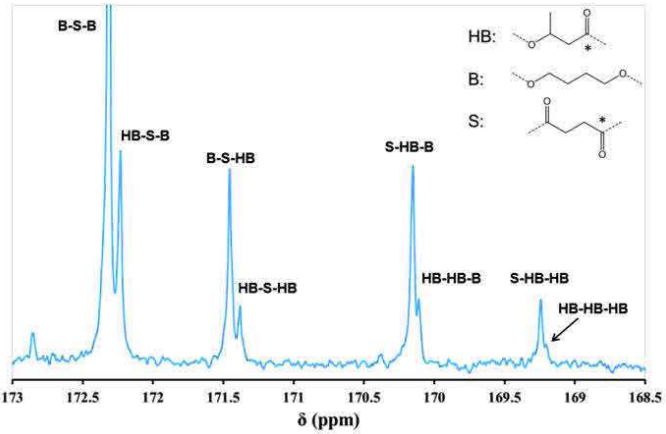

Figure SI.35 : ^{13}C-NMR spectra of poly(HB-co-BS) copolyester in $CDCl_3$ centered on carbonyl peaks and chemical structures corresponding to used abbreviations in the Figure.

➢ *Kinetic of one-step CALB-catalyzed poly(HB-co-BS) syntheses*

Table SI.12 : One-step enzymatic synthesis of poly(HB-co-BS) copolyesters.

Entry	PHB-diol M_n (g/mol) [a]	HB/BS ratio [b]	Reaction time (h)	M_n (g/mol) [c]	M_w (g/mol) [c]	Đ [c]	HB/BS ratio [d]	L_{BS} [e]	L_{HB} [e]	R [e]
1			24	8,000	14,100	1.75	1 / 2.25	6.2	1.2	1.01
2	975	1 / 2.4	48	9,700	18,400	1.90	1 / 2.30	7.2	1.2	0.98
3			72	8,300	17,600	2.12	1 / 2.50	6.4	1.2	1.01
4			24	8,400	14,500	1.73	1 / 1.95	8.7	1.6	0.73
5	2,000	1 / 2.4	48	10,600	21,500	2.03	1 / 2.08	7.5	1.6	0.78
6			72	8,800	17,600	2.00	1 / 2.33	7.7	1.7	0.73

[a] PHB-diol molar mass determined by ^{1}H-NMR. [b] Feed molar ratio between HB and BS segments. [c] Determined by SEC. [d] Experimental molar ratio between HB and BS segments. [e] Sequence distribution study determined by ^{13}C-NMR

➢ *Study on PHB thermal degradation during one-step and two-step processes*

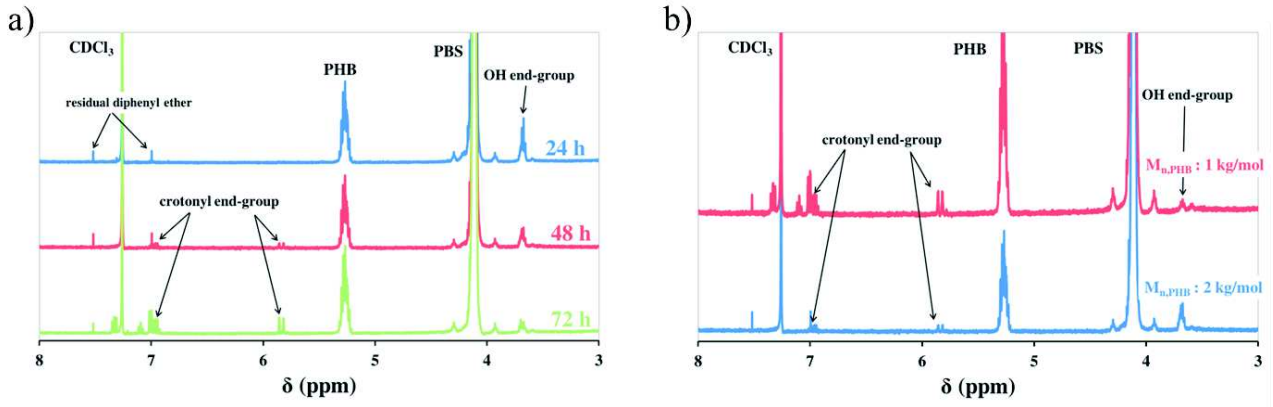

Figure SI.36 : (a) [1]H-NMR spectra of aliquots taken at 24, 48 and 72 h of the one-step reaction of entry 3 (Table 4.2.1); (b) [1]H-NMR spectra of aliquots taken after 48 h of reaction during one-step processes of entry 2 ($M_{n,PHB}$: 975 g/mol) and entry 3 ($M_{n,PHB}$: 2,000 g/mol) in Table 4.2.1.

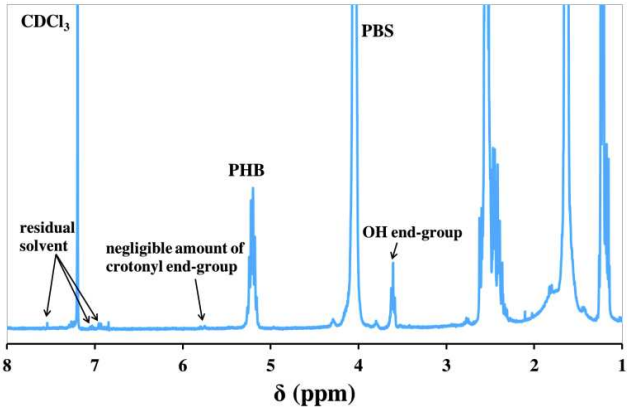

Figure SI.37 : [1]H-NMR spectrum of the poly(HB-co-BS) copolyesters from entry 9 (Table 4.2.1) [copolyester of low molar mass with high PHB content] after 48 h of transesterification synthesized by the two-step process.

➢ *Kinetic of two-step CALB-catalyzed poly(HB-co-BS) syntheses*

Table SI.13 : Influence of the catalyst amount on the kinetic of poly(HB-co-BS) enzymatic synthesis in diphenyl ether with PHB-diol of 975 g/mol and a HB/BS molar ratio of 1/2.4.

Entry	PHB-diol M_n (g/mol) [a]	HB/BS ratio [b]	N435 amount (wt.%)	Reaction time (h)	M_n (g/mol) [c]	M_w (g/mol) [c]	Đ [c]	L_{BS}	L_{HB}	R
1	975	1 / 2.4	5	24	11,300	23,200	2.06	∞	0	0
2				26	7,700	13,500	1.76	67.5	5.7	0.19
3				28	8,100	13,800	1.70	17.8	4.0	0.31
4				32	9,400	16,000	1.70	13.6	2.7	0.45
5				48	11,600	20,400	1.75	7.8	1.6	0.75
6				72	12,300	22,700	1.84	6.0	1.3	0.93
7	975	1 / 2.4	10	24	12,300	26,300	2.14	∞	0	0
8				26	8,900	14,900	1.67	20.9	2.9	0.39
9				28	10,000	17,200	1.72	12.7	2.2	0.54
10				32	9,600	20,000	2.09	8.3	1.6	0.75
11				48	12,600	25,300	2.01	6.9	1.2	0.95
12				72	15,100	27,700	1.84	6.4	1.2	0.99

[a] PHB-diol molar mass determined by [1]H-NMR. [b] Feed molar ratio between HB and BS segments. [c] Determined by SEC.

Table SI.14 : Influence of the PHB-diol molar mass on the kinetic of poly(HB-co-BS) enzymatic synthesis in diphenyl ether with 10 wt.% of N435 and a HB/BS molar ratio of 1/2.4.

Entry	PHB-diol M_n (g/mol)	HB/BS ratio	Solvent	Reaction time (h)	M_n (g/mol)	M_w (g/mol)	Đ	L_{BS}	L_{HB}	R
1	975	1 / 2.4	Diphenyl ether	24	12,300	26,300	2.14	∞	0	0
				26	8,900	14,900	1.67	20.9	2.9	0.39
				28	10,000	17,200	1.72	12.7	2.2	0.54
				32	9,600	20,000	2.09	8.3	1.6	0.75
				48	12,600	25,300	2.01	6.9	1.2	0.95
				72	15,100	27,700	1.84	6.4	1.2	0.99
2	1,400	1 / 2.4	Diphenyl ether	24	12,100	26,600	2.19	∞	0	0
				26	9,200	15,900	1.73	30.3	4.2	0.27
				28	9,900	18,100	1.83	17.4	3.2	0.37
				32	9,500	20,300	2.15	9.9	2.1	0.57
				48	15,800	29,400	1,86	6.6	1.5	0.84
				72	17,900	34,600	1.93	6.2	1.4	0.88
3	2,000	1 / 2.4	Diphenyl ether	24	10,400	20,600	1.99	∞	0	0
				26	8,900	16,500	1.86	-	-	-
				28	9,800	18,800	1.91	16.4	6.2	0.29
				32	11,100	22,600	2.03	22.4	4.1	0.29
				48	13,900	32,500	2.35	11.5	2.7	0.46
				72	11,200	31,300	2.78	9.9	2.4	0.51
4	3,000	1 / 2.4	Diphenyl ether	24	10,000	22,400	2.24	∞	0	0
				26	10,000	20,900	2.09	-	-	-
				28	10,700	23,200	2.17	84.1	12.1	0.09
				32	10,800	25,100	2.32	42.7	9.7	0.13
				48	13,200	33,300	2.53	21.6	6.1	0.21
				72	11,700	32,600	2.81	19.6	4.7	0.27
5	975	1 / 2.4	anisole	24	7,300	15,700	2.16	∞	0	0
				26	6,000	10,800	1.81	66.5	6.0	0.18
				28	6,300	11,200	1.76	35.3	4.4	0.25
				32	7,100	13,000	1.85	21.1	3.2	0.36
				48	8,900	16,500	1.85	9.0	1.9	0.63
				72	10,000	19,500	1.95	6.9	1.4	0.87
6	1,400	1 / 2.4	anisole	24	7,400	14,900	2.02	∞	0	0
				28	7,300	14,100	1.78	-	-	-
				32	8,800	16,300	1.85	27.9	4.7	0.25
				48	11,700	21,300	1.82	10.2	2.1	0.59
				72	10,300	22,400	2.17	7.1	1.4	0.85
7	2,000	1 / 2.4	anisole	24	10,800	22,300	2.07	∞	0	0
				28	9,900	18,300	1.84	107.3	9.7	0.11
				32	11,700	21,500	1.84	33.6	6.1	0.19
				48	13,600	28,100	2.06	12.3	2.5	0.48
				72	11,400	24,800	2.19	7.6	1.6	0.76

Table SI.15 : Influence of the HB/BS molar ratio on the kinetic of poly(HB-co-BS) enzymatic synthesis in diphenyl ether with 10 wt.% of N435 and PHB-diol of 975 g/mol.

Entry	PHB-diol M_n (g/mol) [a]	HB/BS ratio [b]	Solvent	Reaction time (h)	M_n (g/mol) [c]	M_w (g/mol) [c]	Đ [c]	L_{BS} [d]	L_{HB} [d]	R [d]
1	975	1 / 4.8	Diphenyl ether	24	11,200	22,500	2.01	∞	0	0
2				26	9,800	17,600	1.80	31.4	2.9	0.38
3				28	10,600	20,400	1.93	19.0	2.3	0.48
4				32	12,400	25,300	2.05	14.1	1.4	0.78
5				48	16,900	36,000	2.12	11.4	1.2	0.95
6				72	17,600	38,400	2.18	11.3	1.1	0.99
7	975	1 / 2.4	Diphenyl ether	24	12,300	26,300	2.14	∞	0	0
8				26	8,900	14,900	1.67	20.9	2.9	0.39
9				28	10,000	17,200	1.72	12.7	2.2	0.54
10				32	9,600	20,000	2.09	8.3	1.6	0.75
11				48	12,600	25,300	2.01	6.9	1.2	0.95
12				72	15,100	27,700	1.84	6.4	1.2	0.99
13	975	1 / 1.5	Diphenyl ether	24	7,300	13,000	1.79	∞	0	0
14				26	5,500	9,200	1.67	13.2	2.7	0.44
15				28	6,200	10,800	1.74	7.0	2.1	0.61
16				32	6,400	12,000	1.88	5.2	1.6	0.83
17				48	8,200	14,400	1.76	5.4	1.3	0.93
18				72	6,700	13,200	1.99	4.7	1.3	0.98

[a] PHB-diol molar mass determined by ^{1}H-NMR. [b] Feed molar ratio between HB and BS segments. [c] Determined by SEC. [d] Sequence distribution study determined by ^{13}C-NMR.

Table SI.16 : Influence of the solvent on the kinetic of poly(HB-co-BS) enzymatic synthesis with 10 wt.% of N435, PHB-diol of 975 g/mol and a HB/BS molar ratio of 1/2.4.

Entry	PHB-diol M_n (g/mol) [a]	HB/BS ratio [b]	Solvent	Reaction time (h)	M_n (g/mol) [c]	M_w (g/mol) [c]	Đ [c]	L_{BS} [d]	L_{HB} [d]	R [d]
1	975	1 / 2.4	Dibenzyl ether	24	6,100	12,100	1.97	∞	0	0
2				26	5,400	9,300	1.73	21.3	3.0	0.38
3				28	5,900	10,100	1.71	11.7	2.0	0.59
4				32	5,900	10,800	1.83	8.5	1.5	0.80
5				48	6,400	11,700	1.81	6.5	1.2	1.00
6				72	5,900	10,800	1.85	6.5	1.2	1.00
7	975	1 / 2.4	anisole	24	7,300	15,700	2.16	∞	0	0
8				26	6,000	10,800	1.81	66.5	6.0	0.18
9				28	6,300	11,200	1.76	35.3	4.4	0.25
10				32	7,100	13,000	1.85	21.1	3.2	0.36
11				48	8,900	16,500	1.85	9.0	1.9	0.63
12				72	10,000	19,500	1.95	6.9	1.4	0.87
13	975	1 / 2.4	Diphenyl ether	24	12,300	26,300	2.14	∞	0	0
14				26	8,900	14,900	1.67	20.9	2.9	0.39
15				28	10,000	17,200	1.72	12.7	2.2	0.54
16				32	9,600	20,000	2.09	8.3	1.6	0.75
17				48	12,600	25,300	2.01	6.9	1.2	0.95
18				72	15,100	27,700	1.84	6.4	1.2	0.99

[a] PHB-diol molar mass determined by ^{1}H-NMR. [b] Feed molar ratio between HB and BS segments. [c] Determined by SEC. [d] Sequence distribution study determined by ^{13}C-NMR.

➢ *Thermal degradation of homopolyesters and poly(HB-co-BS)*

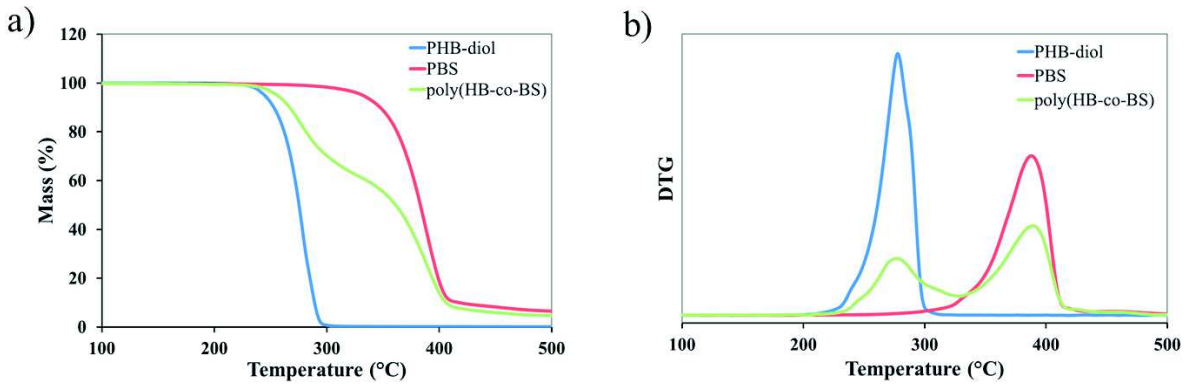

Figure SI.38 : Mass loss curves of PHB-diol, PBS and poly(HB-co-BS) copolyester from thermogravimetric analyses performed under helium at 20 °C/min.

- ***Thermal analysis of poly(HB-co-BS) copolyesters***

Table SI.17 : Evolution of thermal properties of poly(HB-co-BS) copolyesters in diphenyl ether with 10 wt.% of N435, PHB-diol of 975 g/mol and HB/BS molar ratio of 1/1.5, 1/2.4 and 1/4.8.

						1st heating		Cooling		2nd heating				
Entry	Ratio	Reaction time	R	L_{BS}	L_{HB}	T_m	ΔH_m	T_c	ΔH_c	T_g	T_{cc}	ΔH_{cc}	T_m	ΔH_m
	mol.%	h				°C	J/g	°C	J/g	°C	°C	J/g	°C	J/g
1		24	0	∞	0	112	78	93	73	n.o.			113	71
2		26	0.44	13.2	2.7	91	66	42	47	-33	-	-	90	49
3	1/1.5	28	0.61	7.0	2.1	70	46	22	36	-35	10	4	81	42
4		32	0.83	5.2	1.6	61	50	13	12	-37	19	23	73	35
5		48	0.93	5.4	1.3	63	40	9	1	-36	27	25	69	24
6		72	0.98	4.7	1.3	51	55	-	-	-37	33	10	66	6
7		24	0	∞	0	112	78	93	73	n.o.	-	-	113	71
8		26	0.39	20.9	2.9	102	50	63	50	-29	-	-	99	46
9	1/2.4	28	0.54	12.7	2.2	95	40	53	44	-29	-	-	94	40
10		32	0.75	8.3	1.6	85	56	46	42	-31	-	-	86	42
11		48	0.95	6.9	1.2	79	46	25	39	-31	-	-	78	37
12		72	0.99	6.4	1.2	79	43	23	37	-30	13	4	79	41
13		24	0	∞	0	112	78	93	73	n.o.			113	71
14		26	0.38	31.4	2.9	106	62	74	58	n.o.	-	-	106	58
15	1/4.8	28	0.48	19.0	2.3	104	59	69	57	-29	-	-	103	57
16		32	0.78	14.1	1.4	100	54	62	52	-30	-	-	100	55
17		48	0.95	11.4	1.2	95	47	55	48	-32	-	-	96	48
18		72	0.99	11.3	1.1	96	56	49	55	-30	-	-	96	57

Table SI.18 : Comparison of thermal properties of poly(HB-co-BS) copolyesters at different HB/BS molar ratio after 32 h of reaction in diphenyl ether with 10 wt.% of N435 and PHB-diol of 975 g/mol.

					1st heating		Cooling		2nd heating				
Entry	HB/BS ratio	R	L_{BS}	L_{HB}	T_m	ΔH_m	T_c	ΔH_c	T_g	T_{cc}	ΔH_{cc}	T_m	ΔH_m
					°C	J/g	°C	J/g	°C	°C	J/g	°C	J/g
1	1 / 1.5	0.83	5.2	1.6	61	75	13	12	-37	19	23	73	35
2	1 / 2.4	0.79	8.3	1.5	85	56	46	42	-31	-	-	86	42
3	1 / 4.8	0.78	14.1	1.4	100	54	62	52	-30	-	-	100	55

Annexe 9 : Supporting information du sous-chapitre 4.3

➢ *Thermal degradation study of copolyesters*

Table SI.19 : TGA results of poly(HB-co-BA) and poly(HB-co-BS) copolyesters.

Sample	$T_{d,2\%}$	First degradation (PHB)		Second degradation		Third degradation		Residue at 500 °C
		$T_{deg,max,PHB}$	Mass loss	$T_{deg,max}$	Mass loss	$T_{deg,max}$	Mass loss	
	°C	°C	wt.%	°C	wt.%	°C	wt.%	wt.%
Copo-BA-1	213	246	24	332	76	-	-	4.7
Copo-BA-2	227	270	40	313	36	355	17	3.7
Copo-BA-3	227	266	67	313	19	352	8	3.7
Copo-BA-4	205	263	58	199	15	341	8	5.0
Copo-BS-8	230	274	42	380	53	-	-	1.8
Copo-BS-9	241	275	50	378	46	-	-	1.8
Copo-BS-10	244	283	29	384	65	-	-	3.7
Copo-BS-11	254	293	18	390	77	-	-	4.3

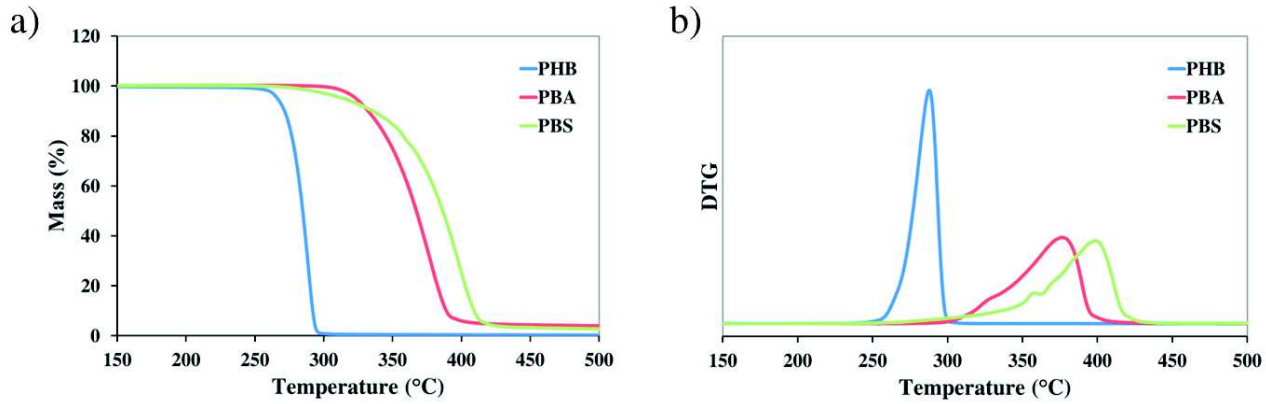

Figure SI.39 : (a) Mass loss and (b) DTG curves of PHB, PBA and PBS homopolyesters under helium.

➢ *Detailed NMR analysis of poly(HB-co-BS) copolyesters*

Poly(HB-*co*-BS) (^{1}H-NMR, $CDCl_3$, δ): 5.26 ppm (1H, -O-C**H**(CH_3)-CH_2-CO-, from HB), 4.12 ppm (4H, -O-C**H**$_2$-CH_2-, from butyl), 2.62 ppm (4H, -CO-C**H**$_2$-, from succinate), 2.45-2.65 ppm (2H, -O-CH(CH_3)-C**H**$_2$-CO-, from HB), 1.7 ppm (4H, -O-CH_2-C**H**$_2$-, from butyl) and 1.27 ppm (3H, -O-CH(C**H**$_3$)-CH_2-CO-, from HB); low intensity resonances ascribed to 1° OH (1,4-BDO) end groups at 3.67 ppm (2H, HO-C**H**$_2$-CH_2-CH_2-CH_2-O-); low intensity resonances ascribed to 2° OH end groups at 1.20 ppm (3H, HO-CH(C**H**$_3$)-CH_2-CO-).

Poly(HB-*co*-BS) (^{13}C-NMR, $CDCl_3$, δ): 172.4 ppm (-**C**O-CH_2-, from succinate), 169.3 ppm (-O-CH(CH_3)-CH_2-**C**O-, from HB), 67.7 ppm (-O-**C**H(CH_3)-CH_2-CO-, from HB), 64.3 ppm (-O-**C**H_2-CH_2-, from butyl), 40.8 ppm (-O-CH(CH_3)-**C**H_2-CO-, from HB), 29.1 ppm (-CO-**C**H_2-, from succinate), 25.3 ppm (-O-CH_2-**C**H_2-, from butyl) and 19.9 ppm (-O-CH(**C**H_3)-CH_2-CO-, from HB); low intensity resonances ascribed to 1° OH (1,4-BDO) end-groups at 64.7 ppm (HO-CH_2-CH_2-CH_2-**C**H_2-O), 62.4 ppm (HO-**C**H_2-CH_2-CH_2-CH_2-O-) and 29.3 ppm (HO-CH_2-CH_2-**C**H_2-CH_2-O-); low intensity resonances ascribed to 2° OH end-groups at 42.9 ppm (HO-CH(CH_3)-**C**H_2-CO-) and 22.6 ppm (HO-CH(**C**H_3)-CH_2-CO-).

- ***FTIR analysis of poly(HB-co-BS)***

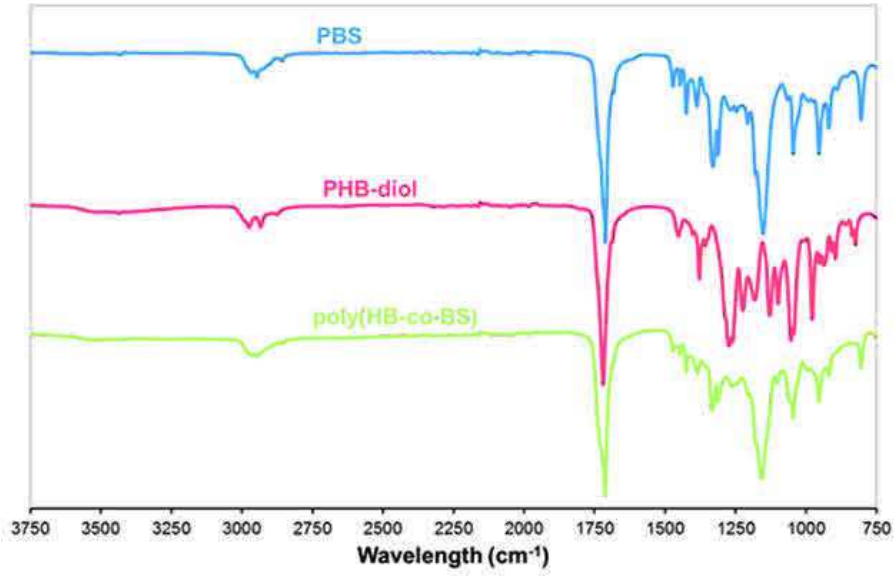

Figure SI.40 : FTIR spectra of PBS, PBH-diol and poly(HB-co-BS).

Annexe 10 : Publication réalisée en collaboration avec le Pr. Müller

Au cours de ma thèse, une collaboration internationale s'est développée entre notre laboratoire et léquipe du Pr. Alejandro J. Müller de l'université du Pays-Basque à San Sebastian. Cette collaboraion a permis d'effectuer des recherces plus poussées et minutieuses sur la microstructure ainsi que ses effets sur les propriétés thermiques et la structure cristalline de certains de nos copolyesters synthétisés par catalyse organométallique.

L'équipe du Pr. Müller s'est notamment focalisée sur l'étude du poly(butylène succinate-*ran*-butylène adipate) de différentes compositions que nous leurs avons fournis. Leur étude utilisant des techniques d'analyses complémentaires à celle évoquée lors de cette thèse (microscope optique polarisé, diffraction des rayons X à température déterminée) complète notre étude qui a été évoqué lors du chapitre 2 (sous-chapitre 1). De plus, l'équipe du Pr. Müller est specialisée dans l'étude et l'analyse des microtructures et donc leur travail apporte une impotante valeur ajoutée.

Ce travail a été valorisé par une publication scientifique publié dans *Macromolecules 2017, 50 (2), 597-608* qui est presentée en annexe ci-après.

Macromolecules

Article

pubs.acs.org/Macromolecules

Tailoring the Structure, Morphology, and Crystallization of Isodimorphic Poly(butylene succinate-*ran*-butylene adipate) Random Copolymers by Changing Composition and Thermal History

Ricardo A. Pérez-Camargo,[†] Borja Fernández-d'Arlas,[†] Dario Cavallo,[‡] Thibaud Debuissy,[§] Eric Pollet,[§] Luc Avérous,[§] and Alejandro J. Müller*[,†,∥]

[†]POLYMAT and Polymer Science and Technology Department, Faculty of Chemistry, University of the Basque Country UPV/EHU, Paseo Manuel Lardizabal 3, 20018. Donostia, San Sebastián, Spain

[‡]Department of Chemistry and Industrial Chemistry, University of Genova, Genova, Italy

[§]BioTeam/ICPEES-ECPM, UMR CNRS 7515, Université de Strasbourg, 25 rue Becquerel, Strasbourg, Cedex 2 67087, France

[∥]IKERBASQUE, Basque Foundation for Science, Bilbao, Spain

Supporting Information

ABSTRACT: Poly(butylene succinate-*ran*-butylene adipate) random copolymers (PBSA) were prepared by melt polycondensation in a wide composition range. Polarized light optical microscopy (PLOM) was employed to observe their superstructural morphology while their thermal and structural properties were studied by differential scanning calorimetry (DSC) and *in situ* synchrotron X-ray diffraction at wide and small angles (WAXS and SAXS). The morphological study revealed negative spherulitic superstructures with (PBS-rich) and without (PBA-rich) ring band patterns depending on composition. The crystallization temperature, melting temperature, and related enthalpies display a pseudoeutectic behavior as a function of composition. WAXS studies demonstrated that these random copolymers are isodimorphic, as their unit cell parameters are composition dependent and switch from PBS-like unit cells to β-PBA-like unit cells around the pseudoeutectic point. For PBA-rich compositions, the inclusion of butylene succinate units in the copolymer selectively promotes the formation of the orthorhombic β-polymorph, instead of the commonly observed monoclinic α-structure. The pseudoeutectic point is located around the 50:50 and 40:60 compositions and is characterized by a remarkable rate-dependent cocrystallization. Parallel DSC, SAXS, and WAXS results for these intermediate compositions show that depending on the cooling rate employed, the materials can exhibit single- or double-crystalline character either upon cooling or during subsequent heating. The structure, morphology, and properties of these versatile random copolymers can be tailored by composition and thermal history.

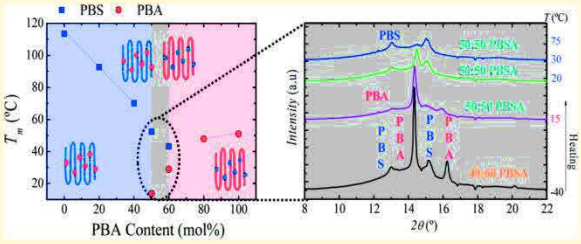

1. INTRODUCTION

Biodegradable and biobased polymers are the choice materials to address environmental concerns and to replace traditional fossil-based polymers.[1] Consequently, they have attracted increasing interest in both practical and fundamental research. Aliphatic (co)polyesters are among the most important biobased and biodegradable materials. Their high potential and improved properties explain their increasing presence associated with a large range of applications in e.g., packaging, agriculture, leisure, textile, and biomedical devices, often for short-term uses.[2]

Most biodegradable polyesters are semicrystalline. Generally, the physical properties of thermoplastic polymers such as thermal behavior, mechanical properties, and biodegradability are significantly influenced by their crystalline structure and morphology, which can be controlled by changing the crystallization conditions.[2]

The copolymerization is an interesting way to modify the crystallization behavior of homopolymers, introducing new monomers and sequences inside the macromolecular architectures. Copolymerization can provide a wide range of new chain structures, such as block, graft, gradient, stars, combs, or random copolymers with diverse crystallization behaviors.[3]

Random copolymers are able to develop isomorphism and isodimorphism.[4,5] In the first case, the comonomeric units must meet strict molecular requirements in order to incorporate into a single-crystalline phase (cocrystallization) over all compositions, with minimum distortion of the unit cell.[5] On the other hand, less strict molecular requirements have to be met by the comonomeric units in the isodimorphic case. Isodimorphic copolymers form two crystalline phases resembling those of the homopolymer constituents.[5] Since both homopolymers of the isodimorphic copolymers can crystallize, the comonomeric

Received: November 12, 2016
Revised: December 23, 2016
Published: January 9, 2017

DOI: 10.1021/acs.macromol.6b02457
Macromolecules 2017, 50, 597−608

units of one type are included in the crystal lattice of the other and vice versa.[6]

On each side of the pseudoeutectic point, the copolymer can crystallize in the crystal lattice of the major component. As the composition of the minor component is increased, a decrease in the melting temperature and crystallinity of the copolymer is usually observed. Pan and Inoue[2] have reviewed such behavior for biodegradable random copolyesters, and recent studies reported isodimorphic crystallization for novel poly(butylene azelate-*ran*-butylene succinate).[5,7]

Poly(butylene succinate-*ran*-butylene adipate) (denoted PBSA in this work) is an attractive biodegradable copolymer, which is commercially available in its 80:20 composition.[2,8,9] Since both main components of this copolymer are biodegradable and miscible and have similar chemical structure (i.e., they only differ in the number of methylene units of their dicarboxylate unit, 2 CH_2 for PBS and 4 CH_2 for PBA),[10] they may display isodimorphic behavior.

The synthesis,[11−15] phase structure,[16] thermal analysis,[13,17] melt rheology,[18] crystallization and morphology,[19] and biodegradability of PBSA copolymers[8,15,20−22] have been reported in the literature, especially for the 80:20 composition, which possesses the best balance between mechanical properties and biodegradability.[8] Moreover, several studies of related blends have also been performed.[10,23,24] Although extensive research has been conducted in PBSA copolymer, its isodimorphic character has not been studied or demonstrated so far.[2]

In the present work, biobased and biodegradable copolymers (random PBSA) have been synthesized with a wide succinate/adipate composition range (i.e., 80:20, 60:40, 50:50, 40:60, and 20:80 molar compositions). The morphology, structure, and thermal properties of these PBSA are studied. The morphological characterization was carried out by polarized light optical microscopy (PLOM). Structural analysis under nonisothermal conditions was performed by differential scanning calorimetry (DSC) and *in situ* synchrotron X-ray diffraction at wide and small angles (WAXS and SAXS).

2. EXPERIMENTAL PART

2.1. Materials. Biobased succinic acid (SA) (99.5%) was kindly supplied by Bioamber (France). SA was bioproduced by fermentation of glucose (from wheat or corn) and obtained after a multistep process based on several purifications, evaporation, and crystallization stages. 1,4-Butanediol (BDO) (99%), methanol (≥99.6%), and chloroform (99.0−99.4%) were purchased from Sigma-Aldrich. Adipic acid (99%), titanium(IV) isopropoxide (TTIP) (98+%), and extra dry toluene (99.85%) were supplied by Acros. All reactants were used without further purification. All solvents used for the analytical methods were of analytical grade.

Organometallic Synthesis of Copolyesters. Aliphatic copolyesters were synthesized by a two-stage melt polycondensation method (polycondensation and postpolycondensation). Syntheses were performed in a 50 mL round-bottom flask with a distillation device in order to remove byproducts of the reaction (mostly water). All reactions were performed with a diol (BDO)/acid (SA and/or AA) molar ratio of 1.1:1. During the first step (esterification), the reaction mixture was maintained under a constant argon flux and stirred at 300 rpm. The temperature of the reactor was set to 200 °C for 3 h. After 3 h of oligomerization, the remaining byproduct of the reaction was removed by distillation under reduced pressure (200 mbar for 5 min), and then the proper amount (0.1 mol % vs the respective amount of diacid) of a 5 wt % solution of TTIP in extra dry toluene was introduced inside the reactor. The reaction mixture was heated to 210 °C under a constant argon flux for 45 min.

In the second step (postpolycondensation), the temperature of the reactor was slowly increased to 230 °C, and the pressure was decreased stepwise over periods of 5 min at 100, 50, and 25 mbar in order to avoid uncontrolled foaming and to minimize oligomer evaporation, which is a potential issue during the melt polycondensation. Finally, the pressure was decreased to 1−3 mbar, and the postpolycondensation continued for about 3−4 h. At the end, the synthesized polyester was cooled, dissolved in chloroform, and precipitated into a large volume of vigorously stirred cold methanol. Thereafter, the precipitate was filtered, washed with methanol, and dried under reduced pressure in an oven at 40 °C for 24 h. A schematic representation of the synthesis is shown in Scheme 1.

Scheme 1. Reaction Procedure for PBSA Synthesis

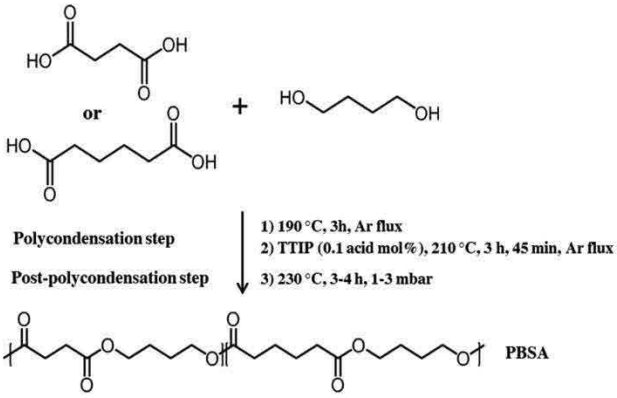

2.2. Chemical Structures Characterizations (SEC and NMR). ^1H and ^{13}C NMR spectra of polyesters were obtained with a Bruker 400 MHz. $CDCl_3$ was used as solvent to prepare solutions with concentrations of 8−10 and 30−50 mg/mL for ^1H NMR and ^{13}C NMR, respectively. The number of scans was set to 128 for ^1H NMR and at least 5000 for ^{13}C NMR. Calibration of the spectra was performed using the $CDCl_3$ peak (δ_H = 7.26 ppm, δ_C = 77.16 ppm). The compositions between succinate and adipate segments in all the PBSA copolyesters employed in the present work were determined using ^1H NMR by comparing the integration of signals at δ = 2.62 ppm and δ = 2.32 ppm assigned to methylene protons in α of ester functions in succinate and adipate segments, respectively (see eq 1).

$$\chi_{\text{succinate}} = \frac{I_{2.62}}{I_{2.62} + I_{2.32}} \quad (1)$$

Number- (M_n) and weight-average (M_w) molecular weights and the dispersity ($Đ$) of the PBSA copolymers were determined in chloroform by size exclusion chromatography (SEC), using a Shimadzu liquid chromatograph. The columns used were PLGel Mixed-C and PLGeL 100 Å. A refractive index detector was employed and chloroform as eluent at a flow rate of 0.8 mL/min. The apparatus was calibrated with linear polystyrene standards from 162 to 1 650 000 g/mol. The molar compositions as well as M_n, M_w, and $Đ$ are shown in Table 1.

Sequence Distribution Study of Copolyesters. The sensitivity of the ^{13}C NMR to small differences in the chemical environment enabled us to determine the different triad structures presented in Figure 2. Three different triads—SBS (succinate−butylene−succinate), SBA (succinate−butylene−adipate), and ABA (adipate−butylene−adipate)—are present in PBSA chains. BDO moieties are present in all three triads and exhibit four distinct ^{13}C chemical shifts according to their surrounding environment. The splitting of signals assigned to PBS and PBA (carbon atoms a_1, a_2, a_3, and a_4 in Figure 2) enable the calculation of the average sequence length of BS and BA units (L_{BS} and L_{BA}, respectively) and the degree of randomness (R) according to eqs 2−4.

DOI: 10.1021/acs.macromol.6b02457
Macromolecules 2017, 50, 597−608

Table 1. Samples Molar Composition, Molar Masses, Dispersity Index, and Sequence Distribution

	molar composition					sequence distribution study		
sample	succinate (mol %)	adipate (mol %)	M_n (kg/mol)	M_w (kg/mol)	$Đ$	L_{BS}	L_{BA}	R
PBS	100	0	29.1	56.2	1.9			
80:20 PBSA	78.6	21.4	29.8	56.9	1.9	4.2	1.3	0.99
60:40 PBSA	58.7	41.3	18.7	30.3	1.6	2.6	1.6	1.01
50:50 PBSA	49.0	51.0	24.7	50.0	2.0	1.9	1.9	1.02
40:60 PBSA	39.3	60.7	30.3	53.8	1.8	1.8	2.4	0.99
20:80 PBSA	20.0	80.0	32.0	55.2	1.7	1.3	3.8	1.03
PBA	0	100	26.8	47.0	1.8			

Scheme 2. (a) Possible Triads of PBSA Copolymers; (b) ^{13}C NMR Spectra of 50:50 PSBA Centered at $\delta \sim 64$ ppm

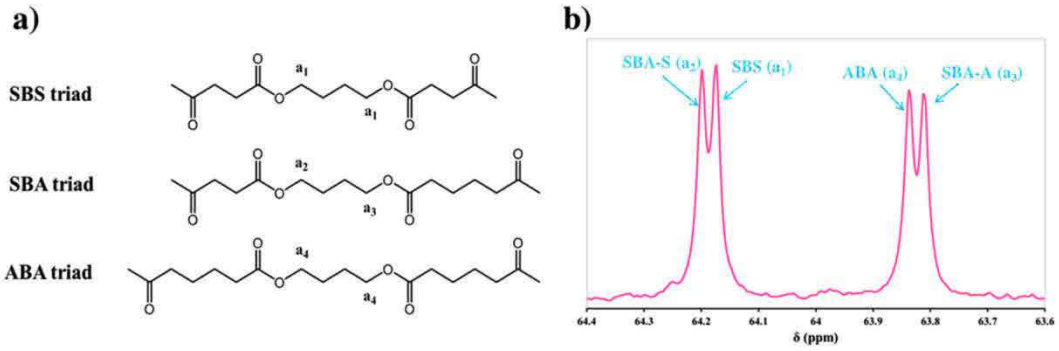

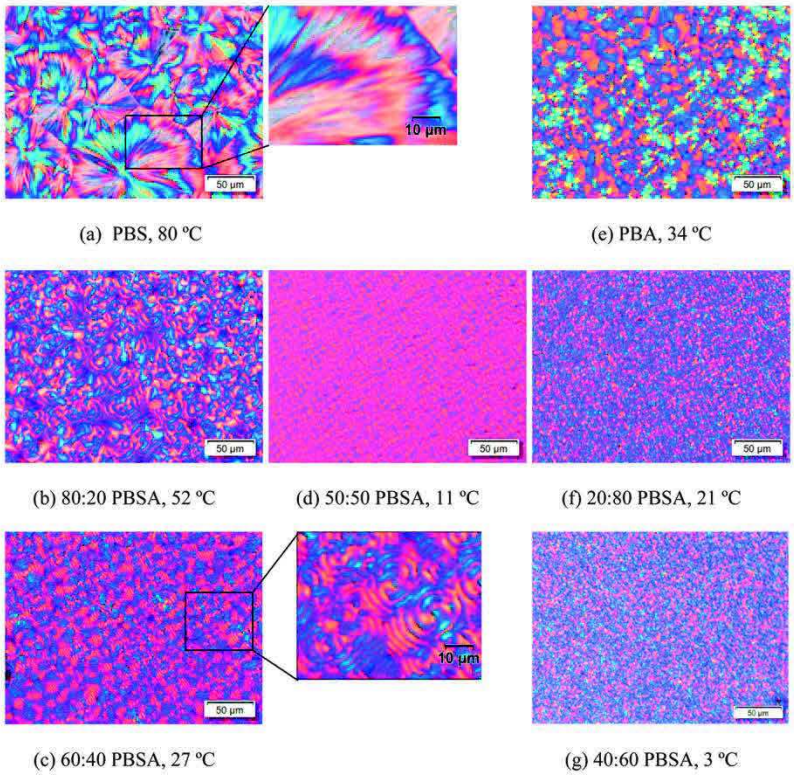

(a) PBS, 80 °C (e) PBA, 34 °C

(b) 80:20 PBSA, 52 °C (d) 50:50 PBSA, 11 °C (f) 20:80 PBSA, 21 °C

(c) 60:40 PBSA, 27 °C (g) 40:60 PBSA, 3 °C

Figure 1. Polarized light optical micrographs for (a) PBS, (b) 80:20 PBSA, (c) 60:40 PBSA, (d) 50:50 PBSA, (e) PBA, (f) 20:80 PBSA, and (g) 40:60 PBSA taken at −40 °C after cooling from the melt at 5 °C/min. The temperature at which the first spherulites appear, or onset crystallization temperature, is indicated under each micrograph.

$$L_{BS} = 1 + \frac{2I_{SBS}}{I_{SBA\text{-}S} + I_{SBA\text{-}A}} \quad (2)$$

$$L_{BA} = 1 + \frac{2I_{ABA}}{I_{SBA\text{-}S} + I_{SBA\text{-}A}} \quad (3)$$

$$R = \frac{1}{L_{BS}} + \frac{1}{L_{BA}} \quad (4)$$

where I_{SBS}, $I_{SBA\text{-}S}$, $I_{SBS\text{-}A}$, and I_{ABA} are integration of peaks assigned to methylene carbons in α of the ester functions ($\delta \sim 64$ ppm) in butyl segments of SBS, SBA, and ABA triads for PBSA copolyesters.

DOI: 10.1021/acs.macromol.6b02457
Macromolecules 2017, 50, 597−608

If R is equal to 1, the terpolyester is randomly distributed. If $R = 2$, the terpolyester is strictly alternated. If R tends to 0, the terpolyester shows a block tendency. L_{BS}, L_{BA}, and R calculated values are summarized in Table 1.

2.3. Polarized Light Optical Microscopy. A polarized light optical microscope, Olympus BX51, was employed incorporating a λ plate in between the polarizers at 45° to facilitate observation and determine the sign of the birefringence. The microscope was equipped with an Olympus SC50 digital camera. A Mettler Toledo FP82 hot stage, which was connected to liquid nitrogen, was coupled to the microscope.

Film samples of PBS, PBA, and their PBSA copolymers were prepared by solution casting using chloroform as a solvent (i.e., 4 wt %). The polymer solution was deposited on a glass slide at ambient temperature to form thin films that were observed uncovered (no cover glass was employed). The cast samples were dried by evaporating the solvent under a hood at controlled temperature for at least 24 h.[25] These uncovered samples were first heated to an adequate temperature in order to erase the thermal history and then crystallized from the melt by cooling to −40 °C at 5 °C/min.

2.4. Differential Scanning Calorimetry. A PerkinElmer 8500 DSC equipped with an Intracooler III was employed in this study. All the experiments were performed under ultrapure nitrogen flow, and the instrument was calibrated with dodecane, indium, and tin standards. Samples of 5 mg were used.

In the nonisothermal scans the samples were melted in the DSC for 3 min at an adequate temperature (e.g., 150 °C for PBS and PBS-rich samples and 90 °C for PBA and PBA-rich samples) to erase any previous thermal history. Then a cooling scan at 5 and 50 °C/min was recorded, followed by a subsequent heating scan at 20 °C/min from −40 °C to the final temperatures given above.

In order to determine the glass transition temperature, the samples were quenched from the melt to −85 °C (employing ballistic cooling) and afterward heated at 20 °C/min. Ballistic cooling is a feature of PerkinElmer 8500 DSC that allows the sample to be cooled at a very fast rate, which is equivalent to 160 °C/min.

2.5. X-ray Diffraction. The samples in DSC pans were examined by simultaneous WAXS/SAXS performed at beamline BM26-B at the European Synchrotron Radiation Facility (ESRF) in Grenoble, France. The energy of X-ray source was 12 keV ($\lambda = 0.1033$ nm), and sample-to-detector distances were 274 and 2946 mm for WAXS and SAXS, respectively. Two Pilatus detectors (300k and 1M) with 172 × 172 μm pixel size were used to record the scattering pattern at wide and small angles. For the temperature-dependent study, the samples were cooled at 5 and 50 °C/min and subsequently heated at 10 °C/min, in a Linkam DSC600 hot stage.

The intensity profile was output as the plot of the scattering intensity (I) vs scattering vector, $q = 4\pi \sin\theta\lambda^{-1}$, where λ is the X-ray wavelength and 2θ is the scattering angle. The scattering vector was calibrated using silver behenate (SAXS) and alumina powder (WAXS). Scattering data were also corrected for background scattering.

3. RESULTS AND DISCUSSION

3.1. Spherulitic Morphology. The morphological study was performed by cooling the samples from the melt to −40 °C at 5 °C/min. Micrographs were taken when spherulites were already impinged, and the onset crystallization temperature is indicated in Figure 1.

Figure 1 shows two kinds of morphologies depending on which is the dominant phase. Therefore, for the PBS or PBA-rich compositions, the morphology approximately resembles that exhibited by the parent homopolymer.

The micrographs shown in Figure 1a−c correspond to PBS-rich compositions (they are generally crystallized at higher temperatures than PBA-rich compositions). All these samples display negative spherulites with more or less defined ring band patterns, as shown in the insets of Figure 1a, d. Ring-banded spherulites have been reported in the literature at temperatures below[19] and up to 80 °C[26] under isothermal conditions for neat PBS. In addition, banding has been also reported for 80:20 PBSA copolymer spherulites by Ren et al.[19]

The ring band patterns in Figure 1a−c go from diffuse (in neat PBS, see Figure 1a and its close-up) to well-defined (in the copolymers, see Figure 1b,c, in which a close-up is inserted) as the BA content increases. Furthermore, a decrease in band spacing, which is related to a decrease in the crystallization temperature,[19] has been observed as PBA content increases (80:20 and 60:40 PBSA). In fact, the onset crystallization temperature also decreases with PBA content (see the onset T_c values below each micrograph in Figure 1). Such morphological changes, added to the increase in the nucleation density as the PBA content is increased, are attributed to changes in supercooling imposed by changing composition.

Figure 1e,f shows the morphologies obtained for PBA-rich compositions, which correspond to negative spherulites without ring band patterns. PBA morphology is a complex subject, since it is reported that PBA in its two polymorphic forms (i.e., α- and β-form) shows negative spherulites without ring band patterns, and when these forms coexist (i.e., mixture $\alpha + \beta$), the ring band pattern appears.[10] However, it is also reported that both α- and β-PBA forms can show banding and mixed morphologies.[27] For instance, according to Liu et al.[27] isothermally crystallized PBA (i.e., with M_n of 5.2 kg/mol) at 30 °C exhibits both ringless α-form and ring-banded β-form spherulites, and this behavior depends on the rate of nucleation and radial growth of α- and β-crystals.

In the present case, in the PBA and PBA-rich compositions, banding is absent, and WAXS results after cooling at 5 °C/min (to be presented below) indicate spherulites with predominant α- or β-phases form, respectively. The increase in nucleation density and the decrease in the onset crystallization temperatures, observed as PBS is added to the PBA-rich copolymers, are attributed to the change in supercooling resulting from the composition changes.

At intermediate compositions (see Figure 1d,g), the high number of nuclei complicates the morphological observations at the micron scale. In spite of this, the birefringent texture observed for the 50:50 PBSA copolymer is similar to those found in PBS-rich compositions, whereas for the 40:60 PBSA copolymer the texture is similar to those present in PBA-rich compositions.

In summary, the superstructural morphology is dominated by the majority component in the copolymer at compositions away from the pseudoeutectic point (lower than 40% of the component in consideration).

As will be demonstrated below, in copolymers with compositions close to 50:50 both PBS-rich and PBA-rich phases can crystallize. It is worth noting that since the PBA-rich phase is molten when the PBS-rich phase starts to crystallize, the latter templates the morphology. Therefore, the PBA-rich phase crystallizes inside the previously formed PBS-rich phase spherulites. This template-like behavior has been reported in PBS/PBA blends,[23] in which PBS forms open structures (i.e., in comparison with the regular spherulites) due to the addition of PBA.

When samples of intermediate composition are heated, changes in birefringence are observed (see Figure S1 in the Supporting Information), and these changes are related to the sequential melting of PBA-rich and PBS-rich phases. Therefore, both PBA- and PBS-rich phases can crystallize when the composition is close to 50:50 (i.e., double crystallization). Even

DOI: 10.1021/acs.macromol.6b02457
Macromolecules 2017, 50, 597−608

though this double crystallization of 50:50 PBSA and 40:60 PBSA is not easy to detect by PLOM, it will be demonstrated below employing X-ray diffraction and DSC experiments.

3.2. X-ray Diffraction Experiments (WAXS and SAXS). *WAXS Experiments.* The WAXS patterns shown in Figure 2

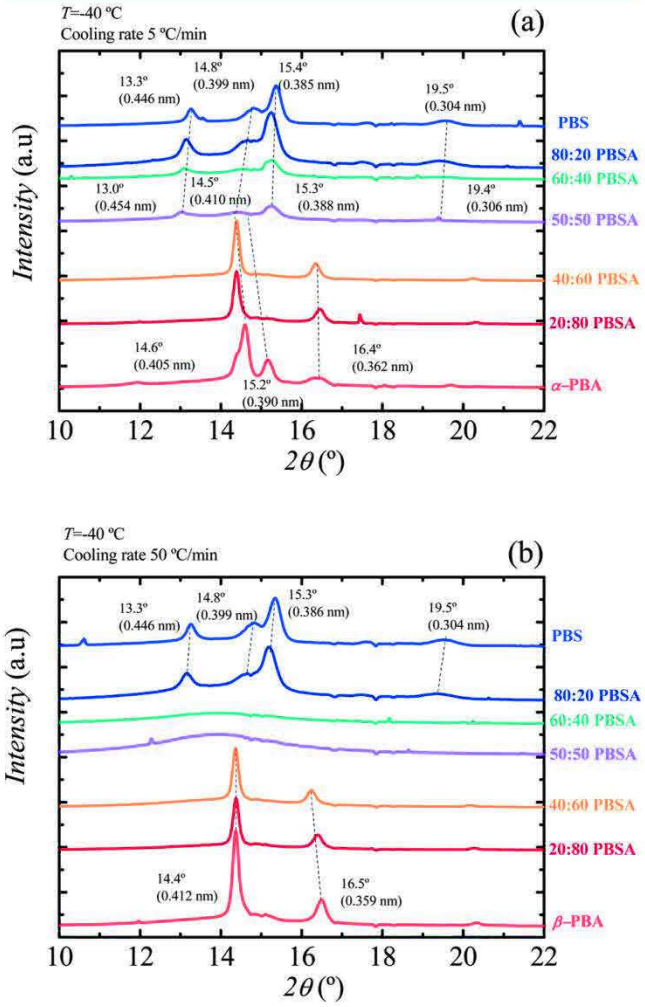

Figure 2. WAXS diffractograms of PBS, PBA, and their copolymers taken at −40 °C after being cooled at (a) 5 and (b) 50 °C/min.

were measured after cooling the samples from the melt to −40 °C at 5 and 50 °C/min (Figures 2a and 2b, respectively). Table S1 in the Supporting Information lists all the reflections and *d*-spacings calculated by employing Bragg's law, which are also labeled in Figure 2.

The most intense reflections observed in the WAXS spectrum of PBS appear at 0.446 and 0.385 nm and correspond to the (020) and (110) planes. Moreover, medium intense reflections were observed at 0.399 and 0.304 nm and can be assigned to the (021) and (111) planes[8,10,13,19,28] of the monoclinic unit cell[13] of α-PBS[19,29] (with the following cell parameters: a = 5.232 Å, b = 9.057 Å, c = 10.900 Å, and γ = 123.87°).[19,28]

In contrast, the most intense reflections observed for neat PBA appear at 0.405 and 0.362 nm, with a medium intense reflection at 0.390 nm, corresponding to the (110), (021), and (020) planes[8,10,13,19,30,31] of the monoclinic unit cell of the α-PBA (with cell parameters a = 6.70 Å, b = 8.00 Å, c = 14.20 Å, and γ = 45.50°).[13]

Figure 2a (for samples cooled at 5 °C/min) reveals that a transformation from α-PBA crystals in neat PBA to β-PBA-rich phase occurs for PBA-rich copolymers (i.e., 20:80 and 40:60 PBSA copolymers). Additionally, a change from β- to α-PBA phase also occurs during heating for the 20:80 PBSA copolymer (see Figure S2).

The more thermodynamically stable α-form in neat PBA is formed preferentially upon slow cooling at 5 °C/min. A switch to the less stable β-phase occurs in PBA-rich copolymers as a consequence of the incorporation of PBS units in chains.

A similar control of PBA polymorphic crystallization in isodimorphic copolymers is reported in the case of in poly(hexamethylene adipate-*ran*-butylene adipate) (P(HA-*ran*-BA), where the increase of HA units in the copolyester favors the formation of the β-PBA form crystals as well.[32] The authors explain this effect by considering that HA units are better "tolerated" in the lattice of β-PBA rather than in the one of α-phase crystals. This is a consequence of lattice matching between β-phase PBA and the crystal structure of PHA.[32]

While in the present case of PBSA copolymers a clear lattice matching between PBS and β-PBA structures is not apparent, from the polymorphic crystallization we can deduce that the free energy penalty for including BS units in the cell of the PBA β-phase crystals is less severe in comparison to the one needed to host them into the α-phase.

It is worth mentioning that the differential partitioning of counits between the different polymorphs has been often invoked to explain the effect of comonomer on polymorph selection in other semicrystalline polymers. An important example is the case of isotactic copolymers of propene with other alkenes (ethylene, 1-butene, 1-hexene), where the orthorhombic γ-form replaces the monoclinic α-phase with increasing counit content.[33,34]

When PBA is cooled rapidly, at 50 °C/min, the most intense reflection appears at 0.412 nm with a medium intense reflection at 0.359 nm, which correspond to (110) and (020) planes of the orthorhombic unit cell of the kinetically favored β-PBA phase (a = 5.06 Å, b = 7.35 Å, and c = 14.67 Å).[27,35−38] The presence of the β-PBA-rich phase can be observed for PBA-rich copolymers (i.e., 20:80 and 40:60 PBSA copolymers) at −40 °C in Figure 2b. If the PBA-rich copolymer samples are subsequently heated, they undergo a series of transformations, from the β phase, passing through a mixture of β + α phases and finally reaching the more stable α-PBA form at higher temperatures (see Figures S2 and S3).

Summarizing the previous results, WAXS experiments show that β-PBA phases are favored either by fast cooling (in both PBA and PBA-rich copolymers) or by the presence of PBS in slowly cooled PBA-rich copolymer samples (i.e., PBSA copolymers cooled at 5 °C/min).

In Figure 2b (i.e., fast cooling rates) the 60:40 and 50:50 PBSA copolymers are not able to crystallize; this result is in line with SAXS and DSC evidence that will be shown below. Nevertheless, according to Figure 2, for both cases (slow and fast cooling), the crystal structure changes from PBS-like unit cells to PBA-like unit cells (either α or β) with increasing PBA composition.

Isodimorphic copolymers are characterized by the inclusion of one of the comonomers in at least one of the present phases. In order to ascertain the possible isodimorphism, the *d*-spacings of the samples were calculated from the main reflections (see Table S1) and plotted in Figure 3. According to Figure 3, *d*-spacing values are not constant with composition but shift in

DOI: 10.1021/acs.macromol.6b02457
Macromolecules 2017, 50, 597−608

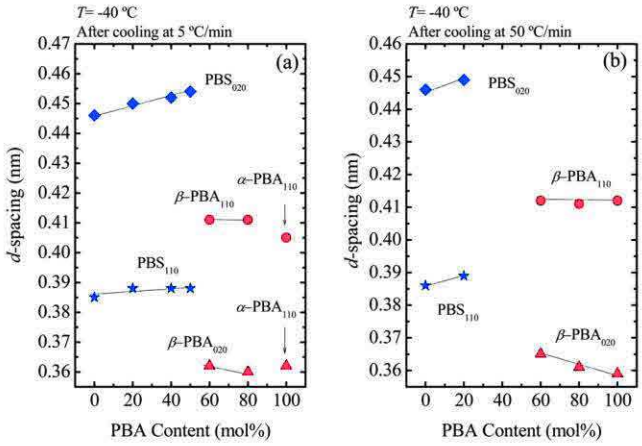

Figure 3. *d*-spacing, obtained after cooling from the melt at (a) 5 and (b) 50 °C/min, of characteristic planes as a function of the PBA content in the PBSA copolymers.

comparison with the main components. These shifts can be interpreted as increases in unit cell dimensions that are needed to accommodate counits of the minority comonomer inside the crystals.

For the PBS-rich phase, Figure 3 shows evidence of clear changes in *d*-spacings with PBA content. These changes can be explained by the inclusion of a small amount of PBA repeating units within PBS-like unit cells. Therefore, cocrystals of PBS and PBA are formed. However, according to the small changes in *d* values and the fact that in PBS-rich compositions WAXS shows the characteristic reflections of PBS unit cells, it can be inferred that comonomer incorporation is limited.

In the case of PBA-rich compositions, the situation is complicated by the change from *α*- to *β*-PBA phases as explained above (see Figure 3a). Nevertheless, the results are consistent with a small inclusion of PBS units within the *β*-PBA unit cells for the 20:80 and 40:60 PBSA copolymers, as judged by the changes in the *d*-spacings of the (020) planes of the *β*-PBA phase unit cells with PBS addition in the copolymer (at least when the samples are cooled at 50 °C/min).

The changes observed in *d*-spacings in Figure 3, together with the DSC results shown below, where a pseudoeutectic point is clearly observed, are consistent with isodimorphic behavior. Furthermore, SAXS results also indicate that two different crystalline phases are formed with distinct lamellar thicknesses that are composition dependent.

SAXS Results. SAXS patterns were obtained under the same conditions as WAXS patterns, since they were performed simultaneously.

The Lorentz representation was chosen to analyze the SAXS results by plotting the product of intensity and the square of the scattering vector q as a function of q. Figure 4 shows clear maxima that represent the scattering from lamellar stacks.

The long periods d^* were estimated by eq 5, and they are listed in Table S2. The experimentally obtained long period values were used for labeling the peaks in Figure 4.

$$d^* = \frac{2\pi}{q_{max}} \tag{5}$$

Figures 4a and 4b show that neat PBA samples (i.e., in its α and β polymorphic forms) have long periods at lower q values in comparison with those of PBS, while the PBSA copolymers

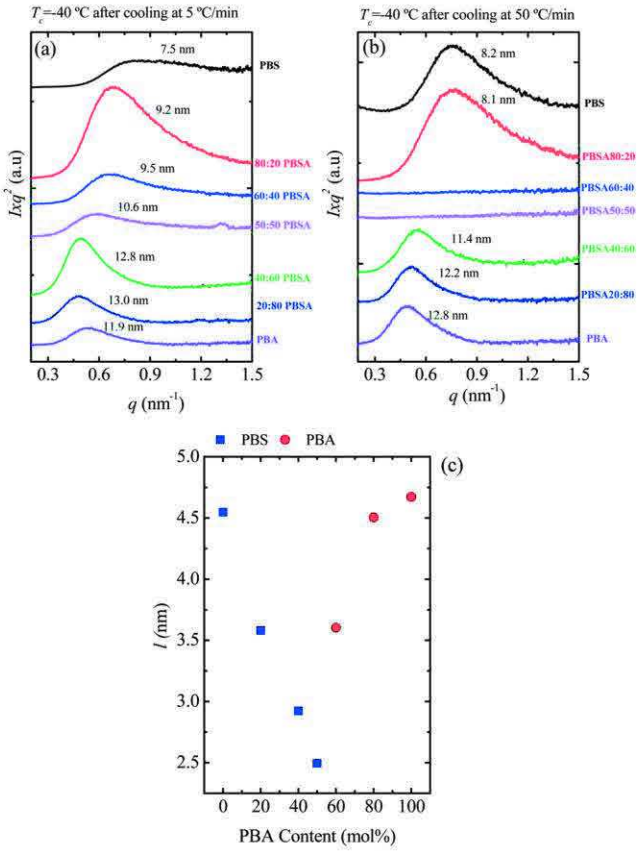

Figure 4. SAXS patterns of PBS, PBA, and their copolymers taken at −40 °C after being cooled at (a) 5 and (b) 50 °C/min. (c) Calculated lamellar thickness for the d^* values presented in (a).

are characterized by long periods located at intermediate q values.

Figures 4a and b show a single long period (d^*) for all the samples (represented by a single maximum in the curve), even at intermediate compositions. These single d^* values are obtained regardless of the previous cooling conditions (i.e., cooling rates of 5 or 50 °C/min) and of composition. Even for those intermediate compositions, where the two phases could potentially crystallize, it would be difficult to observe two long periods since Figure 4 shows that both PBS and PBA homopolymers exhibit similar long periods.

Lamellar thickness values were calculated according to eq 6. They are plotted as a function of PBA content in Figure 4c for samples cooled at 5 °C/min.

$$l = d^* x_v \tag{6}$$

In eq 6, x_v is the crystalline volume fraction, which can be approximated to the mass fraction of crystals (x_m), determined from eq 7, since the density of the different materials has not been measured:

$$x_v \approx x_m = \left(\frac{\Delta H_m^n}{\Delta H_{m,100\%}} \right) \tag{7}$$

where ΔH_m^n is the normalized melting enthalpy of the component under consideration (see Table 2) and $\Delta H_{m,100\%}$ is the enthalpy of fusion of a 100% crystalline sample. Values of 110.5 and 135 J/g determined from the groups contribution

DOI: 10.1021/acs.macromol.6b02457
Macromolecules 2017, 50, 597−608

Table 2. Thermal Transitions and Relevant Enthalpy Values Obtained from the DSC Scans Presented in Figure 5 (T_g) and Figure 6 (Standard Scans)[a]

sample	$T_{g,onset}$ (°C)	$T_{c,end}$ (°C)	$T_{c,peak}$ (°C)	$T_{c,onset}$ (°C)	ΔH_c^n (J/g)	$T_{m,onset}$ (°C)	$T_{m,peak}$ (°C)	$T_{m,end}$ (°C)	ΔH_m^n (J/g)
PBS	−35.2	76.7	80.3	84.6	74	106.4	113.5/109.9	115.3	67
80:20 PBSA	−43.7	48.1	53.4	59.2	55	84.6	92.6	95.2	43
60:40 PBSA	−46.9	24.2	28.5	37.3	41	60.5	70.2/55.3	75.6	34
50:50 PBSA	−49.0	4.9	12.3	20.6	35	4.1	13.8	26.7	0.4
						34.6	52.4/43.7	59.5	26
40:60 PBSA	−52.9	0.4	3.5	7.7	42	25	28.5	32.1	38
						37.2	43.2	48.1	2
20:80 PBSA	−56.8	18.8	21.2	22.8	51	44.4	47.9/42.0	49.6	49
PBA	−59.2	29.3	30.4/34.1	31.4	49	48.3	51.0/54.5/59.1	54.1	53

[a]Onset glass transition temperature ($T_{g,onset}$), onset crystallization temperature ($T_{c,onset}$), peak crystallization temperature ($T_{c,peak}$), normalized crystallization enthalpy (ΔH_c^n), onset melting temperature ($T_{m,onset}$), peak melting temperature ($T_{m,peak}$), and normalized melting enthalpy (ΔH_m^n).

method as proposed by Van Krevelen[39] were used for PBS and PBA, respectively.[8,13,30]

Figure 4c shows how the l values of the PBS-rich composition copolymers decreases with the increase of the PBA content. A similar effect is observed for the PBA-rich copolymers. The reduction in l values is a consequence of comonomer incorporation into the chains that limit the length of crystallizable sequences. In fact, for these PBSA copolymers, the l values exhibit a pseudoeutectic-like behavior as a function of composition.

When the samples are cooled rapidly (see Figure 4b), d^* values experience changes for both homopolymers and random copolymers. At 50 °C/min, the 60:40 and 50:50 PBSA copolymers are not able to crystallize. This is consistent with the WAXS results (discussed above) and DSC data (shown below).

3.3. Standard and Rate-Dependent DSC Experiments.

Figure 5 shows DSC heating traces for the random copolymers and their corresponding homopolymers after they were quenched from the melt (using ballistic cooling as indicated in the Experimental Part). All copolymers exhibit a single glass transition temperature (T_g) in between the T_g values of the homopolymers, as expected for random copolymers (their random sequence structure was determined by ^{1}H NMR, shown above) that form a miscible amorphous phase. The presence of a single phase in the melt was also corroborated by standard (see previous section) and rate-dependent (see section below) SAXS experiments.

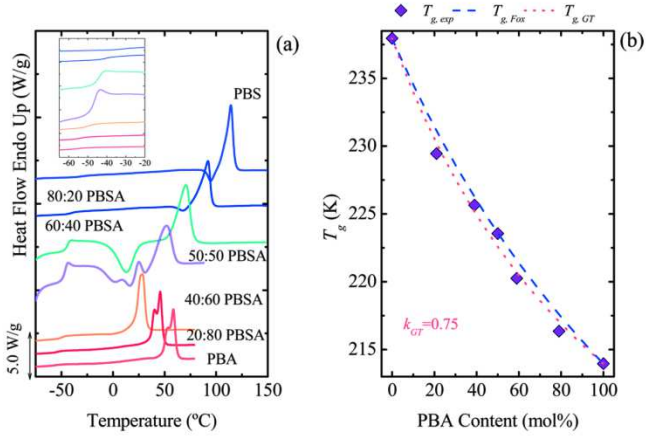

Figure 5. (a) DSC heating scans performed after quenching PBS, PBA, and their copolymers samples. (b) Glass transition temperatures (T_g), taken from (a), as a function of PBA content; the fits to the Fox and Gordon−Taylor equations are also shown.

Figure 5b shows a plot of T_g values versus composition. The T_g values decrease with increasing PBA content, as expected, since there are four methylene groups in the butylene adipate repeating unit, which makes PBA more flexible in comparison with PBS. Such differences in chain flexibility account for the 25 °C difference in between the T_g values of PBA and PBS.[8]

Figure 5a shows that samples that are able to crystallize during the previous ballistic quenching display weak glass transitions that can only be clearly seen if a close-up is made in the curve.[40] In contrast, the intermediate compositions of 60:40 and 50:50 PBSA show a large endothermic jump associated with the change in heat capacity experienced by the material during T_g, followed by cold-crystallization. For these samples, the crystallization during fast cooling was hindered, and this evidences the composition-dependent behavior of the samples.

Figure 5b shows a nonlinear dependence of the T_g as a function of the PBA content that can be approximately described by the semiempirical Fox equation,[41] although it is even better fitted by the Gordon−Taylor equation:[42]

$$T_{g,PBSA} = \frac{w_{PBA}T_{g,PBA} + k_{GT}(1 - w_{PBA})T_{g,PBS}}{w_{PBA} + k_{GT}(1 - w_{PBA})} \quad (8)$$

where $T_{g,PBA}$ and $T_{g,PBS}$ are the glass transition temperature of PBA and PBS, respectively; w_{PBA} is the mass fraction of PBA, and k_{GT} is the Gordon−Taylor parameter.

The Gordon−Taylor equation fitted well the experimental data with k_{GT} = 0.75. As a result, $T_{g,PBSA}$ can be predicted for all composition ranges using eq 8.

Rate-dependent DSC analyses were performed. Cooling rates of 5 and 50 °C/min were selected, whereas the subsequent heating scans were always performed at 20 °C/min. The DSC cooling and heating curves are shown in Figure 6.

Figure 6 shows cooling and heating DSC scans for both 5 and 50 °C/min cooling rates, in which all compositions of PBSA copolymers are able to crystallize. A related remarkable point to consider is that all copolymer samples are able to crystallize, despite their randomness. This is a characteristic behavior of isodimorphic copolymers.[7] Such copolymers can crystallize in unit cells that resemble those of the homopolymers, but with inclusions of the second component repeating units, as demonstrated in the previous section.

Figure 6a shows that all samples exhibit a single crystallization peak during cooling from the melt, which is sharper or broader depending on composition.

DOI: 10.1021/acs.macromol.6b02457
Macromolecules 2017, 50, 597−608

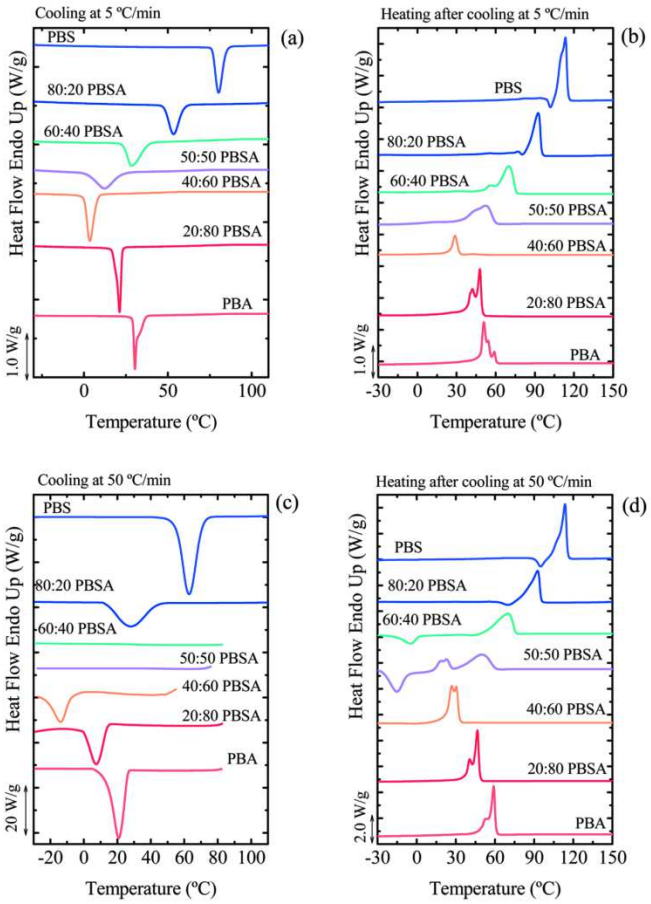

Figure 6. Cooling DSC scans (a, c) from the melt and subsequent heating scans (at 20 °C/min) (b, d) for the indicated homopolymers and random copolymers samples at 5 (a, b) and 50 °C/min (c, d).

The subsequent heating scans are shown in Figure 6b. PBS and PBS-rich compositions exhibit cold-crystallization during heating followed by melting. In contrast, PBA-rich copolymers do not exhibit cold-crystallization. PBA and PBA-rich copolymers display bimodal melting. WAXS analysis (see Figure 2) indicates that these samples are polymorphic. Neat PBA exhibits the α- or β-phase depending on the previous cooling rate (see Figures 2a and 2b, respectively), whereas in the PBA-rich compositions, the β-phase is the dominant polymorphic form regardless of the cooling rate (see Figure 2b). Such predominance of the β-phase is apparently induced by the inclusion of PBS within the crystal lattice of PBA. Therefore, the bimodal melting of the PBA-rich compositions (see Figure 6) is attributed to the polymorphic nature of PBA,[10,30,31,43,44] since a switch from the less stable β-phase to the more stable α-phase typically occurs during heating, especially when the samples were previously cooled at 50 °C/min (see Figure 6b).

For the PBS-rich phase, the α-phase is the dominant one. Therefore, the bimodal melting peaks in these cases are probably due to partial melting and reorganization during the heating scan.[7]

At intermediate compositions (i.e., 50:50 and 40:60 PBSA), both PBS and PBA-like phases have similar chances to crystallize. Figure 6a,b shows broader crystallization and melting peaks and even multiple peaks. A single exothermic peak is always observed during cooling indicating that coincident crystallization of both phases is occurring. This can be demonstrated by the detection of two sequential melting peaks upon heating. In fact, the coincident crystallization and sequential melting can be better observed in Figure S4, where a close-up of the DSC traces of Figure 6a,b is presented. A detailed study of the crystallization and melting of these intermediate compositions can be found in a separate section below.

It is worth noting that in PBS/PBA blends fractionated[10] and sequential crystallization[24] have been reported instead of the coincident crystallization process that has been found in this work for PBSA random copolymers.

Figure 7 shows how the crystallization and melting temperatures and enthalpies (after cooling at 5 °C/min)

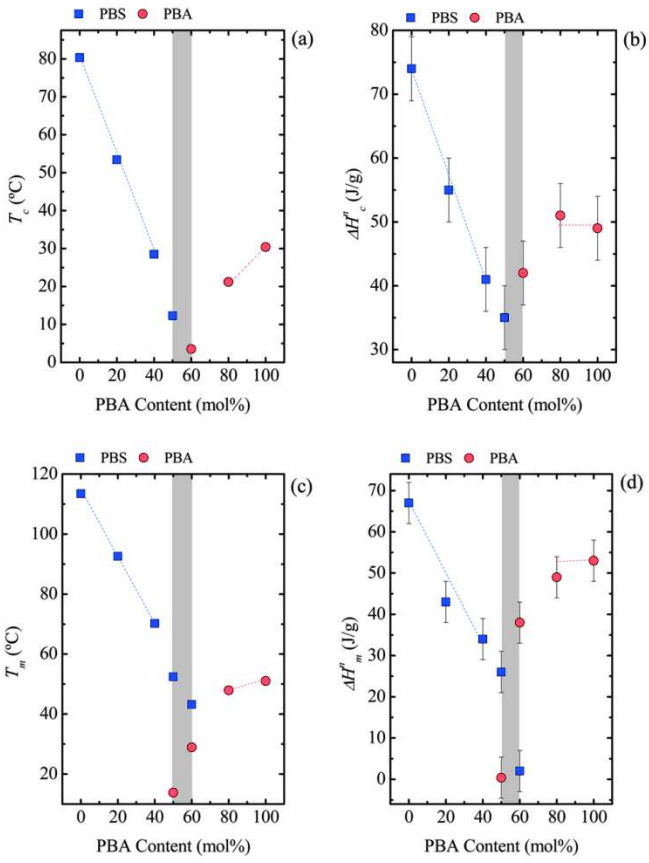

Figure 7. Variation of (a) T_c, (b) ΔH^n_c, (c) T_m, and (d) ΔH^n_m as a function of PBA content taken during cooling at 5 °C/min and in the subsequent heating. The shadowed region indicates the pseudoeutectic point.

depend on the composition of the copolymers (see also Table 2). Figure 7 also shows the characteristic pseudoeutectic-like behavior of isodimorphic random copolymers. Three zones can be distinguished. Left of the pseudoeutectic point, the incorporation of PBA within the copolymer induces the plasticization of PBS, as the random copolymers are miscible. This behavior causes a decrease of the calorimetric properties of PBS with increasing adipate unit content, until they go through a minimum at a copolymer composition close to equimolarity (shadowed region), and then they increase toward the value of PBA. The reductions of melting point and heat of fusion as a function of composition indicate that even though some comonomer incorporation is possible (as indicated by the WAXS results presented above), most of the minority

DOI: 10.1021/acs.macromol.6b02457
Macromolecules 2017, 50, 597−608

comonomer units act as defects that are excluded from the crystalline regions limiting crystallinity and reducing lamellar size (see also the corresponding Figure 4c).[8,13] The miscibility between the two types of comonomer units also induces changes in supercooling as the equilibrium melting point will be a function of composition. These changes in supercooling also contribute to the large dependence of the calorimetric properties on composition.

The pseudoeutectic-like behavior is in agreement with other copolyester systems and in fact was also obtained in PBSA copolymers, but without the sequential melting at intermediate compositions by Tserki et al.[8]

According to the thermal behavior presented in Figure 7, the pseudoeutectic point corresponds to a PBA content of 60 and 50 mol % (see shadowed region). On each side of the pseudoeutectic point, the copolymers crystallize solely in the PBS-like (PBA content <50 mol %) or PBA-like (PBA content >60 mol %) crystal lattice.

The results obtained above by both WAXS and DSC demonstrate that isodimorphic behavior is present in the PBSA copolymer samples in view of their similar chemical structure.

Figure 6c shows that crystallization at intermediate compositions (i.e., PBA content of 40 and 50 mol %) is inhibited, but in the subsequent heating scans (Figure 6d) cold-crystallization and melting peaks are displayed.

Figure 6d shows the subsequent heating scans after cooling at 50 °C/min. Almost all materials show similar curves to those obtained at lower cooling rates. However, for the 60:40 and 50:50 PBSA copolymers, a cold-crystallization is clearly observed followed by one and two melting peaks, respectively.

In the 60:40 case, no evidence of the crystallization of the PBA-rich phase was found (i.e., by WAXS; see Figure S5). In the 50:50 PBSA copolymer case, a cold-crystallization process followed by the sequential melting of the two phases can be observed in Figure 6d. The endothermic peak at low temperature corresponds to the melting of PBA-rich phase crystals, whereas the peak at higher temperatures corresponds to the melting of PBS-rich phase crystals (see Figure 6d). Therefore, the 50:50 PBSA is the only copolymer that is able to develop a double crystalline structure during cold-crystallization from the glassy state. In fact, during the cold-crystallization process, the PBA-rich phase will crystallize first, followed by the PBS-rich phase crystallization. However, the cold-crystallization of the PBS-rich phase and the melting of the PBA-rich phase occur in the same temperature range and are overlapped, as it will be demonstrated below employing temperature-resolved WAXS.

Even though the 40:60 PBSA copolymer crystallizes in a coincident fashion (i.e., the crystallization of both phases occurs in the same temperature range and the exotherms are overlapped into a single process) when it is cooled at 5 °C/min, the PBA-rich phase crystallization is favored over the PBS-rich phase when a cooling rate of 50 °C/min was used. As a result, no PBS-rich phase crystals are formed, and no melting point corresponding to PBS-rich phase is observed in Figure 6d.

3.4. Temperature- and Rate-Dependent Experiments.

DSC Rate-Dependent Experiments. In order to better understand the sequential and coincident crystallization processes of the 50:50 and 40:60 PBSA copolymers, rate-dependent experiments were performed.

Figure 8a shows cooling scans from the melt at different cooling rates corresponding to the 50:50 PBSA copolymer.

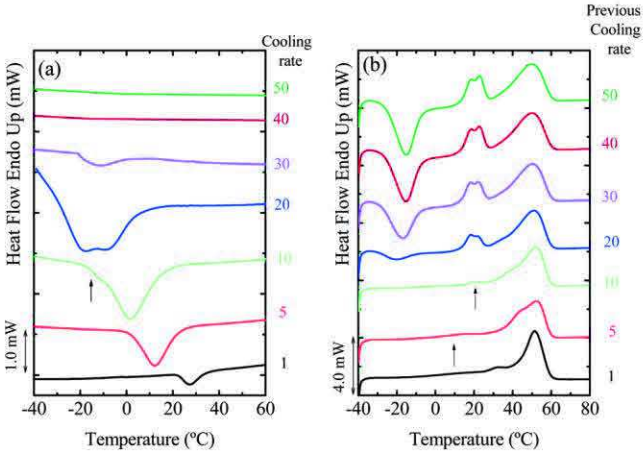

Figure 8. 50:50 PBSA (a) cooling scans to −40 °C at different cooling rates and (b) subsequent heating scans performed at 20 °C/min. The values indicated to the right of each figure indicate the cooling rates applied in °C/min.

Figure 8b, on the other hand, shows the subsequent heating scans performed at the constant rate of 20 °C/min.

Figure 8 shows that when the 50:50 PBSA copolymer is cooled at a very slow rate (i.e., at 1 °C/min), only the PBS-rich phase is able to crystallize, as indicated by the single crystallization exotherm and subsequent melting peak at temperatures that are higher than the melting point of the PBA-rich phase. As the cooling rate is increased, the PBA-rich phase is able to undergo crystallization as well. For the sample cooled at 5 °C/min, even though a single crystallization peak is registered (i.e., coincident crystallization), the subsequent heating shows a very small melting endotherm or shoulder at temperatures that are characteristic of the PBA-rich phase (which is indicated with an arrow and even though it cannot be clearly seen at the scale employed in Figure 8b, it is shown in Figure S4) and a large melting peak at higher temperatures that corresponds to the melting of PBS-rich crystals.

A similar behavior to that observed at 5 °C/min is observed at 10 °C/min, except for the fact that during crystallization, a low temperature shoulder can be seen, which attributed to the crystallization of the PBA-rich phase (signaled with an arrow in Figure 8a). A small melting endotherm at low temperatures can also be seen on the heating curve corresponding to the melting of the small population of PBA-rich phase crystals (also indicated with an arrow in Figure 8b). The bimodality of the crystallization exotherm is easily seen in the sample cooled at 20 °C/min in Figure 8a as well as the evident melting of PBA-rich phase crystals at around 20 °C following a cold-crystallization exotherm.

Increasing the cooling rate to values higher than or equal to 40 °C/min prevents the crystallization of the 50:50 copolymer (also corroborated by WAXS studies). Upon subsequent heating, a very large cold-crystallization exotherm is observed followed by sequential melting. In the next section, WAXS studies during heating show that in such rapidly cooled samples the large cold-crystallization exotherm corresponds to the crystallization of the PBA-rich crystal phase. As temperature is increased, the melting of the PBA-rich crystals overlaps with the cold-crystallization of the PBS-rich phase until temperatures above 30 °C are reached, at which the PBS-rich crystals start melting.

DOI: 10.1021/acs.macromol.6b02457
Macromolecules 2017, 50, 597−608

According to results presented above for the 50:50 PBSA copolymer sample, as the PBS-rich phase crystallization becomes more kinetically limited (upon increasing cooling rates), the PBA-rich phase is able to crystallize. Therefore, the coincident crystallization during cooling from the melt switches to a sequential process when cooled from the melt at 10 or 20 °C/min and finally to a sequential cold-crystallization during heating (for completely amorphous 50:50 PBSA samples).

Similar rate-dependent experiments were performed to the 40:60 PBSA copolymer, and the results are shown in Figure 9.

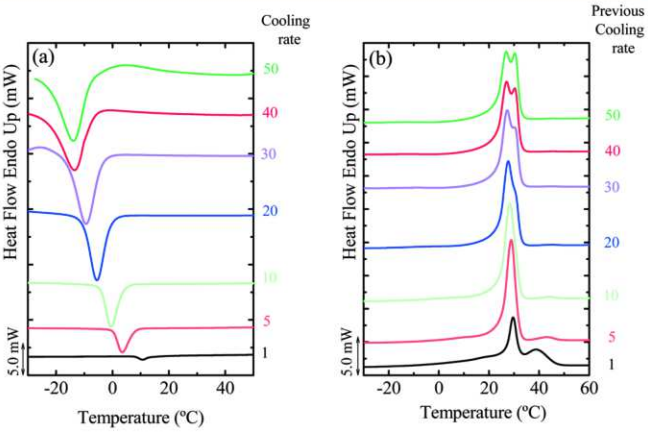

Figure 9. The 40:60 PBSA (a) cooling DSC scans at different cooling rates and (b) subsequent heating scans performed at 20 °C/min. The values indicated to the right of each figure indicate the cooling rates applied in °C/min.

Figure 9a shows a single crystallization peak at all the selected cooling rates for the 40:60 PBSA. At high cooling rates (i.e., >20 °C/min) this peak corresponds to the PBA-rich phase only. This behavior was corroborated by WAXS experiments (see Figure S2), in which β- to α-PBA phase transformation was observed during the heating of the 40:60 PBSA copolymer, whereas such transformation is inhibited when the PBS is able to crystallize.

At low cooling rates (i.e., <20 °C/min) the single crystallization peak (see Figure 9a) corresponds to the coincident crystallization of the PBS- and PBA-rich phases, which melt sequentially in the subsequent heating scans (e.g., 1 °C/min in Figure 9b). As the cooling rate is decreased, the melting peak at higher temperatures, which corresponds to the PBS-rich phase, is increased. Therefore, when PBS is the minority phase (40 mol %), it will only be able to crystallize under favorable thermodynamic conditions, such as slow cooling rates, since it only crystallizes before the PBA-rich phase has started its crystallization.

WAXS Rate-Dependent Experiments. By employing DSC experiments, the conditions to promote double crystallization in the 50:50 and 40:60 PBSA copolymers were determined. These conditions were employed to perform parallel X-ray experiments.

Figure 10a shows WAXS patterns of the 50:50 PBSA copolymer taken during heating immediately after the sample was rapidly cooled from the melt at 50 °C/min. A corresponding DSC heating scan is presented in Figure 10b, indicating the changes experienced by the sample, as determined by the WAXS results of Figure 10a.

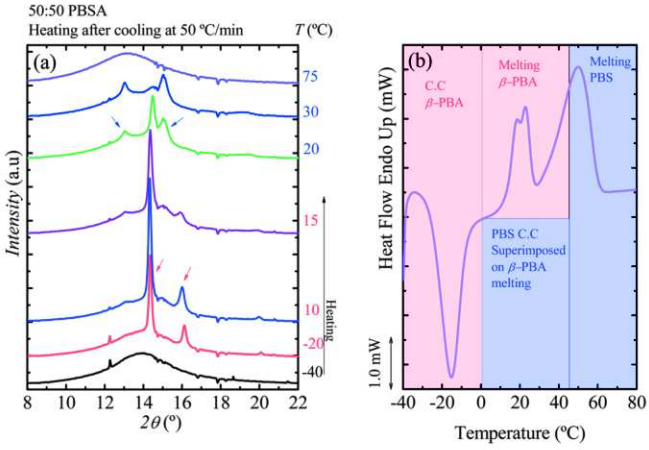

Figure 10. (a) WAXS diffractograms (at different temperatures) obtained during heating after cooling the 50:50 PBSA sample at 50 °C/min and (b) DSC heating scans, for a sample with identical thermal history. The cold-crystallization (CC) and melting processes are indicated. The red shadows as well as red color on the numbers are employed to highlight the PBA-rich phase thermal events while the blue shadows as well as blue color on the numbers are used for the corresponding PBS-rich phase. The heating scans (for both WAXS and DSC) were performed at 10 °C/min. The values indicated to the right of figure (a) indicate the temperature at which the patterns were taken. The arrows indicate the main reflections for PBA (see pattern taken at 10 °C) and PBS (see pattern taken at 20 °C).

Figure 10a shows WAXS spectra obtained during heating for the 50:50 PBSA copolymer from the amorphous state (i.e., T_c of −40 °C), after cooling the sample at 50 °C/min. As the temperature is increased, the PBA-rich phase starts to crystallize at −20 °C, which corresponds to the cold-crystallization shown in Figure 10b. A shoulder at ∼15°, in between the two main reflections of the PBA-rich crystalline phase (∼14° and 16°), and a weak signal at 13°, which correspond to the PBS-rich phase crystals, appear just at the end of the cold-crystallization of the PBA-rich phase at approximately 5 °C (data not shown). Then, an increase in intensity of the PBS-rich crystal reflections and a simultaneous decrease of the PBA-rich crystal reflections are recorded in between 15 and 20 °C, indicating that PBA-rich crystals melt and the PBS-rich phase undergoes cold-crystallization. Finally, at 30 °C, only the signals of the PBS-rich crystals remain, until they disappear at higher temperatures (i.e., >60 °C) upon melting.

It is worth noting that the transition from the β-phase to α PBA-rich phase is inhibited by the crystallization of the PBS.

A different behavior is obtained for the 40:60 PBSA copolymer. When the material is cooled from the melt at 1 °C/min, coincident crystallization of both phases is detected by DSC, as the exotherms corresponding to the crystallization of the two phases overlap (see Figure 9a). However, *in situ* WAXS experiments show that the PBS-rich phase starts its crystallization at slightly higher temperatures (i.e., 2 °C) than the PBA-rich phase. Figure 11a shows representative WAXS diffractograms during cooling from the melt at 1 °C/min. Segmented blue and red lines are used to indicate the PBS and PBA reflections. It can be appreciated that PBS crystal reflections can be first seen at 10 °C as temperature is decreased, while β-PBA reflections only appear at 8 °C. Nevertheless, most of the crystallization process occurs at temperatures below 8 °C in a coincident fashion in agreement with the DSC results.

DOI: 10.1021/acs.macromol.6b02457
Macromolecules 2017, 50, 597−608

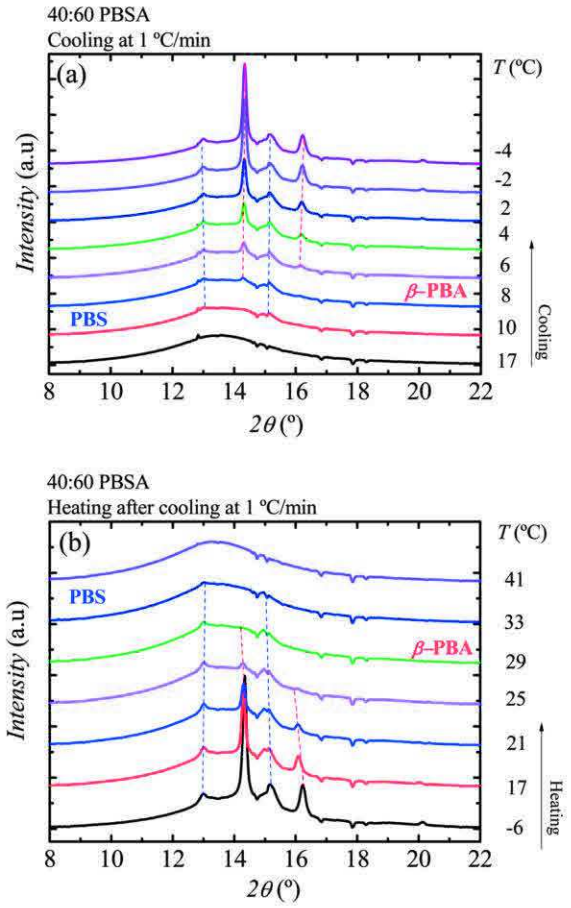

Figure 11. WAXS diffractograms taken during (a) cooling at 1 °C/min and (b) subsequent heating at 10 °C/min for 40:60 PBSA copolymer. The values indicated to the right of each figure correspond to the temperature at which the patterns were taken.

Figure 11b shows WAXS diffractograms for the 40:60 PBSA copolymer taken during heating. The characteristic reflections of β-PBA start to decrease in intensity at 25 °C and disappear completely at 29 °C because the β-PBA rich phase melts. Then, PBS characteristic signals disappear at higher temperatures, as the PBS-rich phase crystals melt, in agreement with the sequential melting detected by DSC experiments (see Figure 9b). It is worth noting that also in this sample β- to α-PBA phase transformation is inhibited by the presence of PBS in the copolymer. The same conditions for the WAXS rate-dependent experiments were used in SAXS, and the results are shown in Figures S6 and S7.

4. CONCLUSIONS

PBSA random copolymers have been successfully synthesized from different biobased or potentially biobased building blocks in a multistep pathway by polycondensation followed by a postpolycondensation step, with a wide succinate/adipate composition range.

The results obtained by DSC and WAXS show that PBSA random copolymers are isodimorphic, since each phase allows the inclusion of the minority comonomer. Moreover, the calorimetric properties exhibit a pseudoeutectic behavior. Around the pseudoeutectic point, which corresponds to two compositions (i.e., 50:50 and 40:60 PBSA), a double crystallization process, which strongly depends on cooling rates, was observed.

For all copolymers, the inclusion of PBS repeating units in the cocrystals forces the PBA-rich phase to cocrystallize in its kinetically favored crystalline phase (i.e., β-PBA). This behavior could be ascribed to a less severe energy penalty for the inclusion of BS units into the PBA-rich β-phase lattice, in comparison to inclusion into the α-phase.

■ ASSOCIATED CONTENT

Supporting Information

The Supporting Information is available free of charge on the ACS Publications website at DOI: 10.1021/acs.macromol.6b02457.

Figures S1−S7 and Tables S1, S2 (PDF)

■ AUTHOR INFORMATION

Corresponding Author

*(A.J.M.) E-mail alejandrojesus.muller@ehu.es.

ORCID

Dario Cavallo: 0000-0002-3274-7067

Luc Avérous: 0000-0002-2797-226X

Alejandro J. Müller: 0000-0001-7009-7715

Notes

The authors declare no competing financial interest.

■ ACKNOWLEDGMENTS

We thank the European Synchrotron Radiation Facility (ESRF) for supporting the X-rays experiments at beamline BM26-B. The BioTeam acknowledges the financial support from the Europeańs Union 7th framework Program for research, technological development and demonstration under grant agreement no. 311815 (SYNPOL Project). In addition, the authors are grateful to the BioAmber company for the supply of biosuccinic acid. The POLYMAT/UPV/EHU team acknowledges funding from the following projects: "UPV/EHU Infrastructure: INF 14/38"; "Mineco/FEDER: SINF 130I001726XV1/Ref.: UNPV13-4E10-1726" and "Mineco MAT2014-53437-C2-P." R.A.P.-C. gratefully acknowledges the award of a PhD fellowship by POLYMAT Basque Center for Macromolecular Design and Engineering.

■ REFERENCES

(1) Sisti, L.; Totaro, G.; Marchese, P. PBS Makes its Entrance into the Family of Biobased Plastics. In *Biodegradable and Biobased Polymers for Environmental and Biomedical Applications*; John Wiley & Sons, Inc.: 2016; pp 225−285.

(2) Pan, P.; Inoue, Y. Polymorphism and isomorphism in biodegradable polyesters. *Prog. Polym. Sci.* **2009**, *34* (7), 605−640.

(3) Xu, J.; Guo, B.-H. Poly(butylene succinate) and its copolymers: Research, development and industrialization. *Biotechnol. J.* **2010**, *5* (11), 1149−1163.

(4) Allegra, G.; Bassi, I. W. Isomorphism in synthetic macromolecular systems. In *Fortschr. Hochpolym-Forsch*; Springer: Berlin, 1969; pp 549−574.

(5) Díaz, A.; Franco, L.; Puiggalí, J. Study on the crystallization of poly(butylene azelate-co-butylene succinate) copolymers. *Thermochim. Acta* **2014**, *575*, 45−54.

(6) Bluhm, T. L.; Hamer, G. K.; Marchessault, R. H.; Fyfe, C. A.; Veregin, R. P. Isodimorphism in bacterial poly(β-hydroxybutyrate-co-β-hydroxyvalerate). *Macromolecules* **1986**, *19* (11), 2871−2876.

(7) Arandia, I.; Mugica, A.; Zubitur, M.; Arbe, A.; Liu, G.; Wang, D.; Mincheva, R.; Dubois, P.; Müller, A. J. How Composition Determines

DOI: 10.1021/acs.macromol.6b02457
Macromolecules 2017, 50, 597−608

the Properties of Isodimorphic Poly(butylene succinate-ran-butylene azelate) Random Biobased Copolymers: From Single to Double Crystalline Random Copolymers. *Macromolecules* **2015**, *48* (1), 43−57.
(8) Tserki, V.; Matzinos, P.; Pavlidou, E.; Vachliotis, D.; Panayiotou, C. Biodegradable aliphatic polyesters. Part I. Properties and biodegradation of poly(butylene succinate-co-butylene adipate). *Polym. Degrad. Stab.* **2006**, *91* (2), 367−376.
(9) Ojijo, V.; Ray, S. S. Poly(Butylene Succinate) and Poly[(Butylene Succinate)-co-Adipate] Nanocomposites. In *Environmental Silicate Nano-Biocomposites*; Avérous, L., Pollet, E., Eds.; Springer: London, 2012; pp 165−218.
(10) Yang, J.; Pan, P.; Hua, L.; Xie, Y.; Dong, T.; Zhu, B.; Inoue, Y.; Feng, X. Fractionated crystallization, polymorphic crystalline structure, and spherulite morphology of poly(butylene adipate) in its miscible blend with poly(butylene succinate). *Polymer* **2011**, *52* (15), 3460−3468.
(11) Fujimaki, T. Processability and properties of aliphatic polyesters, 'BIONOLLE', synthesized by polycondensation reaction. *Polym. Degrad. Stab.* **1998**, *59* (1−3), 209−214.
(12) Montaudo, G.; Rizzarelli, P. Synthesis and enzymatic degradation of aliphatic copolyesters. *Polym. Degrad. Stab.* **2000**, *70* (2), 305−314.
(13) Nikolic, M. S.; Djonlagic, J. Synthesis and characterization of biodegradable poly(butylene succinate-co-butylene adipate)s. *Polym. Degrad. Stab.* **2001**, *74* (2), 263−270.
(14) Ahn, B. D.; Kim, S. H.; Kim, Y. H.; Yang, J. S. Synthesis and characterization of the biodegradable copolymers from succinic acid and adipic acid with 1,4-butanediol. *J. Appl. Polym. Sci.* **2001**, *82* (11), 2808−2826.
(15) Rizzarelli, P.; Puglisi, C.; Montaudo, G. Soil burial and enzymatic degradation in solution of aliphatic co-polyesters. *Polym. Degrad. Stab.* **2004**, *85* (2), 855−863.
(16) Kuwabara, K.; Gan, Z.; Nakamura, T.; Abe, H.; Doi, Y. Molecular Mobility and Phase Structure of Biodegradable Poly(butylene succinate) and Poly(butylene succinate-co-butylene adipate). *Biomacromolecules* **2002**, *3* (5), 1095−1100.
(17) Wang, Y.; Bhattacharya, M.; Mano, J. F. Thermal analysis of the multiple melting behavior of poly(butylene succinate-co-adipate). *J. Polym. Sci., Part B: Polym. Phys.* **2005**, *43* (21), 3077−3082.
(18) Eslami, H.; Grmela, M.; Dubois, C.; Lafleur, P. Melt rheology of biodegradable poly[(butylene succinate)-co-adipate]: Experimental and model predictions. *J. Polym. Sci., Part B: Polym. Phys.* **2010**, *48* (8), 832−839.
(19) Ren, M.; Song, J.; Song, C.; Zhang, H.; Sun, X.; Chen, Q.; Zhang, H.; Mo, Z. Crystallization kinetics and morphology of poly(butylene succinate-co-adipate). *J. Polym. Sci., Part B: Polym. Phys.* **2005**, *43* (22), 3231−3241.
(20) Zhao, J.-H.; Wang, X.-Q.; Zeng, J.; Yang, G.; Shi, F.-H.; Yan, Q. Biodegradation of poly(butylene succinate-co-butylene adipate) by Aspergillus versicolor. *Polym. Degrad. Stab.* **2005**, *90* (1), 173−179.
(21) Hayase, N.; Yano, H.; Kudoh, E.; Tsutsumi, C.; Ushio, K.; Miyahara, Y.; Tanaka, S.; Nakagawa, K. Isolation and characterization of poly(butylene succinate-co-butylene adipate)-degrading microorganism. *J. Biosci. Bioeng.* **2004**, *97* (2), 131−133.
(22) Tomita, K.; Kuroki, Y.; Hayashi, N.; Komukai, Y. Isolation of a thermophile degrading poly(butylene succinate-co-butylene adipate). *J. Biosci. Bioeng.* **2000**, *90* (3), 350−352.
(23) Wang, H.; Gan, Z.; Schultz, J. M.; Yan, S. A morphological study of poly(butylene succinate)/poly(butylene adipate) blends with different blend ratios and crystallization processes. *Polymer* **2008**, *49* (9), 2342−2353.
(24) Wang, H.-j.; Feng, H.-p.; Wang, X.-c.; Guo, P.-y.; Zhao, T.-s.; Ren, L.-f.; Qiang, X.-h.; Xiang, Y.-h.; Yan, C. Effects of crystallization temperature and blend ratio on the crystal structure of poly(butylene adipate) in the poly(butylene adipate)/poly(butylene succinate) blends. *Chin. J. Polym. Sci.* **2014**, *32* (4), 488−496.
(25) Woo, E. M.; Nurkhamidah, S. Surface Nanopatterns of Two Types of Banded Spherulites in Poly(nonamethylene terephthalate) Thin Films. *J. Phys. Chem. B* **2012**, *116* (16), 5071−5079.
(26) Gan, Z.; Abe, H.; Doi, Y. Crystallization, Melting, and Enzymatic Degradation of Biodegradable Poly(butylene succinate-co-14 mol% ethylene succinate) Copolyester. *Biomacromolecules* **2001**, *2* (1), 313−321.
(27) Liu, J.; Ye, H.-M.; Xu, J.; Guo, B.-H. Formation of ring-banded spherulites of α and β modifications in Poly(butylene adipate). *Polymer* **2011**, *52* (20), 4619−4630.
(28) Ye, H.-M.; Tang, Y.-R.; Xu, J.; Guo, B.-H. Role of Poly(butylene fumarate) on Crystallization Behavior of Poly(butylene succinate). *Ind. Eng. Chem. Res.* **2013**, *52* (31), 10682−10689.
(29) Ichikawa, Y.; Kondo, H.; Igarashi, Y.; Noguchi, K.; Okuyama, K.; Washiyama, J. Crystal structures of α and β forms of poly(tetramethylene succinate). *Polymer* **2000**, *41* (12), 4719−4727.
(30) Woo, E. M.; Wu, M. C. Thermal and X-ray analysis of polymorphic crystals, melting, and crystalline transformation in poly(butylene adipate). *J. Polym. Sci., Part B: Polym. Phys.* **2005**, *43* (13), 1662−1672.
(31) Gan, Z.; Kuwabara, K.; Abe, H.; Iwata, T.; Doi, Y. Metastability and Transformation of Polymorphic Crystals in Biodegradable Poly(butylene adipate). *Biomacromolecules* **2004**, *5* (2), 371−378.
(32) Liang, Z.; Pan, P.; Zhu, B.; Inoue, Y. Isomorphic Crystallization of Poly(hexamethylene adipate-co-butylene adipate): Regulating Crystal Modification of Polymorphic Polyester from Internal Crystalline Lattice. *Macromolecules* **2010**, *43* (15), 6429−6437.
(33) Hosier, I. L.; Alamo, R. G.; Esteso, P.; Isasi, J. R.; Mandelkern, L. Formation of the α and γ Polymorphs in Random Metallocene−Propylene Copolymers. Effect of Concentration and Type of Comonomer. *Macromolecules* **2003**, *36* (15), 5623−5636.
(34) De Rosa, C.; Auriemma, F.; de Ballesteros, O. R.; Resconi, L.; Camurati, I. Crystallization Behavior of Isotactic Propylene−Ethylene and Propylene−Butene Copolymers: Effect of Comonomers versus Stereodefects on Crystallization Properties of Isotactic Polypropylene. *Macromolecules* **2007**, *40* (18), 6600−6616.
(35) Pouget, E.; Almontassir, A.; Casas, M. T.; Puiggalí, J. On the Crystalline Structures of Poly(tetramethylene adipate). *Macromolecules* **2003**, *36* (3), 698−705.
(36) Minke, R.; Blackwell, J. Single crystals of poly(tetramethylene adipate). *J. Macromol. Sci., Part B: Phys.* **1980**, *18* (2), 233−255.
(37) Lugito, G.; Woo, E. M. Intertwining lamellar assembly in porous spherulites composed of two ring-banded poly(ethylene adipate) and poly(butylene adipate). *Soft Matter* **2015**, *11* (5), 908−917.
(38) Papageorgiou, G. Z.; Tsanaktsis, V.; Bikiaris, D. N. Crystallization of poly(butylene-2,6-naphthalate-co-butylene adipate) copolymers: regulating crystal modification of the polymorphic parent homopolymers and biodegradation. *CrystEngComm* **2014**, *16* (34), 7963−7978.
(39) Van Krevelen, D. W. Calorimetric properties. In *Properties of Polymers*, 3rd completely revised ed.; Elsevier: Amsterdam, 1997; Chapter 5, pp 109−127.
(40) Zhang, J.; Zhu, W.; Li, C.; Zhang, D.; Xiao, Y.; Guan, G.; Zheng, L. Effect of the biobased linear long-chain monomer on crystallization and biodegradation behaviors of poly(butylene carbonate)-based copolycarbonates. *RSC Adv.* **2015**, *5* (3), 2213−2222.
(41) Young, R. J.; Lovell, P. A. *Introduction to Polymers*, 3rd ed.; Taylor & Francis: 2011.
(42) Gordon, M.; Taylor, J. S. Ideal copolymers and the second-order transitions of synthetic rubbers. i. non-crystalline copolymers. *J. Appl. Chem.* **1952**, *2* (9), 493−500.
(43) Gan, Z.; Abe, H.; Doi, Y. Temperature-Induced Polymorphic Crystals of Poly(butylene adipate). *Macromol. Chem. Phys.* **2002**, *203* (16), 2369−2374.
(44) Dong, T.; Kai, W.; Inoue, Y. Regulation of Polymorphic Behavior of Poly(butylene adipate) upon Complexation with α-Cyclodextrin. *Macromolecules* **2007**, *40* (23), 8285−8290.

DOI: 10.1021/acs.macromol.6b02457
Macromolecules 2017, 50, 597−608

Thibaud DEBUISSY

Développement de nouveaux polyesters par catalyse organométallique et enzymatique

Résumé

Dans un contexte du développement durable, de nouvelles architectures macromoléculaires biosourcées ont été synthétisées à partir de synthons (diacides et diols) pouvant être obtenus par voies fermentaires à partir de sources carbonées issues de la biomasse. Dans un premier temps, différents copolyesters aliphatiques ont été synthétisés en masse, à l'aide d'un catalyseur organométallique à base de titane, à partir de diacides (acides succinique et adipique) et de diols (1,3-propanediol, 1,4-butanediol et 2,3-butanediol) courts. Dans un deuxième temps, des architectures macromoléculaires similaires ont été obtenues par catalyse enzymatique en solution à l'aide de la lipase B de *Candida antarctica.* L'influence de la longueur et de la structure des monomères sur leur réactivité en présence de la lipase a été particulièrement étudiée. Dans un troisième et dernier temps, des architectures macromoléculaires à base d'oligomères hydroxytéléchéliques d'un polyester bactérien : le poly((*R*)-3-hydroxybutyrate) (PHB)tels que des poly(ester-éther-uréthane)s et des copolyesters ont été obtenues soit par couplage de chaîne à l'aide d'un diisocyanate, ou par transestérification organométallique et enzymatique.

Ces études ont permis d'analyser en détail l'effet de l'addition des synthons biosourcés dans les architectures macromoléculaires et notamment sur la structure cristalline, la stabilité thermique et les propriétés thermiques et optiques de ces polymères. De plus, le grand potentiel de la catalyse enzymatique pour la synthèse de polyesters et celui de l'utilisation d'oligomères de PHB pour l'élaboration de nouveaux matériaux performants ont pu être largement démontrés.

Mots-clés : Monomères biosourcés, Copolyesters, Catalyse organométallique, Candida antarctica lipase B, Poly((R)-3-hydroxybutyrate), Relations structure-propriété.

Abstract

In the context of sustainable development, new biobased and aliphatic macromolecular architectures were synthesized from building blocks that can be obtained by fermentation routes using carbon sources from the biomass. First, several aliphatic copolyesters were synthesized in bulk from short dicarboxylic acids (such as succinic and adipic acids) and diols (such as 1,3-propanediol, 1,4-butanediol and 2,3-butanediol) by organometallic catalysis using an effective titanium-based catalyst. In a second time, similar macromolecular architectures were synthesized by an enzymatic process in solution using *Candida antarctica* lipase B as catalyst. The influence of the alkyl chain length and the structure of monomers on their reactivity toward the lipase were particularly discussed. In the third and last part, new macromolecular architectures based on hydroxytelechelic oligomers of a bacterial polyester: poly((*R*)-3-hydroxybutyrate) (PHB), such as poly(ester-ether-urethane)s and copolyesters, were obtained by either chain-coupling using a diisocyanate, or organometallic and enzymatic transesterification, respectively.

These studies permitted to determine a close relationship between the effect of the building blocks structure integrated in the final macromolecular architectures and the intrinsic properties, such as the crystalline structure, the thermal stability and the thermal and optical properties, of these polymers. In addition, the great potential of the lipase-catalyzed synthesis of polyesters and the use of PHB oligomers for developing new high performance materials has been clearly established.

Keywords: Biobased monomers, copolyesters, Organometallic catalysis, Enzymatic catalysis, Candida antarctica lipase B, Poly((R)-3-hydroxybutyrate), Structure-property relationship.